A STUDY OF

THE AERODYNAMIC CHARACTERISTICS OF CAPTOR HOODS

IN

LOCAL EXHAUST VENTILATION SYSTEMS

A THESIS SUBMITTED TO

THE UNIVERSITY OF ASTON IN BIRMINGHAM

FOR THE DEGREE OF

DOCTOR OF PHILOSOPHY

BY

VALIOLLAH YOUSEFI

January 1981

Department of Occupational Health and Safety

A STUDY OF THE AERODYNAMIC CHARACTERISTICS OF CAPTOR HOODS IN LOCAL EXHAUST VENTILATION SYSTEMS

VALIOLLAH YOUSEFI

SUBMITTED FOR THE DEGREE OF DOCTOR OF PHILOSOPHY,

SUMMARY

The research objectives were:-

1) To review the literature to establish the factors which have traditionally been regarded as most crucial to the design of effective exhaust ventilation systems.

2) To design, construct, install and calibrate a wind tunnel.

3) To develop procedures for air velocity measurement followed by a comprehensive programme of aerodynamic data collection and data analysis for a variety of conditions.

The major research findings were:-

a) The literature in the subject is inadequate. There is a particular need for a much greater understanding of the aerodynamics of the suction flow field.

b) The discrepancies between the experimentally observed centre-line velocities and those predicted by conventional formulae are unacceptably large.

c) There was little agreement between theoretically calculated and observed velocities in the suction zone of captor hoods.

d) Improved empirical formulae for the prediction of centre-line velocity applicable to the classical geometrically shaped suction openings and the flanged condition could be (and were) derived.

Further analysis of data revealed that: -

i) Point velocity is directly proportional to the suction flow rate and the ratio of the point velocity to the average face velocity is constant.

ii) Both shape, and size of the suction opening are significant factors as the coordinates of their points govern the extent of the effect of the suction flow field.

iii) The hypothetical ellipsoidal potential function and hyperbolic streamlines were found experimentally to be correct.

iv) The effect of guide plates depends on the size, shape and the angle of fitting. The effect was to very approximately double the suction velocity but the exact effect is difficult to predict.

v) The axially symmetric openings produce practically symmetric flow fields. Similarity of connection pieces between the suction opening and the main duct in each case is essential in order to induce a similar suction flow field.

Additionally a pilot study was made in which an artificial extraneous air flow was created, measured and its interaction with the suction flow field measured and represented graphically.

Key words:- Local exhaust, Captor hood, Centre-line velocity, Guide plate (flange), Extraneous air flow.

ACKNOWLEDGEMENTS:

The author wishes to thank Professor R. T. Booth, Head of Department of Occupational Health and Safety, and all members of the Staff for their help and support, especially Dr. I. Lavery, in the preparation of this thesis.

Also I would like to express my gratitude to my brothers Mr. Abdollah Yousefi and Dr. Rohollah Yousefi for providing financial assistance without which this research could not have been completed. I would like to thank Mrs. Hasleton for typing the thesis.

Finally I owe a great deal to my family, particularly to my wife Nahid for her continuous support.

DEDICATION

I dedicate, with affection this thesis to my late mother and to my family.

NOTATIONS

SYMBOL	DESCRIPTION
A, ARE	Area of Suction Opening
AR	Aspect Ratio (Width/Lenght)
A, B, C, ..A', B', C'..a, b, c.	Constant Variables as stated at the point of appearance
B_i	Biased error
bi, i=1, 2, ..n...	Constant variables
B_t	Characteristic temperature of thermistor expressed in ^{o}K
C_P	Specific heat at constant pressure
Curl	Curl a mathematical term
D	Diameter
Deq	Equivalent diameter for identical Velocity and friction loss.
Div	Divergence a mathematical term
$d\ell$	Element of lenght
$d\vec{s}$	Displacement vector
E(..,..,..), E'(..,..,.)	Point in three dimentional space
F, Fl	Nondimentional variable
F(..,..,), F'(..,..,..)	Points in three dimentional space
f	Friction factor
g	Gravitational acceleration
G, G'..,....	Points in three dimentional space
HL, Hl	Friction loss
HR	Hydraulic radius (Area/Perimeter)
K, k	Constant variable
l	Lenght or an element of lenght
m	Metre
m^2	Square metre
m^3	Cubic metre
ms^{-1}	Metre per second
m^3s^{-1}	Cubic metre per second
n	Constant variable
NTe	Negative resistance temperature coefficient
PTe	Positive resistance temperature coefficient

Notation Continnued (1)

Q, Q_a, Q_m	Measured flow rate
R	The radius of round suction opening
R_{T1}, R_{T2}	The resistance at temperature T1 ($^\circ$K) and T2 ($^\circ$K) respectively
Res	Residuals
RMS	Residual Mean Square
RMSR	Root Mean Square Residual
S_a	Surface Area under the influence of suction
S_p	Static Pressure
t	Time
T	Temperature
T_p	Total Pressure
V, V_x	Point Velocity in front of suction opening
$\bar{V}, V_{BA}, V_{BAR}$	Average Face Velocity
V_c	Centre Point Suction Velocity
$\vec{V}$	Velocity Vector of Air Particle
V_p	Velocity Pressure
V_y	Velocity inside the Duct at y distance from the wall
w	Widht of noncircular Suction Opening
WG	Water Gauge
X, Y, Z	The Cartesian Coordinates of Air Particle in three dimentional Space in front of Suction Opening
p	Pressure Loss
te	Temperature Equivalent
ω	Duct Roughness Factor
η	z/w
ξ	x/w
σ^2	Error Variance
ϕ	Velocity Potential Function
ψ	Stream Function
∇	Gradient Operator
∇^2	Laplacian Operator

LIST OF CONTENTS

LIST OF CONTENTS (contd)

CONTENTS (Contd.)

CONTENTS (Contd.)

CONTENTS (contd)

LIST OF TABLES

LIST OF TABLE (Contd)

LIST OF FIGURES

LIST OF FIGURES (Contd.)

LIST OF FIGURES (Contd.)

FIGURES (Contd).

FIGURES (Contd.)

FIGURES (Contd.)

FIGURES (Contd.)

FIGURES (Contd.)

FIGURES (Contd.)

FIGURES (Contd.)

LIST OF DRAWINGS

LIST OF PICTURE PLATES

LIST OF PICTURE PLATES (contd)

LIST OF APPENDICES

CHAPTER ONE

INTRODUCTION

Extraneous materials carried by air are generally termed "contaminant". The Chapter begins with a survey on the work room contaminant, its production, dispersion and the behaviour of different types of contaminant. Then it is followed by a review of engineering control methods: local exhaust ventilation, especially the application of captor hood and the legal requirement for its use. Present design methods of captor hoods are generally based on recommended capture velocities for certain types of workroom air contaminant. Industrial workroom air consists of a suspension of solid and liquid particles in a gaseous medium i.e. it is an aerosol.

The most important feature of contaminant particles is the difference in behaviour between coarse particles and fine particles (respirable size particles are all in the latter range). The heavy particles move through the air in a definite trajectory sometimes at high speed. Fine particles (e.g. particles of diameter less than 20 micron) on the other hand, move only with the air that contains it. Physical and chemical properties of materials are different when in the form of small particles and dispersed in air. Surface area and effective volume are the most important factors, which are both greatly increased in the form of small particles. The ordinary laws of mechanics giving e.g. a rate of fall through air of fine contaminants, appear no longer to apply. Effective volume, in contrast, governs the design of the control devices. For example if a cubic

particle of one centimetere in size (with one cubic centimetre and 6 cm^2 of effective volume and surface area respectively) is broken into cubes of one micron in size, the total number of cubes will increase to 10^{12} with six square metres of surface area. If assuming a contaminant particle of this size was dispersed at a concentration of 10^8 particles per cubic metre, the control system (e.g. exhaust system) would have to take in 10^4 cubic metres of air in order to collect contaminant which would itself occupy one cubic centimetre. The volume increases in proportion to the dilution.

Turbulence causes diffusion and increases the rate of flocculation. Flocculation of particles is different for different size of contaminant. For example, dusts and smokes behave differently e.g. a cloud of dust becomes finer in particle size as time passes by, whereas in the case of a smoke cloud it is the reverse.

The physical properties of the transport media (i.e. air) are also important in studying the movement behaviour of contaminant particles.

Dispersion of contaminant into the workroom atmosphere may create an unhealthy, unsafe or socially unacceptable environment.

The importance of industrial contamination, both as a health hazard and as an objectionable accompaniment to working conditions has been recognized by researchers. Works are devoted to specifying the conditions under which contaminant may be produced, how it can be dispersed by air currents, how it can be controlled at or near to the source by installing a suitable local exhaust system. Yet, the science of contaminant-control has not been fully developed. Rule-of-thumb methods are still popular among designers.

One of the engineering methods of controlling

industrial contaminants is the application of local exhaust ventilation. Local exhaust ventilation prevents the dispersion of contaminant and ensures that injurious, damaging and hazardous contaminant concentration are maintained at acceptable levels.

A local exhaust ventilation system consists of a hood, a transport duct, a filtration system, an air mover and finally a discharge duct. Exhaust ventilation according to the inlet condition can be classified as:

(i) total enclosure

(ii) booth

(iii) captor hood

(iv) receptor hood

Each group has certain aerodynamic characteristics. In the application of the total enclosure and the booth type of local exhaust system, the source of contaminant is surrounded either totally or partly, respectively.

The receptor and captor hoods on the other hand must be placed either at some distance from the source of contaminant or the source is placed at the face of the hood opening. Except in the case of receptor hoods, where the hood receives the contaminated air as it flows from its point of generation, for the other group of exhaust system, the air must be drawn from the vicinity of the source of the contaminant.

In the case of the captor hood, some of the contaminant may be moving towards the hood but with so low a velocity that it would not move far enough to enter it. Some of the contaminant may move away from the hood so that unless it is accelerated or, if necessary, the direction of its movement is changed, it would never enter the hood.

The moving velocity of air-borne-contaminant generally

is taken as the velocity of air in which it moves and it can be measured by an anemometer or other types of air velocity meter.

The capture velocity at any point in front of the hood is that velocity induced bythe local exhaust system which is necessary to overcome the dispersive forces and unfavourable ambient air movement in order to capture the contaminated air at any point, by causing it to flow into the hood. Tables containing the suggested minimum capture velocities or air flow volume, are given in the Manual On Industrial Ventilation (American Conference of Governmental Industrial Hygienists 1976). The Standard Institutions set some standard capture velocities, for example, American Standard Association recommend a 0.37 ms^{-1} capture velocity for chromic acid mist of 0.1 mg m^{-3} (threshold limit value).

The legal requirement for exhaust ventilation installation is more than a century old. The use of local exhaust ventilation given in Section 63 of the FactoriesAct 1961, entitled "Removal of Dust and Fumes" reads as follows:

> "In every factory connected with any process carried on, there is given off any dust or fumes or other impurity of such a character and to such an extent as to be likely to be injurious or offensive to the persons employed, or any substantial quantity of dust of any kind, all practicable measures shall be taken to protect the persons employed against inhalation of the dust or fumes or other impurities and to prevent it accumulating in any workroom and in particular where the nature of the process makes it practicable, exhaust appliances shall be provided and maintained as near as possible to the point of origin of the dust or fumes or other impurity, so as to prevent its entering the air of any workroom."

Despite the legal requirement and the recognition of the role of local exhaust system and the widespread use of captor hoods to control workroom atmospheric contaminants, the basic principles governing the design and effectiveness of captor hood are not yet properly understood and misconceptions still are prevalent. For example the believe is that positioning a captor hood with high suction velocity at remote distance will give a sufficient control ; or the induced suction velocity is the principal or the only determinant of the effectiveness of captor hood. Whereas, generally suction deficiency arises when the contaminant element fail to move with the induced air movement by suction system. Such a failure is primarily caused by the forces of generation, release and gravitational, as well as extraneous ambient air movement. Also the orientation of the suction inlet, i. e., facing upward, downward, sideways affects the suction efficiency.

Another important factor is the hood aerodynamic efficiency; i. e. the combination of a high enough rate of air intake with the least possible rate of suction and power consumption.

There is a significant differences between results obtained using the empirical formulae given by Dalla Valle et al (1931), Pruzner (1939), Silverman (1941), Drkal (1970 - 1971), and Fletcher (1977, 1978).

A comparison of the results of all these workers (together with the results of the present investigated) for a rectangular hood are shown by Fig.6. 2 page 131 below.. Moreover, most of the researchers did not study the effect of extraneous air movements. There is some in formation available which shows this factor has been taken into account in the study of the velocity distribution at the suction zone (Ladisau Opple 1957). Also Fialkoskaya (1947) studied the effect of a constant cross-current to the vertically positioned hood. The effect of exteraneous air movements appears to be an important factor in the effectiveness of exhaust ventilation for reducing workroom contaminant concentration in the breathing zone of employees.

The application of mathematical analysis in most cases has been confined to the formulation of the problem by forming the differential equations and establishing the boundary conditions. Owing to the complexity of the phenomena and the fact that the analytical solutions are not usually available. Therefore a test of comparison between numerical estimation and experimental measured values are essential. The procedure adopted is to turn to numerical solutions compared with experimental testing and empirical solutions.

This research was based on the objective of comparing theoretical and empirical formulae and assessing the discrepancies of results obtained. In order to achieve the objective, practical tests had to be undertaken. To this end the research facilities were designed and installed. To study the aerodynamic behaviour of air under suction, the following hoods were tested:

(i) Hoods with circular cross section,

(ii) Hoods with rectangular cross section,

(iii) Hoods with square cross section.

The above types of hood were tested with and without flanges.

Aerodynamic measurements consisted of:

(i) Centre-line axis point velocity measurement,

(ii) Horizontal plane symmetry point velocity measurement,

(iii) Vertical plane symmetry point velocity measurement,

(iv) Ellipse locus point velocity measurement.,

(v) The measurement of the angle between the centre line axis and the streamline tangents.

Some of the above tests were repeated for a combined case of suction and a fixed current of blown air representing extraneous air movement.

CHAPTER TWO

LITERATURE SURVEY AND ORIENTATION OF RESEARCH

Introduction.

The many difficult problems affecting the health and safety in industrial plants have been accentuated by the general increase in tempo which has taken place in recent years and much time and effort has been expended in trying to find a solution by management, trade unions and governmental institutions.

Danger related to work is an unwanted and unintended by-product of the work environment.

Environmental factors are increasingly recognized as causative agents in occupational disease e.g. cancer.

The selection and implementation of action against dangerous factors by legislators, administrators and enforcing authorities are different. The choice of preventiv methods are influenced by social and economic considerations as well as scientific considerations (Atherley 1978).

Among industrial workers, foundry men are more prone to lung disease than others (McBain et al. 1962), consequently much work has been done in the study of the characteristics of airborne matter , and in the development of techniques of dust suppression in the foundry trade for example the Harrogate Conference: "Foundry Ventilation and Dust Control" (1955) is one of the standard reference publications. The British Cast Iron Research Association and others devoted a great deal of effort to the rôle of dust both as a health hazard and as an objectionable accompaniment to working conditions (Health and Safety Executive (1975)). In the foundry two important ways of the dispersion of dust were dealt with extensively. The control of dust dispersed

by the high-speed currents of air thrown off from grinding wheel of all types, and the control of the slower speed dust clouds produced at the "Knock-out" and dispersed by general foundry air movement. In these cases, like the majority of other cases, control of workroom contaminants can be accomplished by local exhaust ventilation and application of captor hoods. The type of local exhaust ventilation used in a foundry are of two types: Localised extraction at the work region i. e. the knock-out opertion, and extraction localised at the machines or tools i. e. low volume high velocity system, such a system is available for all types of fetting equipment (e. g. portable grinders, pneumatic chisel, pedestal or bench grinders and swing frame grinders).

The study of the basic principles governing the behaviour of hoods in local exhaust ventilation were presented by Dalla Valle, et al. in 1931. They studied the centre line characteristics of numbers of round, square and rectangular hoods. Furthermore, DalaValle (1946) studied the aerodynamic characteristic for flanged hoods. Alden (1939) treated the data given by DallaValle graphically.

Silverman (1942) followed DallaValle's study with longer and different diameter of round duct and the extention of distance along the centre line axis and different instruments. Pruzner (1939) also followed DallaValle's methods with different instrumentation. More recently Fletcher (1977) studied the centre line velocity character. Table 2. 1 contains the empirical formulae for the centre line velocity variation in front of exhaust hoods and alots. It can be seen that relationship of the fall-off of velocity in the field of suction zones differs from the inverse square law to a larger or smaller extent depending upon the suction profile of the suction orifice. The mathematical solution of the problem concerning the character and dimension of the zone of suction for the different shapes of suction, occurring in practice, is extremely complex.

In studying the aerodynamic characteristics of the suction opening DallaValle et al. considered the following factors:

(i) suction flow rates

(ii) the geometric shape and area of opening

(iii) the transition piece (i.e. reduction or enlarging section conducting the hoods to the main duct system).

They represented their data diagramatically by means of contour lines or curves, each of which represented the geometrical locus of equal velocity. This was the first conceptual study of suction flow pattern. They found that these curves are not influenced by the total air flow through a given hood, nor did the characteristics differ with the geometric shape of the opening. Although rectangular openings exhibit a flattening of their contours this varied with the ratio of the sides. An increase in the area caused a displacement of curves at right angles to the axis of the opening. They concluded that the ratio of the velocity at any point, to the average velocity across the suction opening remains constant for all rates of flow. Also they said that the transition piece has no significant effect upon the distribution of air flow along the suction opening. This means that there is no change in the centre line velocity. They formulated their findings by the assumption that the axial velocity tends towards zero when the distance approaches infinity and also the axial velocity at the face of the suction opening is equal to the average face velocity (see Table 2.1).

Pruzner found that for a given opening the ratio of the

velocity at a point in the suction affected area to the velocity at the cnetre of the suction opening for different flow of suction is practically constant. This principle holds provided that the velocity at any points in the suction affected area, approaches to the mean velocity at the inlet opening. This is in support of the finding made by DellaValle et al. These researchers also found that velocity contour for geometrically similar orifice are the same. In this case, when all linear dimensions are expressed by comparing the value of the ratio of coordinates of the points to the side of rectangular or the diameter of a circle, and the velocity in the form of ratio of velocity at the point to the centre line or average velocity of the opening are compariable, which is another confirmation of results given by DallaValle. Pruzner found that for a rectangular opening with sharp edges the value of centre point velocity is very near to the value of average face velocity ($\bar{V}$) so they used the ratio of 1 for practical purposes. For circular and square openings with sharp edges this ratio is given as 0.945 to 0.95.

Consequently the fall-off of centre line velocity in front of suction openings is characterised by the factors: flow rate, area, and shape of opening. Therefore, Pruzner used the hydraulic radius concept to account for the shape factor. Hydraulic radius is the ratio of suction opening area to its perimeter (HR). The general model of the equation of the variation of axial velocity given by Pruzner is as follows:

$$\frac{V_x}{V_c - V_x} = k(x/HR)^n \qquad (2.1)$$

Where

V_x is the centre line point suction velocity,

V_c is the suction velocity at the centre of opening

x is the X-coordinate of point of velocity measurement,

HR is the hydraulic radius.

k and n were found (see table 2.1) by Pruzner, treating the experimental data derived from testing different types of suction openings.

Silverman appeared to know nothing of Pruzner's work. He extended his research on the basis of DallaValle's methods. He approved the point made by DallaValle on the $V_x/\bar{V}$. which is constant for different Q. But he found that velocity near the opening and at the opening is 1.5 to 1 times the average opening velocity,

and that axial velocity is equal to room-air-current when x approaches infinity. He also found that DallaValle's finding about the transition piece was not valid. He extended his study up to 40" away from the opening (DallaValle studied up to 10" distance from the opening) also he used ducts of 2" to 20" diameter. (DallaValle tested 4, 6, 8, 11.3 and 16" diameter ducts.). He observed that the fall-off of the velocity became asymptotic at a considerable distance from the opening. This asymptote is the ratio of room air movement and the average face velocity of suction opening. He used the flanged opening, and found that it alters the axial velocity and for control at further distances a wider flange was recommended (see Table 2.1 for the formulae)

A theoretical study of round and rectangular slot duct with an imaginary infinite flat plane flange has been undertaken by Fr Von Drkal (1970, 1971) (see Table 2.1.). There has been no complete analytical solution for the problem concerning the round duct. The centre line velocity given by Drkal is as follows:

$$\frac{V_x}{V_{BA}} = 1 - \frac{x/D}{\sqrt{(x/D)^2 + \frac{1}{4}}} \qquad (2.2)$$

Where Vx is the point velocity along the centre line axis ms^{-1}

V_{BA} is the average face suction velocity ms^{-1}

x is the coordinate of the point m and

D is the diameter of suction opening, m.

The most recent study of Fletcher (1977) on the centre-line velocity characteristics of rectangular unflanged hoods and slots showed that for an equal area, and flowrate the velocity at a fixed point is inversely proportional to the ratio of smaller side to larger side of the rectangular hood.

The model used by Fletcher for the treatment of his experimental data is the same as DallaValle's formula for the variation of centre line velocity in front of rectangular hood i.e.

$$\frac{V_x \cdot A}{Q} = \frac{1}{c + d\left(\frac{x}{\sqrt{A}}\right)^n} \qquad (2.3)$$

where: A is the area of suction opening

Q is the suction flowrate

c,d and n are constants which were found by treating the experimental data graphically (Fletcher, see Table 2.1).

Neither DallaValle nor Pruzner referred to the importance of non-directional room air currents. However, the significance of the room air current has been pointed out by Silverman (1942) and Harrold (1941) but the importance of this factor has still not been studied.

The instruments and techniques used by these researchers were quite different. DallaValle used a modified cylindrical pitot tube in conjunction with a sensitive micromanometer (Whalen). This is a device for measuring instantaneous point velocity. Inaccuracy of their measurement was mainly due to calibration and measuring equipment.

After Silverman's investigation DallaValle admitted that the discrepancy of their findings may partly be due to instrument

variation, DallaValle states that:

"At the time of the original work on centre line velocities and velocity contours was undertaken (1928-1929) only the cylindrical pitot-static tube was available for measuring point velocities."

Pruzner used an electro-anemometer for the study of air motion. Silverman used a thermometer-anemometer. These two instruments give the integrated velocity over a much larger area. All the instruments used by these researchers have one common disadvantage in that the measurement of velocities below O.5 ms^{-1}. becomes very difficult.

The thermometer-anemometer and electro-anemometer both suffer an additional disadvantage in that they do not give a directional reading. Fletcher used a constant temperature hot wire anemometer.

The literature survey incidentally revealed that texts and publications dealing the local exhaust systems are sparse.

The evaluation of the efficiency of local exhaust systems is very old. In 1936 Hatch studied the efficiency of local exhaust systems used in granite cutting. DallaValle (1939) studied the design of local exhaust hood and concluded that the frequent ineffectiveness is partly due to the lack of knowledge of factors governing the operation of suction opening. A detailed survey of the use of exhaust system for the control of industrial pollutants has been undertaken by Whitheridge (1945). The conclusion are that most industrial exhaust systems are unsuccessful. McBain et al. (1962) showed that dust control methods were not effective, or the dangerous dust arises from the secondary source of dust e.g. an adjacent dustier area, which either needs an efficient dust control method or the installed one needs to be maintained or the design criteria were wrong and the system requires redesigning and improvement. Gill (1978) points out that the many industrial exhaust ventilation system are unsuccessful, and the main symptom is the inability to capture the contaminant at the point of release i.e. poor capture velocity. Gill summarizes failure points as follows:

(i) faulty design

(ii) faulty installation

(iii) faulty maintenance and care

(iv) faulty procedures

The following is a brief description of the above failure points given after Gill.

Faulty design is due to the following;

1. Inappropriate relative distance suction opening and the source of contaminant.
2. The suction opening is not equipped with any guide plates.
3. Low volume of suction flowrate due to small main duct diameter.
4. An inappropriate fan in the system.
5. Bad ducting design near to the fan, causing reduction of fan performance.
6. Flow fluctuation caused by unaccounted enviromental factors. (i. e. ambient air movement).
7. For a system of too many branches, there is always a risk of an unbalanced system and insufficient fan capacity.
8. At the design stage there has been no allowance for the replacement and make up air for the exhaust volume.

Faulty installations can be due to the following reasons:

1. Bad electrical wiring, especially for the fan.
2. In the case of two stage fans, one stage my be opposing the other.
3. Air leakage through the duct joints.

4. Obstruction in the duct work at installation stage.
5. In cases where dampers are installed, they may not function correctly.

Faulty Maintenance and care.

These may be a combination of some of the instation faults as well as the problem caused by deterioration the following are the most prevailing faults:

1. Dust deposition and air flow restriction in the main duct due to low transport velocity or rough, sticky and damp contaminant or the combination of these.
2. Damage and dent to the duct or hood, causing restriction or leakage.
3. Dust deposition on fan blades reducing its performance.
4. Fan blade corrosion or worn ducts corrosive or abrasive contaminant.
5. Damage to fan motors and poor motor performance.
6. Wrong operation of dampers due to corroded shafts and handles.
7. Faulty filters and air cleaners due to blockage.
8. Faulty weather protection devices due to corrosion or damage.

Faulty Procedures

In some cases the operation of a part or the whole of a system are left to the operators. There is a great danger that the operation may be shut-off perhaps because of noise or draughts. Sometimes the operation may be initiated and left on when the system was designed only for a limited period of operation.

A brief survery of legislation, especially those section concerned with the use of exhaust ventilation, revealed that there has not been any significant change in British legal requirements since 1925 (Dean 1973 and Ezihe 1976).

The American approach to the use of local exhaust ventilation is different. For example, there are several federal and trade association laws, standards and codes of practice. The general problems are:

1. There is no single solution to the difficulties which will meet the requirement of every industry, the fundamental design criteria are not set down universally.
2. There is a significant discrepancy between results obtained with the empirical formulae given for the fall-off of the suction centre line velocity in front of suction hoods.

The following quotation from Dellavalle is evidence of the awareness of the problem by researchers:

"... The Author's quotation is admittedly an overall average for all types of hood whereas silverman's equation applies to a round opening alone. Nevertheless, the differences are far too great to be dismissed for this reason alone".

3. The designers do not have a clear understanding of the physical laws governing local exhaust systems, beacause of their lack of relevant scientific knowledge.
4. Despite the existance of Threshold Limit Values, Standards, and Legal requirements, still designers, managers, employees, inspectors and trade union bodies do not have a clear answer to the following questions:

(i) is a local exhaust system applied to an industrial process for the control of contaminant to an acceptable level efficient?

(ii) What level of the control efficiency is the optimum level?

(iii) What sort of hoods will constitute legal compliance?

(iv) Is the legal requirement specific enough?

Consequently, the design of captor hoods and any other local exhaust ventilation requires an aerodynamic study of their characteristic factors. The pattern of the effect of these factors involved at the intake of the suction opening, requires to be studied. the effect of opening guide plates (i. e. flanges) on the suction pattern and centre line velocity as well as the suction flowrate needs to be established.

Orientation of Research. The research was designed to undertake the above aerodynamic studies. A great deal of time was spent on the preparation and purchase of research facilities. The reasons were the unavailability of equipment and financial restraints. Finally, the research schedule mainly focussed on the following steps:

(i) Design of a compact model scale local exhaust system

(ii) Design, purchase, housing and installation of a research wind tunnel.

(iii) Theoretical, hypothetical and numerical consideration of aerodynamical characteristics.

(iv) Calibration of measuring instruments and wind tunnel.

(v) Preliminary and check up tests both with compact model and wind tunnel.

(vi) A full scale experimental test of aerodynamic characteristic factors of different suction openings.

(vii) Analysis of data.

TABLE 2.1 Formulae for the centre line velocity of a suction opening (a survey of literature)

Year	Investigator or Reporter	Equation	Shape of Opening	Limitation and instruments of measurement	Notation and Remarks
1931	J.M.DallaValle and T.Hatch	$V_x = \frac{F.V_{BAR}}{1 + F}$ $F = 0.03436D^{2.08}x^{-1.91}$	Round Unflanged	(1) Modified pitot tube anemometry (2) Lowest velocity reading 0.5 m/sec (3) $0 \leq x \leq 0.254$ metres	V_x = outward velocity ms^{-1} x = distance m D = diameter m V_{BAR} = Q/area of opening ms^{-1}
		$V_x = \frac{V_{BAR}.F}{1 + F}$ $F = 0.044612A^{1.04}x^{-1.91}F_1$ $F_1 = \frac{1}{1+0.259\left(\frac{AR}{1-AR}\right)^{-1.104}}$	Square or rectangular unflanged	AR=1, 0.75, 0.667, 0.5, 0.333	A = Area of square or rectangular duct (m^2) AR = ω/ℓ ω = Width (m) ℓ = Length (m)
1932	DallaValle	$V_x = \frac{V_{BAR}.F}{1 + F}$ $F = 0.1 A x^{-2}$	For all shapes of opening, unflanged		
1939	A.S.Pruzner	$V_x = \frac{V_c.F}{1+ F}$ $F = k(X/HR)^n$	For all shapes of opening unflanged	(1) Sink point assumption (2) $0 \leq x/HR \leq 4$ (3) Electro-anemometer velocity range 0.15 up to 2.5 m/sec (4) Volume of air with venture nozzle	HR = hydraulic radius = Area/cirxumference or perimeter k and n has to be found V_c = velocity at x = 0.0 OR centre point

TABLE (2.1) continued (1)

Year	Investigator or Reporter	Equation	Shape of Opening	Limitation and Instruments of measurement	Notation and Remarks
1939	A.S.Pruzner	For $^{x}/_{HR} \leq 2$ $k = 0.8, n = -1.4$ For $^{x}/_{HR} > 2$ $k = 1.0, n = -1.7$	For all shapes of opening unflanged	Logarithmically plotted of data	
		$V_x = \frac{0.95V_{BAR}.F}{1+F}$	Square and Round	$V_c = 0.95V_{BAR}$	Two formula one for each sets $k, n, {}^{x}/_{HR}$
		$V_x = \frac{V_{BAR}.F}{1+F}$	For rectangular	$V_c = V_{BAR}$	Two formula one for each set of k,n, and $^{x}/_{HR}$ values
		$V_x = \frac{0.159V_{BAR}}{(HR/x)}$	For slit		
1939	J.L.Alden	$V_x = V_{BAR}.F$ $F = k\left(\frac{x}{\sqrt{A}}\right)^{n}$	Non-dimensional test	$V_c = V_{BAR}$ $V_x = 0.0$ $x \rightarrow \infty$	For replotting DallaValle's data

Year	Investigator or Reporter	Equation	Shape of Opening	Limitation and instruments of measurement	Notation and Remarks
1942a	Leslie Silverman	SAME AS ABOVE $V_x = V_{BAR} \cdot F$ $F = 0.17\left(\frac{\sqrt{A}}{\sqrt{x^2}}\right)^{1.5}$	Round unflanged	(1) 6% average deviaion (2) $0.5 \leq \frac{x}{\sqrt{A}} \leq 3$ (3) Heated thermometer (4) anemometer average velocities over a 1" band were measured	Experiment V_x in fpm, x in inches, Q, in cfm, D, w, ℓ inches
		$V_x = \frac{V_{BAR}}{4.45\frac{x^2}{A}+1}$	Round unflanged	Correction to Dalla-Valle's formula	$x \leq 40"$
		$V_x = \frac{V_{BAR}}{3.1\frac{x^2}{A}+1}$	Flanged round	SIZE — DISTANCE 2" and 4" — 2 - 12" 6" — 3 - 12" 10" — 5 - 25"	
		$V_x = 55.4\, Q/x\ell$	Narow slot flanged $w/\ell \leq 0.5$		
1942 b		$V_x = 46Q/x\ell$ (Theoretically) $V_x = 23.8(\ell w+1)/w)Q/x\ell$ (Experimentally)	Narrow slot " "	$\frac{1}{2}" < w < 2$, Q cfm, ℓ, x in inches, V_x in fpm.	w/ℓ for flanged slot is more critical $x \leq 1"$ $w/\ell \leq 0.2$
1971	Von Fr Drkal	$V_x = V_{BAR} \cdot F$ $F = \frac{1}{\pi}\left(\arctan\frac{\xi+\frac{1}{2}}{\omega} - \arctan\frac{\xi-\frac{1}{2}}{\omega}\right)$ $\eta = x/w, \xi = z/x$ $V_{BAR} = Q/w$	Flanged Rectangular	$\ell >> w$ Flanged width = 4w	V_x Velocity along the direction of x-axis

TABLE 2.1 continued (3)

Year	Investigator or Reporter	Equation	Shape of Opening	Limitation and instrument of measurement	Notation and Remarks
	Continued	$V_z = V_{BAR} \cdot F'$ $F' = \frac{1}{\pi} L_n \left[\frac{(\xi+\frac{1}{2})^2+\eta^2}{(\xi-\frac{1}{2})^2+\eta^2} \right]^{\frac{1}{2}}$		All theoretical consideration	V_z is the velocity along the z-axis
		$V_x' = V_{BAR} \cdot \frac{2}{\pi} \text{arcton} \frac{1}{\xi}$			V_x' is the velocity on x-axis
		$V_z' = V_{BAR} \cdot \frac{1}{\pi} L_n \frac{\xi+\frac{1}{2}}{\xi-\frac{1}{2}}$			V_z' is the velocity in the direction of z-axis (see Fig 3.9 For coordinat)
1970	Von Fr Drkal	$V_x = V_{BAR}\left(1 - \frac{X/D}{\sqrt{(X/D)^2+0.25}}\right)$	Round Flanged	(1)Sink point assumption (2)Axial symmetry condition (3)Ideal fluid	Theoretical compared with empirical
1977	B.Fletcher	$V_x = V_{BAR} \cdot F$ $F = 1/(0.93+8.5\alpha^2)$ $\alpha = \frac{x}{\sqrt{A}} \left(\frac{w}{\ell}\right)^{-\beta}$ $\beta = 0.2\left(\frac{x}{\sqrt{A}}\right)^{-\frac{1}{3}}$	Rectangular Unflanged	(1)AR between 1 and 1/16 Nine shapes (2)Area between 0.0025 to 0.09 M^2 (3)Q regulated by means of valve and measured with orifice plate (4)$0 \leq V_{BAR} \leq 30\ ms^{-1}$ (5)Constant temperature hot-wire anemometer	$\pm$ 5% C.L. Data were treated graphically logarithmically
1978					No formula is given by Fletcher

CHAPTER THREE

THEORETICAL AND HYPOTHETICAL CONSIDERATION OF SUCTION FLOW FIELD

3.1 Introduction

The aim is to find a suitable mathematical expression for velocity distribution around a suction opening. The classical shapes of suction openings are round, square and rectangular. To these suction openings there may be a guide plate or (plates) fixed (generally called flanges). The plates may be perpendicular to the wall of opening or inclined. The suction opening/hood is part of an exhaust system, when the system is operating a known volume of air will be drawn through the hood from the surrounding vicinity.

The displacement of the air particle determines the directions of flow at any point in front of the suction opening. The following discussion is about the streamline and equivelocity locus points of suction opening. The theoretical consideration is general, and can be applied to any sort of suction duct with or without flange.

3.2 Principle of Suction and aerodynamical assumptions.

Principally the suction is an operation to create a zone of low pressure into which air flows and forms a wider zone of weaker suction. This process is continucus until the depre-ssion is filled with replacement air flow from the immediate surrounding vicinity. This flow is orginated from rest. Lamb(1906) defined that any flow originated from rest is irrotational. It is well known that any irrotational flow is a potential flow (Lamb 1906). Also, air under laboratory and industrial ambient air movement conditions can be assumed to behave as incompressible. Therefore it is fair to assume the air motion under suction is steady, inviscid, irrotational and incompresible. It is clear that suction characteristics and aerodynamic assumptions are consistent. Consquently the suction flow is a potential flow.

3.3 Suction Streamline and Potential Curve

Throughout this section and in any other place except where stated to the contrary, the centre of suction opening is the origin. The centre-line-axis of suction opening is the X-axis of a cartesian coordinate system with XZ-plane as horizontal (see Figure 3.1). Let the component of an air particle (A) under the effect of suction be (x,y,z) which are time dependent. Displacement, $\vec{ds}$, of this air particle at instant 't' is

$$\vec{ds} = -\vec{V}(x,y,z,t)dt \qquad (3.1)$$

This equation is the vector form of the differential equation of the streamline. The negative sign means that the direction of the suction motion is toward the origin. In the vicinity of the suction affected area, vector V is defined. The absolute value of vector V is called the spead of air particle, and is measured by any air velocity meters (throughout the thesis the velocity referred to is this measured value except when otherwise stated).

Any curve ψ which will be described by vector V is called a stream function. On the other hand a family of curves for which the velocity of suction at any point of its locus point is constant is called a velocity potential curve (i.e. contour line) and it is defined by ϕ these two families of curves (i.e. ϕ and ψ) are orthogonal in the case of irrotational, incompressible and inviscid flow (Lamb1906). Throughout the thesis the functions $\phi(x,y,z,t)$ and $\psi(x,y,z,t)$ are defined as stream and velocity potential functions of suction flow.

3.4 Hypothesis on Potential Surface and Contour Lines

Generally the researchers in the field of the aerodynamic of suction opening assumed that the potential

surface is the surface of a sphere centred at the centre of the suction duct. In this study this assumption is generalised. The hypothesis is that the potential surfaces take the form of a quadric surface. The general equation of a quadric surface in three dimensional space is as follows:-

$$aX^2+bY^2+cZ^2+dXY+eXZ+fYZ+gX+hY+kZ+\ell = 0 \qquad (3.2)$$

This equation can be written differently as below:

$$\frac{(X-X_o)^2}{A^2} + \frac{(Y-Y_o)^2}{B^2} + \frac{(Z-Z_o)^2}{C^2} = 1 \qquad (3.3)$$

where a,b,c .... ℓ are positive or negative or zero and A,B,C are non-zero values and X_o,Y_o and Z_o are real numbers. If A = B = C the surface is a sphere, while if two of the three numbers are equal, the surface is an ellipsoid of revolution (i.e. spheroid). The intersections of this surface on the XY, XZ and YZ planes are ellipses (or circles in cases of A = B = C) of equations

$$\frac{X^2}{A^2} + \frac{Y^2}{B^2} = 1,\ \frac{X^2}{A^2} + \frac{Z^2}{C^2} = 1,\ \text{and}\ \frac{Y^2}{B^2} + \frac{Z^2}{C^2} = 1, X_o=Y_o=Z_o= 0 \qquad (3.4)$$

Therefore, the potential lines in any planes of coordinates are ellipses (or circles) of the above equations. According to Laplacian requirement in a potential flow (apart from the hydrodynamic requirements, i.e. irrotational incompressible, inviscid and steady state) the stream lines should be orthogonal to potential surfaces.

The potential and streamline complex, of a fully bounded flow out of a channel inside a reservoir is the same as the potential and field distribution of two semi-infinite conducting plates raised to different potentials which have the quadric potential and field distribution in any two dimensional plane (which are orthogonal conic) (Pipes 1946). By analogy the flow of air in front

of the suction duct is a reverse condition of the above flow out of a channel, for any volume of air drawn through the suction opening, and should pass through the surface, bounded to the wall or the suction duct. Therefore, in the case of suction operation, the potential surfaces are the ellipse traces of ellipsoidal surfaces bounded to the wall and streamlines are conic surfaces, so called eliptic hyperboloid of one sheet of equation

$$-\frac{X^2}{A'^2} + \frac{Y^2}{B'^2} + \frac{X^2}{C'^2} = 1 \qquad (3.5)$$

The traces on the ZY plane are ellipses and traces on the XY and XZ planes are hyperbolae. The section made by the planes Y=K (K is a constant) are the hyperbolae

$$\frac{Z^2}{C'^2(1-K^2/B'^2)} - \frac{X^2}{A'^2(1-K^2/B'^2)} = 1 \quad (3.6)$$

The traces on the ZY plane is an ellipse, the section made by any plane X=K are ellipses

$$\frac{Z^2}{C'^2(1+K^2/A'^2)} - \frac{Y^2}{B'^2(1+K^2/A'^2)} = 1 \quad (3.7)$$

These ellipses are also sections of ellipsoid made by any plane X =K.

Theoretically the velocity along the perimeter of this ellipse or velocity over the surface of the ellipsoid of revolution of this ellipse are equal. These conics have a common foci, and the foci are the intersection points of centre plane and the wall of the suction duct.

Practically the velocity along the ellipse and over the ellipsoid is the ratio of volume flowrate and the wall to wall bounded section area of the ellipsoid. This bounded area is equal to the part of the surface created by a complete revolution of the ellipse about its major axis.

In the case of freely suspended suction openings, without flanges the areas are different. The following is the consideration of potential surface area and equipotential lines of suction field in two dimentional flow.

In the case of rectangular ducts the equation of equi-velocity curves in the YZ-plane (see Fig.3.1) is as below:-

$$\frac{X^2}{A^2} + \frac{Z^2}{C^2} = 1 \qquad (3.8)$$

where C and A are semi-major and semi-minor axes of ellipse respectively. Therefore the following equation holds

$$C^2 = A^2 + \left(\frac{FF'}{2}\right)^2 \qquad (3.9)$$

where FF' is the foci distance and in this case is equal to the length (or diameter, in case of round opening) of suction opening where the centre of opening is coincident with the centre of the conic.

Mathematically the area of a complete revolution of this ellipse about its major axis (i.e. Z-axis) is as below

$$2\pi A^2 + (2\pi AC/e)\sin^{-1}e \qquad (3.10)$$

where $e = FF'/QQ'$ is called eccentricity and it is directly related to the flatness of the ellipse (in the case of A=C, the sphere potential surface, the area is $4\pi A^2$ which is the surface area of a sphere of radius A, centred at origin).

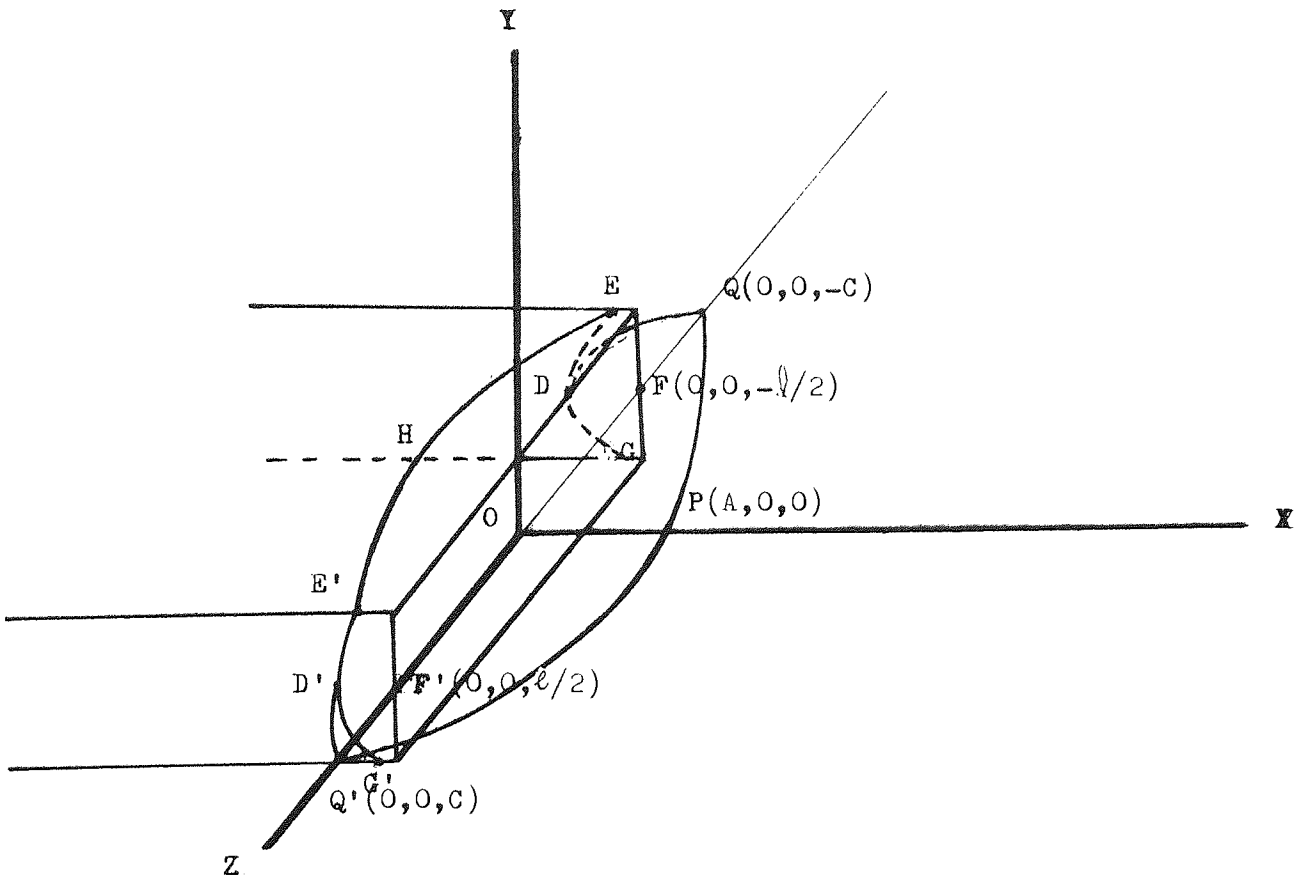

Fig.3.1 Depiction of equivelocity lines in front of a freely suspended rectangular duct.

From Figure 3.1, it can be seen that if 'ℓ', the eccentricity, be very small, the ellipse will be very flat, and if the semi-minor axis be less than or even equal to half of the vertical dimension of the suction duct (i.e. width in the case of the rectangular duct and diameter of a round duct) the area of the ellipsoid bounded by the walls of the duct does not cover the whole surface of the suction opening. In this case the assumption of hyperbola stream lines is not fully applicable to the whole suction zone, instead a radial streamline seems to be a better model.

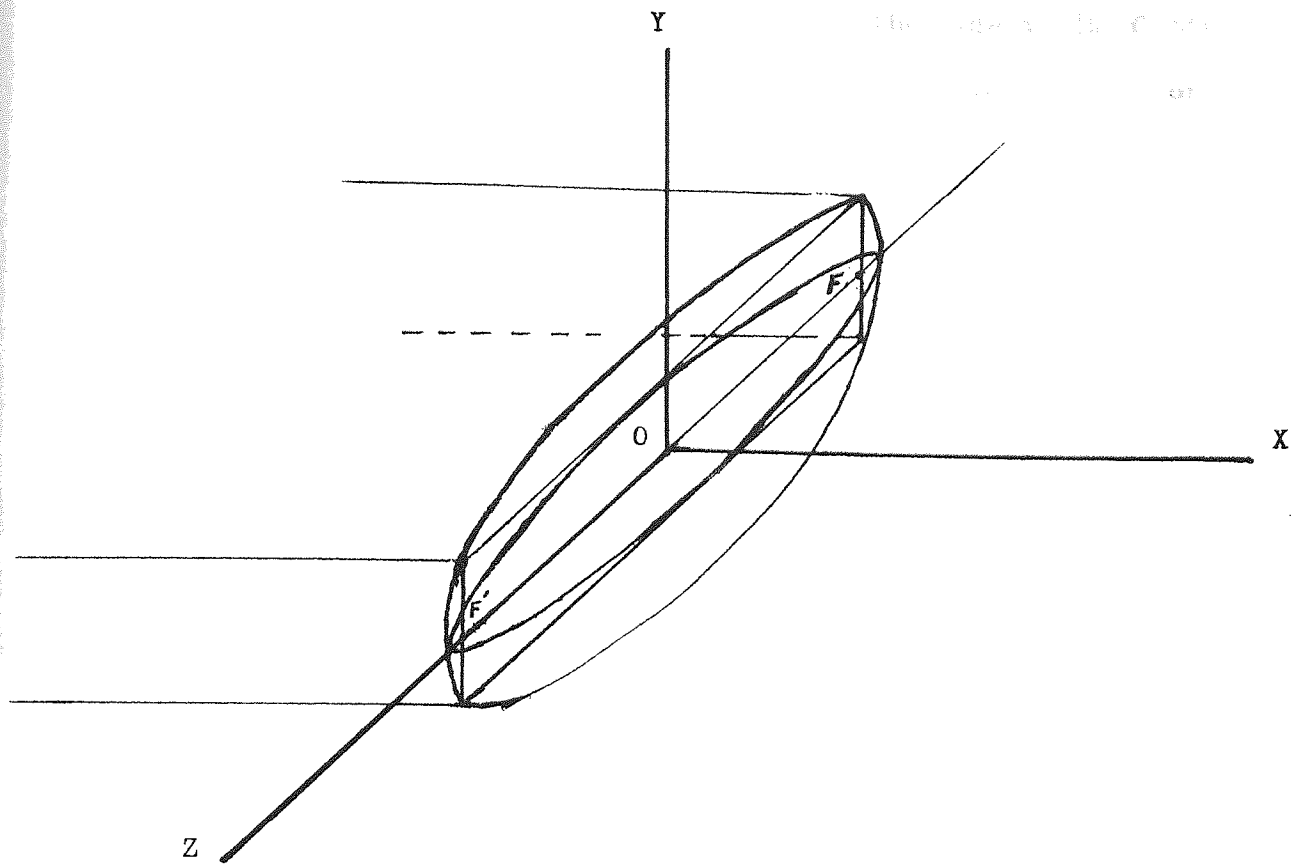

Fig.3.2 Equivelocity line in YZ-plane when the trace of ellipsoid potential surface in XZ-plane is an ellipse of a minor axis greater than the width of a rectangular opening suction duct.

In the case of the semi-minor axis of the YZ-plane ellipse being sufficiently greater than the width of duct opening the surface of the ellipsoid of revolution, covers the whole suction opening area. The angle of revolution for a duct with an infinite flat flange is 180 degrees. Similarly for unflanged (or short lip flanged) suction duct the revolution angle can be determined accordingly.

Let us assume the semi-minor axis is much greater than the half width of rectangular (or the side of square, or radius of round opening) suction duct. As the ellipse of equation

$$\frac{X^2}{A^2} + \frac{Z^2}{C^2} = 1 \qquad (3.11)$$

revolves it generates the ellipsoid

$$\frac{X^2}{A^2} + \frac{Y^2}{B^2} + \frac{Z^2}{C^2} = 1 \qquad (3.12)$$

The surface of this ellipsoid cuts the side walls of the duct along the curve EDG and E'D'G' (Figure 3.1) (in the case of the short lip flat flange the points E and G are the symmetry points of ellipse intersection and flange). For the bottom wall to the top wall revolution, the cutting points of the plane of the revolving ellipse are, first at the vertical wall and then at the horizontal walls of the symmetry planes of walls, for a complete revolution of ellipse. The complete revolution of the ellipse to create the potential surface area is 2π radians. But in the case of suction opening the revolution angle is the angle between the planes through the first and intermediate, and the last and intermediate points of intersection of ellipsoid of a complete revolution. The projection of these points in the XY-plane form an equilateral triangle. The revolution angle is the included angle of equal sides of this triangle. Figure 3.3 shows the position of this triangle relative to the coordinate system with origin at the centre of the suction opening.

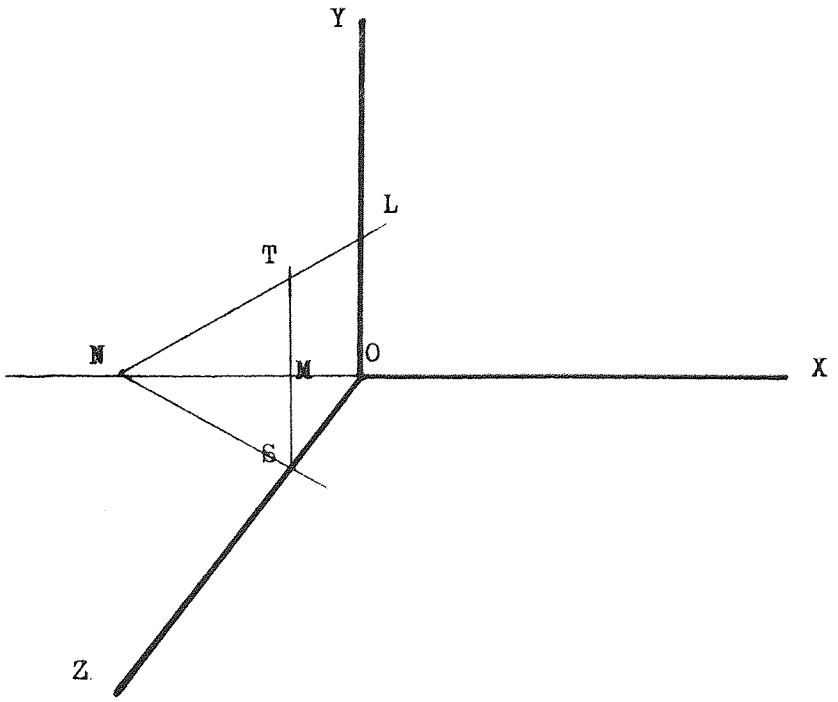

Figure 3.3 Angle of revolution

Points T and S are the projection of first and last intersections of points of wall of duct and ellipsoid in the XY-plane. And point N is the projection of intermediate intersections of the wall and ellipsoid project on the XY-plane whereas this point itself is the symmetry end of the minor-axis of the ellipse trace of ellipsoid of potential surface on the horizontal plane.

Applying the cosine rule to this triangle after the re-arrangement and necessary algebraic calculation of the angle of revolution for generation of the potential surface bounded to the walls of the suction duct yield

$$\alpha = 2\pi - \cos^{-1}\left(\frac{2NS^2 - TS^2}{2NS^2}\right) = 2\pi - \frac{\pi}{2} = \frac{3\pi}{2} \qquad (3.13)$$

which is a constant angle irrespective of the shape of the suction opening. Therefore, the surface area under the influence of suction forces of an unflanged suction opening is

$$S_a = \frac{3\pi A}{2}\left(A + (C/e)\sin^{-1}e\right) \qquad (3.14)$$

This area will be used in the following section.

3.5. Derivation of Potential Function.

In any physical problems involving a vector field, it is important to know not only the vector V at each point A, but also how this vector changes as we move from one point to another. To study this change, we use the partial differential which can be applied to the components of V. Due to dependence of the partial derivative to the basis, a special combination of partial derivatives known as the divergence and curl are used to describe the behaviour of vector fields. In the case of orthonormal basis, the divergence and curl turn out to be independent of basis. The curl and divergence have definite physical significance. The divergence of a vector field is a scalar field which in the case of suction flow,

measure the rate at which fluid is flowing away from the immediate vicinity of each point. The curl of a vector field is, on the other hand, another vector field and measures the tendency of the fluid to rotate at each point. The following mathematical terms are necessary to express before any detailed discussion on potential function.

Mathematically convenient expressions of Curl and Divergence are as follows:

$$\text{Curl}(V) = \nabla \times V \tag{3.15}$$

and

$$\text{Div}(V) = \nabla . V \tag{3.16}$$

where operator ∇ is a symbolic vector (i.e. $\text{grad}\phi = \nabla\phi$) and $\nabla \times V$ and $\nabla . V$ are the cross product and inner product of two vectors ∇ and V respectively. If the partial derivative of ϕ at point A exists, then the scalar field ϕ, whose gradient is $\nabla\phi$ is called the potential function of the vector field $\nabla\phi$. In a potential field equation

$$V = \nabla\phi \tag{3.17}$$

is satisfied over the surface of suction affected area.

Therefore, from the definition of divergence

$$\text{Div}(V) = \text{Div}(\nabla\phi) = \nabla^2\phi \tag{3.18}$$

The operator ∇^2 is called the Laplacian operator.
The partial equation $\nabla^2\phi$ is known as Laplace's equation.
Mathematically a function ϕ is said to be potential (or harmonic) if it satisfies Laplacian equations. A simple partial derivation on hypothetical equations showed that this requirement is not satisfied.

Therefore, the following analysis considered by Drkal (1970) is followed.

Let circle S be the cross section of a suction opening

in the plane of its flange (Figure 3.4). Let δs be an element area of this circle. If q is the velocity of air movement across δs, then in the limit one can consider a point source or a sink point δs of strength $q.\delta s$. For the case of this sink point the stream lines are radially directed toward the origin of the area. The velocities increase as the distance to the origin decreases. Therefore, one can consider, in a 3-dimensional space, a small opening under suction surrounded by an imaginary sphere of radius m, as shown in Fig.3.5. It is clear that all the air entering the duct must pass through the surface of the sphere radius m except at the wall of the pipe cutting through to the centre of the sphere, which in the limit may be considered small enough to be neglected. If Q is the amount of air flowing over the surface of the sphere, the velocity over the surface of the sphere will be given by equation:

$$V = \frac{Q}{4\pi m^2} = K \frac{Q}{m^2} \qquad (3.19)$$

If $\delta\phi$ is the velocity potential due to the sink point at a surface element δs of the flow rate q, the above expression will become

$$V = K \frac{q.\delta s}{m^2} \qquad (3.20)$$

For basic hydrodynamics we have the velocity as the gradient of potential function

$$V = - \frac{\partial(\delta\phi)}{\partial m} \qquad (3.21)$$

Equating these two expressions and integrating along the radial line will yield

$$\delta\phi = \frac{K.q.ds}{m} \qquad (3.22)$$

As Q is equal to the sum of $q.\delta s$ over the area S, then the potential function for the suction opening consisting of an infinite number of sink points will have the mathematical expression

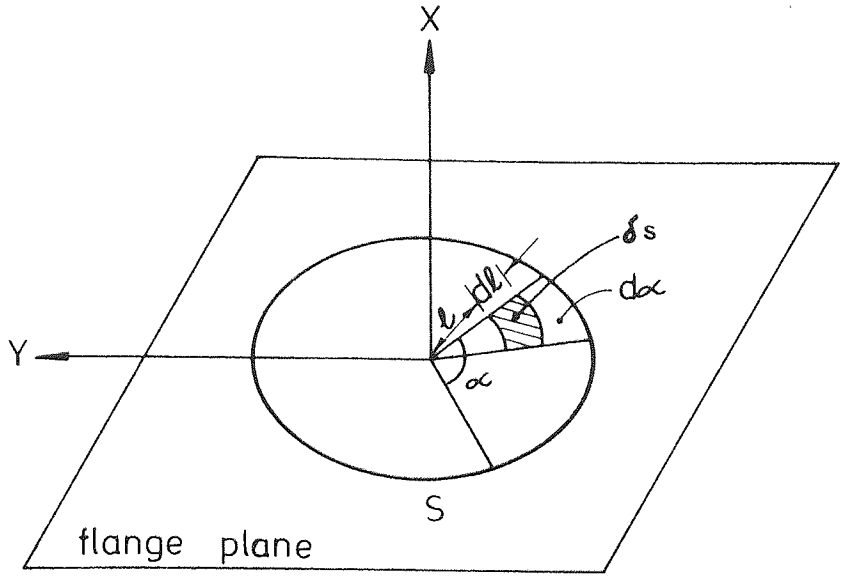

FIG. 3.4. PROJECTION OF ROUND SUCTION OPENING

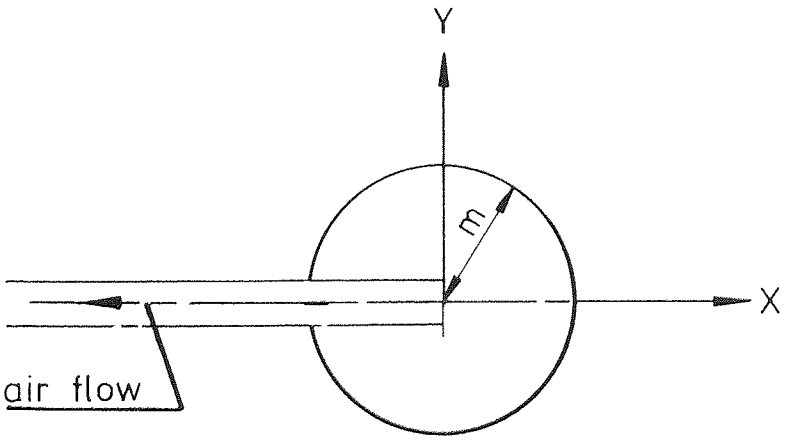

FIG. 3.5 SINK POINT SURROUNDED BY IMAGINARY SPHERE AS EQUIPOTENTIAL SURFACE

$$\phi = K \int_S \frac{q.ds}{m} \qquad (3.23)$$

In a diametrical plane for a circular opening with infinite flat plane flange, we can analogue the flow of air from the open area into a duct with the case of air flowing from one side to the other of a thin plane partition, through an aperature of breadth equal to the diameter of the suction duct (Fig.3.6). In this case the streamlines are hyperbolae and the velocity potential curves are ellipses (Lamb 1906). These conic curves have a common foci at $(0,\pm R)$ (i.e. R is the radius of opening). (Another analogy of suction of air from an open space into a fully bounded duct is with the efflux of a liquid from a small orifice in the wall of a vessel which is kept filled up to a constant level, so that the motion may be regarded as steady).

The issuing fluid is regarded as made up of a great number of elementary streams converging from all sides towards the opening. Its motion is not, therefore, throughout the area of the orifice, everywhere perpendicular to this area, but becomes more and more oblique as it passes from the centre to the sides. Again, the converging motion of the elementary streams must make the pressure at the opening somewhat greater in the interior around the centre than near to the side, where it is approximately equal to atmospheric pressure.

Observing the flow pattern by the aid of smoke filament, clearly it can be seen that the converging motion ceases at a short distance beyond the edge of the opening, and that in the case of circular orifice the jet then becomes approximately cylindrical. The ratio of the area of the sections of the jet at this point called "vena contracta" to the area of the orifice is called the

"coefficient of contraction" (Fig.3.7).

Let us assume that the origin of a cylindrical-polar-coordinate coincides with the centre of suction opening, and the XZ-plane be the horizontal plane with X-axis along the centre line of suction opening (Fig.3.8). Then we can derive the potential function of an axial symmetry suction opening. But because a suction is not quite the same as an aperture in an infinite wall, we can assume that the potential curves would not be ellipses as they are for aperture. Therefore, the aim is to find these curves when the streamlines are approximately hyperbolae.

For the element of area δs of the strength $\delta\phi$ with the average velocity of q passing through the centre of the area, we need to find the effect of the suction at the points A or M (Fig.3.8). Let us take PA equal m, where P is the centre of δs. Applying the cosine rule in triangle OPB (or ONP) and because the triangles ABP (and MNP) are right-angled at B (and N), the following mathematical expressions hold:

$$PB^2 = OP^2 + OB^2 + 2OP.OB\cos(\pi-\alpha) = \ell^2+z^2+2z\ell\cos\alpha \qquad (3.24)$$

$$AP^2 = AB^2 + PB^2 \text{ or } m^2 = x^2 + PB^2 \qquad (3.25)$$

Substituting and rewriting the above relations yield

$$m^2 = x^2 + z^2 + \ell^2 + 2z\ell\cos\alpha \qquad (3.26)$$

The area of δs, the elemented sector of circle S (the area of suction opening) is equal to $\ell\, d\ell\, d\alpha$, and ℓ will vary from zero at the origin up to the value R (radius of opening) and simultaneously α will cover the whole area of circle S, by substitution of these onto equation (3.22), and the following expression will be the general form of velocity potential

$$\phi(x,z,q,R) = K\, q \int_0^R \int_0^{2\pi} \frac{\ell.d\ell.d\alpha}{\sqrt{x^2+z^2+\ell^2+2z\ell\cos\alpha}} \qquad (3.27)$$

Substituting for K and q the mathematical form of velocity potential

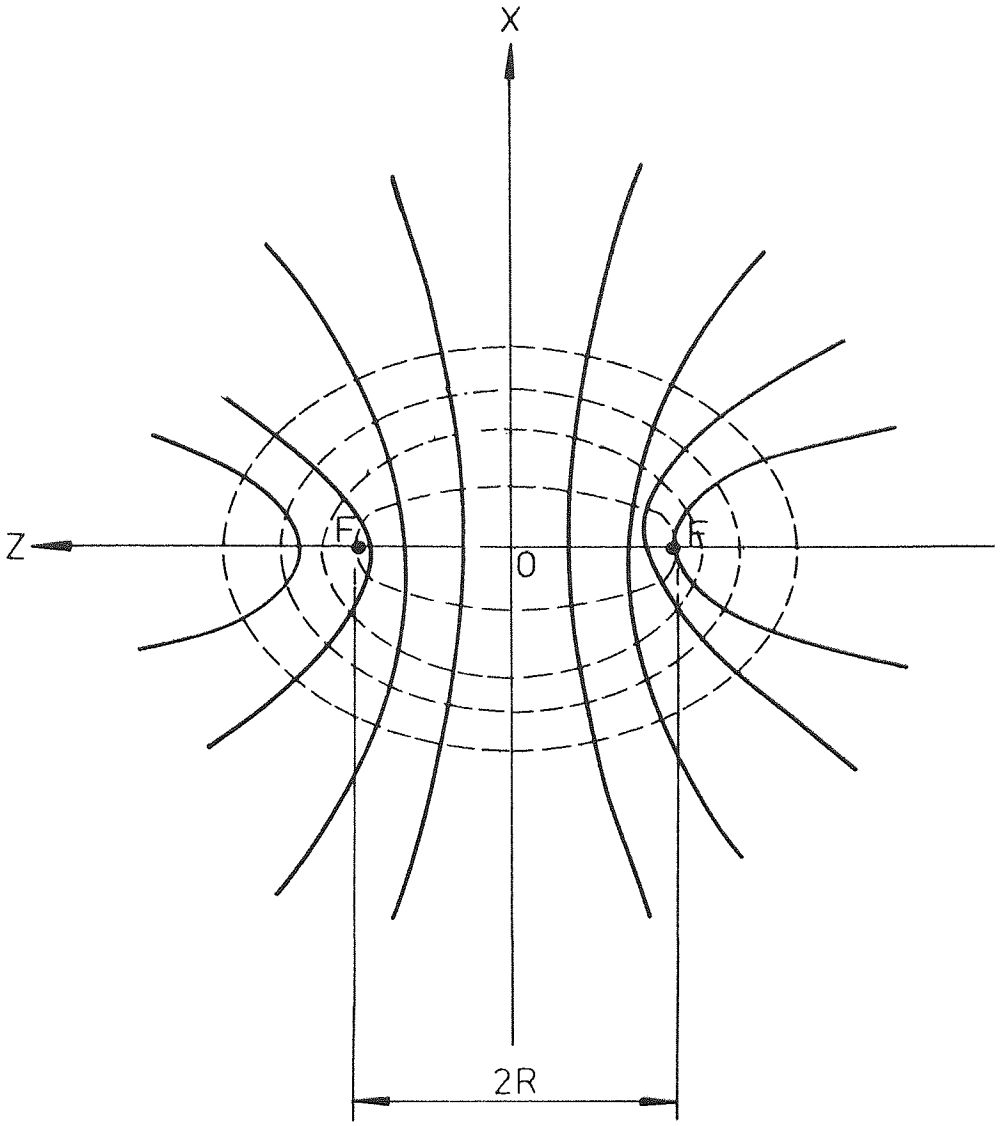

FIG. 3.6 DEPICTING THE STREAMLINE AND EQUIPOTENTIAL LINE OF AIR FLOW THROUGH AN APERTURE IN A WALL

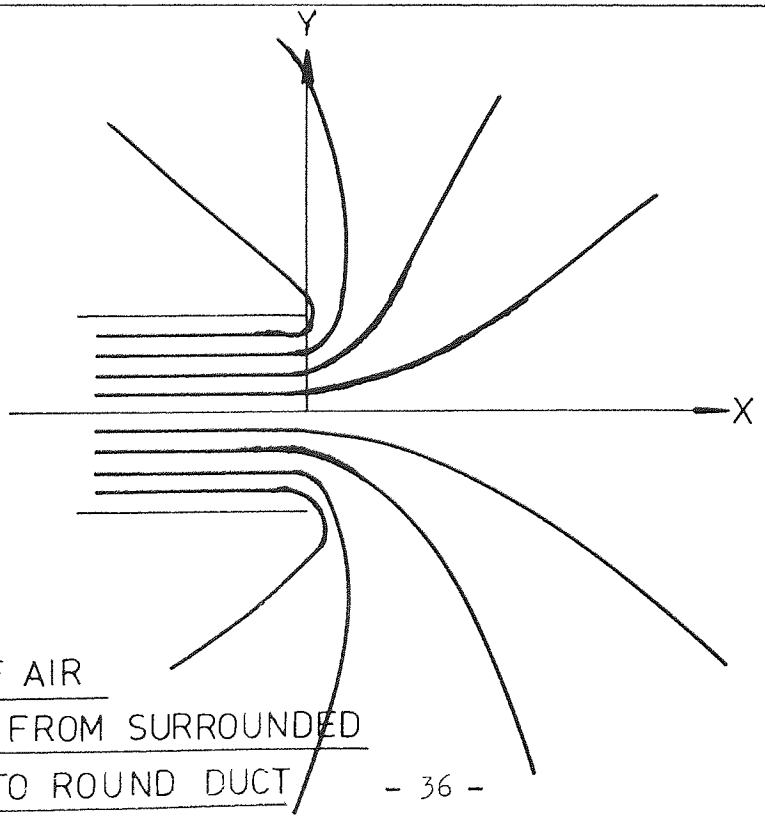

Fig. 3.7. FLOW OF AIR SUCKED FROM SURROUNDED AREA INTO ROUND DUCT

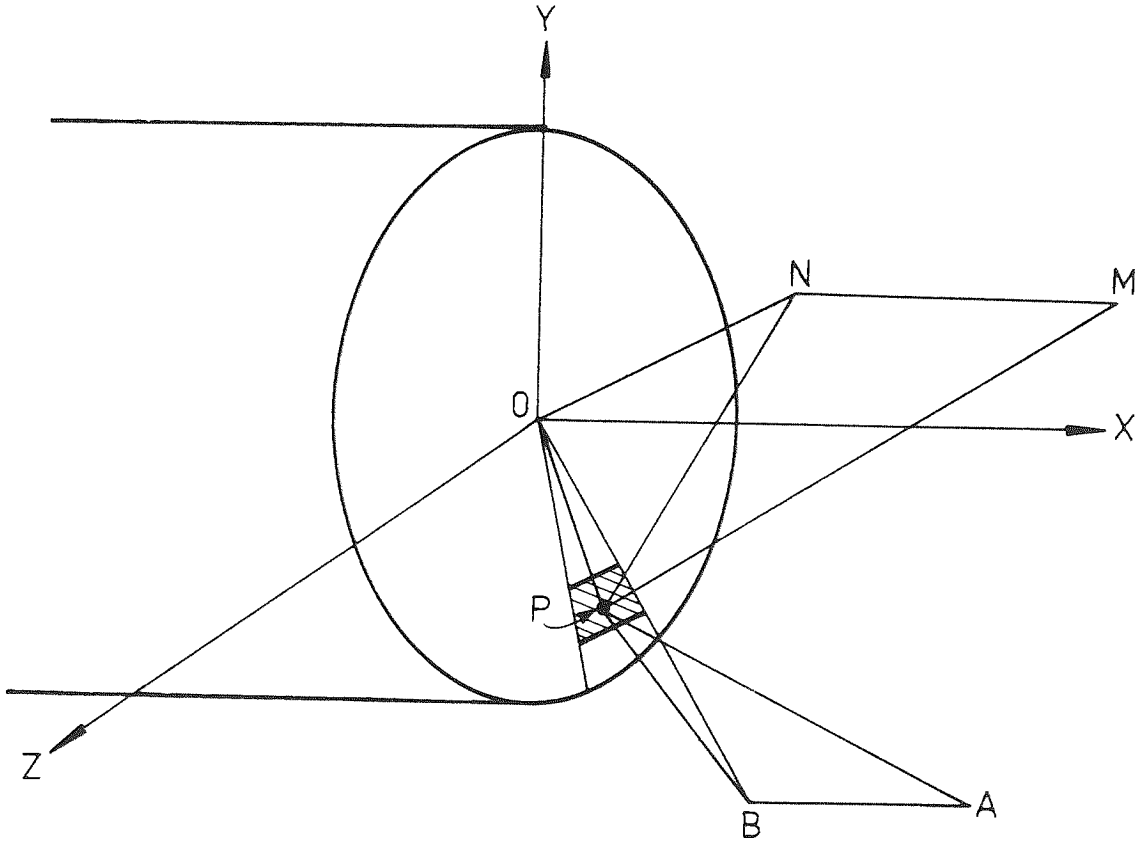

FIG. 3.8. POTENTIAL POINTS IN THE HORIZONTALLY SUSPENDED ROUND DUCT SUCTION AREA

will be

$$\phi(x,z,Q,R) = \frac{Q}{4\pi^2 R^2} \int_0^R \int_0^{2\pi} \frac{\ell d\ell d\alpha}{\sqrt{x^2+z^2+\ell^2+2z\ell\cos\alpha}} \qquad (3.28)$$

The solution for the above integral is not analytically available except for a special condition i.e. z = 0 which represents the centre line points out away from the suction opening. Integration in this case will yield:

$$\phi(x,0,Q,R) = \frac{Q}{2\pi R^2}\left[\sqrt{x^2+R^2} - x\right] \qquad (3.29)$$

This equation also does not satisfy the Laplacian equation. But the component of velocity along the centre line will be the first derivative of this function, viz:

$$V_x = -\frac{\partial\phi}{\partial x}, \quad V_z = -\frac{\partial\phi}{\partial z} \qquad (3.30)$$

Figure 3.9 will illustrate that if the duct end is fitted with a flange the flow volume (Q) will cross the area of a hemisphere, therefore ϕ for a flanged duct will be doubled. Therefore, if denoting the average face velocity due to the flow rate Q by V_{BAR}, the final form of the centre line potential function will be as follows:-

$$\phi(x,0,Q,R) = V_{BAR}\left[\sqrt{x^2+R^2} - x\right] \qquad (3.31)$$

and the $V_x = -\frac{\partial\phi}{\partial x} = V_{BAR}\left(\frac{x}{\sqrt{x^2+R^2}} - 1\right)$ or

$$\frac{V_x}{V_{BAR}} = 1 - \frac{x}{\sqrt{x^2+R^2}} \qquad (3.32)$$

3.6 Numerical Solution.

The general approach and the sink points assumption of round flanged suction hood did not lead to an analytical solution of suction velocity variation in the suction affeated area. Therefore

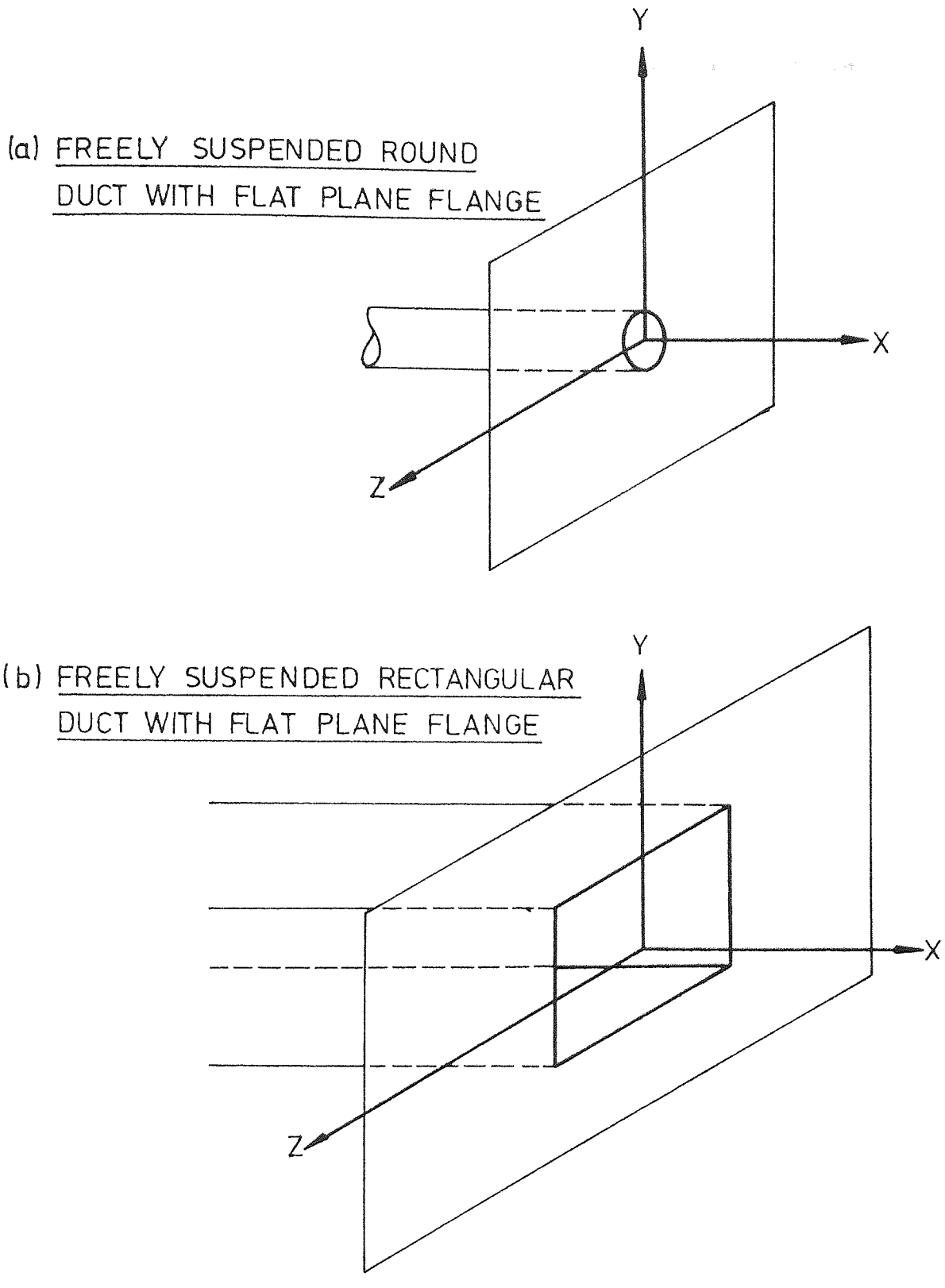

Figure 3.9. Freely suspended duct with flat plane flange.

numerical solution wad turned to. . Equation (3.28) needs to be integrated. The problem was tackled by using computational facilities. The method of computation is called Patterson's method (1968), which is a modified Gaussian quadrature method.

Let us rewrite the equation (3.28) again.

$$\phi(x,z,Q,R) = \frac{Q}{4\pi^2R^2}\int_0^R\int_0^{2\pi}\frac{\ell d\ell d\alpha}{\sqrt{x^2+z^2+\ell^2+2z\ell\cos\alpha}} \qquad (3.33)$$

As previously stated ϕ is the equation of a family of curves which as a whole indicate the situation of a potential flow. Hence ϕ can be used as a basic equation of relative derivative of ϕ along the direction of coordinates attached to a particle in motion to get the velocity component at that point. In the case of equation (3.33) it requires obtaining the derivative of the integral relative to variables x, z for which the boundaries of the integrations are independent of x and z. The relative derivatives yield the following equations:-

$$V_x = \frac{\partial\phi}{\partial x} = \frac{Q}{4\pi^2R^2}\int_0^R\int_0^{2\pi}\frac{\partial}{\partial x}\left(\frac{\ell}{\sqrt{x^2+z^2+\ell^2+2z\ell\cos\alpha}}\right) d\ell d\alpha,$$

$$V_z = \frac{\partial\phi}{\partial z} = \frac{Q}{4\pi^2R^2}\int_0^R\int_0^{2\pi}\frac{\partial}{\partial z}\left(\frac{\ell}{\sqrt{x^2+z^2+\ell^2+2z\ell\cos\alpha}}\right) d\ell d\alpha$$

Therefore the following integrals are required to be integrated numerically

$$\phi(x,z,Q,R) = \frac{Q}{4\pi^2R^2}\int_0^R\int_0^{2\pi}\frac{\ell d\ell d\alpha}{\sqrt{x^2+z^2+\ell^2+2z\ell\cos\alpha}} \qquad (3.34)$$

$$V_x = \frac{Q}{4\pi^2R^2}\int_0^R\int_0^{2\pi}\frac{-x\ell d\ell d\alpha}{(x^2+z^2+\ell^2+2z\ell\cos\alpha)^{3/2}} \qquad (3.35)$$

$$V_z = \frac{Q}{4\pi^2 R^2} \int_0^R \int_0^{2\pi} \frac{-\ell(z+\ell\cos\alpha)\,d\ell\,d\alpha}{(x^3+z^2+\ell^2+2z\ell\cos\alpha)^{3/2}} \qquad (3.36)$$

A computer program (see Appendix 3.1) was written to generate functions under the integral sign for different values of x and z. Then these functions were integrated for a known duct radius and a known volume of suction flow rate. The values of x, z, radius and the suction flow rates can be either inputed from the actual observation or they can be programmed to be calculated as self determining data. In the program a few more calculations like the area of contour surfaces of sphere and ellipsoid shapes, centred at the centre of suction opening and value of equal velocities are included.

Table 3.1 contains some observed velocities (the experimental values have been obtained for the wind tunnel installation described in detail in subsequent chapters) (column 6), hypothetically predicted velocities for sphere and ellipsoid contour surfaces (columns 7 and 8, respectively), and the velocity values along X and Z axes which are integrated numerically (columns 9 and 10), as well as the value of the potential function (column 12) at points of X, Y and Z coordinates testing round fully flat plane flanged hood.

Figure 3.10 shows the graphical representation of the contents of Table 3.1 .

It is clear that for the velocity distribution at the point beyond x greater than the diameter of suction opening the observed and predicted (hypoth ellipse) values are the same, and the theoretical values (derived from numerical solution) are very much lower than the observed and predicted one. Consequently, there is no acceptable agreement between theoretical and practical velocities The prediction based in the spherical potential surface agrees better than the ellipsoid hypothetical potential surface.

TABLE 3.1 The observed, predicted and numercially calculated suction velocities.

1	2	3	4	5	6	7	8	9	10	11	12
D	Q	X	Y	Z	V_m	V_{SPh} at 1.2	$V_{E\ell}$ at 1.2	V_{Nux} at 1.2	V_{Nuz} at 1.2	V_{Nu} at 1.2	ϕ at 1.2
0.152 m	1.02 ms^{-1}	0.107	0.001	0.005	1.4	11.8	8.8	1.082	0.007	1.082	0.142
		0.345	"	"	1.2	1.14	1.0	0.137	-	0.14	0.048
		0.395	"	"	0.85	0.86	0.78	0.105	-	0.11	0.042
		0.445	"	"	0.65	0.68	0.61	0.084	-	0.10	0.038
		0.495	"	"	0.50	0.54	0.50	0.068	-	0.07	0.034
		0.545	"	"	0.34	0.44	0.41	0.056	-	0.06	0.031
		0.595	"	"	0.30	0.38	0.34	0.047	-	0.05	0.028
		0.655	"	"	0.20	0.30	0.28	0.039	-	0.04	0.026
		0.695	"	"	0.18	0.28	0.24	0.035	-	0.035	0.024
		0.725	"	"	0.12	0.26	0.22	0.032	-	0.032	0.023

V_m = Observed velocity ms^{-1}

V_{SPh} = Velocity over spherical potential surface ms^{-1}

$V_{E\ell}$ = " " ellipsoid " " ms^{-1}

$V_{Nux} = \frac{\partial \phi}{\partial x}$ Numerical solution ms^{-1}

$V_{Nuz} = \frac{\partial \phi}{\partial z}$ " "

$V_{Nu} = \sqrt{V_{Nux}^2 + V_{Nuz}^2}$ ms^{-1}

Figure 3.10. Comparison of observed, predicted, and Theoretical point velocity in front of flat flanged round duct

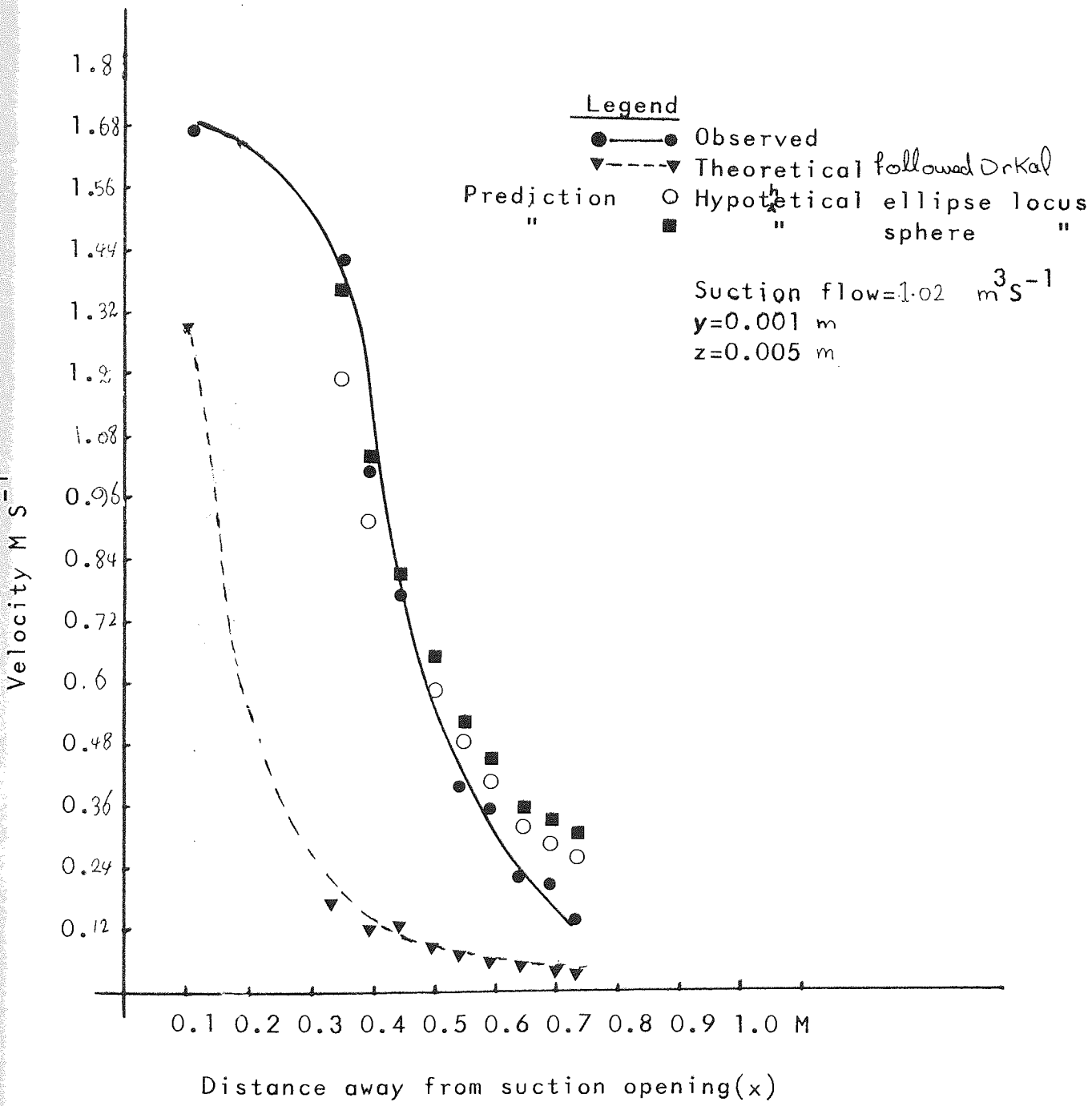

In order to test that the suction field is a potential field, the numerical values of column 12 of Table 3.1 can be used as starting values. The operation is such that the value of ϕ at the intersections 1,2,3 and 4 are ϕ_1, ϕ_2, ϕ_3 and ϕ_4 respectively (see Figure 3.11). It is a characteristic of the Laplacian equation that, provided the mesh of Figure 3.11 is sufficiently fine, the value ϕ_5 will be almost equal to the numerical average of ϕ_1, ϕ_2, ϕ_3 and ϕ_4 as the following reasoning shows.

Figure 3.12 is an enlargement of one square cell of size 'a' from Figure 3.11. Assuming that the variation of ϕ between adjacent intersections of the mesh can be taken as linear with little error, then, for the points A and B, we have

$$\left.\frac{\partial\phi}{\partial x}\right]_A = \frac{\phi_1-\phi_5}{a} \qquad (3.37)$$

$$\left.\frac{\partial\phi}{\partial x}\right]_B = \frac{\phi_5-\phi_3}{a} \qquad (3.39)$$

and for the point 5

$$\frac{\partial^2\phi}{\partial x^2} = \frac{\left.\frac{\partial\phi}{\partial x}\right]_A - \left.\frac{\partial\phi}{\partial x}\right]_B}{a} = \frac{\phi_1+\phi_3-2\phi_5}{a^2} \qquad (3.40)$$

Similarly

$$\frac{\partial^2\phi}{\partial y^2} = \frac{\phi_2+\phi_4-2\phi_5}{a^2} \qquad (3.41)$$

Substituting into a Laplacian equation yields

$$\phi_5 = \frac{\phi_1+\phi_2+\phi_3+\phi_4}{4} \qquad (3.42)$$

The objective of this operation is to adjust ϕ values such that the equation is satisfied throughout the grid. This test itself requires considerable computation and programming which was not the main objective of this research and was not Persued in the Present Thesis.

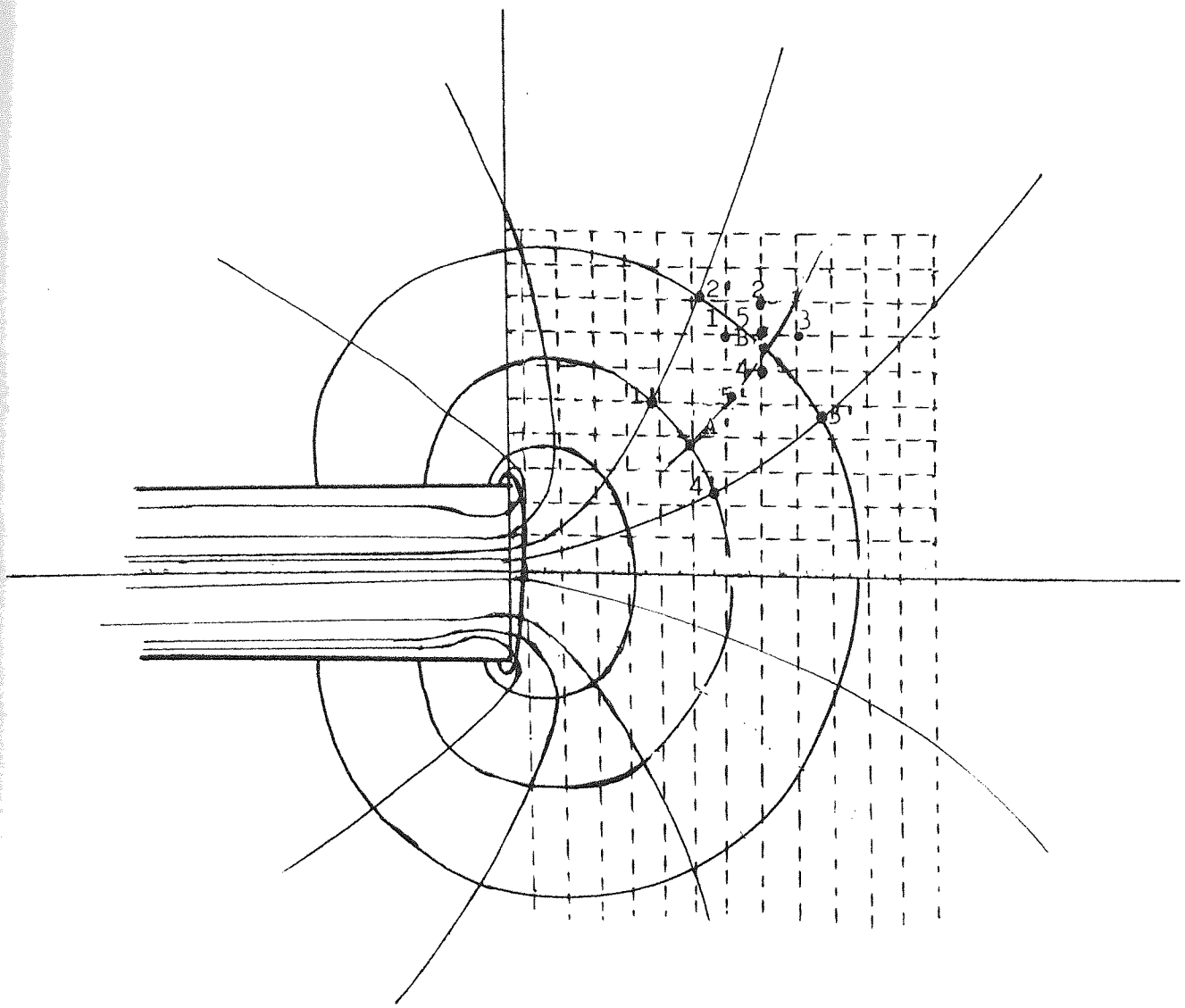

Figure 3.11. a square mesh of size a superimposed upon a pattern of flow of a round suction hood.

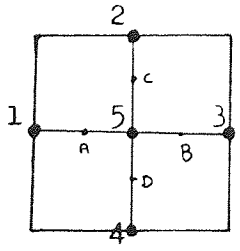

Figure 3.12.Enlargement of square cell of size a from fig3.11.

CHAPTER FOUR

RESEARCH FACILITY;IDENTIFICATION AND DESIGN.

4.1 Introduction.

The research was programmed to be a laboratory based project. At the start of the research, there were no facilities available at all. A great deal of research time was devoted to the identification, design, purchase and manufacture and installation of facilities. The major activities were as follows:

(i) Identification of facility requirement

(ii) Preliminary facility design

(iii) Detailed facility analysis, design calculation and drawing, and installation.

4.2 Basic Research Facility.

The anticipated uses and the desired specifications of facilities, required the survey and the revision of the related type of research sources. Literature survey and the visits to the research centres, led to the wind tunnel as a basic facility.

A number of trade-off wind tunnel was preliminarily studied. Consequently a compact model of exhaust ventilation system was designed and manufactured. Although model studies could give a reliable result within their known limits, it is axiomatic that in many instances, small models do not act at all like their full-sized original under conditions which seem at first sight to be similar, and that hasty conclusions from model experiments are very unsafe indeed. For example, in the field of natural ventilation it has been shown that the model tests do not show agreement with full-scale measurement (AMCA 500-75, 1975).

Therefore, a versatile full scale wind tunnel was preferred to a model.

In industrial applications of exhaust ventilation systems mostly the flow in a horizontal duct is of practical interest. Also, the study of aerosols' transport and capture involve the consideration of body forces on the particle themselves, for larger particles often the gravitational force dominates and the particles tend to settle as they flow. In laboratory cases, the rapid and easy modification of the test section and other major components in order to accommodate various types of research programme , reveals that such a modification will be difficult and complicated immensely if the test section were vertical.

Although both vertical and horizontal test section are of interest, cost, convenience and flexibility consideration indicate that a horizontal test section is a more practical section. Therefore, the wind tunnel system was based on the horizontal duct section.

4.3 Wind Tunnel Assembly & its Limitations and Requirements

The wind tunnel assembly consists of:

(i) a main duct system;

(ii) air cleaner;

(iii) silencers;

(iv) air mover, and

(v) discharge and accessory sections

Drawing No.1 shows the general assembly of the wind tunnel. The main tunnel consists of three round ducts flanged and fitted together followed by air cleaners, silencer, fan and motor, ended up to the output side silencers.

The general limitations were as follows:

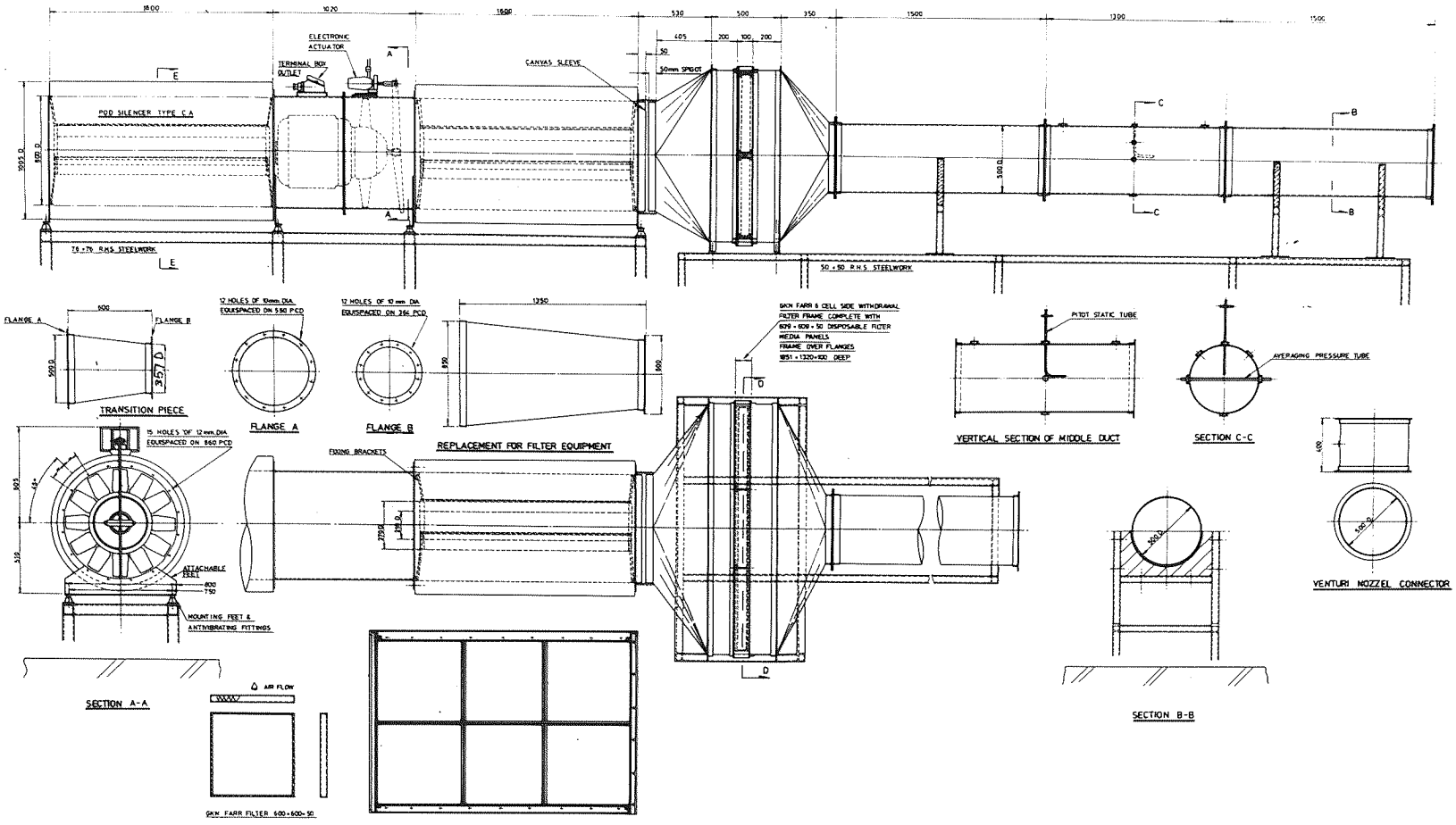

TITLE WIND TUNNEL GENERAL ARRANGEMENT		NOTE ALL DIMENSIONS IN MILLIMETRES
		SCALE 1 10
ASTON UNIVERSITY DEPARTMENT OF SAFETY & HYGENE		DRAWING No 1

(i) The size of the tunnel was limited to the available installation spaces.

(ii) The suction flow rate was limited to the laboratory volume.

(iii) Wind tunnel room is a closed chamber.

The general requirements were as below:

(i) A fully developed flow section was required for flow metering.

(ii) Recirculation was inevitable.

(iii) In the case of dust generation, a desired efficiency for a dust filtration was essential.

(iv) Air cleaner replacement and its maintenance required special consideration.

(v) A quiet, aerodynamically efficient and stable moving fan was absolutely essential.

(vi) A reliable suction flowrate control facility was essential.

(vii) Noise reduction was essential.

(viii) Communication, safety and personal protection facilities were required.

(ix) A multiple number of suction opening simulation were required.

Table 4.1 contains the comparative information on the past and present research facilities.

The size and the length of the wind tunnel assemblies were based on the considerations of above limitations, requirements and comparison.

TABLE 4.1

A Summary of Past and Present Research Facilities:- Wind Tunnels, Captor Hoods, and Velocity or Flow Ratus

RESEARCHER	SYSTEM DIMENSIONS						FAN TYPE	VELOCITY OR VOLUME FLOW RATE	FLOW RATING	FLOW CONTROL	MAXIMUM DISTANCE OF VELOCITY STUDY	REFERENCE
	MAIN DUCT		TEST DUCT AND HOOD									
	DIAMETER	LENGTH	SHAPE	SIZE	RANGE OF AREA	ASPECT RATES						
DALLAVALLE	30", 8" (0.76m, 0.2m)	40ft (12m)	Round	4", 8", 8", 11.3", 16"	12.56 to 200.0 square inches (0.008m^2 to 0.129m^2)	-	Not Known	2000 cfm (0.9m^3/sec)	ORIFICE PLATE AND VINTURE NOZZLE	VARIABLE SPEED MOTOR	CENTRELINE VELOCITY 10" (0.254m)	J.M. DALLAVALLE and T.HATCH (1931)
	"	"	Square	4", 6", 8", 10"	16 to 100 square inches	1	"	"	"	"	"	"
	"	"	Rectangular	4.1" x 5.5" 6 x 8 7.5 x 10 12 x 16 4 x 6 5 x 7.5 6 x 9 12 x 18 18 x 27 4 x 8 5 x 10 6 x 12 8 x 18 15 x 30 3 x 9 4 x 12 5 x 15 8 x 24	22.6 to 4.86 square inches	4(0.75), A 5(0.66), 4(0.5), (0.4), 4(0.3)	"	"	"	"	"	"
PRUZNER	Not reported	Not reported	Round	Not reported	Not clearly reported	-	Not reported	588.5 cfm (1000m3/h 0.27m3/se initial velocity of 5m /sec	Venturi nozzle	Not reported	Up to the distance which velocity is 10% of initial velocity	A.C. PRUZNER and INSTITUTE FOR THE PROTECTION OF LABOUR (1939)
			Square	"	"	1.0						
			Rectangular and orifices of equal area of different shape	"	"	1,0.5, 0.3, 0.1						
					of 0.0314 m^2	0.0125 (Slit)						
SILVERMAN	8"	Not reported	Round	2" to 20"	3.14 to 31.4 square inches	-	Planning mill exhaust fan	Not reported	Venturi nozzle	Not reported	50" (1.016 m)	E. SILVERMAN (1941)
			rectangular or slot type	30" x 2" 20" x 2" 10" x 2" 19.5 x 1.5 19.5 x 1 19.75 x 0.5	19.5 sq. in. to 60 sq. in. (0.0126m^2 to 0.3871m^2)	0.067 0.1 0.2 0.079 0.051 0.025						
FLETCHER	Not reported	Not reported	Rectangular and square	9 - Different	0.0025 m^2 0.09 m^2	1, 0.06	Not reported	Average face velocities range 2 to 30 m/sec	Orifice plate	Valve	Not reported	B. FLETCHER (1977)
YOUSEFI	0.5 m	0.3 m of one 1.5 m in the middle of 2 ducts of 1.5 metre straight duct	Round	0.152	0.018 m^2 to 0.1639 m^2	-	Variable pitch aerofoil fan	9.72 m/sec.	pitot-static anemometry and averaging pressure tube anemometry	Electrical Actuator for variable pitch control		Y. YOUSEFI (Present Research)
				0.343								
				0.457								
	"	"	Rectangular	0.098 by 0.203	0.0199 m^2,	0.5	"					
				0.152 by 0.254	0.0387 m^2,	0.6	"					
	"	"	square Bell mouth flanged Rectangular flared to round hood	0.535 x 0.535	0.2862 m^2 square section	1	"	7.5 m/sec.				
				0.25 by 1.145	Same area as square section of bell mouth hood	0.22	"					

A The number before brackets represent the number of hoods of equal aspect ratio (ratio of width to length of opening)

4.4 Design Consideration.

In order to study the aerodynamic characteristics of suction openings, a number of classical-geometry shaped openings required to be tested. Due to the fact that geometrically similar openings behave the same (DallaValle 1939) only a limited number of similar openings have been chosen to be studied in detail.

The suction openings were classified according to the cross section of the opening, and its preceding duct cross section. If the cross section of the opening and preceding duct are alike and of equal area, it is called a suction duct, otherwise it is called a hood or a suction opening.

There were two types of ducts i.e. round and rectangular cross sections and two types of hoods i.e. square bell-mouth flanged and oblong cross section hood, whose opening area was equal to the square cross section area of the square hood. Drawing Nos.1,2 and 3 show the size and dimension specification of the main wind tunnel section and accessories, hoods and ducts.

The bell mouth flanged hood is designed to the specification given by the American Conference of Governmental Industrial Hygienists for calibration of velometers. It is meant to be used for the calibration of air velocity meters as well as a test hood. The oblong hood is designed as a typical industrially used exhaust hood. Flange plates designed to be fitted to the hood (see Drawing No.2 and Figure 4.1).

Design calculation (see Section 4.7) was based on the calculation of pressure drop. A flowrate of 4.72 $m^3 s^{-1}$ through the system is the maximum nominal value for the design calculation. The main wind tunnel duct diameter was chosen in such a way that the minimum transport velocity is to be equal to the transport velocity (i.e. 22.86 m s^{-1}) recommended for heavy or moist dust

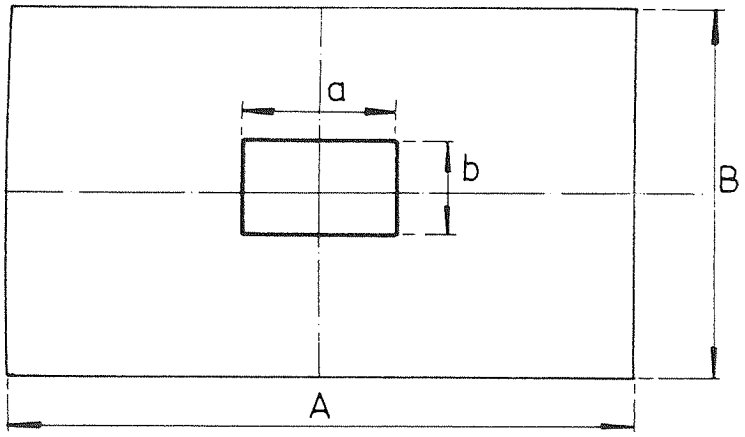

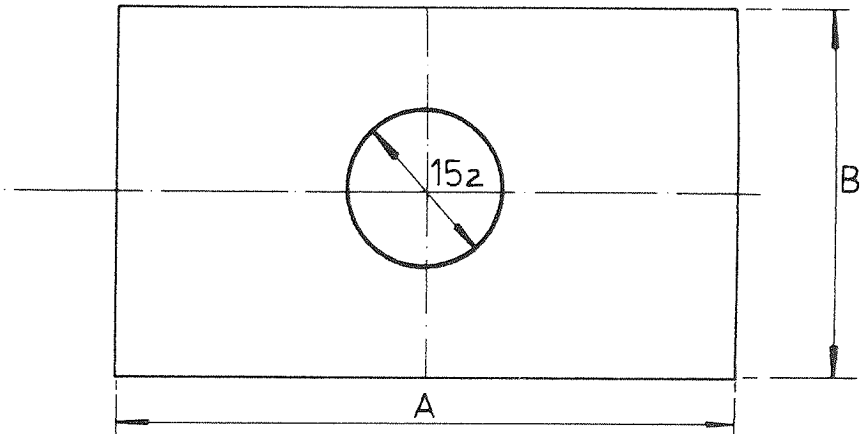

I	A = 1220	a = 254	A/a = 4·8
	B = 610	b = 152·4	B/b = 2·4
II	A = 910	a = 203·2	A/a = 4·4
	B = 610	b = 101·6	B/b = 3·0

$A / D = {}^{913}/_{152} = 6$

$B / D = {}^{608}/_{152} = 4$

NOTE : All measurements are in millimetre

FIG. 4.1 FLAT FLANGE PLATES FOR RECTANGULAR DUCTS AND ROUND DUCTS

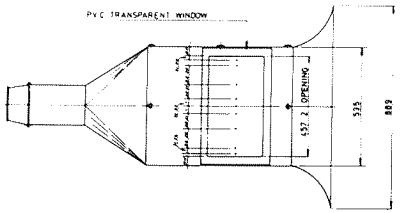

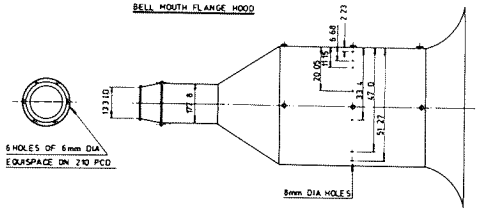

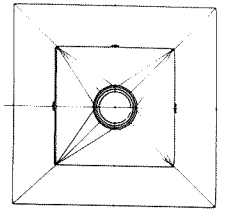

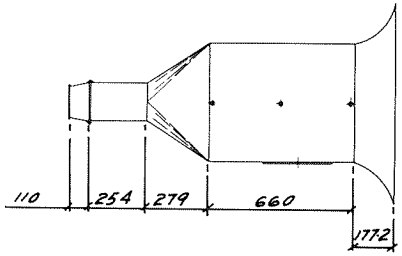

HOOD WITH RECTANGULAR OPENING WITH EQUAL AREA SQUARE SECTION OF BELL MOUTH HOOD

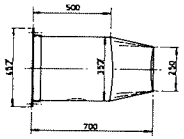

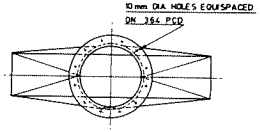

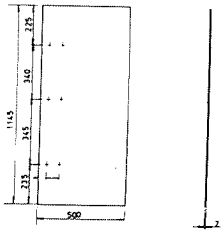

FLAT PLANE FLANGE ATTACHMENT FOR RECTANGULAR HOOD

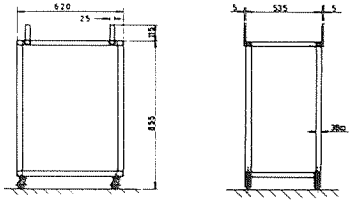

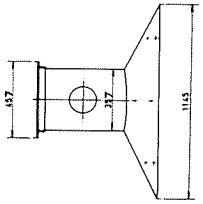

SIDE BRANCH ATTACHMENT FOR VENTILATION RIG

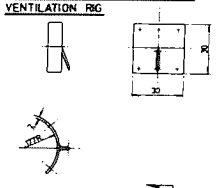

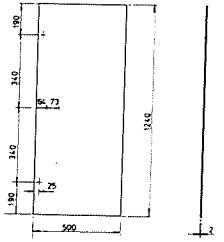

PLANE SCHEMATIC VIEW OF WIND TUNNEL

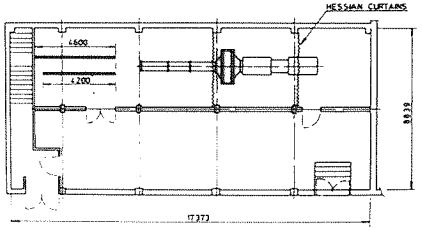

SECTIONS OF SILENCERS

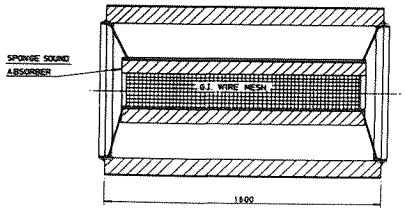

SECTION F-F

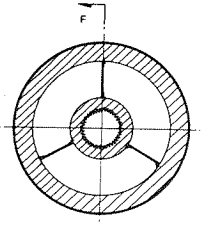

SECTION E-E (DRG.No 1)

TITLE HOODS, FLANGE ATTACHMENT AND DETAILS OF WIND TUNNEL		NOTE DO NOT SCALE ALL DIMENSIONS IN MM
UNIVERSITY OF ASTON DEPARTMENT OF SAFETY & HYGENE		SCALE 1:10 DRAWING No. 2

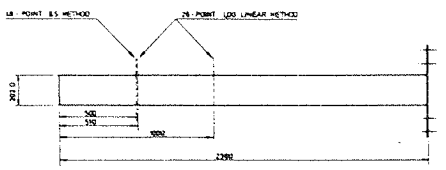

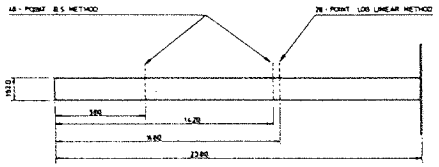

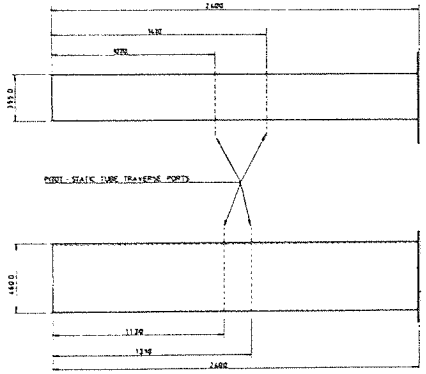

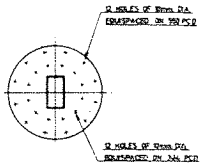

REC 1

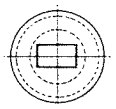

REC 2

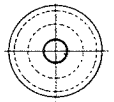

ROU 1

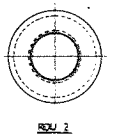

ROU 2

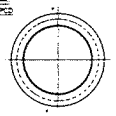

ROU 3

12 HOLES ON INNER AND OUTER PCD'S ON REC 1, REC 2, ROU 1, ROU 2 ARE IDENTICAL

12 HOLES OF 10mm DIA EQUISPACED ON 1560 PCD SEE REC 1

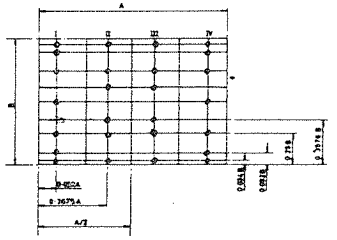

TRAVERSE POSITION OF 28 POINT LOG LINEAR METHOD

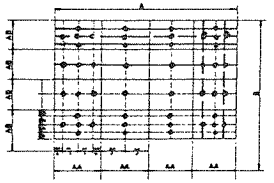

TRAVERSE POSITIONS OF THE 48 POINT B.S METHOD

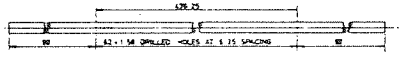

AVARAGING PRESSURE TUBE

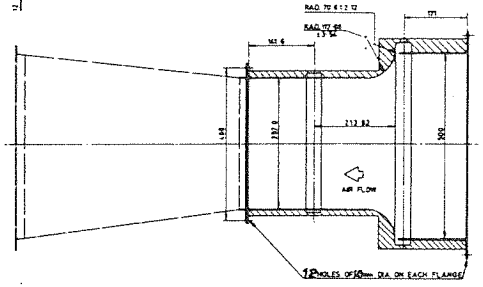

TRANSITION PIECE (see DRG. No. 1)

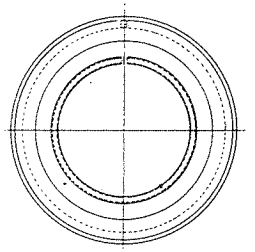

VENTURI NOZZEL B.S. 1042

TITLE		NOTE ALL DIMENSION IN MILLIMETRES
UNIVERSITY OF ASTON DEPARTMENT OF SAFETY & HYGENE		SCALE 1 : 10 DRAWING No. 3

(ACGIH 1974). Therefore, the main duct section of 0.5 m diameter and 4.3 m length, consisting of 3 sections, has been designed to be the main wind tunnel ducting. Middle plane of the middle duct proved a good traverse plane for a reliable flow metering cross section. Traverse ports are drilled and tapped at two perpendicular planes and two 45 degree planes. Two more vertical traverse ports are drilled at equidistance from the middle cross section for further pressure tube traverses (see Drawing No.1, Section C-C, and vertical section of middle duct).

In the case of the natural air suction, a transition piece as a replacement for air cleaner, was designed (see Drawing No.1). This duct enlarges the duct diameter to fit the silencer, with a minimum addition to the overall duct length, and pressure losses and commonly used enlargement ratio of 0.025 m diameter increase for 0.05 m of length.

In the case of generation of dust particulate, at the design stage, provision of cleaning air has been made. The wind tunnel room is a closed chamber. The sucked air is recirculated into the room. Therefore, consideration of minimising the recirculation of contaminant is required. The restriction of space, the maintenance and economic aspect, called for a survey on the type of filter for the best fit to the wind tunnel system. Here the nature of particulate (i.e. toxicity, concentration, size, physical, chemical and biological character) is not known, therefore a disposable type of filter was thought to be a better way of cleaning air for recirculation. A market survey showed that G.K.N.Filtration Limited manufacture a disposable filter of nominal dimension 0.609 × 0.609 × 0.5 m. This is a relatively inexpensive filter and the efficiency is fairly good, also it does not require a substantial length of filter compartment.

It was, therefore, decided to design the filter section compartment to fit the above mentioned filter plates. The filter panel is a disposable type pleated media filter. It is a multilayer and a high efficiency strainer filter.It gives a good filtration with a low pressure drop, while maintaining efficiency. The flat folder media provided a large media area within a compact preformed panel. Each filter is constructed of sturdy rigid durable cardboard filter frame with rib supports holding a man-woven fabric media in 0.5 m deep pleats with wire back for maximum support and at the same time guarantees uniform air flow across the filter. The construction of this type of filter allows a minimum of 16 media pleats per 0.3 linear meter of filter and over 0.42 square meter of filter media per square meter of face area. The filter compartment of the area 1.68 m^2 with the maximum average face velocity of 2.8 m s^{-1} of six of this disposable filter, is the designed air cleaner. The efficiency of the purchased filter for the research wind tunnel is 80% for 3 micron and 99.5% for 60 micron of British Standard recommended test material.

In order to reduce the fan noise two silencers for inlet and discharge section of fan was purchased. The silencer was made by Woods of Colchester, and it is of Ca type silencer, consisting of a 20 gauge galvanised cylindrical steel casing, and sound absorbent lining material of polyeurethane foam and one inner cylinder compartment is the final part of silencer (see Drawing No.2). For the purchased fan (detail will follow), the attenuation provided by the silencers is as measured by the manufacturer and are given in the following table. The test is based on the methods specified by British Standard 848 Part 2, 1966.

TABLE 4.2 Fan Noise Rating (Woods of Colchester)

Sound level dB at distance:	Mid-Octave hand frequency H_z 125	250	500	1000	2000	4000
1 metre	92	93	90	86	86	86
2 "	85	86	83	79	79	79
3 "	81	82	79	75	75	75
4 "	79	80	77	73	73	73

Plotting the measured sound level at 1 metre distance on the noise rating chart, gives a contour indicated of the approximate sound level of 91 dB. A further reduction at 4 metre distance indicates an A-weighted equivalent of 80 dB (see Figure 4.2).

In order to test the noise level in different rooms and area of the neighbourhood of the wind tunnel room, a test was carried out. Airborne noise was generated according to the B.S.2750, 1956 specification. The measurements were done accordingly. The data was treated following the existing code of practice and standard. The following conclusion was based on room reverberation time and transmission loss measurements.

The predicted levels do not exceed the recommended maximum noise level for offices i.e. noise rating of 40 dB even at the full output of the tunnel (see Figure 4.3).

Although the noise level at the suction zone is not very high it masks communication and warning alarms. In order to attract the attention of an operator working in the wind tunnel room to fire alarm, telephone and person to person communication, a system has been installed by Bilsom International Limited. The system gives full speech, attention and warning facilities to people working in the wind tunnel laboratory and the adjacent room. The complete wiring and communication microphone positions are shown by Figure 4.4 .

FIGURE 4.2 FAN NOISE RATING

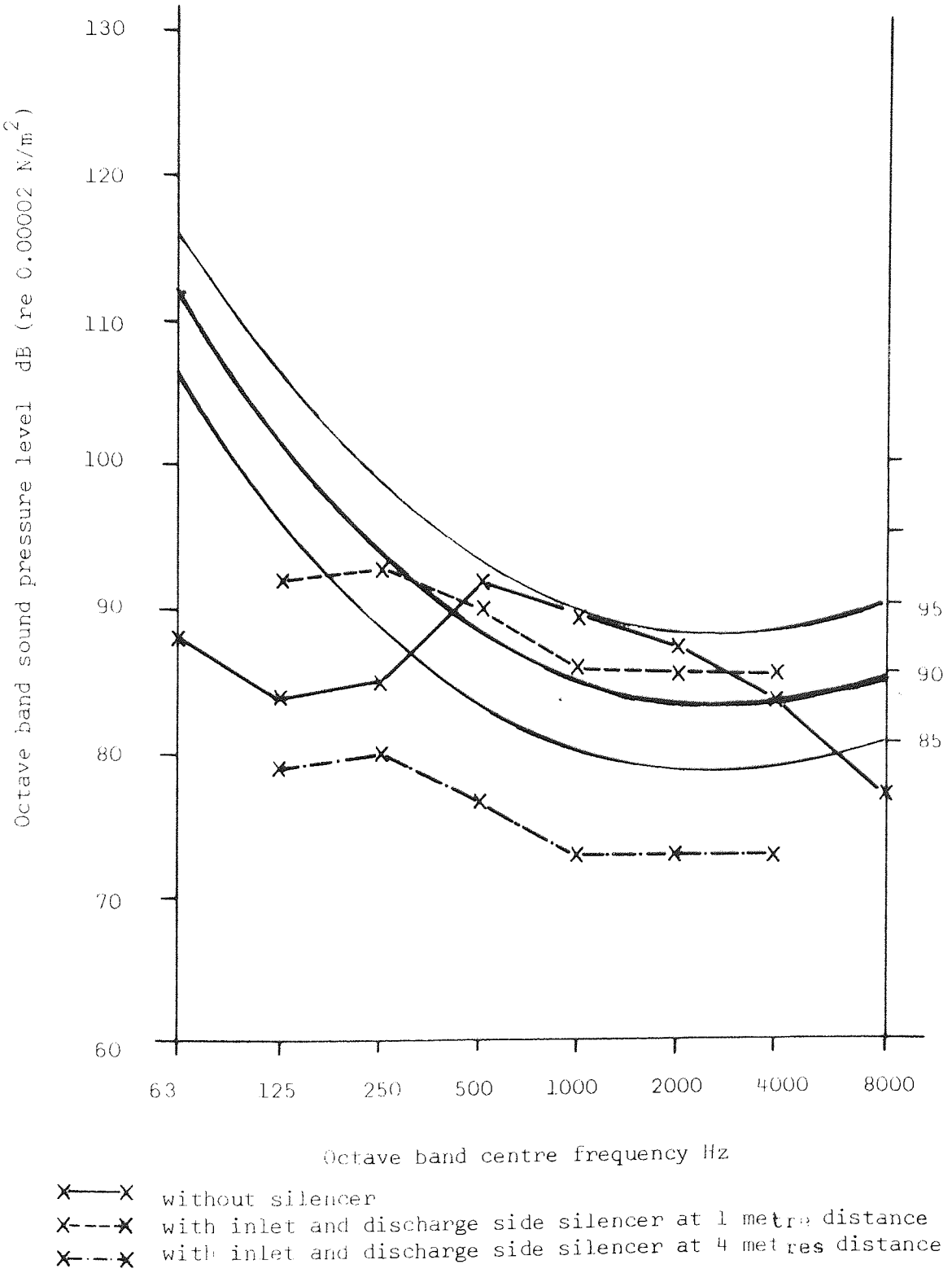

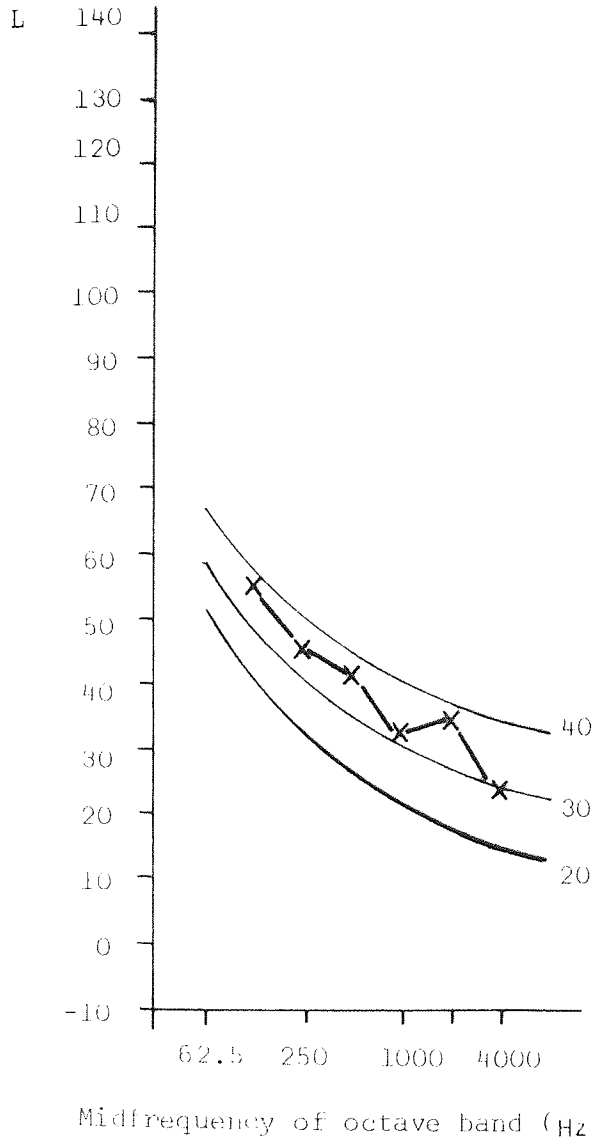

	criterion
broadcasting studio	15
concert hall, legitimate theatre 500 seats	20
class room, music room, TV studio, conference room 50 seats	25
sleeping room (see for corrections below)	25
conference room 20 seats or with public address system, cinema, hospital, church, courtroom, library	30
living room (see for corrections below)	30
private office	40
restaurant	45
gymnasium	50
office (typewriters)	55
workshop	65

Corrections for dwellings		
(a) Pure tone easily perceptible		-5
(b) Impulsive and/or intermittent		-5
(c) Noise only during working hours		+5
(d) Noise during 20% of time		+5
	6%	+10
	1.5%	+15
0.02% +30	0.5%	+20
	0.1%	+25
(e) Economic tie		+5
(f) Very quite surburban		-5
surburban		0
residential urban		+5
urban near some ind.		+10
area of heavy ind.		+15

Figure 4.3 Curves for rating noises for acceptability. The ordinate L is octave-band sound pressure level in dB relative to 2×10^{-4} μm^{-2}. The parameter is noise rating number NR. The table opposite gives criteria for various circumstances together with corrections applicable to dwellings only.

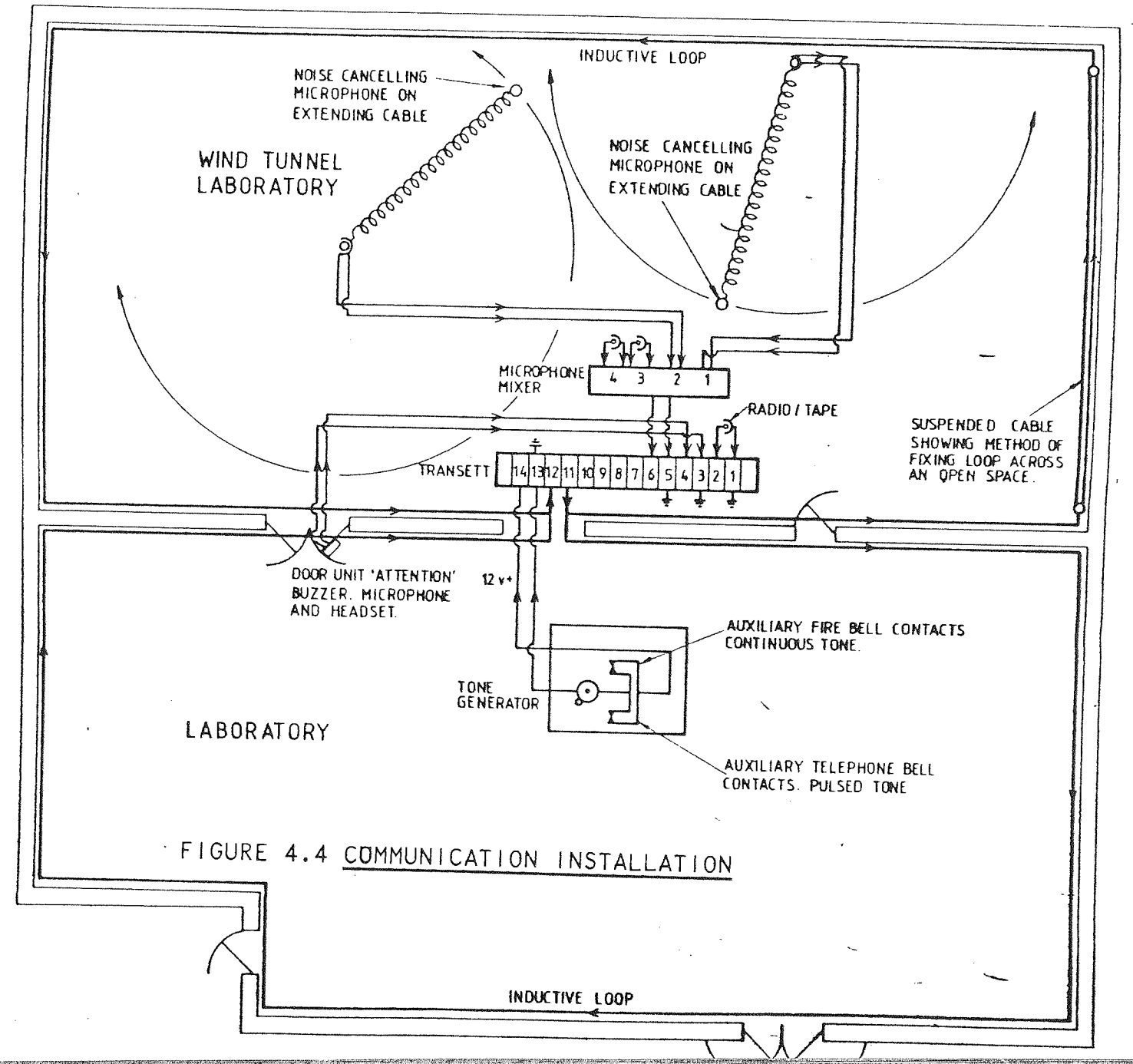

FIGURE 4.4 COMMUNICATION INSTALLATION

An inductive loop has been wired around each of the laboratories, from the output terminals on the Transett unit. When an input is provided an A.F. current passes through the loop and generates an electromagnetic field inside the area of the loops. This A.F. field is detected by the headsets and converted to sound pressure waves, audible to the headset wearer.

Person-to-person communication is provided by the installation of two noise cancelling microphones by speaking into the microphone. The outputs from these microphones are fed via a mixer to appropriate terminals on the Transett. There is full duplexing i.e. each can hear the other speaking without releasing the press to speak microphone switch. These signals automatically override the lower priority signal at terminals on the Transett.

The attention of the operator(s) in the wind tunnel room may be gained by pressing the button on the door unit. This will override the previous two channels. Conversation may be carried out between a person at the door unit and operator inside the wind tunnel room who will be using the noise cancelling microphones.

Telephone ringing gives a pulsed signal to the terminals, giving a pulsed tone in all the headsets. The input is superimposed on any of the others. Telephone conversation cannot be overheard over the system - only the bell signal. Likewise,in the event of a fire alarm signal a continuous signal will be presented to the same terminals, giving a continuous tone in all the headsets within the area of either loop. This signal overrides all others. The headset wearer while being protected against noise, can hear paging, alarms, warnings, instructions and background music and/or radio.

The headset has a limiting circuit which prevents the

sound pressure level of a signal, at the ear, from exceeding 80 dB(A) regardless of how far the individual headset volume control is adjusted. The headset receiver is a battery operating circuit. The on/off switching is carried out automatically by the head band. The head band is self adjusting.

4.5 Design Calculation and Fan Selection.

The loss due to different cross sectional area of duct is different. Even for two ducts of the same cross section area of different shapes, the loss due to friction is different.

In a ventilation system there are two types of friction loss. Losses due to friction in straight pipes and ducts, which are called the major losses and losses associated with sudden changes in the cross section either by enlargement or connection and elbows, air cleaner, discharge duct etc., which are called minor losses. Losses can be calculated from the energy balance for a control volume between two points in a flow system.

In calculating the losses certain assumptions are necessary. These assumptions are as follows:

(i) flow, is a fully developed flow (i.e. there is no well defind boundary layer).

(ii) fluid is incompressible

(iii) and the flow is a turbulent flow in a constant diameter duct

The pressure losses are known to depend on:

(i) duct diameter (D)

(ii) average velocity across the cross section of the duct (V)

(iii) length of duct (L)

(iv) viscosity of moving media (i.e. air) (μ)

(v) density of moving media (i.e. air) (ρ)

(vi) duct wall roughness (ε)

It is customary to write the losses in the form

$$H_L = K \text{ (velocity pressure)}^2 \quad \text{OR}$$

$$H_L = f \frac{L}{D} \frac{V^2}{2g} = F(D,V,L,\mu,\rho,\varepsilon)$$

where K is called the pressure factor, f and g are friction factors and gravitational acceleration respectively. The value of the pressure factor is given for commercial pipe fitting in engineering handbrooks. The following table lists some approximate K values:-

TABLE 4.3 Values of pressure factor "K" for duct fittings, etc.

Fitting and duct	K
90 degree elbow	0.9
45 " "	0.42
Sharp edge entrance to circular pipe	0.50
Round entrance to circular pipe	0.25
Sudden expansion	$(1-A_1/A_2)^2$
	A_1 = upstream area
	A_2 = downstream area

Alternatively combined charts for friction losses in straight ducts are given by different sources. The American Society of Heating, Ventilating and Air Condition Association (ASHRA), American Conference of Governmental Indistrial Hygeinists (ACGIH), Institute of Heating and Ventilation Engineers (IHVE), and British Institute of Standards etc., give the relevant charts, tables etc., for engineers' reference.

In this research a metric version of all charts and tables, given by ACGIH and the others, were used for the design calculation.

Tables 4.4 to 4.8 are summaries of the design calculation for the wind tunnel asemblies. Design calculation showed that a fan

Table 4.4 Loss calculation for main duct section, filter section and silencer (for fan duty of 1 cubic meter per second)

a	b	c	d	e	f	g	h	i	j	k	l	m	n
Opening, Duct section	Volume of air through section cubic metre per second (m^3/s)	Size and equivalent circular size millimeter (mm)	Area square metre (m^2)	Average velocity metre per second (m/s)	Velocity pressure millimeter of water gauge (mm WG)	Friction loss in velocity pressure (k)	Length of straight duct metre (m)	Friction loss in velocity pressure per metre	Friction loss per length of duct	Total friction loss mm WG	Total loss of each section mm WG	Reference, tables, charts, graphs, etc.	Remarks
Round lip flanged	1.0	510	0.2043			0.49	-	-	-	0.62		ACGIH	
Straight section consist of 3 - straight round duct	"	500	0.1963	5.09	1.26	0.032	4.30	0.052	0.28	0.28	0.897	Fig MG.5,6	ACGIH
Filter section: expansion	"	1800 by 1200 by 500 equiv. 1611.6	2.0398	0.049	0.00015	0.1 regain	0.35	ng*	ng	ng		BS.CP352 103:1950	taper angle α = 50
straight	"	"	"	"	"	0.01	0.2	ng	ng	ng		Fig MG.9	
filter	"	"	media area 5 x 1.654	"	"	"	0.1	-	-	3.0 max.		GEN Farr	
straight	"	"	2.0398	"	"	0.01	0.2	ng	ng	ng		Fig M.59	
contraction	"	800	0.50264	1.99	0.24216	0.05	0.405		0.012	0.012	3.012	ACGIH	taper angle 8°
silencer	"	800	0.50264	1.99	0.24216	-	1.60	-	3.5 Max	3.5	3.5	Chart 4 Woods of Colchester	

* ng = negligible

Grand Total = 7.409

(0.29 in wg)

Table 4.5

Loss calculation of square hood with bell mouth flange (see drawing No 2), Fan duty $1M^3$/sec. (see Figure 11)

a	b	c	d	e	f	g	h	i	j	k	l	m	n
Opening, Duct section	Volume of air through section cubic metre per second (m^3/s)	Size and equivalent circular size millimeter (mm)	Area square metre (m^2)	Average velocity meter per second (m/s)	Velocity pressure millimeter of water gauge (mm WG)	Friction loss in velocity pressure (k)	Length of straight duct metre (m)	Friction loss in velocity pressure per metre	Friction loss per length of duct	Total friction loss mm WG	Total loss of each section mm WG	Reference, tables, charts, graphs, etc.	Remarks
Entrance bell shape curved	1	890 x 890	0.7920	1.2	0.0975	0.04	0.1778	-	-	0.0298	0.0298	Fig. 4.8	ACGIH
Square duct	1	535	0.2862	3.49	0.7468	0.05	0.66	0.037	0.0244	0.0244	0.0244	Fig. MS5	"
Contraction to round	1	177.8	0.0248	-	-	-	0.279	-	-	-	85.45	St Venant equation	Dallavale 1935
Round	1	177.8	0.0248	40.32	99.46	1	0.254	1	25.26	25.26	25.26	Fig. MS.5	ACGIH
Further contraction	1	127.0	0.0127	78.74	379.31	0.06	0.11	-	22.76	22.76	22.76	Fig. 6-6	ACGIH Taper angle 9 degrees
Expansion (Abrupt)	1	152.0	0.0181	55.248	186.73	0.88	Free inlet inside larger duct	-	-	28.137	28.137	$(1-\frac{A1}{A2})^2 \times \frac{v^2}{2g}$	W F Hughes & A Brighton Schaum's outline series

Grand Total = 133.52 mm WG (5.26" WG)

Table 4.0 Loss calculation due to 1st round test section coupled with Bell mouth flanged hood (Fan duty $1 m^3/sec$)

a	b	c	d	e	f	g	h	i	j	k	l	m	n
Opening and duct section	Volume of air through section m^3/s	Size on equivalent circular size mm	Area of cross section square metre	Velocity metre/sec	Velocity pressure mm WG	Loss factor k	Length of straight duct section metre	Friction loss in velocity pressure per metre length	Friction loss per length of duct	Total friction loss mm WG	Total loss of each section	Reference, tables, charts, formulae, etc.	Remarks
Round straight duct	1	152.0	0.0181	55.248	186.73	0.93 entrance loss factor	1.19	-	-	1.44 0.084	1.44 0.084	Lee's equation	Dallavalle 1935
Abrupt expansion:	1	357	0.10009	9.99	6.1053	$V_2/V_1=0.18$ $K = 0.67$ $K(VP_1-VP_2)$	-	-	-	30.32	30.32	I.H.V.E. Guide Book	
within transition piece	1	Tapered expansion to 500	0.1963	5.09	1.5851	$D_2/D_1 = 1.4$ $= 15$ $k = 0.7$	0.6	-	5.6	5.6	5.6	Fig 6-6	
at the end of transition piece	"	"	"	"	"	$D_2/D_1=1.4$ $L/D_1 = 1.6$ $k = 0.47$ regain	-	-	2.87 regain	2.87 regain	2.87 regain	Fig 6-6	
										Grand Total = 34.04 mm WG (1.28 WG)			

Table 4.7 — Loss calculation due to rectangular hood tapered to round duct with equal opening area as square section of bell shaped flange hood.

a	b	c	d	e	f	g	h	i	j	k	l	m	n
Opening, Duct section	Volume of air through section cubic metre per second (m^3/s)	Size and equivalent circular size millimeter (mm)	Area square metre (m^2)	Average velocity meter per second (m/s)	Velocity pressure millimeter of water gauge (mm WG)	Friction loss in velocity pressure (k)	Length of straight duct metre (m)	Friction loss in velocity pressure per metre	Friction loss per length of duct	Total friction loss mm WG	Total loss of each section mm WG	Reference, tables, charts, graphs, etc.	Remarks
Rectangular opening	1.0	1145x250 equiv.=4104	0.2862	3.49	0.7468	α= 3degree k = 0.8	-	-	-	0.149	0.15	Fig 6-10 entry loss	ACGIH
	4.72	"	"	16.49	16.64	"	-	-	-	13.31	13.31	"	"
Reducing Taper section within & at the end of section	1.0	"	"			α= 3degree 0.8	0.2	-	-	"	0.15	"	
	4.72	"	"			"	"	-	-	"	13.31		
Straight round section	1.0	357.	0.28038	3.57	0.78	0.75	0.5	-	-	0.58	0.58	Fig 6-5	ACGIH
	4.72	"	"	16.83	17.34	"	0.5	-	-	13.0	13.0	"	"
Transition section:													"
Within section	1.0	500				D_2/D_1=1.4 α=15, K=0.7	0.6	-	5.6	5.6	5.6	"	"
	4.72	"					0.6		12.61	12.61	12.61		
At the end of the section	1.0		0.1963	5.09	1.58	D_2/D_1= 1.4 L/D_1 = 1.6 k = 0.47 regain	-		2.87 regain	2.87 regain	2.87 regain	"	
	4.72		"	24.04	35.36		-		0.37 regain	0.37 regain	0.37 regain	"	
										Total = 3.61 mm WG @ 1.M^3/sec (0.14 mm WG) 51.86 mm WG @ 4.72 M^3/sec (2.04 mm WG)			

Table 4.8 Loss calculation for main duct section, filter section and silencer fan duty 4.72 m^3/s (1000 cfm)

a	b	c	d	e	f	g	h	i	j	k	l	m	n
Opening, Duct section	Volume of air through section cubic meter per second (m^3/s)	Size and equivalent circular size millimeter (mm)	Area square meter (m^2)	Average velocity meter per second (m/s)	Velocity pressure millimeter of water gauge (mm WG)	Friction loss in velocity pressure (k)	Length of straight duct meter (m)	Friction loss in velocity pressure per meter	Friction loss per length of duct	Total friction loss mm WG	Total loss of each section mm WG	Reference, tables, charts, graphs, etc.	Remark
Round lip flanged	4.72 (10000cfm)	510	0.2043	-	-	0.49	-		17.33	17.33		ACGIH, I.H.V.E.	50 mm lip flange
(see drawing No. 1) Round straight duct with two flange coupling and gaskets		500	0.1963	24.04	35.37	0.032	4.30	1.13	4.87	4.87	22.20	Fig. MS.5,6	
(see drawing No 1) Filter Section: expansion	"	inside dimensions 1800 by 1200 by 500 equiv. 1611.6	2.0398	0.43	0.0114	0.1 Regain	0.350	-	+0.0011	+0.0011		BSCP352.103 1958	taper angle α = 50
straight	"	"	"	"	"	0.01	0.20	0.000114	negligible	* ng		Fig. MS.9	
filter	"	"	media area = 6x1.654	"	"	-	0.1	-	-	3.0		GKN Farr	For 1.5m/s
straight	"	"	2.0398	"	"	0.01	0.2	0.000119	negligible	ng		Fig. MS.9	
contraction	"	800	0.50264	9.39	5.39	0.05	0.405	-	0.27	0.27	3.27	ACGIH	Taper angle 4 degree
Silencer (drawing No. 1) Section F-F, E - E Drawing No. 2)	"	"	"	"	"	"	1.60	-	3.5	3.5	3.5	Chart 4 woods of Colchester	

* ng = negligible

Grand Total = 28.97 mm WG

(1.14 inches of water)

of duty 4.72 $m^3 s^{-1}$ for a system resistance of 172.72 mm WG (fan total pressure) will be a sufficient air moving device for this wind tunnel system.

Apart from the above requirements, the following characteristics were considered for the selection of fan:

(i) low sound level ratings

(ii) reliable and accurate volume control

(iii) stable at various system pressures with required flowrate

(iv) stable speed of rotation

(v) minimum power requirement

(vi) good efficiency at all operating conditions with minimum power requirement

Studying the commercially available data on fan characteristics considering the above factors, a variable pitch angle fan was the best selection of the air moving devices for this wind tunnel system.

Generally, variable pitch fans are special models in which the blade angle can be continuously varied while the fan is running. The other unique feature of this type of fan is the ability to control the volume flow down to zero even at constant system pressure, and to produce reverse flow if required. Noise level falls with reduction of volume flow, whereas it tends to rise with other volume control devices (i.e. damper or vane control (Noon (1976), Daly (1978)).

The selected fan is a single stage varofoil fan of diameter 800 mm and 12 blades with a constant impeller speed of 295 rpm of minimal duty. The total inward and outward movement of impeller is 15.5 mm over 48 seconds. This movement is equal to -8 to 10 degrees of pitch angle alteration. The impeller is directly fitted to the shaft of the constant speed motor. The

wings are clamped to the hub of the impeller. Pitch angle control is via the actuating beam which may be controlled pneumatically, electrically or mechanically. The response between the control action and pitch angle movement is linear (Noon).

4.6 Electric actuator and supply panel.

The electro-mechanical actuator of the pitch is manufactured by Drayton Controls. The model designation is POWERACTOR VA1 and consists of a reversible geared motor driving a rack to provide a linear movement.

The actuator has a full potentiometric feedback making it suitable for modulating, on/off, or floating control applications. The 135 ohm range corresponds to the total actuator movement.

An electric supply panel coupled with a remote control system and on/off switch has been made by Satchwell Control Systems Limited. Further facility of this control panel is the possibility of adjusting the pitch angle to give a known linear centre line velocity at any desired measuring point using a Prosser Scientific Air Velocity Meter type 501F or any equivalent velocity meter to give an equivalent voltage response to its sensor. This facility is especially useful to adjust the pitch angle in order to provide a certain control velocity at any desired position in the suction field.

4.7 Support system.

The silencers, motor, fan, air cleaner section and ducts are mounted firmly on a antivibration mounting metalastik on the steel rectangular hollow section frame (Drawing No.5). Steel supports for each section on the wind tunnel system are individually

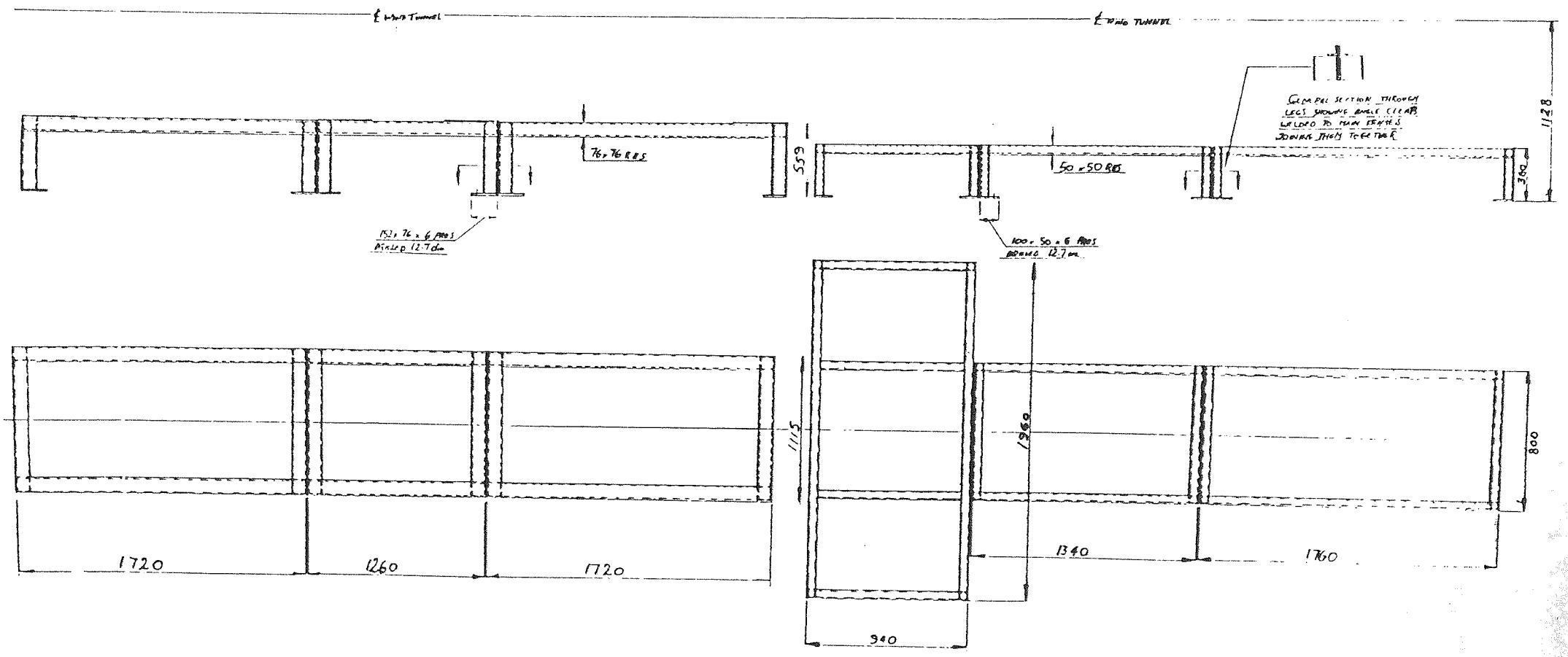

DRAWING No. 5 STEEL SUPPORT

screwed into the floor. The ducts are laid on a properly shaped wooden mounting support which in turn lies on the cross steel bars (Drawing No.1 Section B-B).

A portable and adjustable steel support used for the support of test ducts under study.

A wheeled steel support for Square Bell Mouth hood is the other moveable support stand (Drawing No.2).

4.8 Coordinator.

For placing the measuring sensor at a known position relative to the coordinates origin (centre of suction) a probe carriage holder has been made (Drawing No.4). By means of the machined clamps to adopt the air velocity measuring (guard) tubes and steel rods the sensors can be placed at either horizontal or vertical positions in the suction field. The rods fit together at right angles, and are fixed to a support moving side to side which is the means of adjustment in the Z-axis direction.

Displacing the horizontally fitted rods up and down will provide the movement in the Y direction. The whole system is mounted on a three wheel base moving inward and outward over two angular tracks fixed permanently along the centre line of the wind tunnel system at a distance of 2 x 36.25 mm apart (Drawing No.4). This movement is the adjustment in the X-axis direction.

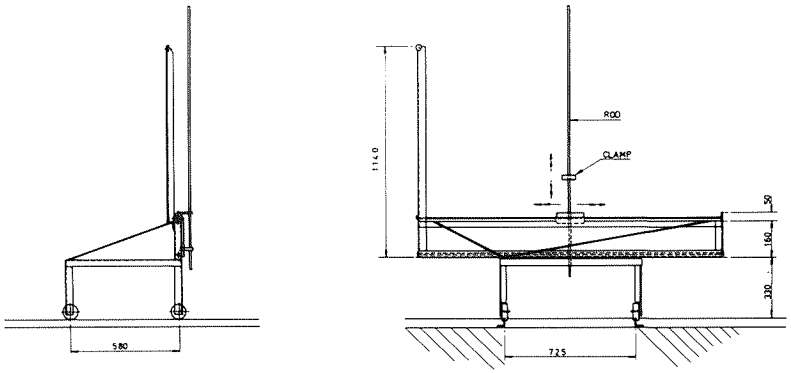

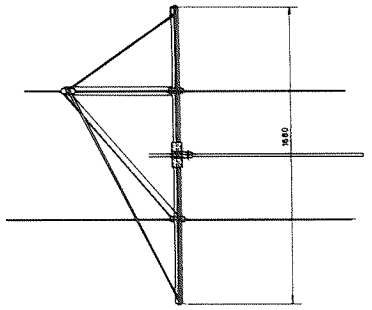

PROBE HOLDER CARRIAGE CORDINATOR

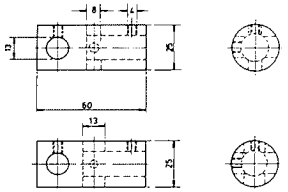

CYLINRICAL CLAMPS

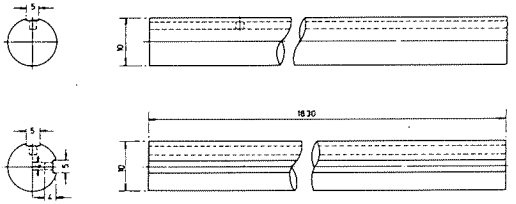

HORIZONTAL & VERTICAL CLAMPING STEEL RODS WITH GROVES & HOLES AT 15mm. INTERVALS

TITLE		NOTE ALL DIMENSIONS IN MILLIMETRES
UNIVERSITY OF ASTON DEPARTMENT OF SAFETY & HYGENE		SCALE 1 10 DRAWING No 4

CHAPTER FIVE

MEASUREMENT PROCEDURE, INSTRUMENTS, FACILITIES CALIBRATION AND RECIRCULATION

5.1 Measurement Procedure

5.1.1 Introduction

Generally in ventilation and air conditioning work, there are four common positions for measuring air velocity:

1. in a duct
2. at the face of a supply outlet
3. at an intake or suction opening
4. in an open space or room

Duct velocity is usually high enough to permit direct impact measurement by the pitot tube and manometer, while room air velocities range down to barely perceptible air movement which is difficult to measure by a pitot-static tube. The measurement of an air velocity of 0.25 ms^{-1} (50 fpm) is quite different from the measuring of 5 ms^{-1} (1000 fpm) and calls for different instrument characteristics. A second problem arises from the fact that the air velocities in various parts of a stream are often different, and these velocity variations greatly complicate effective measurement. The advantages and limitations of the various instruments become apparent when the methods of calibration and methods of application of the instruments are investigated, hence the problem has been approached from that angle.

5.1.2 Fluid Flow in ducts and Methods of Measurements.

Fluid flow in a duct is a complex phenomena. Despite extensive studies during the past 50 years, existing knowledge is far from complete and recourse is made to a semi-empirical

equation to describe velocity profiles (Miller et al. 1968).

For a flow of fluid entering a duct, the viscosity causes a boundary layer to form on the wall with zero velocity at the wall.

Methods for measuring the average velocity for circular ducts are

i) Log linear rule method (Figure 5.1 Six Points reading)

ii) Tangential rule method (Figure 5.2 ten Points reading)

iii) Direct use of mean velocity

iv) Averaging pressure tube method

Some of these methods all involve the use of pressure tubes, a description of pressure tubes will follow later).

When the upstream straight length of duct is greater than ten pipe diameters, the velocity distribution will generally have settled down sufficiently for the mean velocity to be determined from a reduced number of measurement points (i.e. ten points or six points).

The general method of obtaining the flow rate in a rectangular duct is to divide the duct into a number of equal areas geometrically similar to that of the full section. Measurements of velocity are then made in each area, which are then averaged to give the mean velocity in the duct and hence the flow rate.

British Standard 848 Part 1: 1963 recommends 16 rectangles for pitot measurements. The perimeter rectangles which usually contain the steepest velocity gradients, are subdivided so that 3 measurements are made to obtain the mean velocity. A single measurement is used for the velocity of each of the centre rectangles. Then 48 points of measurement of velocity pressure for the duct under investigation would be required. Myles et al.(1966) extended the log-linear theory and developed an integration.

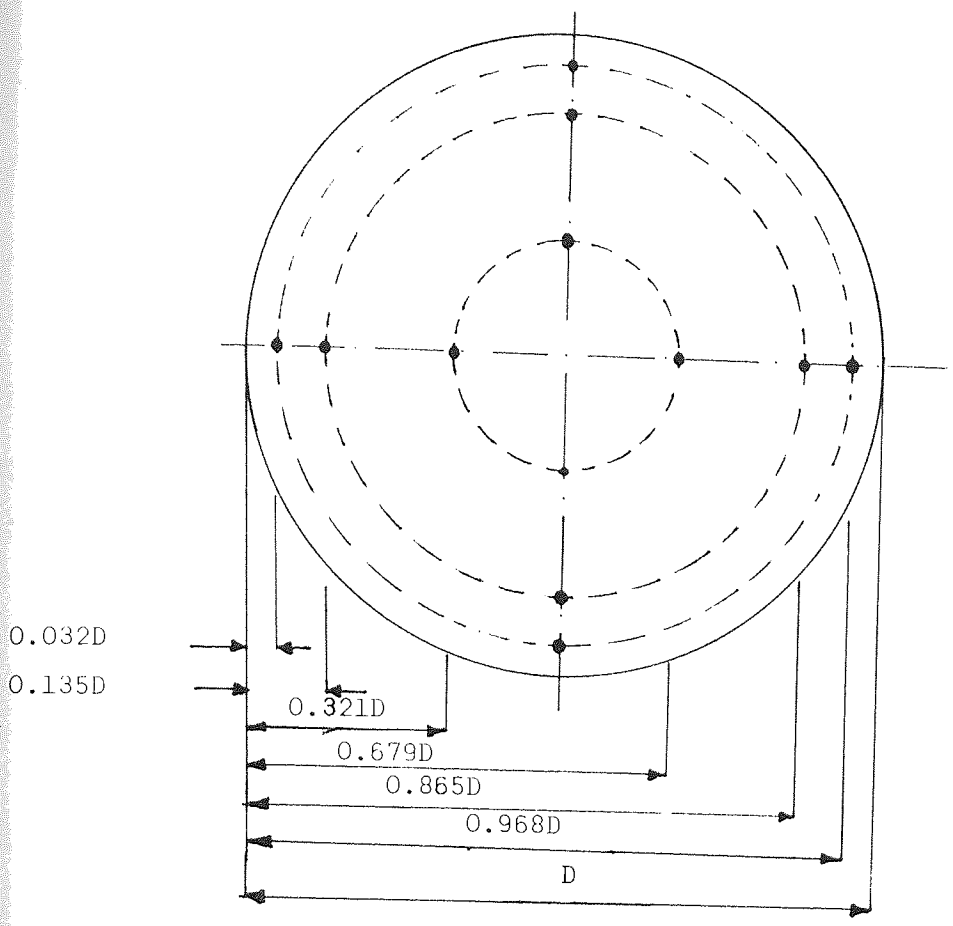

FIGURE 5.1 Positions at which pitot tube measurements should be taken when using log-linear rule.

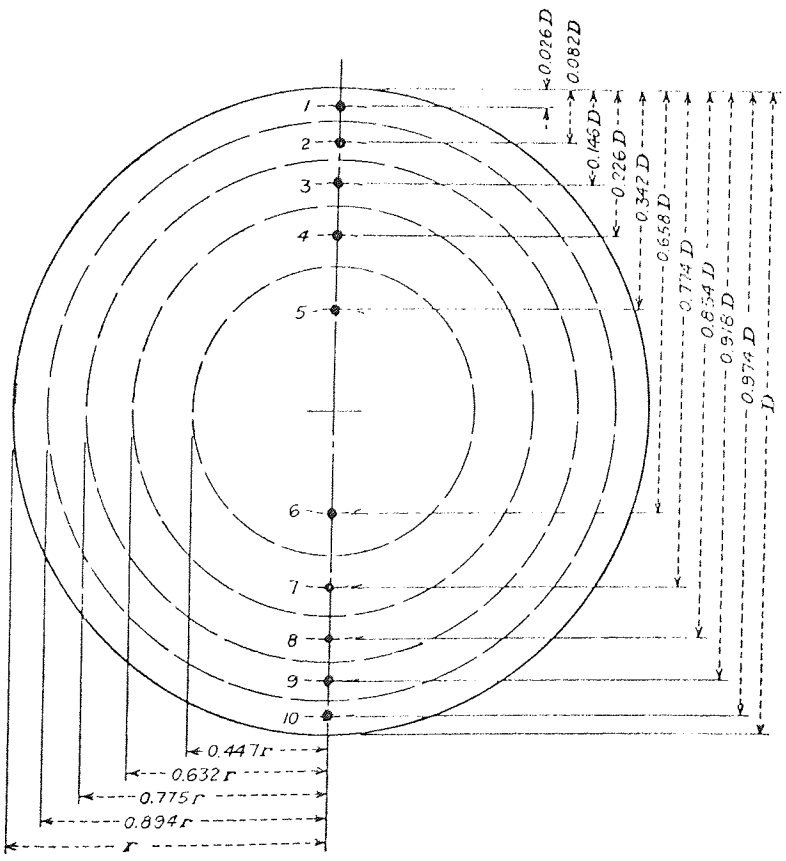

Figure 5.2 Locations for Pitot Tube Tip When Making a 10-Point Traverse (tangential rule)

technique for measuring the volume in rectangular ducts. This technique involved 26-points pitot-tube measurements. (The position of traversing points for both B.S. and 26-points derived from theoretical considerations (ibid) are shown in Drawing No. J, Figures 5.26,)

Tests carried out by Myles indicate that under stable flow conditions the 26-point method was as accurate as the B.S.48 point method, although both methods deviated on average by approximately +1.5% when compared with the flows obtained from orifice plate measurements. Tests carried out by Legg (1970) showed that the two methods are in close agreement and concluded that 26-point traverse would be satisfactory for obtaining the reference volume.

In 1968 Miller et al. revised the existing method of flow metering, and they developed a method of flow measuring for any duct cross-section. The following is a summary of their findings:

i) the log-linear rule is a good method for velocity measurement near any duct wall, and can be applied with reasonable accuracy to the remainder of the duct;

ii) the log law can be used to find the position of the mean velocity in any two-dimensional or circular region;

iii) at high Reynolds numbers, corner region can be approximated to circular regions.

The measurement at the face of outlets and intakes of suction are more or less the same as the measurement inside the duct.

There is not any set method of measuring the open space or room current movement.

5.2 A review of existing methods of measuring air speed.

The methods of air velocity measurements can be divided into the following groups. In each of the groups a different effect

arising from the air motion is measured. These are:

(i) visualisation of actual transport or displacement of the air for example by the motion of smoke;

(ii) the pressure effects associated with the motion;

(iii) the rate of cooling of a hot body;

(iv) the force exerted by the flow on a suitably mounted body, such as a plate;

(v) the change of the speed of sound in an air stream;

(vi) the deflection of the path of ions in an electric field.

Some methods can be classified as coming under more than one of these headings, and an arbitrary choice has to be made. The following sections are descriptions of some of the instruments depending on these effects though not necessarily in the same order as the above list.

5.2.1 Pressure tubes.

There are a variety of pressure tubes. The following description refers to some of the tubes extensively used in this research or used by previous researchers.

(i) The Standard Pitot tube.

Air velocity is measured by means of a pitot tube shown schematically in Figure 5.3. This instrument consists of two independent concentric tubes bent into an upside-down "L" in diagram. In use the tube is inserted into a duct and directed along the axis so that it points upstream. The two terminals S and T are connected to a suitable gauge, and the deflection observed is an indirect measure of the speed with which the air is moving.

The theory of measurement of this device is that the point T measures the total pressure within the duct which consists of a dynamic or impulsive pressure, and S static pressure. The

Figure 5.3 PRINCIPLE OF OPERATION OF THE PITOT STATIC TUBE

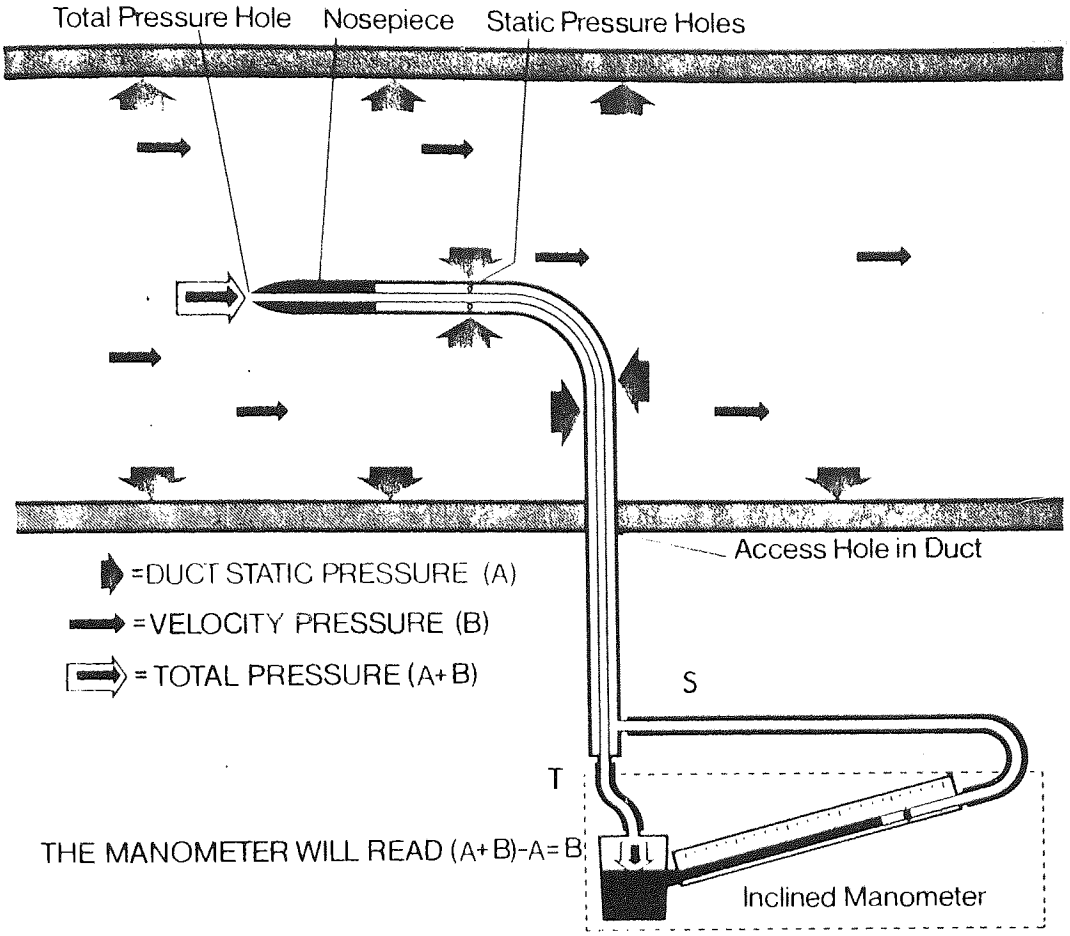

former is accurately measured only when the tube is pointed upstream, but the latter is a pressure which at a given point is the same regardless of direction. If, therefore, the total pressure is denoted by T_P, the velocity pressure by V_P and the static pressure by S_P, then the pressure measured at a point is

$$T_P = V_P \pm S_P \qquad (5.1)$$

depending on whether the duct is under positive or negative pressure. By using Bernoulli's equation V_P will be directly converted in terms of velocity as follows:-

$$V_P = c \frac{\rho V^2}{2g} \qquad (5.2)$$

where c = pitot tube coefficient = 1 with a tolerance of $\pm \frac{1}{2}\%$. Information regarding the detailed design of pitot tubes is given in such references as British Standards (BS 1042 and BS 848).

ii) Modified Pitot Tube.

One of the difficulties of the ordinary pitot tube is the fact, that the total and static pressure are not measured at identical points. Consequently in regions where the air movement changes rapidly as at an opening under suction, the ordinary pitot cannot be used. For such a condition DallaValle (1932) used a modified tube shown in the following figure. The tube consists of a thin brass cylinder, approximately 3.1 mm (one-eighth of an inch) in diameter with two independent compartments closed at one end. Two small holes 0.5 mm (0.02 inch) in diameter are drilled at its midsection and a pointer is fastened near the closed end in the direction of the holes. Using this tube, the readings are a measure of velocity pressure.

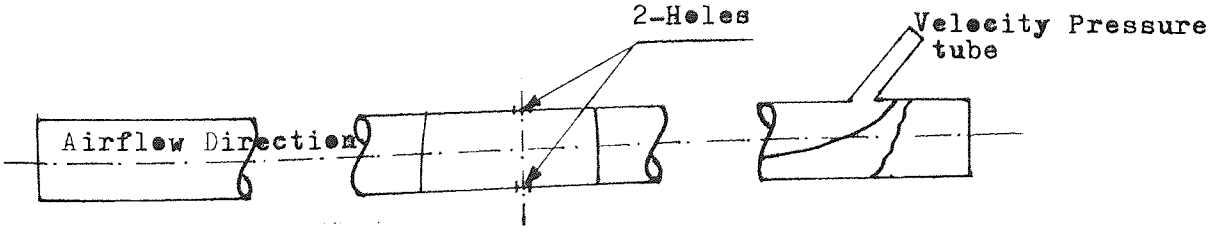

DallaValle's modified Pitot tube

(ii) Averaging pressure tube.

The rate of airflow in a duct is an integration of the product of the velocity and the area through which the velocity exists. This is given by

$$Q = \int_A V \, dA \qquad (5.3)$$

The velocity can be calculated from the relationship between the velocity pressure and velocity. Velocity pressure can be measured by the pressure difference between the total pressure and the static pressure. These relationships are as follows:

$$V_P = T_P - S_P = \tfrac{1}{2}\rho V^2 \qquad (5.4)$$

$$V = \sqrt{\frac{2V_P}{\rho}} \qquad (5.5)$$

Velocities across the duct are measured at small discrete intervals. After this measurement a velocity profile can be constructed and the integral for the flow rate of airflow can be evaluated by a graphical method. In 1966 William reviewed the existing system of flow meters, and showed that the rate of air flow is measured by the product of the cross-sectional area of the duct and the mean of the velocities measured by a mechanical device.

Mean of the velocities measured at small discrete distance intervals across the duct has the form of:-

$$\bar{V} = \frac{V_1 + V_2 + \ldots V_n}{n} = \frac{\sum_{i=1}^{n} V_i}{n} \qquad (5.6)$$

where $$V_i = \sqrt{\frac{2V_{P_i}}{\rho}} = \sqrt{\frac{2}{\rho}} \sqrt{V_{P_i}} \quad ; i = 1, \ldots n \qquad (5.7)$$

therefore

$$\bar{V} = \sqrt{\frac{2}{\rho}} \sum_{i=1}^{n} \sqrt{\bar{V}_{P_i}}/n \qquad (5.8)$$

This is a laborious process in flow rate measurement, both in terms of measurement and a lengthy arithmetical operation is involved to obtain the mean velocity.

In the above expression, it can be assumed that the mean velocity of airflow in a duct is the square root of the average of the velocity pressure times a constant instead of the average of the individual square roots of the velocity pressure times the same constant. This statement can be expressed mathematically as below:

$$\bar{V} = \sqrt{\frac{2}{\rho}} \sqrt{\frac{\sum_{i=1}^{n} V_{P_i}}{n}} \qquad (5.9)$$

William showed that this averaging of velocity pressure can be done by mechanical means. The averaging pressure tube flowmeter is the result of his research (Drawing No. 3 and Fig. A 5.18). The flowmeter is mainly a tube with small holes drilled equally spaced, on the longitudinal side of the tube facing the airstream. The average velocity pressure will be measured by the connection of the two ends of the tube to one side of a manometer and the other side to a number of static pressure holes on the circumference of the duct. However, this method of flowmetering raises the following questions:

i) is this pressure difference, a true average of individual pressures?

ii) is the difference between the average of the individual square roots of velocity pressure and the square root of the average of the velocity pressures as measured by this flowmeter significant?

William experimented on the size of tube and size of holes. He found that the tube gives a good estimate of the

for the arithmetical mean of the pressure imposed on each hole. For the second type of uncertainty, he evaluates the differences mathematically, provided that the flow distribution is known. However, this distribution is not known properly, uncertainties exist between the relationship of the velocity and the distance from the wall of a duct at which the velocity is measured. Two widely accepted relationships are:

i) Power law

$$\frac{V_y}{V_c} = \left(\frac{Y}{R}\right)^{\frac{1}{m}} \qquad (5.10)$$

ii) Log-linear relationship for a fully developed and symmetrical flow with respect to the axis of the duct

$$V_y = a + b \log(^{y}/_{D}) \qquad (5.11)$$

where m,a and b are constants, Y is the points distance from the wall and D(=2R) is the duct diameter. But flow in a duct at different positions has a different pattern. For a turbulent but not 'fully developed' (asymmetrical) flow at a short distance from a right angle bend, the relationship is uncertain. At this sort of duct cross-section, the flow is subjected to the effect of swirling created by the bend. The degree of influence of swirling on the performance of the flowmeter depends on the mean air velocity, the size of duct, the length of the straight duct before and after the flowmeter and the different configuration of bends upstream from the flowmeter.

The other types of errors are instrumental and human errors. These errors can be taken into account by an experimental coefficient which can be defined by:

$$c = \frac{Q_a}{Q_m} \qquad (5.12)$$

William studied the suitability of the averaging pressure tube and concluded that the averaging pressure tube flowmeter is more suitable

for flowmetering than any other method because it is simple and robust, and virtually creates no resistance to the airflow, requiring only a short distance of lengths of duct before and after the measuring point and is consistent in its performance. The accuracy of the averaging pressure tube flowmeter given by William is $\pm$ 6.5% for air velocities from 3 to 7 ms^{-1}.

(iv) Prandtl Pressure Tube type 607.

Appendix 5.2 gives an illustration of the tube. Flow streamlines were studied by means of this pressure tube. The procedure was as below:

(i) A protractor was fixed flat on a clamp reading 90° from the Z-axis (see Plate Nos.3 and 4 also 9 to 16)

(ii) The pressure tube was fixed to this clamp.

(iii) A pointer was fixed to the stem of pressure tube in order to point to the graduation on the protractor when the tube was rotated.

(iv) Then two legs of the pressure tube were connected to the ports of a micromanometer to read the pressure difference.

(v) A zero pressure difference measurement indicates flow stream direction.

(vi) The angle of rotation of the pressure tube from the centre line stream position will be the angle of tangential velocity line to the streamline at the tip of the pressure tube point of measurement.

5.2.2 Manometers.

Manometers are pressure sensing devices. They are of different types with different characteristics and sensitivity. The following is a brief description of those manometers which wereused in this research and by the other researchers quoted in this thesis.

(i) Micromanometer. This is a pressure sensitive device, which indirectly measures the motion of a fluid medium.

The Furness Control 5-range Micromanometer type MDC was used for measuring pressure difference.

The MDC micromanometer is a sensitive pressure measuring device. The instrument is capable of measuring pressure down to ± 0.001 mm WG (0.12 m s^{-1} of air velocity measurement).

A most useful and valuable feature of this instrument is the built-in calibration check facility, which enables the calibration to be checked in a matter of seconds, whilst the instrument is being used under operation conditions.

The five ranges are 0.1,0.3,1.0,3.0 and 10.0 mm WG for full scale readings. The minimum of 0.001 mm WG and maximum of 10 mm WG (12 m s^{-1}) are the covering ranges of pressure readings with this instrument. The accuracy of the instrument is 1% of the scale in use except in the 1 mm WG range and below, where the accuracy is ± 5%.

An electronic output signal is provided for recording pressures. The instrument was calibrated at the factory, the calibration was checked in the laboratory and at the factory again during the occasion of a visit to the factory. Checking has been done against a master standard of accuracy of 0.1% for full scale deflection of the range of MDC.

The micromanometer was used for calibration of inclined manometers as well as for the low velocity and pressure difference measuring instrument used throughout the experiments.

(ii) Liquid Manometers. Liquid manometers are used in connection with pressure tubes for pressure readings. When the tube is connected to a pressure source, the liquid column will be displaced

by an amount sufficient to balance the force acting upon it. Then the vertical distance between the liquid levels indicates the amount of pressure exerted by the fluid. The graduation of tubes is conventionally in water gauge (WG). Tubes can be U shaped or inclined. The inclined tubes are more sensitive than U-tubes. A manometer, which is mounted on a right-angled wedge-shaped block with a rise of 2.54 cm. (one inch) for 2.54 cm. (10 inches) of tube length has a sensitivity ten times as great as a vertical manometer. U-tubes may also be sloped to give sensitivities twenty times as great as vertical tubes, but such sensitivities do not guarantee accurate readings.

In use, a sloping manometer should always be carefully levelled.

iii) Wahlen Gauge. DallaValle (1932) used a Wahlen gauge for pressure difference measurements. The instrument is very sensitive and the range of velocity measurements is from 0.5 to 20.3 ms^{-1} (100 to 4000 feet per minute).

The gauge is shown schematically in Fig.5.4 and consists of two large bulbs filled with coloured alcohol connected by an inverted U-tube containing kerosene. The bulb B is so connected to the U-tube that it can be moved in a vertical direction by means of vernier calipers mounted on a framework. A stopcock is provided near the bottom of the stem connection of the bulb B so that when pressure is applied to the bulb the liquids will not be violently disturbed. Before use an initial reading is taken with both bulbs open to the atmosphere by bringing the meniscus at D to the hair-line. The difference between initial and connected to pressure source readings is the actual displacement in terms of the heavier liquid.

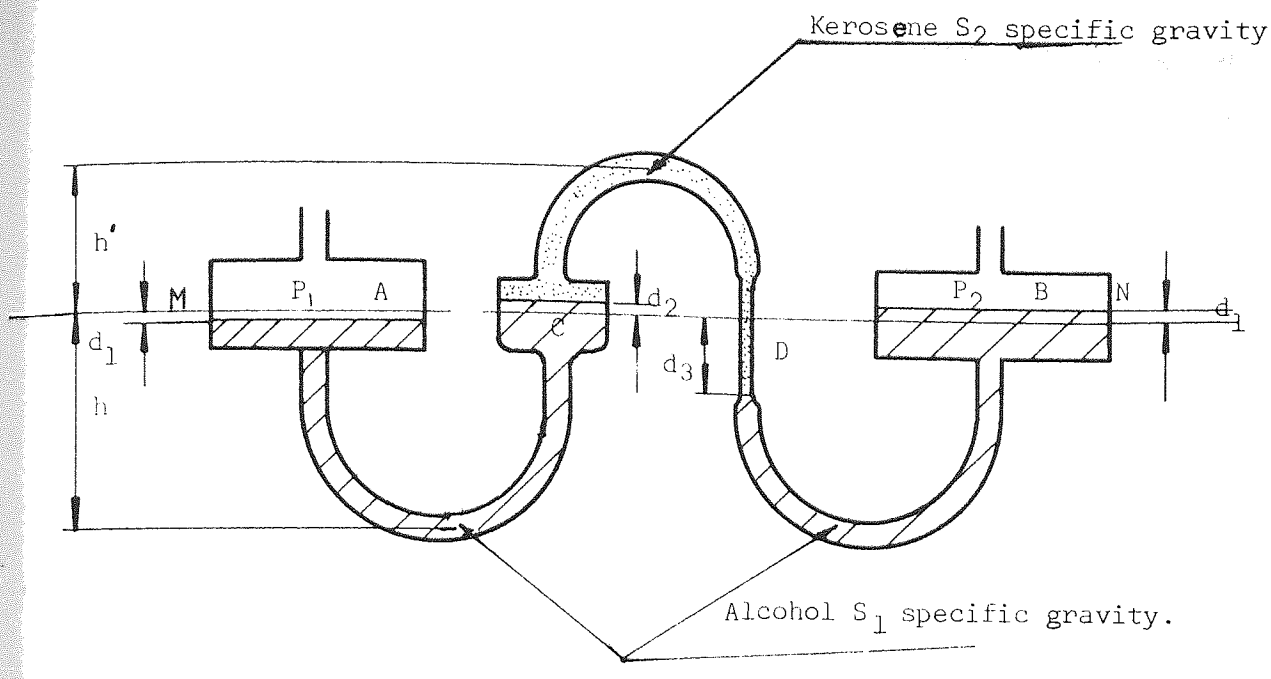

Notation: S_1 specific gravity

Area A = Area B = A_1

Area C = A_2

Area D = A_3

$b = S_1 - S_2$, $P = P_1 - P_2$

MN=liquid level when $P_1 = P_2$

$$d_3 = \frac{p - 2d_1S_1 - d_2b}{b}$$

$A_1d_1 = A_2d_2 = A_3d_3$ = constant so

$$d_3 = \frac{P}{b\left(1 + \frac{A3}{A2}\right) - 2S_1\frac{A3}{A1}}$$

Figure 5.4 WAHLEN GAUGE

The reading may be converted to inches of water by multiplying the difference by the specific gravity of the alcohol. This is a null method based instrument. However, accurate readings depend upon a knowledge of the specific gravity of the alcohol over the range of temperature the instrument is to be used, and upon maintaining the instrument level at all times. DallaValle states that the zero readings should be taken frequently during experiments since the meniscus at D tends to vary.

From the relationship (see Fig.5.4) it is clear that the sensitivity of the gauge depends chiefly on a low specific gravity difference between the liquids, b, and on the ratio of the areas of the large bulbs to the area of the D-tube.

The liquids used in the Wahlen gauge should be allowed to stand in the presence of each other in a stoppered bottle for some time. This permits the liquids to reach a stable condition and reduce the variation of the meniscus at D due to the solubility of kerosene in alcohol (DallaValle).

(iv) Inclined manometer. The Air Flow Development Ltd., portable test comprising of two adjustable manometers Mark MK were used for measuring the pressure difference in pitot-tube anemometry in this research. This consists of two limbs (short and long) and a rapid levelling device and a control knob for zero adjustment. The limbs are adjustable to four different inclinations covering the ranges 0 up to 500 mm WG. The gauge fluid is a blend of paraffin (kerosene) having a specific gravity of 0.784 at 20°C dyed deep orange-red giving an extremely clear and free moving meniscus. The instrument panel is levelled by the adjustment of two knobs and two very sensitive spirit levels.

Zero adjustment is effected quickly and accurately by rotating a knob on the panel. This actuates a mechanism to dis-

place liquid in the reservoir tank. There is no gland through which leakage can take place.

The scales are photo-etched and are of curved section which serves as a clamp to press the glass tube into the supporting groove. As the edge of the scale is actually in contact with the glass, possible errors in reading due to parallax are reduced to a minimum. The scale longths are 320 mm and 643 mm. An Aneroid barometer range 58 to 83 cm Hg and two thermometers of ranges 0 to 60 °C and 0° to 400 °C are the other useful devices comprising this portable test set. Type 504 industrial manometers cover the range of zero up to 75 mm WG. The limb is at a fixed inclination angle. Zero adjustment is effected quickly and accurately by rotating the knurled collar at the tapping connection to displace the reservoir tank within the instrument case. All pressure connection was done by P.V.C. flexible tubing grade 5 mm. bore by 2 mm. wall.

5.2.3 Direct air velocity meters.

The following direct air velocity meters were used for the point velocity readings.

(a) Thermistor air velocity meter manufactured by Prosser Scientific Instrument, types AVM501F and AVM502.

(b) Simon Shielded hot wire anemometer type 5115F manufactured by Tinsley Co.

Thermistors are thermally sensitive resistors. They have, according to the type, (Negative (NT_e) or positive (PT_e)) resistance/temperature coefficients (see Fig.5.5.1C)

These sensors are suitable for measuring the velocity of liquid or gases as well as temperature (Fig.5.5.1(A) shows probe outline).

The relationship of the resistance at a temperature

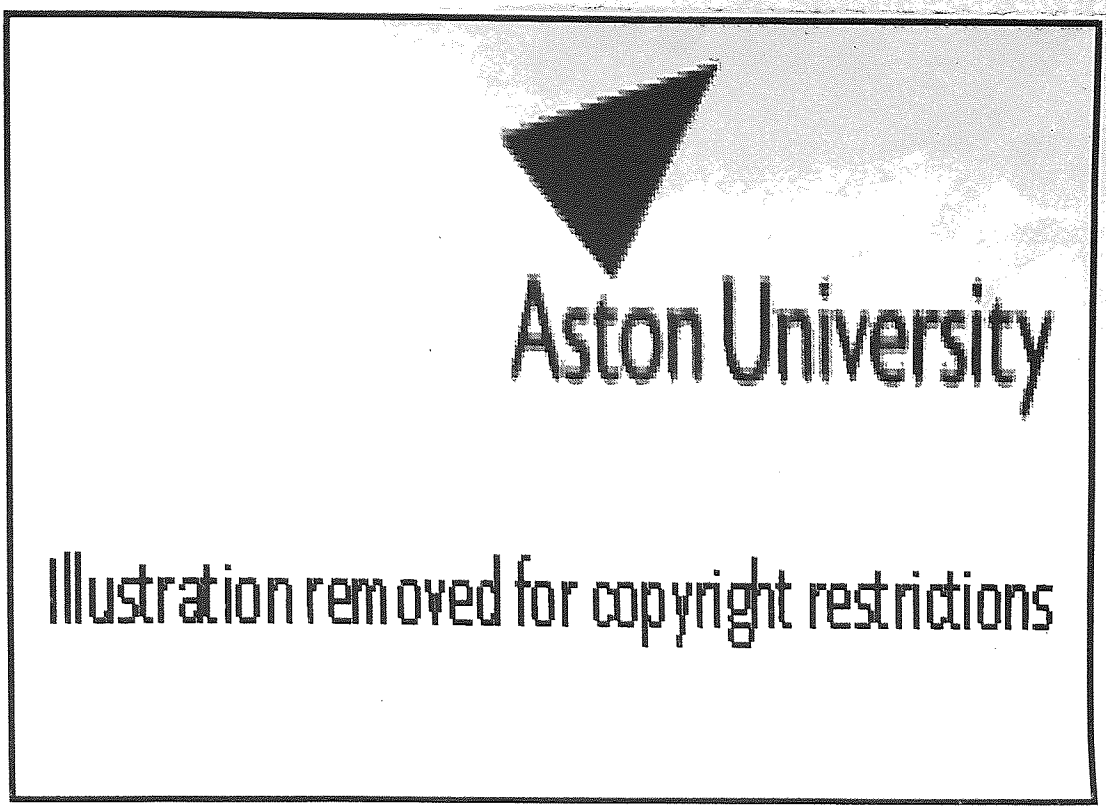

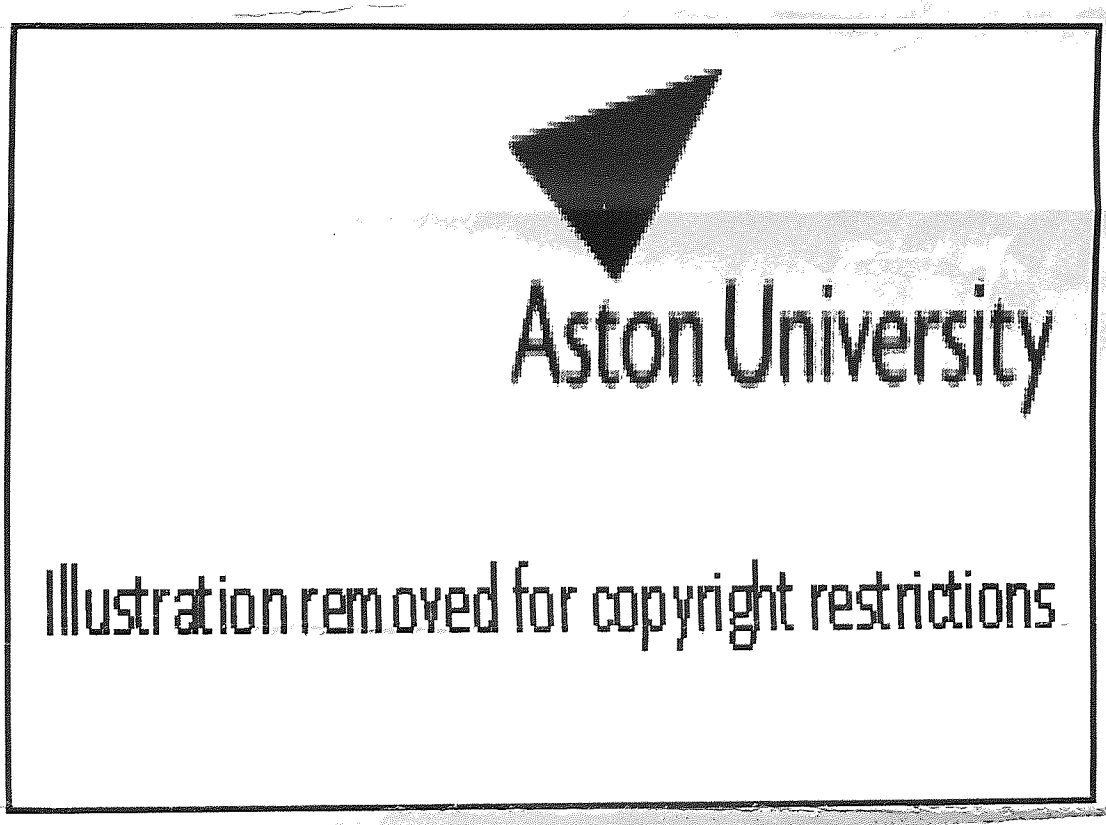

Figure 5.5.1 Characteristics of Unencapsulated glazed bead suspended beyond of glass probe (Code P23) for Katharometry, anemometry and other flow measurements.
(From ITT, Thermistor Data Booklet 1977/78)

T_1(°K) to the resistance at any other temperature T_2(°K) is as below (Thermistor Data 1977-78):

$$R_{T_1} = R_{T_2} \exp\left(\frac{B_t}{T_1} - \frac{B_t}{T_2}\right) \qquad (5.13)$$

where B_t is a characteristic temperature of the thermistor expressed in °K, and R_{T_1} and R_{T_2} are resistance at temperature T_1 and T_2 respectively.

The type of thermistor used in this research is a directly heated bead. The bead is an encapsulated glazed bead suspended beyond the end of a probe lead (see Fig.5.5.1A). The lead is made of platinum iridium alloy.

These types of thermistors are resistance matched within 1% of each other as suffix MP_c or alternatively matched at a constant current as suffix MPH. The AVM's thermistors are of the type P_{23} and MP_c which have 1.7K ohms nominal resistance at 25°C and 5 mA constant current. The constant temperature bridge is shown in Fig.5.5.2.

(i) Theory of operation of direct velocity meters. Thermistor AVM velocity meters have a sensor element which is heated up by means of a battery or mains source. As the impinging air velocity increases, the sensor will cool with a resulting decrease in resistance. The resistance drop causes a voltage drop, changing the input to the differential amplifier. This results in an increase in the output of the amplifier so the current through the sensor is increased. The gain of the amplifier is sufficient to keep the two inputs 1 and 2 balanced (see Fig.5.5.2). Therefore, any change in the sensor resistance is immediately corrected by an increase or decrease in the current through the sensor. The output of the system is the voltage output of the amplifier which in turn is the voltage required to derive the necessary current through the

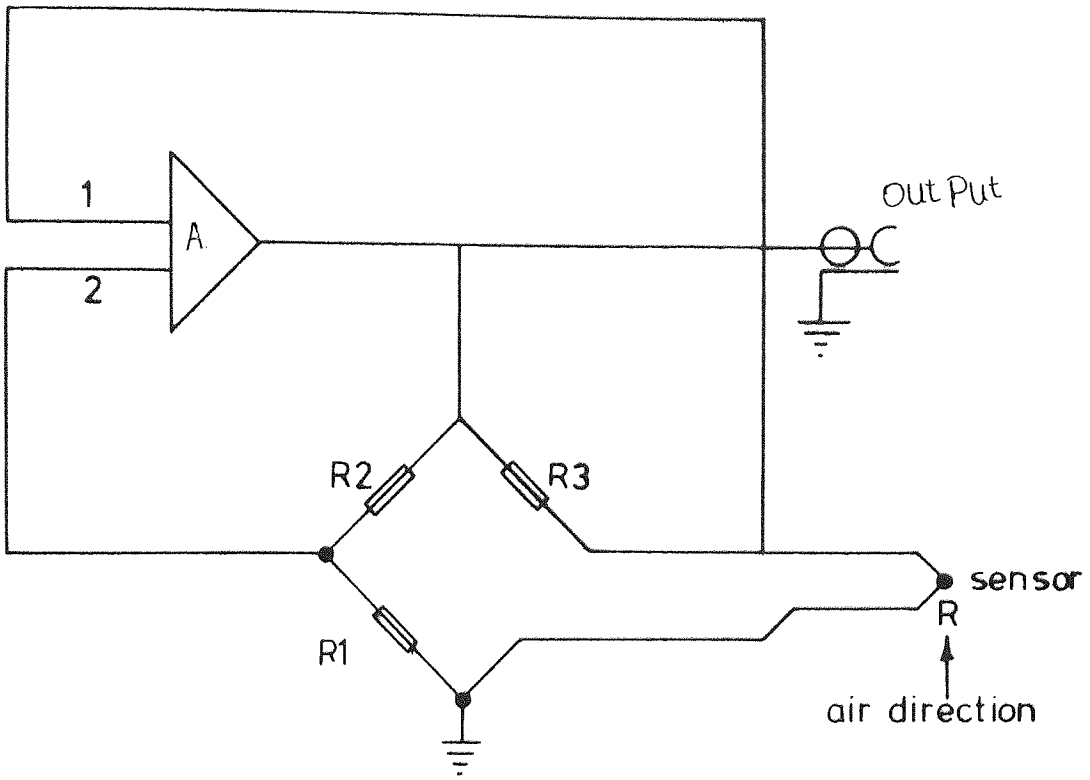

A = Amplifier

R1, R2, R3, & R are resistances

FIGURE 5.5.2 CONSTANT TEMPERATURE TYPE BRIDGE

sensor (Plate No.2 shows the physical size of the bead).

The Simon Shielded hot wire anemometer was developed at the National Physical Laboratory (Omer 1966). The anemometer operates on the hot wire principle. Impinged air tends to cool the heated wires which are heated up with a standard current of 0.5 amps, standardization being affected by operating the switch and adjusting the coarse and fine current controls, until the galvanometer gives a specified reading. The head consists of a hot wire about 3 cm. long mounted in one bore of a very small twin bore silica tube; the other bore contains the thermocouple which is used to determine the temperature of the hot wire. The silica tube protects the hot wire against deposits and ensures permanency of calibration. The standing e.m.f. of the thermocouple is backed off by the zero setting control, while the anemometer head is covered. The output from the thermocouple is read on the 15 cm. scale length of the reflecting galvanometer. The relationship between air speed and the galvanometer reading is non-linear, hence direct readings are not possible, but calibration figures are provided by manufacturers, enabling the air speed to be determined from any scale readings (see Appendix 5.1).

(ii) General limitation of direct measuring velocity meters. Each direct measuring velocity meter has certain characteristics which limit its accuracy. These are:

(a) the short length and compression of the scale in certain ranges which reduces the precision of the reading.

(b) The fluctuation of the pointer during a velocity measurement, limits the certainty of the exact point to be read.

(iii) Measurement accuracy. Any measurement depends on a number of factors. These are:

(a) the accuracy of instrument

(b) the ability of the observer to record that he sees on the instrument

(c) the actual fluctuations of the air flow

The user of the instrument has very little control over the accuracy of the instrument. The general procedure is to accept the manufacturer's estimate or arrange for calibration by a specialist. For the instruments used, a detailed factory calibration chart and data as well as the laboratory calibration were applied (Appendix 5.1).

5.2.4 Comparison of Devices for measuring air flow, and their choice.

In Table 5.1 are given the principle characteristics of some of the devices used for the measurement of airflow. It can be seen from the table that both the standard pitot and special tubes have accuracies dependent on the sensitivity of the manometer used.

Considering the requirements and limitations of research facilities, the preferred methods of measurement are:

(i) Pressure tubes i.e. pitot static tube and averaging pressure tube in conjunction with inclined manometers and MDC micromanometer. A single horizontally traversed averaging pressure tube was fixed at the middle of the test section of the wind tunnel.

(ii) Direct velocity measuring instruments i.e. AVM Thermistor air velocity meters, Simmon Shielded hot wire anemometer type 5115F and velometer.

The considerations given to the choice of these instruments was that a conventional and practically accurate instrument should be employed in the laboratory test so that industrial usage may be followed. Therefore, any systematic errors arising will be comparable with those arising in normal use and the accuracy of results is directly appicable.

The instruments are all calibrated, the detail of the

TABLE 5.1 Comparison of some of the air velocity measuring instruments and air flow pattern study technique.

(1) Device	(2) Method of Use	(3) Range of air velocities or volumes which can be measured	(4) Calculations based on	(5) Accuracy obtainable	(6) Skill Required	(7) Reference
1 Pitot tube	Used for measuring velocity pressure in ducts pointed against direction of air flow.	200 feet per minute. Upper limit not determined.	Formula $V=4.043\sqrt{VP(\text{m m } H_2O)}$ m/sec (or V (fpm) = $4009\sqrt{VP(\text{inch WG})}$)	Depends on sensitivity of the manometer used.	Some. Location of tube is important.	Owen (1966) Dalla Valle (1935)
2* Special simple tube	Used for measuring point velocities and velocity of air in ducts. Requires special mounting.	100 feet per minute. Upper limit not determined.	Formula or curve. Device requires calculation against a standard pitot.	Depends on sensitivity of the manometer used.	Considerable. The device is sensitive to direction of flow and requires careful mounting.	Dalla Valle (1932)
3* Venturi	Fixed convergent and di vergent tubes forming part of the duct system	Can be built to handle any volume of air flow	Formula $Q = \frac{21.2\, d_A^2 \sqrt{h}}{\left(\frac{d_A^4}{d_B^4} - 1\right)^{\frac{1}{2}}}$ d_A = diameter of main (inches) d_B = diameter of throat (ins.)	Device is very accurate for volume determination (0.5 - 5 percent error)	No skill required. Manometer scale can be made to read volume directly.	BS (1042)

CONTINUED.....

TABLE 5.1 CONTINUED(1)

Averaging pressure tube	Used for measuring the average total pressure across the cross section of air flow.	No specific ranges	$\bar{V} = \sqrt{\frac{2g}{\rho}}\sqrt{\frac{\sum_{i=1}^{n} VPj}{n}}$ where: $\bar{V}$ mean velocity of air flow, velocity pressure at discrete interval distance across the duct.	Depends on sensitivity of the manometer used. The accuracy of better than ±6.5 percent for air velocities from 3 to 7 mm/sec is reported.	Virtually none.	Y.L. William (1966)
Hotwire anemometer	Used for measuring the velocity of fluid.	different but not very high	Not a direct way of convertion exists.	Depends on the sensitivity of incorporated auxiliary equipment.	Some.	1. Dryde H.L. and Keautbe A.M. (1929) 2. N.A.S.A. (1929)
Hot film sensor	Used for measuring the velocity of fluid medium	Output is non linear, therefore it is possible to make the measurement over a wide range of flow velocities. ie. few feet per minute up to supersonic velocity.	The output is non linear. A linearizer can be employed.	Depends on sensitivity of additional instruments	Considerable.	1. P. Freymuth (1968) 2. L. King (1914) 3. D. Collins & M. Williams (1957)
7* Laser Doppler anemometer	Used for measuring the velocity of fluid medium.	0 up to supersonic velocities.	$\Delta\nu = (ks - ko)\, v$ where v is the velocity of the scatterer $ko = 2\pi/\lambda$, λ is the wavelength of the incident radiation. ko is the scattered wave vector $\Delta\nu$ is the doppler shift.	Depends on the sensitivity of auxiliary equipment or infra-red analyser	Considerable.	J.A. Abbiss, T.W. Chubb and E.R. Pike (1974)
8* Tracing technique	Used to evaluate air flow patterns.	Any volume of air flow. An air change of every ten minutes of a room of 7000 cubic feet has been reported.	Evaluation of aerosol concentration and deposition of aerosol particles.	Depends on chromatograph and flame photometer.	Considerable.	1. David A. Frazer (1965) 2. J. Higgins & S.E.H. Shuttleworth (1958) 3. L.F. Daws (1970) 4. L.F. Daws & A.D. Penwarden (1965)
9* Ionization Anemometer	Used for the measurement of air movement. Instrument is omni-directional or uni-directional.	Region 0 to 300 ft/min.	The transport of ions in air can easily be measured in terms of an electric current and the effect of air movement upon the transport measured as a change in value of that current. Mobility of ion in air are dependent upon	The instrument is rapid in response and equally sensitive over the whole range of velocities covered.	Considerable. Air movement across the parallel plate cage prevents some of the ions from reaching the collecting electrode.	J.E. Lovelock and E.M. Wasilewska (1945) W.L. Welman and J.E. Lovelock (1955).

CONTINUED.....

TABLE 5.1 CONTINUED(2)

			the temperature, pressure and relative humidity of the air			
Shielded hot-wire anemometer	Used for the measurement of air movement	Three ranges: 0 to 0.4 ft/sec 0 to 2 ft/sec and 0 to 5 ft/sec (0 to 1.5 m/sec)	The relationship between the air speed and the galvanometer reading is non-linear, hence direct reading is not possible, but calibration figures are available enabling the air speed to be determined.	Instrument is rapid in response and equally sensitive over the whole range of velocities covered. Sensitivity is ample, the maximum speed in each range being measureable with an error of less than 0.5 percent.	Some. Hot wire should be vertical when measurements are taken.	E. Owen and R.C. Parkhurst (1966)
Thermistor AVM 501F and AVM 502	Used for the measurement of fluid movement.	0 to 10 ms^{-1} 0 to 30 m/sec 0 to 0.5 m/sec 0 to 5 m/sec	Direct dial reading and calibration line is provided for each instrument.	Depends on ambient radiation temperature. Overall accuracy is 15% of reading or $Vt \pm 0.03\ V_m$ where: Vm measured velocity Vt = Vm (1+0.01(T-20.0)) Vt is true velocity.	None.	Manufacturer Instruction booklet 1976
Smoke	Used for observation of air flow pattern.	Any	Visual observation of air movement.		None.	
Heated Thermometer anemometer *	Used for measuring the mean air movement velocity over the the area accompanied by the heated thermometer bulb.	10 to any velocities provided an adequate voltage is applied to the heating elements.	$\frac{\text{Net milliwatts}}{th - ta} = ko + ki\sqrt{V}$ Where: th = heated temperature ta = ambient air ko, ki = instrument constant V = air velocity fpm net milliwatts = electrical heat input to the bulb alone. or velocity should be read from table or chart corresponding to temperature difference = th-ta	For velocity less than 100 ft/m no correction required For high velocities a correction of 30% required for stem correction. In laboratory a sensitivity of 2% is obtainable in all velocities by using precision voltmeter and thermometer. -	Some. Positioning and distance from the reference thermometer.	1. P. Yaglou (1938) 2. L. Silverman (1941, 1942)

* This instrument was not employed in this research.

calibration is given by Appendix 5.1.

5.3 Calibration of Wind Tunnel Assemblies.

5.3.1 Introduction.

The purpose of this calibration was to study the flow conditions and flow rates in the main duct section i.e. middle duct (see Drawing No.1) for different system assemblies. The requirements are as below:

i) To use a method accurate and rapid enough to rate the airflow through a duct assembly.

ii) To find the pitch angle setting of different duct assembly for an equal suction flow rate.

iii) To find the flow conditions for a uniform steady state required for the calibration of anemometers.

Methods are discussed in previous sections.

The third requirement has been discussed previously, where it was concluded that the averaging pressure tube has distinct advantages and it was applied to fulfil the first and second requirements.

Generally, there were two types of wind tunnel assemblies:

i) All the ducts of the assemblies were of round cross section.

ii) The suction openings were of non-circular cross section.

Procedures of calibrations are as below.

5.3.2 Calibration of Wind Tunnel for Testing Round Ducts.

The first type of wind tunnel assembly under test consists of three sizes of round suction opening, with or without flat plane flanges. These ducts are assembled on to the main duct via a transition piece (Drawing No.1). Due to difference

of test duct size and length, the flow rates at the main duct section were widely different, therefore the descriptions are given separately.

(i) Smallest size and shortest length round test duct. This duct was used as a by-pass duct for the square duct as well as an individual test section. This is a duct of 152 mm. inner diameter and 1.19 metres length (Row 1, (See Drawing No 3)). This duct was attached to the main wind tunnel via the transition piece. The position of the flowmetering plane of the main duct was less than 10-diameters distant from the first change of the cross section (i.e. transition piece of enlargement section). Consequently, the flow at this measuring plane was found to be very fluctuating. Therefore, flowmetering by pitot-tube was very much affected by pulsations, hence erroneous, but flowmetering with an averaging pressure tube showed less fluctuation and was more stable than pitometry. Figures 5.6 and 5.7 are the calibration lines and pressure measurement recordings respectively for the wind tunnel assembly testing this round duct.

(ii) Middle size round test duct. This is a duct of 343 mm. internal diameter and 2.4 metres length (Row 2, (See Drawing No. 3)). Due to long length and large diameter of test duct, the flow condition at the main duct was more settled. Figures 5.8 and 5.9 show the calibration line and pressure fluctuation tracing. As it can be seen from these figures, the flow condition at the main duct was fairly laminar.

(iii) Largest size round test duct. This is a duct of 457 mm. internal diameter and 2.4 metres length (Row 3, (See Drawing No. 3)).

For a number of flow rates, as with the other test duct under test, flowmetering at the main duct section was carried

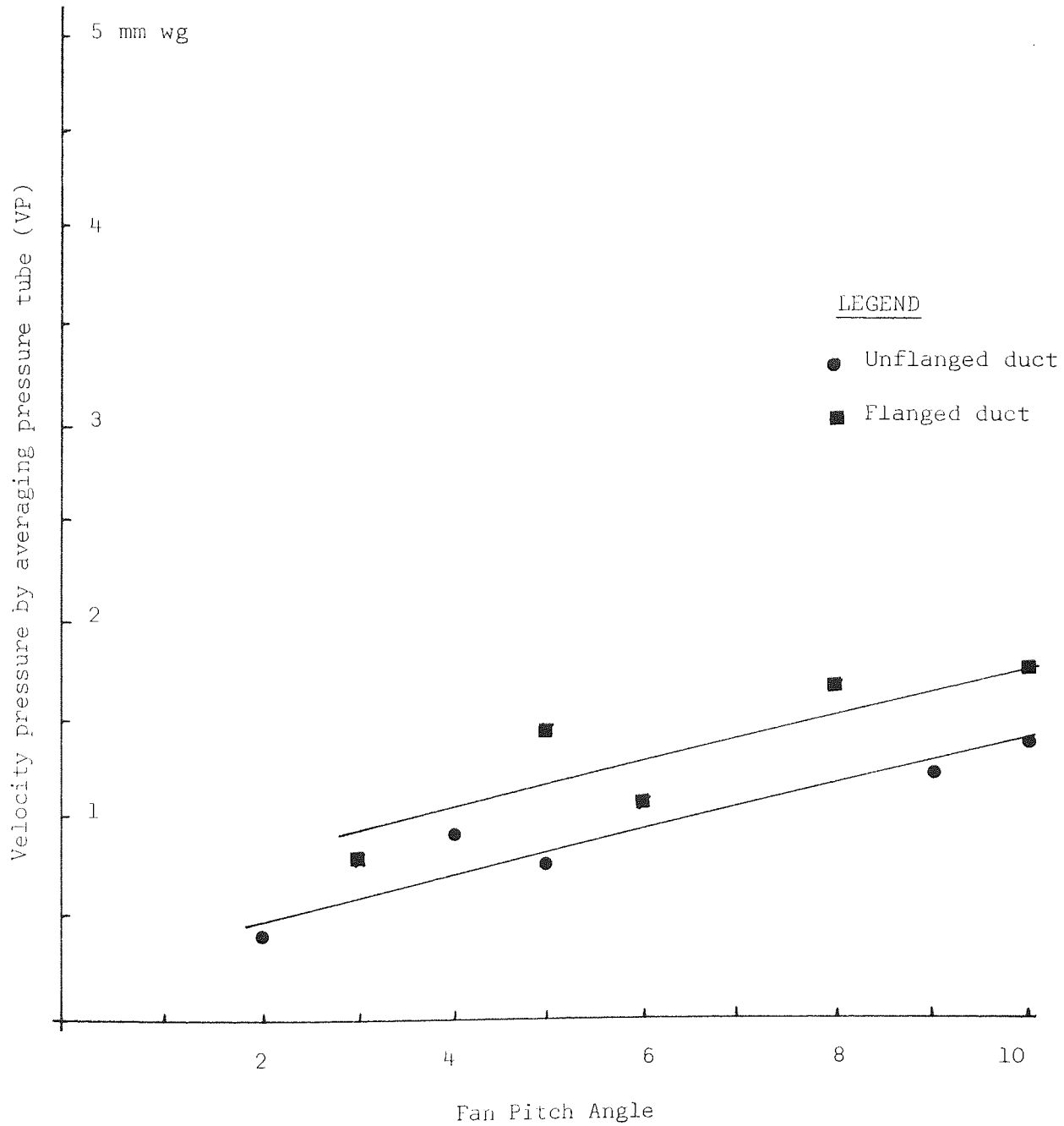

FIGURE 5.6 CALIBRATION OF WIND TUNNEL WITH ROUND DUCT ASSEMBLY (D = 152mm)

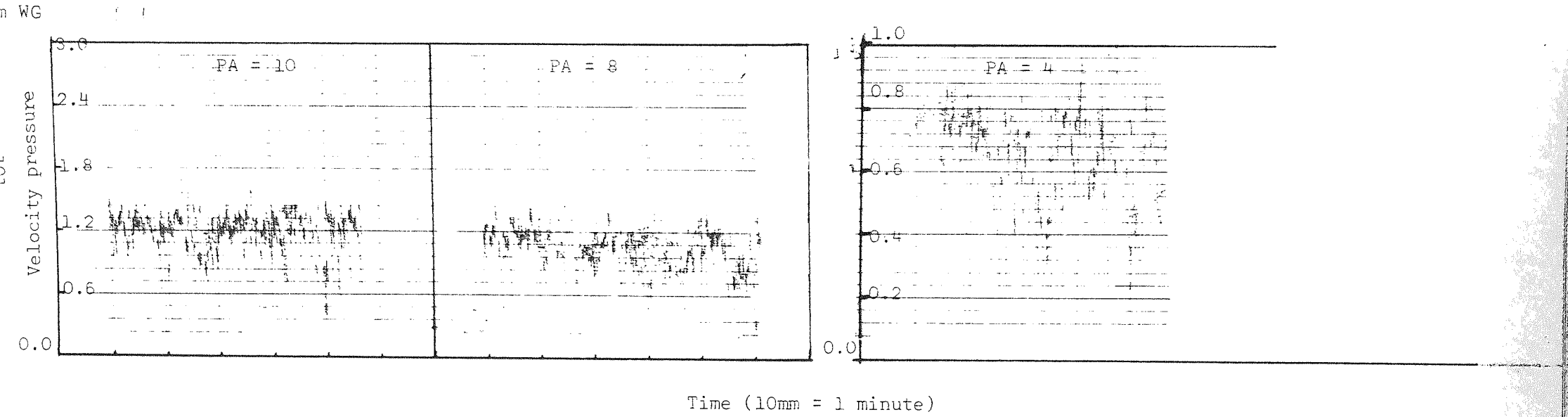

FIGURE 5.7 VELOCITY PRESSURE FLUCTUATION AT MAIN DUCT SECTION USING AVERAGING PRESSURE TUBE, TESTING ROUND DUCT (D = 152 mm, PLAIN OPENING)

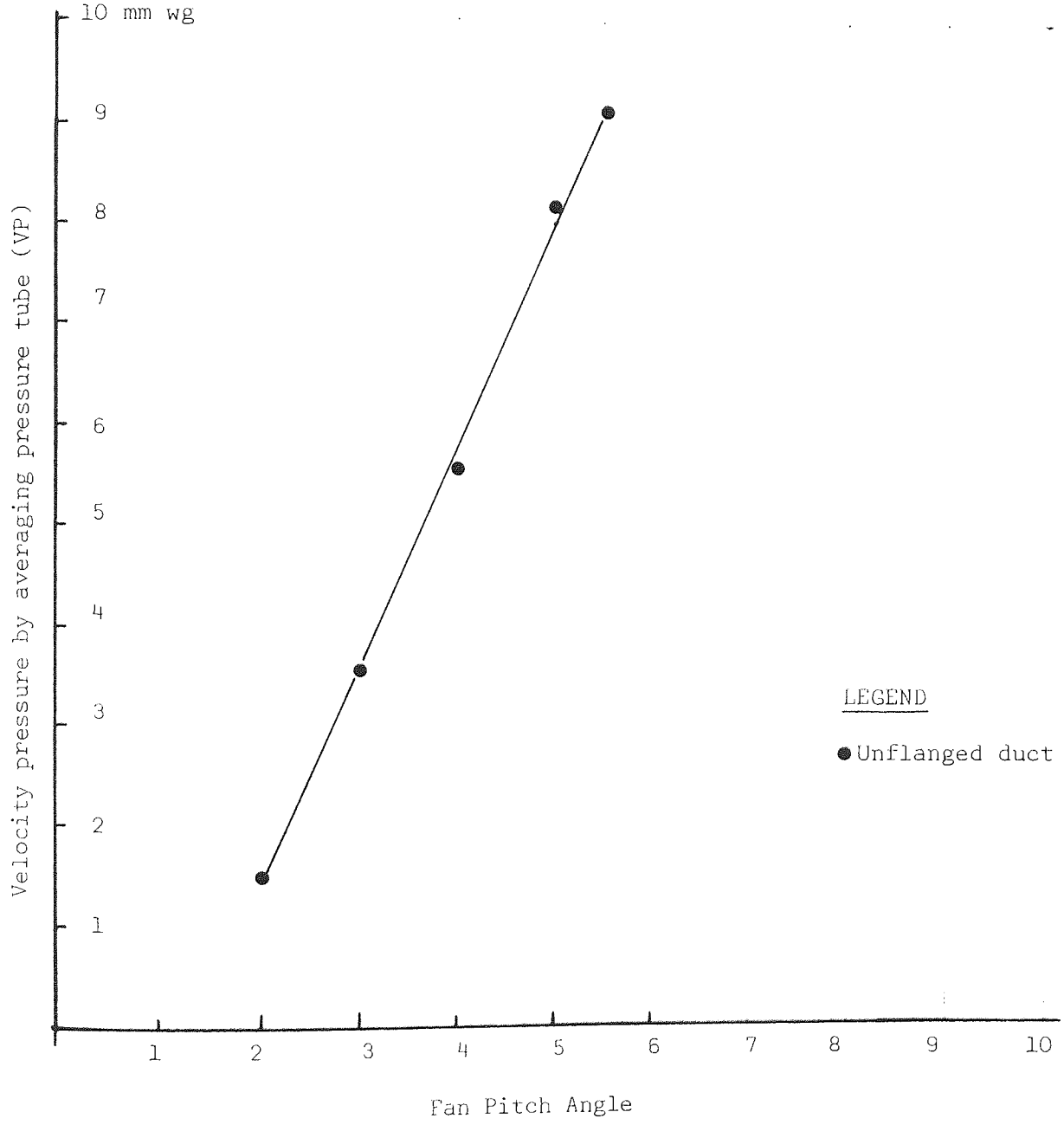

FIGURE 5.8 CALIBRATION OF WIND TUNNEL WITH ROUND DUCT ASSEMBLY (D=343 mm, PLANE OPENING)

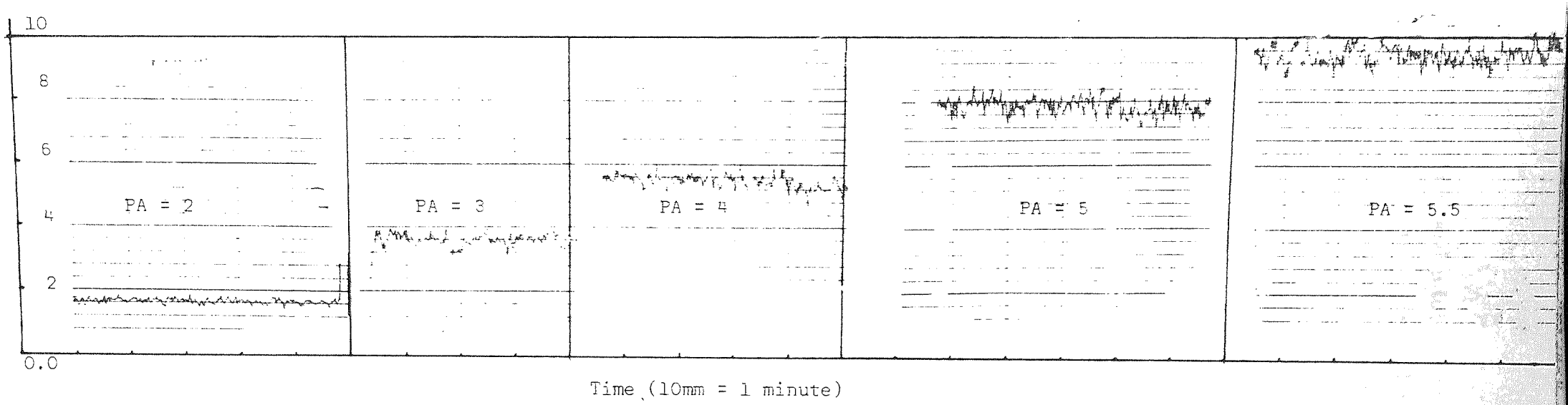

FIGURE 5.9 VELOCITY PRESSURE FLUCTUATION USING AVERAGING PRESSURE TUBE, TESTING ROUND PLAIN OPENING DUCT (D=343mm)

out by both averaging pressure tube and pitot-static tube. Figures 5.41, 5.42 and 5.43 show the calibration line and pressure recorded traces. As it can be seen from the plotted data and traces, the flow at the main test duct was very nearly laminar. Figures 5.46 5.47, 5.48, show a comparison of velocity pressure fluctuations using averaging presure tube and pitot-static tube. Fig. 5.13, shows the the velocity profile using AVM501F, which shows the state of fully developed airflow inside the main duct for the range of suction flow rates. In Figure 5.11 the high flow rate point and low static pressure readings are the outliers and it is due to the experimental errors.

5.3.3 Calibration of wind Tunnel for testing Non-circular Test Ducts.

The second type of wind tunnel assembly consisted of three different suction openings, with or without flange. These ducts were coupled to the main duct via the same transition piece as previous test duct assemblies. Description of calibrations is as follows:

(i) Testing Rectangular Ducts. There were two rectangular test ducts which required calibration (Drawing No. 3, Rec. 1 and Rec. 2). The calibrations were performed for both plane and flanged opening ducts. The pressure measurement of the main duct section was recorded. Figures 5.14 to 5.17, and 5.19 show the flow condition and calibration line at the main duct section respectively. Nonlinearity of Figure 5.19 is partly due to extent of the laminar development length (See insertion in Fig. 5.13).

For the case of Rec. 2 duct, the flow condition at the main duct section was less turbulent than in the case of the Rec. 1 duct. Also in the cases of flat flanged ducts, the flows closely resemble those for unflanged ducts (Figures 5.14 to 5.17).

(ii) Rectangular Hood. Two calibration tests were performed for this hood, one with and the other without flange. Figures 5.20 and 5.21 show the calibration line and traces of velocity pressure recording respectively. As these Figures

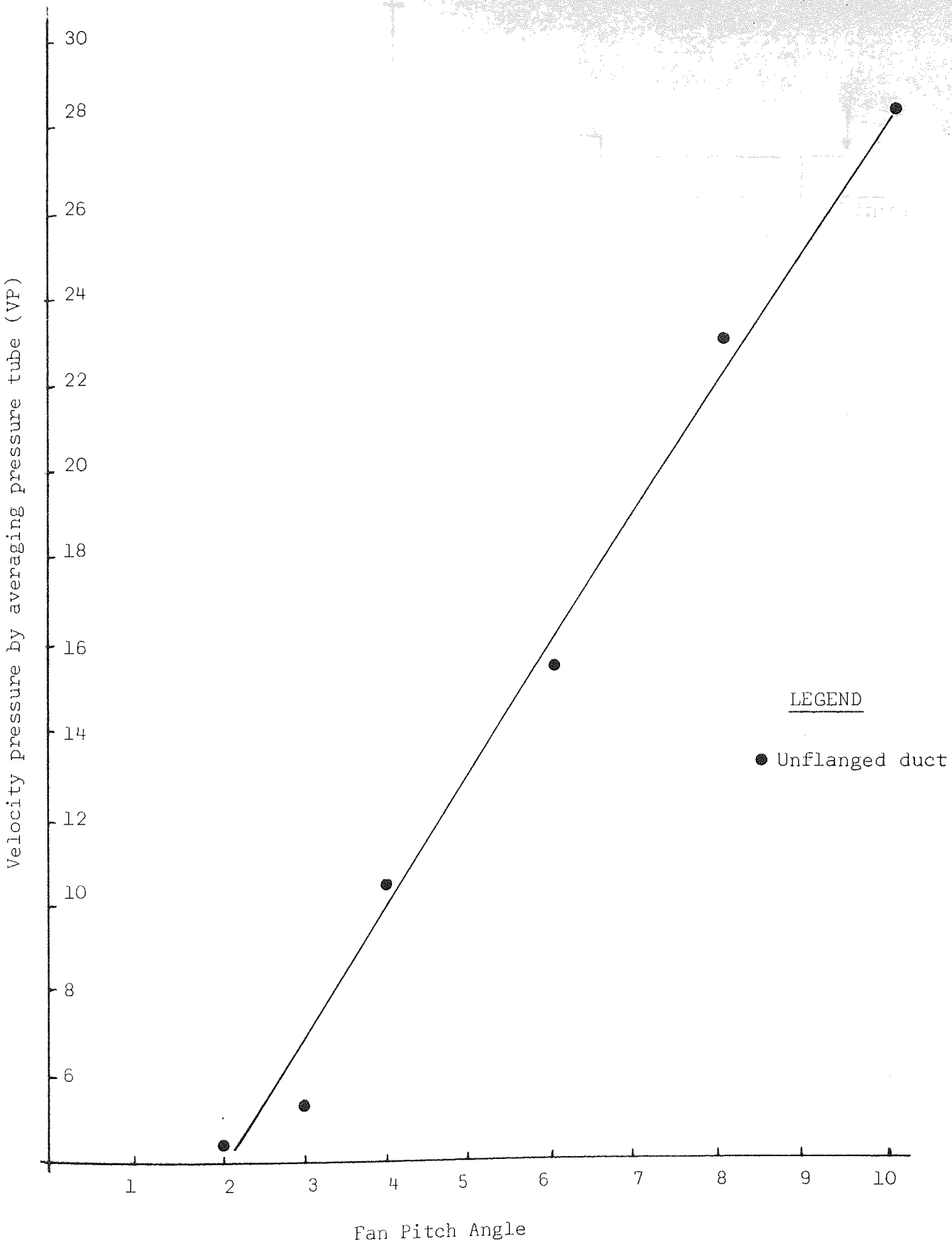

FIGURE 5.10 CALIBRATION OF WIND TUNNEL WITH ROUND DUCT ASSEMBLY (D=457 mm PLANE OPENING)

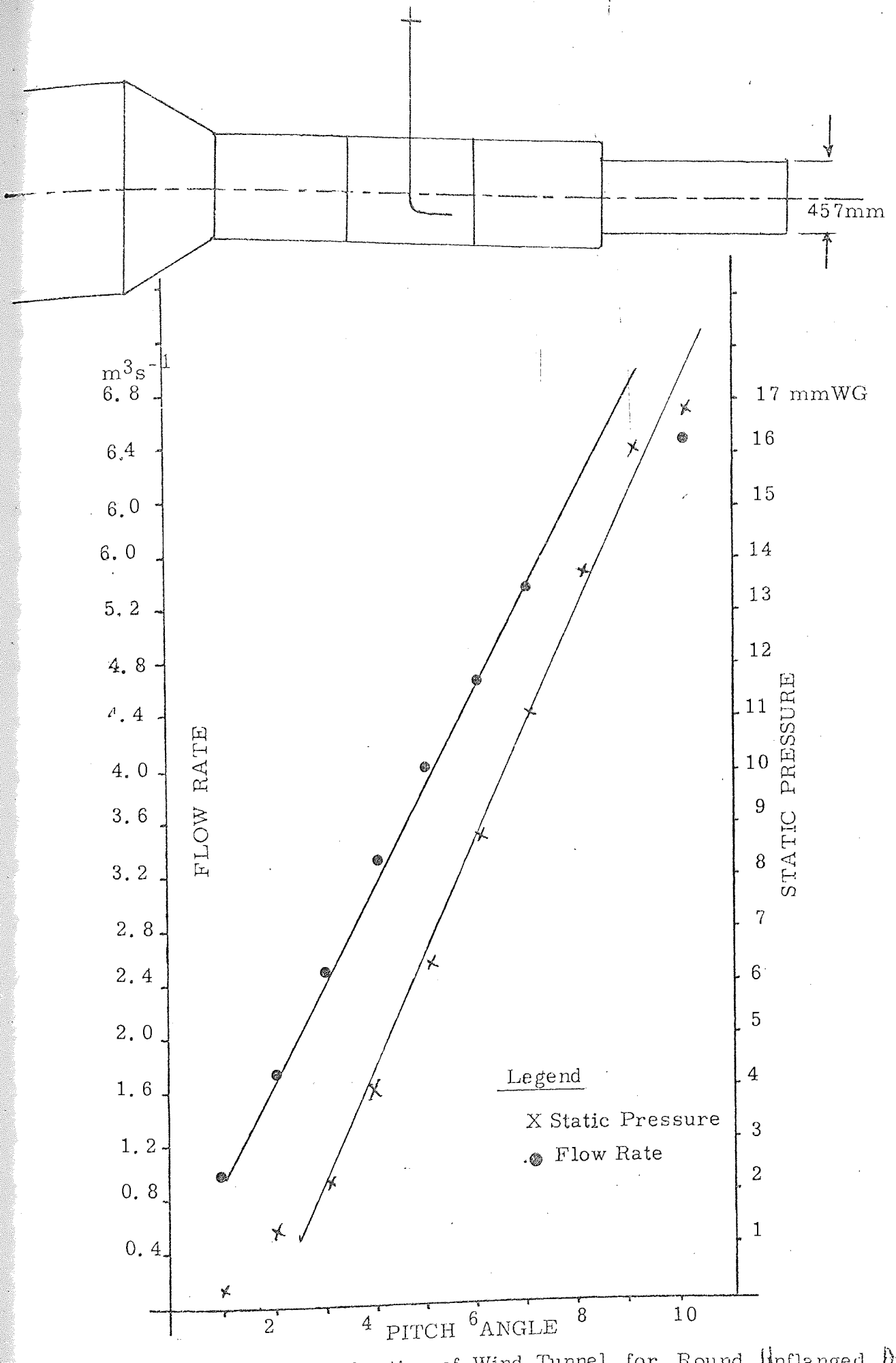

Figure 5.11 Calibration of Wind Tunnel for Round Unflanged Duct

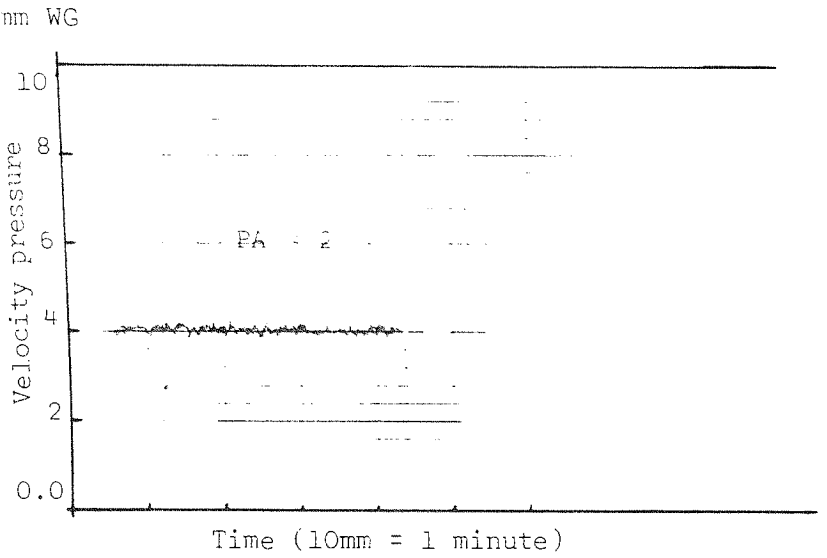

FIGURE 5.12 VELOCITY PRESSURE FLUCTUATION USING AVERAGING PRESSURE TUBE, TESTING ROUND PLAIN OPENING DUCT (D = 457 mm)

Figure 5.13 VELOCITY PROFILE IN THE MAIN DUCT BY DIRECT VELOCITY MEASUREMENT (AVM501F) IN HORIZONTAL TRAVERSE

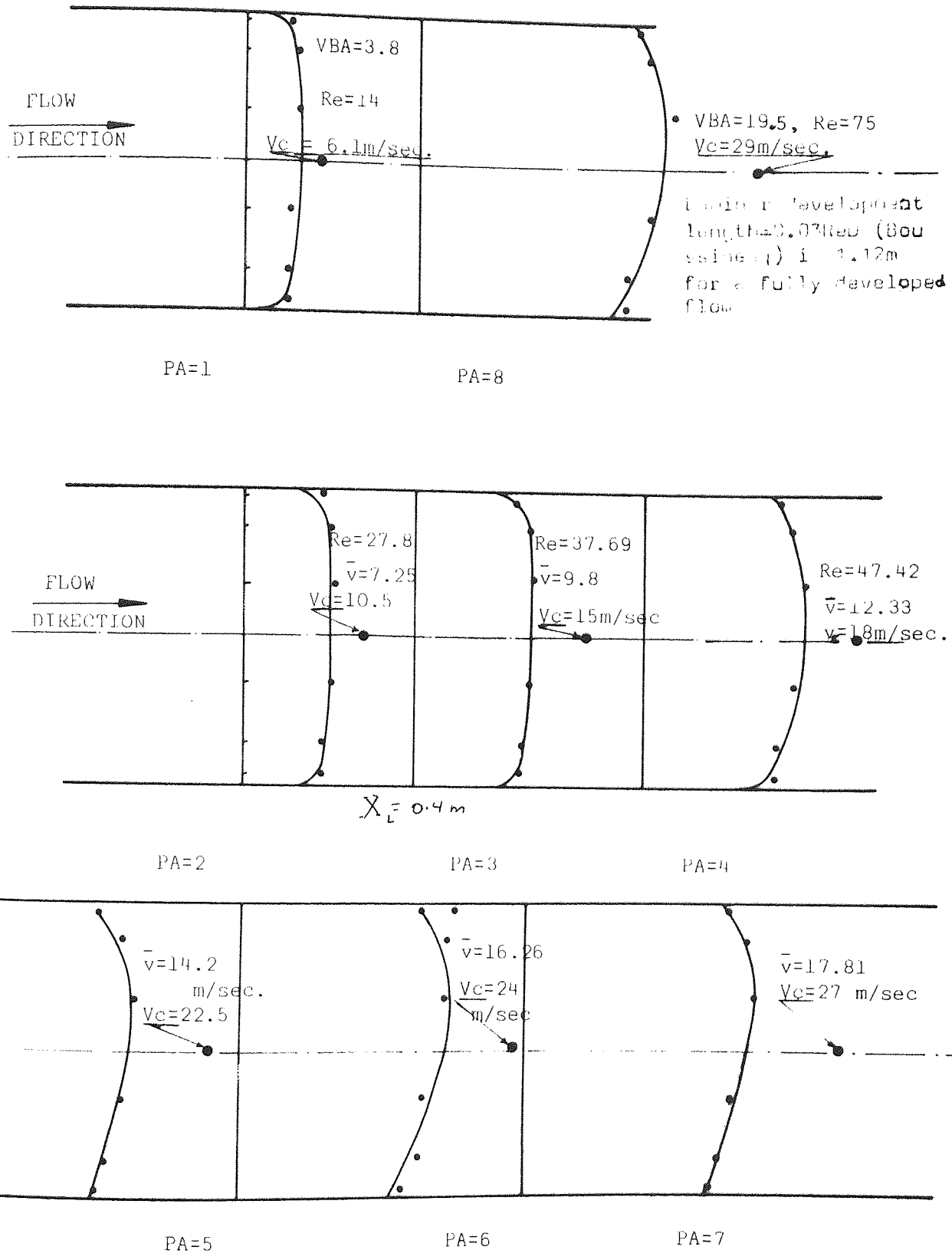

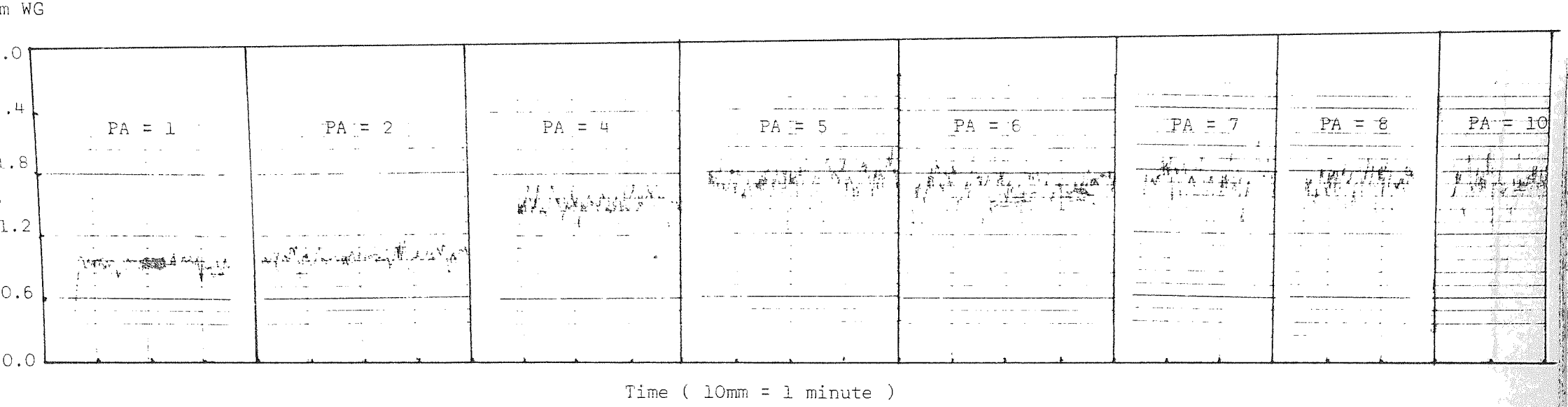

FIGURE 5.14 VELOCITY PRESSURE FLUCTUATION AT MAIN DUCT SYSTEM, TESTING RECTANGULAR DUCT (101.6mm BY 203.2mm, UNFLANGED OPENING) USING AVERAGING PRESSURE TUBE

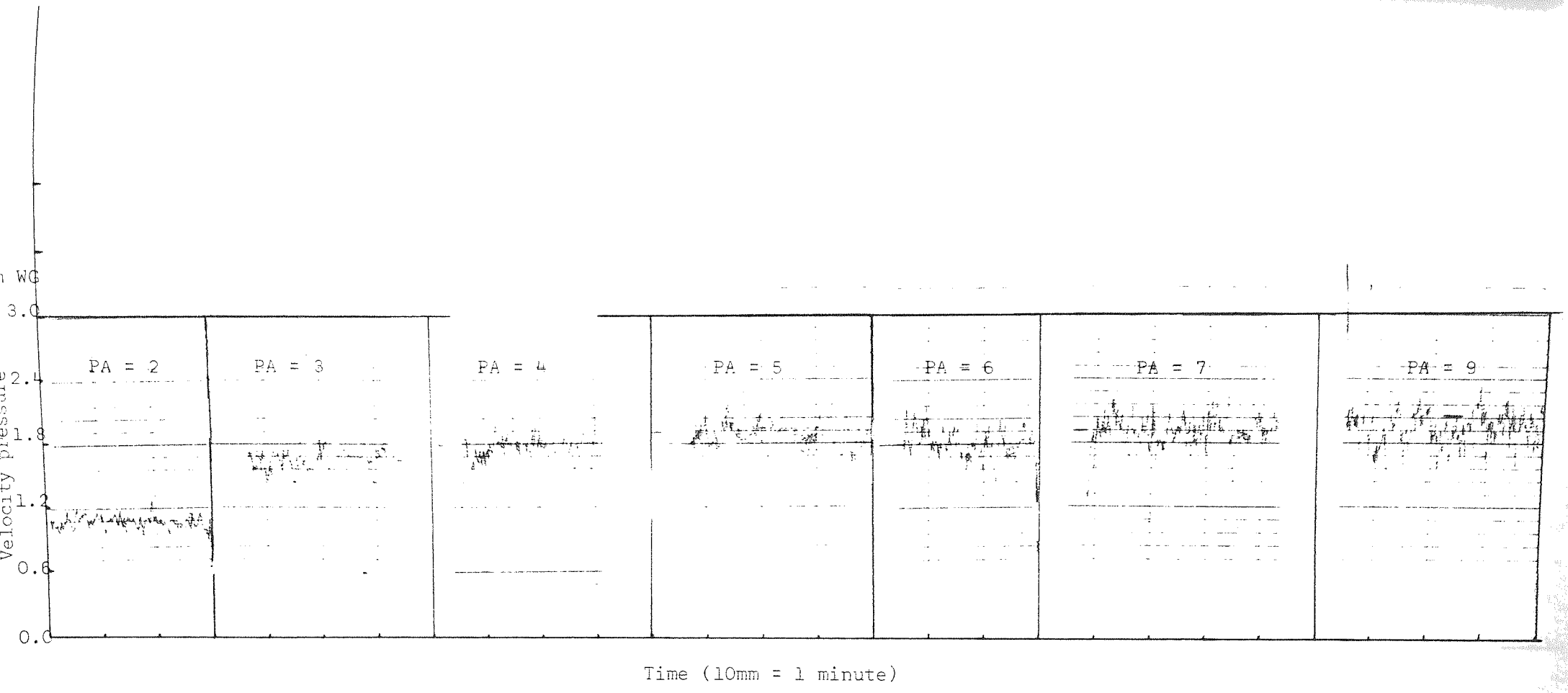

FIGURE 5.15 VELOCITY PRESSURE FLUCTUATION AT MAIN DUCT SYSTEM, TESTING RECTANGULAR DUCT (101.6mm BY 203.2mm FLANGED OPENING) USING AVERAGING PRESSURE TUBE

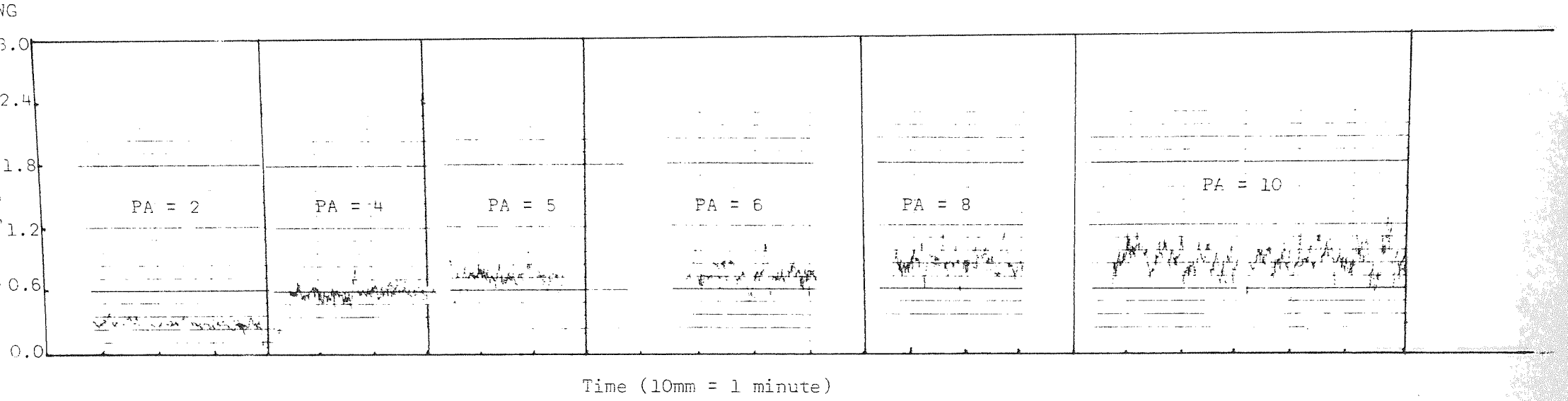

FIGURE 5·16 VELOCITY PRESSURE FLUCTUATION AT MAIN DUCT SYSTEM, TESTING RECTANGULAR DUCT (152.4mm by 2.54mm UNFLANGED OPENING) USING AVERAGING PRESSURE TUBE

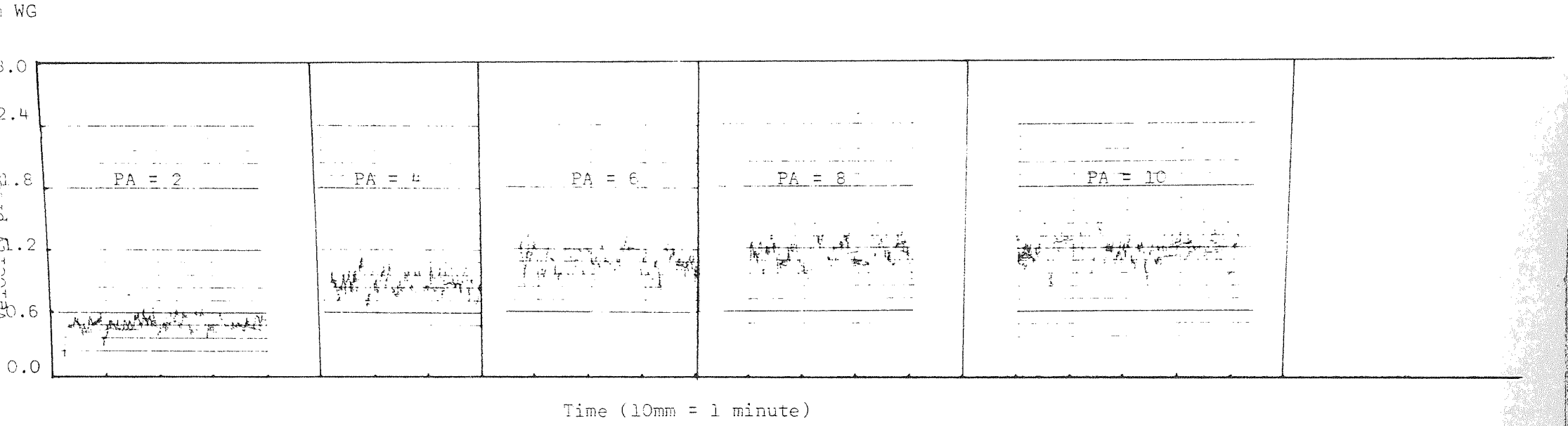

FIGURE 5.17 VELOCITY PRESSURE FLUCTUATION AT MAIN DUCT SYSTEM, TESTING RECTANGULAR DUCT (152.4mm BY 254.0mm FLANGED OPENING) USING AVERAGING PRESSURE TUBE

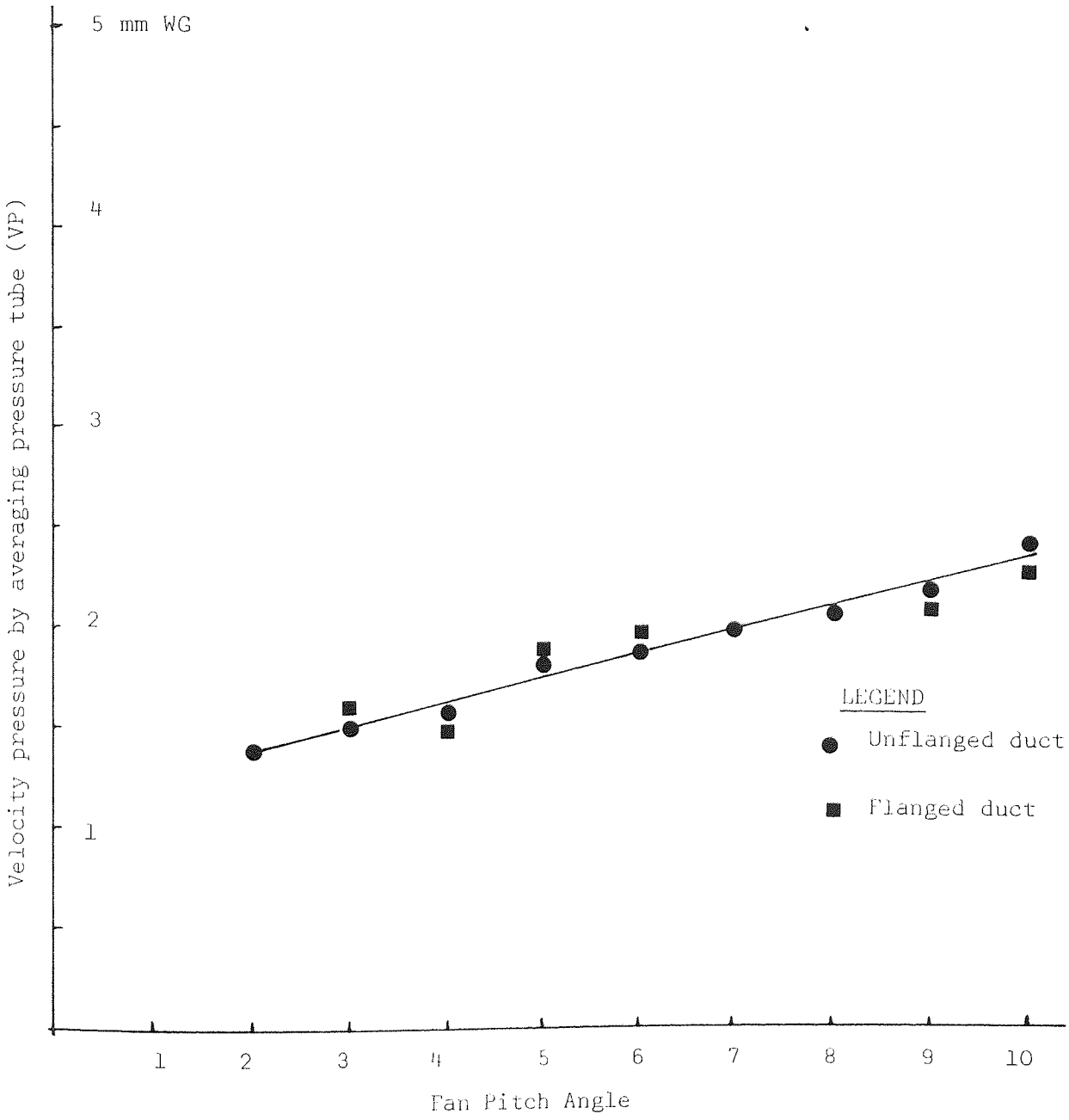

FIGURE 5.18 CALIBRATION OF WIND TUNNEL WITH RECTANGULAR DUCT ASSEMBLY

(101.6 mm by 203.2 mm)

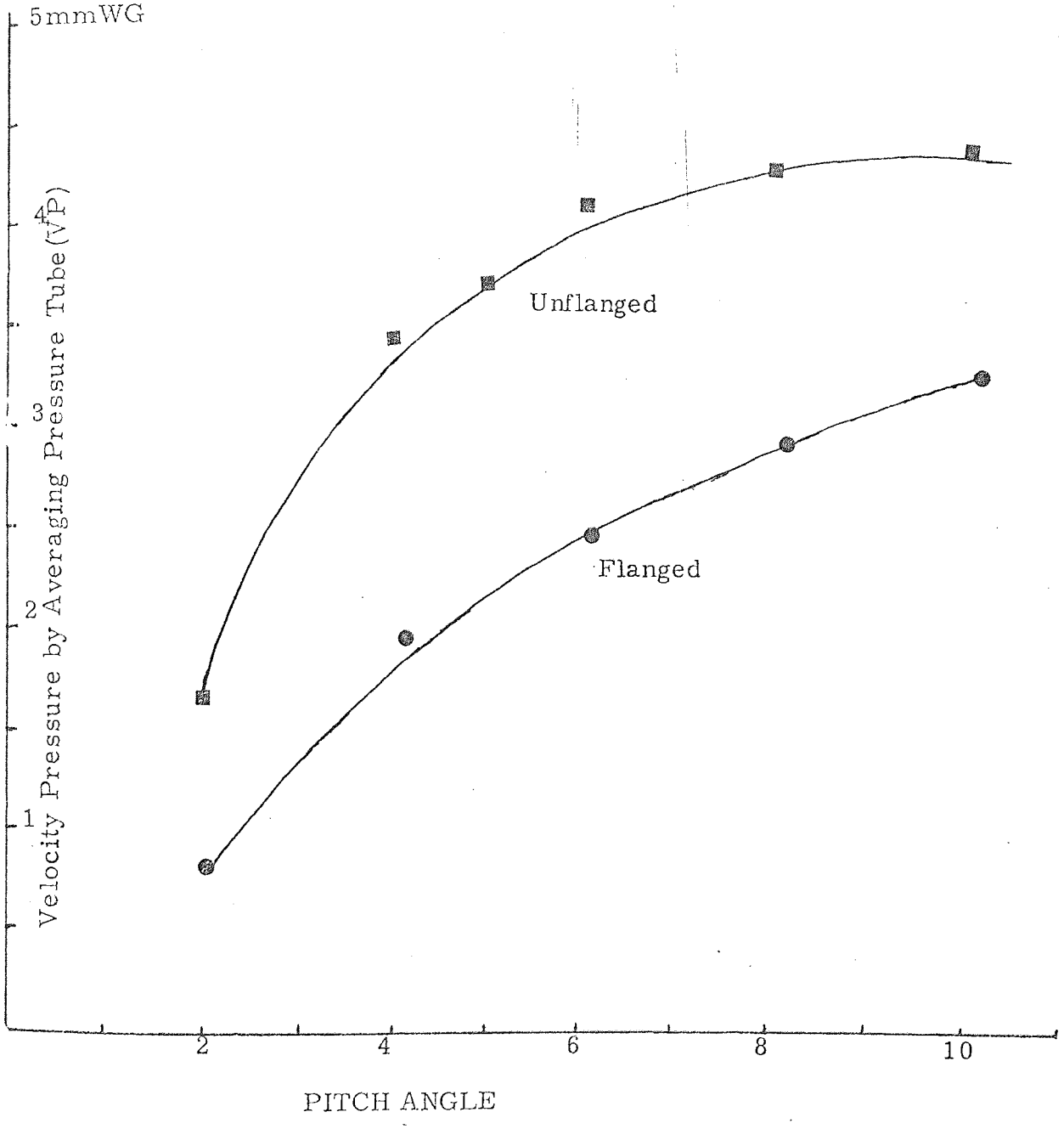

Figure 5.19 Calibration of Wind Tunnel With Rectangular Duct Assembly

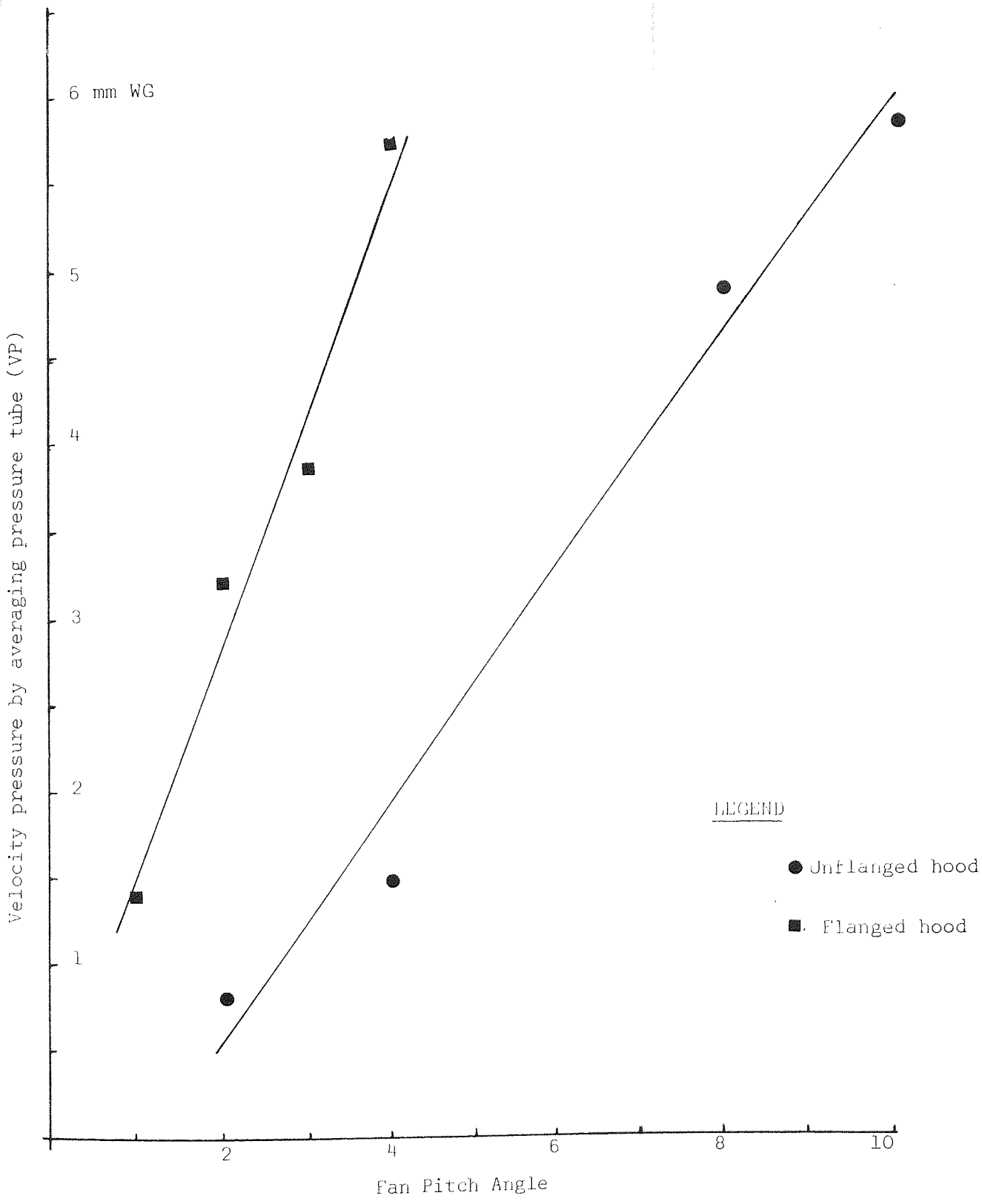

FIGURE 5.20 CALIBRATION OF WIND TUNNEL WITH RECTANGULAR DUCT ASSEMBLY (250 mm BY 1145 mm)

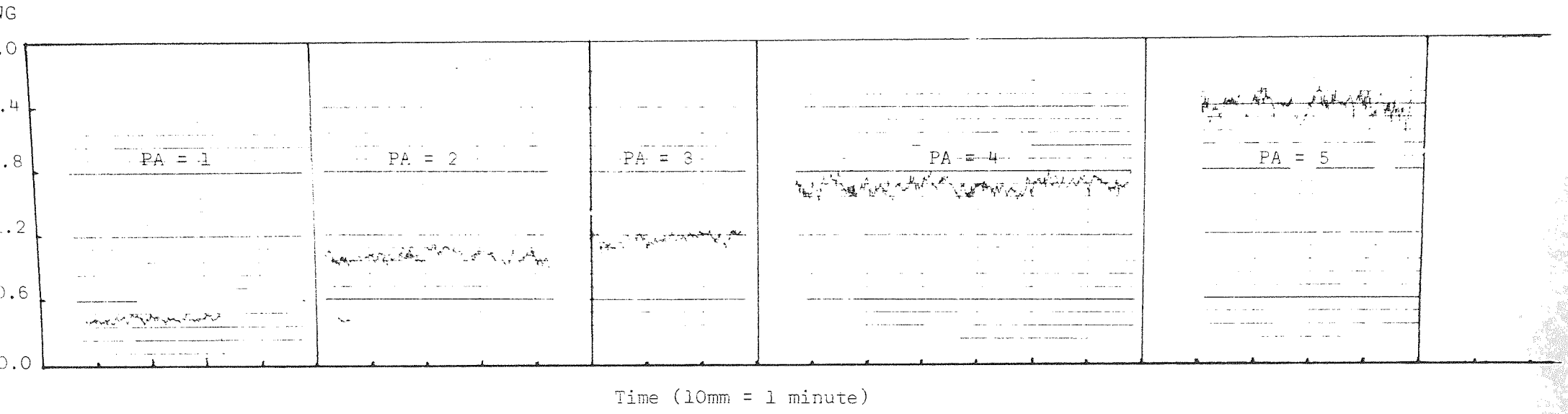

FIGURE 5.21 VELOCITY PRESSURE FLUCTUATION AT MAIN DUCT SYSTEM, TESTING RECTANGULAR HOOD (250mm BY 1145mm FLANGED OPENING) USING AVERAGING PRESSURE TUBE

show the flows are not very turbulent. Although the fluctuation for low flow rate is less, its intensity is not greater than the case for rectangular ducts (see Figures 5.18 to 5.21).

(iii) Square Hood. The square hood was designed for use in calibrating air velocity measuring devices. It is flanged and the flange is shaped elliptically to preserve the streamlines of the air flow. The flanged opening area is 0.7821 m^2. The square section has an area of 0.28622 m^2. Drawing (2) shows the design details.

Testing consists of the study of the velocity profile across the square duct, flow rate measurement for each known pitch angle setting of the fan, symmetry study at the suction zone, and finally visualization and observation of streamlines of air flow.

The pitot-tube anemometry was set in British Standard (BS 848: Part 1 1963) and was the method used to obtain the average velocity at the centre cross-section of the stream (Drawing No.2). Velocity pressure and static pressure respectively were determined by placing the standard pitot-static tube at the location shown by Figures 5.26,5.27 and Drawing No.3.

For each flow rate (or fan pitch angle setting) a total number of 48-velocity pressure readings plus 48-static pressure readings were recorded. Then velocity was computed from the formula. The average velocity for this cross-section of the stream was obtained from the arithmetical average of the point velocities, and then the volume flow as obtained by multiplying the area of the airway by the average velocity. This procedure was continued for ten different pitch angles. Figure 5.28 shows the plot of the flowrate (shown by · and +) computed from V_c and V_{BAR} respectively and SP (shown by X) for each system set up.

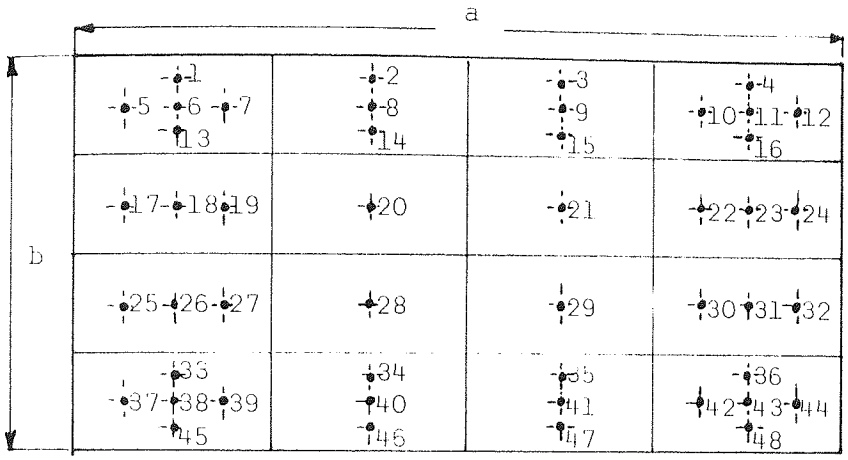

Position in rectangular airways for pitot measurement

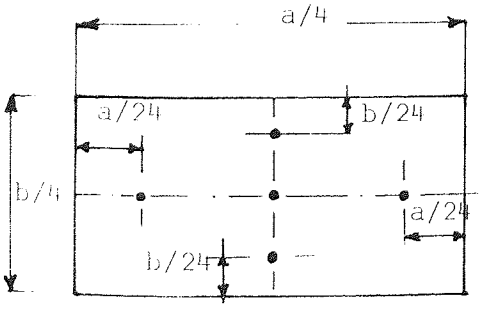

Arrangement of pitot tube positions for each corner panel of the airway.

FIGURE 5.22 BRITISH STANDARD METHOD FOR AIRFLOW TESTING IN RECTANGULAR AIRWAY

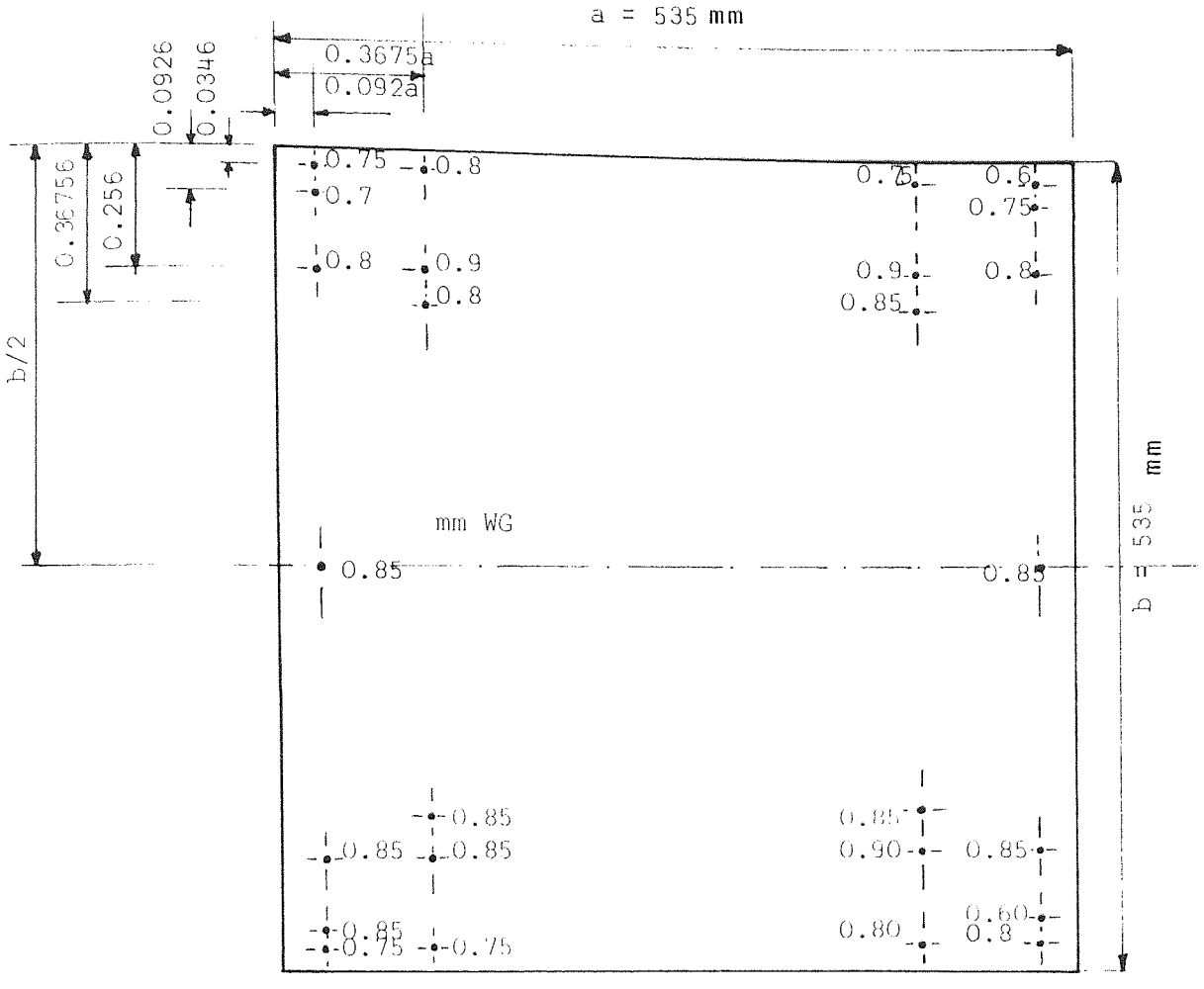

PA = 10

Q = 1.016 $m^3 s^{-1}$

$\bar{V}$ = 3.616 ms^{-1}

FIGURE 5.23 POINT VELOCITY PRESSURE READING BY 26-POINT MEASURING METHOD (HORIZONTAL TRAVERSE PITOMETRY)

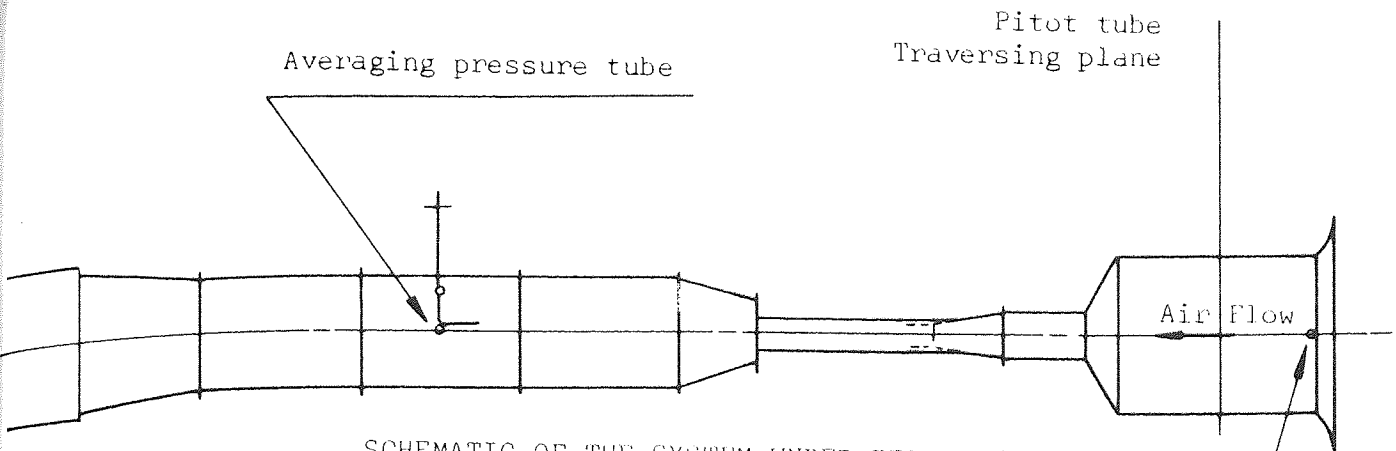

SCHEMATIC OF THE SYSTEM UNDER TEST

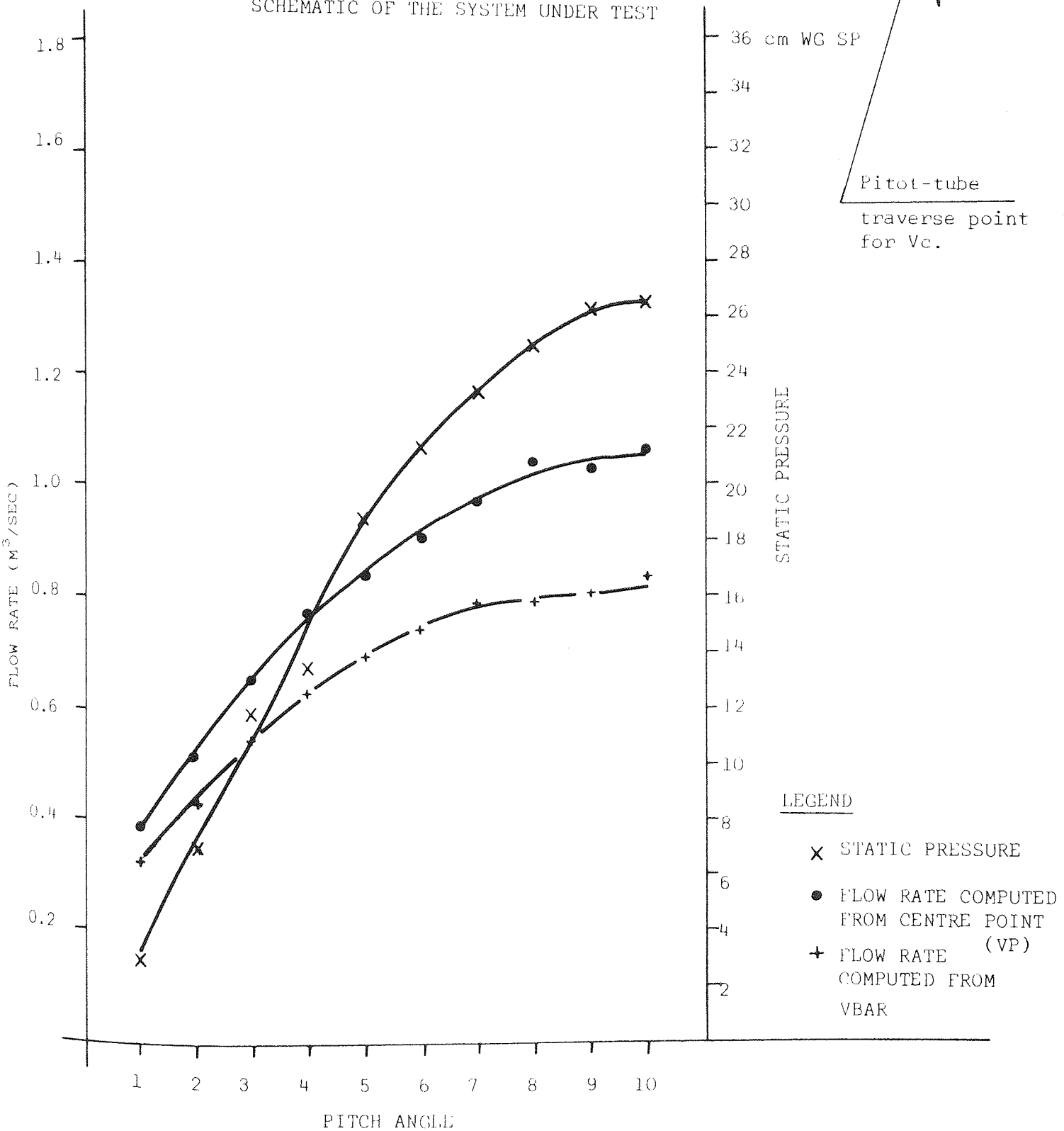

FIGURE 5.24 CALIBRATION OF WIND TUNNEL FOR SQUARE BELL MOUTH HOOD UNDER

5.3.4 Discussions and conclusions.

The following points may be drawn from the wind tunnel calibration.

i) The velocity at the centre region is fairly uniformly distributed. This means that the velocity at points 20,21,28 and 29 (see Fig.5.22) at the cross section deviated by up to a maximum of 0.167 m s^{-1} which is within the accuracy range of log-linear pitot-static tube anemometry (i.e.2%, Owen et al. 1966). The case was better with a 26-points method (see Fig.5.23).

ii) Because the square duct is not absolutely geometrically symmetric i.e. at the corner as well as the throat area, the distribution of the velocity at each symmetry point of the diagram is not always the same. However, for quite a number of locations, velocities were virtually the same.

iii) The centre line velocity computed from the centre point velocity pressure readings, with a pitot-static tube, was compared with the average velocity calculated from 48-points reading. The ratio of centre velocity (V_c) to average velocity (V_{BAR}) has an average of 0.87545 (duct coefficient). Ignoring the unreliable values corresponding to low pitch angles, the average will be 0.896 which can be taken as a good ratio between the centre velocity and the average velocity for the whole range of flow rates for a square flanged hood (Fig.5.25).

iv) For the study of the effects of equal flow rates through different suction systems one has to set the two systems to an equal suction flow rate. To do this a simple and accurate method is required. For the reasons stated on averaging pressure tubes (§5.1.3(ii)), this method has

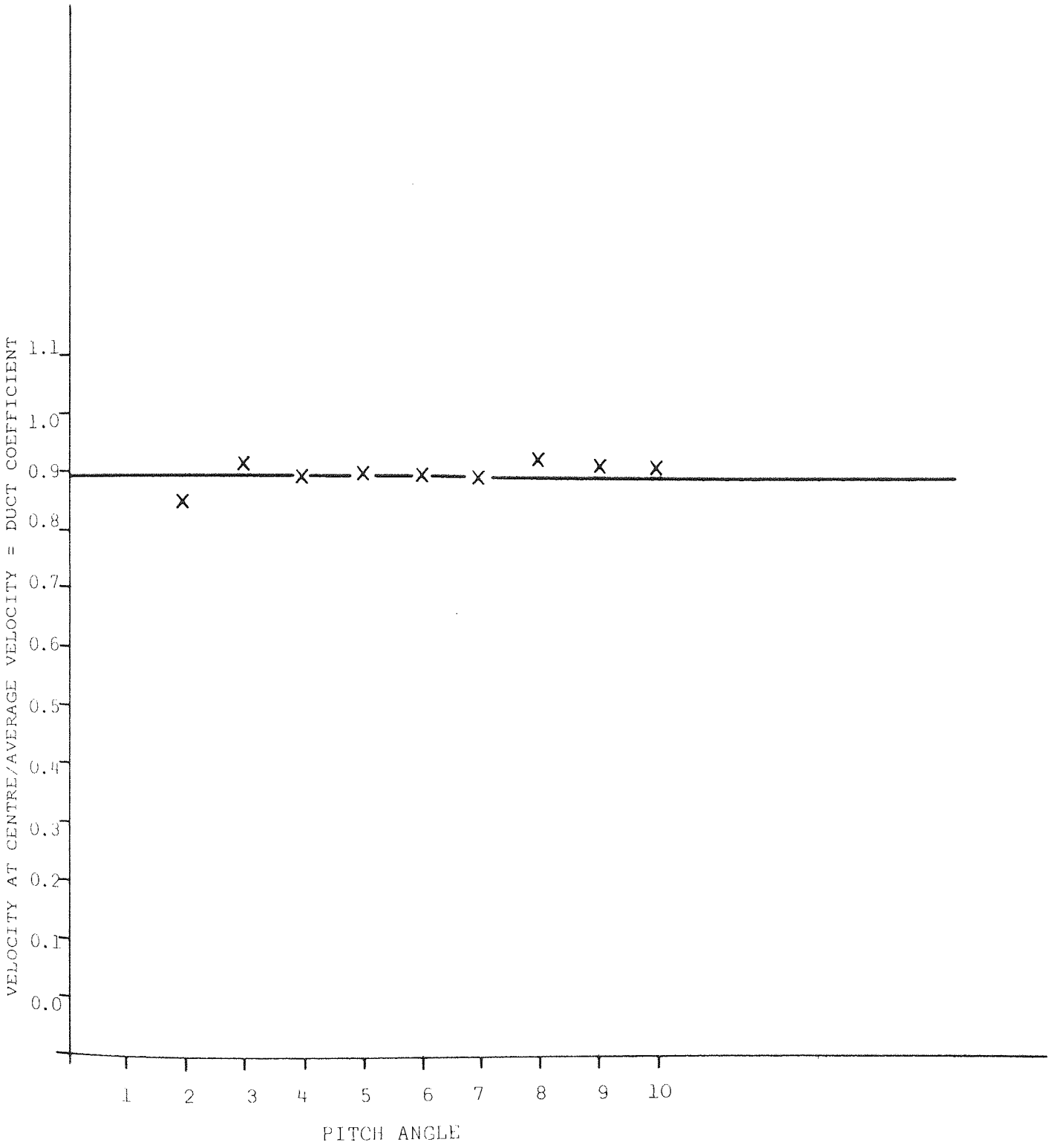

Figure 5.25 RATIO BETWEEN VELOCITY AT THE CENTRE OF HOOD TO THE AVERAGE VELOCITY VERSUS EACH DIFFERENT FLOW RATE SETTINGS.

iv) contd.

been chosen. Velocities obtained with averaging pressure tube in conjunction with the pitot-tube for the static pressure readings (or 3-wall static port connected to a single tube) are related to the average velocities obtained by pitot-static anemometry (see Figures for calibrations of wind tunnel). Figures 5.26, 5.27 and 5.28 show the calibration lines and velocity pressure tracing respectively, when testing the square hood (see also schematic in Fig.5.24). Fig.5.25 shows the duct coefficient for the whole range of the operation capacity of the fan.

Therefore, if one wishes to study the effect of a known volume flow rate (e.g. 0.9 m^3/s^{-1}) on the velocity distribution at the suction zone to compare with other openings, the first step is to find the corresponding velocity pressure by averaging pressure tube combinations (i.e. 1.5 mm.WG), then from the wind tunnel calibration lines find the corresponding fan pitch angle. Finally, by adjusting the pitch angle setting and observing the pressure reading gauge approaching this value. Checking for the equilibrium and stable condition, is the final step of the suction flow rate setting. With one or two more pressure readings, by switching the fan on and off, if the readings are the same, this means that the whole system is set up to the required conditions (i.e. 0.9 m^3s^{-1}).

5.4 Recirculation Air Velocity

5.4.1 Introduction

As previously mentioned (research facilities section), the wind tunnel room is a closed chamber. The air drawn in, passes over the filtration section and through the system over the motor through the silencers, and is finally discharged into the room. This recirculation caused some directly opposite movement to the suction air flow. To slow down this disturbance airflow, two

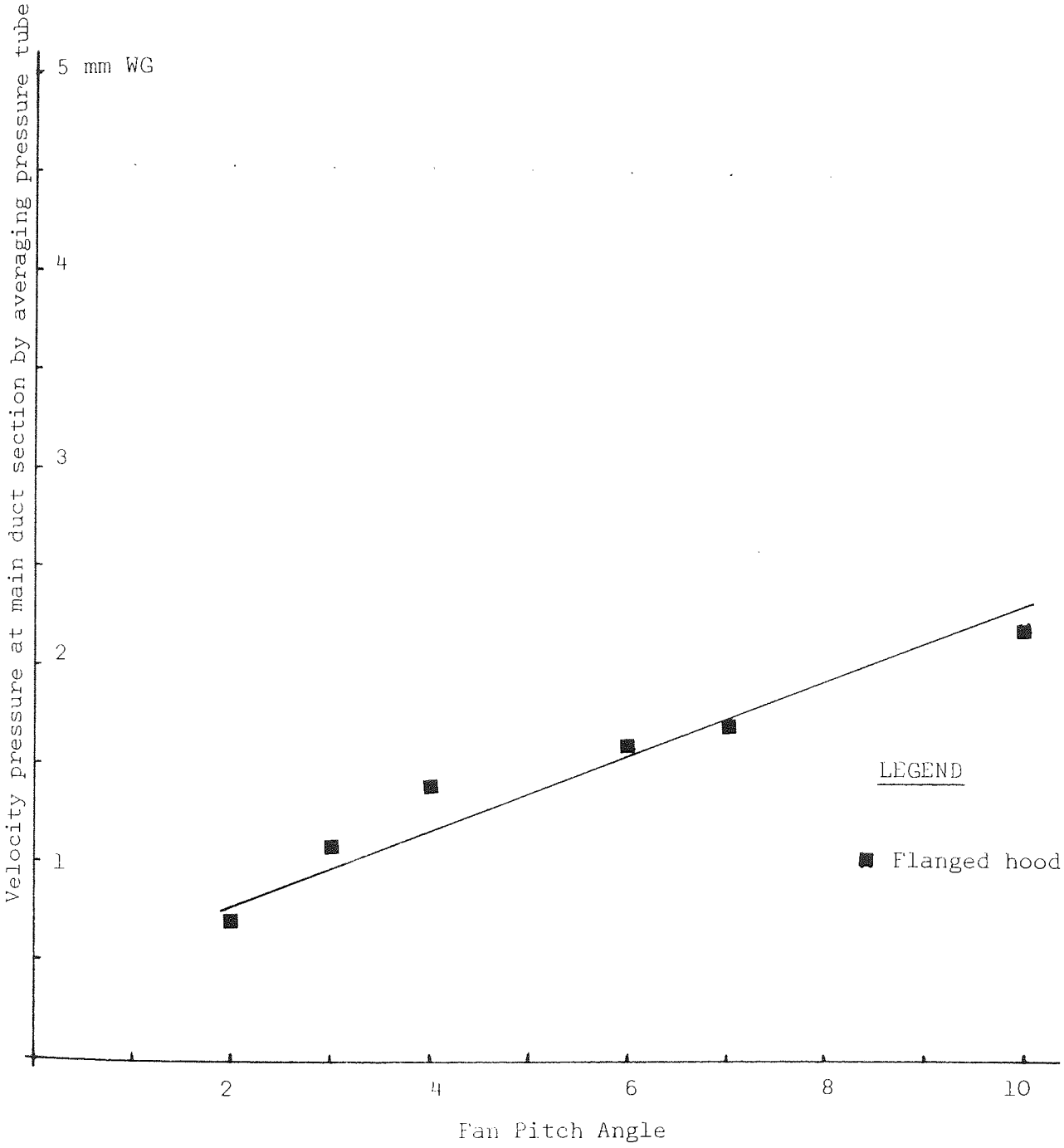

FIGURE 5.26 CALIBRATION OF WIND TUNNEL WITH SQUARE BELL-MOUTH FLANGED HOOD ASSEMBLY (SQUARE SECTION 535 mm)

Points 1 and 2 were connected to a T piece with rubber tube and then connected to the pressure reading meter.

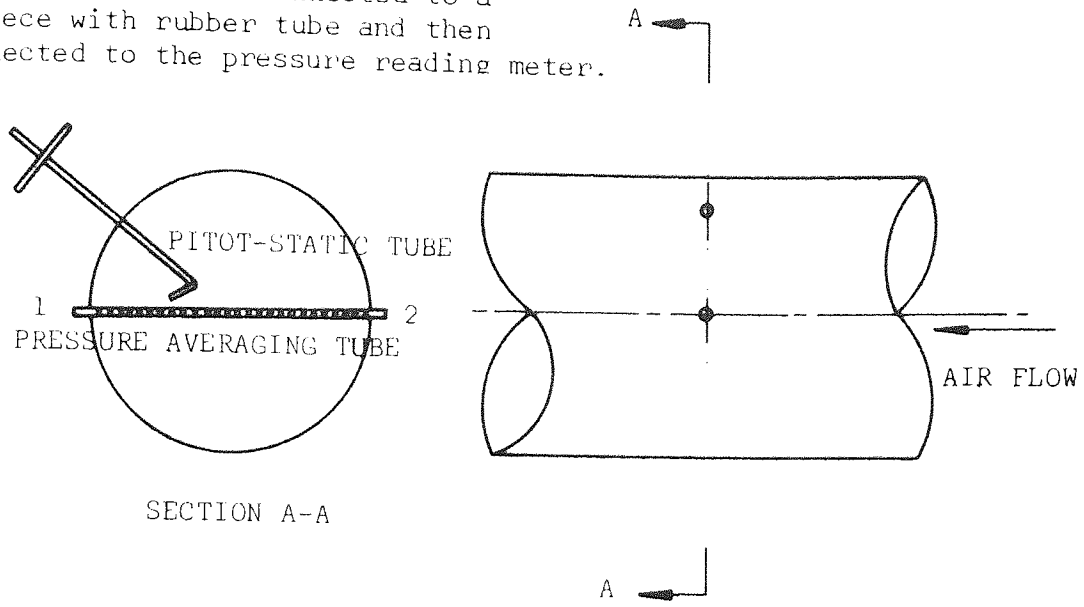

The rest of system is as schematic of figure 5.11

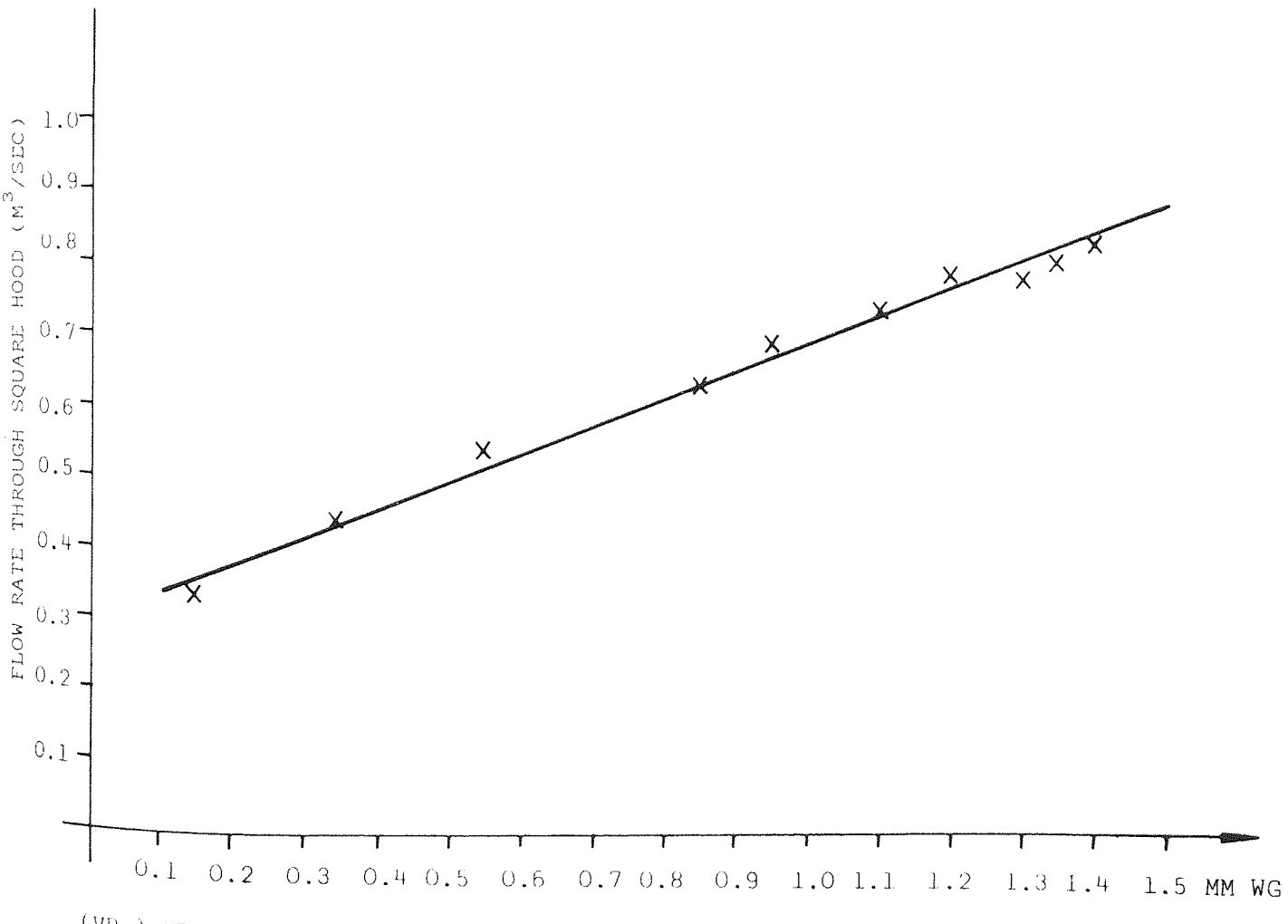

FIGURE 5.27 FLOW RATE AT HOOD FACE RELATED TO AVERAGING PRESSURE READING

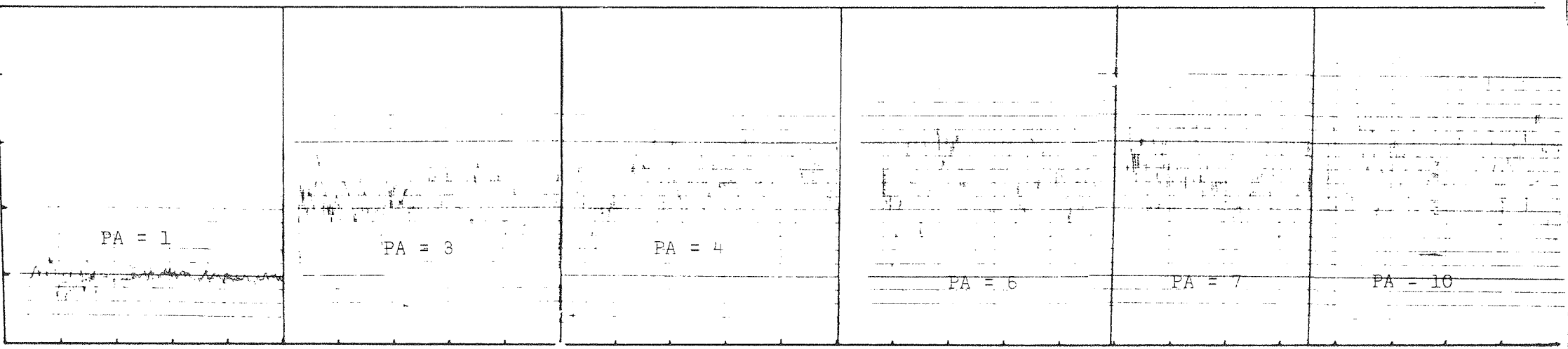

Time (10mm = 1 minute)

FIGURE 5.28 VELOCITY PRESSURE FLUCTUATION AT MAIN DUCT SYSTEM, TESTING SQUARE BELL-MOUTH FLANGED HOOD (SQUARE SIZE 535mm)

(hessian) curtains were fitted across the airflow.
To study the extent of the disturbance caused by recirculation air speed, one velometer was placed at the coordinate point (-3.40, 0.57, 0.665 meters) relative to the origin which is the centre of the suction opening. The test data was compared with the variation of turbulence caused by average human inhalation and exhalation. The following is the description of these tests.

5.4.2 Recirculation Cross Current.

As previously stated the cross current caused by recirculation was measured by a velometer direct air velocity meter. At a fixed position and for a number of suction flowrates, for the largest round test duct, the variation of velocity was recorded.
Figure 5.29 shows the relationship of suction flowrate and recirculation velocity measured at point (-3.40, 0.57, 0.665 meters). It can be seen that there is a linear relationship between the fluctation of velocity and flowrate. Also this the velocity measured at a significant distance away from the suction zone area which is almost negligible velocity.

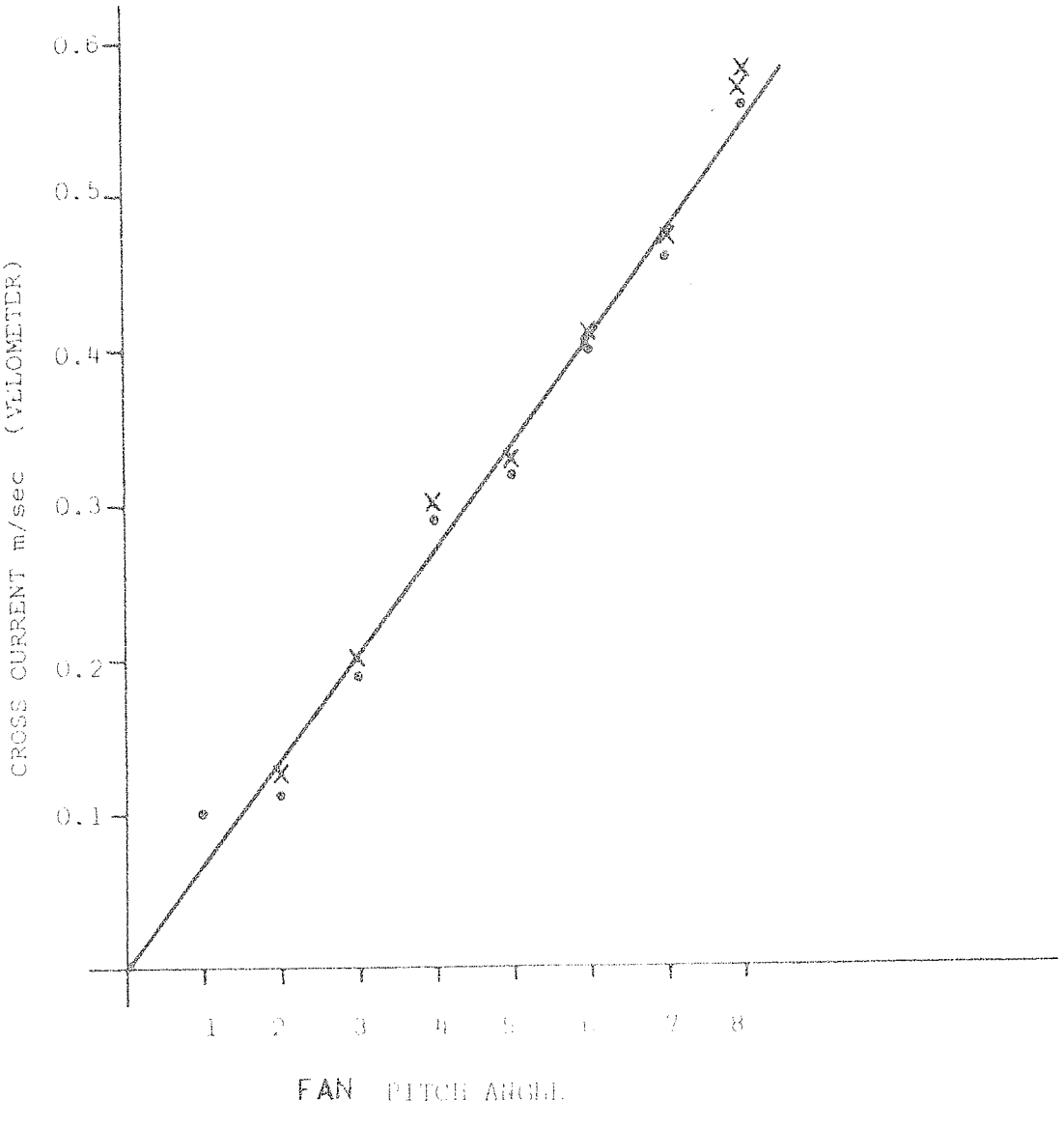

FIGURE5.29 VELOCITY OF RECIRCULATION AIR AT THE POINT OF COORDINATE (-3.40, 0.57, 0.865 meter) RELATIVE TO THE ORIGIN (0.0, 0.0, 0.0) WHICH IS THE CENTRE OF ROUND SUCTION OPENING (D=0.457 m)

CHAPTER SIX

AERODYNAMIC STUDIES, TYPES OF TREATMENT, STATISTICAL AND METHODOLOGY OF ANALYSIS OF DATA

6.1 Aerodynamic Studies

6.1.1. Introduction

As stated in chapter 2 above DallaValle et al (1939) stated that the frequent ineffectiveness of local exhaust ventilation could be partly attributed to the lack of sufficient knowledge of factors governing the operation of suction. The literature survey showed that, although attention has been drawn to the role and significance of these factors, and some investigations have been made, there is a lack of consistency between the relationships found by different investigators. The mathematical models given by different investigators are different. The discrepancies in applying these formulae are far too great to be dismissed (Figures 6.1, 6.2 and 6.3). The present study was undertaken in order to obtain detailed and reliable data on the aerodynamic characteristics of simply shaped captor hoods, i.e. round, square and rectangular suction openings, which could by analysed mathematically and statistically to present a new empirical relationship.

In operation, an exhaust opening creates an air velocity at the point of contaminant generation which in the case of a well designed, installed, maintained and adjusted system is sufficiently great to carry the contaminant into the collecting system. Although the minimum air velocity at a point, required or the efficient removal of contaminant particulates depends upon a number of removal of contaminant particulates depends upon a number of factor, capture efficiency constitutes the primary specification upon which the design of captor hoods must be based.

Figure 6.1 Variation of centre line velocity in front of square bell mouth flanged hood (AR=1.0, W=0.89m, L=0.89m, HR=0.222m, Q=1.198$m^3 s^{-1}$)

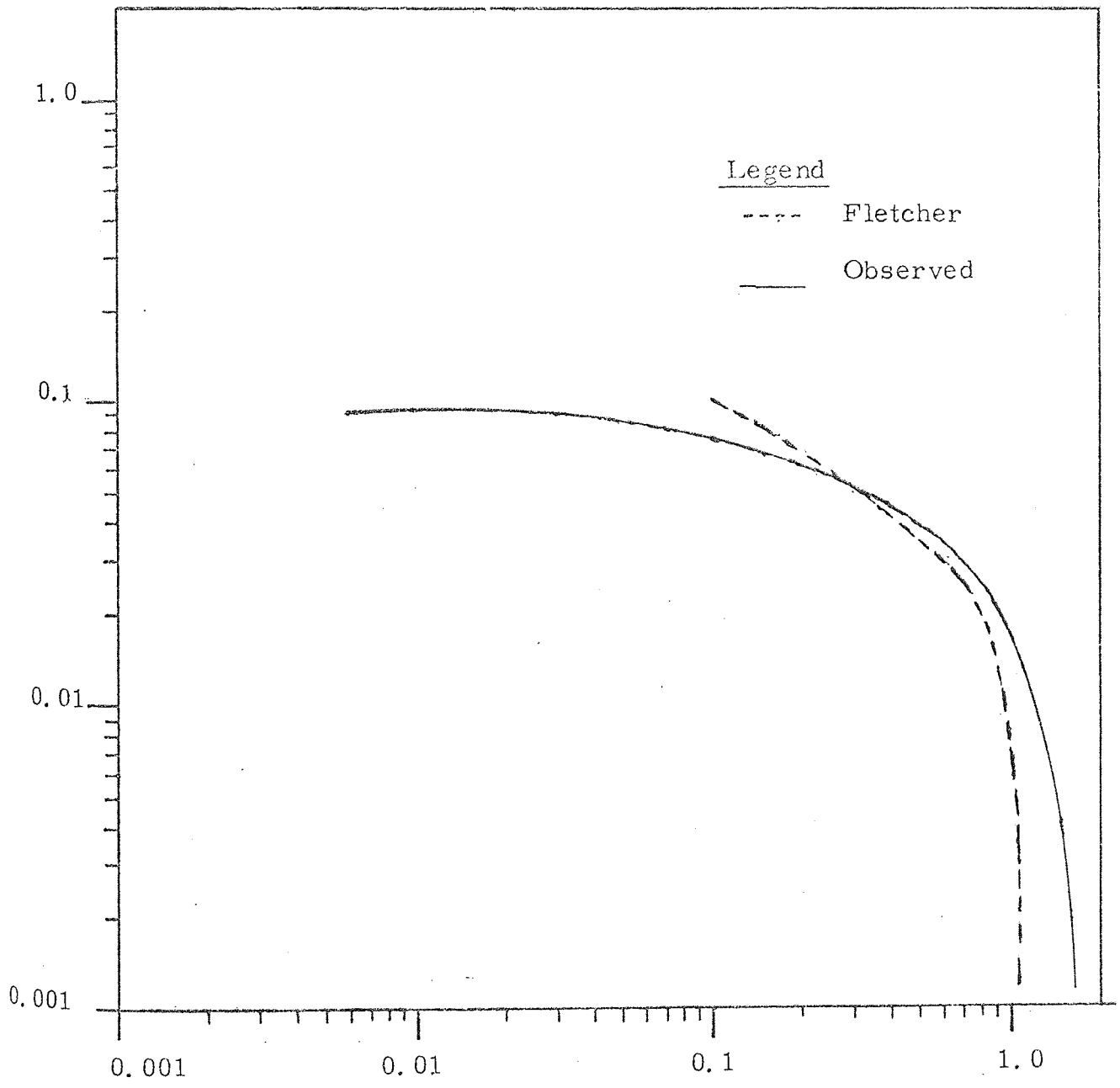

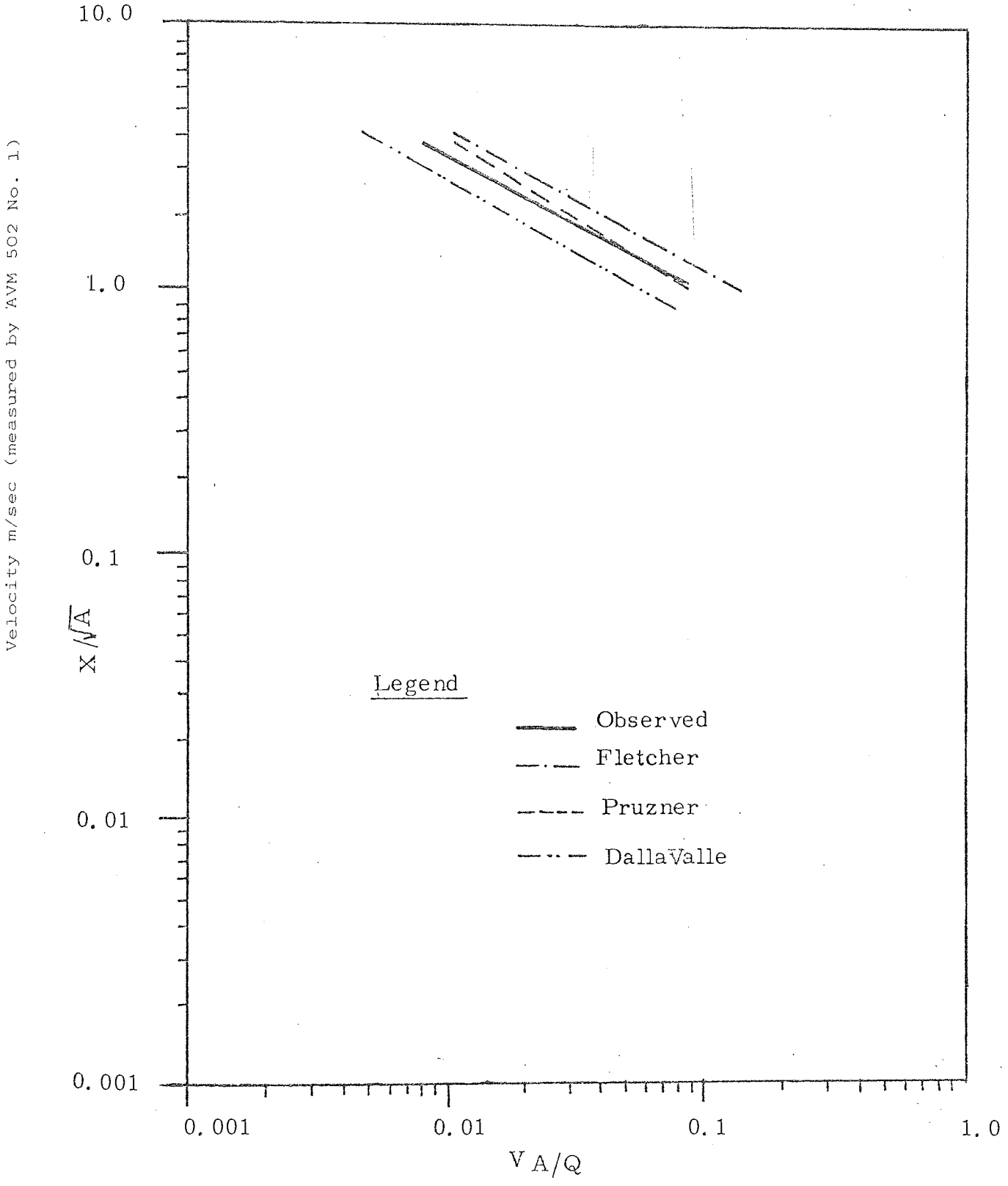

Figure 6.2 Variation of centre line velocity in front of unflanged rectangular suction opening (AR= 0.6 W=0.152m L =0.254m HR=0.048m

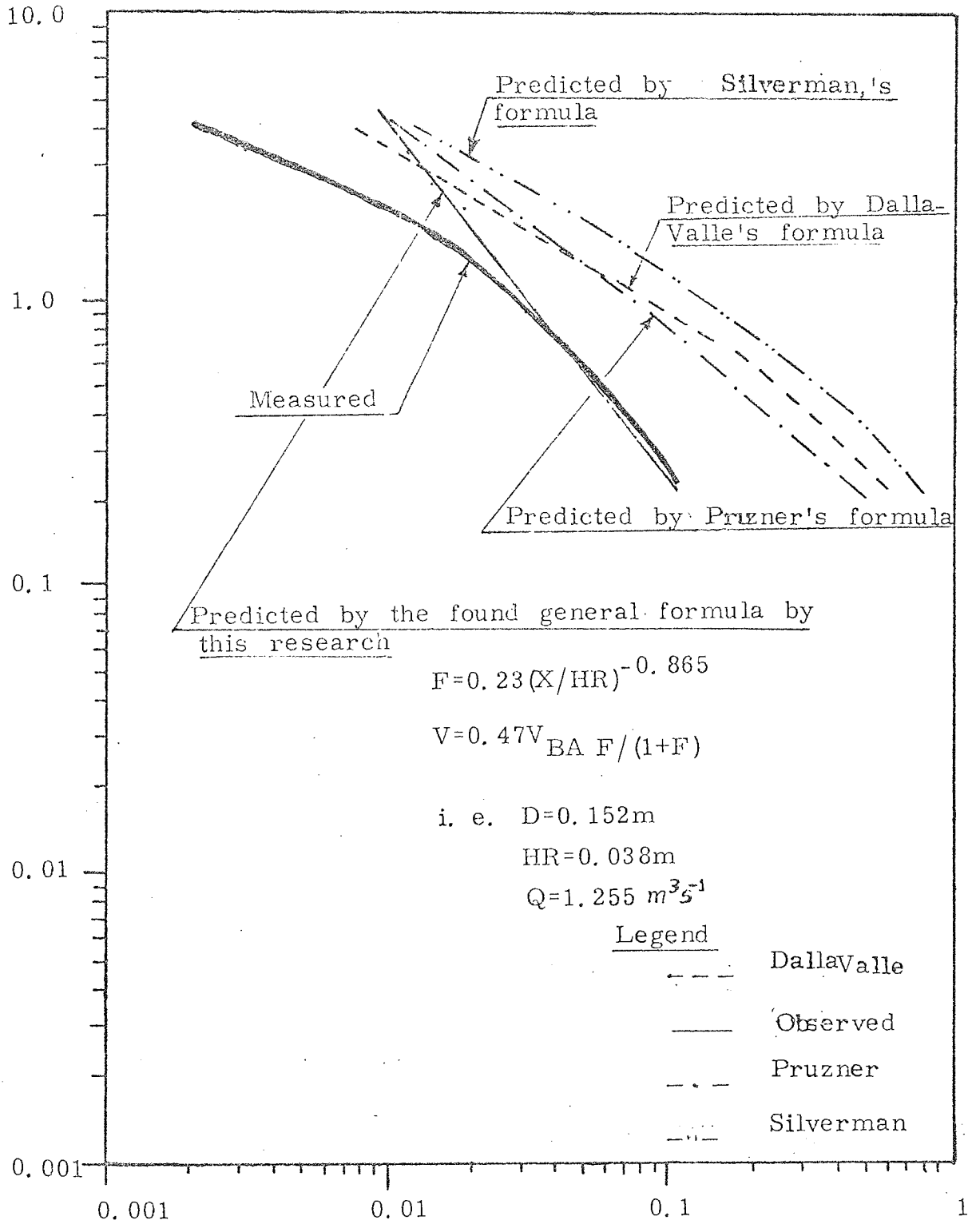

Figure 6.3 Variation of centre line velocity in front of unflanged round suction opening (D=0.152m, HR=0.038m, $Q=1.255\ m^3s^{-1}$).

upon which the design of captor hoods must be based.

The point air velocity in the zone of influence of a suction opening depends upon a number of factors which must be considered in the design stage. The most important factors are:

i) the shape, size and state of opening (i.e. flanged or plain);

ii) the distance of the point of the hygienically safe position of work (i.e. coordinates relative to the centre of suction opening);

iii) the position of hood relative to the source of pollutant; and

iv) the total airflow through the suction opening.

The above factors constitute what may be termed the aerodynamic characteristics of suction openings, and their influence upon the air velocity at the point of pollutant generation should determine the choice of hood and minimum airflow requirements.

6.1.2 Experimental Set-up.

The wind tunnel as an exhaust system consisted of 4.30 metres length of 0.5 metre diameter round duct followed by filtration compartment, silencer, fan and motor and then the discharge side silencer (see Drawing No.1). Indrawn air was recirculated into the room. The disturbance caused by circulation of air was controlled by means of two fully crossed hessian curtains. Variation of the rate of air flow through the system was obtained by means of a remote control device by varying the fan blade pitch angles, and the measurement of flow through the system was achieved by means of an averaging pressure tube inserted in the middle section of the main duct system. The test ducts were coupled to the main duct via a transition piece. Details on the physical dimensions and cali-

brations were discussed in earlier chapters.

6.1.3 Procedure of Air velocity measurement.

The test section to be studied was connected to the wind tunnel system and air was drawn through it at a measured rate. Six identically calibrated air velocity meters (AVM502) and one Simmon shielded hot wire anemometer which was calibrated by the manufacturer and at the laboratory, were the main measuring instruments. The sensor probes of the (AVM502)'s and hot wire were fixed to the specially built clamp adopted to the size of the probe stem (see Plate Nos. 1 to 19). The clamps themselves were fixed to a horizontally placed rod, which in turn was fixed to a vertically placed rod, this rod itself was fixed to a carriage which could be moved from side to side. The whole system was fixed to a base which was itself mounted on three wheels. The wheels were placed on two tracks which were fixed on the floor and centre lined up with the main duct of the wind tunnel. The carriage can be rolled in and out along the centre line of the whole duct system. Therefore, any instrument fixed to the probe holding carriage can be moved at any point in 3-dimensions . This movement and consequently the position of probes at each instance, is in just one plane, and along one axis. In some cases a bank of six AVM502 probes, one hot wire anemometer head, and sometimes a small pitot-static tube, sensor of AVM501F, and a prandtl pressure tube were vertically placed on the suction zone. The air velocity response readings from the gauges were recorded for each coordinate set up. Readings were taken as far out from the face of the suction area as possible, the limiting factor being the sensitivity of the Simmon Shielded hot wire anemometer (i.e. 0.002 ms^{-1}). The gauges were placed on a bench far away from the suction influenced zone.

All probes were connected to the gauges by means of extension cables and accessory devices (i.e. multiplexer as intermediate set up to a single gauge for six probes of AVM502, see plate 1 and Appendix 5.2. Careful location of sensors with reference to the coordinate system with origin at the centre of the opening, and the X-axis coincident with the duct centre line, was obtained by means of the mentioned probe carriage coordinator. The true position of the probes was ± 2 mm. deviation from the set up position. The coordinate measurements were taken by means of a conventional tape measure. The steel rods were of sufficient thickness to withhold the required weight without any significant deviation from vertical. The vertical and horizontal position of the rods was also checked conventionally. To counter balance the weight of the clamps and probes on the horizontal rod, a weight was hung in the opposite direction to the horizontal and vertical rods. Its distance and height was chosen in such a manner as to guarantee not to create any obstruction to the air flow in the suction zone and also far away from the measuring sensors. This counter weight also helped to stop the whole measuring sensor from shaking in the case of high suction flow rate.

For visualisation of streamline, a smoke tube or smoke generator probe was fixed to the probe carriage system. Picture plate 3 shows the probes, pressure tubes and smoke generator source fixed to the carriage coordinator.

6.1.4 Types of air velocity (or flow) measurements.

Table 6.1 gives the types of experimental test and for each duct under test the following types of measurements were performed:

(i) Centre line velocity measurement
(ii) XZ-Plane velocity measurement
(iii) XY-Plane velocity measurement
(iv) Ellipse locus point velocity measurement.
(v) Velocity pressure with pitot tube at a distance very close to the opening for average face velocity and centre point velocity readings. (see plates Nos. 2-19).

6.2 Types of Data Treatments.

Tables 6.2 and 6.3 are the example of the types of data collection. These types of experimental data were treated both graphically and statistically.

6.2.1. Graphical Representation

Graphs of velocity versus distance; velocity versus non-dimensional ratio (X/HR); velocity versus nondimentional ratio (X/Deq) and(V/V_{BA}) versus $(X/\sqrt{A})$ are some of the types of graphs which were prepared. Graphs based on logarithmic scales of velocity and of distance are the other type of presentation. In any graph the symbol of a hexagon with a vertical line on it represents the observed velocity.

6.2.2. Statistical Treatment

The task is to determine the functional relation between the suction velocity and a number of variable related to the suction aerodynamic characteristics with the help of experimental data. The problem to which attention is given is that of data fitting.

The most common method for fitting is least squares. Those values of the parameters are chosen which give the best fit of the experimental data to a model using the least square criterion.

The literature survey on the existing empirical and theoretical structural formulae on the suction aerodynamic character showed that all these equations are of nonlinear form (Table 2.1). Therefore, data treatment calls for considerable computation.

A literature survey of data fitting computation showed that the existing computer package programmes are quite sufficient for the treatment of data. The package used is the Statistical Package for the Social Sciences (SPSS), (section nonlinear regression (1977,1979)).

Appendix 6.1 is the computation programme and the example of the statistical consideration of the nonlinear regression analysis. The package was not available at Aston Computing Centre, therefore data were processed and prepared using the available computing facilities at Aston, then the prepared files were asked by the Centre to be transferred to the University of Manchester Computer Centre for the final treatment.

6.3 Methodology of non-linear regression analysis of data.

The aim is to determine the functional relation between the point velocity at the suction zone and a number of independent variables with the help of experimental data. The mathematical form of the functional relation is written in the form of a regression function:

$$V = f(x,D,V_{BA},HR,AREA,AR;b_1,b_2,b_3,b_4,b_5,b_6)$$

where the function f is given mathematically, but the unknown parameters, $b_1,b_2,\ldots b_i$, ..m have to be estimated from a set of observed velocities,V, and associated independent variables (i.e. x,D,V_{BA}, HR,AREA,AR). The method of estimation most frequently employed for the estimation of the b_i in the above expression, is the method of Least Squares:- with this method the differences V-f, between the observed velocities, V, and The responses computed from the associated inputs, through the regression function, are formed using a trial set of parameters $b_2,\ldots b_i$. The sum of squares of

These differences is then an i-variables function of the trial parameters and minimized as a function of these parameters.

Table 2.1 shows that the 'f' functions are non-linear in parameters. When the regression function is non-linear in the parameters, both the theory and the practice of the estimation procedure is considerable more difficult. This section is concerned with the methodology of non-linear regression analysis to produce a set of curves based on the least squares assumption. From these equations aerodynamic parameters may be derived. It is a numerical technique of computing Least Square estimate for solutions of the system of non-linear equations. Appendices 6.2. to 6.3 are the SPSS programme and residual output.

Appendix 6.3 gives the extract from the SPSS computational output. These data provide information on decision criteria.

6.3.1. Decision Criteria

Decision should be based on the following questions:

(i) which of the models give a better prediction i.e. better fitted to data or less RMSR;

(ii) Which model provides highest precision (i.e. lowest standard error);

(iii) Which model minimises bias (i.e. the difference of estimator and response is as close to zero as possible);

(iv) Which model is more unbiased than the other (i.e. the difference of major factors very close to zero).

Let us discuss a little about the lack of fit and errors involved in data fittings. Statistically the error of an incorrect model is of two types, biased error and random error.

The residuals contain all available information on the way in which the fitted model fails to properly explain the observed variation in the dependent variables.

Random error has a zero mean, and this is true whether

the model is correct or not, in contrast, biased error is just due to the lack of fit. Biased error for a correct model is zero, otherwise its value depends on the true model and the value of independent variable.

Other property of random error is that they are correlated and the sum of square of random error has expected or mean value of $(n-2)\sigma^2$, where σ^2 is the error variance. As the equation of residual mean square:

$$\text{Residual mean square (RMS)} = \frac{\text{Residual sum of square}}{\text{Residual degree of freedom}}$$

has expected or mean value σ^2 if the postulated model is the correct form, or $\sigma^2 + \Sigma$ (Biased error)$/(n-2)$ if the model is not correct. Therefore, a correct model is equivalent to zero biased error, and residual mean square can be used as an estimate of the error variance σ^2. However, if the model is not correct, that is

$$\text{Biased error} = B_i \neq 0$$

then the residuals contain both random (q_i) and systematic (B_i) components. Therefore the RMS no longer provide a satisfactory measure of the random variation present in the observation. Since, however, the mean square is a random variable it may, by chance, not have a large value even when bias does not exist. In order to find where and how the model is inadequate, calls for the examinations of residuals.

6.4 The examination of residuals.

The residual is the difference between predicted and observed values i.e. prediction-observation = Residual = Res. It may be called the observed error if the model is correct. In examining the residual, the following assumptions have been made:

i) errors are independent;

ii) errors have zero mean;

iii) errors have a constant variance σ^2

iv) error follows a normal distribution.

Thus if the fitted model is correct, the residuals should exhibit tendencies to confirm the above assumptions, or at least should exhibit a denial of the assumptions. This is the concept that one should apply in examining the residuals. This is equivalent to the question "Do the residuals make it appear that our assumptions are wrong?". After examining the residuals, we shall be able to conclude either:

i) the assumptions appear to be violated or

ii) the assumptions do not appear to be violated,

this means that on the basis of the data we have seen, we have no reason to say that they are incorrect.

Ways of examining the residuals are all graphical, are easy to do, and are usually very revealing, when the assumptions are violated.

One way of plotting the residuals is against the independent variable.

The scale unit of residual (abscissae) plot is the root mean square residual (RMSR).

Two vertical bands were examined i.e. $\pm\frac{1}{2}$ RMSR and ± 1 RMSR (see Appendix 6.2).

6.5 Ranking. Appendix 6.3 is an extract of data from SPSS computation output. The values of columns 8, 10, 11, 12, 14 and 15 were ranked. For values on column 8, ranking starts from 1 corresponding to the lowest value and highest rank to the high value of RMSR. For columns 10 and 11 rank 1 for the smallest value and up to the highest rank of the larger numbers. Conversely for the values on column 12, 1 corresponds to the cases of the highest value and higher ranks to lower values.

Finally, for columns 14 and 15 ranks of 1 for the minimum values of about 90° and highest rank for smallest value of angle.

These ranked values for each model are then averaged. Bias tests suggest that if the model is a perfect one the difference between initial values of parameters and the final value of parameter must be zero or very close to zero. To perform the bias test, column 7 was calculated, then squared, and averaged and square rooted, then these values for each model were ranked again i.e. rank of one for the smallest value and highest rank for the largest value. Finally, the best fitted model will be chosen among the others on the basis of these final values of rank. In principle the model which has the lowest mean rank and the lowest root mean square is the best fitted model.

Table 6.1 The type of ducts, instruments and flow rates under the experimental test.

TEST ORDER	HOOD OR DUCT	DIMENSION	AREA	DESCRIPTION OF MEASUREMENT	FAN PITCH ANGLE	AVERAGING PRESSURE TUBE FLOW RATING	TYPE OF AIR VELOCITY METERS	REMARKS
1	2	3	4	5	6	7	8	9
1	Round duct.	0.152 M	0.018 M^2	Velocity measurement in Horizontal plane along duct's centre line	9	0.835 cubic meter	1. Four AVM 502 2. One AVM 501F 3. One Hotwire anenometer	Air flow pattern was visualised by smoke filament and pictured.
2	"	"	"	Centre line velocity measurement.	"	"	"	"
3	"	"	"	Ellipse focus point velocity reading	"	"	"	
4	"	"	"	Horizontal plane velocity reading	2, 4, 5, 9, 10	0.5, 0.66, 0.71, 0.87, 0.94	"	
5	"	"	"	Centre line velocities	8.5	0.87	"	Flow rate sets same as square bell mouth hood.
6	"	"	"	" " "	10	0.94	"	"
7	Same duct with plate rect. Flange size 0608 by 0.913 m.	"	"	" " "	3, 5, 6, 8, 10	0.74, 0.87, 0.92, 1.0, 1.02	"	Log-liner pitot-static tube anenometry.
8	"	"	"	" " "	2, 5, 6, 8, 10		1. Six new AVM 502. 2. Pitot-static tube 3. Hot wire anenometer	-
9	Unflanged	"	"	" " "	"		"	
10	Rectangular duct	0.1524 by 0.254 M (6" by 10")	0.0387	" " "	2, 4, 6, 8, 10	0.68, 1.078, 1.209, 1.32, 1.4	"	Position of probes are same as test No. 9
11	"	"	"	" " "	10	1.4	"	All probes moved away from duct face.

Continued.....

Table 6.1 Continued(1)

12	"	"	"	Horizontal plane velocity reading.	10	1.4	"	"
13	"	"	"	" "	"	"	"	"
14	"	"	"	Ellipse focus in horizontal plane	"	"	"	"
15				Horizontal plane velocity reading.	"	"	"	"
16	"	"	"	Vertical plane velocity reading.	"	"	"	For comparison with test 15
17	"	"	"	" " "	10, 5		"	"
18	"	"	"	Horizontal plane velocity reading.	10, 5		"	"
19				Ellipse focus points in horizontal plane.	5	"	"	"
20	Rectangular duct with flat rect. flange.	"	"	Ellipse focus points in horizontal plane.	"	"	"	Fan pitch angle is same as test No. 19.
21	"	"	"	" " "	10		"	A blower was used as a extraneouse source of air flow crossing the suction air flow.
22	"	"	"	Centre line velocity reading.	10, 6, 8, 4, 2, 0.		"	" Also flow pattern was pictured.
23	"	"	"	Ellipse focus point	2, 4, 6, 10.		"	-
24	Unflanged.	"	"	" " "	10		"	Fan pitch angle is the same as test No23, & 26 points log linear pitometry was undertaken.
25	Rectangular	0.1m x 0.2m (4" x 8")	0.0206	Horizontal plane velocity reading.	"		"	"
26	"	"	"	Angle of streamline at a fixed point for different flow rate.	1 to 10		-	-
27	"	"	"	Centre line velocity with and without cross blowing	4, 5, 7, 9, 10, 8, 6, 4, 2.		"	26-point log-linear pitot-static tube anenometry for all the PA's has been done cross blowing was an for all measurements of this test.
28	"	"	"	Horizontal plane velocity.	7, 10.			Flow pattern was pictured.
29	"	"	"	Vertical plane velocity.	"		"	
30	"	"	"	Ellipse focus points in horizontal plane.	10		"	Prandtl tube type 607 for direction of air flow was used.

Continued.....

Table 6.1 Continued(2)

31	Same duct with flange (0.61x0.91)	"	"	Ellipse focus points in horizontal plane.	"			Pitch angle is the same as Test No. 30.
32	"	"	"	Horizontal plane with and without cross blowing.	"	"	"	" and 26-point anenometry.
33	"	"	"	Just blower is switched on	-	-	"	Position of measurements are the same as the last position of reading of test No. 33.
34	"	"	"	Vertical plane reading with and without blowing.	10			Flow pattern was photographed.
35	"	"	"	Centre line with and without cross blowing.	10, 2, 4, 6, 8, 5.		"	-
36				Horizontal line with and without cross blowing.	8			Flow pattern was pictured.
37	Rectangular opening hood flared to round duct.	0.25 by 1.145	0.2862 m^2	Centre line velocity with and without cross blower.	8, 10, 6, 2, 4.		"	Pitch angle is the same as the test No. 36.
38	"	"	"	Horizontal plane reading.	4, 8.		"	-
39	"	"		Vertical plane reading with and without blower.	"		"	-
40	"	"		Ellipse focus points as well as vertical plane reading.	8		"	-
41	Top flange plate fixed	"	"	Centre line velocity.	8, 6, 5, 5, 2.		"	Pitch angle 8 is the same as test No. 40.
42	"	"	"	Ellipse focus point.	7.5		"	-
43	"	"	"	Centre Line	5, 2, 3, 7.5		"	-
44	Another side plate fixed	"	"	" " "	"		"	-
45	Third plate fixed.	"	"	Horizontal plane.	7.5, 6.			
46	"	"	"	Vertical plane.	4, 2.5, 2.		"	
47	Fully flanged rectangular duct flared to round.	"	"	Centre line with and without blower.	2, 4, 6, 7, 10.		"	Pitch angle 2 settings is the same as test No. 46. Flow pattern was photographed.

Continued.....

Table 6.1 Continued(3)

48	"	"	"	Horizontal plane measurement of blowing velocity distribution.	-		"	"
49	"	"	"	Above pluse suction.	4		"	"
50	"	"	"	Ellipse focus point in horizontal plane.	"	"	"	Flow direction angle was measured with prandtl tube type 607.
51	Round duct	0.343 meter	0.0924 square meter.	Centre line measurement with and without blower.	2, 3, 4, 5, 5.8, 7.		"	6-point log-linear pitometry for hath test duct and main duct has been done
52	"	"	"	blower velocity at centre line position.	-	-	"	Position of probes are same as test No. 51.
53	"	"		horizontal plane with and without blower.	7		"	Flow pattern was photographed.
54	"	"	"	Vertical plane.	"	"	"	"
55	"	"	"	Horizontal plane ellipse focus point.	"	"	"	"
56	"	"	"	Centre line.	2, 3, 4.		"	-
57	"	"	"	Horizontal plane position readings.	10		"	-
58	Round duct.	0.457		Centre line velocity reading	2, 3, 5, 6, 8, 10.		"	6-joint vertical plane pitometry for both main duct and test duct has been done. Position of blower is the same for all suction and blower crossing tests.
59	"	"		Horizontal plane measurement for both blower on and off.	10			
60	"	"		Vertical plane reading	"	"	"	
61	"	"		Horizontal plane	5.8		"	Flow rate fixed to the same flow rate of duct 0.343 for pitch angle 7.
62	"	"		Ellipse focus point	"	"	"	Direction of air flow was measured with pressure tube type 607. Air flow pattern was photographed.
63	"	"		Symmetry point velocity reading.	"	"	"	
64	Square bell mouth shaped entry hood.	0.89 by 0.89 hood opening Duct size	0.2862	Centre line.	10, 8, 4, 10.		"	Flow pattern has been photographed.

Continued.....

Table 6.1 Continued(4)

		0.535 by 0.535						
65	"	"	"	Horizontal plane with and without blower.	10		"	
66	"	"		Just blower flow.	-		"	
67	"	"	"	Inside square section.	10, 8, 4.		Pitot-static tube	26-point and B.S. 48-point log-linear pitometry has been taken down for comparison.

TABLE 6.2 Corrected velocity measurement at symmetry point in the suction affected area in front of different size, shape and opening conditions (ie flanged, and unflanged) for equal volume of suction flow.

Suction duct under test	Main Duct and Fan Condition			Point velocity and temperature measured by six AVM 502 air velocity meters																REMARKS
				Probe Number P1					No. P2		No. P3		No. P4		No. P5		No. P6			
	Pitch Angle	Velocity mmw Pressure	Air °C Temperature	Temperature °C	Velocity m sec⁻¹	XP1 (Cm) Coordinate	YP1 (Cm) Coordinate	ZP1 (Cm) Coordinate	Temperature °C	Velocity m sec⁻¹	Temperature °C	Velocity m sec⁻¹	Temperature °C	Velocity m sec⁻¹	Temperature °C	Velocity m sec⁻¹	Temperature °C	Velocity m sec⁻¹		
Round Duct Unflanged D = 0.457m	0.8	1.5	19	20	4.5	8.5	0.1	0.1	22	2.55	20.5	1.3	20	0.8	20	0.48	23	0.33		$XP_2 = XP_1 + 6.8$, $XP_3 = XP_2 + 8.5$, $XP_4 = XP_3 + 9.8$, $XP_5 = XP_4 + 10.3$ $XP_6 = XP_5 + 10.4$
	"	"	"	21	4.6	"	"	"	22.5	2.56	21.0	1.31	20.5	0.85	20.5	0.47	23	0.32		
	"	"	"	21.5	4.47	"	"	-3.5	23.0	2.49	21.0	1.30	"	0.82	21.0	0.42	24.0	2.91		
	"	"	"	"	4.54	"	"	-8.0	23.5	2.48	21.5	1.30	21.0	0.79	"	0.42	"	0.23		
Round Duct Unflanged D = 0.152 m	10	1.5	22	26.0	2.12	"	"	4.0	24.5	3.97	24.0	2.1	24.0	1.23	23.0	0.67	28.5	0.26		
	"	"	"	25.5	2.37	"	"	0.1	27.5	1.18	26.0	0.69	25.0	0.5	25.0	0.32	28.5	0.24		
	"	"	"	24.0	2.29	"	"	-3.5	27.5	1.1	24.5	0.61	25.5	0.51	25.0	0.29	"	0.26		
	"	"	"	24.5	2.09	"	"	-8.0	26.5	0.96	24.5	0.56	24.5	0.48	24.5	0.31	27.5	0.23		
Rectangular Duct uflan. 4" by 8"	3.3	1.5	20	23	Off scale	"	"	-3.5	24.0	2.39	23.0	0.93	22.5	0.56	23.0	0.35	25.5	0.23		
	"	"	"	"	"	"	"	0.1	24.5	2.51	"	0.97	23.5	0.57	23.0	0.33	25.0	0.21		
	"	"	"	24	4.37	"	"	8.0	25.0	1.68	24.0	0.83	24.0	0.55	23.0	0.27	25.5	0.21		
Rectangular unflan. 6" by 10"	1.8	1.5	22	25	Off Scale	"	"	0.1	27.0	3.0	26.0	1.17	25.0	0.74	25.0	0.4	27.5	0.3		
	"	"	"	"	"	"	"	-3.5	"	2.89	25.5	1.1	"	0.68	"	0.37	"	0.26		
	"	"	"	"	"	"	"	-8.0	"	2.78	"	1.03	"	0.65	"	0.35	"	0.24		
Square bell mouth flanged	10	1.5	22	28.5	2.06	"	"	4.0	28.0	1.4	26.5	1.48	25.5	0.69	25.5	0.58	28.0	0.3		
	"	"	"	27.0	2.14	8.5	0.1	0.1	"	1.51	26.5	1.01	26.0	0.76	26.0	0.45	"	0.27		
	"	"	"	26.5	2.08	"	"	-3.5	"	1.4	27.0	1.03	"	0.85	"	0.47	29.0	0.41		
	"	"	"	27.0	2.03	"	"	-8.0	28.5	1.25	26.5	0.96	26.5	0.76	"	0.44	28.5	0.38		

TABLE 6.3 Corrected velocity measurement at symmetry point in the suction affected area in front of different size, shape and opening conditions (ie flanged and unflanged) for equal volume of suction flow.

Suction duct under test	Main Duct			Point velocity and temperature measured by six AVM 502 air velocity meters												REMARKS
				Probe No. P1				No. P2		No. P3		No. P4		No. P5		No. P6		
	Pitch Angle	Velocity mm W6	Air temperature °C	Temperature °C	Velocity m sec^{-1}	XP1Cm Coordinate	YP1Cm Coordinate	ZP1Cm Coordinate	Temperature °C	Velocity m sec^{-1}	Temperature °C	Velocity m sec^{-1}	Temperature °C	Velocity m sec^{-1}	Temperature °C	Velocity m sec^{-1}	Temperature °C	Velocity m sec^{-1}	
Rectangular opening to round duct (C.25xl.145)	1.3	1.5	20	23.5	3.3	7.5	0.1	0.1	25.5	2.11	23.5	1.24	23.5	0.99	23.5	0.64	26.0	0.53	$XP_2=XP_1+6.8$, $XP_3=XP_2+8.5$, $XP_4=XP_3+9.8$, $XP_5=XP_4+10.3$, $XP_6=XP_5+10.4$
	"	"	"	23.0	3.19	7.5	0.1	-3.5	25.0	2.06	23.5	1.14	22.5	0.92	22.5	0.56	25.0	0.42	
	"	"	"	22.5	3.07	"	"	-8.0	24.5	1.93	23.0	1.03	22.5	0.87	22.5	0.53	25.0	0.39	
	"	"	"	23.5	3.06	"	0.1	8.0	26.0	2.07	24.0	1.04	23.5	0.85	23.5	0.57	26.0	0.41	
Unflanged	"	"	"	24.0	3.1	8.5	0.1	0.1	26.0	1.9	24.5	1.04	24.0	0.82	"	0.54	26.5	0.39	
	"	"	"	24.5	3.01	8.5	0.1	-3.5	"	1.89	24.5	1.02	24.0	0.84	24.0	0.53	26.0	0.38	
	"	"	"	24.5	2.93	"	"	-8.5	"	2.07	"	"	23.5	0.81	24.5	0.51	27.0	0.37	
	"	"	"	25.0	3.04	"	"	8.5	25.5	1.95	25.0	0.89	24.5	0.78	"	0.52	27.0	0.39	
Flanged Rectangular Duct 6"x10"	1.3	1.5	22	21.5	Off Scale	"	0.1	8.0	23.5	3.62	22.0	1.43	"	0.96	21.5	0.51	24.0	0.35	
	"	"	"	"	"	"	"	0.1	23.0	4.12	21.5	1.60	21.5	1.09	21.5	0.56	"	0.33	
	"	"	"	"	"	"	"	-3.5	23.5	3.93	22.0	1.62	21.5	1.01	"	0.51	24.0	0.32	
	"	"	"	22.0	"	"	"	-8.0	24.0	3.85	22.0	1.58	22.0	1.0	21.5	0.49	24.5	0.43	
Flanged Rectangular Duct 4"by8"	"	1.5	18	18.5	Off Scale	"	"	8.0	21.0	2.73	20.0	1.15	20	1.0	19.5	0.48	22.5	0.33	
	"	"	"	"	"	"	0.1	0.1	23.0	4.33	21.5	1.52	20.5	1.0	20.5	0.52	23.5	0.36	
	"	"	"	"	"	"	"	-3.5	23.0	4.12	22.0	1.51	21.5	0.99	21.0	0.48	23.5	0.32	
	"	"	"	21.5	"	"	"	-8.0	"	3.8	"	1.48	"	0.91	"	0.46	"	0.3	
Flanged round duct D=0.152(6")m	10	1.5	22	23.0	Off Scale	8.5	0.1	4.0	24.5	3.97	24.0	2.08	24.0	1.23	23.0	0.67	26.5	0.51	
	"	"	"	24.5	"	"	"	0.1	25.0	5.0	24.5	2.19	24.5	1.25	24.0	0.64	26.5	0.49	
	"	"	"	26.5	"	"	"	-3.5	26.5	5.54	"	2.09	25.0	1.21	24.5	0.63	27.0	0.45	
	"	"	"	"	"	"	"	-8.0	"	5.11	"	1.88	"	1.21	"	0.61	27.5	0.43	

REMARKS

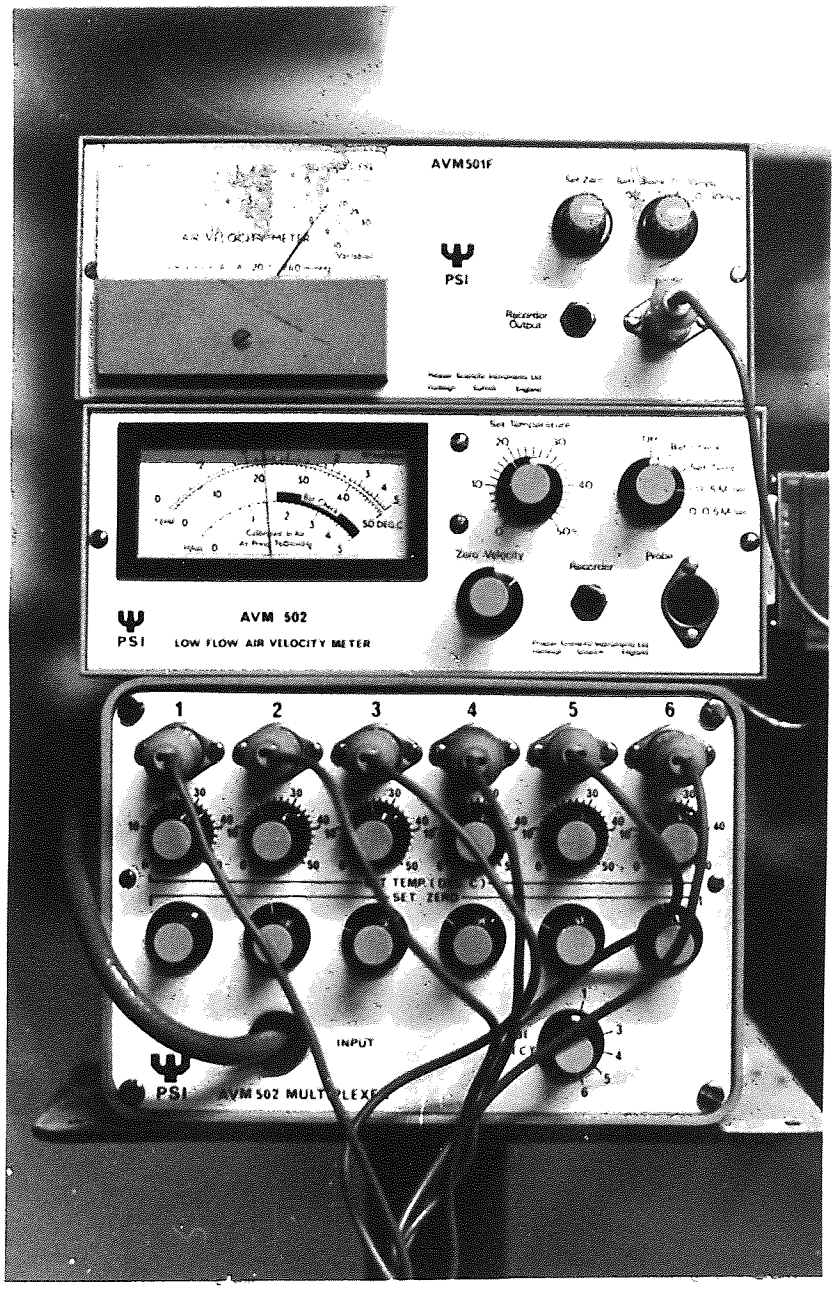

PLATE 1. Air velocity metering gauges placed on a bench at a distance far from suction affected area.

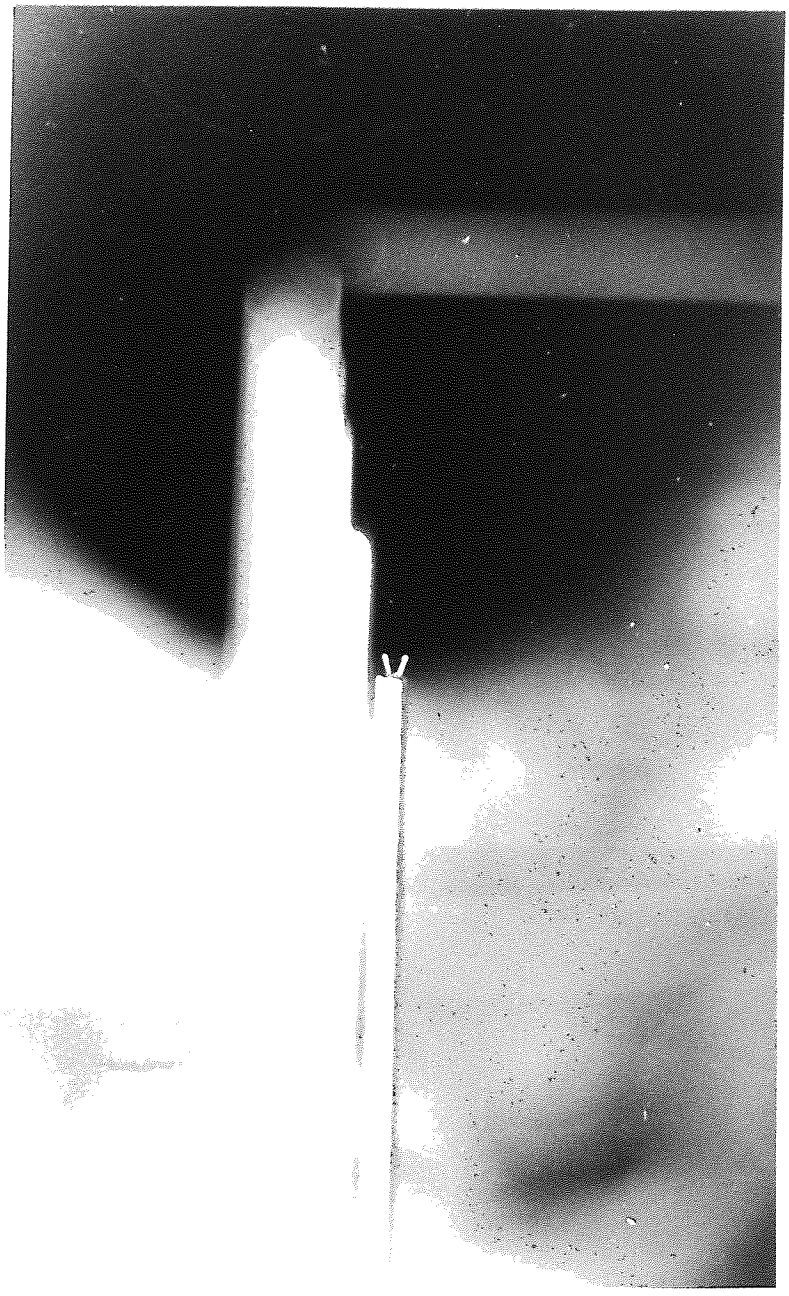

PLATE No 2 Physical size of thermistor bead as sensor of AVM 502 velocity meter

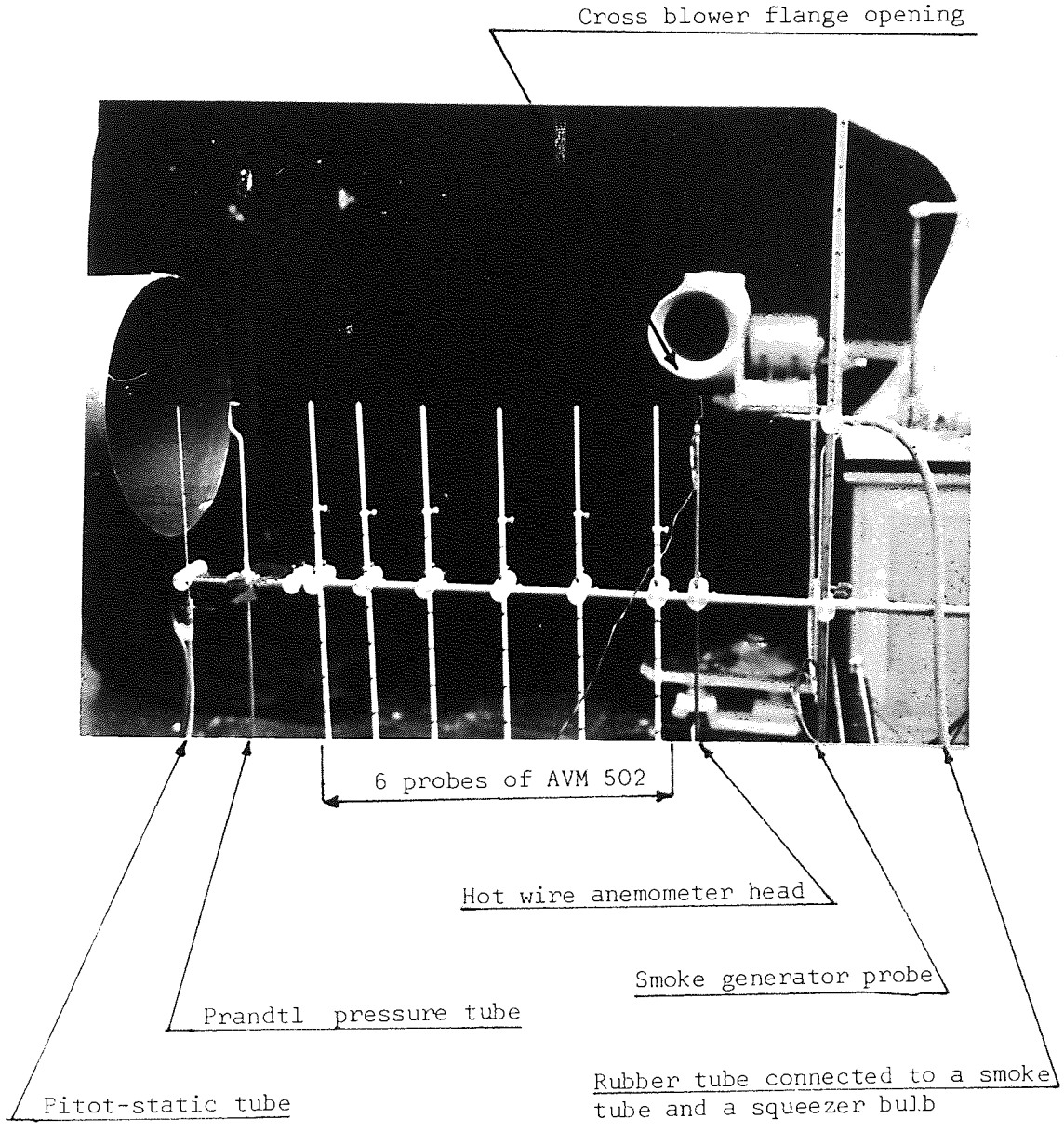

PLATE 3. Arrangement of air velocity measurement, testing round opening suction duct.

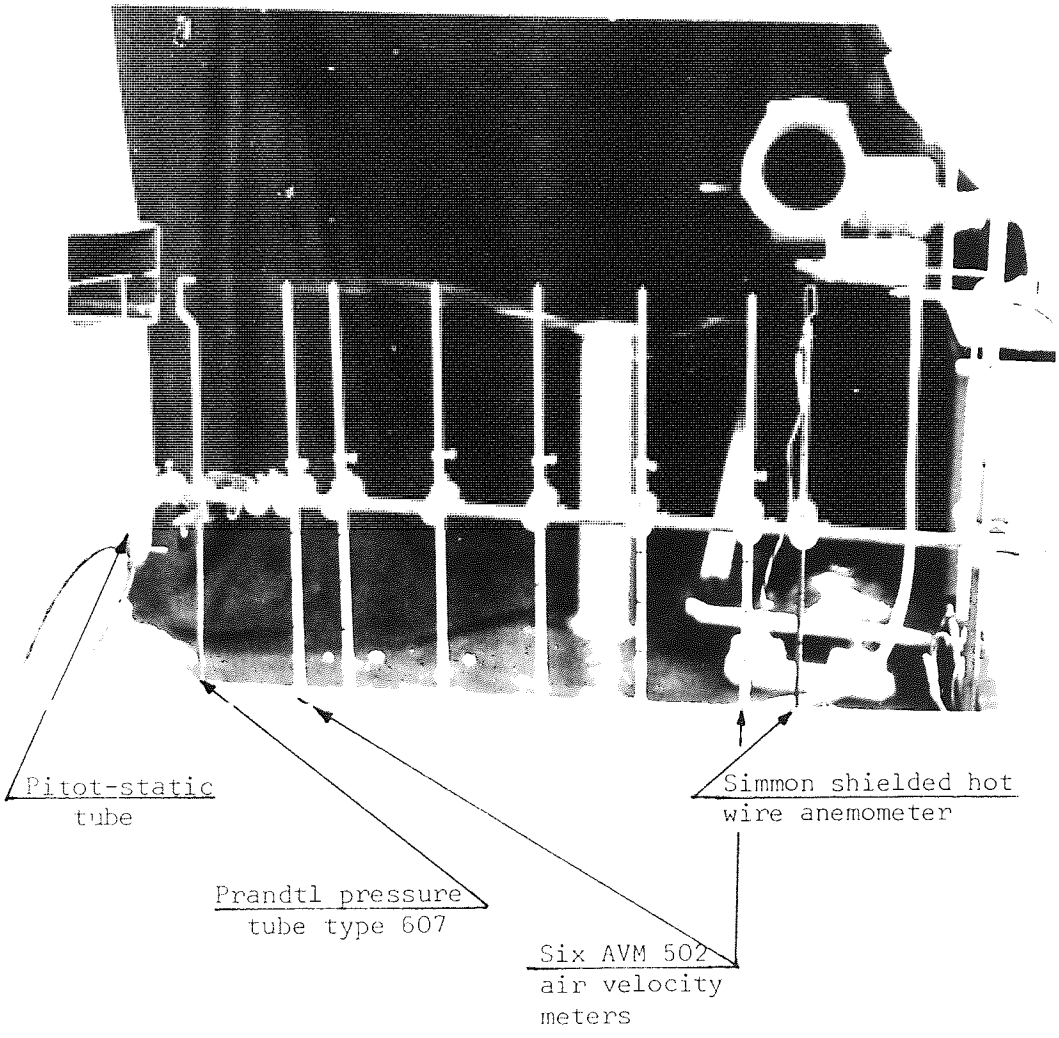

PLATE NO.4 Air velocity measurement arrangement, testing rectangular opening suction duct.

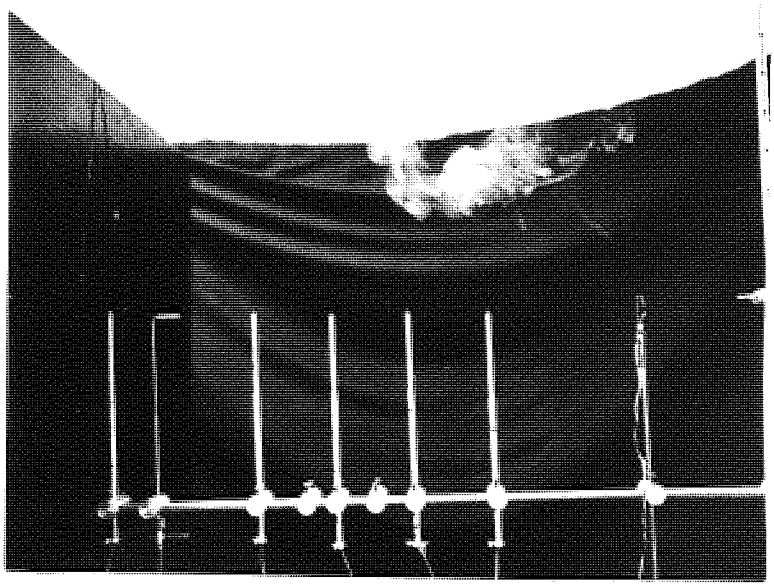

Plate No 5 Smoke generated at 0.86 m distance from the centre of suction opening along the centre line axis when the suction is nil.

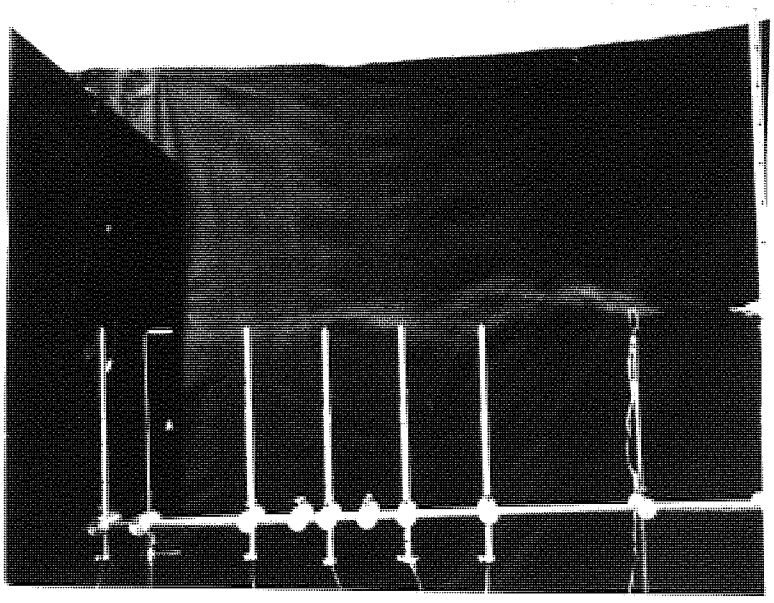

Plate No 6 Stream line and suction effect of 1.06 $m^3 sec^{-1}$ suction flow rate in front of flat plate flanged round duct (D = 0.152m) at 0.86 meter distance from the centre

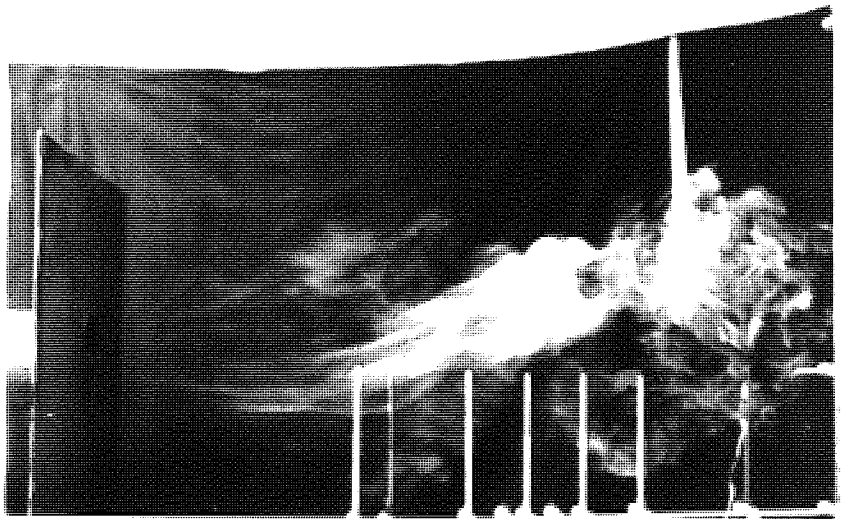

PLATE NO 7. The distance of smoke generation point was increased from 0.86m to 1.28meter along the centre line axis of suction opening when 1.06$m^3 sec^{-1}$ of air is drawn in through the system as plate number 6.

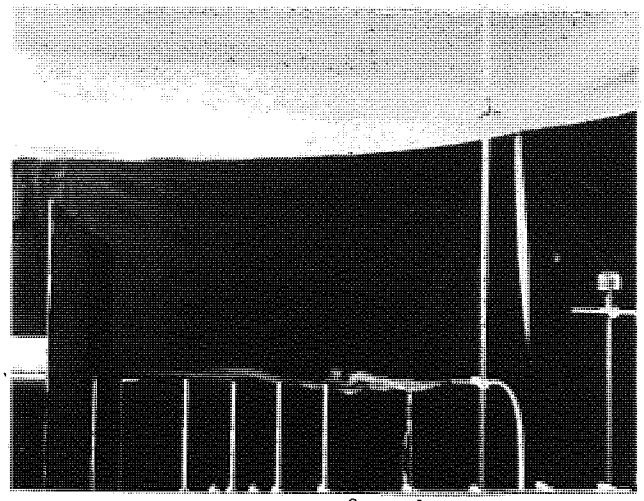

(a) Suction flow rate is $0.71 m^3 sec^{-1}$, smoke tube at 0.812m

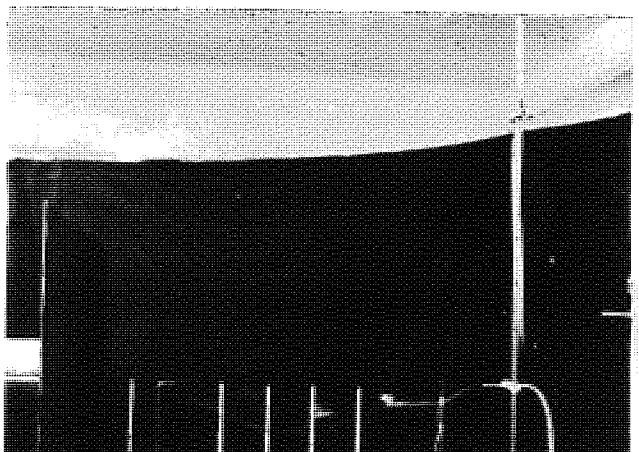

(b) Suction flow rate is $0.71 m^3 sec^{-1}$, smoke tube at 0.9m

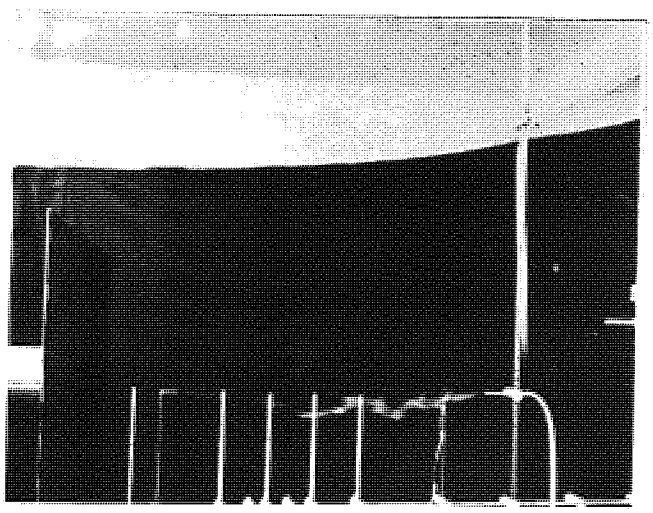

(c) Suction flow rate increased from 0.71 to $0.83 m^3 sec^{-1}$, but smoke tube is at the same position as above (ie 0.9m along centre line axis)

Plate No 8.1 Comparison of suction effect in front of flanged round duct (D=0.152m)

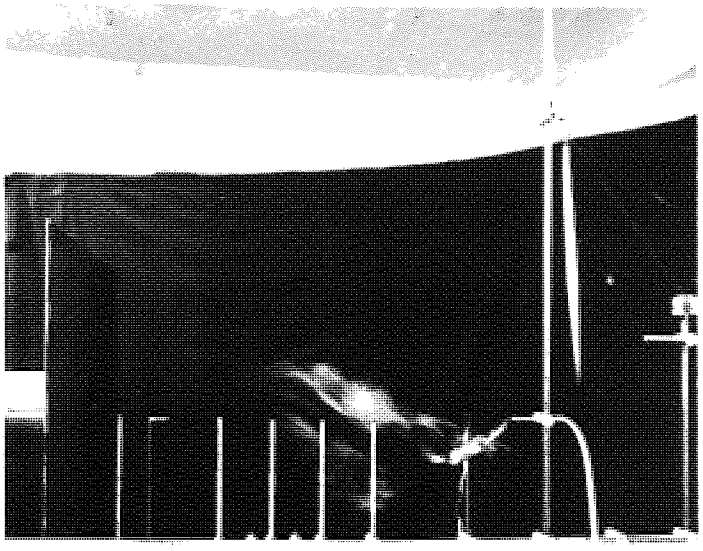

(a) Suction flow rate is $0.97m^3sec^{-1}$, smoke is generated at 0.85 meters from the centre of suction opening along centre line axis.

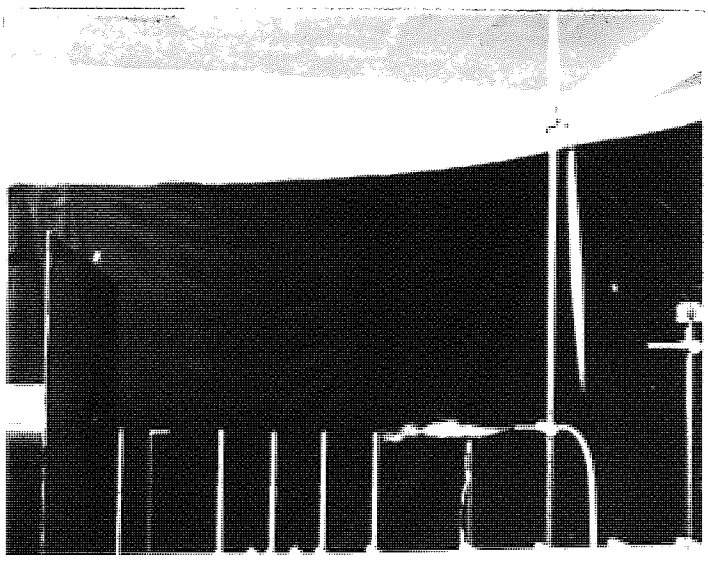

(b) Suction flow rate increased from 0.97 to $1.03m^3sec^{-1}$, but smoke generation position kept the same as above experiment (ie 0.85m)

PLATE NO.8.2. Comparison of the effect of suction in front of flanged round duct.

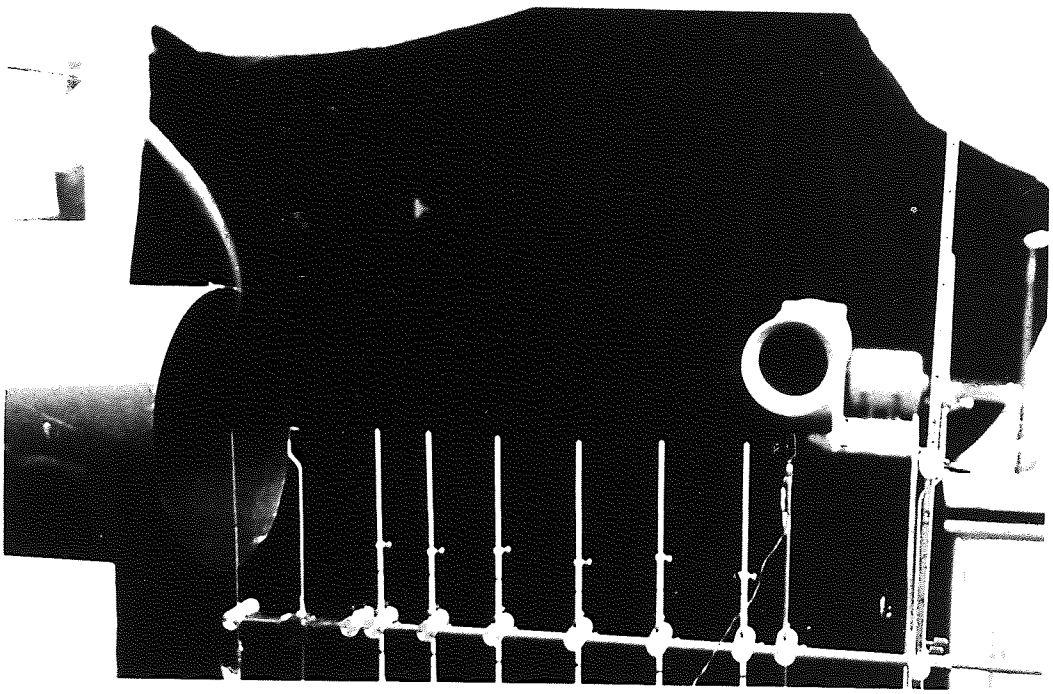

PLATE NO 9 Trace of smoke filament as stream line of suction in front of unflanged round duct (D = 0.343m)

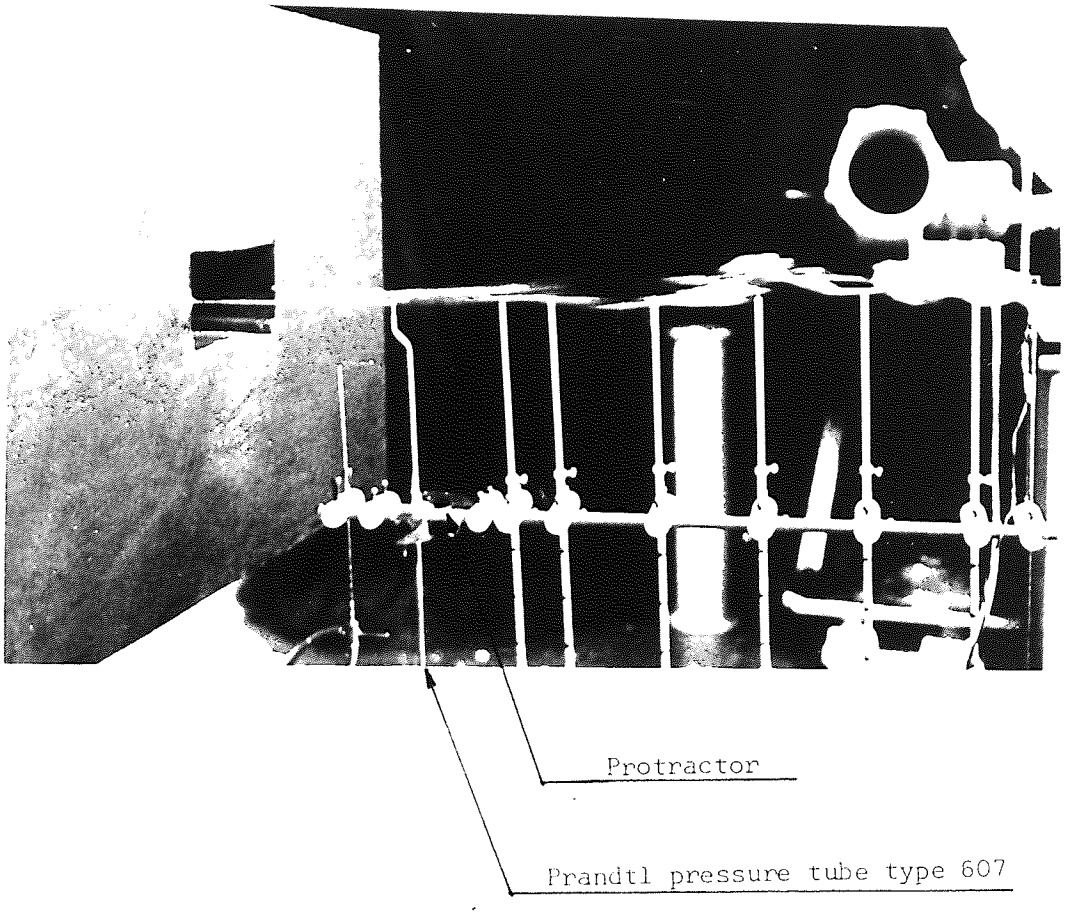

PLATE NO. 10 Smoke trace shows the centre line axis stream line in front of flanged rectangular opening suction duct (AR = 0.6)

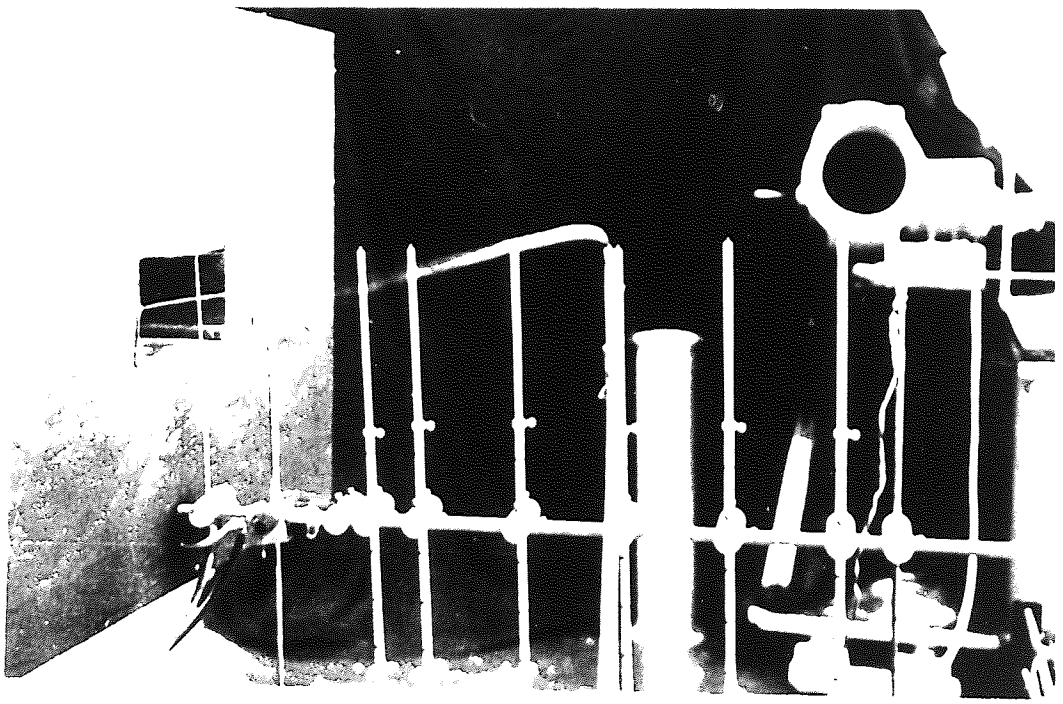

PLATE NO.11 Visualization of stream line in xy plane in the suction affected area in front of flanged rectangular opening suction duct.

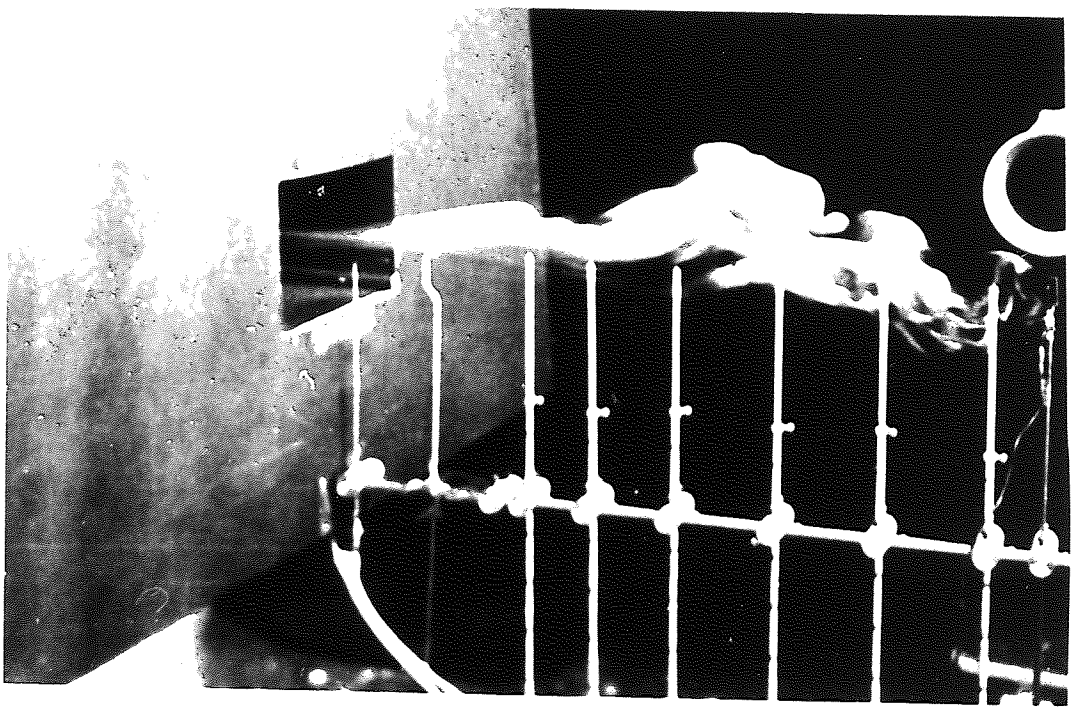

PLATE NO 12 Suction effect of flanged rectangular duct

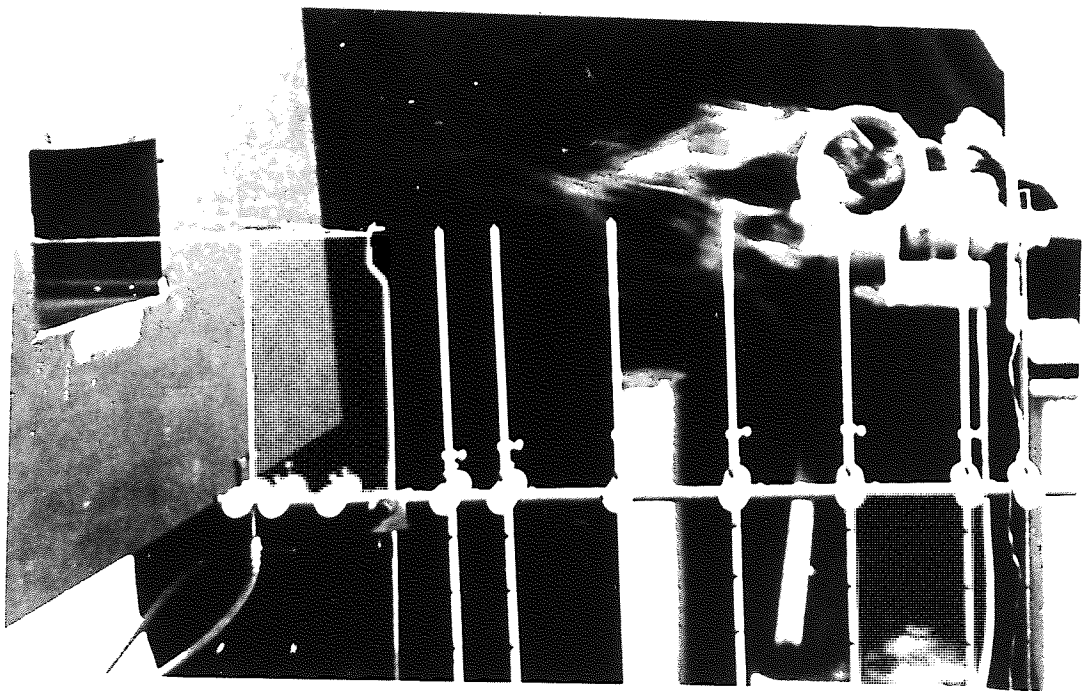

PLATE NO.13 The position of smoke source and suction flow rate is the same as the plate no. 12 but cross blowing is switched on.

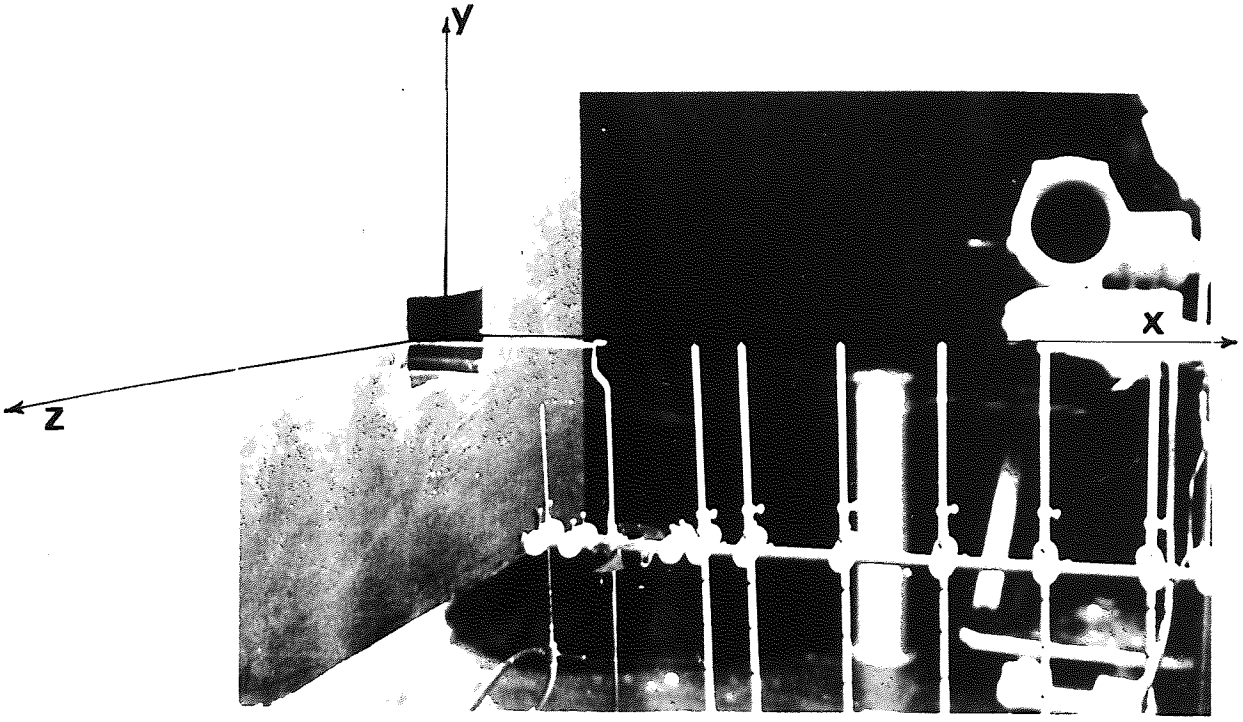

PLATE NO.14 The arrangement of velocity measurement in XZ plane on the locus point of ellipse of major axis along the length of duct and foci at the edge of suction duct.

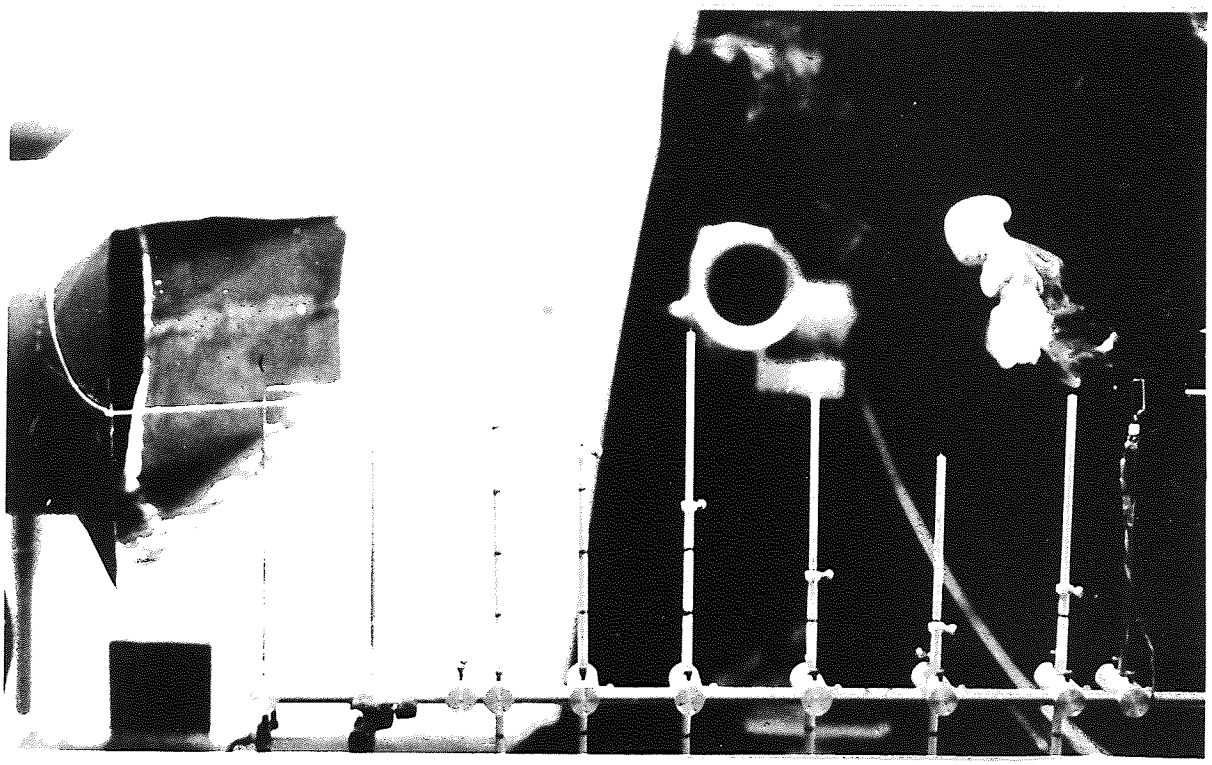

PLATE No. 15 Rise of smoke cloud in front of rectangular hood with no suction.

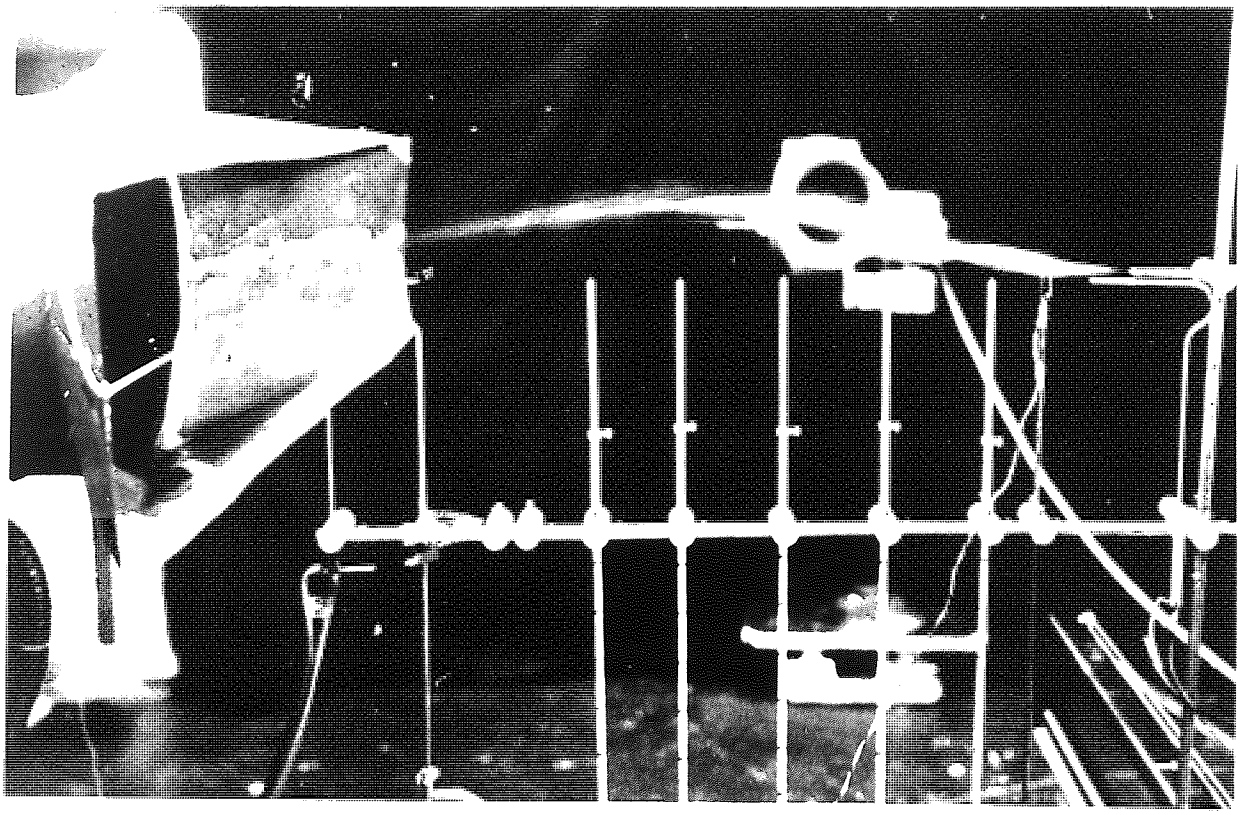

PLATE NO. 16 Illustration of capture (stream line) of smoke generated at the same position and place in front of rectangular hood as plate no 15 .

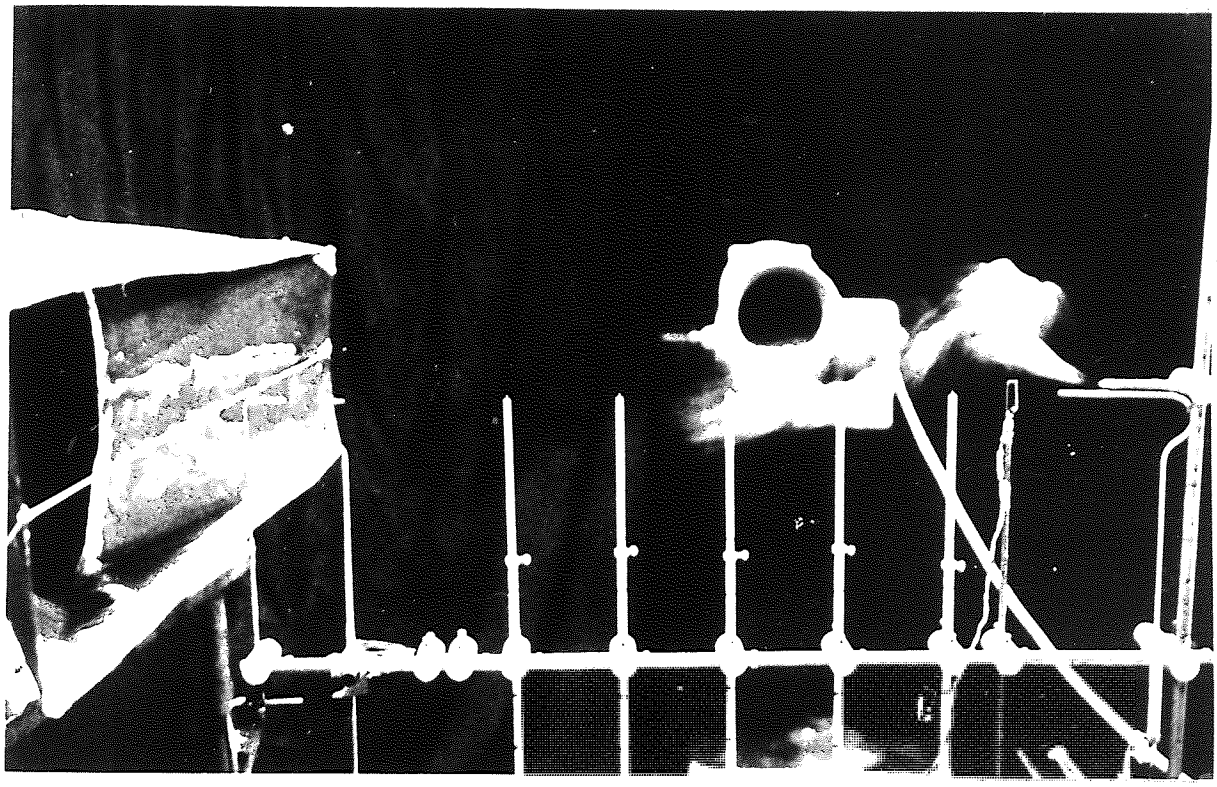

PLATE NO.17 The position of generation of smoke and the flow rate of suction are same as the plate number 16 , but the suction is crossed by a blow air flow as extraneous air movement.

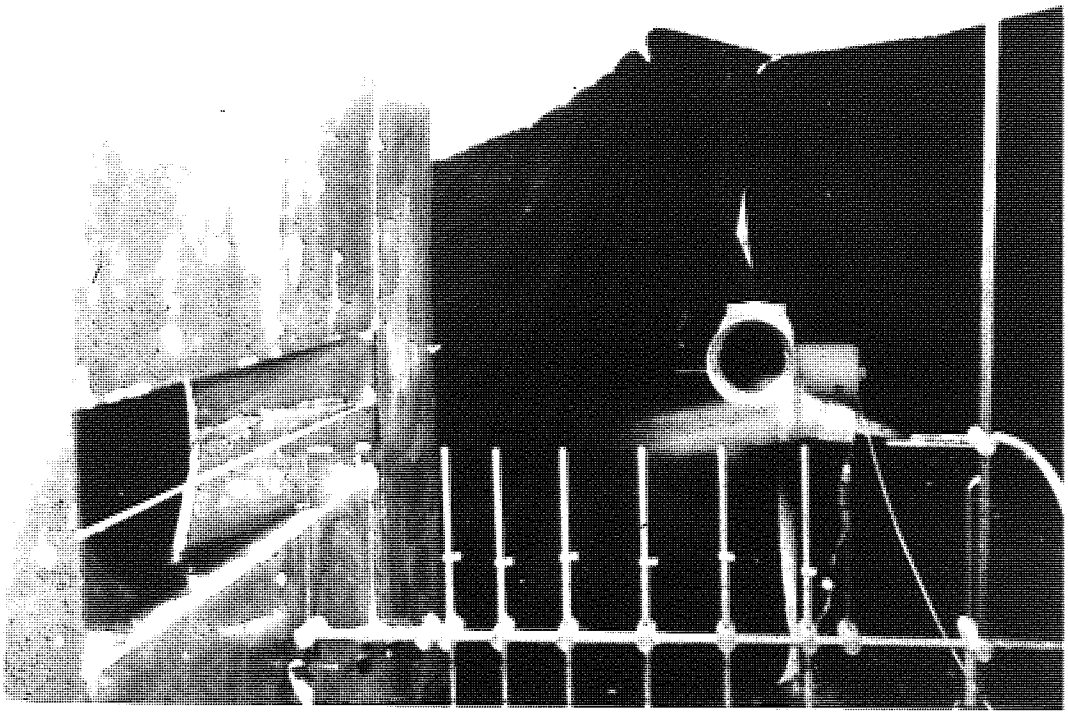

PLATE No. 18 This plate shows the capture effect and the position of probe of the air velocity meters for the point velocity measurement in front of rectangular flanged hood.

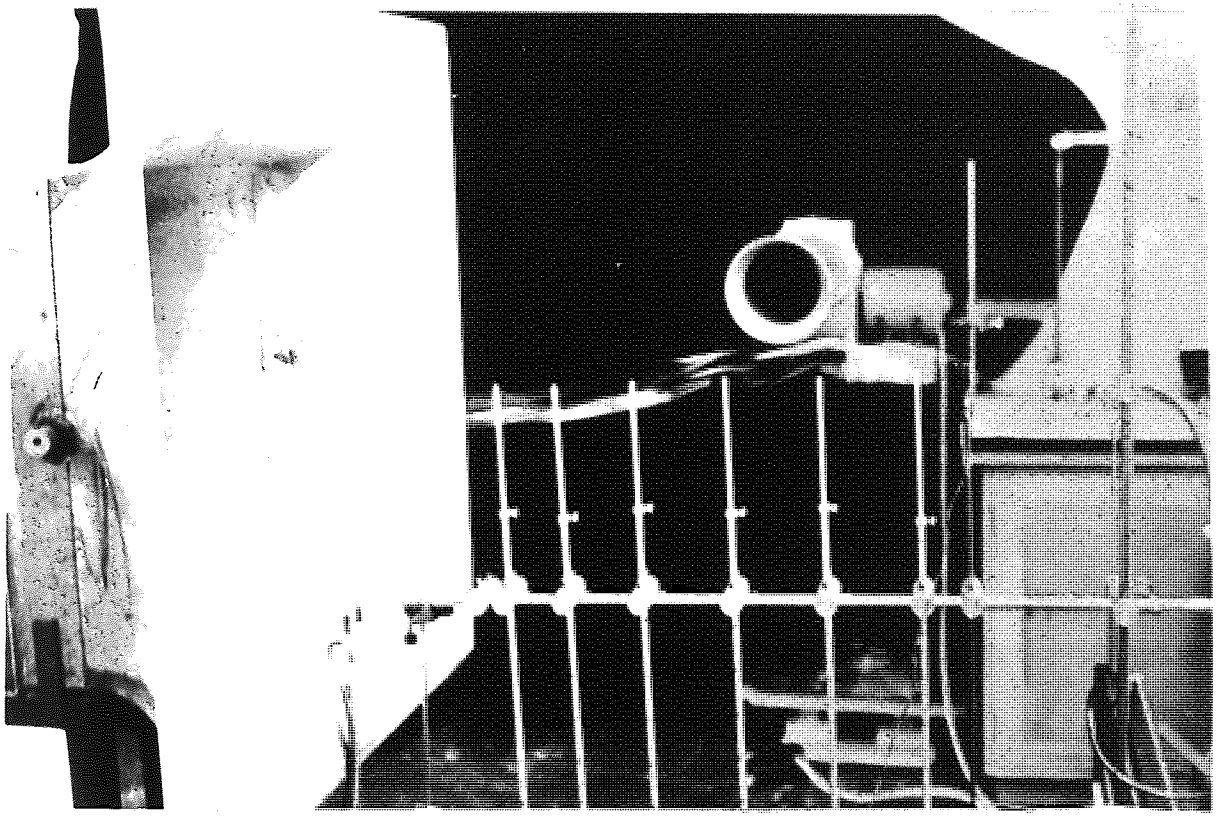

PLATE NO.19 This plate shows the shape of flange and the stream line of the capture of smoke in the centre line axis in front of square flanged hood.

CHAPTER SEVEN

EXPERIMENTAL RESULTS AND DISCUSSION

7.1 Introduction

Experimental data (see table 6.2) were collected by testing a range of different suction opening for different suction flows, different planes of measurement, different axis of measurement and different condition of opening (i.e. flanged or unflanged).
These data were treated statistically and graphically. The following sections are devoted to the description of the presentation, results and discussion of the study of the aerodynamic characteristics of suction openings.

7.2 Centre-Line Velocities

Since captor hoods ordinarly draw contaminated air from the area directly in front of the suction opening, the chief factor governing the suctinn efficiency is the distribution of air flow in this region, which flow is customarily represented by centre-line curves, the following are the results of centre-line velocity measurement and analysis.

7.2.1 Rectangular Duct No.1(see drawing No. 3)

Photographic plate No.4, Table 7.1 and Figures 7.1 to 7.19 are the measuring arrangement, best empirical formulae and graphical representation of data collected by testing the rectangular duct of aspect ratio 0.6 (ratio of small side to large side of opening) respectively.
The entries of the final empirical formulae in Table 7.1 are in descending order of testing the decision making criterion, (see Chapter six , section 6.3.1)
Figure 7.1 and 7.4 show the closeness of fit. Figure 7.2 and 7.6 show that the transformation of variable in order to check the linearity of relationship is not very satisfactory, especially for low suction flow. Figure 7.3 is the velocity versus a non-dimentional factor for a general comparison of velocity variation of different geometrical suction openings. Figure 7.5 shows the discrepancies of the observe, calculated and

Predicted velocities. Descriptions of other Figures will follow accordingly.

7.2.2. Discussion

The empirical formulae given in Table 7.1 are chosen from the others, on the basis of the decision criterion (see chapter 6, section 6.3, 6.4 and 6.5). The statistics of each model were ranked in order to find the best fit, least biased and most precise model. Measurement were taken for two conditions.

(i) Flow rate the same and position of measurement varied.

Treating this data for the curve fitting of models given by Table 2.1 and appendix 6.1 resulted entirely different equations. Table 7.1, column 3 contains these reconciled equations. For example Pruzner gives the following equation for the X/HR greater than 2

$$\frac{V}{V_{BA}} = \frac{(X/HR)^{-1.7}}{1+(X/HR)^{-1.7}} \qquad (7.1).$$

Whereas the analysis resulted the following:

$$\frac{V}{V_{BA}} = 0.29\ \frac{10.9\ (X/HR)^{-2.21}}{1+10.9\ (X/HR)^{-2.21}} \qquad (7.2).$$

For the X/HR=5 above equations resulted 0.0608 and 0.0687 for V/BA respectively, Which it means approx. 11.5% difference based on new equation. Figures 7.1 to 7.3 show the attenuation of centre-line velocity versus the distance.

(ii) The position of measurements kept unchanged, but the suction flow rates varied (i.e. Q=0.71 to 1.46 $m^3 s^{-1}$, see figures 7.4 and Table 7.2).

Table 7.1 columns 1 and 5 containe the new equation for the analysis. Equations in column 1 are for the analysis of data collected by above experiment. Reconciled equation for Pruzner model is as below:

$$\frac{V}{V_{BA}} = 0.39 \frac{11.28(X/HR)^{-2.38}}{1+11.28(X/HR)^{-2.38}} \qquad (7.3)$$

This equation results $V/V_{BA} = 0.0767$ for $X/HR=5$, which means an approximate 20.73% difference based on the equation.

The equations of column 5 of Table 7.1 are the results of analysis of the combined data of experiments (i) and (ii). The reconciled equation for Pruzner model is as follow:

$$\frac{V}{V_{BA}} = 0.66 \frac{3.82\ (X/HR)^{-2.129}}{1+3.82\ (X/HR)^{-2.129}} \qquad (7.4)$$

for $X/HR=5$, the ratio V/V_{BA} becomes 0.0728 which means an approximate 16.48% difference based on the results obtained by the application of new equation.

In practice in order to predict the centre line velocity in front of a rectangular suction opening of 0.6 and 0.048m aspect ratio and hydraulic readius respectively. Any of the equations given in column 5 Table 7.1 can be used without a significance difference of prediction.

Figures 7.1, 7.4 and 7.5 show the comparision of prediction and the observed velocities.

Figures 7.4 shows that the effect of flowrate is linear, and velocity attenuation lines are parallel. This suggests that the ratio of point velocty and average face velocity must be constant. Table 7.2 contains theses ratios (i.e. the row-values) which are practically the same and the column-values descreases as the distance of measure-ments from the centre of suction opening increases (i.e. as expected).

From Figure 7.5 it can be seen that DallaValle's equation gives low velocity, conversely Fletcher's formula results in high velocity and Pruzner's formula results in a better prediction but is not very close.

Finally, the following equation can be chosen equally as a reconciled mathematical expression for prediction of the centre line velocity variation in front of rectangular unflanged ducts of aspect ratio 0.6(HR=hydraulic radius of 0.048m).

$$\beta = 2.09(X/A)^{-0.07}$$

1 $$\alpha = 2.496(X)\ (AR)^{\beta}/\sqrt{A}$$

$$\frac{V}{V_{BA}} = 1/(1.52+8.65\alpha^2)$$

$$F=3.82(X/HR)^{-2.129} \qquad F=1.62(X/HR)^{-2.378}$$

2 $$\frac{V}{V_{BA}} = 0.66F/(1+F) \qquad \text{"OR"} \qquad V=0.697V_{BA}F/(0.255+1.775F)$$

$$F_1 = 1/(1+0.254((1+AR)/AR)^{0.98})$$

3 $$F = 0.18A^{1.01}X^{-2.129}F_1$$

$$\frac{V}{V_{BA}} = 0.66F/(1+F)$$

$$F = 8.011(X^2/A)^{1.065} + 1.51$$

4 $$\frac{V}{V_{BA}} = 1/F$$

The numbers of equations are referred to the types of models tested.

7.2.3 Rectangular Duct No.2 (Rec.2, see drawing No.3)
Figures 7.20 to 7.25 are the graphical representation of data collected by measuring the centre-line velocity in front of rectangular unflanged duct of aspect ratio 0.5 (HR=0.034m) for different suction flow rates. Figure 7.2.1 shows the prediction (i.e. $Q=0.97m^3s^{-1}$) of centre-line velocity using DallaVelle, Flectcher and Pruzner formulae as well as the prediction using the presently found empirical formulae (i.e. F=7.29) $F=7.29(X/HR)^{-2.34}$, $V=0.33V_{BA}\ F/(1+F)$, RMSR=0.136).

Figure 7.20 shows the general trend of centre-line velocity attenuation which is very much the same as the Figure 7.1. Table 7.1 also contains the best fitting empirical formulae for these data.(Column 7).

7.2.4 Discussion

The following equations are the reconciled empirical formulae for the prediction of centre-line velocity in front of unflanged rectangular ducts of aspect ratio 0.5(HR=0.034m)

$$F=7.29(X/HR)^{-2.34}$$

1 $$V=0.33\ V_{BA}F/(1+F)$$

$$\beta=-0.206(X/\ A)^{-3.24}$$

2 $$\alpha=1.26X(AR)^{\beta}/\sqrt{A}$$

$$V=V_{BA}/(8.5\alpha^{2}-0.903)$$

3 $$V=V_{BA}/(16.8X^{2.24}/A+2.999)$$

$$F1=1/(1+0.249((1-AR)/AR))$$

4 $$F=0.21A^{0.985}X^{-2.24}F1$$

$$V=0.33V_{BA}F/(1+F)$$

Same models, treatment and geometrical shape, but different aspect ratio and hydraulic radius and suction flowrates result in different parameters. For example the reconciled equation for Pruzner's formulae is as below

$$\frac{V}{V_{BA}}=0.33\ \frac{7.29(X/HR)^{-2.34}}{1+7.29(X/HR)^{-2.34}} \qquad (7.5)$$

Comparing equations 7.3 and 7.5 the parameters difference are obvious. The difference of parameters 0.39 and 0.33 and power indices -2.38 and -2.34 are not significant. Whereas the coefficients of (X/HR) 11.28 and 7.29 in equations 7.3 and 7.5 respectively are significantly different which is not due to the suction flowrate.

For example substituting 5 for X/HR in equation 7.5 results $V/V_{BA}=0.0479$. This means an approximate of 26.93

difference based on prediction obtained from equation 7.5 , which is slightly more than the % obtained by using equation 7.3. This differences is due to the difference on hydraulic radius 0.048m and 0.034m respectively for ducts of aspect ratio 0.6 and 0.5.

The root mean square residuals are higher than those for the treatment of previous duct centre line velocity data, but still are within the range of magnitude of ambient room air movement (i.e. zero to 0.5m s^{-1}). Comparing Figures 7.4 and 7.20 and 7.21 show that the centre line velocity at a chosen point and the same suction flow rate is different. This velocity is high corresponding to the high aspect ratio.
Looking at these Figures, it is clear that the general trend of velocity distribution for similar suction openings is the same.

Figure 7.22 shows that there is no significant difference between the velocity prediction by any of the equation 1 to 5. This Figure also shows that prediction by DallaValle, is low at closer points and high at further points from the opening, but does not deviate very much. On the other hand predictions by Pruzner and Fletcher are very much overestimated, but for the further points away from the suction opening the predictions are the same.

Figure 7.21 shows the prediction of centre-line velocity using the presently found formulae. It can be seen that the prediction results are overestimated for low suction flow rates, whereas the prediction is good for high suction flow rates. Finally in Figure 7.23 which shows the logarithm of velocities versus the logarithm of distances for different suction flow rate, the lines are not straight. Especially at the further distance points (e.g. points beyond 0.63m from the face of the openings) scatter is more. Comparing Figures 7.2, 7.6 (for suction opening of AR=0.6) with this Figure, it indicates that linearity is better for ducts of high aspect ratio. This discrepancy could be due to the experimental error rather than a dependence on the size of the suction opening.

7.2.5 Rectangular Ducts.

The independent measurements of centre-line velocities in front of two unflanged rectangular ducts (Rec.1 and Rec.2 see drawing No.3) were treated combindly Figure 7.26 is the graphical representation of data.
The following empirical formulae are the mathematical expressions of centre-line velocity with the variables related to the velocity.

$F=0.162(X/HR)^{-2.044}$

1 $V=11.13V_{BA}F/(1+F)$

RMSR=0.19

$\beta=-0.73(X/A)^{0.115}$

2 $\alpha=0.624X(AR)^{\beta}/\sqrt{A}$

$V=V_{BA}/(1.4+8.42\alpha^2)$

RMSR=0.11

$F=7.084X^{1.56}/A^{-3.566}$

3 $V=V_{BA}/F$

RMSR=0.18

$F1=1/(1+0.569((1-AR)/AR)^{1.225})$

4 $F=0.904A^{1.45}X^{-2.14}F1$ "OR" $\frac{1}{F1}=(1+1.034((1-AR)/AR)^{0.67})$

$V=0.64V_{BA}F/(1+F)$ $F=0.068X^{-2.019}A^{1.38}F1$

RMSR=0.1 $V=V_{BA}F/(1+F)$

RMSR=0.004

7.2.6 Discussion

The positions of centre-line velocity measurement for each duct under test operation was unchanged, only the suction flow rate was altered. After the completion of measurement recordings, line velocities in front of unflanged rectangular ducts, taking into account the effect of suction flow rates, and different aspect ratios and hydraulic radius (i.e. AR=0.5,0.6 and HR=0.034,0.048m).

Equation Nos. 2(Section 7.2.2), 1(Section 7.2.4) and 1 (above equation) are the arising empirical equations for the centre-line velocity measurement of tessing three rectangular suction openings by treating the data individually and combined respectively.

These are of the same mathematical model but with different parameters and root mean square residuals (RMSR). The power index of variable (X/HR) have the values 2.129, 2.34 and 2.044. These figures suggest that centre-line point velocity is inversely propertional to the square of the ratio of points distance from the centre of the suction opening to its hydraulic radius. Rearranging the equation 1 (Section 7.2.4) Yields:

$$V=1.8V_{BA}(X/HR)^{2.04}/(1+0.162(X/HR)^{2.04}) \qquad (7.6)$$

Figures 7.25, 7.26 show the prediction velocities using all the above equations. As the RMSR is a precision measure for curve fitting, i.e. the smaller the RMSR the better the fit of the data to the model. Consequently either the above or the following equation can be chosen as the best fitted model for the prediction of centre-line velocity in front of rectangular suction opening.

$$\frac{1}{F1} = 1+1.034((1-AR)/AR)^{0.67}$$

$$F=0.068X^{-2.019}{}_{A}{}^{1.38}{}_{F1}$$

$$V=V_{BA}F/(1+F)$$

Figure 7.25 shows the discrepancies of observed and predicted velocities by DallaValle, Pruzner and Fletcher formulae.

7.2.7 Rectangular Hood

This is a hood of dimension 0.25x1.145m, rectangular opening abruptly reduced to a round duct (see Drawing No.2). This hood has the smallest aspect ratio in comparison with the other suction openings (i.e.AR=0.218) and the highest hydraulic radius HR=0.103m). Analysing the data on centre-line velocities, measured in front of this hood, the following empirical formulae arise as the reconciled equation or the prediction of centre line velocity.

$$F = 0.33(X/HR)^{-2.55}$$

1 $$V = 28.96V_{BA}F/(1+F)$$

RMSR = 0.37

$$\beta = 0.72(X/A)^{-0.119}$$

$$\alpha = 2.48\ X\ (AR)^{\beta}/\sqrt{A}$$

2 $$V = V_{BA}/(8.645\alpha^2-0.238)$$

RMSR = 0.39

$$F_1=1/(1+0.352((1-AR)/AR)^{1.03})$$

3 $$F =0.0103A^{1.104}X^{-2.56}F_1$$

$$V =25.83V_{BA}F/(1+F)$$

RMSR = 0.4

$$V = V_{BA}/(8.13X^{2.24}/A-0.254)$$

4

RMSR = 0.37

$$F = 0.0082(D_{eq})^{2.148}X^{-2.56}$$

5 $$V = 23.96V_{BA}F/(1+F)$$

RMSR = 0.38

Figures 7.27, 7.28 and 7.29 are the graphical representations of centre-line velocity attenuation.

7.2.8 Discussion.

Figure 7.27 shows that the velocity attenuation is not very sharp, and suction flow rate has a fair linear effect on the attenuation. Figure 7.28 shows how prediction velocities calculated using DallaValle, Pruzner and Fletcher formulae, are all underestimated. Although Fletcher's prediction values do not deviate very much from the corresponding observed values they still are low. This Figure shows that the prediction velocities using the found formulae are very much closer to the corresponding observed centre-line velocity. Although the range of RMSR statistics is not very wide, each individual RMSR value is a bit high i.e.0.37 to 0.4 ms^{-1}. Figure 7.29 shows that the variable transformation does not indicate

a linear relationship between centre-line velocity versus the distance. Table 7.6 contains the best empirical formulae, resulting from treating the experimental centre-line velocities. These formulae show that the centre-line velocity is proportional to the inverse of the square of distance of the measurements.

7.2.9 Testing Round Duct No.1.

This is a round duct of 0.152 m diameter and hydraulic radious 0.038 m. The centre-line velocity along its axis was measured for a number of suction flow rates, (i.e. 1.255 m^3s^{-1} to 2.1 m^3s^{-1} for 7 different air flows). The following equations give the best fitting mathematical relationship of variables studied.

1

$$F = 3.497(X^2/A)^{1.86} + 9.73$$
$$V = V_{BA}/F$$
RMSR = 0.2

2

$$F = -0.031(D_{eq})^{2.21}X^{-0.874}$$
$$V = -9.39V_{BA}F/(1+F)$$
RMSR = 0.65

3

$$F = 0.33(D/X)^{0.915}D^{0.154}$$
$$V = V_{BA}F/(1+F)$$
RMSR = 0.64

4

$$\beta = 0.2(X/A)^{-0.33}$$
$$\alpha = 1.99\ X\ (AR)^{\beta}/\sqrt{A}$$
$$V = V_{BA}/(9.28+7.78\alpha^2)$$
RMSR = 0.4

5

$$F_1 = 1$$
$$F = -0.047A^{1.88}X^{-0.876}F_1$$
$$V = -18.35V_{BA}F/(1+F)$$
RMSR = 0.7

7.2.10 Discussion

Figures 7.30 to 7.32 are the graphical representation of data on centre-line velocity in front of round unflanged ducts (D=0.152m). Figure 7.30 shows that the decay of velocity versus distance from the centre of suction opening is not quite the same as for the rectangular duct (see Figures 7.4 for Q=1.255 m^3s^{-1} and 7.21, for Q=1.2m^3s^{-1}). As the distance increased the drop in velocity shaper than for the same point in front of the rectangular opening duct.

The band of the asymptotes of velocity attenuation in front of a round duct is narrower than that of the rectangular duct. This means that in this case the effect of increase of suction flow rates at further distances away from the centre of suction opening, is insignificant, whereas the case is different in front of rectangular suction openings.

Figure 7.31 shows that the calculated velocities using existing formulae for prediction of centre-line velocity in front of round ducts are either overestimates or underestiamtes. The RSMR statistics of different arising formulae are significatnly different. These differences are clear from the Figure 7.31. In this case testing the Silverman model gives a better fitted model to the observed velocities (Figure 7.31).

$$V=V_{BA}/(3.497((X^2/A)^{1.86}+9.78)$$

Figure 7.32 is a non-dimentional logarithmetic representation of centre-line velocity in front of this round unflanged duct. It is clear from this Figure and Figure 7.23, that the trend is not the same, which is namely due to the different shape of opening (i.e. round and rectangular).

Finally, the empirical formulae show that velocity is not proportional to the inverse square of distance as it is in the case of rectangular suction openings ducts and round ducts for corresponding equations, (See Table 7.1 columns referred to rectangular ducts and the round ducts for corresponding equations)

7.2.11 General Discussion

(i) Generally the treatment of the combined data collected from the measurement of centre-line velocities in front of two rectangulars and one round duct, yield the following mathematical relationships:

$$F=36.73(D_{eq}/X)^{0.815}D^{3.82}$$

1 $V=V_{BA}F/(1+F)$

RMSR=0.75

$$F=3.196(X^{0.89})/A+2.058$$

2 $V=V_{BA}^{F}$

RMSR=0.7

$$F=0.722(D_{eq})^{6.71}\ X^{-2.03}$$

3 $V=0.74V_{BA}F/(1+F)$

RMSR= 4.32

$$F=0.215(X/HR)^{-0.869}$$

4 $V=0.49V_{BA}F/(1+F)$

RMSR=0.83

$$F1=1/(1-0.42((1-AR)/AR)^{2.899})$$

5 $F=31.9A^{2.076}X^{-1.15}F1$

$V=0.33V_{BA}F/(1+F)$

RMSR=0.6

(ii) In order to find a most general formula for prediction of centre-line velocity in front of any shape of opening, any area any aspect ratio and any hydraulic reduis for different suction flow rates, the data on centre-line velocities were treated combindly. The

following formulae are the best empirical equation for the reconcilation, and the prediction of centre-line velocity in front of any shape of suction openings (i.e. rectangular openings of AR=0.218, 0.5, 0.6 and round duct D=0.152m of hydraulic radius 0.103m, 0.034m, 0.048m, 0.038m respecti-vely):

$$F=0.23(X/HR)^{-0.865}$$

1 $$V=0.47V_{BA}F/(1+F)$$

RMSR=1.17

$$F=1.775(D_{eq})^{10.05}X^{-2.064}$$

2 $$V=1.92V_{BA}F/(1.+F)$$

RMSR=4.4

$$F1=1/(1-0.097((1-AR)/AR)^{-0.826})$$

3 $$F=0.0035A^{1.396}X^{-2.66}F1$$

$$V=82.6V_{BA}F/(1+F)$$

RMSR=4.23

$$F=9.851(D/X)^{0.807}D^{3.106}$$

4 $$V=V_{BA}F/(1+F)$$

RMSR=0.86

$$V=V_{BA}/(27.7(X^2/A)^{0.45}+2.38)$$

5 RMSR=1.13

$$\beta=10.36(X/A)^{-0.765}$$

6 $$\alpha=1.952X(AR)^{\beta}/\sqrt{A}$$

$$V=V_{BA}/(4.283+110.96\alpha^2))$$

RMSR=0.9

Figure 7.33 shows how the observed velocities correspond to the predicted values for rectangular duct of aspect ratio 0.6, using the following equation:

$$F=0.23(X/HR)^{-0.865}$$

$$V=0.47V_{BA}F/(1+F)$$

$$RMSR=1.17$$

Table 7.10 contains the general empirical equations for the prediction of centre-line velocities in front of any type of suction duct, tested in this research.
Therefore above equation seem to be a good general equation for the prediction of centre-line velocity in front of unflanged suction opening.
In this equation the independent variables are average face velocity, the X-coordiante of the centre-line points and the hydraulic radius. The important role of the hydraulic radius is that, it is a factor of the combined effect of the size and the shape of the suction opening. As for the whole analysis of models studied, the independent and dependent variables were tried to be transfered into the non dimentional form, the ratio X/HR and V/V_{BA} in this equation are the examples. The practical application of this equation is that:

(i) In order to evaluate and apraise the suction velocity along the centre line in front of a known shape, and size of an existing opening the following measurements are required:

(a) Suction flow rate.

(b) The shape and the dimension of opening.

(c) The X-coordinate of the point at centre line axis.

The flow can be measured by flow meters, the shape and the size of opening can easily be known either by direct measurement or from the design information. Therefore a point velocity measurement can be compared to the corresponding predicted one.

(ii) At the design stage if the control area is defined, the type of the taxicity, the size, and the concentration of the contaminant are known a control point velocity may be decided accordingly. Therefore the designer requires to consider the following points:

(a) Average face velocity

(b) The shape and the size of the suction opening (i. e. HR)

Therefore the designer has more freedom on recommending the shape and the size of the suction opening and the flow rate.

7.3 Effect of flow rate on streamlines

A pressure tube (prandtl tube type 607, Appendix 7.1) was used to study the direction of streamlines. As previously mentioned, this tube was placed near the centre of the suction opening. The procedure was that if the tip of the tube is aligned with the direction of air movement then the pressure difference reading should be zero. The assumption is that the streamline along the centre-

line of the suction duct is a straight line and it is asymptote of the family of hyperbolic streamlines of common foci at the edge of the suction duct. The angle of tangent at the point of measurement on streamlines can be read off from the pointer fixed to the tube above the face of a protractor. When the pressure reading by manomenter was zero the reading of angle was recorded.

In Practice the streamline of suction was observed by the generation of smoke filament at the point of interest. The shape of the streamlines was consistently hyperbolic (see plates Nos. 9 and 11) irrespective of the shape of the opening and the opening conditions (i. e. flanged or unflanged).

At a fixed point in front of a rectangular opening, the measurement was undertaken for a number of different suction flow rates in order to study the effect of flow rate on corresponding streamlines. As the flow rate was increased the angle of streamline from the asymptote (i. e. centre-line axis) was decreased. As the surface area of po tential surface was the same and only the flow of suction was varied, the velocity at this point, theoretically must change directly proportional to the flow rates. This relationship is shown in Figures 7. 6 and 7. 8. The latter is the flow rate-streamline relationship. As can be seen from this Figure, the streamlines passed through a fixed point in front of the suction opening for different suction flow rate are asymptotic to the centre-line streamline (i. e. centre-line axis). Hence, as the flow rate increase the streamlines passing at a known point (i. e. position of pressure tube) will separate

from the centre-line axis. This means that the angle of the tangent to the streamline with X-axis will increase. consequently the increase of flow rate corresponds to widening the suction affected area along the Z-axis. Assuming the velocity distribution lines in Figures 7.6 are straight, then Figure 7.7 can be produced. The vertical axis represents the intercept value of the velocity-distance lines with the right hand vertical line of Figure 7.6 The right hand vertical line of Figure 7.6. The Figure 7.7. shows that the increase in flow rate will increase the centre point velocity linearly.

7.4 Effect of Geometric Shape of Suction Opening

The centre-line velocities of all openings studied, do differ in their distribution in the suction affected area. The Figure 7.34 shows the effect of geometric shape of opening on centre-line velocities of round, rectangular and square ducts for the same position of velocity measurement, and an equal suction flow rate. As can be seen for an equal flow of suction at a fixed point of velocity measurement for different rectangula suction opening, (i. e. different aspect ratio (AR) and hydraulic radius (HR) velocity is higher corresponding to high values of AR or HR In the case of sound suction ducts centre-line velocities at the same points for an equal flow of suction, are higher corresponding to the high diameter of suction opening. Figure 7.34 shows that for the square bell-mouth flanged duct the velocity distribution at the points along the centre-line axis does not fall off very sharply. The distribution of centre-line point velocity in front of a sqaure bell-mouth flanged duct of which its squared cross-

section has an area equal to a rectangular opening which is abruptly reduced to a round duct, is consistently lower than the velocity in front of rectangular hood (Figure 7.34). This means that for two openings of equal area, drawing equal volume of air, the centre-line velocity at the same distance from the face in front of duct with low AR, is greater than in front of duct of high AR. Although square hood is flanged but later on it will be shown that this difference is not only due to the flanges.

7.5 Effect of Flanges.

In Chapter Four it was stated that in the case of an aperture in the wall, the wall can be assumed as a flat plane flange for a horizontally placed duct. Thus the streamlines are of the form of hyperbolae. Photographic plate Nos.9,11 (Chap.6) show the tendency of movement of a smoke filament toward the suction opening which confirms the validity of the hyperbola assumption. The study of the size of flange was not the objective of this research, the conventional size was chosen, the purpose of this experiment was to simulate a large enough flat flange to the suction opening in order to satisfy approximately the unlimited flange assumption considered in Chapter Four. The following is the description of the test.

7.5.1 Centre-line Velocity in Front of Flanged Rectangular Duct.

(i) Flanged rectangular duct Rec 1 (see Drawing No. 3) For a number of different suction flow rates, the centre-line velocity was measured. The Table 7.4 contains the empirical equation obtained from the analysis of data.

Figures 7.14 and 7.16 show the illustrations of the effect of flange on the centre-line velocity. It can be seen that the effect of the flange is clearly obvious and at distances close to the opening a more than 50% increase was observed. Apart from this increase, the affected area in front of flanged suction duct will increase. Figure 7.36 shows that velocity distance lines

are not linear. Figures 7.35 to 7.38 show the effect of flow rate on the centre line velocity in front of flanged duct. Comparing Figures 7.4 and 7.35 it is clear that the flow effect is the same for flanged. This means that the relationship of suction flow rate and point velocity is linear and direct. Figure 7.35 shows that the velocities at the same point in front of the suction duct, are reduced in proportion as the volume flows of suctions are decreased. In the case of flanged ducts, the asymptote band is slightly wider than in the unflanged cases.

(ii) Flanged Rectangular duct No.2. Figures 7.24, 7.39 and 7.40 show the effect of flange on centre-line velocity in front of a rectangular duct of aspect ratio 0.5. Figure 7.39 also shows the velocity distributed along the centre-line axis in front of an unflanged duct of aspect ratio 0.5 as well as the centre-line velocity for different flow of suctions. This Figure shows that at a point of distance greater than 0.51 m, velocity in front of anunflanged duct is higher than in front of a flanged duct but not by very much, this could well be due to experimental error.

On Figure 7.40 the predicted centre-line velocities using different empirical equations are plotted too. Table 7.5 contains the empirical equations for flanged and unflanged rectangular duct of aspect ratio 0.5. The statistic RMSRsof all these fitted equations are small and very close together. This means that the velocity prediction with either of these equations does not differ significantly. Almost all of these equations overestimate the centre-line velocity in front of flanged rectangular ducts (i.e. AR = 0.5). The overestimation increases with distance.

7.5.2 Effect of Flange on Centre-line Velocity in Front of Rectangular Hood.

Table 7.6 contains all the empirical equations for centre-line velocity in front of the flanged rectangular hood, which reduced abruptly to a round duct(i.e.AR = 0.218, HR = 0.103 m). Figures 7.41 , and 7.42 are the graphical representations of data. Figure 7.41 is the illustration of velocity versus a non-dimensional value (X/HR) for general comparison. Figure 7.42 shows the variation of velocity at centre-line points for different flows of suctions. It shows that the velocity attenuation is gradual and smooth. The velocity does not reach to a minimum at a distance unlike in unflanged cases. For two nearly equal suction flow rates (i.e. Q = 1.944 $m^3 s^{-1}$ and 2.01 $m^3 s^{-1}$) the centre-line velocities were plotted in this graph. As can be seen in the case of unflanged hoods, the velocity drops very sharply at distances up to 0.30 m whereas, for flanged hoods the velocity decreases very gradually. For the region up to 0.37 m distance from the centre of opening, the velocity in the case of an unflanged hood is higher than for its flanged counterpart. This observation in the case of this hood is mainly due to the shape, length and diameter of the opening, reduction throat and round duct size. In the case of the unflanged hood the air rushes into the duct from all directions, therefore the vortex at centre plane and at the vertical central area is higher than in the case of the flanged hood. In the case of flanged hoods there is no suction beyond the edge of the suction duct.

The other effect of the flange is the increase of velocity at farther points along the centre axis compared with the unflanged case. This means a better suction at greater distance. Flanges also widen the asymptote band, and increase of flow rate corresponds to the increase of velocity at farther distance than the unflanged hood.

Although the RMSR statistics of curve fitting of each model are very close together, they are very high compared with unflanged cases. This means that though the results of the application of each model are very similar, they all result either in overestimations or underestimations as the case may be. Figure Rehf 2 shows how a model for high flow rate results in over-estimation and conversely in underestimation for low suction flow rates.

7.5.3 Effect of Flange on Centre-line Velocity in Front of a Round Duct.

In this case a round duct of diameter 0.152 m was flanged with a flat plane flange of 0.608 m by 0.915 m size. (see Fig 4.1) The measurement of centre-line velocity was carried out for a number of suction flow rates. Figures 7.43 and 7.44 are the graphical representations of collected data. These date were analysed statistically. Table 7.7 contains all flanged and un-flanged empirical formulae for the prediction of centre-line suction velocities.

Figure 7.43 shows how a flanged affects the centre-line velocity in front of round ducts. The velocity at a point on centre-line axis for 1.255 $m^3 s^{-1}$ flow of suction through un-flanged duct is very much lower than the velocity at the same point on the centre-line axis for 1.06 $m^3 s^{-1}$ suction flow rate through the flanged duct.

The decay of velocity in front of a flanged round duct is very smooth and gradual whereas it is very sharp and sudden in the case of an unflanged duct. The suction affected area is ex-tended in front of the flanged duct considerably compared with the unflanged duct. Even at the far distance point in front of the flanged duct the suction centre line velocity is nearly 30% more

than with unflanged duct cases (i.e.velocities at 0.71m is 0.285ms^{-1} and at 0.723m is 0.08ms^{-1}, for 1.06m^{3}s^{-1} and 1.255m^{3}s^{-1}for flanged and unflanged ducts respectively). Figure 7.43 shows the plot of velocities obtained using the Drkal theoretical formula. It can be seen that the velocities are overestimation for points of distance less than D and underestimation otherwise. The following equation produced a better fit to the data than the others.

$$V = V_{BA}/(7.76(X^2/A)^{0.86}+1.82)$$
$$RMSR = 0.85 \text{ ms}^{-1}$$

Figure 7.43 shows the closeness of the fit. Figure 7.44 shows the effect of flow of suctions on centre-line velocity distribution. As it was expected the effect of various flow rates on the centre-line velocity in front of flanged round duct is the same as the unflanged round duct.

7.5.4 Centre-line velocity in front of a square bell mouth flanged opening.

The centre-line velocity in front of square shape opening for various suction flowrates was measured. A total of 189 sets of readings was treated, following equations were found:

$$\frac{V}{V_{BA}} = \frac{1}{1+9.01(X/HR)^{1.87}}$$

RMSR = 0.0729,

Both above equations are for the case $X/HR < 2$

"OR"

$$F=0.31(X/HR)^{-0.98}$$
$$V=0.96V_{BA}F/(1+0.31F)$$
$$RMSR = 0.048$$

$$\beta = 0.175(X/\sqrt{A})^{-0.39}$$
$$\alpha = (x/\sqrt{A})(AR)^{-\beta}$$
$$V = V_{BA}/(0.64+2.01\alpha^{1.29})$$
$$RMSR = 0.085$$

7.6 General Empirical Formulae For Flanged Suction Openings.

The analysis of the combination of data collected from each individual experiment on different geometry flanged suction opening was performed. The following are the findings of each combination.

7.6.1 The Treatment of Data from Rectangular Flanged Duct (AR = 0.6) and Rectangular Flanged Hood (AR = 0.218)

A similar test and models of analysis result in the following:-

$$F = 89.72(X/HR)^{-3.0028}$$

1 $$V = 0.34V_{BA}F/(1+F)$$

$$RMSR = 0.795$$

$$F = 4.108(X^2/A)^{1.085} + 2.77$$

2 $$V = V_{BA}/F$$

$$RMSR = 0.676$$

$$F = 11.31\ X^{3.018}/A+2.78$$

3 $$V = V_{BA}/F$$

$$RMSR = 0.789$$

$$\beta = -0.58(X/A)^{-1.122}$$

4 $$\alpha = 0.916(AR)^{\beta}X/\sqrt{A}$$

$$V = V_{BA}/(12.033\alpha^2-4.65)$$

$$RMSR = 0.7$$

$$F_1 = 1/(1+0.1036((1-AR)/AR)^{0.84})$$

5 $$F = 0.4086(A)^{1.23}X^{-3.36}F_1$$

$$V = 0.336V_{BA}F/(1+F)$$

$$RMSR = 0.81$$

Figure 7.45 shows the predicted and observed velocity plots for different suction flow rates. As it shows, the following equation is a better fitting empirical formula for the observed velocity in front of flat plane flanged rectangular suction openings (i.e. AR = 0.5, 0.218 (for flange sizes see Figure 4.1 and Drawing No. 2)).

$$F = 11.31X^{3.018}/A+2.78$$

$$V = V_{BA}/F$$

$$RMSR = 0.8\ m\ s^{-1}$$

7.6.2 Velocity in Front of Flanged Round and Rectangular Hoods.

Figure 7.46 and 7.47 are the plots of the combined data collected from the measurement of velocity in front of round flanged and rectangular hoods with flat plane flanged suction openings for different suction flow rate. The following are the preferred empirical formulae:-

1

$$F_1 = 1/(1+0.1225((1-AR)/AR)^{0.96})$$
$$F = 0.52\,A^{1.071}X^{-1.746}F_1$$
$$V = 0.548V_{BA}F/(F+1)$$
$$RMSR = 0.96$$

2

$$F = 2.09(X/HR)^{-1.65}$$
$$V = 0.55V_{BA}F/(1+F)$$
$$RMSR = 1.12$$

3

$$V = V_{BA}/(5.46X^{1.81}/A+1.84) \quad \text{"OR"} \quad V=V_{BA}/(1.83+7.54(X^2/A)^{0.869})$$
$$RMSR = 0.95 \qquad\qquad RMSR = 0.96$$

4

$$\frac{V}{V_{BA}-V} = 1.337X^{-2.21}A^{2.57}/(1+0.038((1-AR)/AR)^{0.24}),$$
$$RMSR = 0.225$$

5

$$\beta = 0.074(X/A)^{0.178}$$
$$\alpha = 0.947(AR)^{\beta}X/\sqrt{A}$$
$$V = V_{BA}/(1.87+9.53\alpha^2)$$
$$RMSR = 0.987$$

6

$$F = 1.0019(D_{eq})^{2.634}X^{-1.75}$$
$$V = 0.55\,V_{BA}F/(1+F)$$
$$RMSR = 0.95$$

7

$$F = 0.375(D_{eq}/X)^{0.909}(D_{eq})^{0.701}$$
$$V = V_{BA}F/(1+F)$$
$$RMSR = 1.42$$

Figures 7.46 and 7.47 show how good the fit is for predicted velocities calculated from the empirical equation with the observed values. Consequently the following seems to be the best one:

$$V = V_{BA}/(1.83+7.54(X^2/A)^{0.869})$$
$$RMSR = 0.96$$

7.6.3 Test of Rectangular Flanged and Round Flanged Suction Openings.

A similar combination of data for testing the rectangular flanged duct and round flanged duct yield the following empirical equations:

$$F = 1.79(X/HR)^{-1.54}$$

1 $$V = 0.56V_{BA}F/(1+F)$$

RMSR = 0.9

$$V = V_{BA}/(7.13(X^2/A)^{0.807}+1.8)$$

2

RMSR = 0.812

$$V = V_{BA}/(3.46X^{-1.63}/A+1.8)$$

3

RMSR = 0.78

Figure 7.48 shows how close the predicted values of velocities are to the observed values.

7.6.4 Centre-line Velocity in Front of all Shapes of Suction Openings.

Finally the treatment of the combined data from the experiments of centre-line velocity measurement of all flat plate flanged and geometrically different suction openings, yield the general empirical formulae given by Table 7.9. Figure 7.49 gives the plots of observed and predicted velocities. It can be seen from this Figure how well the empirical formulae fit the observed values. Equations with low RMSR give the best fit and the following is the preferred one:-

$$F_1 = 1/(1+0.075((1-AR)/AR)^{3.16})$$

$$F = 3.42A^{1.58}X^{-1.8}F_1$$

$$V = 0.54V_{BA}F/(1+F)$$

RMSR = 0.86

The following equations are only marginally worse than the above one.

$$F = 7.016(X^2/A)^{0.818} + 1.81$$

$$V = V_{BA}/F$$

RMSR = 0.902

$$F = 1.001(D_{eq})^{2.45}X^{-1.61}$$

$$V = 0.56V_{BA}F/(1+F)$$

RMSR = 0.915

7.6.5 Effect of Geometry of the Flanged Suction Opening.

For an equal flow rate, the centre-line velocity along the centre-line axis at the same points of measurements in front of flanged suction openings of different geometry was measured. Figure 7.50 illustrates the centre-line velocity decay for an equal suction flow rate in front of flanged, round (D = 0.152 m), rectangular ducts (AR = 0.5,0.6), rectangular hood (AR = 0.218), and square hood (AR = 1). This Figure shows that:

i) Centre-line velocity in front of the round duct for most distances is higher than the velocity in front of other suction openings, whereas the reverse was the case for the unflanged suction opening (see Figure 7.34).

ii) Flanged rectangular opening of higher aspect ratio induced higher centre-line velocity except at points very close to the opening.

iii) For two flanged suction openings of equal area (of opening without flange and different aspect ratio (i.e. AR = 0.218 and 1) for an equal suction flow rate, the hood with low aspect ratio, induces higher velocity along the centre-line than the other, which is a confirmation of conclusion drawn by Fletcher (1978).

7.7 Symmetry Test.

For a known suction flow rate measurements of velocity at geometrical symmetry points in XOZ and XOY planes were undertaken. Figure 7.10 shows that the velocity distribution at symmetry points is nearly symmetrical. The comparison of Figures 7.4 and 7.10 shows that the trend of velocity decay remains the same for centre-line velocity and symmetry points velocity distribution for points of measurements in a horizontal plane. Figure shows the velocity distribution at symmetry points, and taking into account the execution, the instrument and measurement

errors, the distributions are very nearly symmetrical. This Figure supports the claim made by looking at the Figure 7.10 about the symmetry velocity distribution in a horizontal plane at symmetry points.

For the same flow of suction, measurement of velocity at vertical plane symmetry points was undertaken. Figures 7.13 and 7.15 are the graphical representation of measured data. These figures show that the general trend of velocity decay at a distance is the same as centre-line velocity decay. In the vertical plane, points of measurements are symmetrical geometrically but are not symmetrical aerodynamically (Figure 7.15). Due to this difference, apart from the experimental error, velocity distribution at vertical symmetry points do not show consistency, in some contrast to the reasonable consistency for the horizontal symmetry points.

In the case of round suction openings, owing to their axial symmetry, velocity at symmetry points in suction affected area should be the same. Figures 7.51 and 7.52 clearly show this fact.

7.8 Contour Lines.

In any plane in the region of the suction affected area, locus points of equal velocity may be drawn. Representation of aerodynamic characteristics of suction opening by means of contour lines offer a fairly simple means of comparing graphically various types of suction openings. Figures 7.53 and 7.54 are the centre-planes measuring points and graphical depiction of contour surface and contour line respectively. Contour line in one centre-plane determines the shape of contour surface of round suction openings, owing to their axial symmetry. For a geometrically similar suction opening with changes in the magnitude of suction flow rate,

the geometrical form of potential and streamlines are unchanged. In cases of square and rectangular suction openings, however, the distribution of air flow at the corners differs from the distribution in the centre-plane. The effect of the corners is to reduce the effective area of the opening which results in a general outward displacement of contour lines as compared with those for round openings of the same area (DallaValle 1931). There is a flattening of contour line along the long side and a corresponding shortening in the plane bisecting the short side (Ibid). Along the axis there is an inward displacement of contour lines as compared with round opening having the same area (Ibid). An increase in the area of the opening, with the geometric shape remaining the same, causes an outward displacement of the contour lines at right angles to the axis of the opening (Ibid).

DallaValle concluded that there is a considerable advantage to be gained in using a large opening for the collection of contaminated air at some distance from the suction opening. Also he concludes that a large opening not only gives a wider and better contour distribution for the same quantity of flow, but reduces the loss of energy at the suction opening entrance.

The effect of the extent of the abruptness of the connection of suction opening to the main duct of exhaust system on the distribution and shape of the velocity contours is of importance since the location of hoods often limits the amount of transition space available.

The procedure for the preparation of contour lines is that, first velocity-distance curves for a number of 2-dimensional centre-plane points will be prepared (Figures 7.10, 7.15 7.55 and 7.56), then by extrapolation, the coordinates of the equal velocity points will be obtained (Figure 7.55). The following

sections are the descriptions of contour line considerations of suction openings under test.

7.8.1 Contour Lines for Square Bell-Mouth Flanged Hood.

This square hood has a flanged face opening of $0.7921m^2$ area. Drawing $0.83m^3s^{-1}$ air through it gives the centre-plane velocity distribution as Figure 7.55 Extrapolating the coordinates of points of equal velocities of 0.5, 1, 1.2 and 1.4 ms^{-1} from Figure 7.55 and plotting these coordinates in another chart (Figure 7.56) by joining the equal velocity points, the contour line will be drawn. This Figure shows that the lines at short distances from suction openings are very flat which is a confirmation of points made by DallaValle. If one wishes to use this hood to control a known contaminant with a nominal capture velocity and a known area and distribution of pollutant generation, it is necessary to position the source of pollutant somewhere in the area of the appropriate contour-line and the suction face. This placing of contaminant source means that any airborne material released at this area will be subjected to a velocity equal or greater than the figure of corresponding contour velocity.

7.8.2 Contour Lines for Rectangular Opening.

Figure 7.9 was prepared in a similar manner as the above procedure. Also for the rectangular suction opening contour surfaces cannot be created by the rotation of contour lines in one plane, therefore it is required to prepare two centre-plane contour lines.

Figure 7.19 clearly shows that the equipotential lines are of different shapes according to the distances from the suction opening.

7.8.3 Contour Lines for Round Duct with Bell-shape Flange.

A compact ventilation rig was designed and constructed at the early stage of research. Figure 7.59 shows the main duct and the different flange arrangements. Figures 7.57 and 7.58 are the XY-centre-plane velocity-distance curve and the contour lines respectively. Comparing Figures 7.9, 7.56 and 7.58 it will be clear that there is no obvious similarity between these contour lines, mainly because of the difference of size, shape and flange condition.

7.8.4 Effect of the type of the Flange.

Figure 7.59 shows the flange types to fit the round suction ducts. The actual flange openings areas are approximately the same. For a fixed fan setting and different suction opening conditions, centre-line velocity and suction flow rates were measured. As the figure shows, suction flow rates for different opening conditions are different (see inserted values along the centre-line axis of duct). This means that the flange will cause a significant change in resistance to the suction system. This is another confirmation of a point stated by DallaValle about transition and high entry loss due to flange. Although the suction flow rates for equivelocity lines of Figures 7.59 and 7.61 is different, yet comparison of the shape and curvature of lines will show the effect of bell mouth flange on the suction velocity distribution. Consequently the effect of flange depends upon its size, shape and the angle of fitting to the suction opening.

7.8.5 Matching the theoretical sense and practical values.

There is a need for one simple method directing and helping to reconcile the theoretical pattern and experimental plotted pattern, and closing the ubiquitous gap between practice and theory. The hypothesis employed and the models used were based on the ellipsoidal

and hyperbolic potential and stream functions. To prove the correspondence, the measuring points were located on the perimeters of ellipses centred at the centre of the suction duct opening with all ellipses having common foci at the edge of the duct. The following descriptions are based on the analysis of experimental data.

(i) Rectangular Opening. Table 7.11 contains the XZ-plane, ellipse locus points velocity measurement in front of a rectangular duct.The duct was unflanged, and velocities were measured with identical measurements for a fixed flow of suction. The area of ellipsoid bounded by the walls of the duct was calculated for each contour line (column 5 Table 7.11). Then the equivelocity of each contour was calculated accordingly, (see column 6 Table 7.11). This velocity was compared with the average measured velocties at the locus of ellipse contour line. Column 8 of Table 7.11 gives the percentage deviation on average measured velocities. The columns 5,6 and 8 also contain the corresponding sphere surface area of $\frac{3\pi}{2}$ radians revolution of a circular contour line velocity and percentage deviation respectively. As these percentage values show, the elliptical contour lines seem a better depiction of equivelocity points in front of unflanged rectangular suction ducts. Data were fitted to a conic curve in the XZ-plane. For a fixed fan pitch angle testing unflanged and flanged opening (i.e. different suction flow rate and different system pressure loss) the velocity measurements at ellipse locus point was treated equally. The following equations were obtained:

$$\frac{V}{V_{BA}} = \frac{Z^2}{1.68} - \frac{X^2}{5.643E13} \quad (Q = 1.506 m^2 s^{-1}, RMSR=0.03, unflanged)$$

and

$$V = \frac{Z^2}{0.021} - \frac{X^2}{2.37}, \quad (Q = 1.28 m^3 s^{-1}, RMSR=1.31, flanged)$$

Consequently for flanged ducts the hypothesis of hyperbola seems to be valid.

A set of 164 velocity readings in the XZ-plane on the locus points of ellipses in front of rectangular flanged suction opening was analysed. The following mathematical relations have been found

(i) contd.

1 $$\frac{V}{V_{BA}} = \frac{X^2}{53.1} + \frac{Z^2}{2.02}$$

RMSR = 0.034

2 $$F = (1+1.034((1-AR)/AR)^{1.085})$$

$$P_1 = 0.91\ X^{-1.5}\ A^{1.28}/F$$

$$V = P_1 V_{BA}/(1+P_1)$$

RMSR = 0.016

3 $$F = 0.1185(D_{eq}/X)^{1.55} D^{0.029}$$

$$V = V_{BA} F/(1+F)$$

RMSR = 0.52

4 $$F_1 = 1/(1+0.217((1-AR)/AR)^{1.004})$$

$$F = 0.445A^{0.8}X^{-3.73}F_1$$

$$V = 0.084V_{BA}F/(1+F)$$

RMSR = 0.47

5 $$F = 2420.9(X/HR)^{-3.73}$$

$$V = 0.084V_{BA}F/(1+F)$$

RMSR = 0.46

A combined velocity measurement in XZ- and XY-planes in front of flanged and unflanged rectangular ducts is treated too yielding the following equations:-

6 $$\frac{V}{V_{BA}} = \frac{X^2}{10.51} + \frac{Y^2}{0.75} + \frac{Z^2}{3.67}$$

RMSR = 0.161 (Unflanged rectangular AR = 0.5)

and

7 $$\frac{V}{V_{BA}} = \frac{X^2}{35.63} + \frac{Y^2}{6.07} + \frac{Z^2}{35.8}$$

RMSR = 0.03 (Flanged rectangular AR = 0.5)

Equation (6) shows that although RMSR (corresponding to the unflanged duct) is low enough to justify the closeness of fit the locus points are not the surface of an ellipsoid or sphere. On the other hand in the case of flanged ducts (i.e. equation (7)), the fit is very good, also because the parameters of X^2, Z^2 are nearly equal therefore the locus points are the surface of an ellipsoid, which is a confirmation of the hypothetical assumption (see earlier chapters).

(ii) Round Opening (unflanged).

The procedure of velocity measurement on the locus of an ellipse is the same as that previously mentioned for the rectangular duct. Table 7.12 shows the comparison of measured and theoretically expected velocities. It can be seen that at locus points of ellipses of semi-minor axis

less than the diameter of the suction opening, ellipsoidal potential surfaces give a better representation than the spherical surfaces. On the other hand when the semi-minor axis of ellipse locus points are

greater than the diameter of the suction duct, the spherical surfaces give a better representation of the potential surfaces.

7.9 Effect of Extraneous Air Movement on Hood Performance.

Extraneous air movement is a haphazard and unstable air current of unknown origin. It may be moving toward the suction opening, or in the opposite direction to the suction, or crossing the suction flow field at any angle with respect to the suction opening centre-line axis. The degree of the effect of extraneous air movement depends on the magnitude of its movement or its flow rates and the angle of interaction. Therefore, the effect can be in favour (positive) unfavour (negative) or inert (neutral). The unfavourable effect is of some concern. In the industrial situation, the estimation of existing extraneous current is not possible. Any information on the aerodynamic behaviour of extraneous air movement is intuitive and rule of thumb. Therefore, laboratory simulation is not possible.

In this research, a blower was used as a source of extraneous air current. A small wind tunnel was used as blower

device (Appendix 5.2). The outlet duct was short enough to locate it easily. The blower outlet was placed at a known, fixed position (i.e. 0.66 m, 0.001 m, -1.13 m) relative to the centre of the suction opening. Figure B1 shows the arrangement of the test and the velocity profile of blower.

7.9.1 Test Method

In order to study the effect of draught on the flow pattern of suction, the blower was positioned at a known place and with its inlet damper it was set to a fixed volume blowrate. The position and blowrate were kept the same for all the suction opening testings. The average face velocity of blow was 3.1 ms^{-1} (the area of flanged blower outlet is 0.028 m^2) The AVM502 air velocity meters were fixed in series to the carriage and in operation the carriage was moved inward and outward to the suction or blower opening and velocity readings were recorded. The velocity in the XZ-plane was measured. Four types of velocity measurement was undertaken:

i) Blow velocity in XZ-plane,

ii) Suction velocity in XZ-plane

iii) Suction opening-centre-plane velocity measurement both for blow velocity and suction velocity individually

iv) Combined suction-blow velocity in XZ-plane

In order to visualize the suction and suction-blow flow field, smoke was generated at points in the potential field. Picture plate No's 7 to 19 (Chapter 6) are the illustrations of streamlines in front of different suction openings. Plate Nos. 5 to 7 show the effect of suction flow rate, and the distance of the suction opening from the source

of the smoke cloud. Plate 5 shows the smoke cloud after the travel of a distance which moves from the effect of the initial velocity of generation, starts to rise vertically in the calm room ambient conditions. Plate 6 shows how this cloud is sucked inward. As the distance from the suction opening decreases, the cloud's density will decrease and eventually turn to thin line traces. In order to see the effect of distance on the suction efficiency, the source of smoke generation was moved away. Plate No.7 shows this effect. As can be seen, the smoke cloud at distances 0.86m downward is effectively sucked, and at further distances, the suction efficiency will reduce significantly. Plates 8.1(a), 8.1(b), 8.1(c) (Chapter 6) show how the distance and suction flow rate affect the suction efficiency. Plates 8.1(a) and 8.1(b) show the effect of distance on suction efficiency. Plate 8.1(c), 8.2(a), 8.2(b) show how a small increase of suction flow rate, increases the suction efficiency. Plates Nos.12,13,15,16 (Chapter 6) show the suction effect in front of rectangular suction openings. Plates 12 and 13 show how the smoke cloud in the zone of the suction-blow flow field is dispersed and suction efficiency reduced by the existence of the cross blow. Plates 15,16 and 17 show how smoke rises in the clam condition, is sucked inward by the application of suction and suction stream lines are diverted due to the cross blow respectively.

Figures 7.62, 7.14, 7.17, 7.18, 7.63, 7.64, 7.65, 7.66 and 7.67 are the graphical representations of velocity measurements in front of rectangular suction openings unflanged and flanged respectively.

7.9.2 Discussion

Figure 7.62 shows the profile of blow velocity in the area in front of suction opening.

Figure 7.14 is the blow velocity profile along the

centre-line axis of the suction opening, which shows how velocity increases as the points of measurement get nearer to the position of blow opening axis and then after reaching its peak (i.e. around 3 ms^{-1}) decreases as the points goes away from this axis. Figures 7.17 and 7.18 are the resultant velocity distribution and the resultant velocity variation in the XZ-plane at symmetry points of the blow-suction flow field (i.e. suction flow rate = 1.28 $m^3 s^{-1}$ and blow flow as before) respectively. As it should be in the case of suction the velocity at symmetry points are equal, whereas looking at Figure 7.17 it can be seen that the blow flow has violated this symmetry condition. For example velocity at point (0.21 m, 0.001 m, -0.2 m) is the maximum whereas in the case of suction flow only the peak velocity corresponds to the point (0.2 m, 0.001 m, 0.0 m) (i.e. point at suction centre-line axis).

The effect of blow on suction is followed as combining two flow fields. Fig. 7.17 shows the variation of the resultant velocity at symmetry points. As the points moved at the positive direction along the Z-axis, effect of blow field decreases. Points around the intersection of centre-lines (i.e. x = 0.66 m, y=0.001m, z = 0.0m) are subjected to the highest blow velocity and relatively high centre-line point velocity. Therefore the direction of the movement of resultant velocity at this region will be the direction of highest velocity component. Hence, for points in the region of negative direction of Z-axis, blow field and suction field both are nearly in the same direction extended up to the suction centre-line region so that the resultant velocities will increase (i.e. favourable condition or at least for the points in the region of $x \leq 0.66$ m and $z \leq 0.0$ m). For the points in the region $z \geq 0.0$ m suction flow is in the opposite direction to the blow flow. Therefore, the

resultant is under the effect of the direction of the dominant flow.

The condition of the points in this region is different due to their distance from the suction face. Because the suction effect at farther distant points is less (i.e. as it was found inversely proportional to the square of distance), this effect can be seen by looking at points of positive Z in Figure 7.17 . Therefore, if one wishes to place a source of contaminant in the region of this combined flow field, this figure can be some guide of how the airborne material is going to be subjected to the resultant velocity. Figure 7.18 shows the actual variation of the velocity of this combined flow field. This figure also shows the region of the minimum combined velocity(at points in the region of 0.46m), positive velicity (at points with $x \leq 0.40$m) and negative velocity region. Therefore, the suction efficiency of this combined flow fields will be zero for the points at the minimum and negative velocity regions, and increases as the points move away from the minimum velocity regions to the positive velocity region.

Figure 7.5 shows how suction flow rate will broaden the positive velocity region and reduce the maximum escape velocity (i.e. see intersection points of blow centre-line axis and velocity curve for $Q = 1.68\ m^3s^{-1}$).

Figure 7.64 is the suction velocity profile in front of flanged rectangular duct for $1.4\ m^3s^{-1}$ flow of suction. Superimposing this figure and Figure B1, one can trace the resultant velocity paths. Figure 7.7 is the graphical comparison of suction and suction-blow velocity variation at suction centre-line points.

Figure 7.66 is the variation of the velocity of the combined suction-blow flow field in XY-plane in front of a flanged

rectangular suction opening. Although the velocity variation in the XY-plane in front of a rectangular suction opening is different from velocity variation in the XZ-plane, still the combined flow of suction and blow has the same trend of resultant velocity as the previous experiment (i.e. Figure 7.63). Figure 7.67 is the XY-centre-plane combined velocity variation in front of rectangular flat flanged duct (i.e. AR = 0.5).

The position of blower and the blow flowrate is the same as the other experiments. As the blow duct is axially symmetrical and blow affected area is conical, therefore, deformation of the curves in Figure 7.67 compared with Figure 7.17 is mainly due to the difference of velocity variation between the two centre planes XZ and XY.

The curves in Figure 7.67 show that if a source of contaminant be placed in the XY-plane at a known coorcinate (i.e. x = 0.655m, z = 0.001m) any airborne particles will be subjected to the corresponding velocity to the y coordinate of the curve points (i.e. minimum velocity of 0.28 ms^{-1} and maximum velocity of 0.625 ms^{-1} corresponding to y = 0.24m and 0.049m respectively).

Due to the unknown character of real states of extraneous air movement, treatment of the combined velocity of suction-blow flow field was not undertaken in order to find a generalized mathematical formula.Nevertheless,the graphical representation of data showed that, in order to study the effect of extraneous air movement,first one needs to identify, monitor and measure the air velocity and prepare the velocity profile curve for extraneous air movement. Then assuming the velocity profile of suction flow is known and unchanged, superimposing these profiles the effect of extraneous air movement will be illustrated graphically. Consequently the positive region will

be identified and the effectiveness of suction in case of interaction of any air movement will be appraised.

TABLE 7.1 Empirical formulae for centre line velocity in front of different geometrically shaped suction opening

(UNFLANGED)

Rectangular duct AR = 0.6 CENREC1 various flow rate	RM SR	Rectangular duct AR = 0.6 ONE FLOW REXY1	RM SR	Rectangular duct AR = 0.6 CE126	RM SR	Rectangular duct AR = 0.5	RM SR
$F=0.248(D_{eq})^{2.056}X^{-2.38}$ $V=0.39V_{BA}F/(1+F)$	0.09	$F=7.15(X^2/A)^{1.104}+3.423$ $V=V_{BA}/F$	0.04	$\beta=2.09(X/A)^{-0.09}$ $\alpha=2.496X(AR)^{\beta}/\sqrt{A}$ $V=V_{BA}/(1.52+8.65\alpha^2)$	0.09	$F=7.29(X/HR)^{-2.34}$ $V=0.33V_{BA}F/(1+F)$	0.14
$F=11.28(X/HR)^{-2.38}$ $V=0.39V_{BA}F/(1+F)$	0.09	$F=0.15(D/X)^{1.97}D^{0.17}$ $V=V_{BA}F/(1+F)$	0.05	$F=3.82(X/HR)^{-2.129}$ $F=0.66V_{BA}F/(1+F)$	0.09	$F_1=1/(1+0.249(1-AR)/AR))$ $F=0.21A^{0.985}X^{-2.24}F_1$ $V=0.33V_{BA}F/(1+F)$	0.14
$F=12.03X^{2.36}/A+2.55$ V_{BA}/F	0.09	$F=10.9(X/HR)^{-2.21}$ $V=0.29V_{BA}F/(1+F)$	0.04	$F_1=1/(1+0.254((1-AR)/AR)^{0.98})$ $F=0.18A^{1.01}X^{-2.129}F_1$ $V=0.66V_{BA}F/(1+F)$	0.10	$F=10.57(X^2/A)^{1.1197}+2.999$ $V=V_{BA}/F$	0.14
$F=0.165(D/X)^{2.01}D^{0.16}$ $V=V_{BA}F/(1+F)$	0.09	$F=0.37(D_{eq})^{2.015}X^{-2.21}$ $V=0.29V_{BA}F/(1+F)$	0.04	$F=8.011(X^2/A)^{1.065}+1.51$ $V=V_{BA}/F$	0.09	$\beta=0.206(X/A)^{-3.24}$ $\alpha=1.26X(AR)^{\beta}/\sqrt{A}$ $F=1/(8.52\alpha^2-0.903$ $V=V_{BA}F$	0.14
$F=0.313A^{0.96}X^{-2.38}F_1$ $F_1=1$ $V=0.39V_{BA}F/(1+F)$	0.09	$F=10.02X^{2.21}/A^{+3.42}$ $V=V_{BA}/F$	0.04	$\frac{V}{V_{BA}-V}=P_1$ $F=1+0.998((1-AR)/AR)^{0.976}$ $P_1=0.85X^{-2.01}A^{1.496}/F$	0.004	$F=16.8X^{2.24}/A+2.999$ $V=V_{BA}/F$	0,14
$\beta=0.2(X/A)^{-0.33}$ $\alpha=1.088X(AR)^{\beta}/\sqrt{A}$ $V=V_{BA}/(1.065+19.69\alpha^2)$	0.114	$F=10.02X^{2.21}/A^{+3.42}$ $V=V_{BA}/F$	0.04			$F=0.23(Deq)^{2.06}X^{-2.24}$ $V=0.33V_{BA}F/(1+F)$	0.138
$F=1.62(X/HR)^{-2.38}$ $V=0.697V_{BA}F/(0.255+1.77F)$	0.09	$F_1=1$ $F=0.38A^{0.88}X^{-2.21}F_1$ $V=0.29V_{BA}F(1+F)$	0.04	$F=9.88X^{2.129}/A+1.51$ $V=V_{BA}/F$	0.088		
		$\beta=0.2(X/A)^{-0.33}$ $\alpha=1.104X(AR)/\sqrt{A}$ $V=V_{BA}/(1.58+20.06\alpha^2)$	0.05	$F=0.18(D_{eq})^{2.07}X^{-2.129}$ $V=0.664V_{BA}F/(1+F)$	0.088		
				$F=0.18(D_{eq}/X)^{2.04}D^{0.164}$ $V=V_{BA}F/(1+F)$	0.089		

TABLE 7.1 Continued (1)

Combination of AR=0.6,05		Rectangular Hood AR = 0.218		Round duct AR=1,D=0.152M	
UFCE56	R_N SRS	BOLO	RM SR	URS152N	RM SR
$P_1 = 0.0684X^{-2.019}A^{1.36}/F$ $F = (1+1.034((1-AR)/AR)^{0.6})$ $V=PV_{BA}/(1+P_1)$	0.004	$\beta = 0.72(X/A)^{0.129}$ $\alpha = 2.48(AR)^{\beta}X/\sqrt{A}$ $V = V_{BA}/(8.645\alpha^2-0.238)$	C.39	$F=3.497(X^2/A)^{1.86}+9.78$ $V=V_{BA}/F$	0.2
$\beta=-0.73(X/A)^{0.115}$ $\alpha= 0.624(AR)^{\beta}/\sqrt{A}$ $V= V_{BA}/(1.4+8.48\alpha^2)$	0.11	$F = 8.13X^{2.24}/A-0.254$ $V = V_{BA}/F$	0.37	$F=0.033(D/X)^{0.92}D^{0.154}$ $V=V_{BA}F/(1+F)$	0.64
$F_1=1/(1+0.569((1-AR)/AR)^{1.23})$ $F =0.904(A)^{1.45}X^{-2.14}F_1$ $V =0.636V_{BA}F/(1+F)$	0.11	$F_1= 1/(1+ 0.35((1-AR)/AR))$ $F = 0.0103A^{1.104}X^{-2.56}F_1$ $V = 25.83V_{BA}F/(1+F)$	0.40	$F=-0.031(D_{eq})^{2.21}X^{-0.87}$ $V=-9.39V_{BA}F/(1+F)$	0.65
$F =0.914(D_{eq})^{3.024}X^{2.14}$ $V = 0.636V_{BA}F/(1+F)$	0.11	$F = 0.33(X/HR)^{-2.54}$ $V = 28.9V_{BA}F/(1+F)$	0.37	$\beta=0.2(X/A)^{-0.33}$ $\alpha=1.99(AR)^{\beta}X/\sqrt{A}$ $V=V_{BA}/(9.28+7.7\alpha^2)$	0.38
$F = 0.48(D/X)^{2.05}D^{0.82}$ $V = V_{BA}F/(1+F)$	0.11	$F = 6.99(X^2/A)^{1.121}-0.254$ $V = V_{BA}/F$	0.37	$V=V_{BA}\left(1-\frac{X/D}{\sqrt{(X/D)^{1.36}-0032}}\right)$	671.7
$F = 0.162(X/HR)^{-2.074}$ $V = 11.13V_{BA}F/(1+F)$	0.19	$F = 0.008(D_{eq})^{2.146}X^{-2.56}$ $V = 23.96V_{BA}F/(1+F)$	0.38		
$F = 7.085X^{1.562}/A-3.566$ $V = V_{BA}/F$	0.18				

TABLE 7.1 Continued (2)

Combination of AR=0.5, 0.6, 1(D=0.152) UFCES56RO	RMSR
$F = 36.73(D/X)^{0.815}D^{3.82}$ $V = V_{BA}F/(1+F)$	0.85
$P_1 = 2.015X^{-1.284}A^{1.979}/F$ $F = 1-0.799((1-AR)/AR)^{0.17})$ $P_1 = V_{oo}/(100-V_{oo})$ $V_{oo} = 100V_o, V_o=V/V_{BA}$	0.016
$F = 3.196(X^{0.89})/A+2.058$ $V = V_{BA}/F$	0.70
$F = 0.215(X/HR)^{-0.869}$ $V = 0.49V_{BA}F(1+F)$	0.83
$F_1=1/(1-0.42((1-AR)/AR)^{2.9})$ $F = 31.9A^{2.08}X^{-1.15}F_1$ $V = 0.33V_{BA}F/(1+F)$	0.60
$F = 28.73(X^2/A)^{0.45}+2.24$ $V = V_{BA}/F$	0.80

TABLE 7.1 Continued (3)

Rectangular Hood (AR=0.218) and Round ducts (0.152m)	RM SR	Rectangular (AR=0.6,0.5) and Rectangular Hood	RM SR	Combination of tests on Round D=0.152 and Rectangular AR=0.6,0.5,0.218	RM SR	Round ducts, Rectangular ducts and Rectangular hood are tested for equal flow of suction.	RM S^R
UFRHRON		UF56RH		UFCEALL		QQES	
$V=V_{BA}/(4.18(X^{0.79}/A)-3.87)$	0.6	$V=V_{BA}/(7.23(X^{1.67}/A)-1.99)$	0.327	$F=0.228(X/HR)^{-0.865}$ $V=0.474V_{BA}F/(1+F)$	1.17	$F_1=1/(1+0.561((1-AR)/AR)^{0.00007})$ $F=0.006A^{-0.37}X^{-1.987}F_1$ $V=1.58V_{BA}F/(1+F)$	0.2614
$F=11.214(D/X)^{0.96}D^{3.29}$ $V=V_{BA}F/(1+F)$	0.9	$F_1=1/(1+0.0936((1-AR)/AR)^{0.828})$ $F=0.0046A^{1.43}X^{-2.056}F_1$ $V=86.99V_{BA}F/(1+F)$	0.235	$F=1.775(D_{eq})^{10.05}X^{-2.064}$ $V=1.92V_{BA}F/(1+F)$	4.42	$F=(1+0.995((1-AR)/AR)^{1.0004})$ $P_1=1.17X^{-0.587}A^{0.3191}/F$ $P_1=V_{oo}/(100-V_{oo})$ $V_{oo}=100V_o, V_o=V/V_{BA}$	5.23
$V=V_{BA}/(2.26(X^2/A)^{2.28}+9.52)$	1.21	$\beta=0.288(X/A)^{-0.893}$ $\alpha=1.025(AR)^{\beta}X/\sqrt{A}$ $V=V_{BA}/(0.0723+11.08\alpha^2)$	0.26	$F=9.85(D/X)^{0.807}D^{3.11}$ $V=V_{BA}F/(1+F)$	0.86		
$\beta=73.97(X/A)^{35.79}$ $\alpha=1.129(AR)^{\beta}X/\sqrt{A}$ $V=V_{BA}/(6.112+9.128\alpha^2)$	1.82	$F=0.0102(D_{eq})^{3.33}X^{-1.99}$ $V=105.05FV_{BA}/(1+F)$	0.27	$F=27.7(X^2/A)^{0.45}+2.38$ $V=V_{BA}F/(1+F)$	1.13	$F=0.0007(D_{eq})^{-0.728}X^{-1.51}$ $V=15.47V_{BA}F/(1+F)$	0.342
		$V=V_{BA}/(12.64(X^2/A)^{0.97}-1.989)$	0.327	$F=2.33X^{0.635}/A-2.075$ $V=V_{BA}/F$	0.804	$\beta=-0.4116(X/A)^{-0.4376}$ $\alpha=0.5612X(AR)^{\beta}/\sqrt{A}$ $V=V_{BA}/(1.138+9.55\alpha^2)$	1.023
		$F=2.45(D/X)^{2.24}D^{1.72}$ $V=V_{BA}F/(1+F)$	1.62	$\beta=10.36(X/A)^{-0.765}$ $\alpha=1.052X(AR)^{\beta}/\sqrt{A}$ $V=V_{BA}/(4.283+110.97\alpha^2)$	0.935	$F=0.016(X/HR)^{-0.748}$ $V=46.02V_{BA}F/(1+F)$	0.945
		$F=0.043(X/HR)^{-2.725}$ $V=V_{BA}(126.6)F/(1+F)$	0.74			$V=V_{BA}(4.9(X^2/A)^{0.257}-0.735)$	0.986
						$F=0.024(D/X)^{2.696}D^{-3.59}$ $V=V_{BA}F/(1+F)$.	0.38

TABLE 7.2 **Variation of flow rates and the ratio of point velocity to the average face velocity.**

X Coordinate of point of measurement (metres)	Q Flow rate $m^3 s^{-1}$				
	0.71	1.12	1.25	1.37	1.46
	Ratio of point to average face velocity				
0.25	0.061	0.072	0.071	0.072	0.074
0.355	0.032	0.035	0.035	0.035	0.036
0.455	0.016	0.019	0.0197	0.0199	0.0195
0.555	0.011	0.011	0.0127	0.0129	0.0128
0.61	0.008	0.0101	0.01045	0.0114	0.0115

TABLE 7.3 Centre-line velocity in front of flat plane flanged suction openings.

Rectangular duct AR = 0.6 FS9V7	RM SR
$F=0.0056(D_{eq})^{2.08}X^{-2.76}$ $V=19.35V_{BA}F/(1+F)$	0.268
$F_1=1/(1+1.02((1-AR)/AR)^{0.99})$ $F=0.0219A^{1.23}X^{-2.76}F_1$ $V=14.57V_{BA}F/(1+F)$	0.279
$\beta=0.2(X/A)^{-0.33}$ $\alpha=1.347X(AR)/\sqrt{A}$ $V=V_{BA}/(12.32\alpha^2-8.38)$	0.22
$F=0.692(X/HR)^{-2.76}$ $V=21.99V_{BA}F/(1+F)$	0.263
$F=0.531(D/X)^{2.893}D^{0.18}$ $V=V_{BA}F/(1+F)$	0.275
$V=V_{BA}/(34.44(X^2/A)^{0.46}-40.5)$	0.176
$F=6.041X^{0.927}/A-40.5$ $V=V_{BA}/F$	0.176

Rectangular duct AR = 0.5 XYF5480	RM SR
$F=0.0327(D_{eq})^{1.96}X^{-2.44}$ $V=0.2986V_{BA}F/(1+F)$	0.089
$F_1=1/(1+0.236((1-AR)/AR))$ $F=0.279A^{0.98}X^{-2.44}F_1$ $V=0.2986V_{BA}F/(1+F)$	0.094
$F=4.837(X^2/A)^{1.22}+3.34$ $V=V_{BA}/F$	0.088
$\beta=23.61(X/A)^{-1.45}$ $\alpha=1.14X(AR)^{\beta}/\sqrt{A}$ $V=V_{BA}/(7.79+8.51\alpha^2)$	0.089
$F=0.252(D/X)^{2.22}D^{0.149}$ $V=V_{BA}F/(1+F)$	0.09
$F=11.33X^{2.44}/A+3.35$ $V=V_{BA}/F$	0.088

Rectangular hood AR = 0.218 FFRHCEN	RM SR
$F=0.11574(D/X)^{1.43}D^{-0.593}$ $V=V_{BA}F/(1+F)$	1.167
$F_1=1/(1+0.93((1-AR)/AR)^{0.9})$ $F=0.707A^{0.92}X^{-3.68}F_1$ $V=0.325V_{BA}F/(1+F)$	1.163
$F=0.37(D_{eq})^{2.1}X^{-3.68}$ $V=0.32V_{BA}F/(1+F)$	1.117
$F=15.4X^{-3.68}/A+3.07$ $V=V_{BA}/F$	1.096
$\beta=0.2(X/A)^{-0.33}$ $\alpha=X(AR)^{0.112}/\sqrt{A}$ $V=V_{BA}/(2.187+8.46\alpha^2)$	1.2
$F=246.03(X/HR)^{-3.68}$ $V=0.325V_{BA}F/(1+F)$	1.096

Round SRFC152	RM SR
$F=4.48X^{1.73}/A+1.82$ $V=V_{BA}/F$	0.85
$F=7.76(X^2/A)^{0.86}+1.82$ $V=V_{BA}F$	0.85
$F=2.073(X/HR)^{-1.72}$ $V=0.55V_{BA}F/(1+F)$	0.85
$F=0.362(D_{eq})^{2.07}X^{-1.72}$ $V=0.55V_{BA}F/(1+F)$	0.86
$F_1=1/(1+(1-AR)/AR))$ $F=0.031A^{0.36}X^{-1.73}F_1$ $V=0.55V_{BA}F/(1+F)$	0.86
$\beta=0.2(X/A)^{-0.33}$ $\alpha=0.95X(AR)^{\beta}/\sqrt{A}$ $V=V_{BA}/(1.87+9.53\alpha^2)$	0.923

TABLE 7.3 Continued (2)

Rectangular duct and Rectangular Hood AR = 0.6, 0.218 FL6RE	RMSR
$F=89.72(X/HR)^{-3.003}$ $V=0.34V_{BA}F/(1+F)$	0.795
$F=0.174(D/X)^{1.7}D^{-0.075}$ $V=V_{BA}F/(1+F)$	0.896
$F=11.31X^{3.018}/A+2.78$ $V=V_{BA}/F$	0.789
$F=4.108(X^2/A)^{1.085}+2.77$ $V=V_{BA}/F$	0.876
$\beta=-0.58(X/A)^{-1.122}$ $\alpha=0.916X(AR)^{\beta}/\sqrt{A}$ $V=V_{BA}/(12.03\alpha^2-14.65)$	0.703
$F_1=1/(1+0.104((1-AR)/AR)^{0.84})$ $F=0.4086(A)^{1.23}X^{-3.36}F_1$ $F=0.336V_{BA}F/(1+F)$	0.806

Rectangular and Round suction opening AR=0.6, 1(D=0.152m)	RMSR
$F=3.46X^{1.63}/A+1.8$ $V=V_{BA}/F$	0.78
$F=1.79(X/HR)^{-1.54}$ $V=0.56\ V_{BA}F/(1+F)$	0.9
$F_1=1/(1-0.44((1-AR)/AR)^{21.56})$ $F=2.883\ A^{1.53}X^{-1.8}\ F_1$ $V=0.54V_{BA}F/(1+F)$	0.76
$\beta=6.83(X/A)^{-1.32}$ $\alpha=0.938(AR)^{\beta}X/\sqrt{A}$ $V=V_{BA}/(9.53\alpha^2+1.76)$	0.9
$F=0.155(D/X)^{0.91}D^{0.235}$ $V=V_{BA}F/(HF)$	1.32
$F=7.13(X^2/A)^{0.81}+1.8$ $V=V_{BA}/F$	0.812

TABLE 7.3 (Continued 2)

Centre-line velocity in front of flat plate flanged suction openings

Rectangular Hood and Round duct AR=0.218,1(D=152 m)	RM SR
$F_1 = 1/(1+0.12((1-AR)/AR)^{0.9590})$ $F = 0.52A^{1.07}X^{-1.746}F_1$ $V = 0.548V_{BA}F/(1+F)$	0.96
$F = 2.09(X/HR)^{-1.65}$ $V = 0.55V_{BA}F/(1+F)$	1.12
$V = V_{BA}/(5.46X^{1.81}/A+1.84)$	0.95
$V = V_{BA}/(7.54(X^2/A)^{0.87}+1.83)$	0.96
$\beta = 0.074(X/A)^{0.178}$ $\alpha = 0.95X(AR)^{\beta}/\sqrt{A}$ $V = V_{BA}/(1.87+9.53\alpha^3)$	
$F = 0.375(D/X)^{0.91}D^{0.7}$ $F = V_{BA}F/(1+F)$	1.42
$\frac{V}{V_{BA}-V} = 28.7(D_{eq})^{7.1}X^{-2.213}$	0.222
$F = 1/(1+0.038((1-AR)/AR)^{0.241})$ $\frac{V}{V_{BA}-V} = 1.54X^{-2.21}A^{2.57}/F$	0.225
Rectangular Duct,Rectangular Hood Round duct,AR=0.6,0.218,2(D=0.152)	RMSR
FL6RERO	
$F=4.47(X)^{1.74}/A+1.83$ $V=V_{BA}/F$	0. 899
$F=1.001(D_{eq})^{2.46}X^{-1.61}$ $V=0.56V_{BA}F/(1+F)$	0.915
$\beta=0.2(X/A)^{-0.33}$, $\alpha=0.94X(AR)^{\beta}/\sqrt{A}$ $V=V_{BA}/(1.88+8.98\alpha^2)$	0.969
$F=1.925(X/HR)^{-1.53}$, $V=0.56V_{BA}F/(1+F)$	1.05
$F=0.37(D/X)^{0.92}D^{0.715}$ $V=V_{BA}F/(1+F)$	1.29
$F_1=1/(1+0.075((1-AR)/AR)^{3.16})$ $F =3.42(A)^{1.58}X^{-1.8}F1$ $V =0.54V_{BA}F/(1+F)$	0.86

TABLE 7.4 *Empirical formulae for centre-line velocity in front of rectangular duct (AR = 0.6, HR= 0.048 M, Area =0.039 M^2, D_{eq} = 0.191 M)*

Order	Unflanged suction opening	Root Mean Square Residual	Flat plane flanged opening	Root Mean Square Residual
1	$F = 3.82(X/HR)^{-2.129}$ $V = 0.66V_{BA}F/(1+F)$	0.09	$F = 0.692(X/HR)^{-2.76}$ $V = 21.99V_{BA}F/(1+F)$	0.263
2	$F_1 = 1/(1+0.25((1-AR)/AR)^{0.98})$ $F = 0.18A^{1.01}X^{-2.129}F_1$ $V = 0.66V_{BA}F/(1+F)$	0.1	$F_1 = 1/(1+1.02((1-AR)/AR)^{0.98})$ $F = 0.0219A^{1.23}X^{-2.76}F_1$ $V = 14.57V_{BA}F/(1+F)$	0.279
3	$\beta = 2.09(X/A)^{-0.07}$ $\alpha = 2.496(AR)^{\beta} X/\sqrt{A}$ $V = V_{BA}/(1.52+8.65\alpha^2)$	0.09	$\beta = 0.2(X/A)^{-0.33}$ $\alpha = 1.347(AR)X/\sqrt{A}$ $V = V_{BA}/(12.32\alpha^2-8.38)$	0.22
4	$F = 8.011(X^2/A)^{1.065}+1.51$ $V = V_{BA}/F$	0.09	$F = 34.44(X^2/A)^{0.46}-4.05$ $V = V_{BA}/F$, $X^2/A \geq 1.44$	0.176
5	$F = 0.18(D_{eq})^{2.07}X^{-2.129}$ $V = 0.66V_{BA}F/(1+F)$	0.088	$F = 0.0056(D_{eq})^{2.08}X^{-2.76}$ $V = 19.35V_{BA}F/(1+F)$	0.268
6	$F = 0.16(D_{eq}/x)^{2.04}D_{eq}^{0.164}$ $V = V_{BA}F/(1+F)$	0.089	$F = 0.531(D_{eq}/X)^{2.893}D_{eq}^{0.18}$ $V = V_{BA}F/(1+F)$	0.275

TABLE 7.5 Centre-line velocity in front of rectangular duct (AR = 0.5, HR = 0.034 M, Area = 0.021 M^2, D_{eq} = 0.135 M)

Order	Unflanged	Root Mean Square Residual	Flanged (plane flat 0.61 m by 0.81 m	Root Mean Square Residual
1	$F = 7.29(X/HR)^{-2.34}$ $V = 0.33V_{BA}F/(1+F)$	0.14	Overflow detected during the last iteration	
2	$F_1 = 1/(1+0.249((1-AR)/AR)$ $F = 0.21A^{0.985}X^{-2.24}F_1$ $V = 0.33V_{BA}F/(1+F)$	0.14	$F_1 = 1/(1+0.236((1-AR)/AR))$ $F = 0.279A^{0.98}X^{-2.44}F_1$ $V = 0.299V_{BA}F/(1+F)$	0.094
3	$\beta = -0.206(X/A)^{-3.24}$ $\alpha = 1.26X(AR)^{\beta}/\sqrt{A}$ $F = 1/(8.52\alpha^2-0.903)$, $V=V_{BA}/F$	0.14	$\beta = 23.61(X/A)^{-1.46}$ $\alpha = 1.14(AR)^{\beta}\ X/\sqrt{A}$ $V = V_{BA}/(7.79+8.51\alpha^2)$	0.089
4	$F = 16.8X^{2.24}/A+2.999$ $V = V_{BA}/F$	0.14	$F = 11.33X^{2.44}/A+3.35$ $V = V_{BA}/F$	0.088
5	$F = 0.231(D_{eq})^{2.057}X^{-2.24}$ $V = 0.33V_{BA}F(1+F)$	0.138	$F = 0.0327(D_{eq})^{1.98}X^{-2.44}$ $V = 0.2986(V_{BA})F/(1+F)$	0.089
6	$F = 0.13(D/X)^{2.12}D_{eq}^{0.17}$; $D=D_{eq}$ $V = V_{BA}F/(1+F)$	0.136	$F = 0.252(D/X)^{2.22}D^{0.149}$ $V = V_{BA}F(1+F)$, $D = D_{eq}$.	0.09

TABLE 7.6 Centre-line velocity in front of rectangular hood (AR = 0.218, HR = 0.103 M, Area = 0.286 M^2, D_{eq} = 0.41 M)

	Unflanged	Root Mean Square Residual	Flat plane flanged (1.24m by 2.145m)	Root Mean Square Residual
1	$F = 0.33(X/HR)^{-2.54}$ $V = 28.9V_{BA}F/(1+F)$	0.37	$F = 246.03(X/HR)^{-3.68}$ $V = 0.325V_{BA}F/(1+F)$	1.096
2	$F_1 = 1/(1+0.35((1-AR)/AR)^{1.03})$ $F=0.0103A^{1.104}X^{-2.56}F_1$ $V = 25.83V_{BA}F/(1+F)$	0.4	$F_1 = 1/(1+0.93((1-AR)/AR)^{0.9})$ $F = 0.707A^{0.92}X^{-3.68}F_1$ $V = 0.325\ V_{BA}F/(1+F)$	1.163
3	$\beta = 0.72(X/A)^{-0.119}$ $\alpha = 2.48(AR)^{\beta}X/\sqrt{A}$ $V = V_{BA}/(8.64\alpha^2-0.238)$	0.39	$\beta = 0.2(X/A)^{-0.33}$ $\alpha = x(AR)^{0.112}/\sqrt{A}$ $V = V_{BA}/(2.187+8.46\alpha^2)$	1.2
4	$F = 8.13X^{2.24}/A-0.254$ $V = V_{BA}/F$	0.37	$F = 15.4X^{-3.62}/A+3.07$ $V = V_{BA}/F$	1.096
5	$F = 0.008(D_{eq})^{2.148}X^{-2.56}$ $V = 23.96V_{BA}F/(HF)$	0.38	$F = 0.37(D_{eq})^{2.1}X^{-3.68}$ $V = 0.32V_{BA}F/(1+F)$	1.117
6	$F = 0.5(D/X)^{4.923}D^{0.17}$ $V = V_{BA}F(1+F), D = D_{eq}$	0.504	$F = 0.1157(D_{eq}/X)^{1.43}D_{eq}^{-0.503}$ $V = V_{BA}F/(1+F)$	1.167

TABLE 7.7 Centre-line velocity in front of round duct (D = 0.152 M, AR = 1, Area = 0.018 M^2)

	Unflanged	Root Mean Square Residual	Flanged (Flat Plane 0.608 m by 0.913 m	Root Mean Square Residual
1	Some of the predictions are zero		$F = 2.073(X/HR)^{-1.72}$ $V = 0.55V_{BA}F/(1+F)$	0.85
2	$F_1 = 1/(1+0.259((1-AR)/AR))$ $F = -0.047A^{0.86}X^{-0.876}F_1$ $V = -18.35V_{BA}F/(1+F)$	0.66	$F_1 = 1/(1+((1-AR/AR))$ $F = 0.031A^{0.36}X^{1.73}F_1$ $V = 0.55V_{BA}F/(1+F)$	0.86
3	$\beta = 0.2(X/A)^{-0.33}$ $\alpha = 1.99(AR)^{\beta}X/\sqrt{A}$ $V = V_{BA}/(9.28+7.78\alpha^2)$	0.381	$\beta = 0.2(X/A)^{-0.33}$ $\alpha = 0.95X(AR)^{\beta}/\sqrt{A}$ $V = V_{BA}/(1.87+9.53\alpha^2)$	0.923
4	$F = 3.497(X^2/A)^{1.86}+9.78$ $V = V_{BA}/F$	0.2	$F = 7.76(X^2/A)^{0.86}+1.82$ $V = V_{BA}/F$	0.85
5	$F = -0.0307(D_{eq})^{2.21}X^{-0.874}$ $V = -9.39V_{BA}F/(1+F)$	0.65	$F = 0.362(D_{eq})^{2.07}X^{-1.72}$ $V = -0.55V_{BA}F/(1+F)$	0.86
6	$F = 0.033(D_{eq}/X)^{0.915}D_{eq}^{0.154}$ $V = V_{BA}F/(1+F)$	0.636	$F = 0.13(D_{eq}/X)^{0.904}D_{eq}^{0.135}$ $V = V_{BA}F/(1+F)$	1.53

TABLE 7.8 Centre-line velocity in front of rectangular ducts (AR = 0.6,0.5)

	Unflanged	Root Mean Square Residual
1	$F = 0.162(X/HR)^{-2.07}$ $V = 11.13V_{BA}F/(1+F)$	0.19
2	$F_1 = 1/(1+0.569((1-AR)/AR)^{1.23})$ $F = 0.904(A)^{1.45}X^{-2.14}F_1$ $V = 0.636V_{BA}F/(1+F)$	0.11
3	$\beta = -0.73(X/A)^{0.115}$ $\alpha = 0.624(AR)^{\beta}X/\sqrt{A}$ $V = V_{BA}/(1.4+8.48\alpha^2)$	0.11
4	$F = 7.085X^{1.56}/A-3.566$ $V = V_{BA}/F$	0.18
5	$F = 0.48(D_{eq}/X)^{2.05}D_{eq}^{0.82}$ $V = V_{BA}F/(1+F)$	0.108
6	$F = 0.914(D_{eq})^{3.024}X^{-2.14}$ $V = 0.636V_{BA}F/(1+F)$	0.108

TABLE 7.9 Centre-line velocity in front of rectangular openings (AR = 0.6,0.50 and 0.218)

	Unflanged	Root Mean Square Residual
1	$F = 0.043(X/HR)^{-2.725}$ $V = 126.6V_{BA}F/(1+F)$	0.74
2	$F_1 = 1/(1+0.098((1-AR)/AR)^{0.828})$ $F = 0.0046A^{1.43}X^{-2.056}$ $V = 86.99V_{BA}F/(1+F)$	0.235
3	$\beta = 0.288(X/A)^{-0.893}$ $\alpha = 1.025(AR)^{\beta}X/\sqrt{A}$ $V = V_{BA}/(0.0723+11.08\alpha^2)$	0.26
4	$F = 7.23(X^{1.67}/A)-1.99$ $V = V_{BA}/F$	0.327
5	$F = 2.45(D_{eq}/X)^{2.24}D_{eq}^{1.72}$ $V = V_{BA}F/(1+F)$	1.62
6	$F = 0.0102(D_{eq})^{3.33}X^{-1.99}$ $V = 105.05V_{BA}F/(1+F)$	0.27

TABLE 7.10 Centre-line velocity in front of different geometry of suction openings (rectangular, rectangular hood, round)

	Unflanged	Root Mean Square Residual	Flanged	Root Mean Square Residual
1	$F = 0.228(X/HR)^{-0.865}$ $V = 0.474V_{BA}F/(1+F)$	1.17	$F = 1.925(X/HR)^{-1.53}$ $V = 0.56V_{BA}F/(1+F)$	1.05
2	$F_1=1/(1-0.097((1-AR)/AR)^{-0.826})$ $F =0.0035A^{1.396}X^{-2.66}F_1$ $V =82.6V_{BA}F/(1+F)$	4.233	$F_1= 1/(1+0.075((1-AR)/AR)^{3.16})$ $F = 3.42A^{1.58}X^{-1.8}F_1$ $V = 0.54V_{BA}F/(1+F)$	0.86
3	$\beta =10.36(X/A)^{-0.765}$ $\alpha =1.052X(AR)^{\beta}/\sqrt{A}$ $V =V_{BA}/(4.283+110.96\alpha^2)$	0.935	$\beta = 0.2(X/A)^{-0.33}$ $\beta = 0.943(AR)^{\beta}X/\sqrt{A}$ $V = V_{BA}/(1.88+8.98\alpha^2)$	0.969
4	$F =27.7(X^2/A)^{0.452}+2.38$ $V = V_{BA}/F$	1.13	$F = 7.016(X^2/A)^{0.818}+1.81$ $V = V_{BA}/F$	0.902
5	$F = 1.775(D_{eq})^{10.05}X^{-2.064}$ $V = 1.92V_{BA}F/(1+F)$	4.42	$F = 1.001(D_{eq})^{2.45}X^{-1.61}$ $V = 0.56V_{BA}F/(1+F)$	0.915
6	$F = 9.851(D_{eq}/X)^{0.807}D_{eq}^{3.106}$ $V = V_{BA}F/(1+F)$	0.857	$F = 0.37(D_{eq}/X)^{0.92}(D_{eq})^{0.715}$ $V = V_{BA}F/(1+F)$	1.29

TABLE 7.11 Velocity at locus of ellipse and circle contour line in front of rectangular unflanged duct for a fixed flowrate of suction

Measuring Instrument	X coordinate metre	Y coodinate metre	Z coordinate metre	Suction flow rate $m^3 s^{-1}$	Area of ellipsoid of revolution for 270°	Expected velocity over the surface of ellipsoid	Measured velocity on locus of ellipse in XZ-plane	% Deviation based on measured velocity	Remarks
	1	2	3	4	5	6	7	8	9
AVM 502 Proba No.1	0.292	0.001	0.001	1.217	1.002	1.214	1.316	19.05	ellip-soid
	0.242		-0.155				1.394		
	0.192		-0.215		0.8036	1.5144	1.68	-0.96	sphere
	0.142		-0.255				1.8		
	0.142		0.23				1.327		
	0.192		0.21				1.469		
Average of velocity readings							1.5		
AVM502 Probe No.2	0.342	0.001	0.001	1.217	1.717	0.71	0.889	37.17	ellip-soid
	0.292		-0.155				1.083		
	0.242		-0.123		1.023	1.104	1.231	2.13	sphere
	0.192		-0.255				1.38		
	0.192		0.23				1.15		
	0.242		0.21				1.035		
Average of velocity readings							1.128		
AVM502 Probe No.3	0.442	0.001			1.8732	0.65	0.391	-8.28	ellip-soid
	0.392						0.563		
	0.342				1.841	0.66	0.731	-10.17	sphere
	0.292						0.787		
	0.392						0.509		
	0.342						0.624		
Average velocity readings							0.6		

TABLE 7.11 (contd)

Case Number	X coordinate metre	Y coordinate metre	Z coordinate metre	Suction flow rate $m^3 s^{-1}$	Area of ellipsoid of revolution of 270°	Expected velocity over the surface of ellipsoid	Measured velocity of locus of ellipse in XZ-plane	% Deviation based on measured velocity	Remarks
	1	2	3	4	5	6	7	8	9
AVM502 Probe No.4	0.542	0.001	0.001	1.217	2.8007	0.4345	0.314	-11.98	ellipsoid
	0.492	"	-0.155		Sphere		0.336		
	0.442	"	-0.213		2.7686	0.439	0.392	-13.14	sphere
	0.392	"	-0.255				0.45		
	0.492	"	0.23				0.384		
	0.442	"	0.21				0.452		
				Average of six measurement			0.388		
AVM502 Probe No.5	0.642	0.001	0.001	1.217	3.9167	0.311	0.245	2.96	ellipsoid
	0.592		-0.155		sphere		0.858		
	0.542		-0.213		3.8844	0.313	0.314	2.34	sphere
	0.492		-0.255				0.36		
	0.492		0.23				0.384		
	0.542		0.21				0.362		
				Average of velocity readings			0.3205		
AVM502 Probe No.6	0.742	"	0.001	"	5.22	0.233	0.183	-0.47	ellipsoid
	0.692		-0.155		sphere		0.218		
	0.642		-0.213		5.1886	0.23455	0.23	-1.1	sphere
	0.592		-0.255				0.253		
	0.592		0.23				0.276		
	0.642		0.21				0.231		
				Average of velocity readings			0.232		
Pitot tube	0.153	0.001	0.001	0.87	0.2506	3.87	2.51	-54.21	ellipsoid
					sphere				
					0.22062	4.4		-75.36	sphere

TABLE 7. 12 Velocity at locus of ellipse and circle contour line in front of unflanged round duct D = 0.457 m) for a fixed flow rate of suction.

Measuring instrument	X-coordinate metre	Y-coordinate metre	Z-coordinate metre	Flow rate m^3/S	Area of potential surfaces m^2	Expected velocity m/sec	Measurement velocity m/sec	% Deviation based on measurement value	Remarks
	1	2	3	4	5	6	7	8	9
AVM502 Probe No. 1	0.44	0.001	0.001	2.917	1.713	1.703	2.19	26.18	ellipsoid
	0.34	"	0.285	"			2.178		
	0.20	"	0.38	"	1.82	1.598	2.2	30.7	sphere
	0.2		-0.41	"			2.2		
	0.395		-0.215	"			2.775		
						Average	2.307		
AVM502 Probe No.2	0.509	"	0.001	"	2.85	1.025	1.443	30.45	ellipsoid
	0.409	"	same				1.45		
	0.269	"	as above respect-ively		2.44	1.195	"	18.89	sphere
	0.464	"	"				1.575		
							1.474		
AVM502 Probe No.3	0.595	"	"	"	3.74	0.78	0.931	24.14	ellipsoid
	0.495						0.931		
	0.355				3.34	0.87	1.095	14.95	sphere
	"						1.095		
	0.55						1.089		
							1.028		
AVM502 Probe No.4	0.695	0.001	0.001	2.917	4.96	0.59	0.766	20.27	ellipsoid
	0.595	"	0.285	"			"		
	0.455	"	0.38	"	4.55	0.64	0.876	13.51	sphere
	0.455	"	-0.41	"			0.821		
	0.65	"	-0.25	"			0.77		
							0.74		

TABLE 7.12 (contd)

Measuring Instrument	X-coordinate metre	Y-coordinate metre	Z-coordinate metre	Flow rate m^3/S	Area of potential surfaces m^2	Expected velocity m/sec	Measurement velocity m/sec	% Deviation based on measurement value	Remarks
	1	2	3	4	5	6	7	8	9
AVM502 Probe No.5	0.795	0.001	same	"	6.36	0.46	0.657	32.35	ellipsoid
	0.695	"	as above	"			"		
	0.555		respect-		5.96	0.49	"	27.94	sphere
			ively						
	"	"	"	"			0.712		
	0.75						0.715		
							0.68		
AVM502 Probe No.6	0.895	"	"	"	7.96	0.37	0.538	33.92	ellipsoid
	0.795	"	"	"	7.55	0.39	0.54	30.36	sphere
	0.655						0.563		
	0.655						0.565		
	0.85						0.616		
							0.56		
Mat wire anemometer	0.945	"	"	"	8.82	0.33	0.41	36.54	ellipsoid
	0.845	"	"	"			0.5		
	0.785	"	"	"	8.42	0.35	"	32.69	sphere
	0.785	"	"	"			0.6		
	0.905	"	"	"			0.39		
							0.52		
Pitot Tube	0.205	0.001	0.001	"	0.718	4.059	4.429	8.35	ellipsoid
					0.396	7.36		-66.17	sphere

Figure 7.1 Centre line velocity in front of unflanged rectangular suction opening(AR=0.6,HR=0.048m)

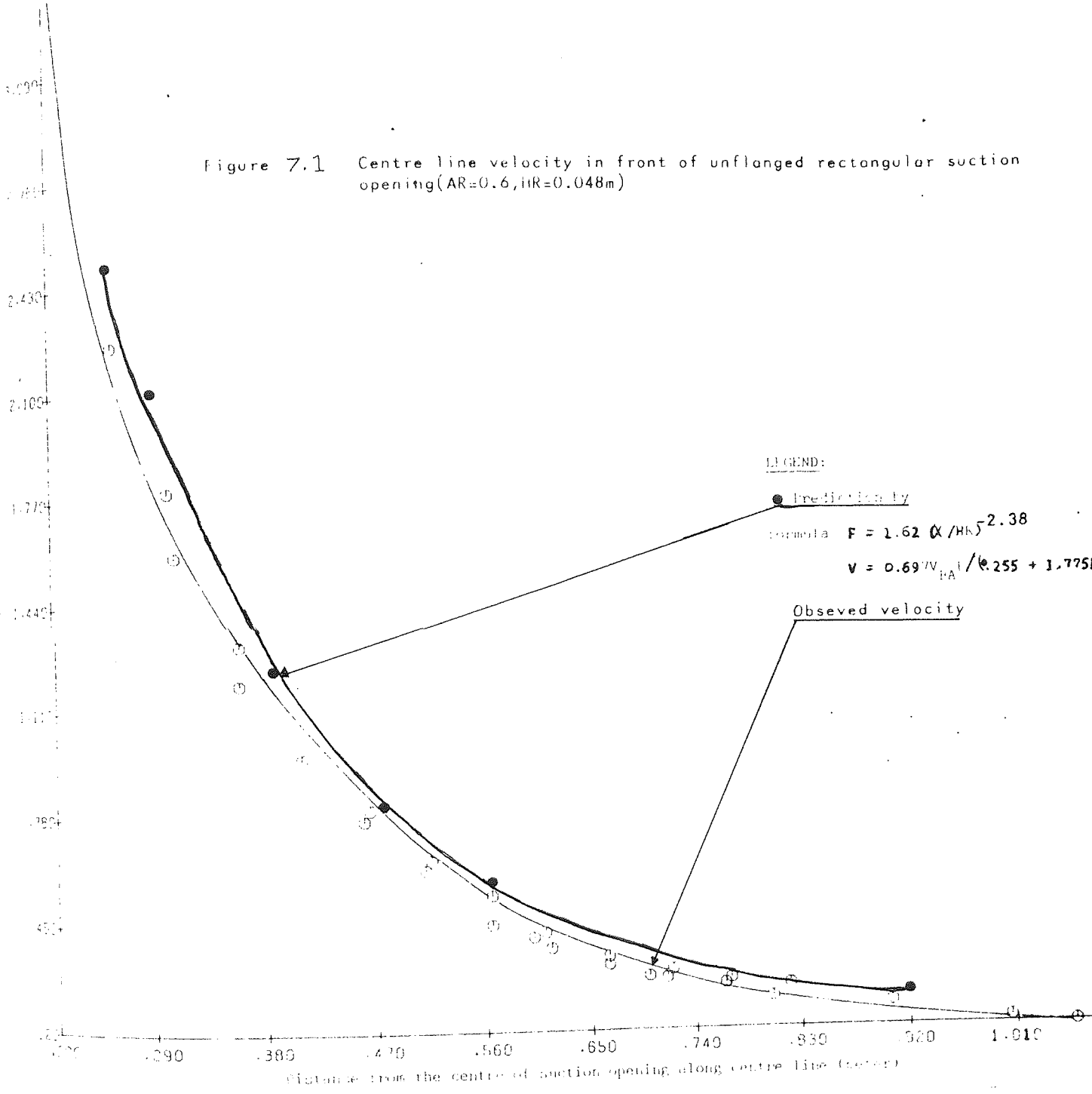

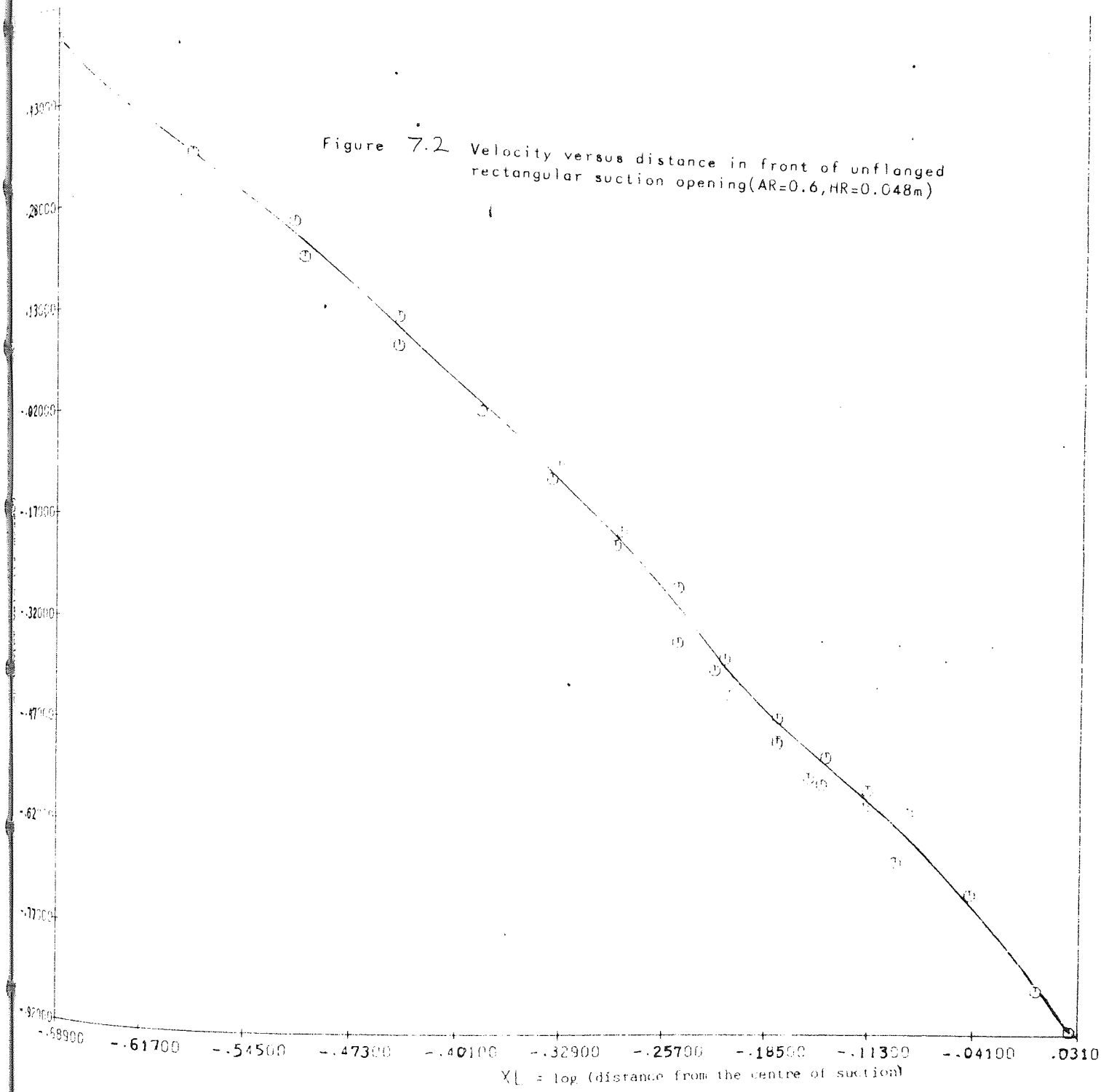

Figure 7.2 Velocity versus distance in front of unflanged rectangular suction opening(AR=0.6,HR=0.048m)

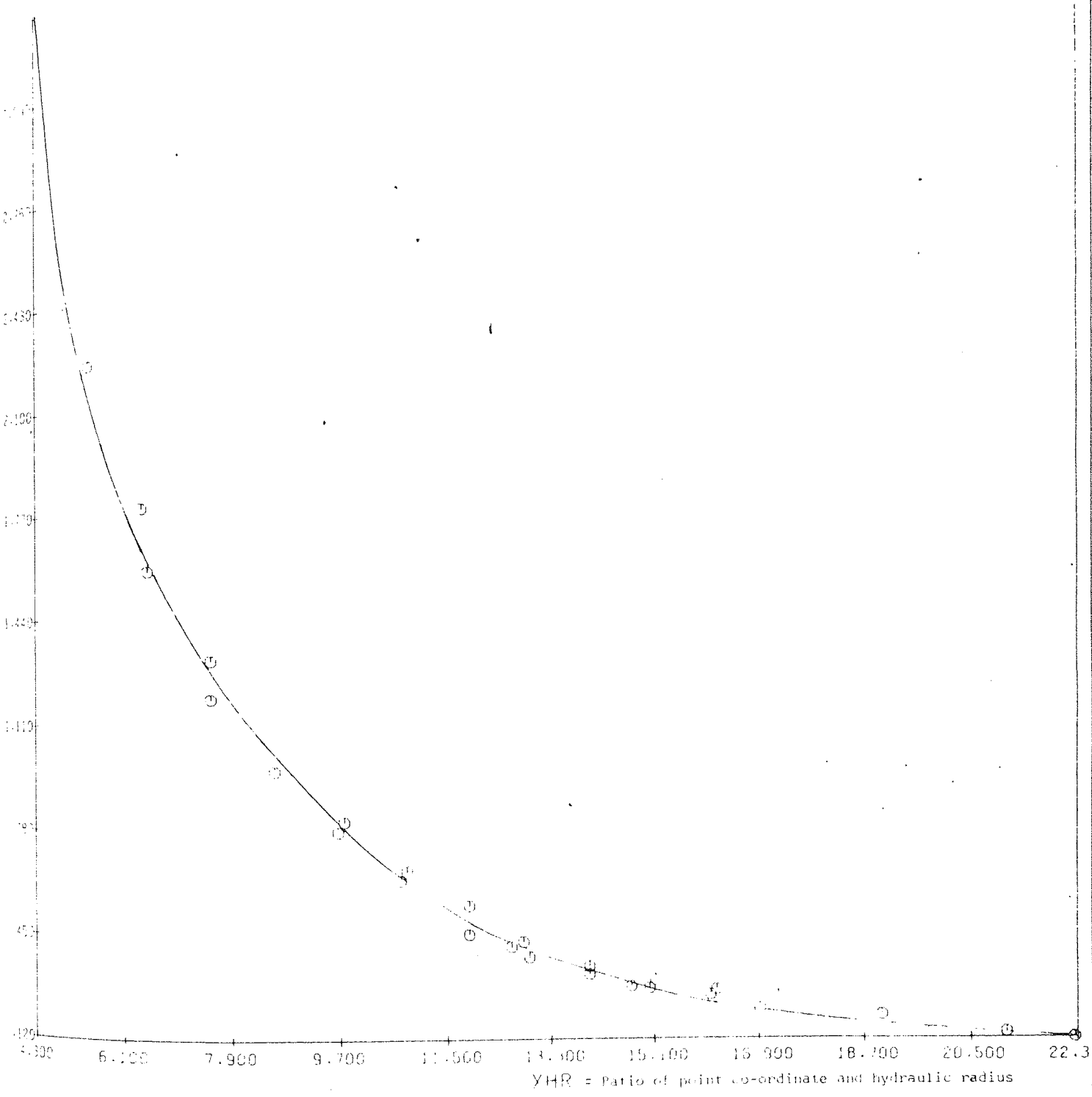

Figure 7.3 Centre line velocity in front of rectangular duct.

Figure 7.4 Velocity versus distance in fronf of rectangular suction opening (e.g.Centre line velocity, AR=0.6, HR=0.048m)

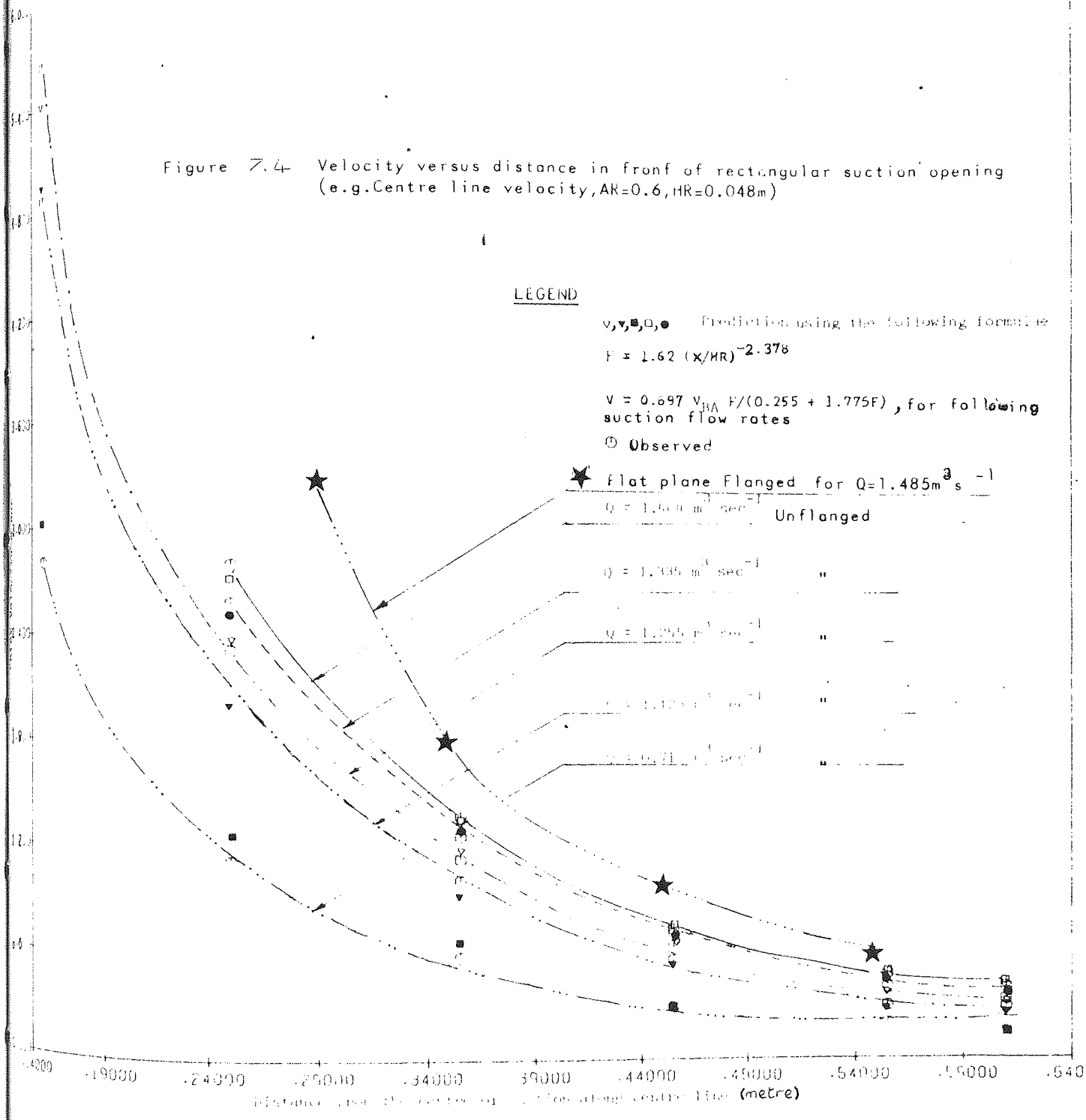

Figure 7.5 Centre line velocity in front of unflanged rectangular suction opening(AR=0.0,HR=0.04M)

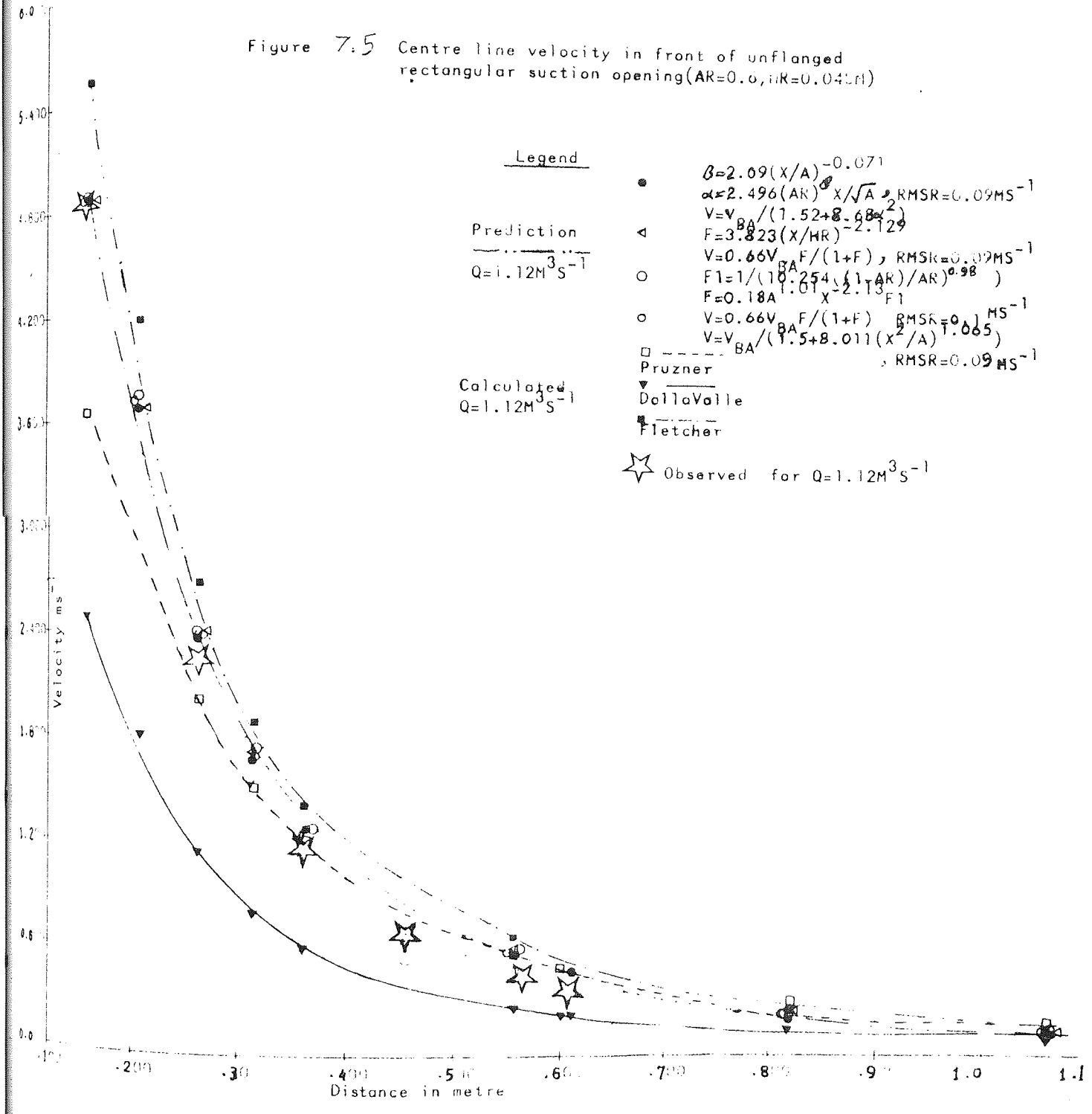

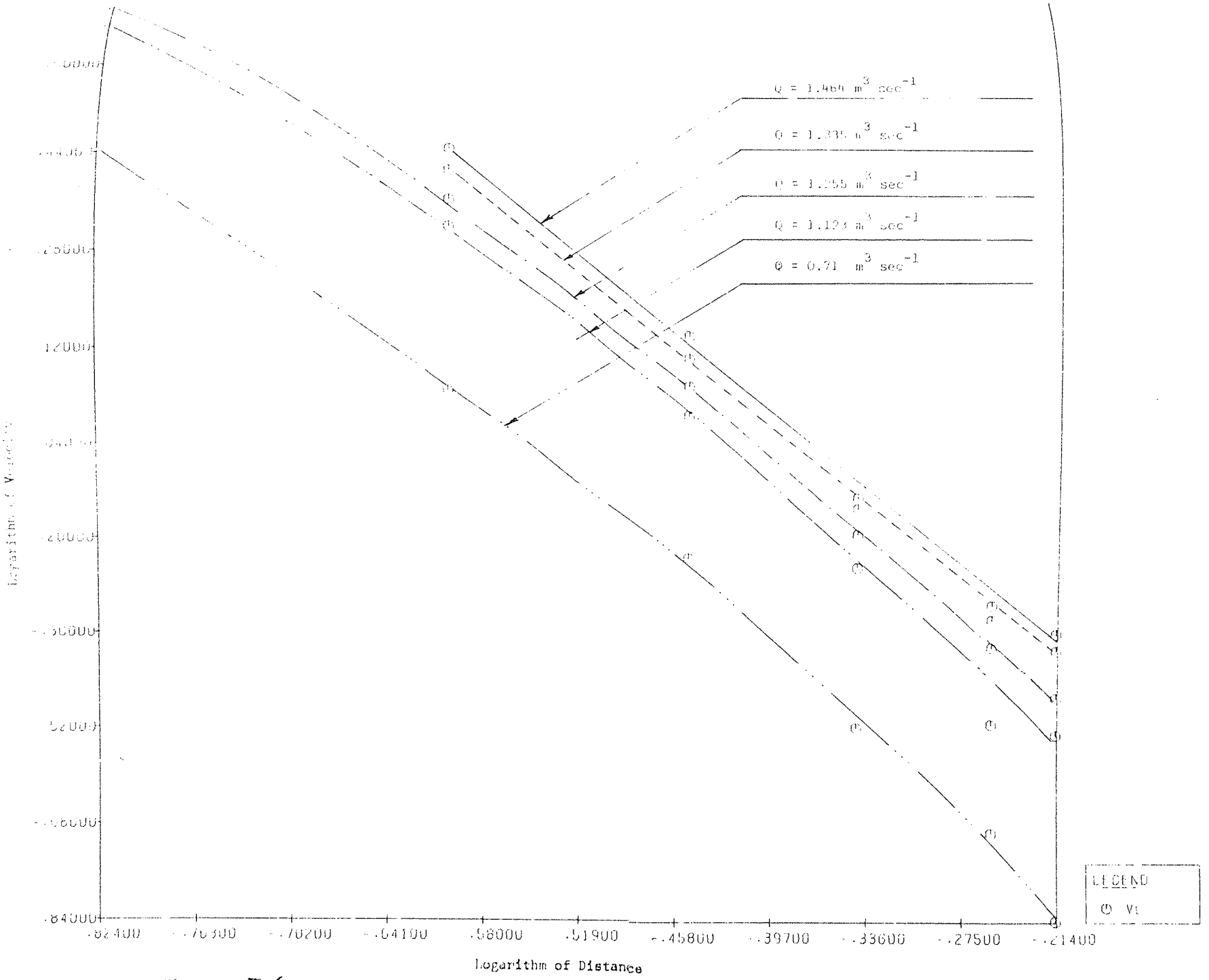

Figure No. 7.6 Decay of centre line velocity with distance from the suction face (aspect ratio 0.6)

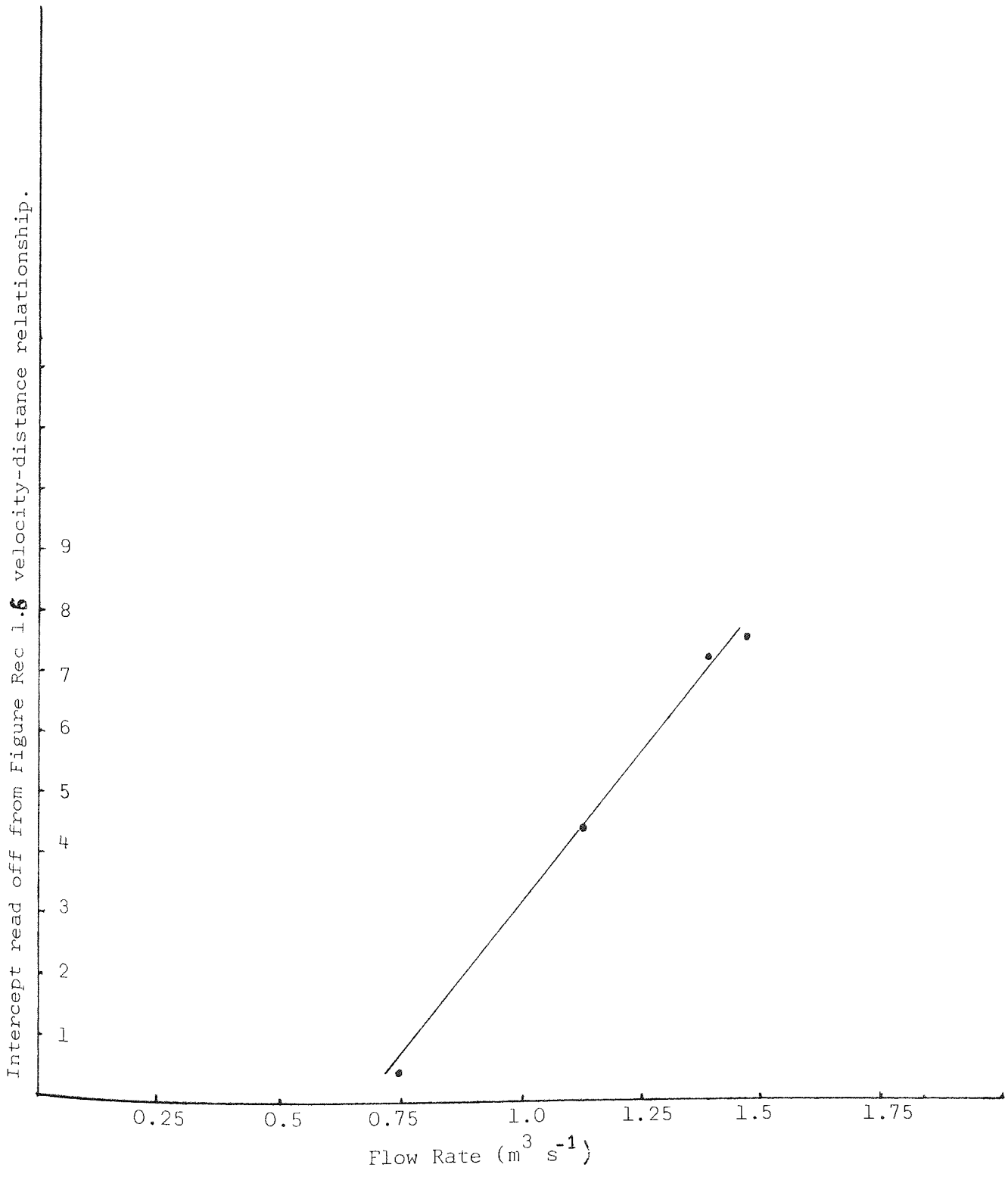

Figure Rec. 7.7 Flow rate-centre line velocity curve relationship.

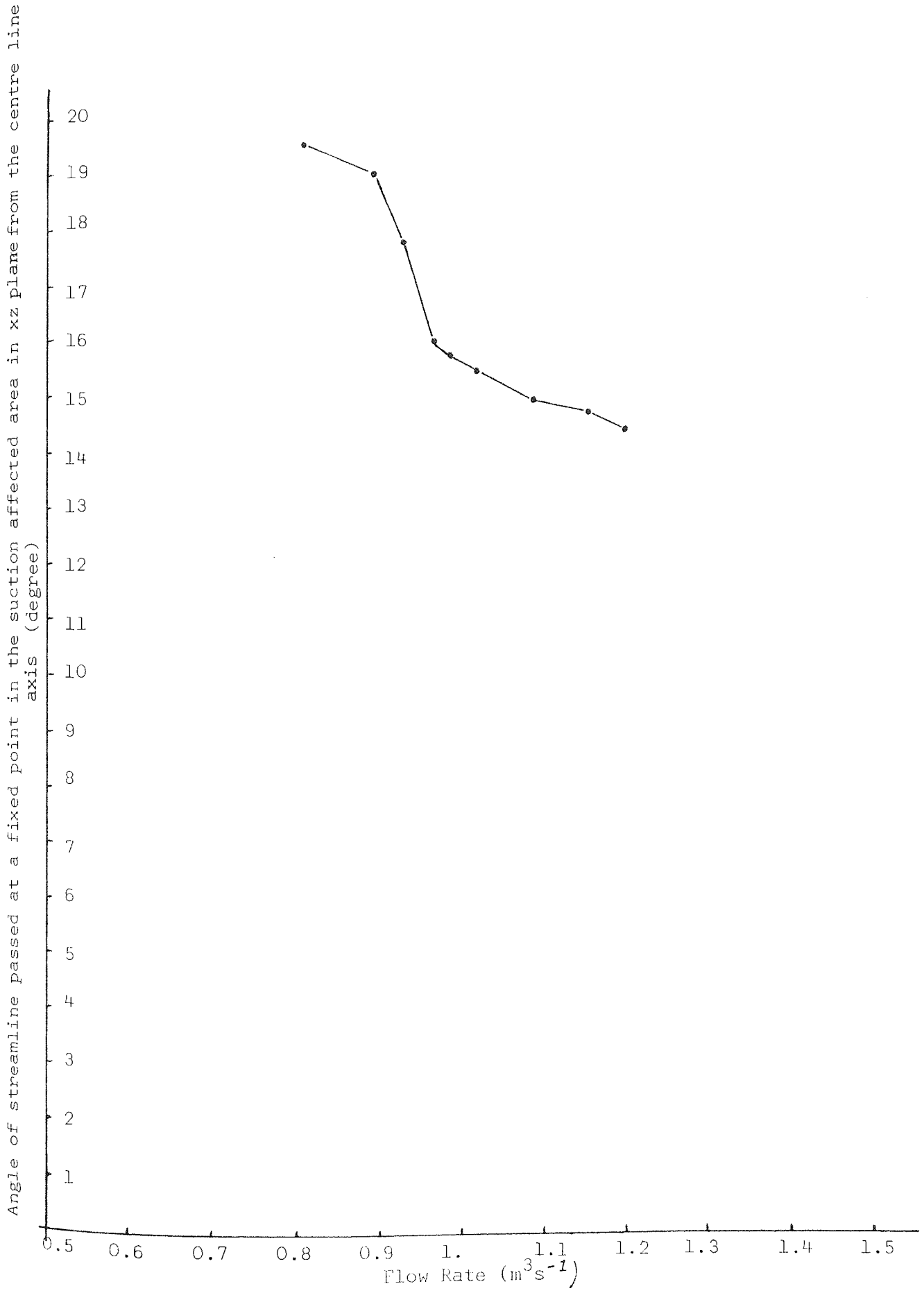

Figure 7.8 Angle of stream line from centre line versus flow rate of suction in front of rectangular suction duct (AR = 0.6, HR = 0.048m)

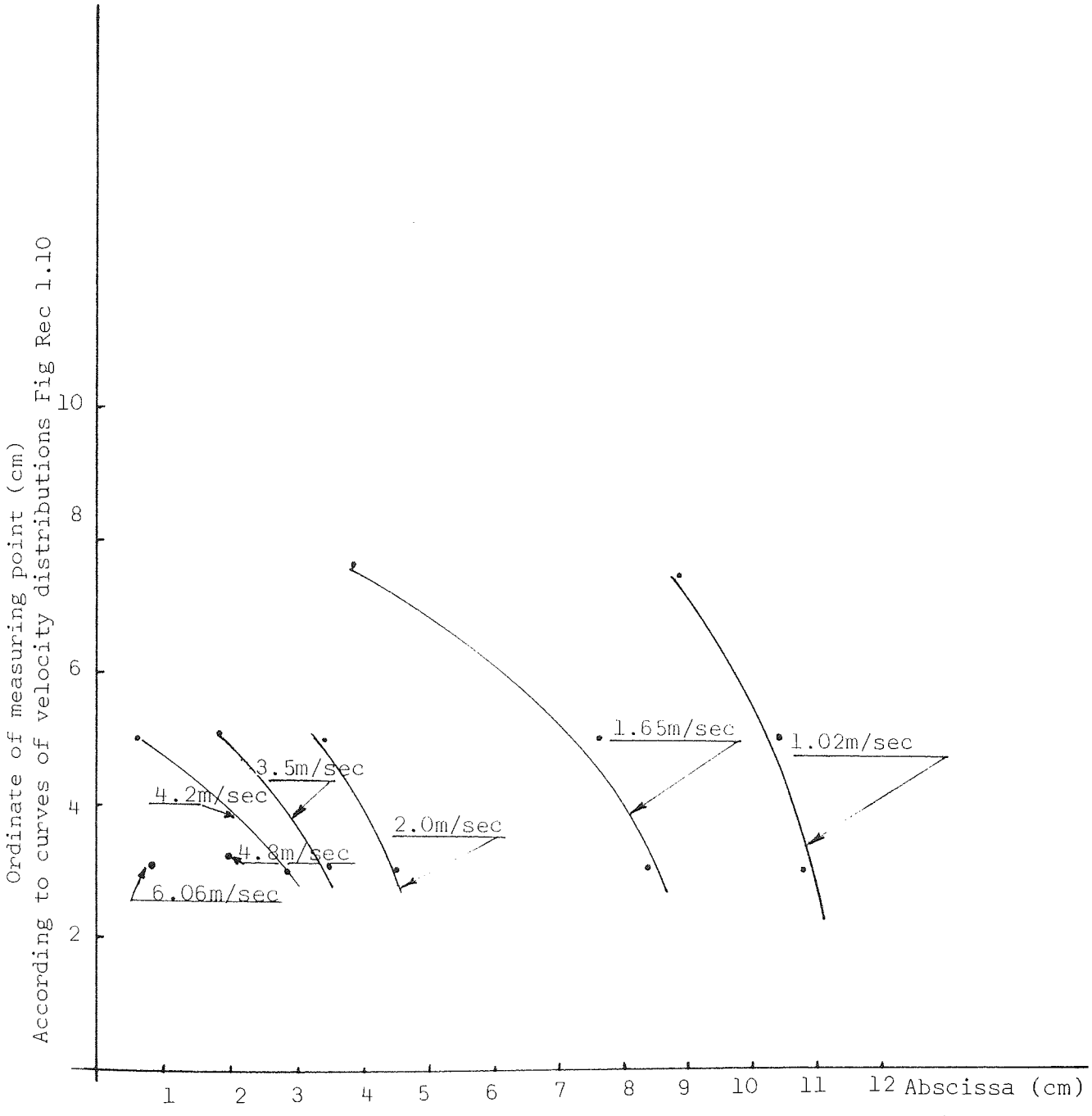

Read off from Figure Rec 1.10 for equal velocity lines and different ordinates points.

Figure 7.9 Vertical plane equivelocity point in front of rectangular opening suction duct (AR = 0.6, HR = 0.048m)

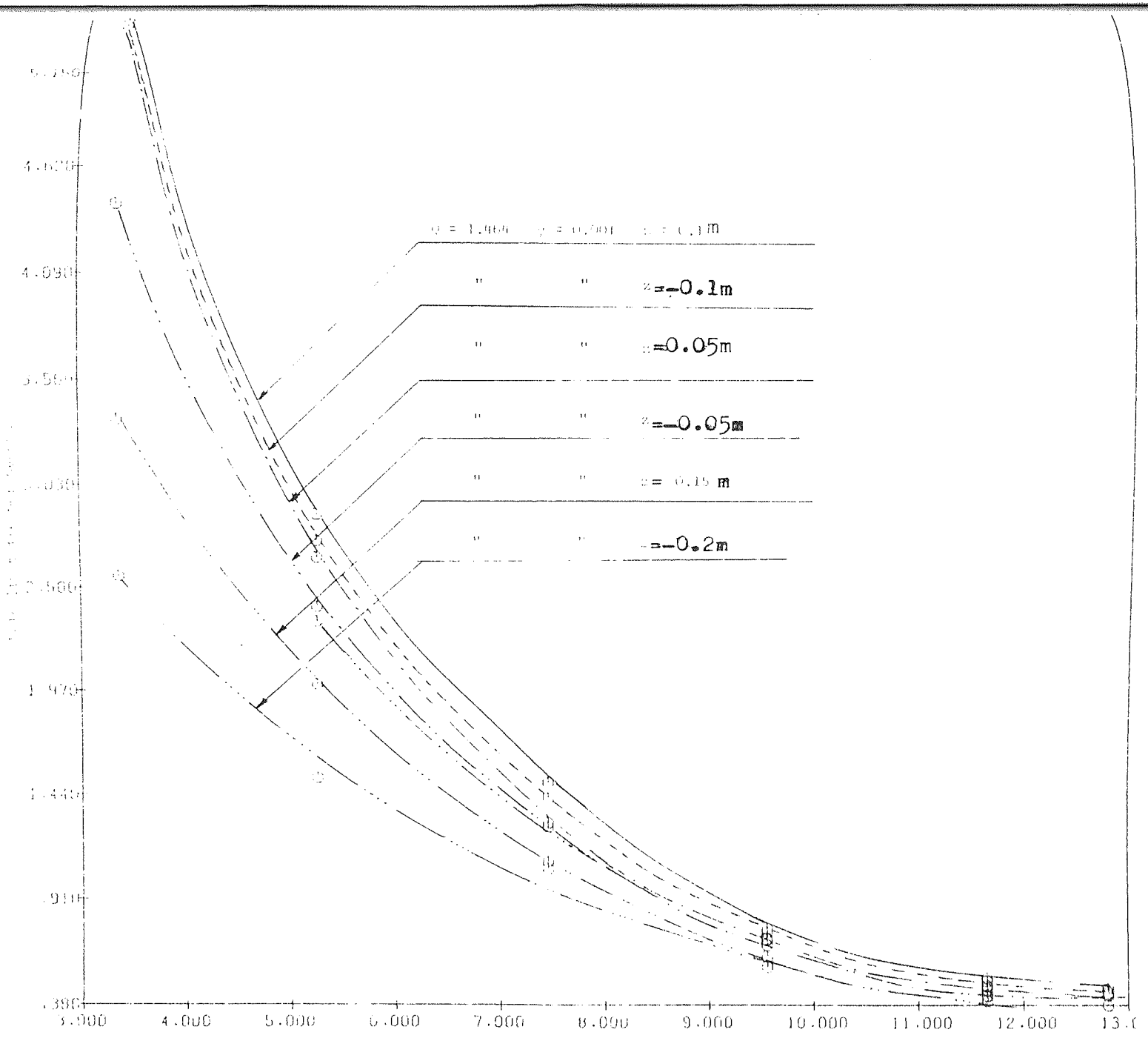

Figure 7.10 Velocity-distance in symmetry position in front of rectangular opening duct (AR=0.6, HR=0.048 metres)

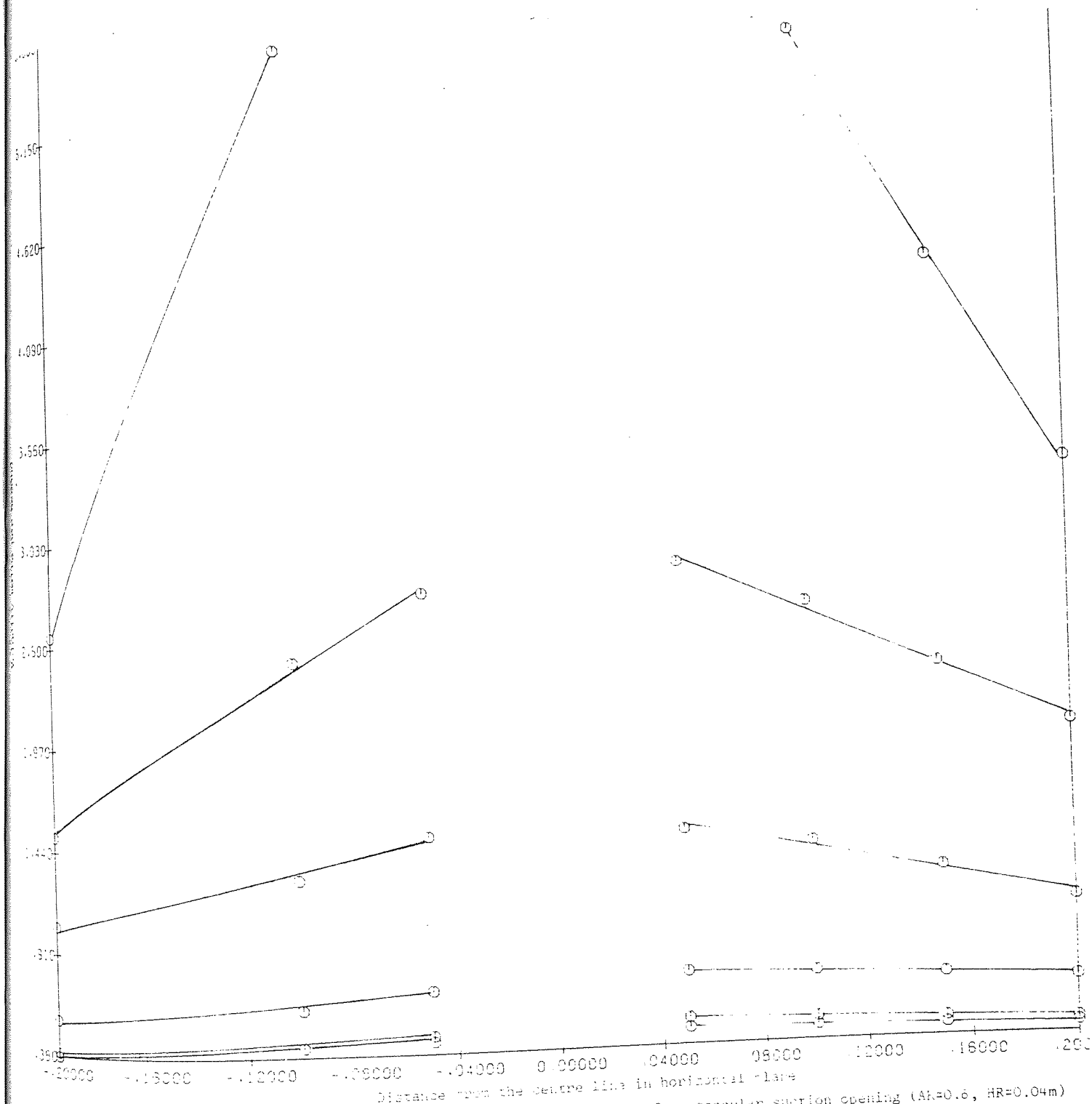

Figure Rec 7.11 Velocity measured at symmetry points in front of rectangular suction opening (AR=0.6, HR=0.04m)

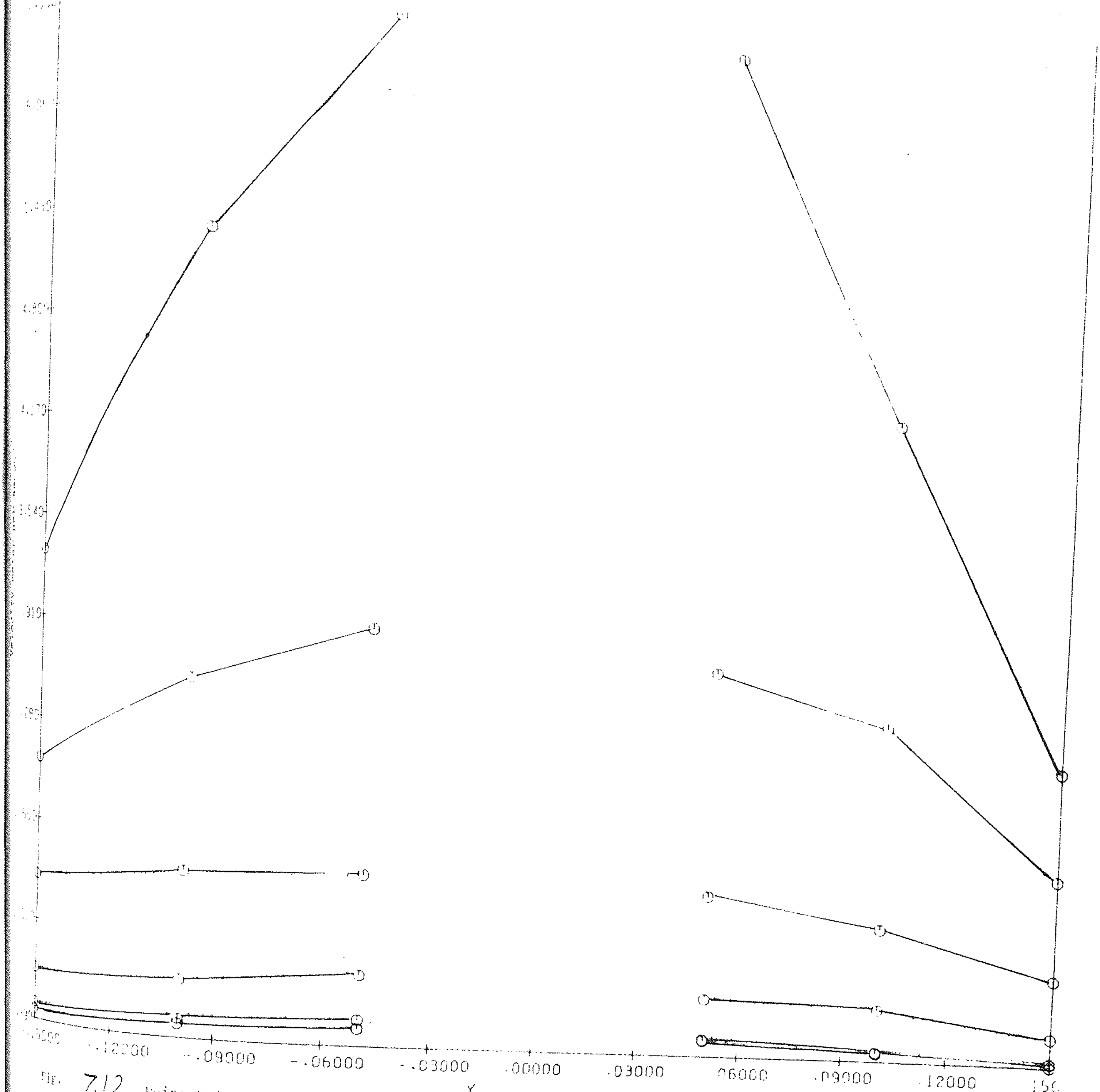

Fig. 7.12 Point Velocity at vertical plane symmetry point in front of rectangular opening suction duct (AR=?, HF=0.?? m)

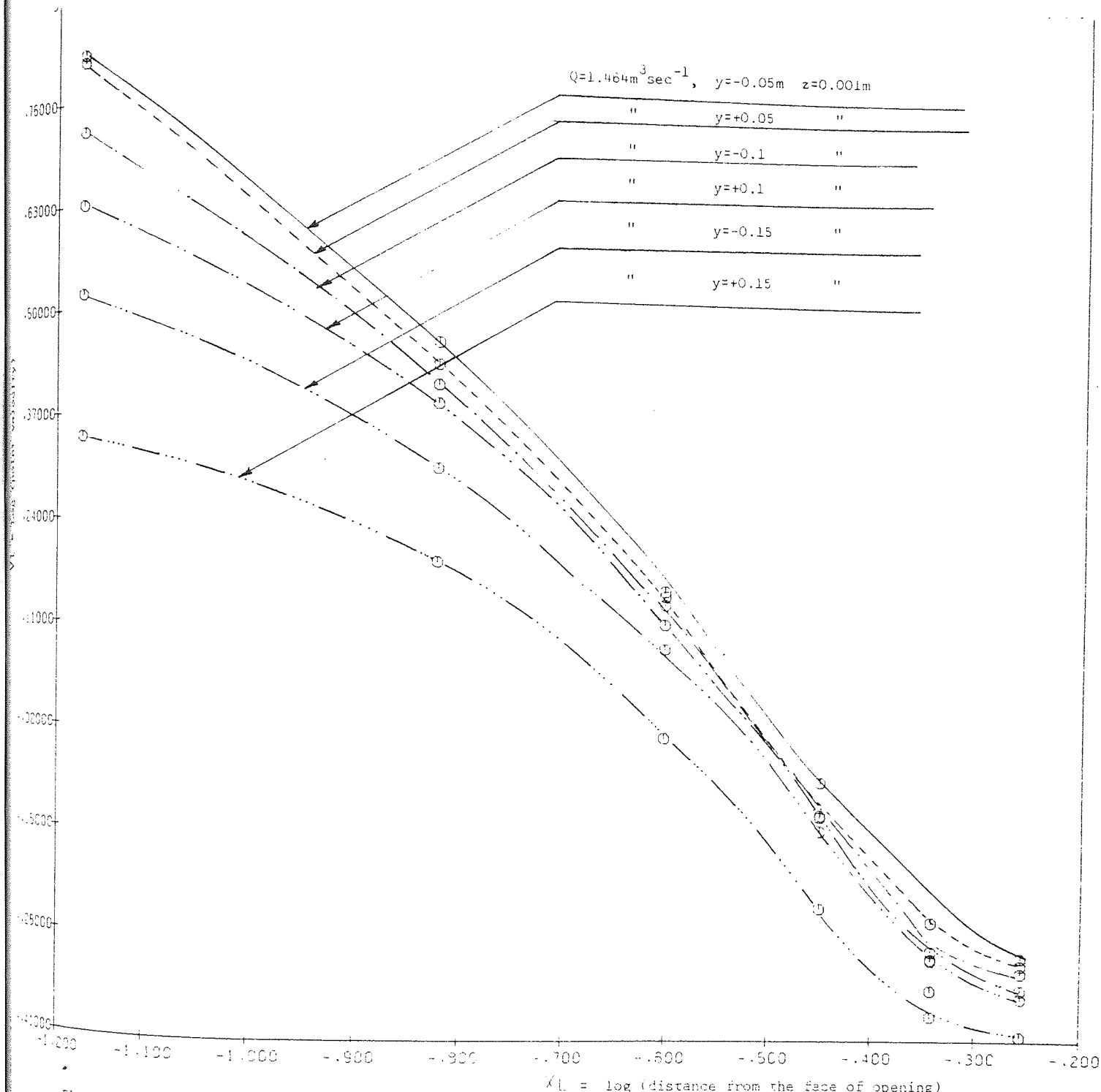

Figure 7.13 Logarithmical representation of velocity - distance in front of rectangular opening at symmetry points.

FIGURE 7.14 Blowing velocity distribution along the centre line of suction opening

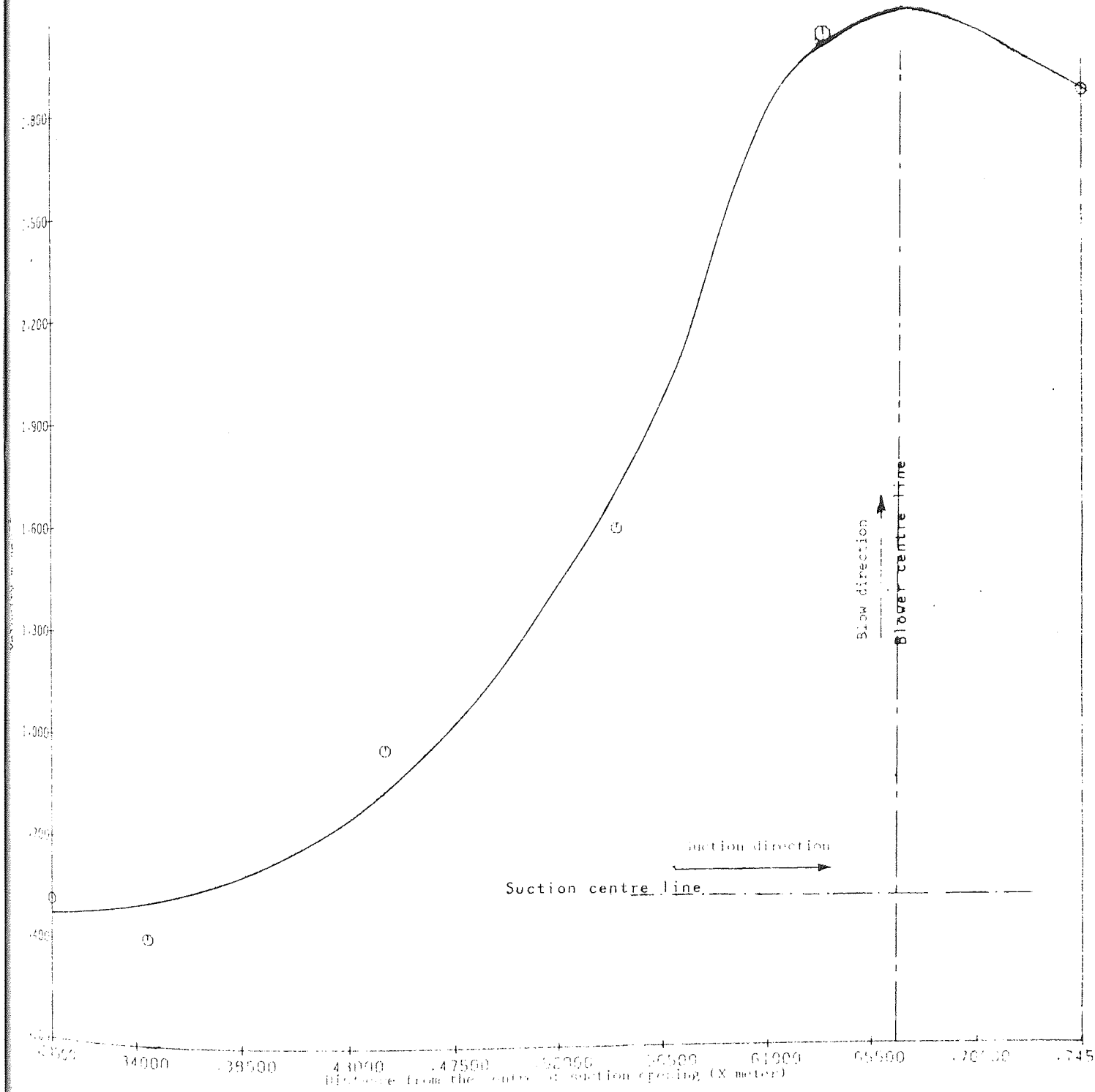

FIGURE 7.15 Velocity distribution in front of rectangular opening suction duct at vertical symmetry points (AR=0.6, HR=0.048m)

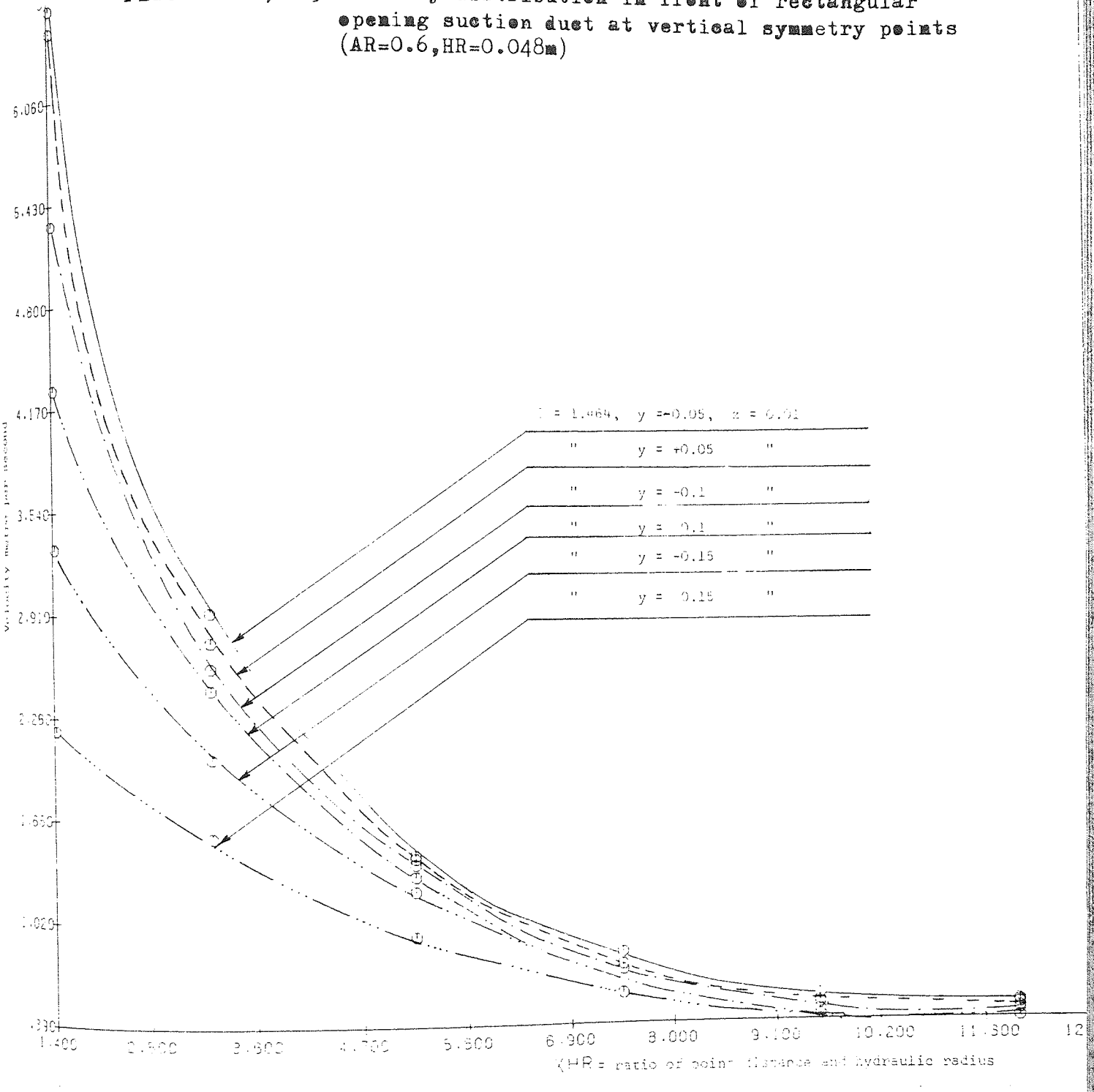

FIGURE 7.16

Illustration of the effect of flange on centre line velocity for a fixed volume of suction (AR=0.6, HR=0.048m)

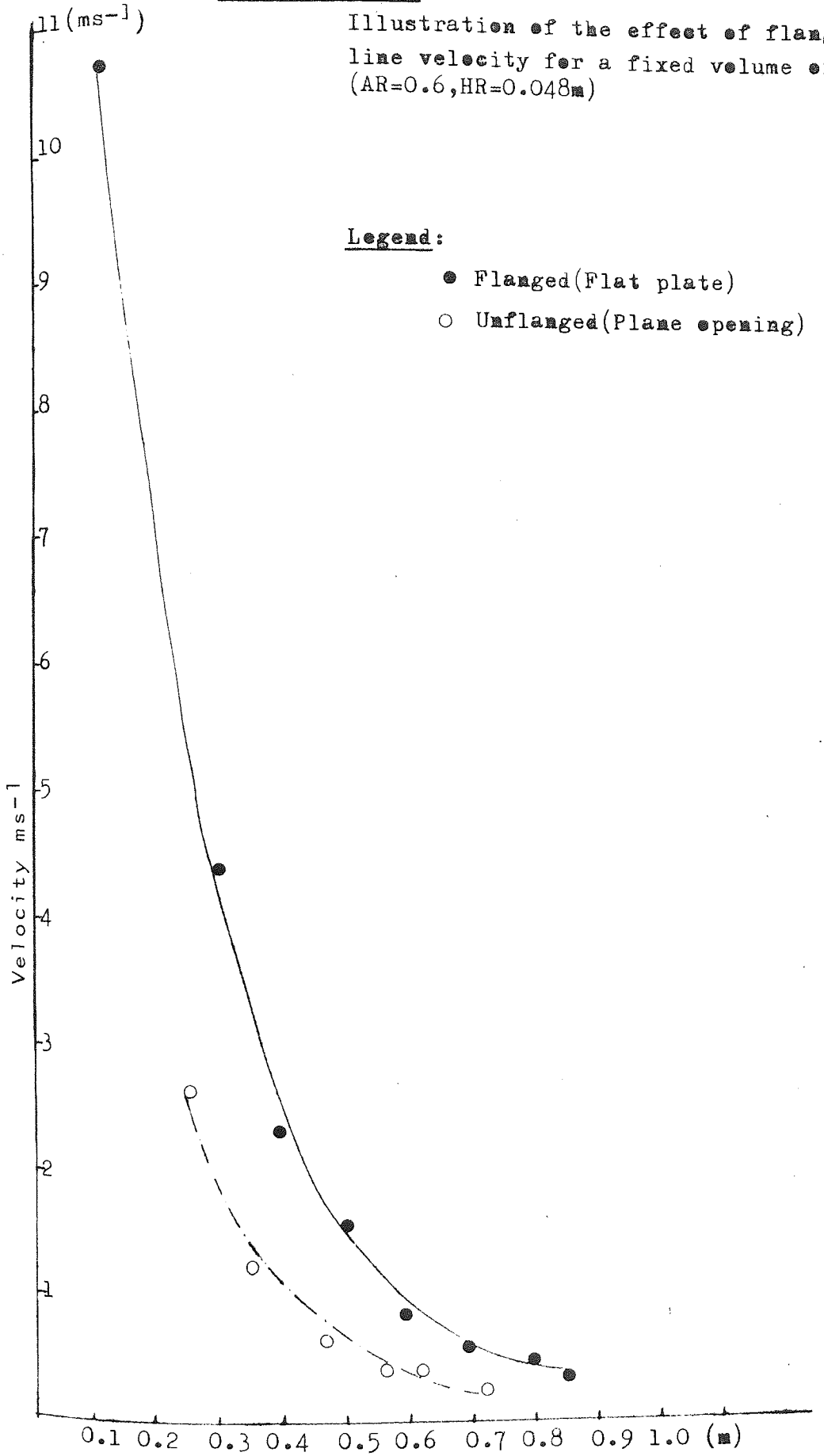

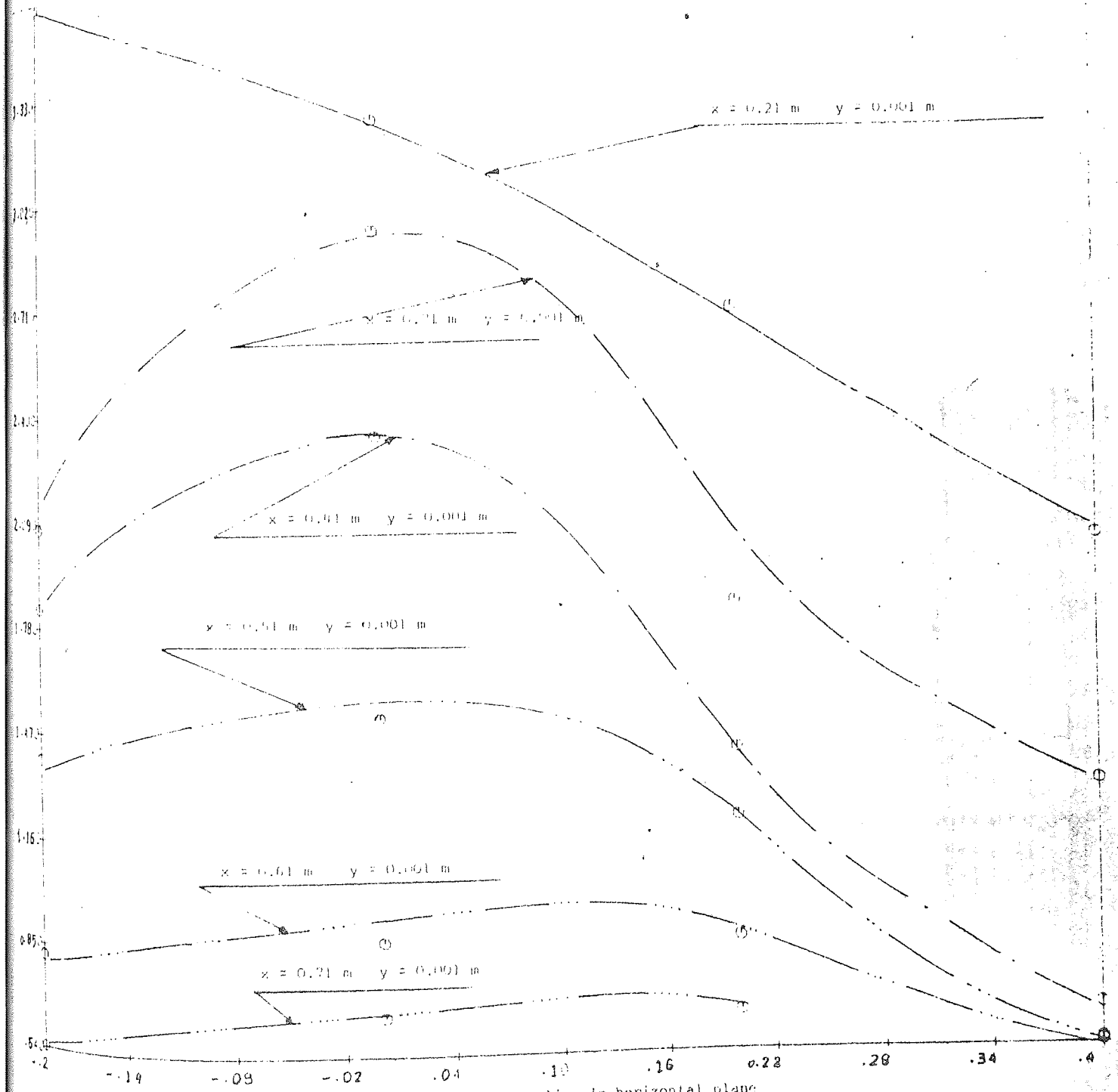

Figure 7.17 - Velocity distribution in XZ - plane in front of unflanged duct opening (AR = 0.6)

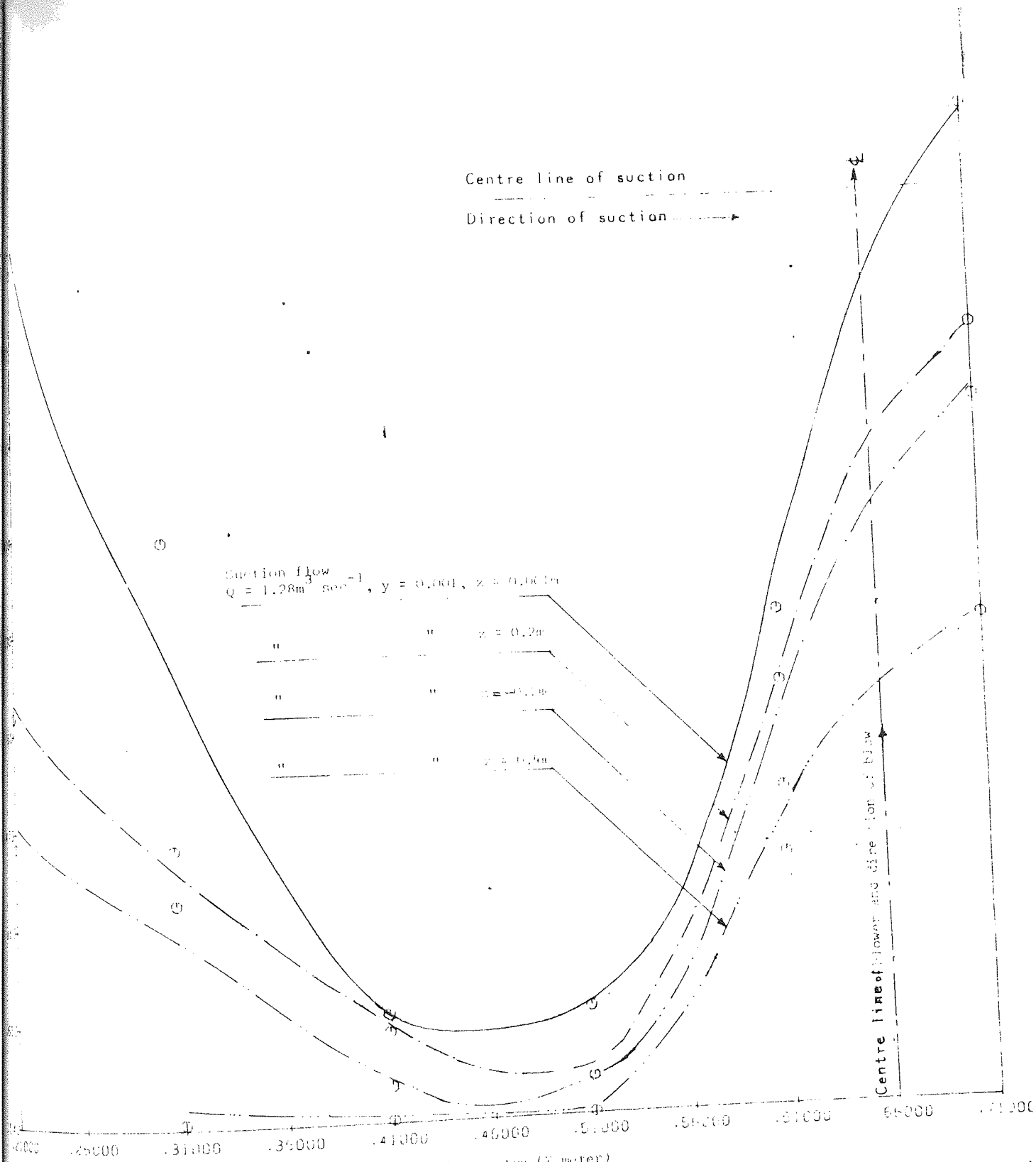

Distance from the centre of suction opening (X meter)

Figure 7.18 Combined suction and cross blow velocity distribution in horizontal plane in front of unflanged rectangular suction opening (AR = 0.6, W = 0.0060)

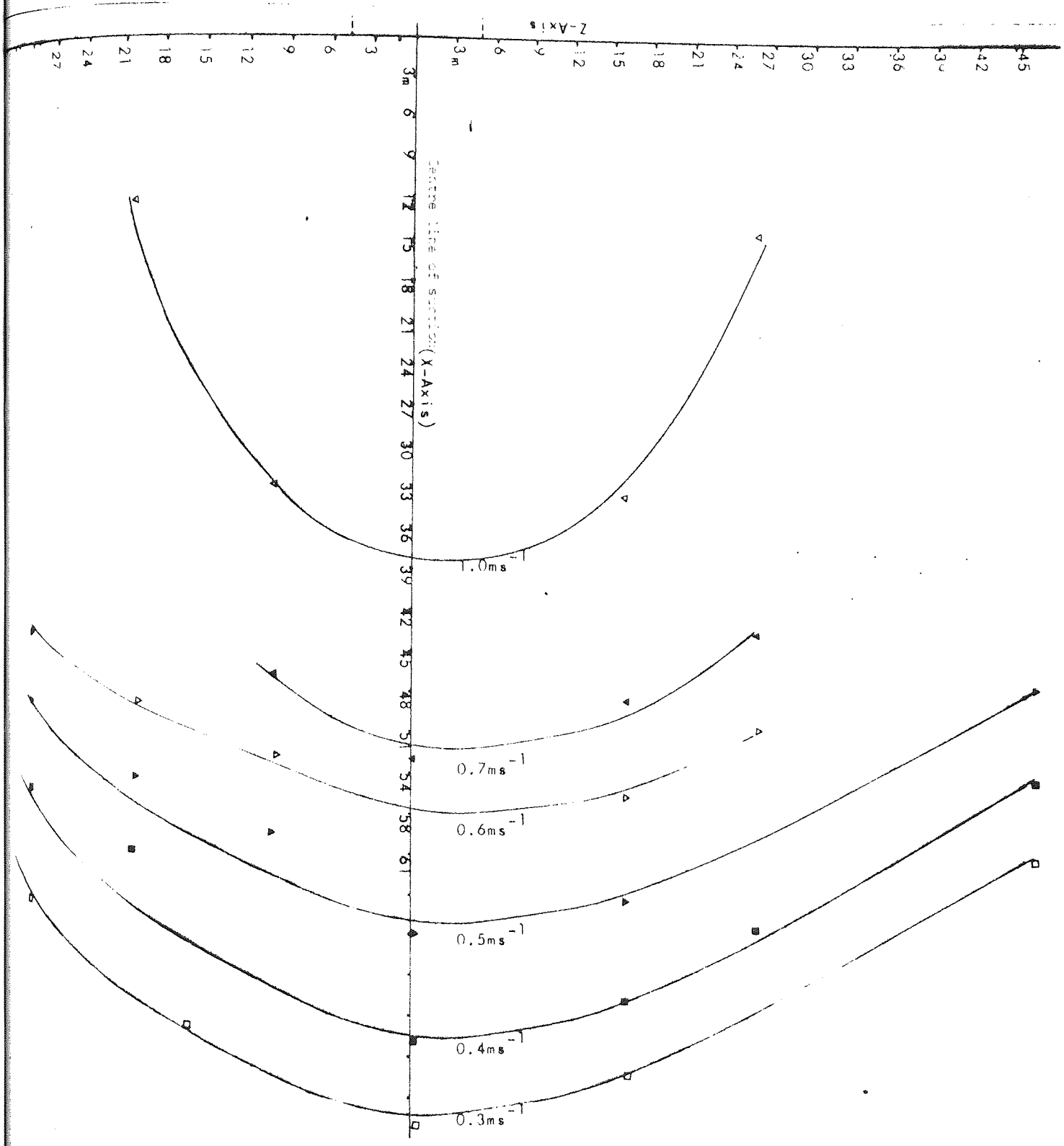

Figure 7.19 Contour line in front of unflanged rectangular suction opening (AR=0.6)

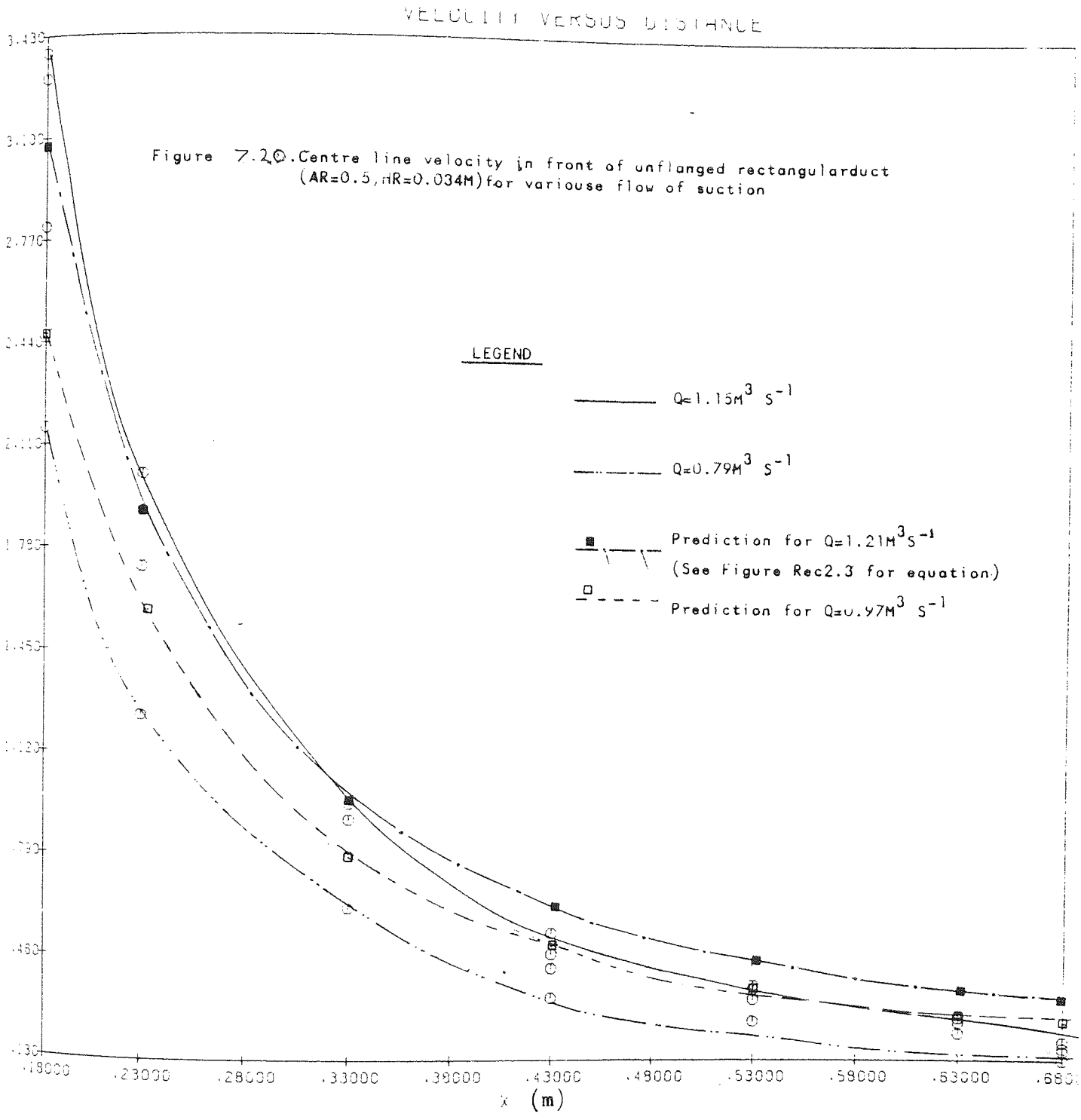

Figure 7.20. Centre line velocity in front of unflanged rectangular duct (AR=0.5, HR=0.034M) for variouse flow of suction

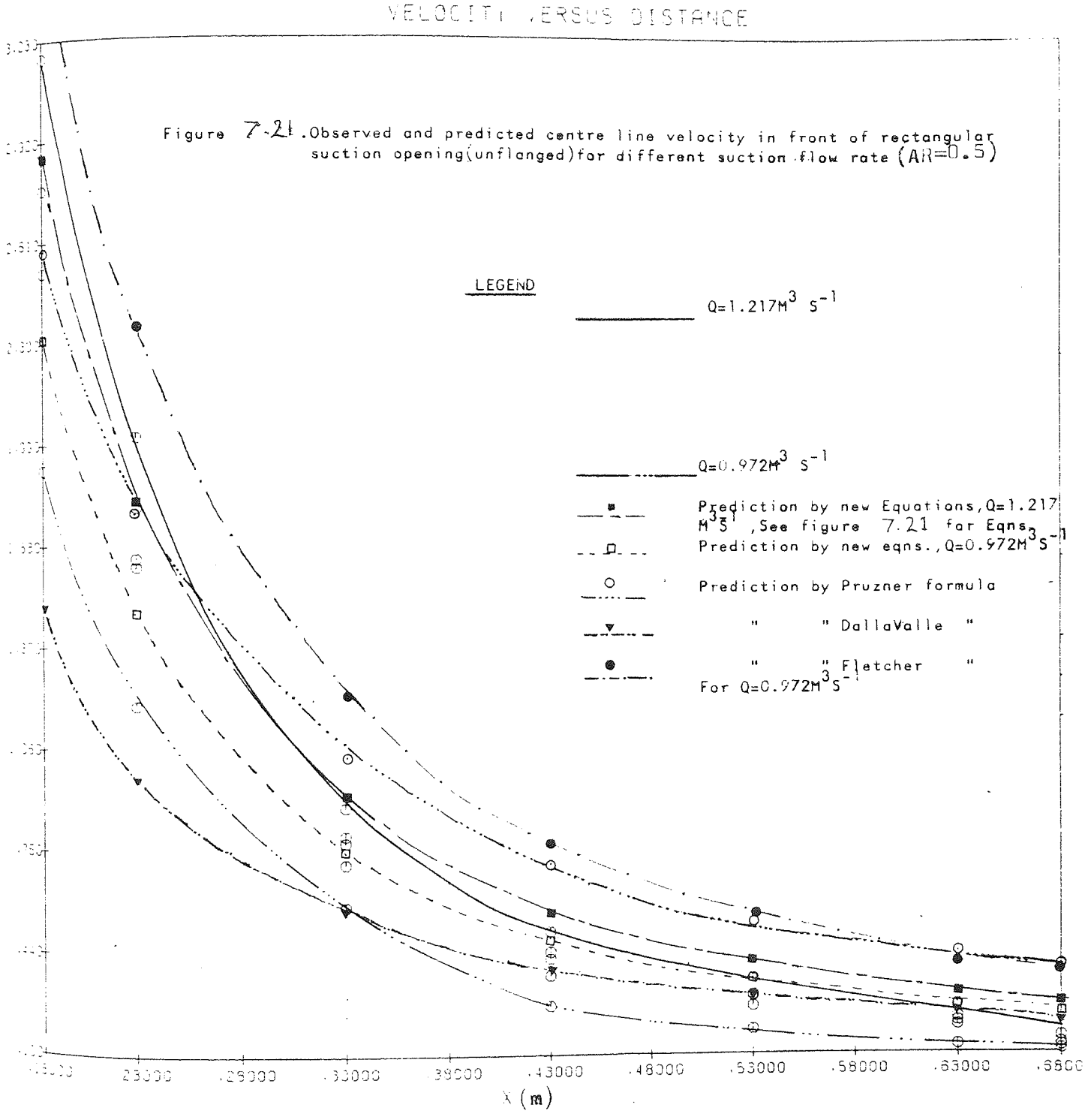

Figure 7.21 .Observed and predicted centre line velocity in front of rectangular suction opening(unflanged)for different suction flow rate (AR=0.5)

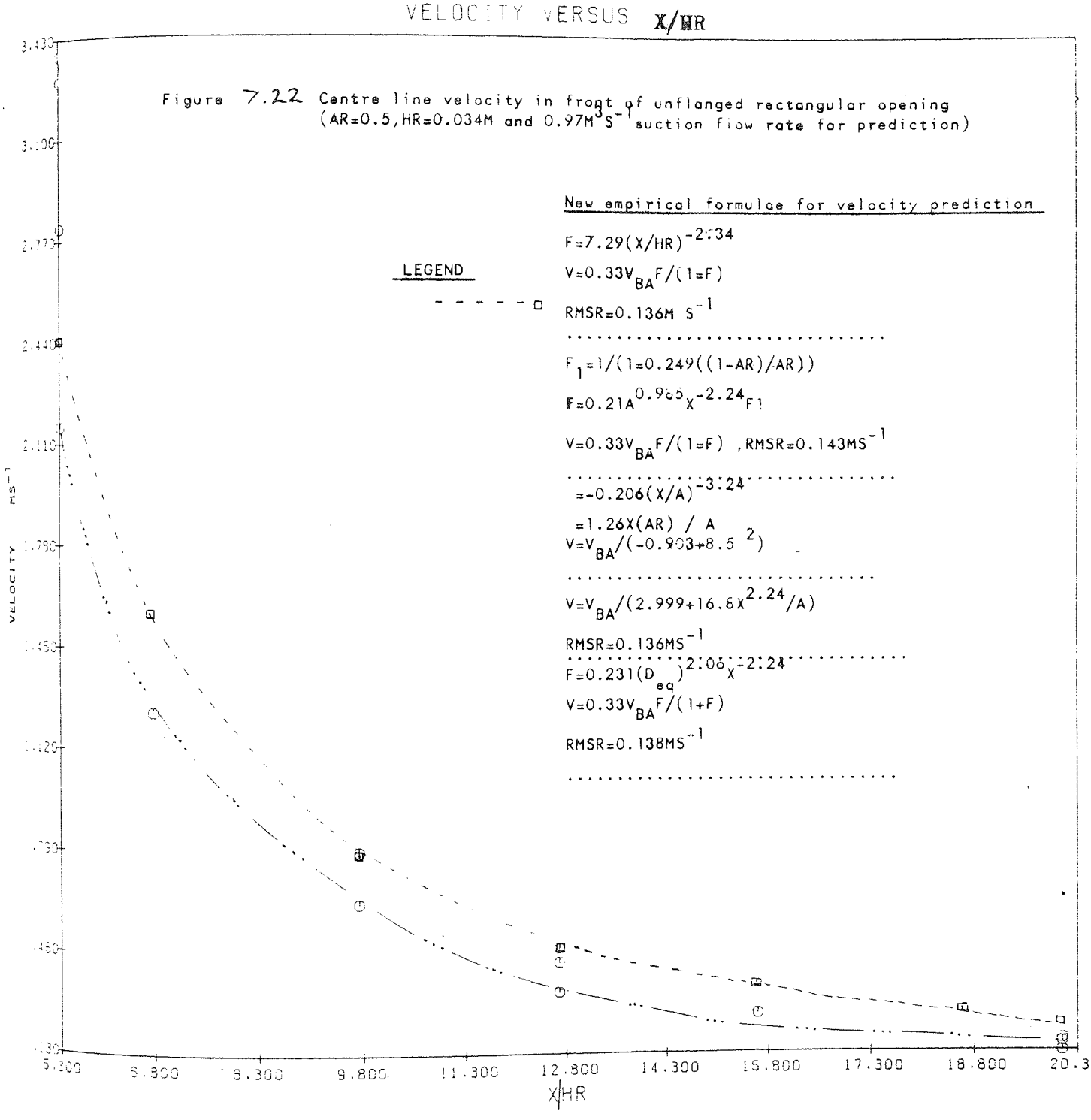

Figure 7.22 Centre line velocity in front of unflanged rectangular opening (AR=0.5, HR=0.034M and 0.97M^{3}S^{-1} suction flow rate for prediction)

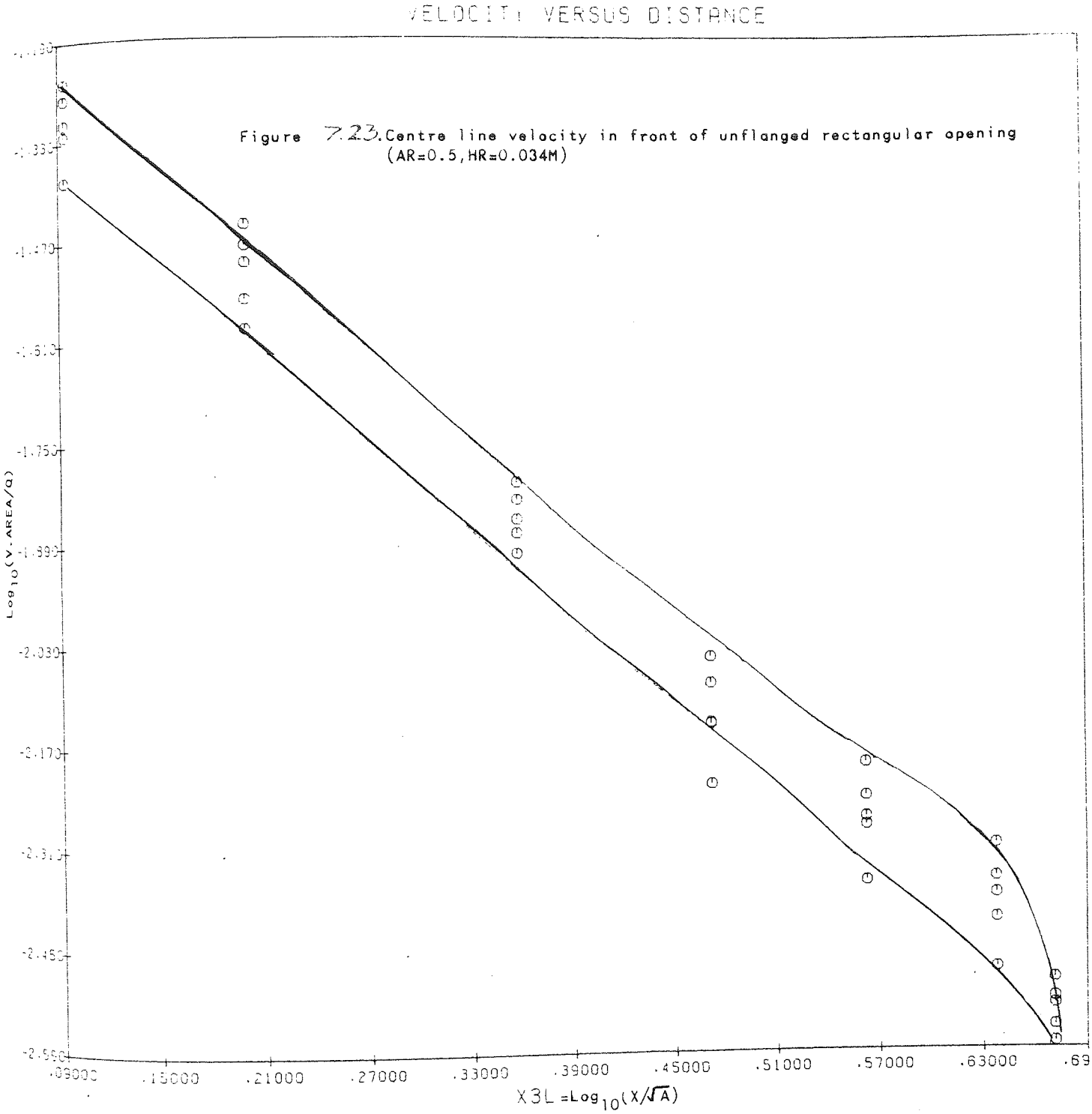

Figure 7.23. Centre line velocity in front of unflanged rectangular opening (AR=0.5, HR=0.034M)

Figure 7.2.4 Comparison of velocity decay along centre line axis of rectangular duct with and without flat plane flange and for the same volume of suction.

(AR=0.5)

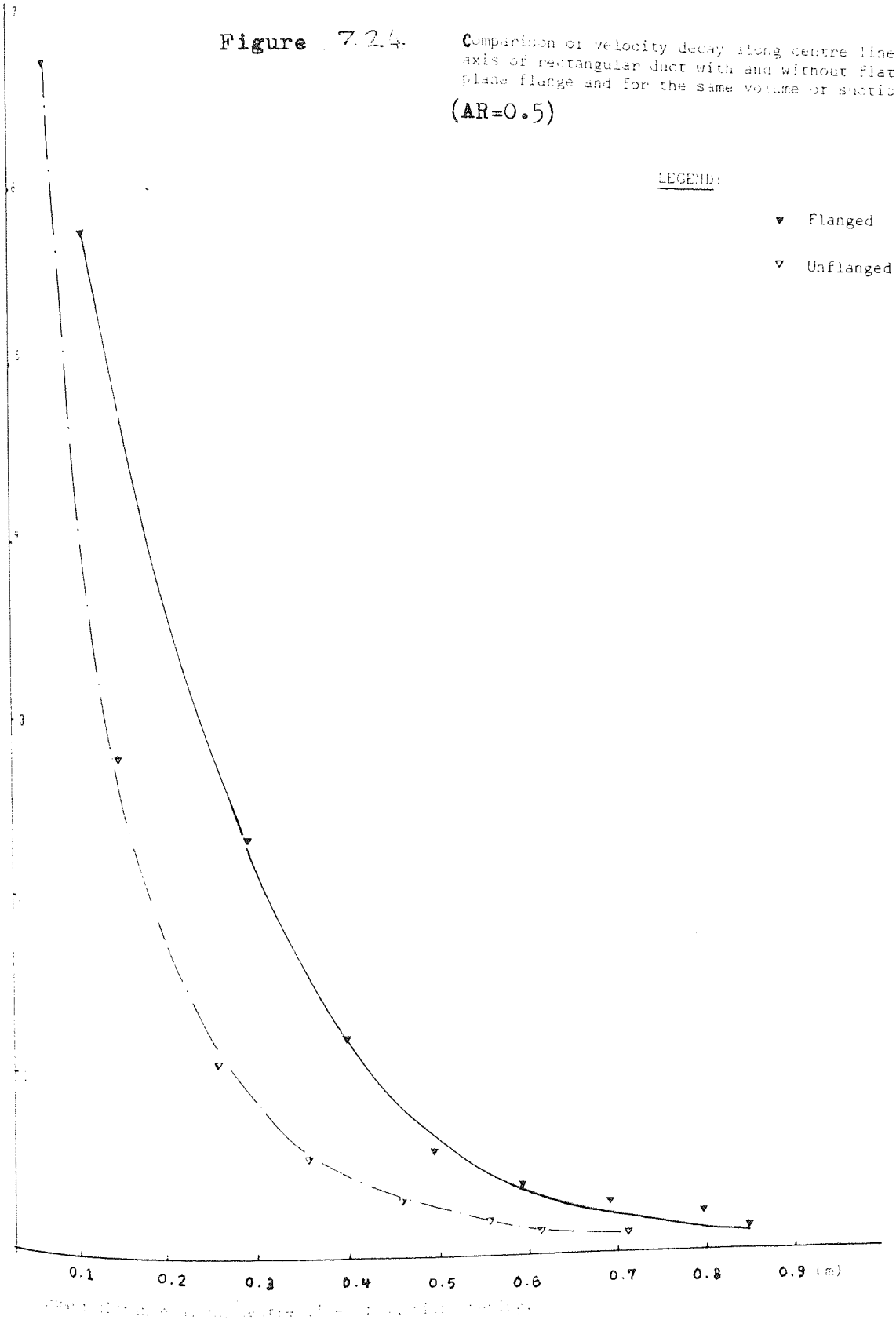

VELOCITY VERSUS DISTANCE

Figure 7.25. Centre line velocity versus distance in front of unflanged rectangular suction openings, AR=0.5, 0.6, for different suction flow rates.

Note: Prediction is for $1.46 M^3 S^{-1}$ suction flow rate

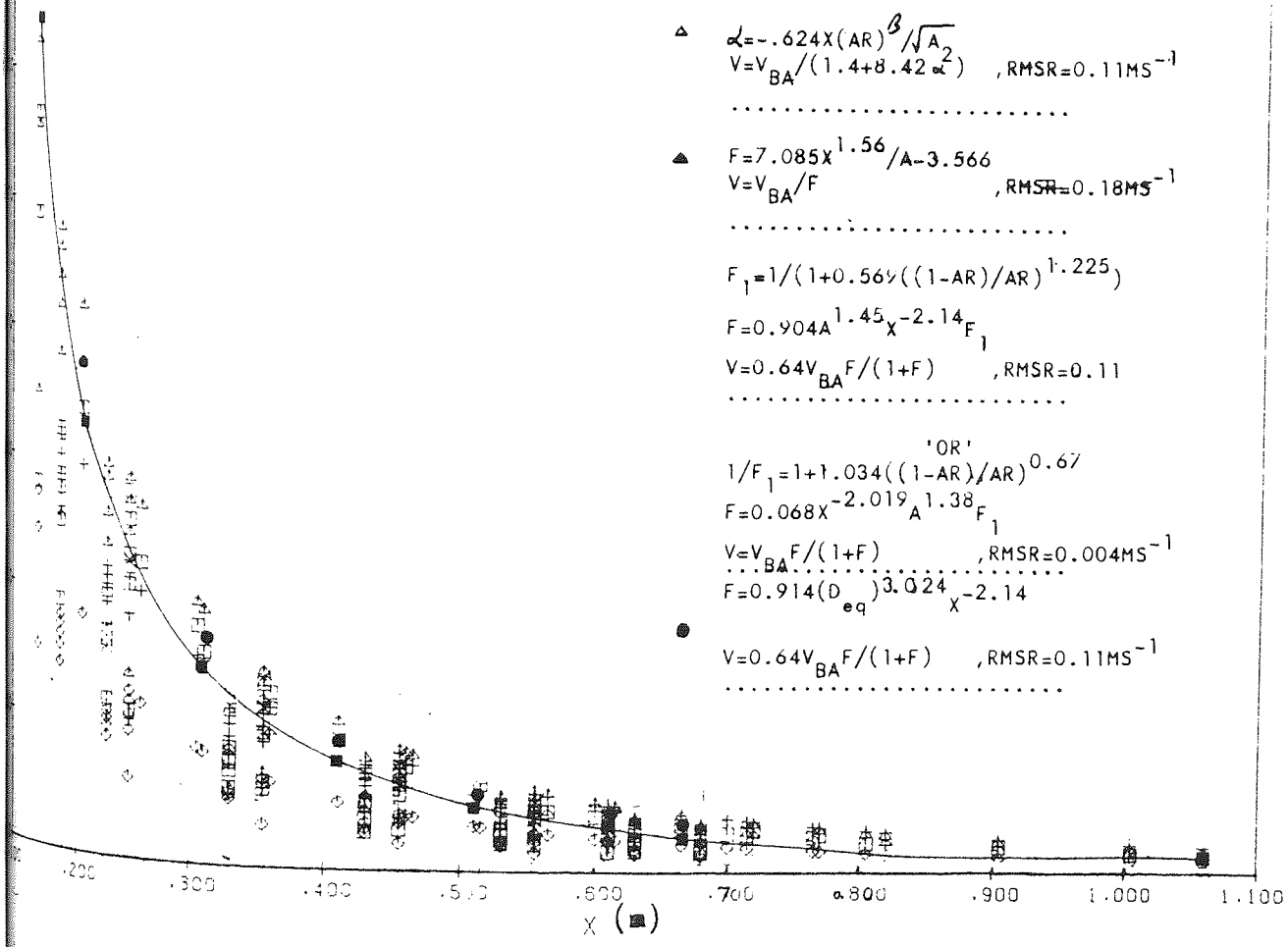

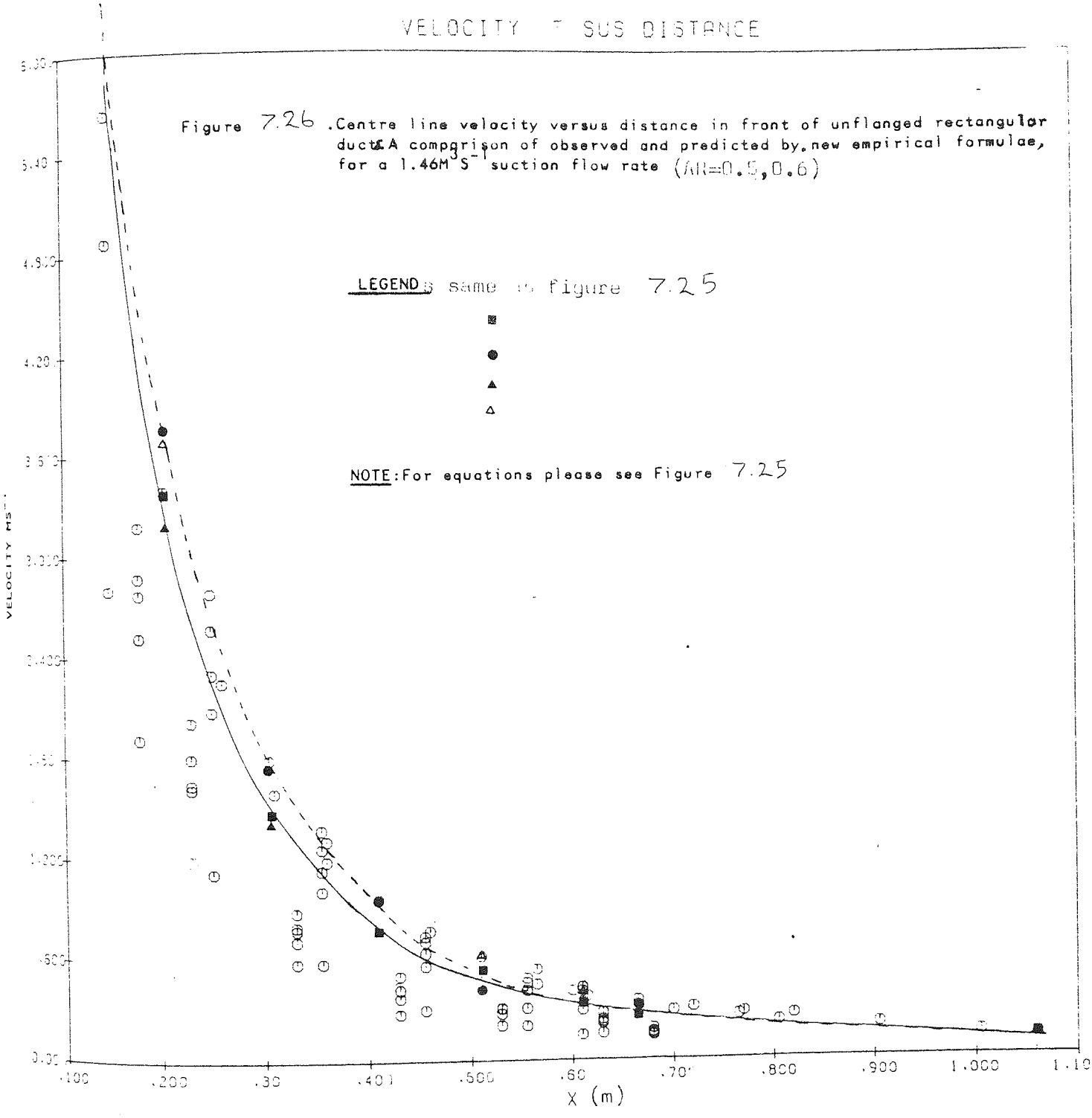

Figure 7.26 .Centre line velocity versus distance in front of unflanged rectangular duct. A comparison of observed and predicted by new empirical formulae, for a 1.46M^3S^{-1} suction flow rate (AR=0.5,0.6)

LEGEND: same as Figure 7.25

NOTE: For equations please see Figure 7.25

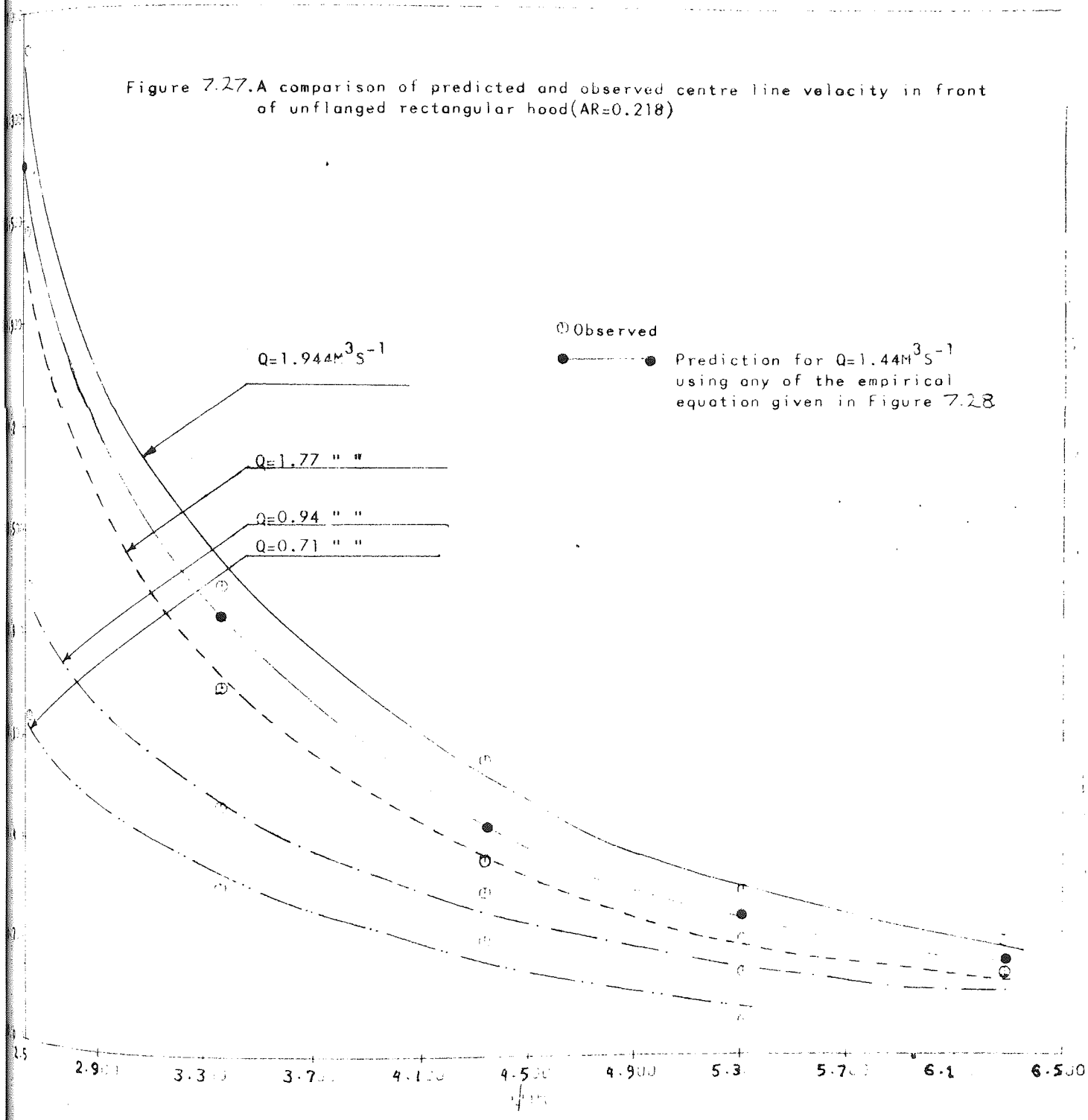

Figure 7.27. A comparison of predicted and observed centre line velocity in front of unflanged rectangular hood(AR=0.218)

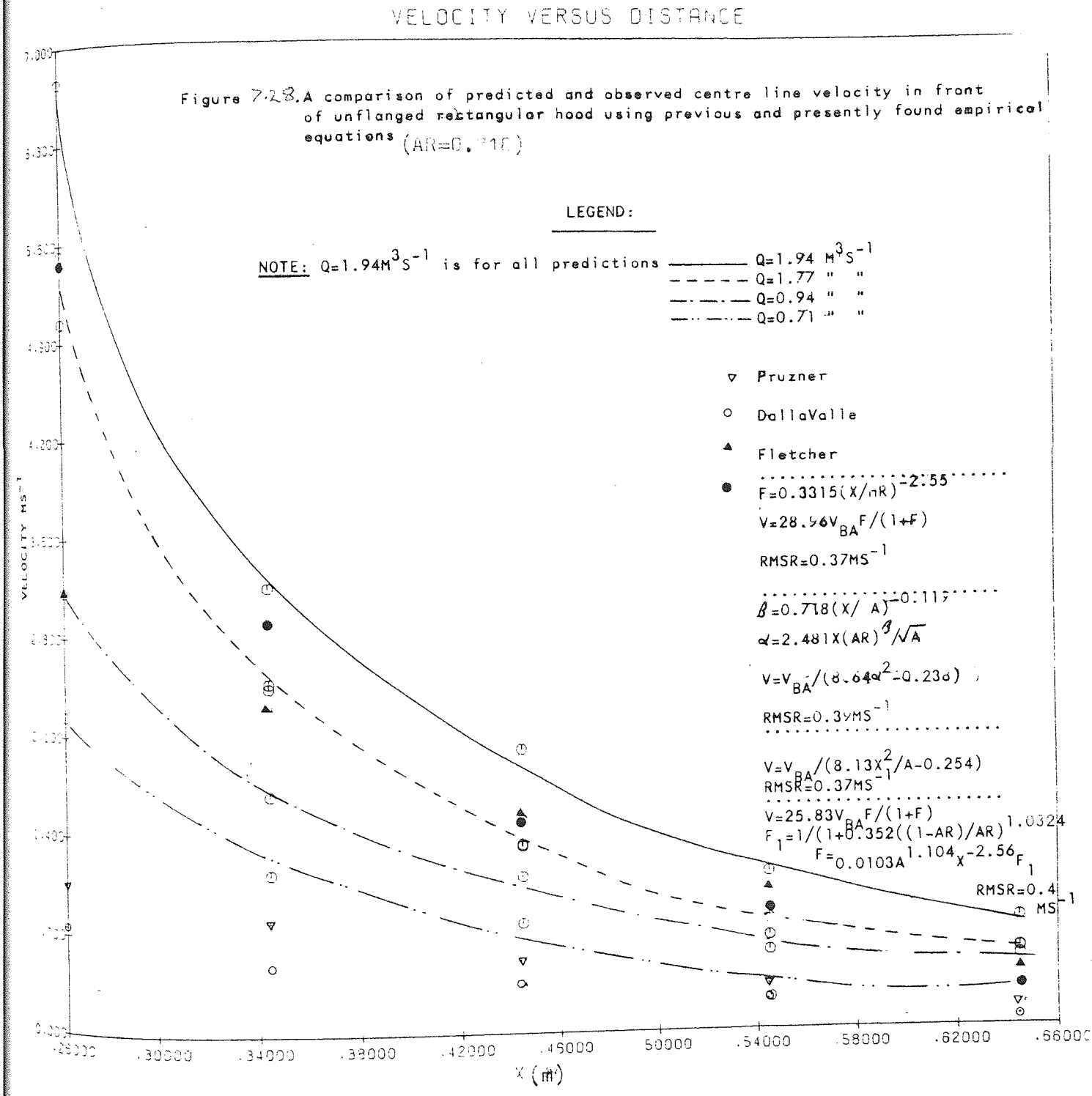

Figure 7.28. A comparison of predicted and observed centre line velocity in front of unflanged rectangular hood using previous and presently found empirical equations (AR=0.210)

figure 7.29. Centre line velocity in front of unflanged rectangular hood(AR=0.218) for different flow of suction

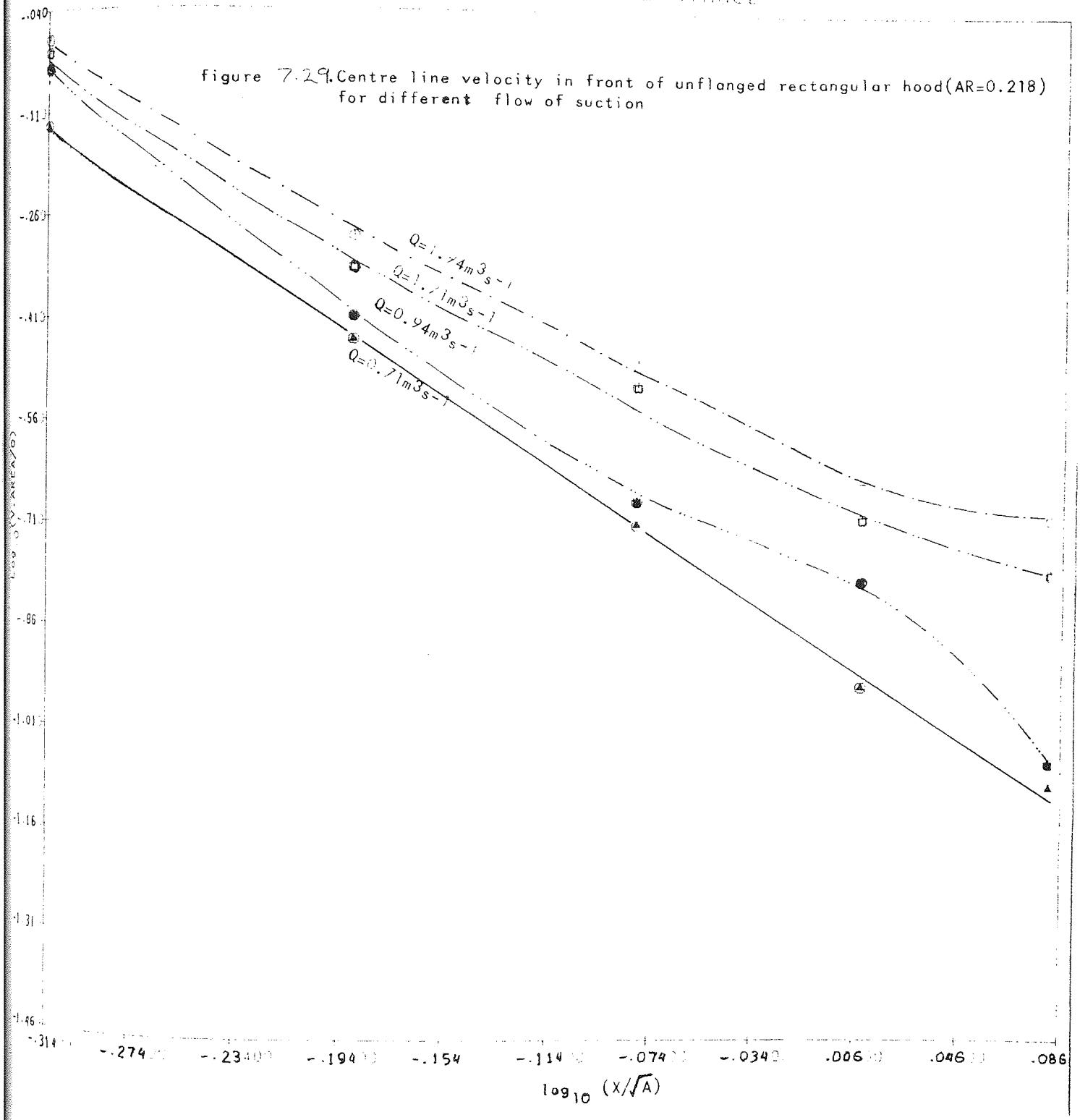

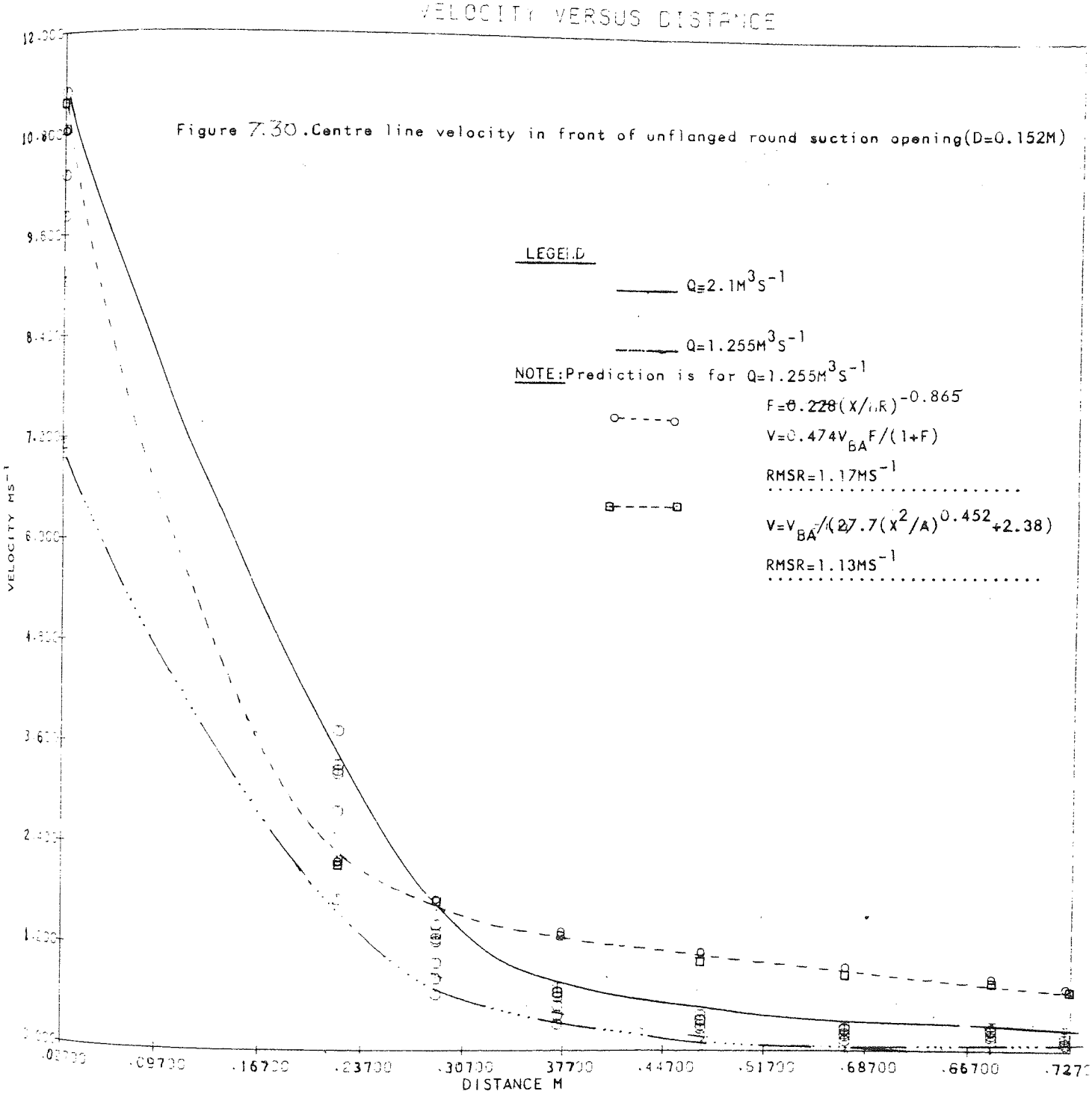

Figure 7.30. Centre line velocity in front of unflanged round suction opening(D=0.152M)

Figure 7.31 .The observed and predicted centre line velocity in front of round unflanged suction opening(D=0.152M)

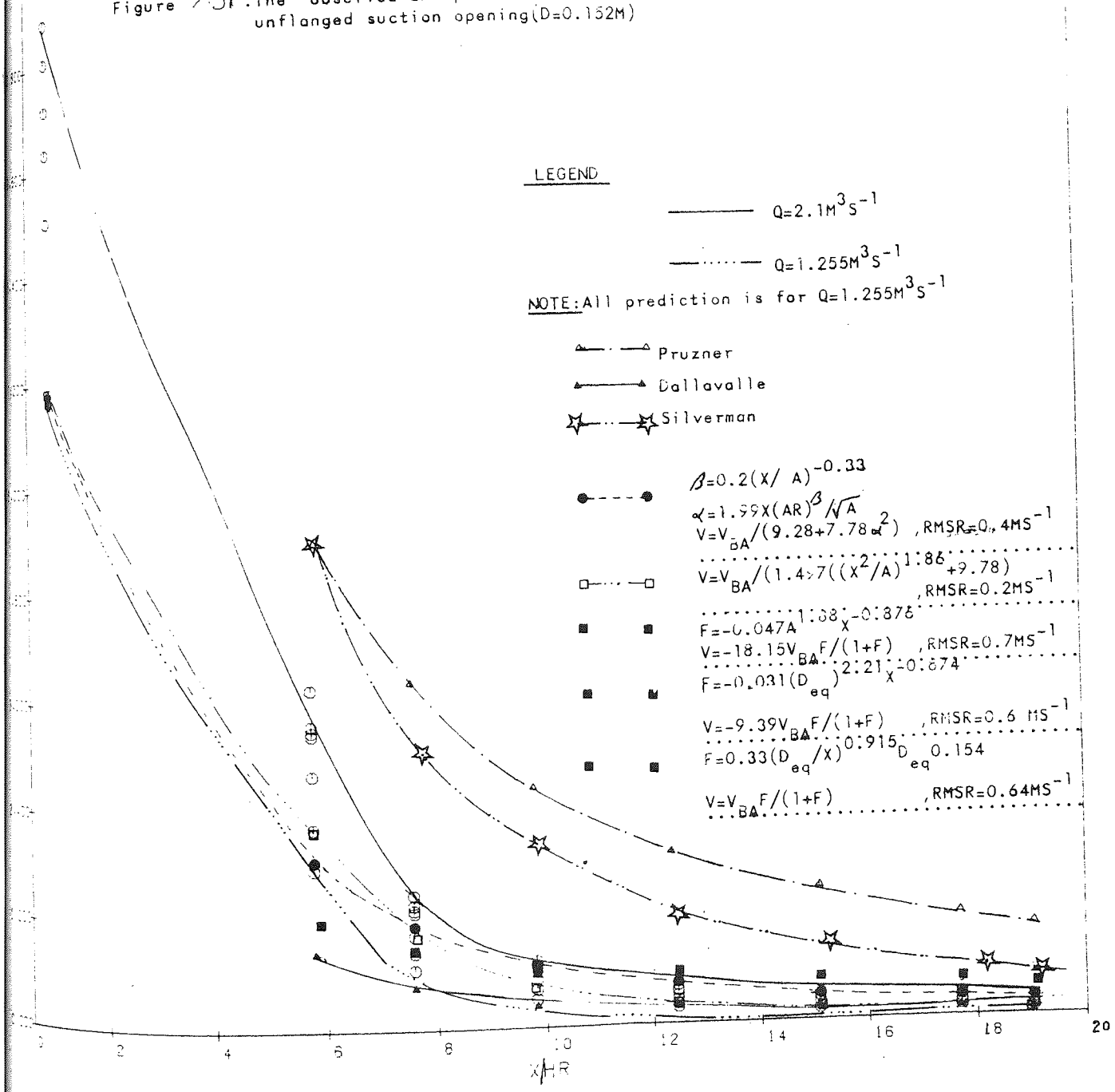

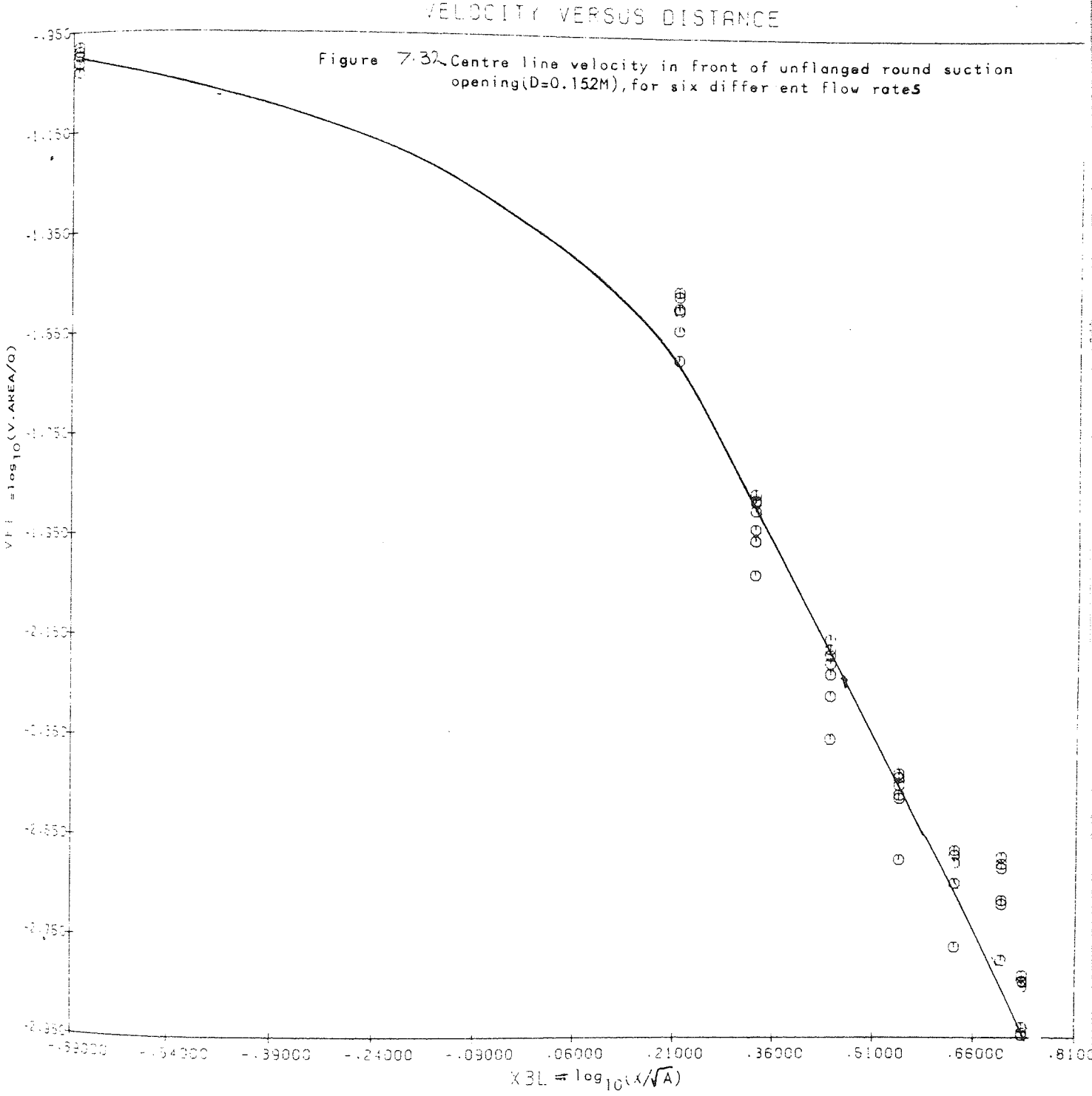

Figure 7.32 Centre line velocity in front of unflanged round suction opening(D=0.152M), for six differ ent flow rates

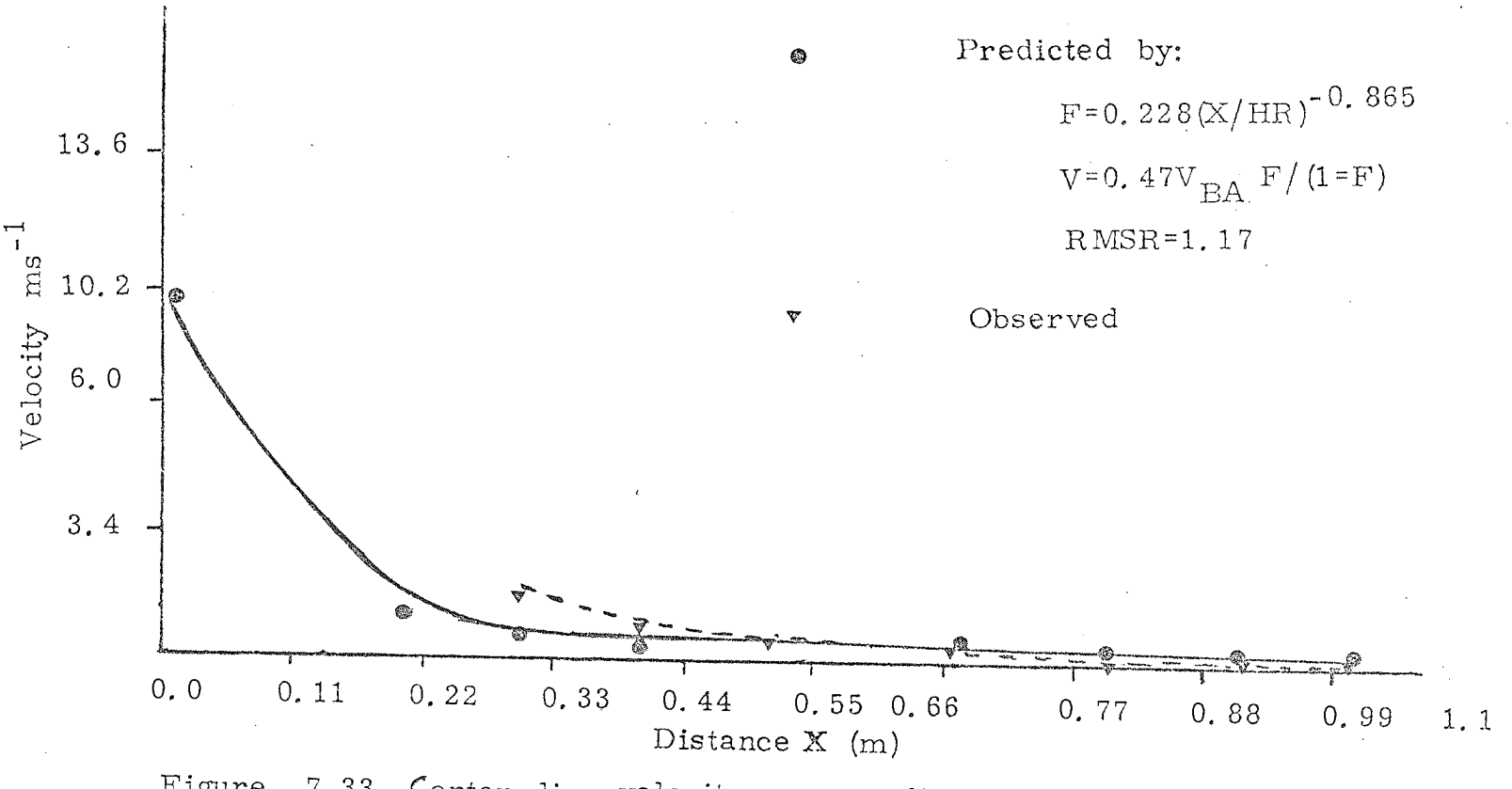

Figure 7.33 Center line velocity versus distance in front of different geometry shaped suction openings (AR=0.5, 0.6, 0.218, 1 (D=0.152).

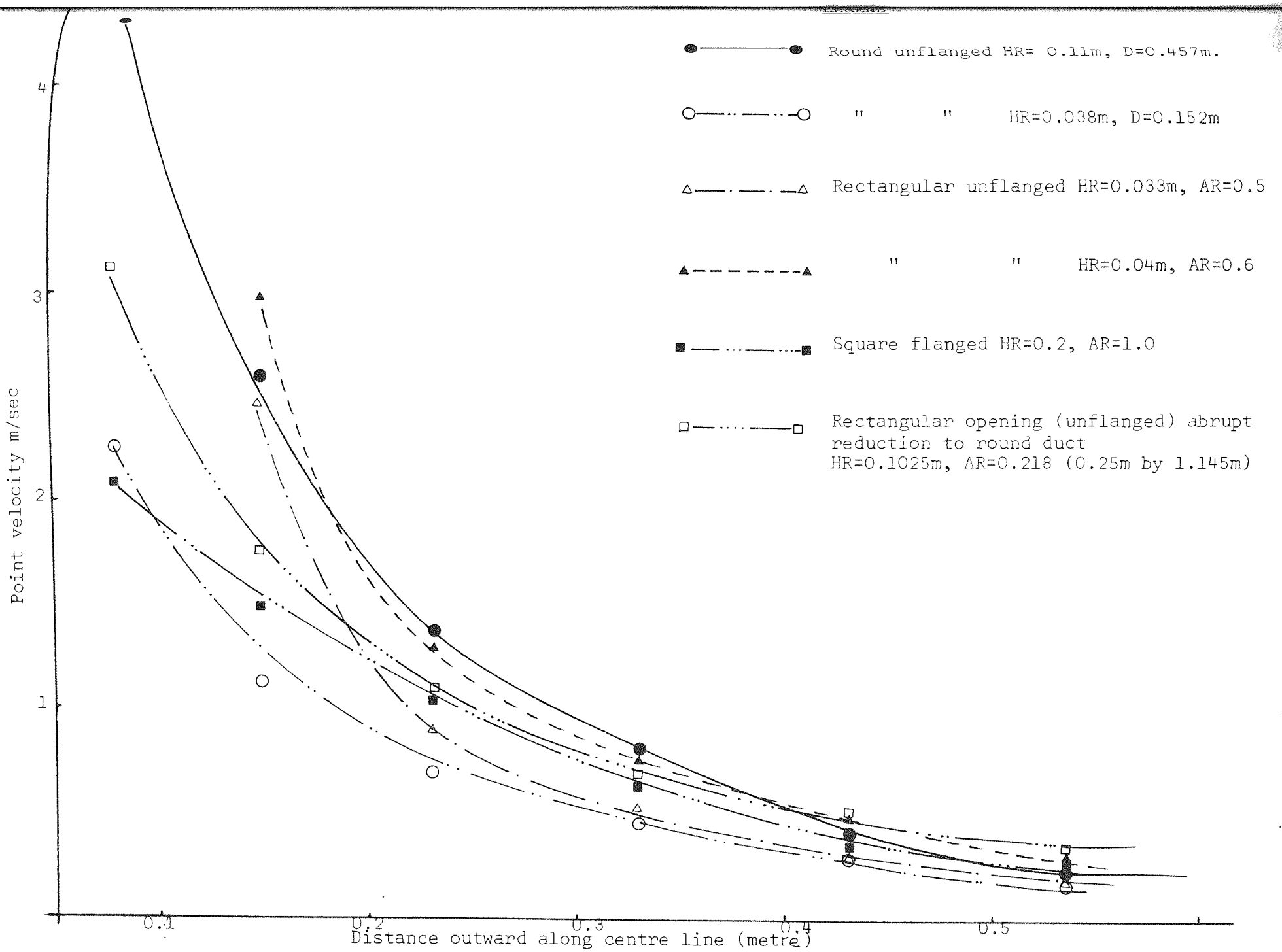

Figure 7.34 Centre line velocity characteristics of different suction opening under the same flow rate of suction.

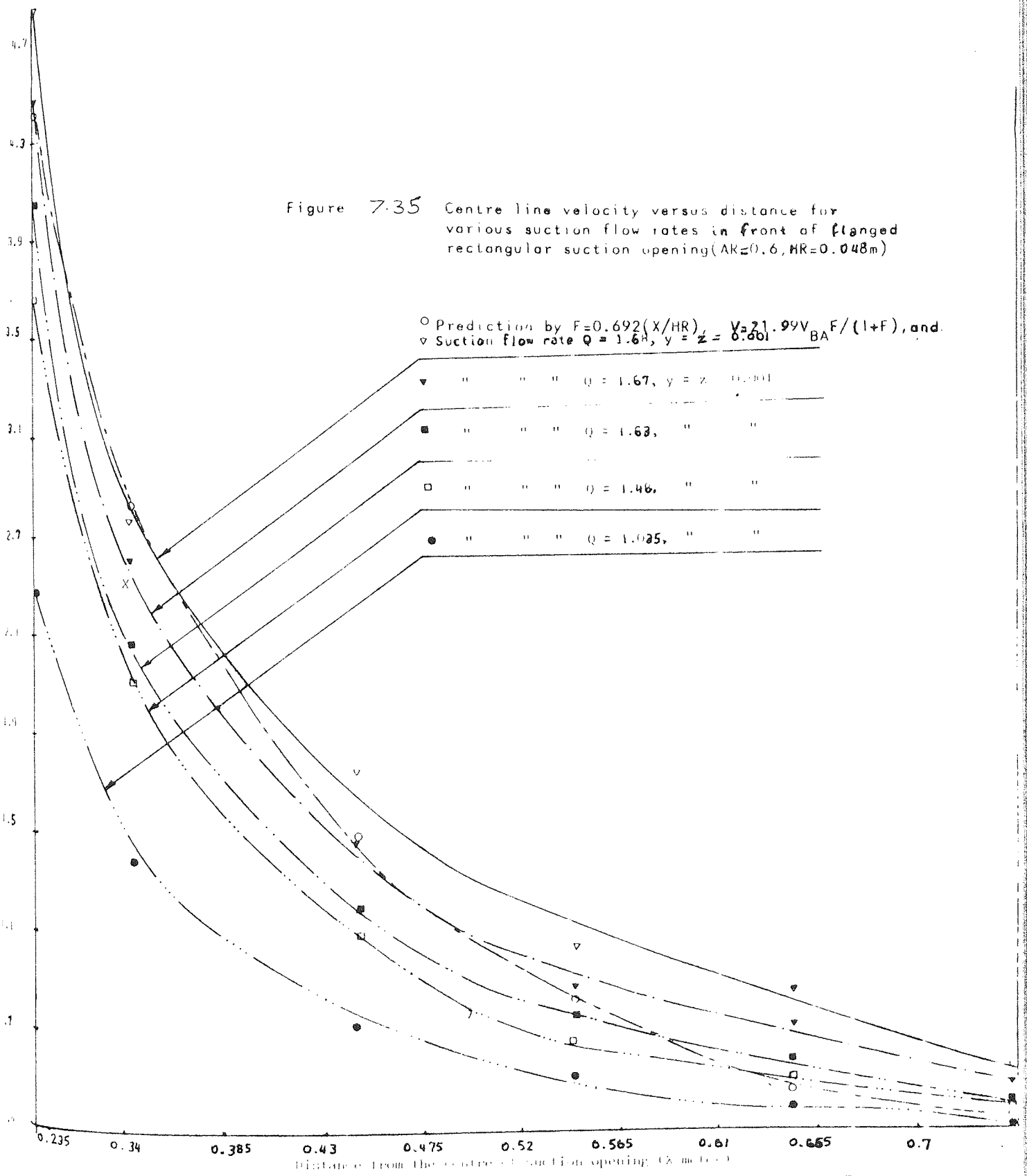

Figure 7.35 Centre line velocity versus distance for various suction flow rates in front of flanged rectangular suction opening(AR=0.6, HR=0.048m)

Figure 7.36 Centre line velocity for different flow of suction followed Dalla Valle's methods of plot(AR=0.6)

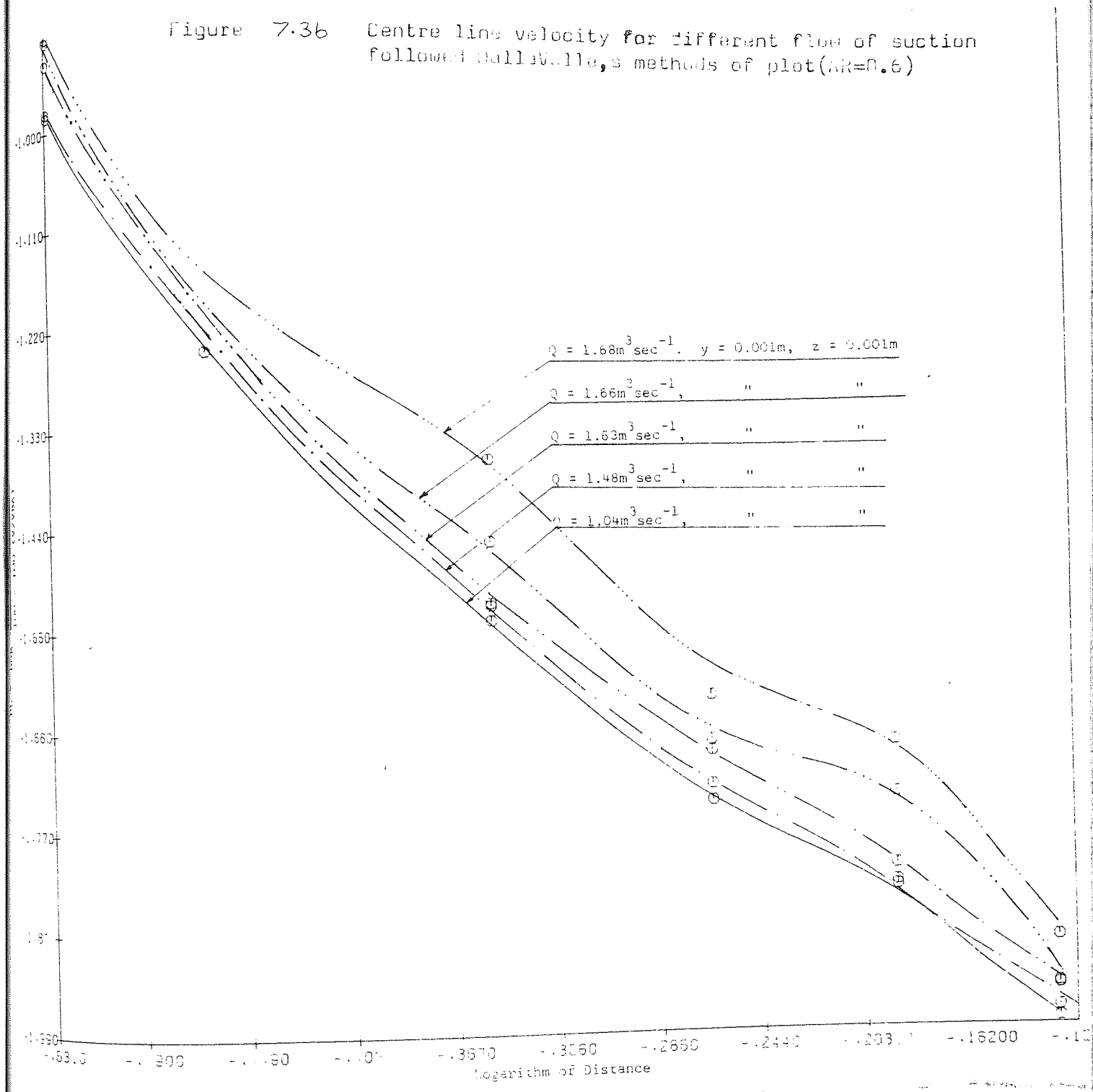

Figure 7.37 The plot of centre line velocity followed Pruzner method of treating the data(AR=0.6)

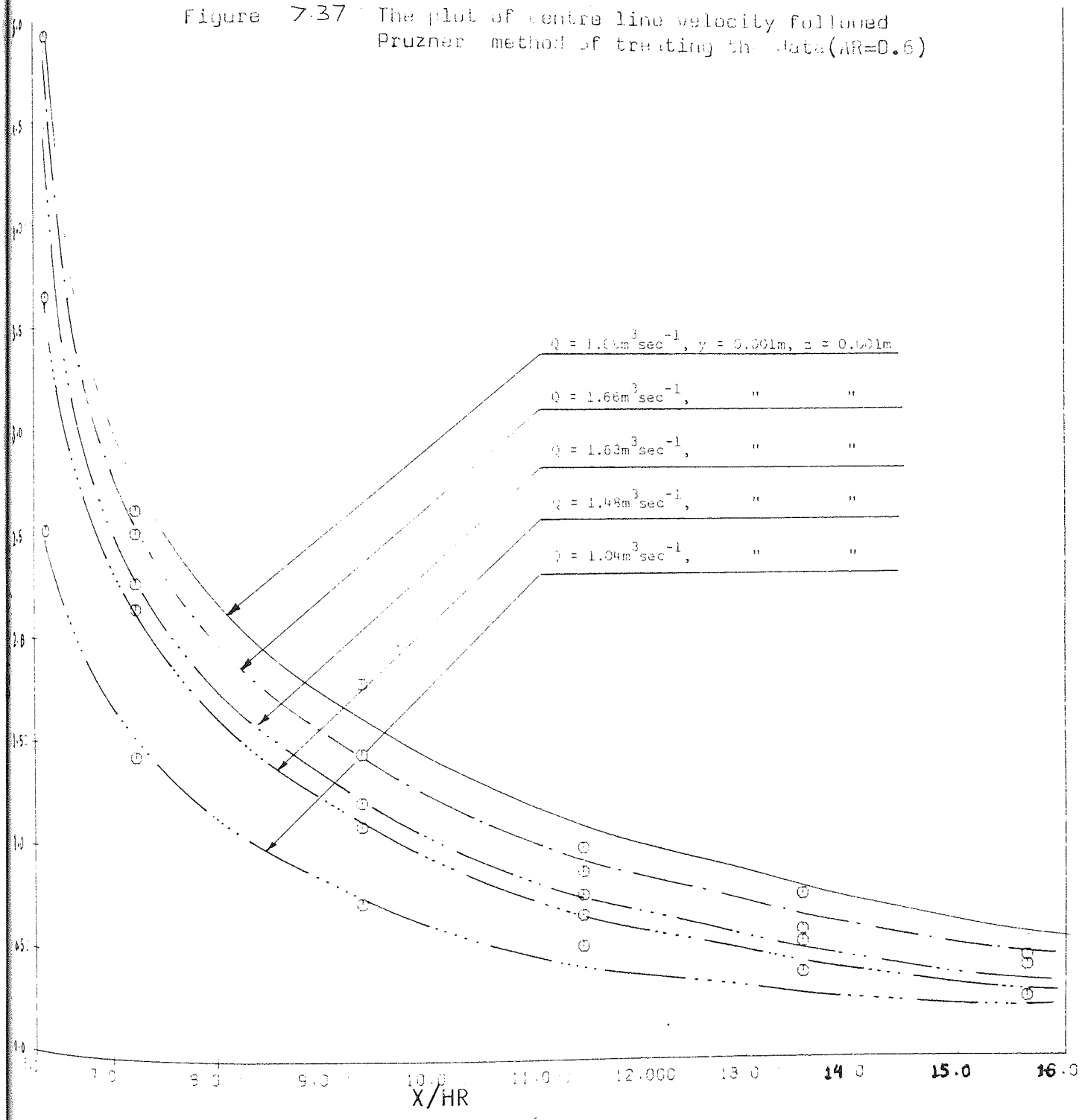

Figure 7.38 Plot of centre-line velocity followed the way Silverman treated the measured point velocity (A=0.5)

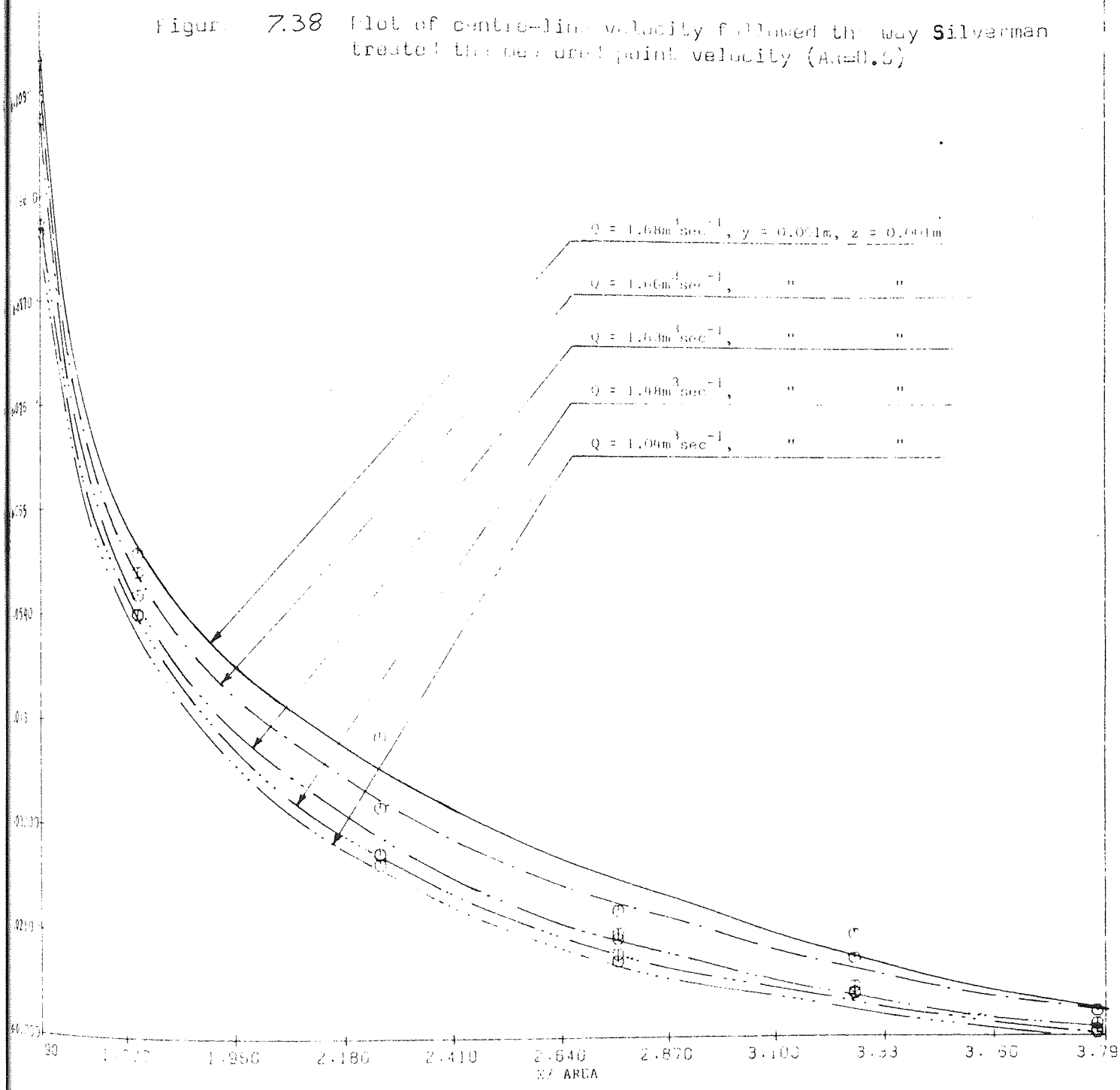

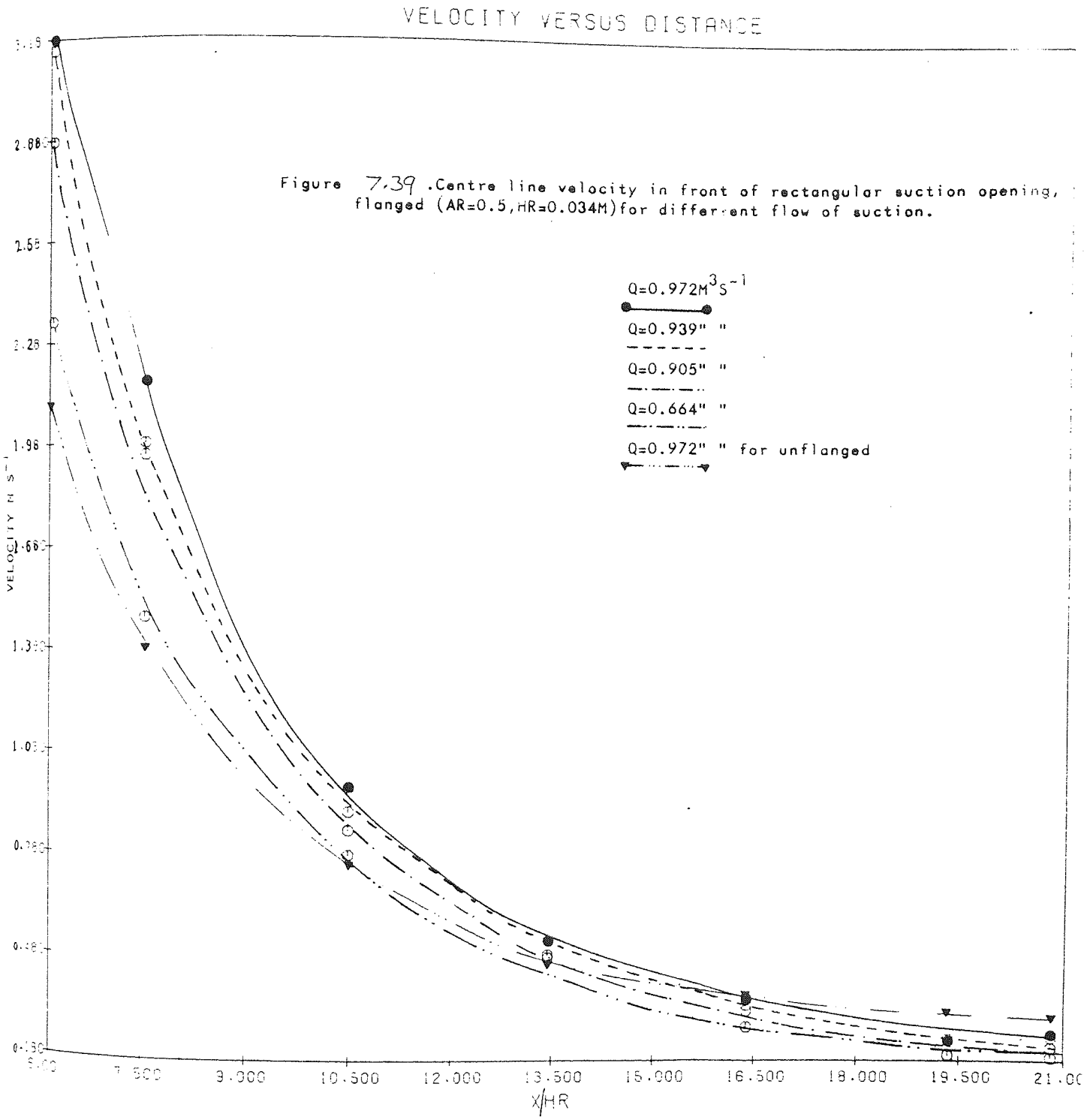

Figure 7.39 .Centre line velocity in front of rectangular suction opening, flanged (AR=0.5, HR=0.034M) for different flow of suction.

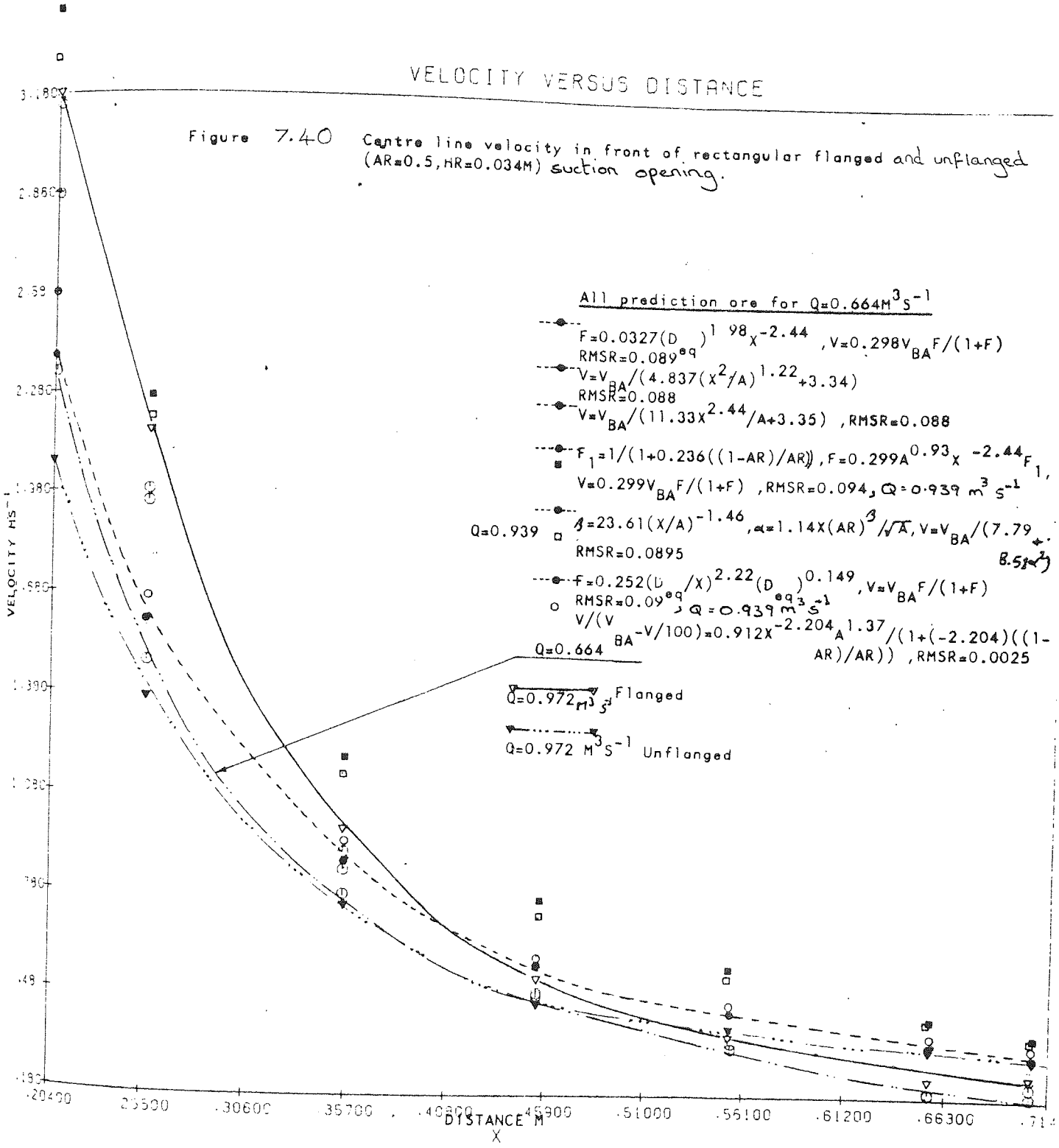

Figure 7.40 Centre line velocity in front of rectangular flanged and unflanged (AR=0.5, HR=0.034M) suction opening.

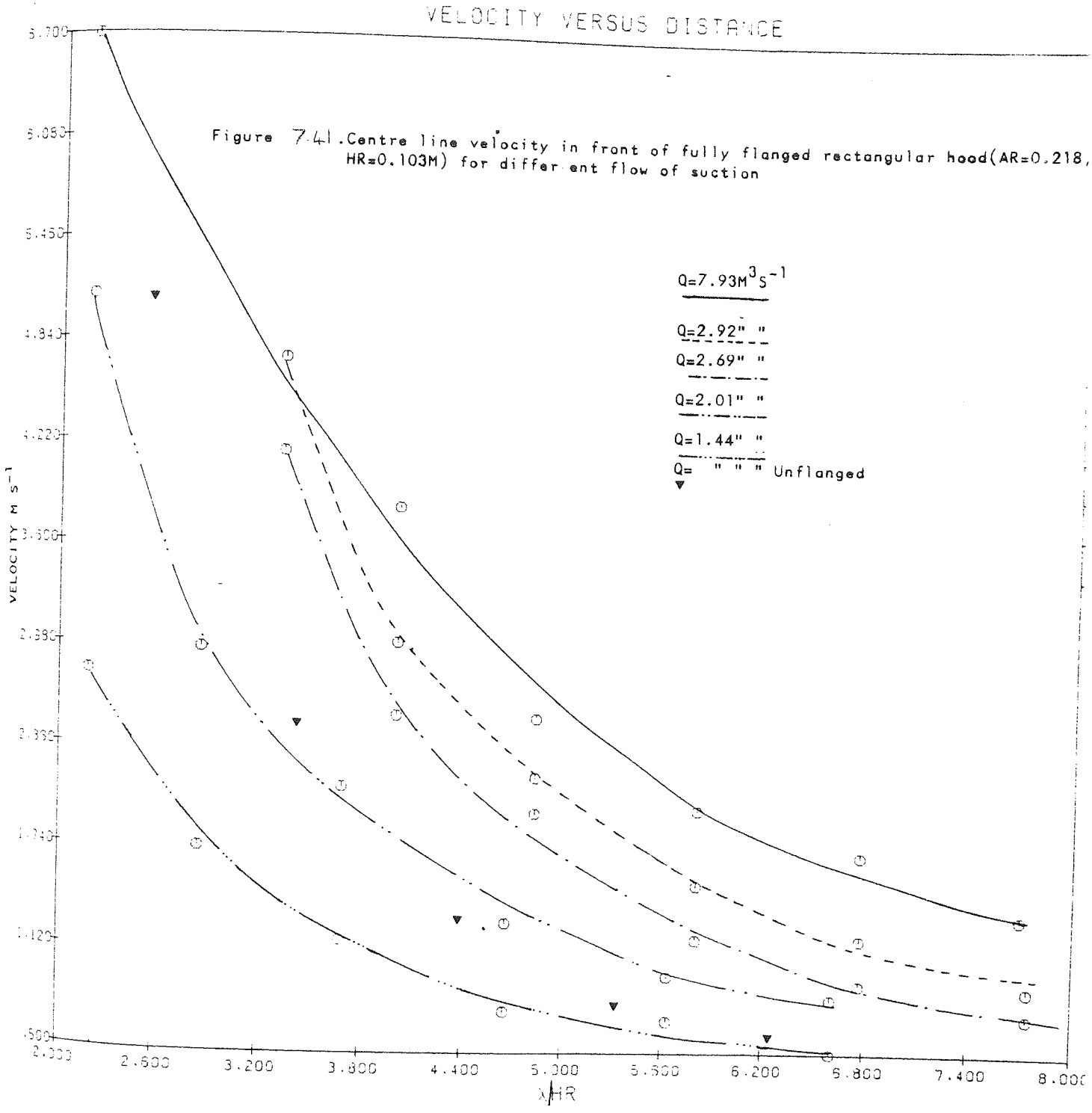

Figure 7.41. Centre line velocity in front of fully flanged rectangular hood(AR=0.218, HR=0.103M) for different flow of suction

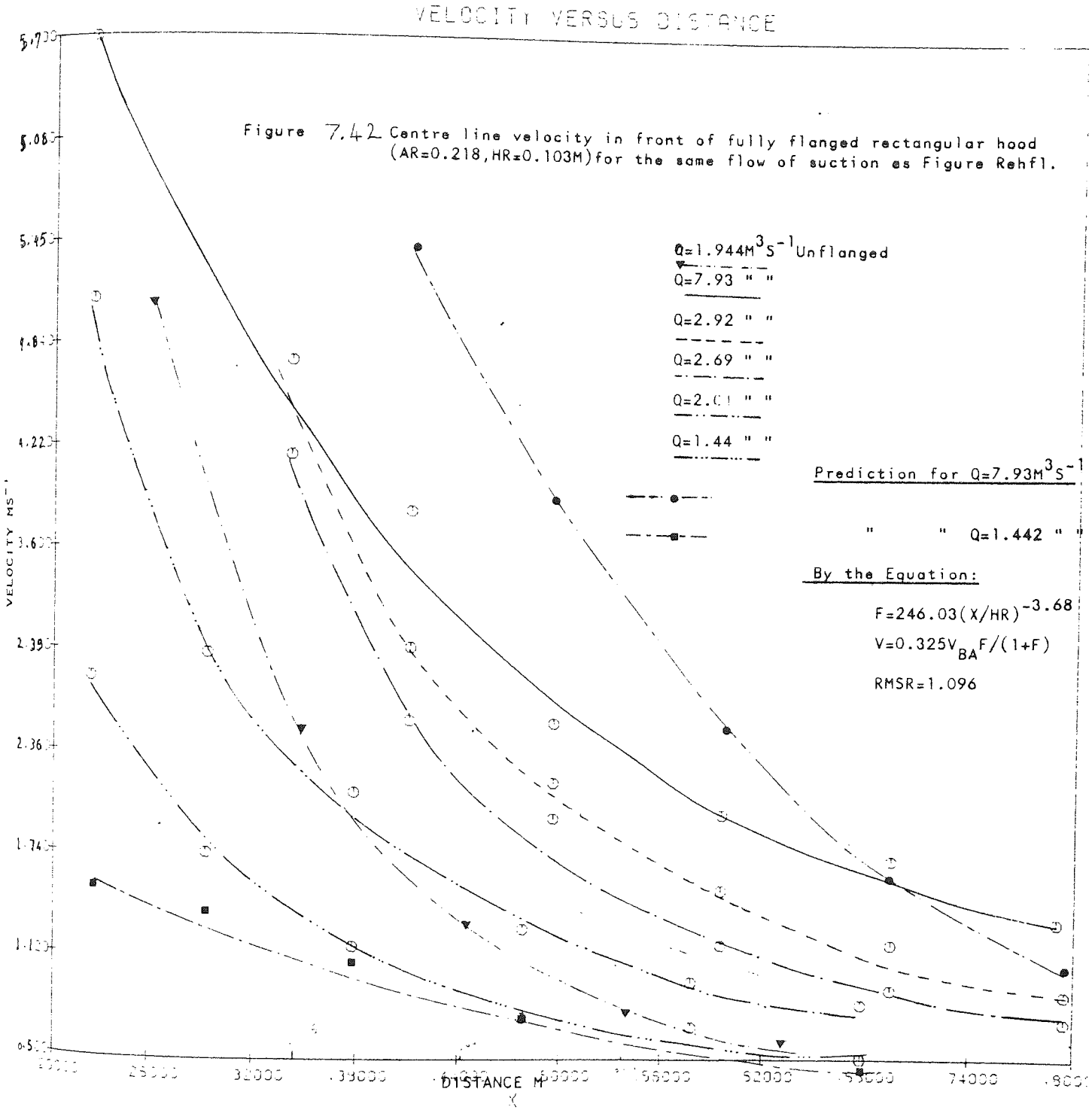

Figure 7.42 Centre line velocity in front of fully flanged rectangular hood (AR=0.218, HR=0.103M) for the same flow of suction as Figure Rehfl.

Figure 7.43 .Centre line velocity in front of flat plane flanged round suction opening for different suction flow rate(D=0.152M)

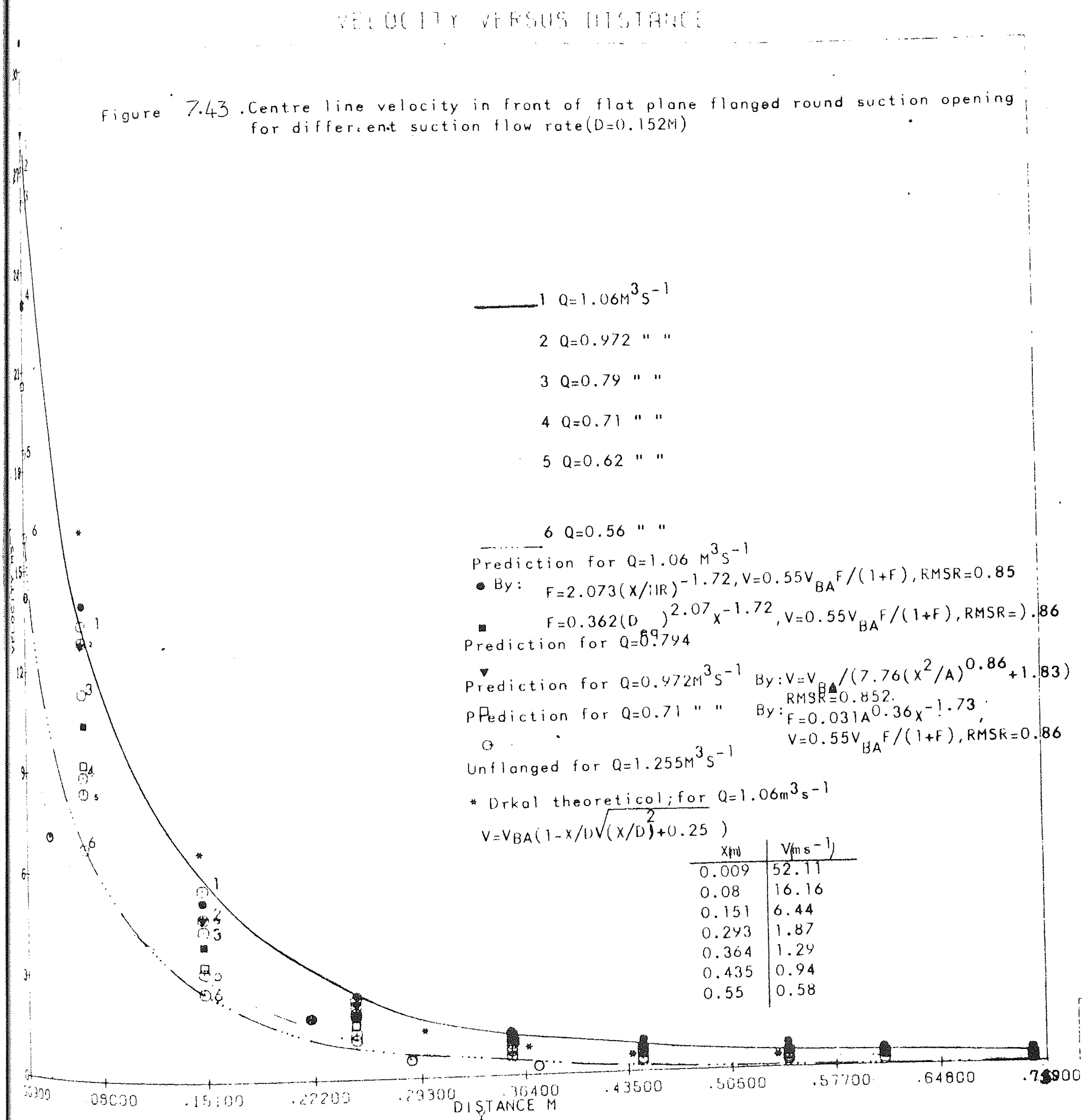

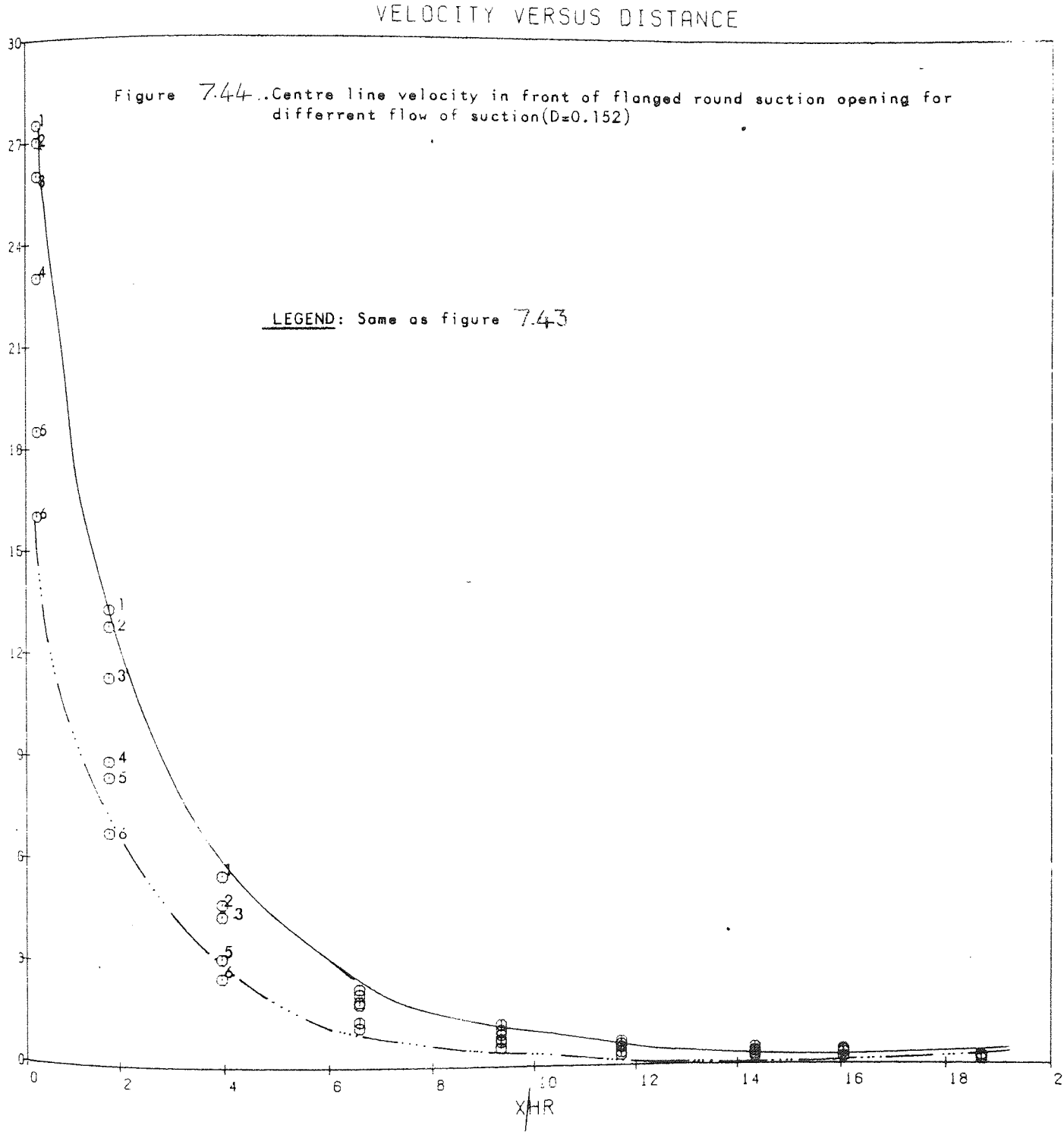

Figure 7.44 ..Centre line velocity in front of flanged round suction opening for differrent flow of suction(D=0.152)

LEGEND: Same as figure 7.43

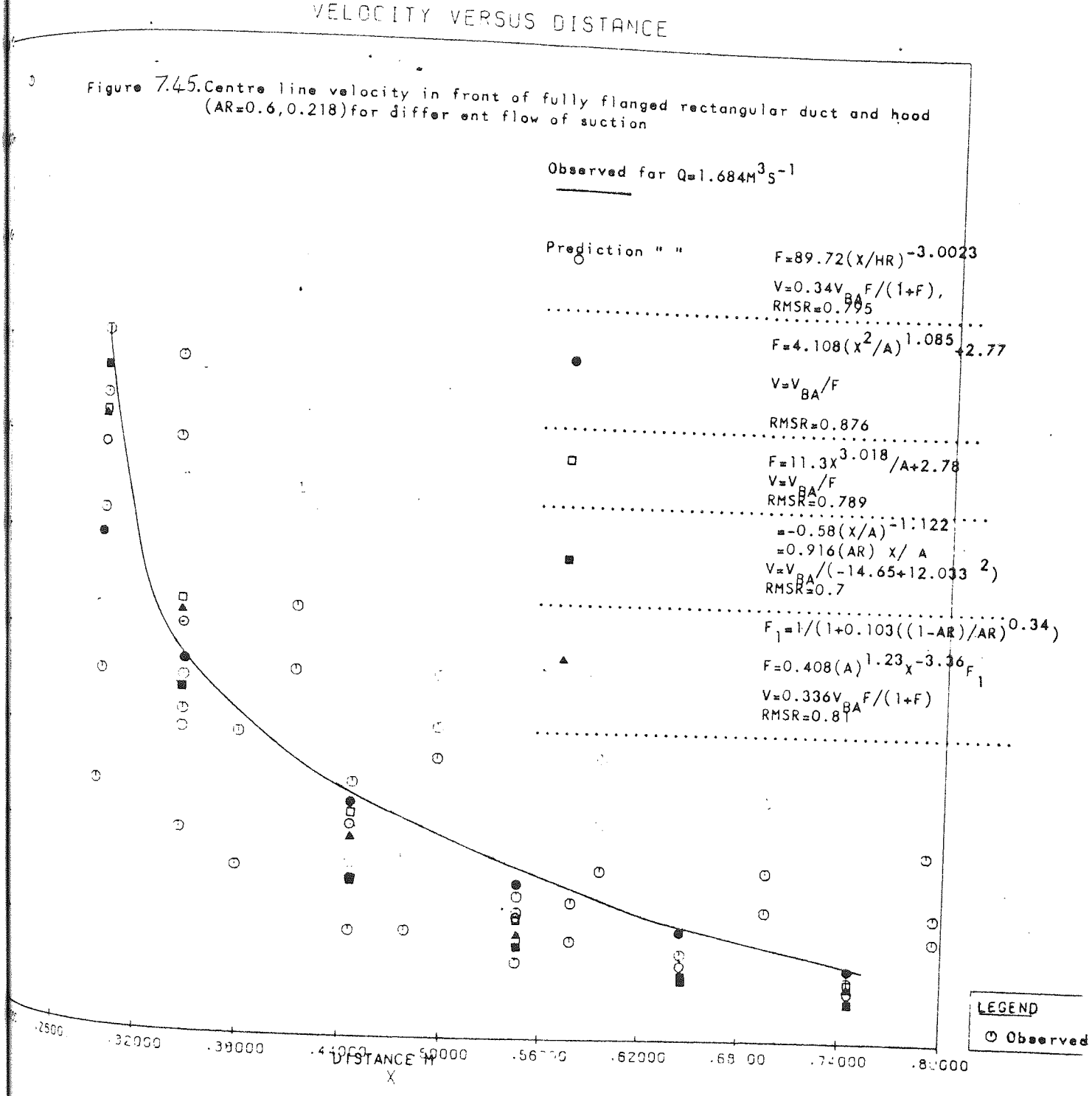

Figure 7.45. Centre line velocity in front of fully flanged rectangular duct and hood (AR=0.6, 0.218) for differ ent flow of suction

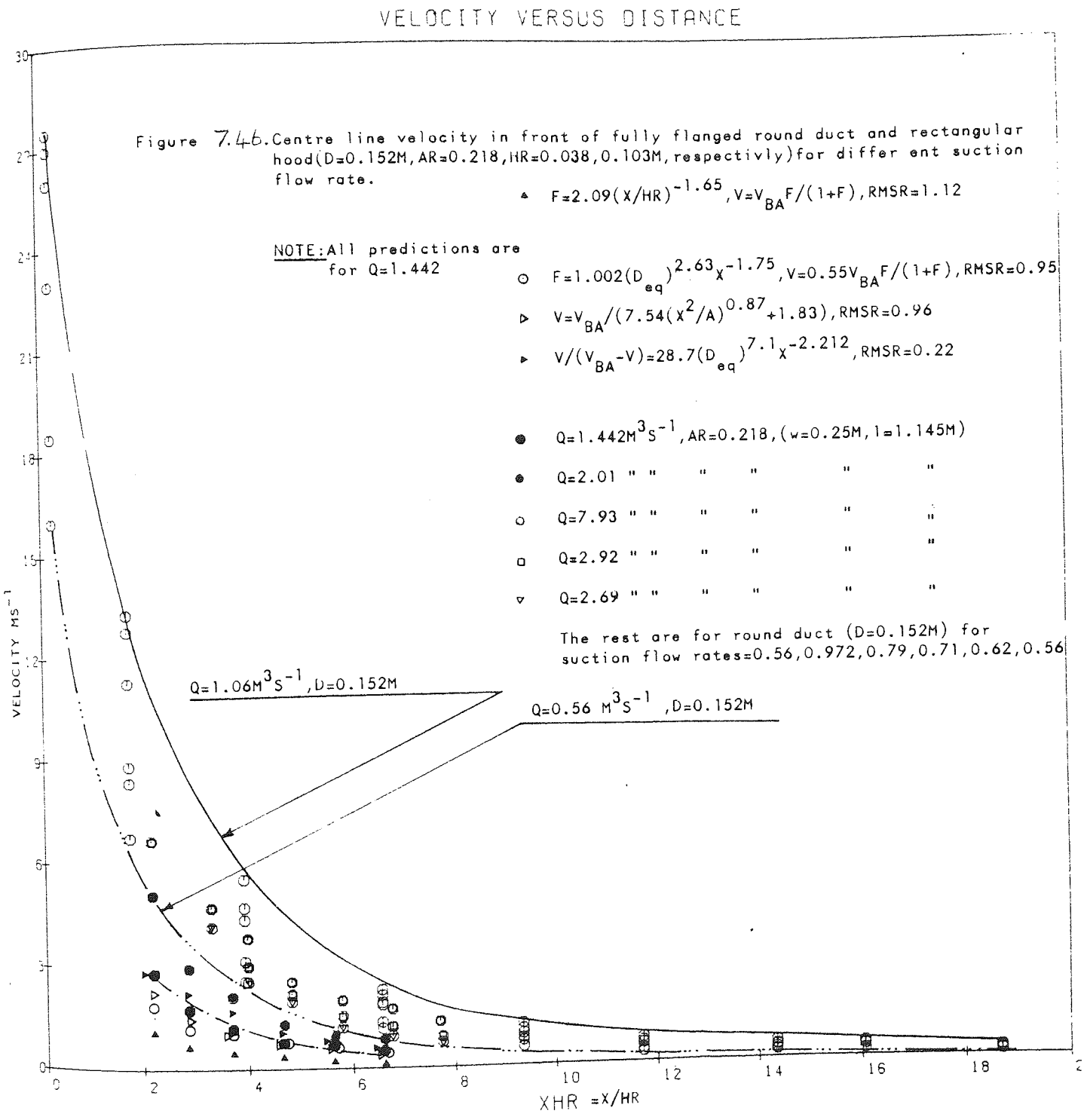
VELOCITY VERSUS DISTANCE
Figure 7.46. Centre line velocity in front of fully flanged round duct and rectangular hood(D=0.152M, AR=0.218, HR=0.038, 0.103M, respectivly) for differ ent suction flow rate.
NOTE: All predictions are for Q=1.442
▲ F=2.09(X/HR)^-1.65, V=V_BA F/(1+F), RMSR=1.12
○ F=1.002(D_eq)^2.63 X^-1.75, V=0.55V_BA F/(1+F), RMSR=0.95
▷ V=V_BA/(7.54(X^2/A)^0.87+1.83), RMSR=0.96
▸ V/(V_BA-V)=28.7(D_eq)^7.1 X^-2.212, RMSR=0.22
● Q=1.442M^3S^-1, AR=0.218, (w=0.25M, l=1.145M)
● Q=2.01 " " " " " "
○ Q=7.93 " " " " " "
□ Q=2.92 " " " " " "
▽ Q=2.69 " " " " " "
The rest are for round duct (D=0.152M) for suction flow rates=0.56, 0.972, 0.79, 0.71, 0.62, 0.56
Q=1.06M^3S^-1, D=0.152M
Q=0.56 M^3S^-1, D=0.152M
VELOCITY MS^-1
XHR =X/HR
0
2
4
6
8
10
12
14
16
18
3
6
9
12
15
18
21
24
27
30

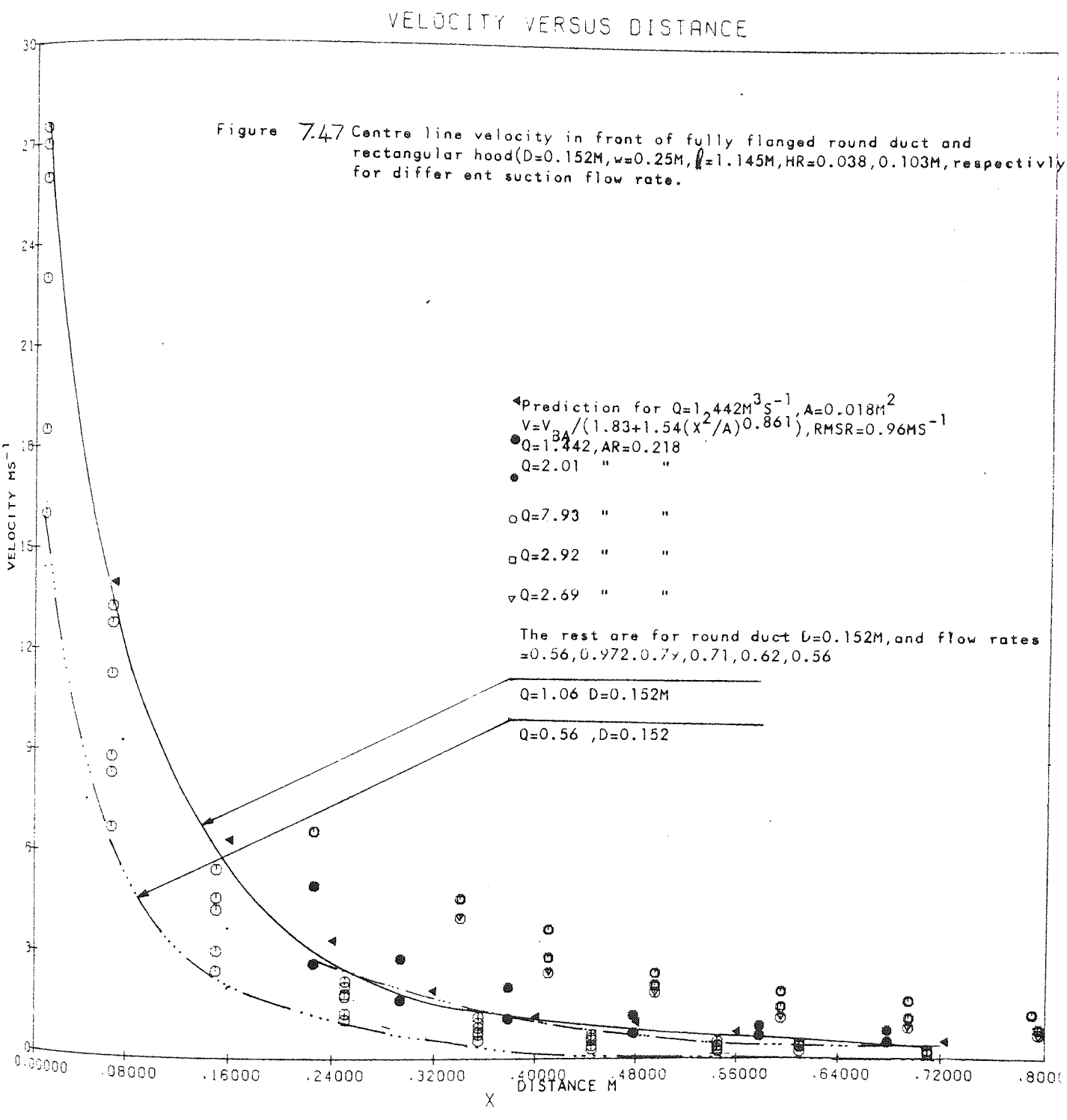

Figure 7.47 Centre line velocity in front of fully flanged round duct and rectangular hood(D=0.152M, w=0.25M, ℓ=1.145M, HR=0.038, 0.103M, respectivly for differ ent suction flow rate.

Figure 7.48 Centre line velocity in front of flanged rectangular ducts(AR=0.6, 0.5 and roundduct(D=0.152m)for different flow of suction

* Prediction for $Q=1.065M^3S^{-1}$ By:

■ $F=1.79(X/\sqrt{A})^{-1.54}$, $V=0.56V_{BA}F/(1+F)$, RMSR=0.9

◁ $V=V_{BA}/(7.13(X^2/A)^{0.807}+1.8)$, RMSR=0.812MS^{-1}

▶ $V=V_{BA}/(1.86+3.46(X^{1.63}/A)$, RMSR=0.73 " "

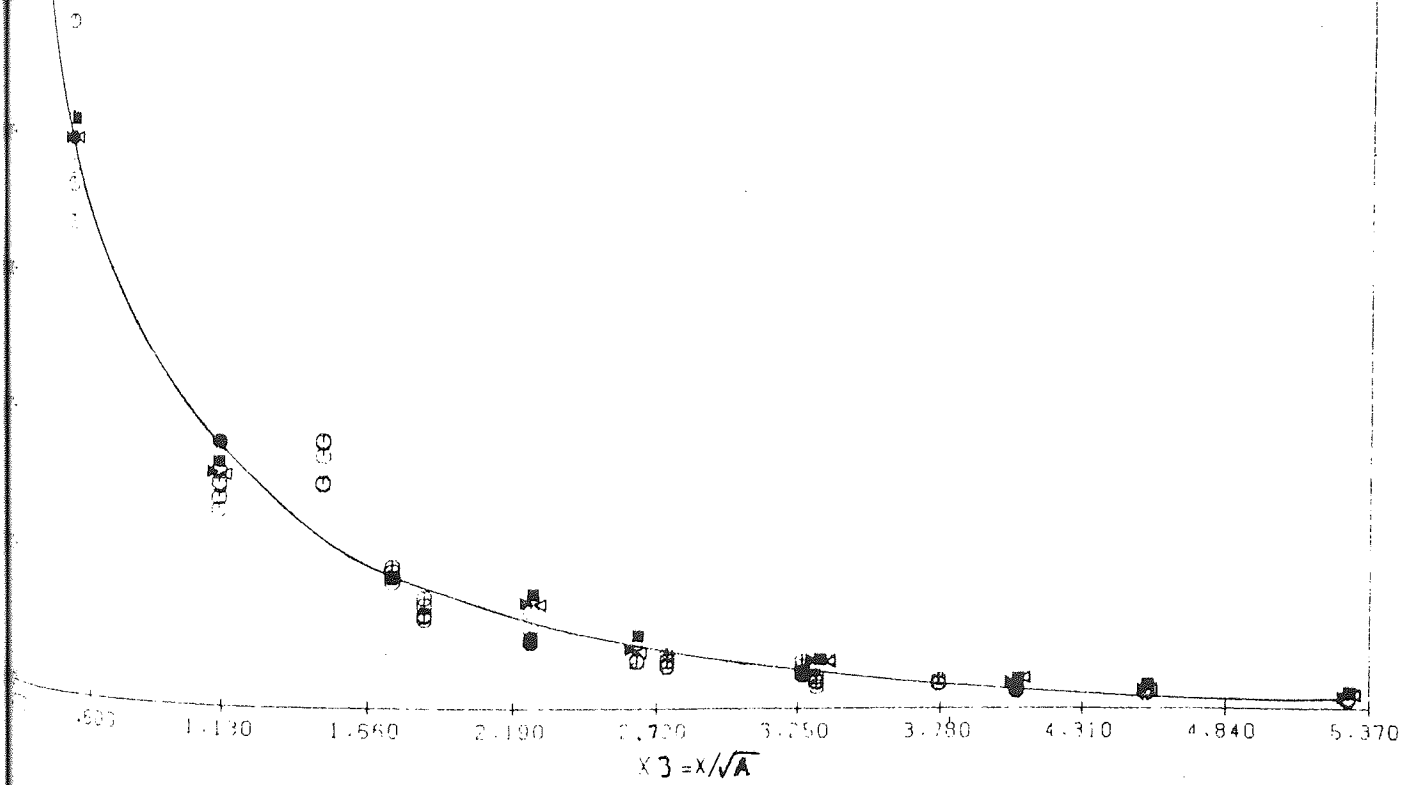

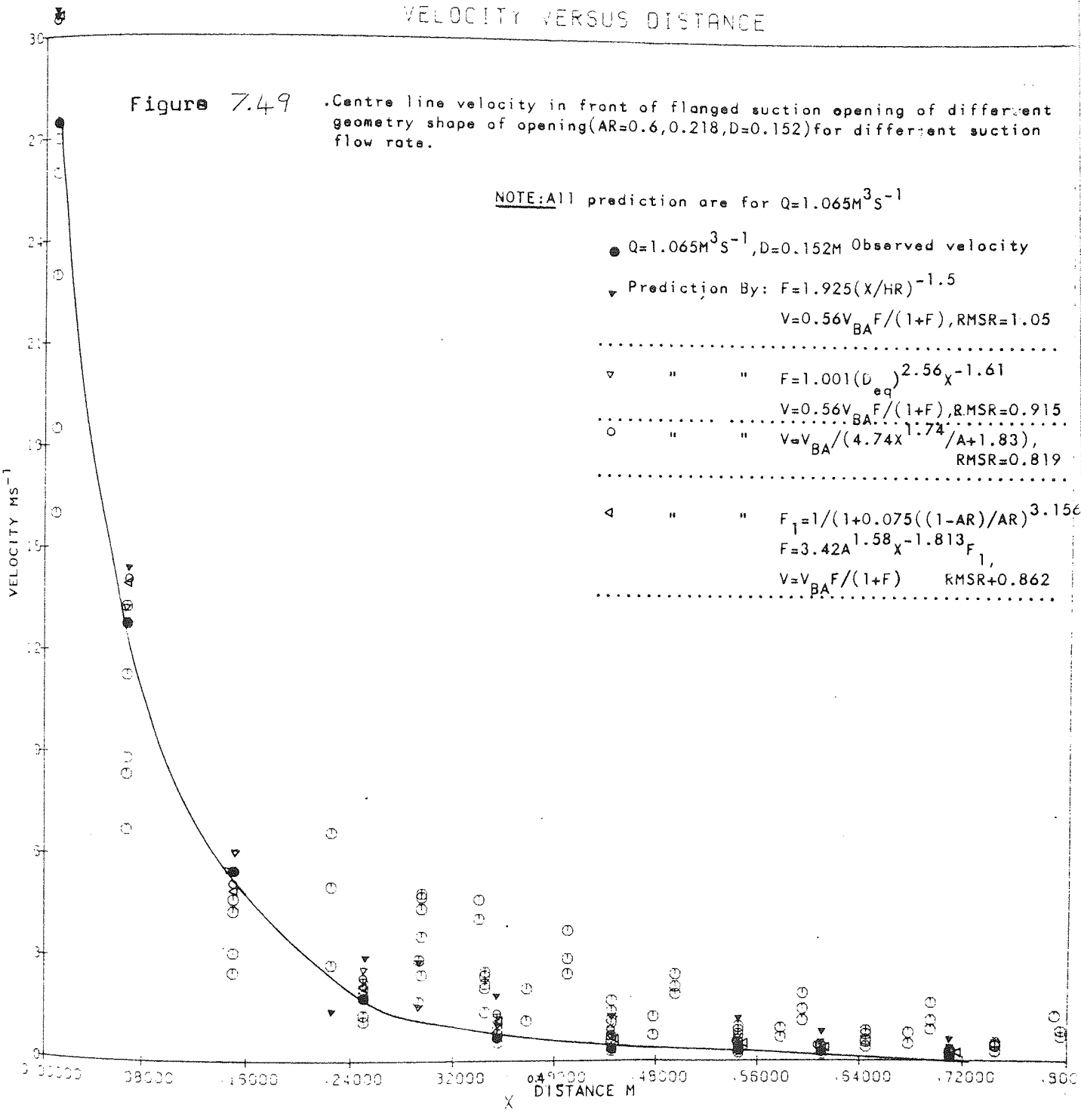

Figure 7.49 .Centre line velocity in front of flanged suction opening of different geometry shape of opening(AR=0.6,0.218,D=0.152)for different suction flow rate.

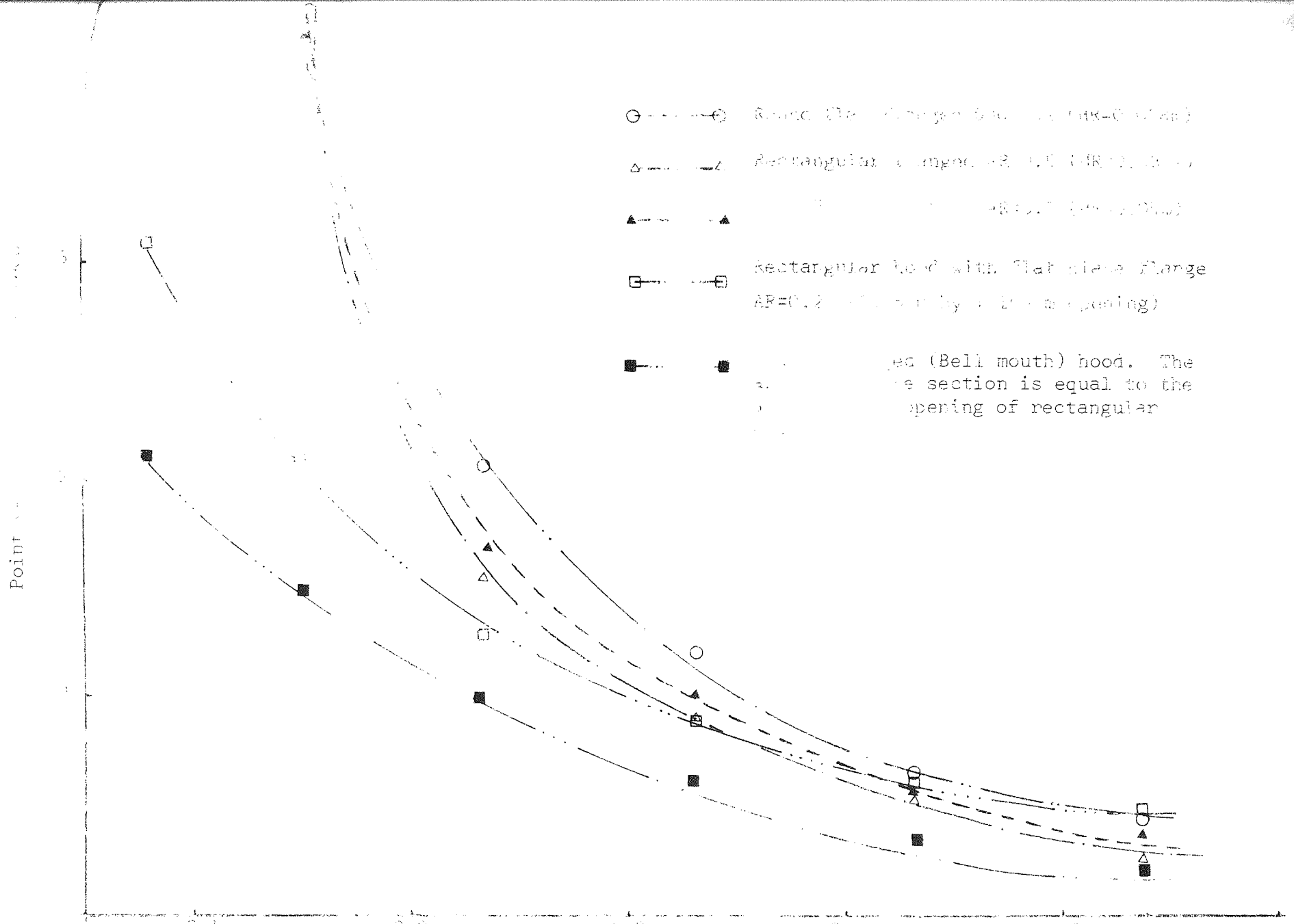

Figure 7.50. Centre line velocity of flanged (flat plane) suction openings drawing in the same volume of air

SYMMETRY TEST IN XOY PLANE OF ROUND DUCT

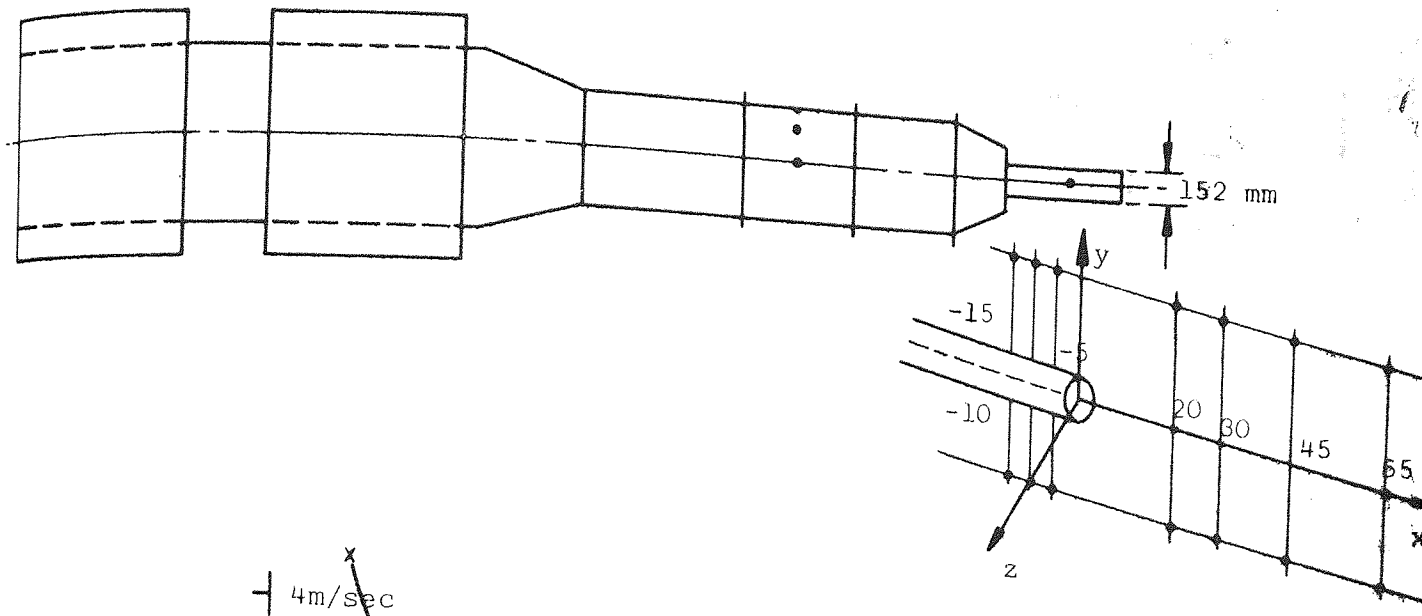

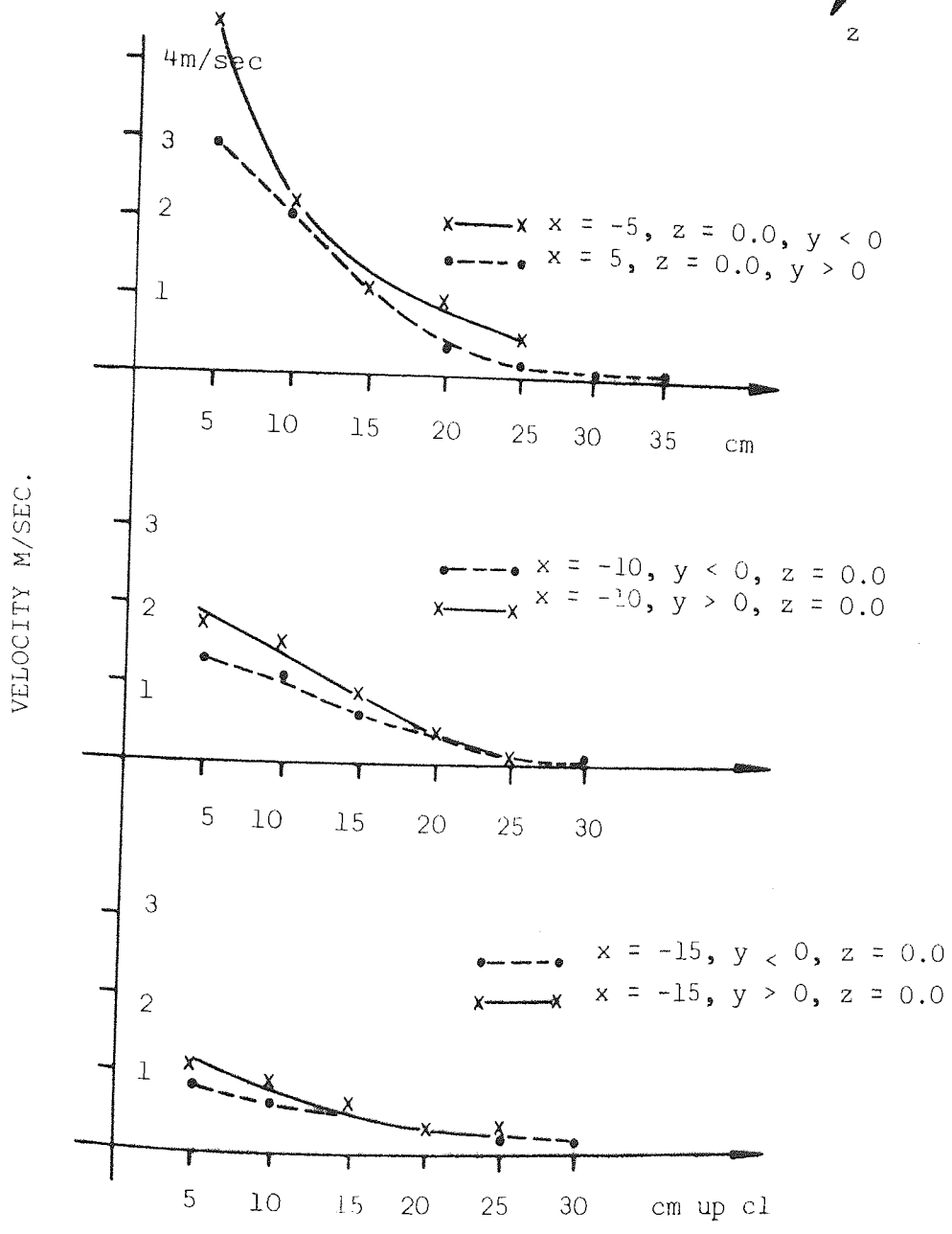

HORIZONTAL DISTANCE FROM SUCTION FACE

Figure 7.51. VELOCITY VERSUS DISTANCE (VERTICAL PLANE THROUGH CENTRE LINE XOY PLANE)

Figure 7.52 VELOCITY READING AT SYMMETRY POINTS AT SUCTION ZONE IN HORIZONTAL PLANE

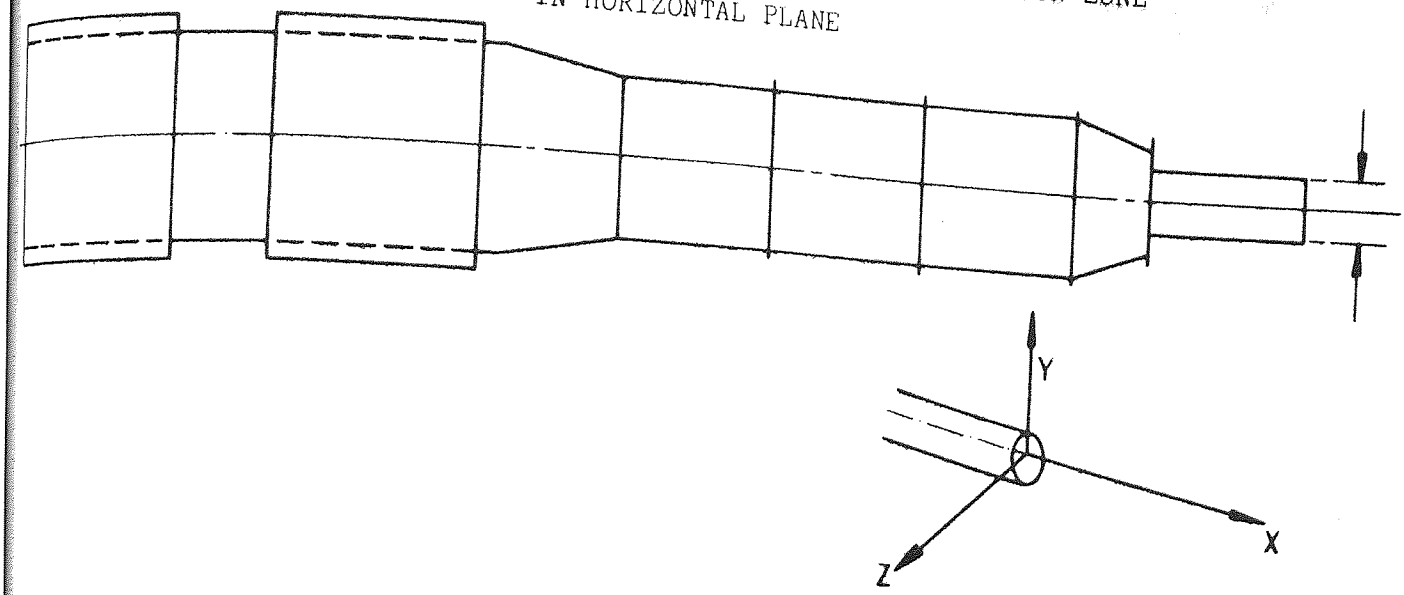

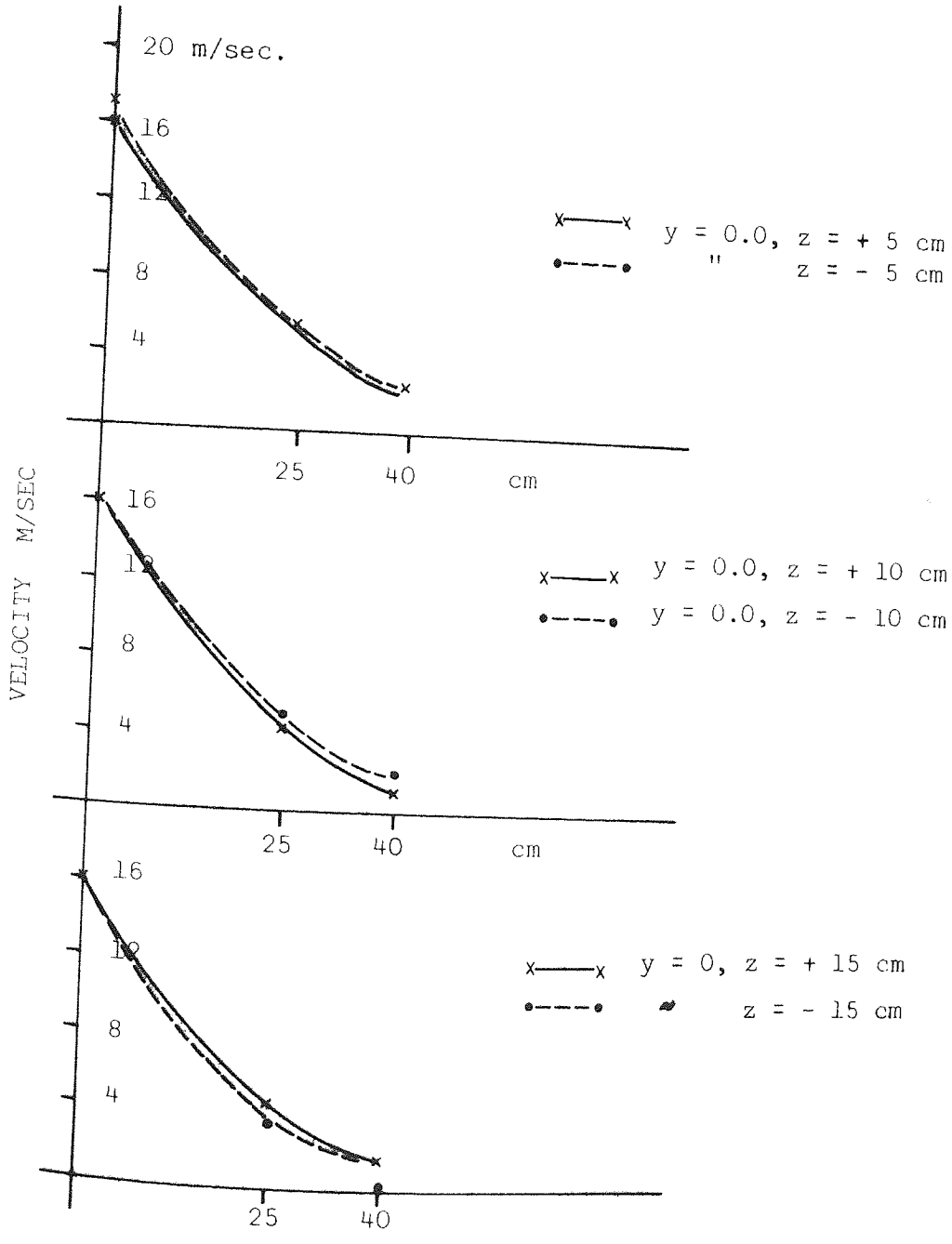

DISTANCE ALONG CENTRE LINE AWAY FROM SUCTION APERTURE.

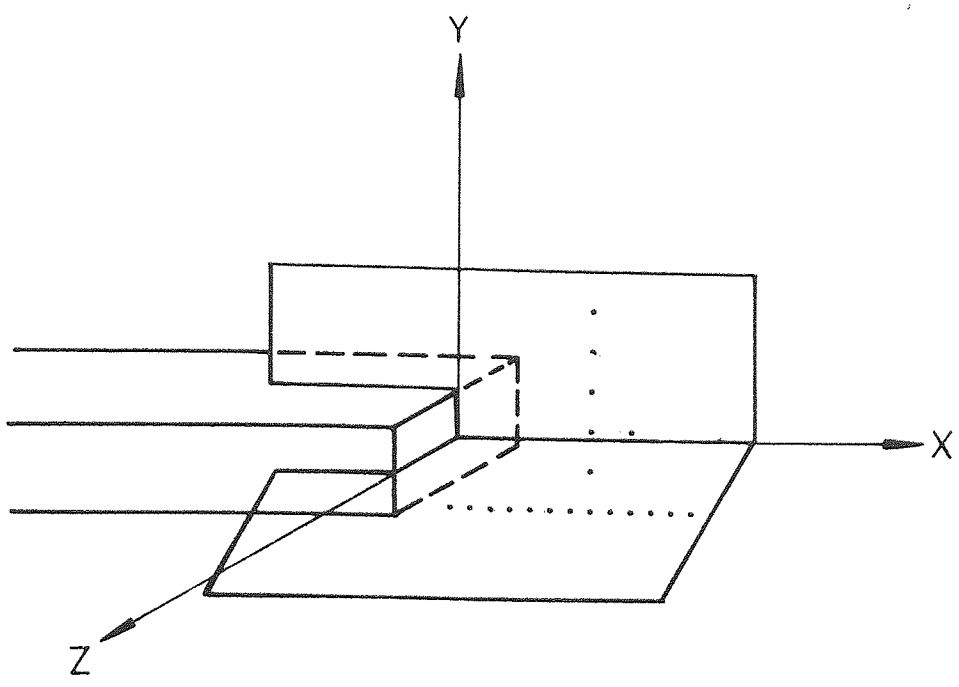

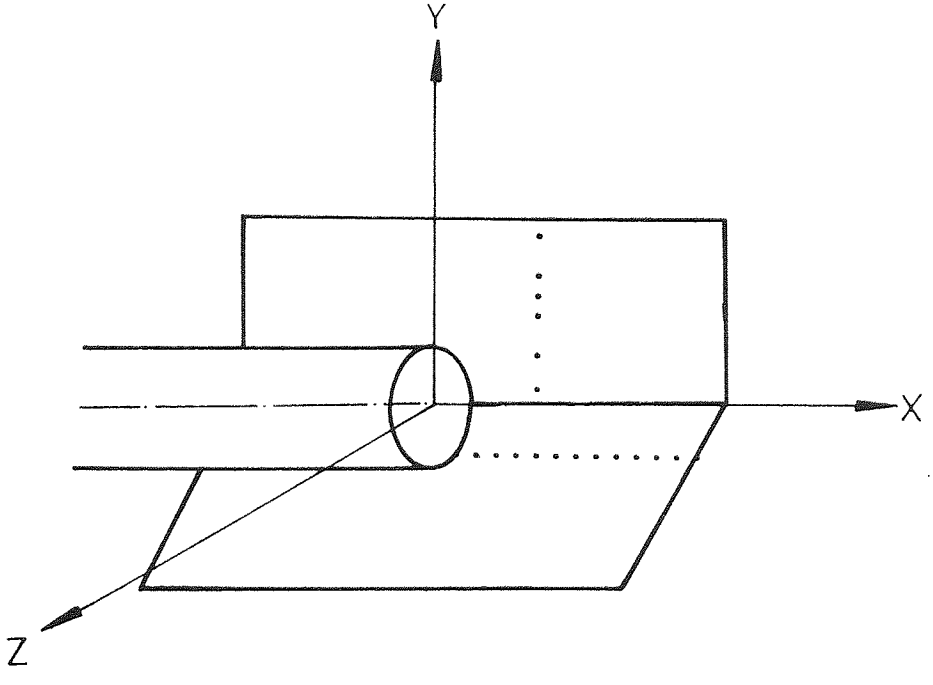

Figure 7.53 PLANE OF VELOCITY MEASURING POINTS

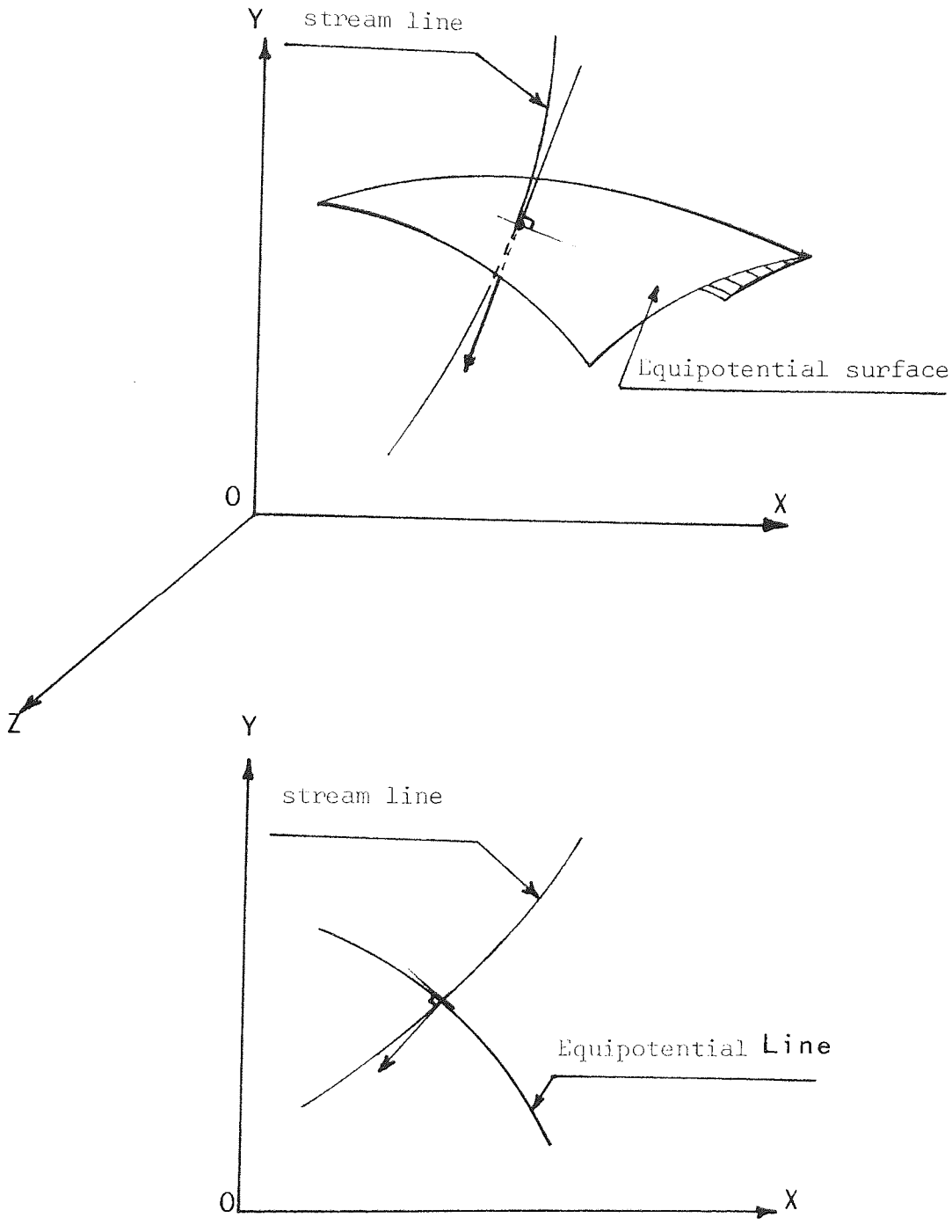

Figure 7.54 GRAPHICAL DEPICTION OF EQUIPOTENTIAL SURFACE AND LINE (CONTOUR SURFACE AND LINE)

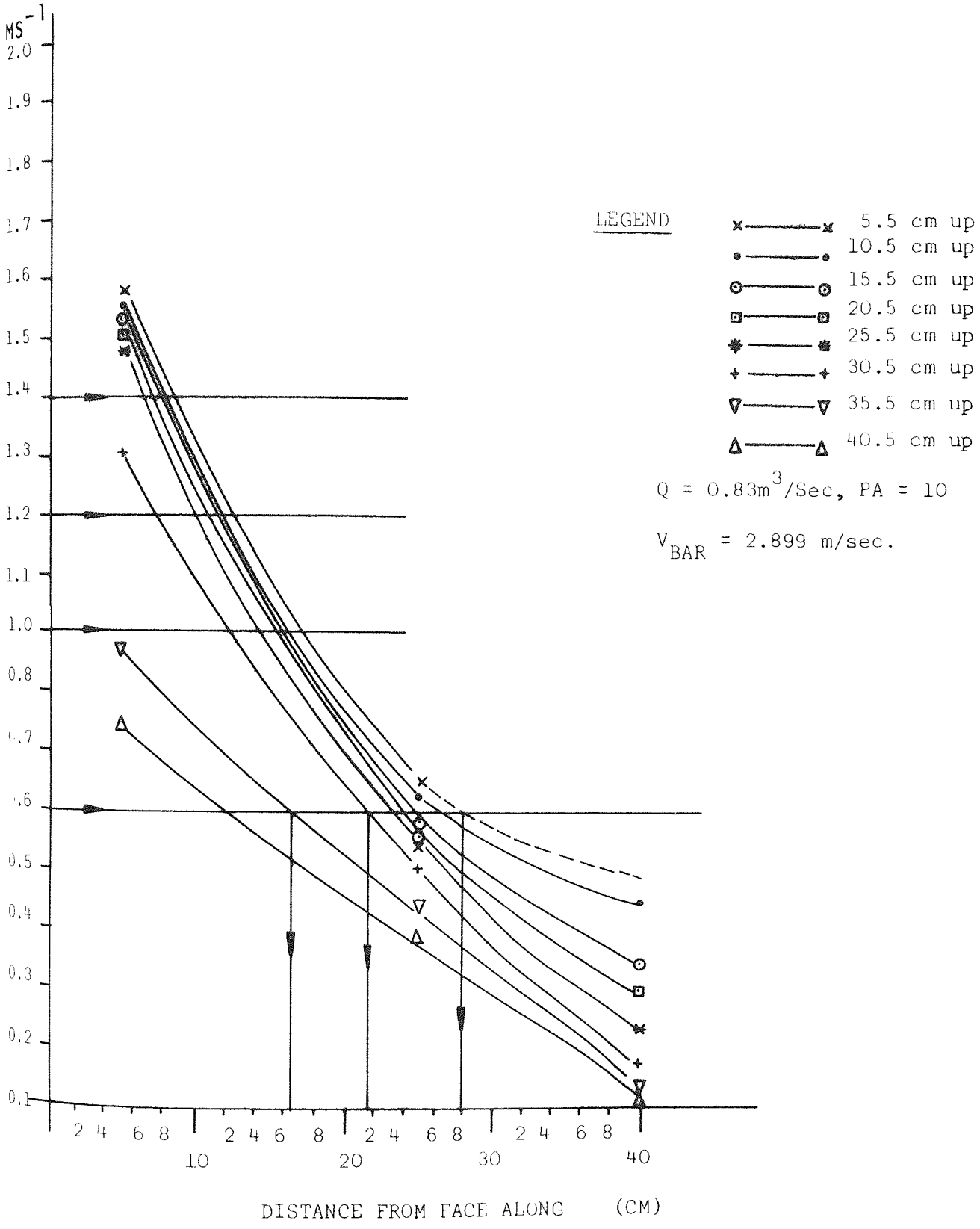

Figure 7.55 VELOCITY ATTENUATION VERSUS DISTANCE, BELL MOUTH HOOD

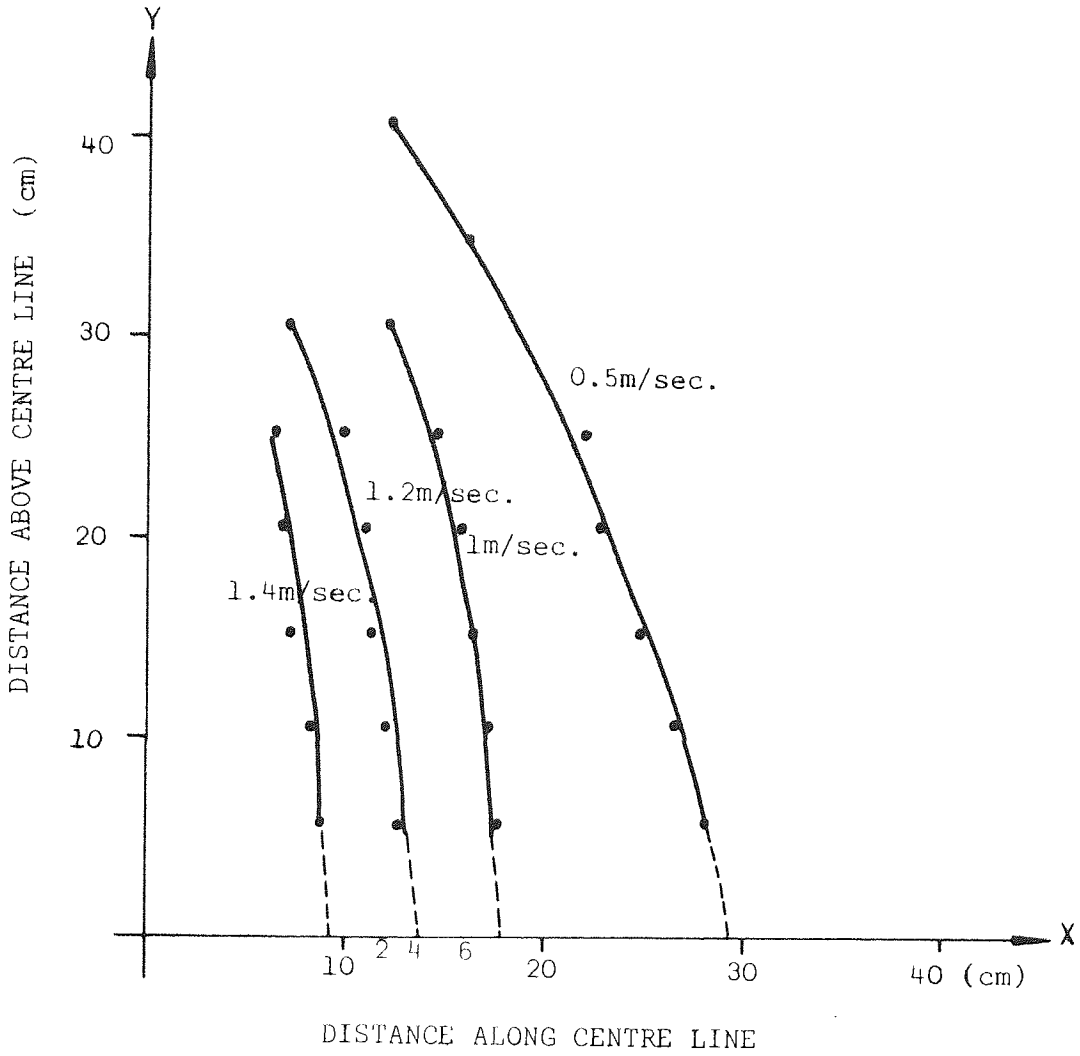

Figure. 7.56 CONTOUR LINE FOR BELL-MOUTH FLANGED SQUARE HOOD.

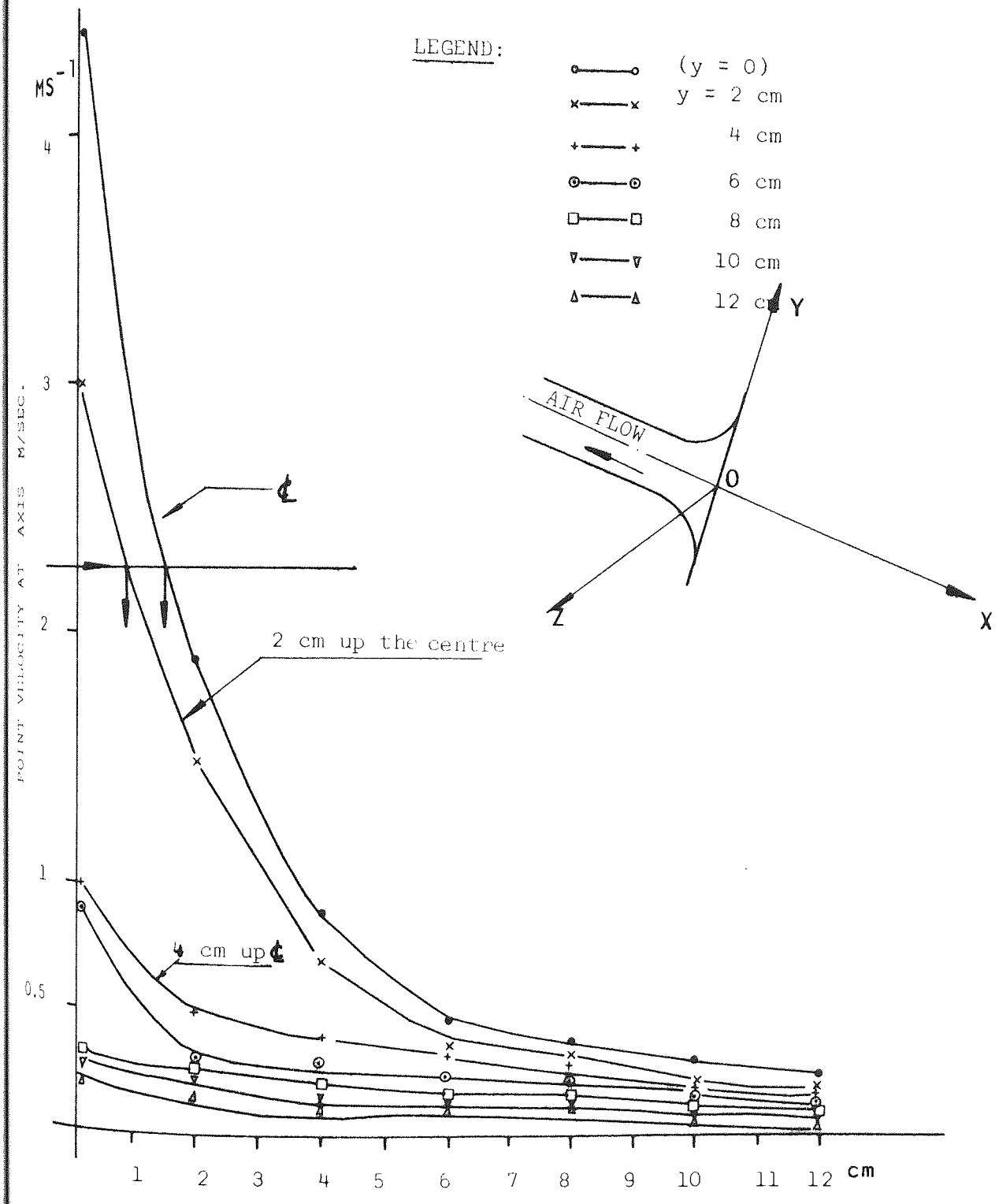

Figure 7.57 POINT VELOCITY FOR ROUND DUCT BELL MOUTH FLANGED.

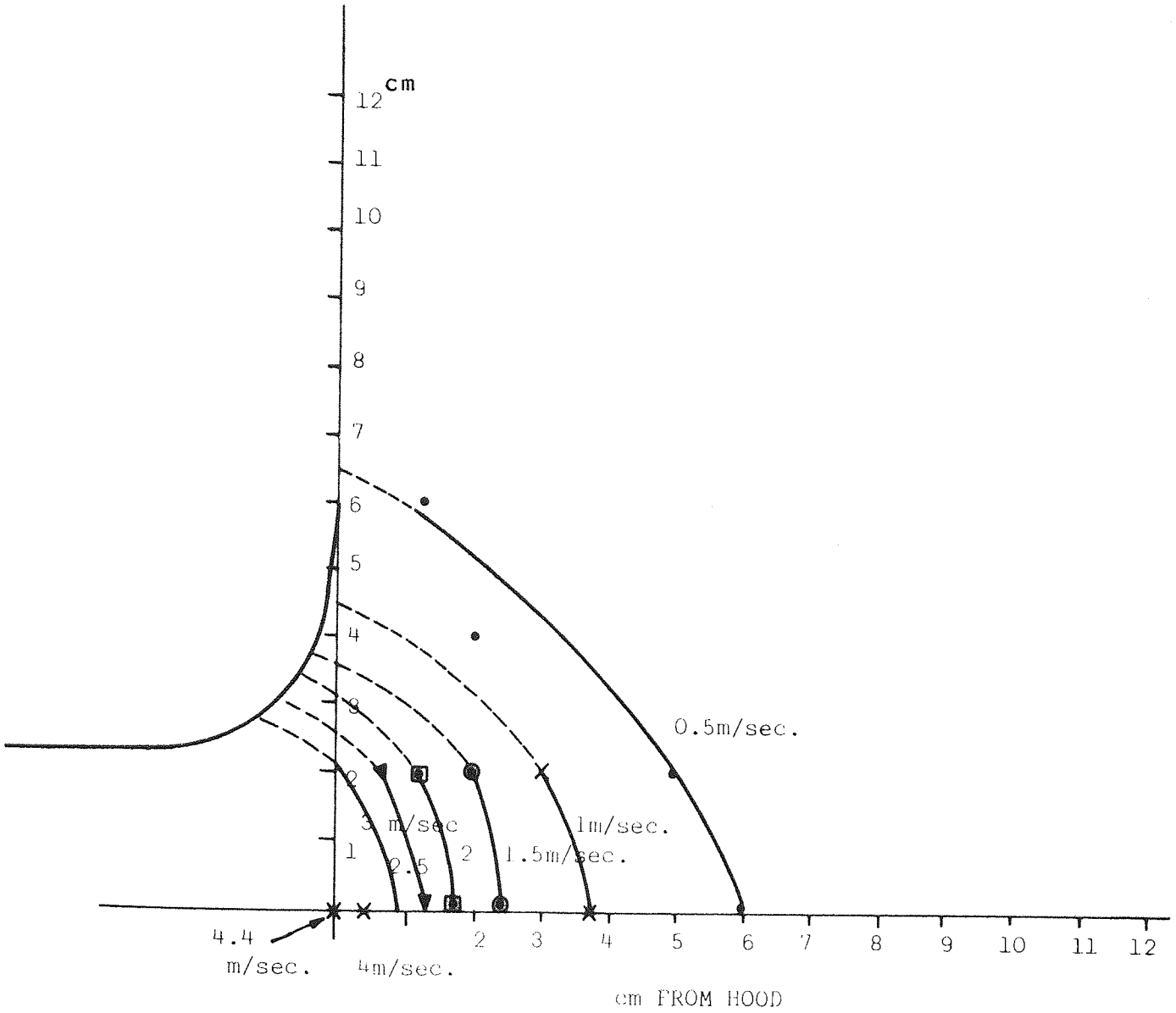

Figure 7.58 CONTOUR LINE FOR BELL MOUTH FLANGED ROUND DUCT

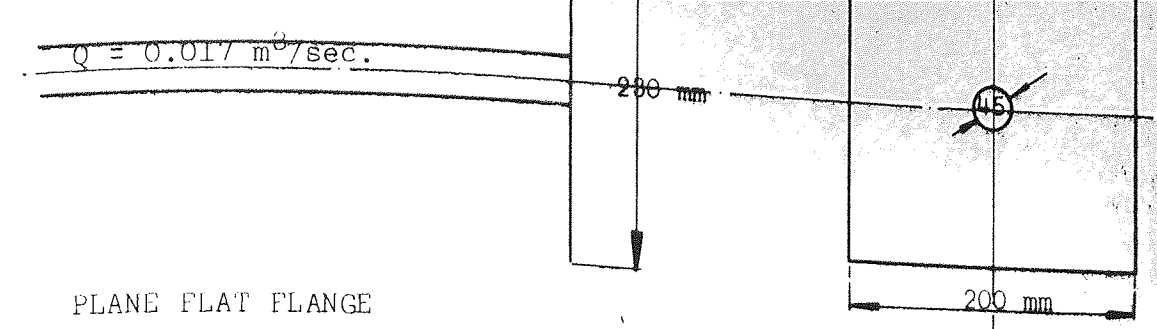

PLANE FLAT FLANGE

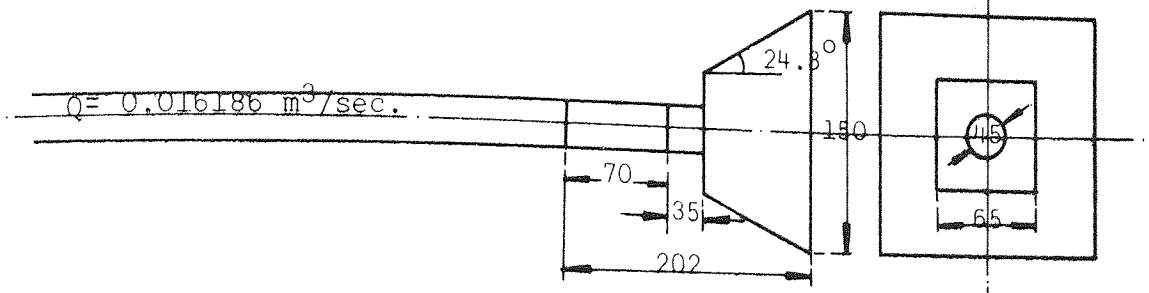

PYRAMID FLANGE

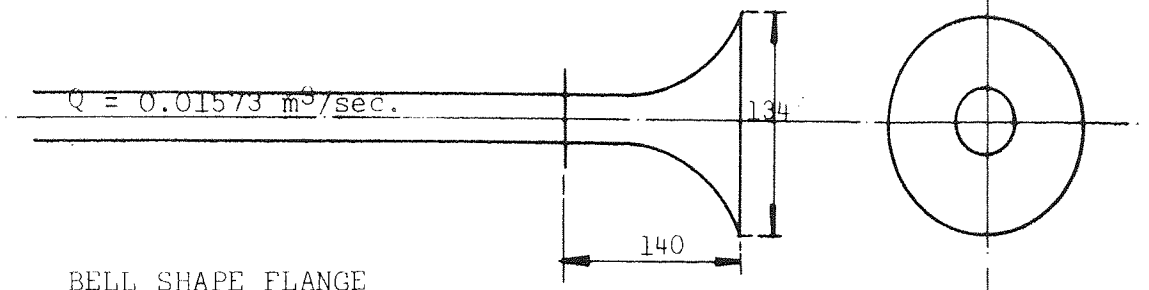

BELL SHAPE FLANGE

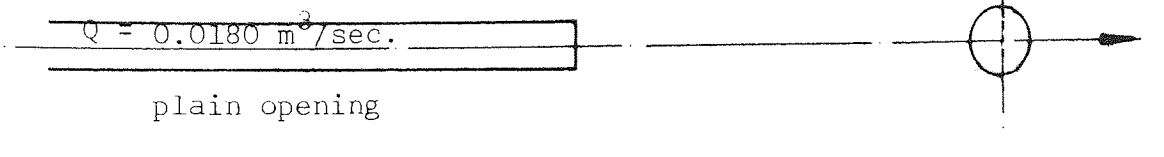

plain opening

Figure 7.59 COMPARISON OF VELOCITY ATTENUATION AT DISTANCE (CENTRE LINE AXIS) FOR DIFFERENT FLANGES

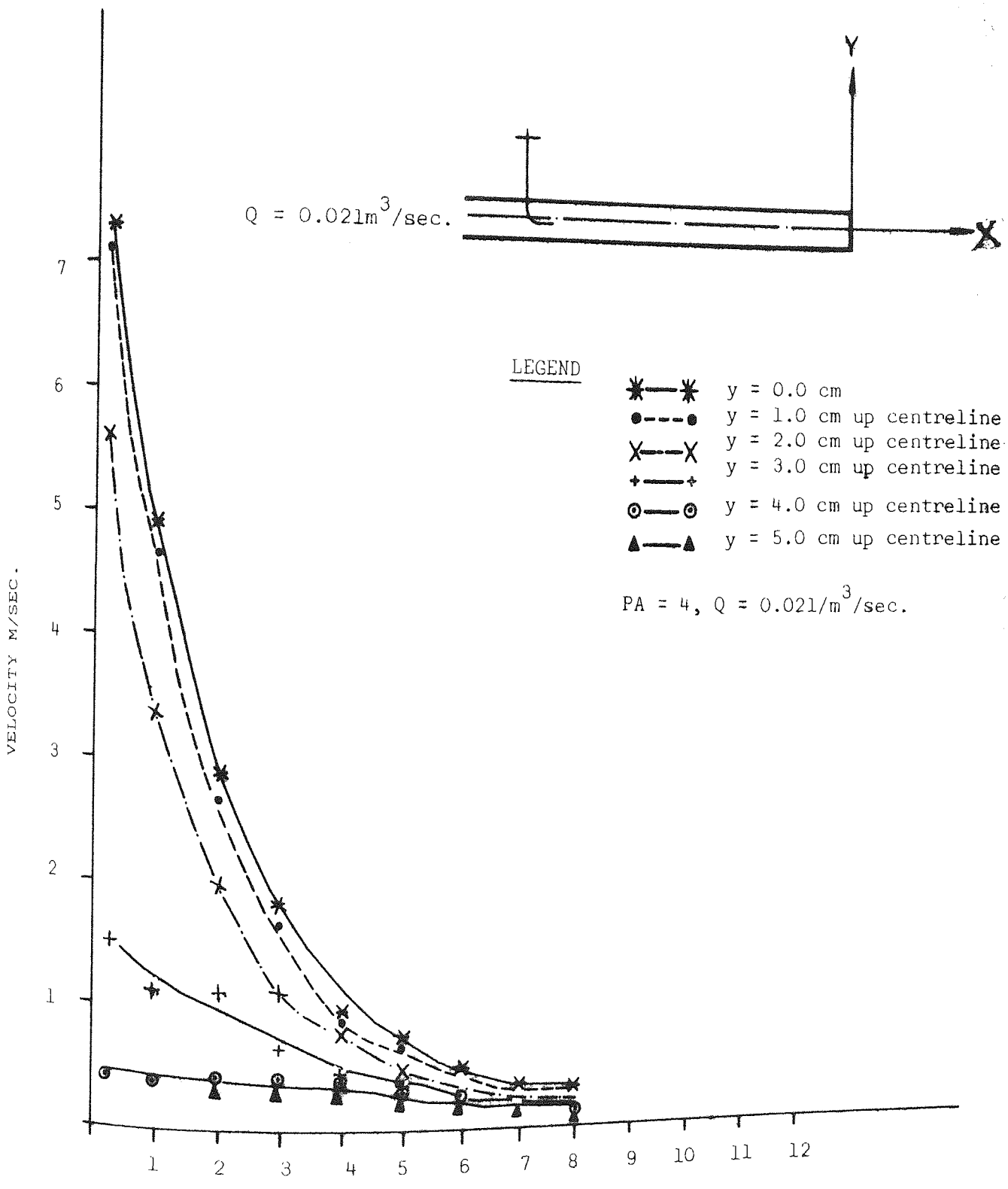

Figure 7.60 VELOCITY VERSUS DISTANCE IN XY- CENTRE PLANE

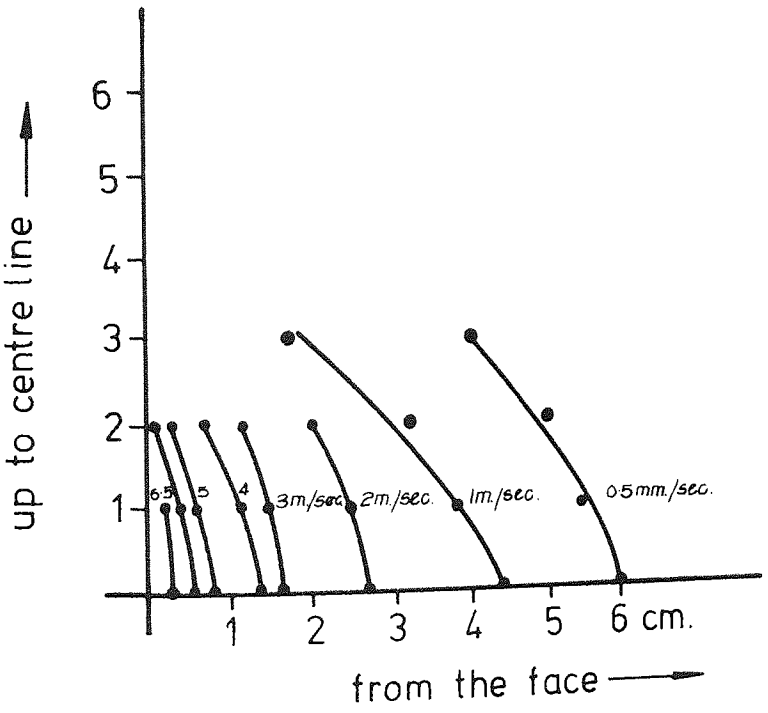

FIGURE 7.61 CONTOUR LINE FOR ROUND DUCT BASED ON FIGURE 7.8

Figure 7.62. Blow velocity profile

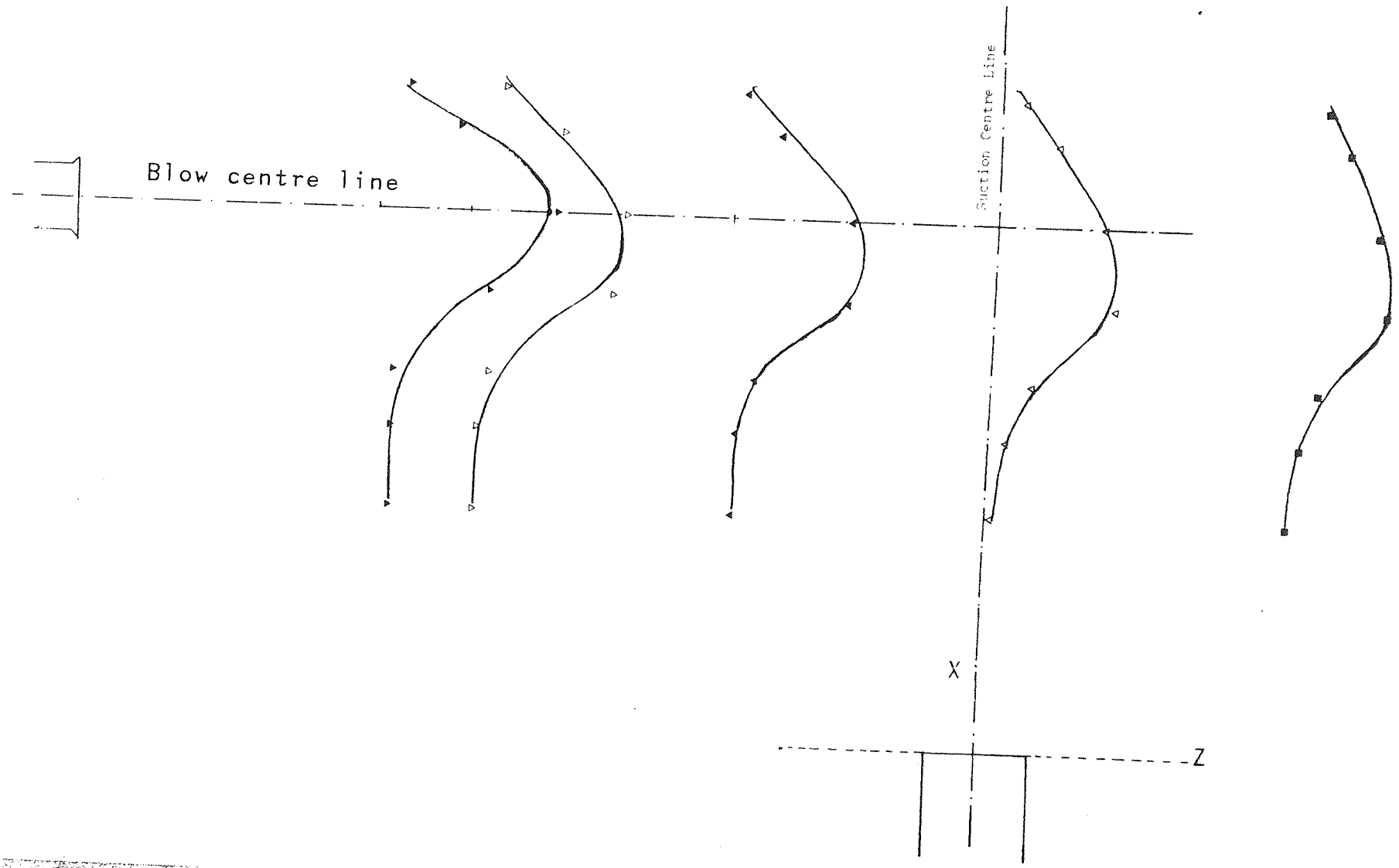

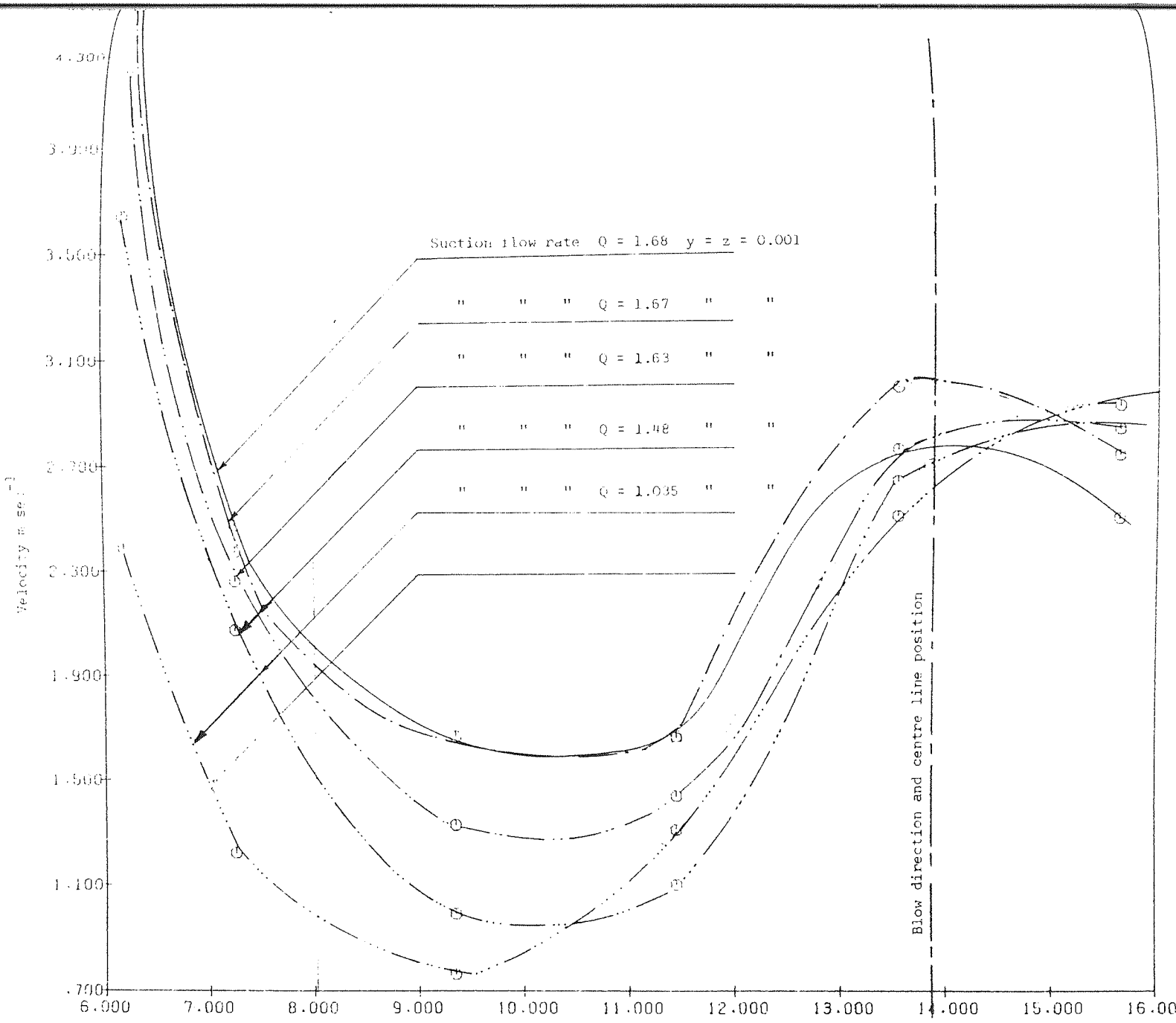

Figure 7.63 Combined suction and cross blow air movement in front of flanged rectangular suction opening (AR=0.6, HR=0.048m)

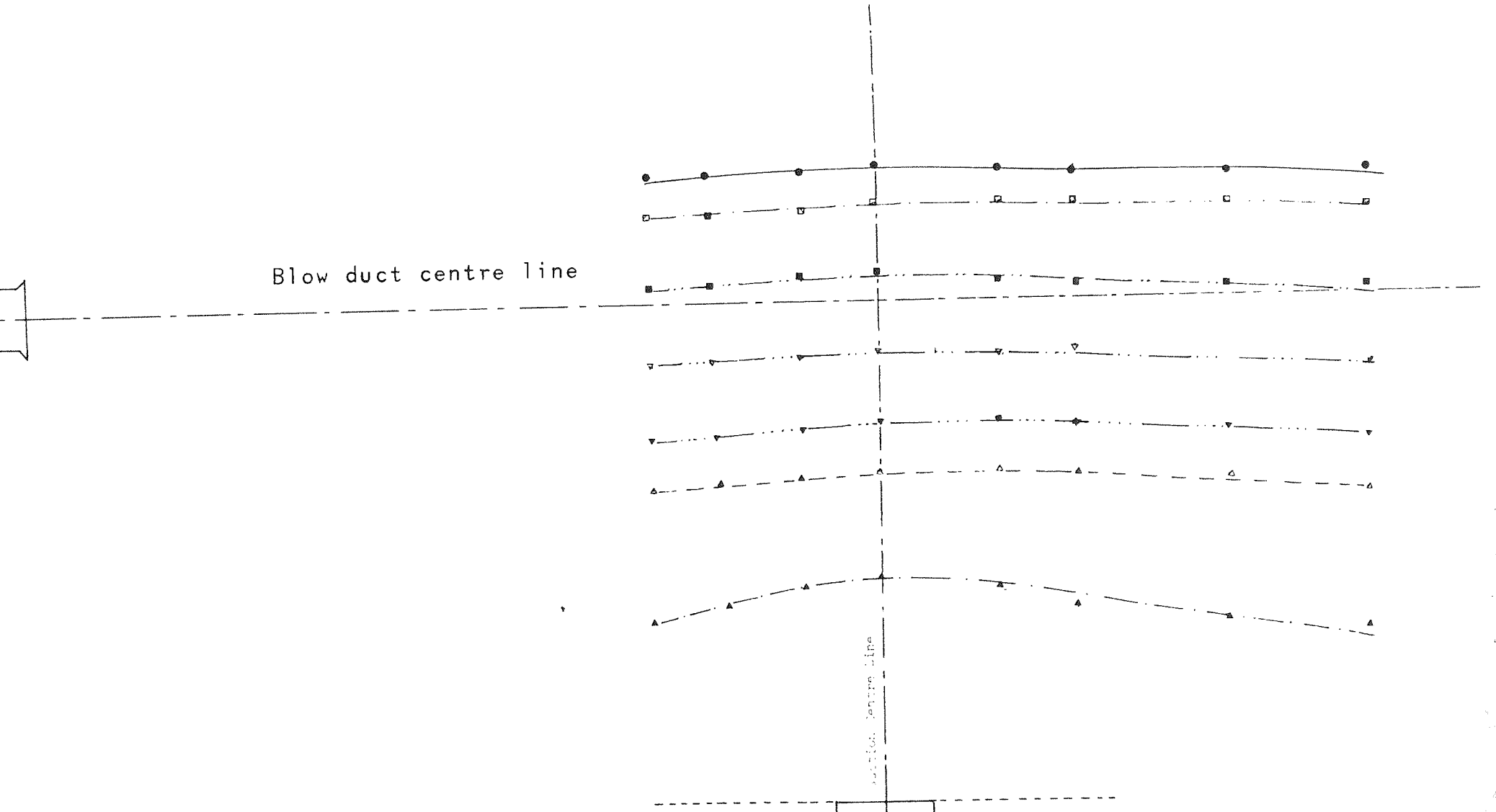

Figure 7.64 Suction velocity profile in front of rectangulare duct(AR=0.6,Q=1.4M^{3}S^{-1})

Figure 7.65 Comparison of centre line point velocity with and without a perpendicular extraneous air flow (i.e. Blow, AR = 0.6, HR = 0.048 m)

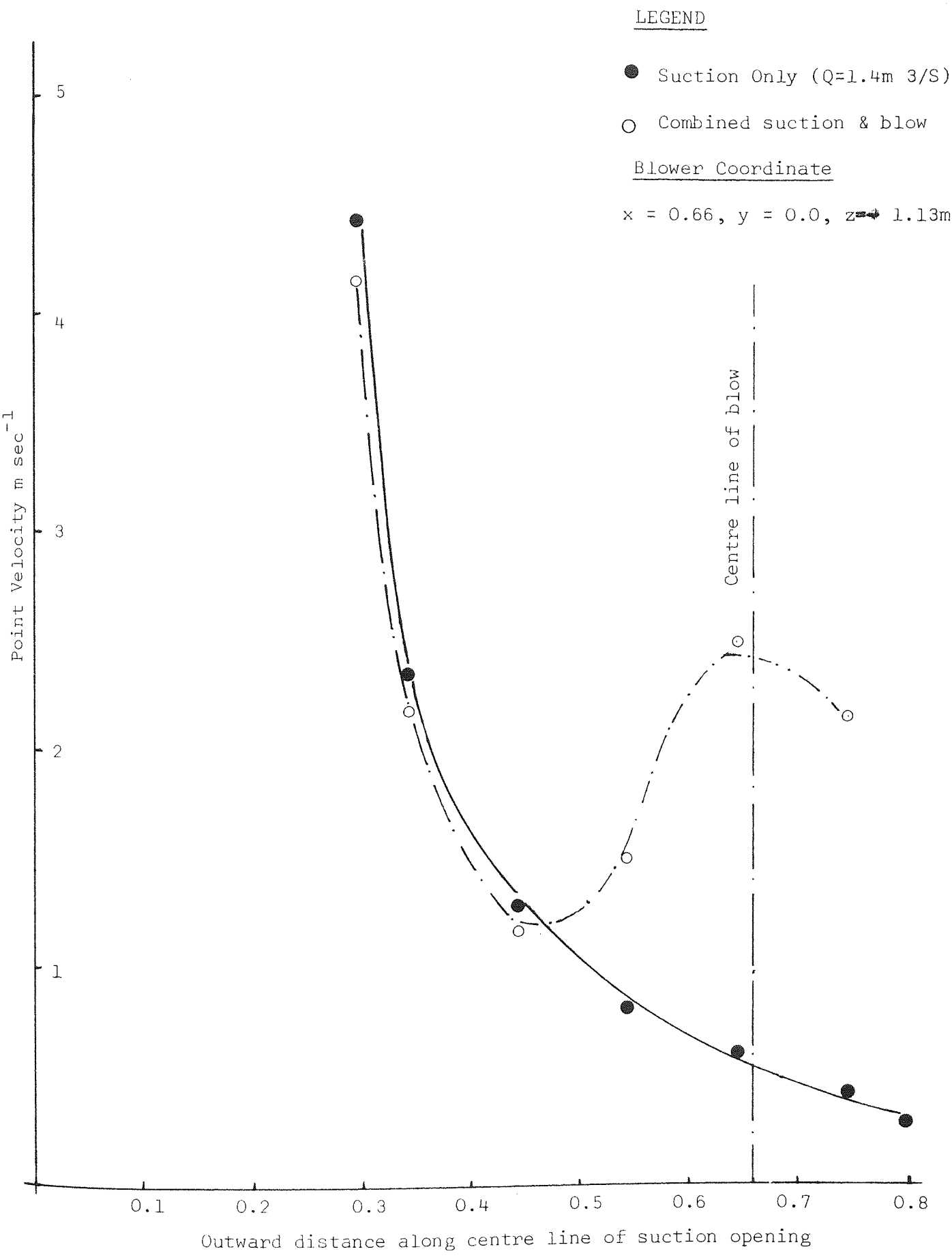

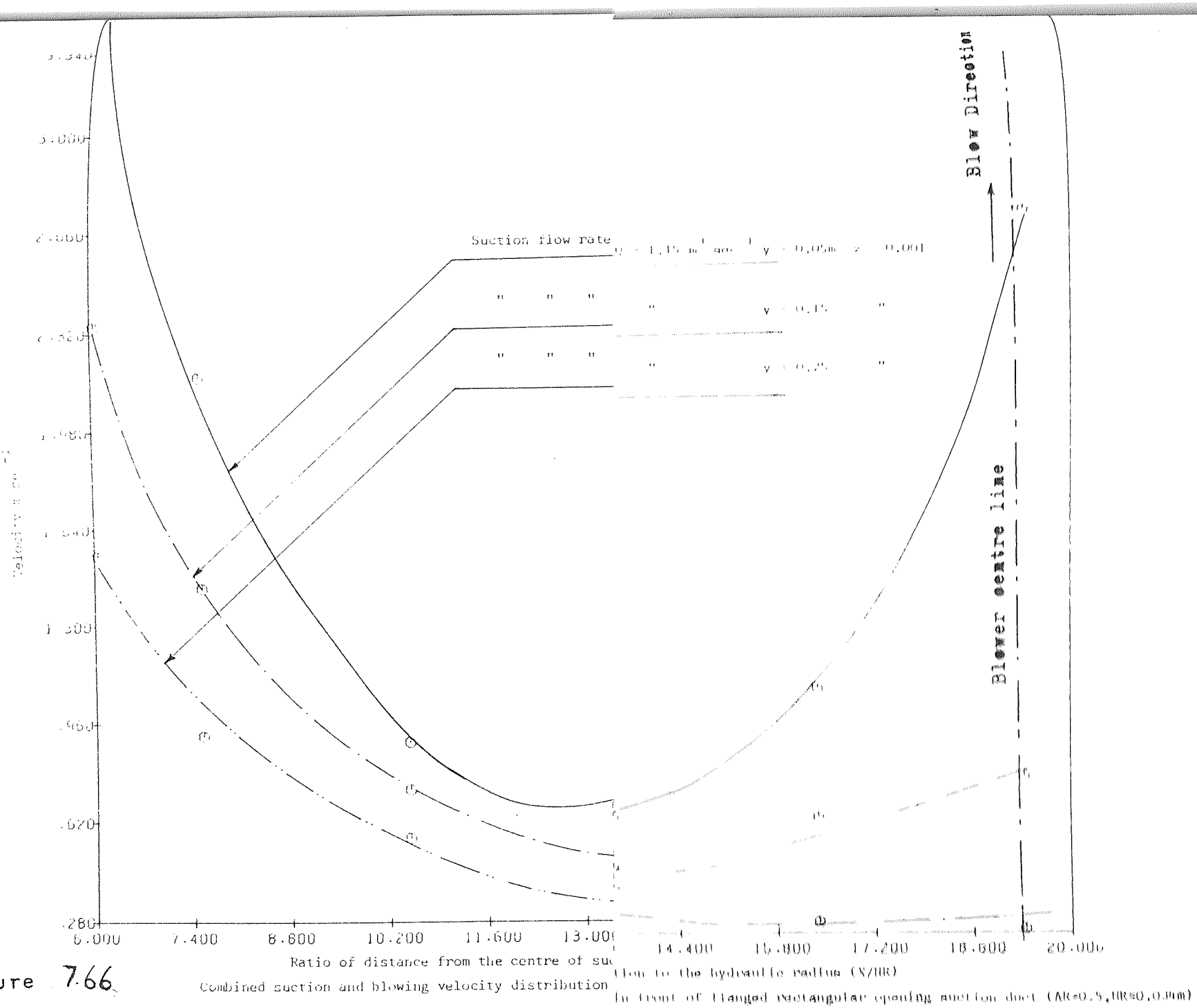

Figure 7.66 Combined suction and blowing velocity distribution in front of flanged rectangular opening suction duct (AR=0.5,HR=0.0m)

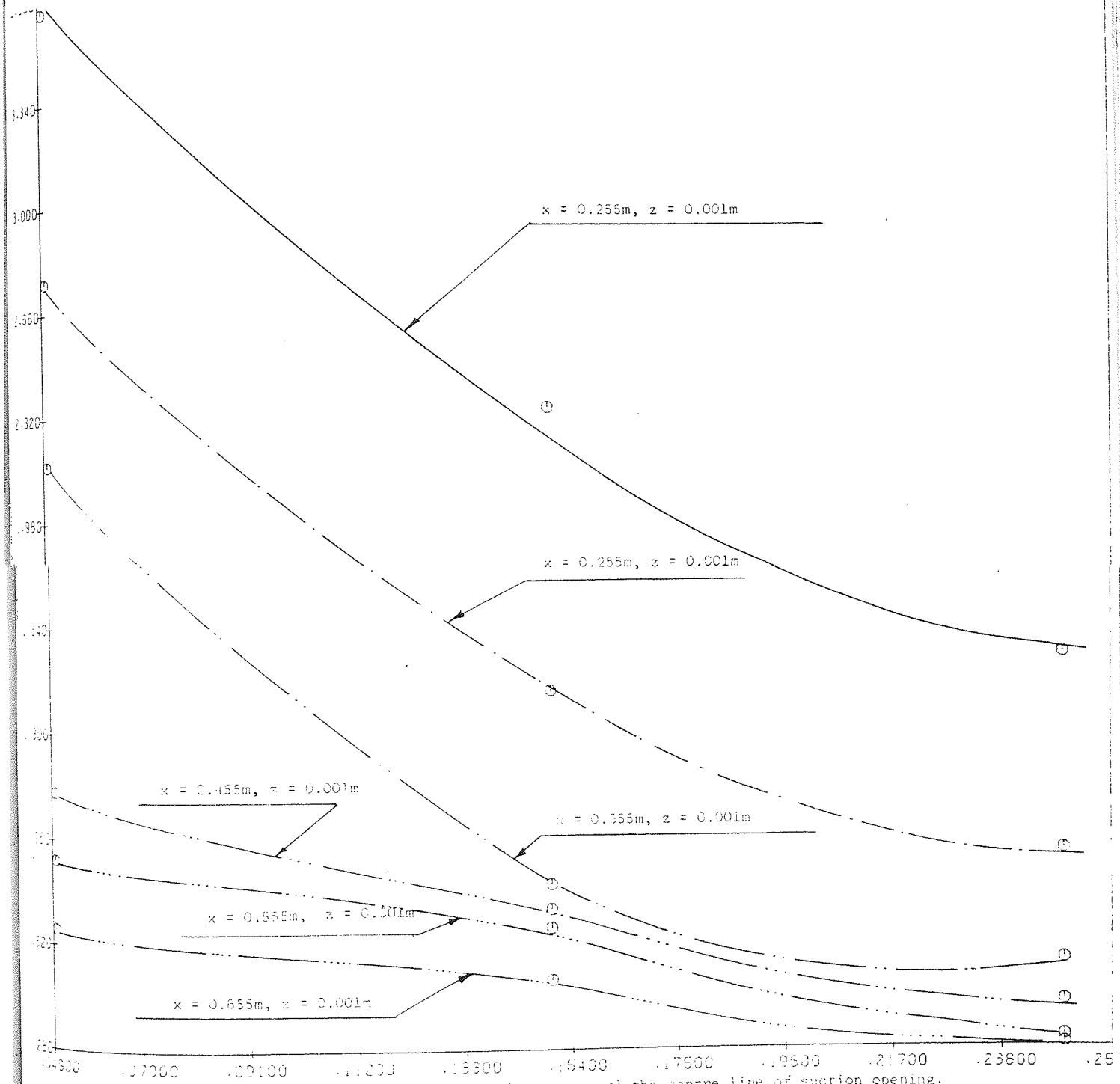

Distance away from ( ) , meter) the centre line of suction opening.

Figure 7.67 Combined suction and blowing velocity in vertical plane in front of flanged rectangular opening (AR = 7.5, HR = 0.034m)

CHAPTER EIGHT

REVIEW, CONCLUSIONS AND SUGGESTIONS FOR FUTURE WORK.

8.1 Review of major points from previous Chapters.

1. Contaminant particles of respirable size move with the air that it contains, and the velocity of airborne particles generally is taken as the velocity of movement. Surface area and effective volume of small contaminant particles are important factors from the point of view of hygiene and safety. Effective volume, particularly, must be taken into account in the design of the local exhaust ventilation.

2. Engineering methods of control of localised sources of airborne industrial pollution rely on the application of local exhaust ventilation. However despite legal requirements, recognition of the rôle and the widespread use of the local exhaust ventilation, the effectiveness in practice of a captor hood cannot be taken for granted.

3. A number of researchers have, so far, studied the aerodynamic characteristics of local exhaust hoods. The consistency between the available empirical formulae is not good. This is mainly due to the fact that the aerodynamic study of the local exhaust hood, as an engineering contaminant control measure, has not been sufficiently advanced or properly undertaken.

4. A thorough theoretical and practical study of the aerodynamic characteristics of the captor hood was, therefore, essential.

The streamlines and potential surfaces of flow field in front of a rectangular captor hood were assumed to be of the form of quadric surfaces of equifoci as below:-

$$-\frac{X^2}{A'^2} + \frac{Y^2}{B'^2} + \frac{Z^2}{C'^2} = 1, \quad A' < \omega/2 \qquad (8.1)$$

and

$$\frac{X^2}{A^2} + \frac{Y^2}{B^2} + \frac{Z^2}{C^2} = 1, \quad A >> \omega/2 \qquad (8.2)$$

4. contd.

where $C = C' = \ell/2$ and ω and ℓ are the width and length of a rectangular suction opening respectively. Therefore, the effective surface area under the influence of suction forces of an unflanged rectangular opening (Figures 3.1 and 3.2) are

$$S_a = \frac{3\pi A}{2}\left(A + \frac{C}{e}\sin^{-1}e\right) \qquad (8.3)$$

where S_a is the surface area of an ellipsoid, centred at the centre of the suction hood,

A is the semi-minor axis along the X-axis of ellipse,

C " " " major " " " " Z- " " "

e " " eccentricity of ellipse $(= {}^{\omega}/_{2}C)$

On the other hand, the potential surface and streamlines in front of flanged round hoods have been assumed by researchers, to be spherical surfaces and diametrically straight lines. On the basis of this assumption, the potential surface is as follows:

$$\phi(x,z,Q,R) = \frac{Q}{4\pi^2R^2}\int_0^R\int_0^{2\pi}\frac{\ell\,d\ell\,d\alpha}{\sqrt{x^2+z^2+\ell^2+2z\ell\cos\alpha}} \qquad (8.4)$$

This integral is not analytically soluble, except for z = 0 cases, which results in:-

$$\phi(x,0,Q,R) = \frac{Q}{4\pi^2R^2}\left(\sqrt{x^2+R^2} - x\right) \qquad (8.5)$$

Consequently, from the definition of potential surfaces, the theoretical centre line point velocity in front of flat flanged round duct is as follows (Drkal 1971):

$$\frac{V_x}{V_{BA}} = 1 - \frac{x}{\sqrt{x^2+R^2}} \qquad (8.6)$$

Generally, equation (8.4) has been used for the numerical solution of velocity contours and potential strength in front

4. contd.

of a round flanged captor hood. Applying the gradient concept of a potential field, and using the equation (8.4), the following equations will result:-

$$V_x = \frac{\partial \phi}{\partial x} = \frac{Q}{4\pi^2 R^2} \int_0^R \int_0^{2\pi} \frac{-x\ell d\ell d\alpha}{(x^2+z^2+\ell^2+2z\ell\cos\alpha)^{3/2}} \qquad (8.7$$

and

$$V_z = \frac{\partial \phi}{\partial z} = \frac{Q}{4\pi^2 R^2} \int_0^R \int_0^{2\pi} \frac{-(z+\ell\cos\alpha)\ell d\ell d\alpha}{(x^2+z^2+\ell^2+2z\ell\cos\alpha)^{3/2}} \qquad (8.8)$$

The equations 8.4, 8.7 and 8.8 were integrated numerically, then the point velocity was calculated as below:-

$$V = \sqrt{V_x^2 + V_z^2} \qquad (8.9)$$

5. As the main philosophy of the research programme has been that a better understanding of the aerodynamics behaviour of suction flow, which can be achieved with a process of first identifying the variables which appear in the conventional prediction equations, and then subjecting each one to close examination. After literature survey theoretical considerations, and numerical solution, the practical examination and appraisal methods followed. In order to test the rôle of variables and appraise the existing empirical and theoretical formulae, a model ventilation rig, and a full-scale wind tunnel and test ducts and hoods were designed and manufactured.

A coordinating carriage probe holder was designed in order to position the probe sensor of the meter at a known place in 3-dimensional space in front of suction hoods.

Consideration was given in the choice of instrumentation to select a conventional and practically accurate instrument such that errors would be comparable to those arising in industrial practice.

5. contd.

Measurement procedures, measuring devices, their limitations and merits were reviewed.

All research facilities were calibrated.

For reference flow metering, the averaging pressure tube in conjunction with micromanometer and inclined manometers proved to be very convenient and practically accurate. For average main duct cross section velocity up to 30 ms^{-1} a maximum 5% and minimum -7% deviation, based on averaging pressure readings, was observed. This deviation compared with $\pm$ 6.5% (for average velocity up to 7 ms^{-1} stated by William) demonstrated that this method is more reliable than it was thought to be.

Calibration of AVM502 velocity meters proved that there is a one to one corresponence of AVM502 velocity readings and pitometry methods. It was found that there is no significant difference between each calibrated AVM502 instrument.

A Simon Shielded hot wire anemometer was used for measuring a very low air movement, (i.e. with velocity down to 0.002 ms^{-1}).

The suction flow rates through each suction assembly was set fixed remotely by means of electric actuators, which changes the fan's pitch angle to a required position.

As the wind tunnel room is a closed chamber, the re-circulated air velocity was monitored for the maximum fan duty (i.e. 4.72 m^3s^{-1}). Accepting the allowable turbulence at suction affected area as similar to the turbulence caused by human inhalation-exhalation, it was found that the back blow of recirculation air movement after passing through two crossed curtains is negligible.

5. contd.

The measurements consisted of points, coordinates, velocity and temperature in the suction affected area, for different suction opening, different entrance condition (i.e. flanged or unflanged) and suction flowrate. The same types of measurements were repeated in the case of suction-blow flow field for a fixed volume blow rate.

6. The experimental data was corrected to STP as well as for instrument temperature. These corrected data were treated graphically as well as statistically. Statistical package (i.e. SPSS) used for non-linear least square curve fitting. The requirement of the package was that it should test a model to fit to the data. The models were chosen from the existing empirical formulae as well as for the theoretical one.

The statistical inference was based on the following decision making criteria:

i) Best fit (i.e. residual analysis, low RMSR);

ii) High precision (i.e. low standard error and RMSR);

iii) Minimum bias (i.e. differences of estimated and response parameters be as close to zero as possible;

iv) Less bias (i.e. the difference of major factors be very close to zero).

The graphical examination of residuals combined with ranking procedure based on the above criteria, the best empirical equation examining the different models are chosen.

Graphical representation of data showed that:

i) The general pattern of the velocity distribution in front of similar suction openings is the same

ii) In front of rectangular suction opening, for an equal

6. contd.

ii) contd.

suction flowrate, and at the same distance from the opening, the velocity is high corresponding to the high aspect ratio (the ratio of small side to large side).

iii) For different suction flowrates the velocity versus distance relationships are similar, in agreement with the assumption that the point velocity is directly proportional to the suction flowrate.

iv) A comparison of numerically obtained point velocity and experimental velocity showed that, there is not a good agreement between the theoretical and observed velocity.

v) For the round flanged suction hood and for the points at distance greater than the radius of the suction opening, the spherical potential surfaces represent better the real situation than ellipsoidal surfaces.

vi) On the other hand the ellipsoidal potential surfaces for the points at distances greater than the half width of the rectangular opening seems to be a better assumption than spherical surface area.

The treatment of data showed that:

i) For prediction of centre line velocity in front of rectangular unflanged hoods (i.e. AR = 0.5,0.6), the following equations can equally be used:

6. contd.

$$F_1 = 1/(1+1.034((1-AR)/AR)^{0.67})$$

(1)
$$F = 0.068X^{-2.019}A^{1.38}F_1$$
$$V = V_{BA}F/(1+F)$$
$$RMSR = 0.004\ ms^{-1}$$

(2)
$$V = 1.8V_{BA}(X/HR)^{2.04}/(1+0.162(X/HR)^{2.04}$$
$$RMSR = 0.19\ ms^{-1}$$

(See Figure Rec 12.1)

ii) For unflanged round suction opening the following equation can be used for the centre line velocity prediction (see Figure Rof 1.2)

$$\begin{cases} V = V_{BA}/(9.78 + 3.497(X^2/A)^{1.86}) \\ RMSR = 0.2\ ms^{-1} \end{cases}$$

iii) For all shapes of unflanged hoods (i.e.AR = 0.5,0.6, 0.218, D = 0.152 m) the centre line velocity can be predicted from the following equations:

$$F = 0.23(X/HR)^{-0.865}$$

(1)
$$F = 0.47V_{BA}F/(1+F)$$
$$RMSR = 1.17\ ms^{-1}$$
(See Figure A1)

$$\beta = 10.36(X/A)^{-0.765}$$

(2)
$$\alpha = 1.052(AR)^{\beta}X/\sqrt{A}$$
$$V = V_{BA}/(4.283+110.96\alpha^2)$$
$$RMSR = 0.9\ ms^{-1}$$

Any guide plate (i.e. flange) fitted to the suction opening has the following effects:

i) Any type of guide plate fitted to a suction opening causes some increase of the total pressure of the fan.

ii) An equal suction flow rate through suction hood creates higher point velocity in the case of the flanged condition, than the unflanged hood.

iii) The flange causes the velocity fall-off to become gradual and smooth.

6. contd.

iv) For two hoods of different geometrical shape (i.e.square (AR = 1), and rectangular, abruptly reduced to round (AR = 0.218)), but equal opening area (i.e. 0.2862 M^2) which are flanged differently (i.e. bell mouth lip, and flat plate respectively), and withdrawing the same volume of air, they induce different velocity at the same distant point from the suction face. Graphical representation of velocity (see Figure Qef) showed that the velocity at the same point in front of the hood with lower aspect ratio, is higher than the velocity in front of the other. This difference is partly due to flange size, shape and the angle of fitting and partly due to different shape of hood opening, and the transition piece.

The treatment of velocity measurement in front of flanged hood showed a distinct difference of mathematical pattern of the variables involved. The following are the best empirical equations:

i) Rectangular flanged hoods:

AR = 0.6, Flange size 0.61m by 1.22m

$F = 0.692(X/HR)^{-2.76}$

(1) $V = 21.99V_{BA}F/(1+F)$

RMSR = 0.263 ms^{-1}

$F_1 = 1/(1+1.02((1-AR)/AR)^{0.99})$

(2) $F = 0.0219A^{1.23}X^{-2.76}F_1$

$V = 14.57V_{BA}F/(1+F)$

RMSR = 0.279 ms^{-1}

AR = 0.5, Flange size 0.61m by 0.91m

$F_1 = 1/(1+0.236((1-AR)/AR))$

(3) $F = 0.279A^{0.93}X^{-2.44}F_1$

$V = 0.299V_{BA}F/(1+F)$

RMSR = 0.094 ms^{-1}

ii) Round flanged (i.e. flange size 0.608m by 0.913m)

6. contd.

ii) contd.

$$V = V_{BA}/(7.76(X^2/A)^{0.86}+1.82)$$
$$RMSR = 0.85\ ms^{-1}$$

iii) For all shapes of hood (i.e.AR = 0.218,0.5,0.6,1(D=0.152m))

$$F = 1.825(X/HR)^{-1.53}$$

(1)
$$V = 0.56V_{BA}F/(1+F)$$
$$RMSR = 1.05\ ms^{-1}$$

$$F_1 = 1/(1+0.075((1-AR)/AR)^{3.16})$$

(2)
$$F = 3.42A^{1.58}X^{-1.8}F_1$$
$$V = 0.54V_{BA}F/(1+F)$$
$$RMSR = 0.86\ ms^{-1}$$

$$F = 7.016(X^2/A)^{0.818}+1.81$$

(3)
$$V = V_{BA}/F$$
$$RMSR = 0.902\ ms^{-1}$$

See Figure 7.49 for graphical representation.

7. In the graphical representations of velocity measurement of symmetry points in front of axially symmetric suction hoods as well as rectangular suction openings, it was noted that the velocity at symmetry points in front of a round duct are practically the same. The trend of velocity fall-off in centre plane or any plane parallel to the centre plane are the same regardless of the shape of suction opening or suction opening condition (i.e. flanged or unflanged).

8. The type of flanges has a significant effect on the fall-off of suction velocity (i.e. centre line point velocity) as well as hood entrance loss, and consequently the suction flowrate. This effect on round suction duct (D = 0.045m) was examined (see Figure 7.59).

9. Treatment of data collected by testing rectangular suction opening, flanged with flat plane flange, showed that the

9. contd.

hyperbola streamline and ellipsoidal contour surface assumptions are valid. The following equation was obtained:

$$V = \frac{z^2}{0.021} - \frac{x^2}{2.37} \qquad (Q = 1.28\ m^3 s^{-1}), RMSR = 1.31\ ms^{-1}$$

and

$$\frac{V}{V_{BA}} = \frac{X^2}{35.63} + \frac{Y^2}{6.07} + \frac{Z^2}{35.8}, \quad RMSR = 0.03\ ms^{-1}$$

$AR = 0.5$

10. In order to study the effect of extraneous air movement, a combined suction-blow flow field was examined. Due to the lack of knowledge on the aerodynamic characteristics of industrial extraneous air movement, laboratory simulation was not persued. A graphical representation was made. It was noted that in order to appraise the effectiveness of a local exhaust captor hood, one needs to prepare the detailed velocity profile of all suction, blow and the combination of suction-blow flow fields. Then by knowing or deciding the position of the source of contaminant relative to the suction opening, it is possible to appraise the effectiveness of the existing or design local exhaust system appropriately.

8.2 Conclusions.

From the research findings the following conclusions can be drawn:

1. The discrepancies of centre line velocity prediction by existing empirical formulae are very high and cannot be dismissed.
2. With the designed research facilities, the suction flow rate setting and its metering was done in a more reliable

2. contd.

and convenient manner than the previous researchers were able to perform.

3. The averaging pressure tube proved to be practically accurate, convenient to use and less vulnerable to flow fluctuation despite being a relatively inexpensive flow metering device.

4. There is not a good agreement between theoretically based and experimentally measured centre-line point velocity in front of flat plane flanged round duct which can be due to the invalidity of the sink points assumption or insufficient size of flange or finally due to the experimental errors of measurements.

5. The main aerodynamic factors (i.e. shape, size, suction flowrate, points distance and velocity and suction face average velocity) of a captor hood were identified and examined. The following conclusions were drawn accordingly:

   i) Point velocity in front of any size, shape and suction opening condition, is directly proportional to the suction flowrate.

   ii) For a fixed Point and different suction flowrate, the ratio of point velocity and average suction face velocity is constant (see Table 7.2)

   iii) The shape and the size of suction opening are two interacting factors which required to be studied both individually and interactively in the case of uncircular suction openings.

   iv) The geometrically similar suction opening without the similarity of the immediate connection piece to the main duct, does not produce a similar flow pattern. For example in front of the rectangular duct for an equal suction flowrate, the centre line velocity increases as aspect ratio increases. On the contrary, in front of rectangular suction hood, which is abruptly reduced to a round duct, this proportionality does not hold for all points along the

5. contd.

iv) contd.

centre-line axis. For points of distance less than the width of suction opening the point velocities are directly related to the aspect ratio, whereas for the rest of the points the case is reversed. This transition point seems to move away from the face of the suction opening when the hood is flanged (flat plate flange).

v) Any guide plate(s) fitted to the suction opening, improve the effective suction affected area, and suction flow rate for a fixed fan duty. The magnitude of these alterations depend upon the size, shape (i.e. bell mouth or pyramid) and the inclination angle of guide plate fitting relative to the suction centre plane.

vi) Flanging causes the velocity attenuation to become gradual and smooth, and results in a higher velocity at the same farther distant point as in front of an unflanged hood (both withdrawing the same volume of air).

vii) For two suction opening, withdrawing the same volume of air, the velocity attenuation in front of the duct with larger opening area is gradual and wider than the others.

viii) The validity of the hypothesis of the ellipsoidal potential function and hyperbolic streamlines in front of the flat plate flanged rectangular suction opening, was empirically tested.

ix) In front of axially symmetric suction openings point velocities at symmetry points are practically equal.

5. contd.

x) In front of the round flanged duct, spherical potential surfaces seem to be a better assumption than ellipsoidal ones.

6. In studying the interaction of extraneous airflow and suction flow, theoretically one needs to study the aerodynamic behaviour of combined airflows. Practically the hygienists require a graphical comparison of velocity profiles of suction flow, extraneous flow, and the combined flow at a fixed position. These velocity profiles reveal the critical zones of area, and the extent of the flow interaction. On the other hand, a designer needs to acquire practial information on the aerodynamics behaviour of the extraneous air movement in order to design a local exhaust ventilation hood, to be able to control the contaminant by contracting the unfavourable airflow.

7. Consequently the following empirical equations could be introduced for the prediction of centre-line velocity in front of any shapes of suction openings:

$$F = 0.23(X/HR)^{-0.865}$$
$$V = 0.47V_{BA}F/(1+F) \qquad \text{For unflanged hood}$$
$$RMSR = 1.17ms^{-1}$$

$$F = 1.925(X/HR)^{-1.53}$$
$$V = 0.56V_{BA}F/(1+F) \qquad \text{For flat plane flanged hoods}$$
$$RMSR = 1.05\ ms^{-1}$$

8.3 Suggestion for Future Work.

This research was designed to test a number of classically shaped openings. It was mainly concerned on identification and examination of some but not all the aerodynamic factors.

Although much additional work is required on the study

of the aerodynamic characteristics of captor hoods in local exhaust ventilation systems, priority should be given to major aerodynamic factors.

On the shape of the captor hood, further tests should be carried out on a number of geometrically different shapes, for a fixed suction flowrate.

On the size of the captor hood, tests should cover a number of geometrically similar shapes of different aspect ratios (on different hydraulic radius) for a fixed suction flow rate.

On the suction flowrates, the above tests should be repeated for a number of different suction flowrates.

On the type, size and inclination angle of guide plate fittings, tests should be carried out on a number of geometrically similar hoods.

In all the above studies, the point velocity in the suction affected area, should be measured in order to stuay the effects of aerodynamic factors on suction potential flow field.

Included in the above studies, tests should be undertaken to investigate the streamline function in the field of suction flow field.

Theoretical work should be undertaken to check the validity of the suction flow field as a potential field, hence establishing the mathematical function for contour lines, contour surfaces, and streamlines and stream tubes for suction processes.

Furthermore, a study of the aerodynamic characteristics of aerosol particles, followed by the study of the movement of dust laden cloud under the effect of suction flow field, is

strongly recommended.

Appropriate tests are required to be undertaken on the suction-blow flow field behaviour.

APPENDIX 3.1

Computer programme for the numerical solution of potential field in front of fully flanged round duct.

```
      PROGRAM BNAGF(INPUT,OUTPUT,VVBOUG,TAPE1=INPUT,TAPE2=VVBOUG)
      DIMENSION D(9 ),Q(12) ,TX(10),TY(10),TZ(10),VXYZ(10),R(10),Z(10),
     1MA(10,9),EC(9,10),SELX(10,9),SELY(10,9),SSPH(10),VELX(10,9,12),
     2VELY(10,9,12),VSPH(10,12),POTFU(12,9)
      D01DAF DRKAL FORMULA
      COMMON /RZ/R(10),Z(10),I
      INTEGER NOUT,IFAIL,NPTS,N,KM,M,K
      REAL YA,YB,ABSACC,ANS,PHI1,PHI2,F  ,V1,V2
      REAL YA,YB,ABSACC,ANS2,PHI1,PHI2,F2,V1,V2
      REAL X,Y,R,Z    ,MA
      EXTERNAL F,G,H,PHI1,PHI2
      DATA NOUT/2/
      WRITE(2    ,99999)
      YA=0.0
201    FORMAT(F5.3,2X,F5.3,2X,F5.3,2X,F4.2)
      WRITE(2,500)
500  FORMAT(1H ,1X,5H SELX,2X,5H SELY,3X,4H SSP,3X,5H VELX,3X,5H VELY,3
     1X,5H VSPH,3X,5H VXYZ,3X,6H POTFU,2X,2H R,6X,2H Z,6X,2H Q)
      READ(1,502)(D(L),L=1,9)
      READ(1,503)(Q(M),M=1,12)
      READ(1,201) (TX(J),TY(J),TZ(J),VXYZ(J),J=1,10)
502  FORMAT(1X,F5.3,8(2X,F5.3))
        DO 13 JJ=1,3
      DO 11 L=1,9
      YB=D(L)/2
503  FORMAT(12(1X,F4.2))
      DO 12 M=1,12
      DO 9 II=1,10
      I=II
      R(I)=TY(I)
      Z(I)=TX(I)
      MA(I,L)=(R(I)**2.0+D(L)**2.0/4.0)**(1.0/2.0)
      EC(I,L)=D(L)/(2.0*MA(I,L))
      SELX(I,L)=2.0*3.1415*Z(I)**2.0+(2*3.1415*MA(I,L)*Z(I)*ASIN(EC(I,L)
     1))/EC(I,L)
      SELY(I,L)=2*3.1415*MA(I,L)**2.0+3.1415*Z(I)*Z(I)*(ALOG10((1.0+EC(I
     1,L))/(1.0-EC(I,L)))/EC(I,L))
      SSPH(I)=4*3.1415*Z(I)*Z(I)
      VELX(I,L,M)=Q(M)/SELX(I,L)
      VELY(I,L,M)=Q(M)/SELY(I,L)
      VSPH(I,M)=Q(M)/SSPH(I)
      YB IS IN METER
      ABSACC=0.000000001
      IFAIL=1
         IF(JJ.EQ.2)GOTO 233
         IF(JJ.EQ.3)GOTO 244
      CALL D01DAF(YA,YB,PHI1,PHI2,G,ABSACC,ANS,NPTS,IFAIL)
      PHI(1) LE X AND X LE PHI(2),PHU(1) IS 0 PHI(2) 2PI
      YB GE Y AND Y GT OR E YA YA IS 0,YB IS RADIUS OF DUCT
233     GOTO 235
            IFAIL=1
      CALL D01DAF(YA,YB,PHI1,PHI2,F,ABSACC,ANS,NPTS,IFAIL)
      PHI(1) LE X AND X LE PHI(2),PHU(1) IS 0 PHI(2) 2PI
      YB GE Y AND Y GT OR E YA YA IS 0,YB IS RADIUS OF DUCT
244     GOTO 235
            IFAIL=1
      CALL D01DAF(YA,YB,PHI1,PHI2,H,ABSACC,ANS,NPTS,IFAIL)
```

```
  YB GE Y AND Y GT OR E YA YA IS 0,YB IS RADIUS OF DUCT
  P=Q(M)
  T=D(L)/2.0
  POTFU(M,L)=Q(M)*ANS/(4.0*3.1415*3.1415*D(L) **2.0)
  WRITE(2,600)SELX(I,L),SELY(I,L),SSPH(I),VELX(I,L,M),VELY(I,L,M) ,V
 1SPH(I,M)   ,VXYZ(I),POTFU(M,L),R(I),Z(I),Q(M)
  IF(IFAIL)10,10,20
20 WRITE(2    ,99997) IFAIL
PHI(R,Z)=(Q/4*3.14159**2*R**2)*DOUBLE INTEGRALOF(L/SQRT(Z**2+L**2+R**2
+2*R*LCOSALPHA)
600 FORMAT(1H ,2X,8(F6.3,1X),3(F6.3,1X))
10 CONTINUE
9 CONTINUE
12 CONTINUE
11 CONTINUE
13      CONTINUE
40 STOP
99999 FORMAT(4(1X/),'001DAF DRKAL FORMULA RESULTS',/1X)
99997 FORMAT(1H ,'CONVERGENCE NOT OBTAINED IFAIL= ',I4/)
  END



  REAL FUNCTION PHI1(X)
  REAL X
  SET LOWER LIMIT OF INNER INTEGRAL.
  PHI1=0.0
  RETURN
  END



  REAL FUNCTION G(X,Y)
        REAL X,Y
    COMMON /RZ/R(10),Z(10),I
   G=-Y*(R(I)+Y*COS(X))/(Y**2.0+Z(I)**2.0+R(I)**2.0+2.0*R(I)
 1*Y*COS(X))**1.5
   RETURN
   END



  REAL FUNCTION PHI2(X)
  REAL X
  SET UPPER LIMIT OF INNER INTEGRAL.
  PHI2=2.0*3.14159
  RETURN
  END

  BOUNDARY 0 TO R AND 0 TO 2PI
  REAL FUNCTION F(X,Y)
  COMMON /RZ/R(10),Z(10),I
  REAL X,Y
  F=Y/SQRT(Z(I)**2+Y**2+R(I)**2+2*R(I)*Y*COS(X))
  RETURN
   END
  REAL FUNCTION H(X,Y)
        REAL X,Y
    COMMON /RZ/R(10),Z(10),I
   H=-Y*Z(I)/(Y**2.0+Z(I)**2.0+R(I)**2.0+2.0*R(I)
 1*Y*COS(X))**1.5
   RETURN
   END
```

APPENDIX 5.1

CALIBRATION OF EQUIPMENT AND STATISTICAL ANALYSIS

1. Introduction.

In appraising a ventilation system using some measuring device, the observed value may have the magnitude of true value $\pm$ e, where e is the error of measurement. Each anemometer has its own associated error, and each contributes to the overall certainty in the final results. Calibration is generally defined as the determination of the true values of reading of a measuring instrument.

Calibration of anemometers should be made in a uniform airflow condition. Ideally an anemometer should be calibrated in the situation in which it is going to be used. Generally, that is not possible. The following are the requirements of calibration:

i) the calibration test section must have a uniform airflow both across the air stream and in line with the airflow;

ii) a satisfactory means of precisely metering the airflow;

iii) a means of regulating and effecting airflow through the tunnel.

Therefore, the conventional ducted air wind tunnel is the preferred situation. A literature survey showed that the calibration wind tunnel recommended by the American Conference of Governmental Industrial Hygienist (ACGIH) for calibration of velometers is the most feasible type of calibration wind tunnel.

A bell-mouth flanged square cross-section hood (see Drawing No.2) was designed to satisfy the first requirement.

A standard pitot-static tube was used for rating the airflow following B.S. method for pitometry.

An electrical actuator to alter the fan pitch angle is the means for fulfilment of the third calibration requirement.

2. Calibration of air velocity meters.

There were four types of direct air velocity meters:

i) Prosser Scientific Instrument Ltd.air velocity meter type AVM501F

ii) " " " " " " " " AVM502

iii) Simmon Shielded hot wire anemometer

iv) Salford Electrical Instrument Ltd., volometer (AEI)

2.1 Calibration of AVM501F.

Two calibration lines were provided for each scale ranges 0 to 10 m s^{-1} and 0 to 30 m s^{-1} (Figures 5.31 and 5.32). For the first line, measurements were taken at the face of the bell-mouth shaped flanged square hood. The AVM's probe was placed at the symmetry position as was the pitot-static tube. Flow was adjusted to give ten different flow rates. Then velocity reading and velocity pressure reading from micromanometer were recorded. These readings were corrected for standard air temperature and pressure (STP). The final velocity values were plotted against each pair of readings (see Fig.5.31). This method was repeated for the 0 to 30 m.sec^{-1} range. The test section at this time was the centre cross plane of main duct section (Drawings No.1). In a horizontal traverse plane at the centre line, the velocity was recorded with both pitot tube and AVM alternatively. Then these readings were corrected for STP and the final pairs of velocities were plotted (Figure 5.32). Figures 5.31 and 5.32 are the calibration lines for each range of scale readings.

2.2 Calibration of AVM502.

The wind tunnel assembly is given by Fig. 5.33 One standard pitot-static tube was firmly placed at the symmetry location as the probe of AVM502. Both probe and tube were positioned in the centre horizontal plane inside the hood.

Velocity pressure at the point of the pitot tube were read with both inclined manometer and micromanometer, the latter was recorded too.

The flow fluctuation was traced by chart recorder. Figure 5.34 shows the flow fluctuations. At low flowrate (i.e. P A = 2) the fluctuation was virtually nil and the maximum fluctuation corresponded to the high pitch angle setting (i.e. PA = 10). Maximum velocity variation was ranged about up to 0.08 $m.s^{-1}$ (see Fig. 5.34). Velocity (or velocity pressure) across the traverse plane and along the symmetry points along the flow stream was uniform up to a certain distance from the walls and up to the reduction section zone.

The velocity pressure readings were converted into velocity and then corrected for temperature and pressure to standardize to 20 °C and 760 mm Hg of atmospheric pressure. These velocities were used as the true velocity for calibration setting of AVM502 probes. Each of the readings from the scale deflection of AVM pointer and the corresponding recorded voltages were used to prepare a graphical representation of voltage-velocity relationship (see Fig. 5.50)

The velocity and temperature readings were substituted in the following equation

$$V_{true} = V_{measured} (1 + 0.01(T-20))$$

to correct the measured velocity for the deviation of temperature

from the standard calibration temperature (i.e. 20°C). And then this value was again corrected for air density to standardize at STP. Then the final corrected velocities were plotted. Fig. 5.35 shows the corrected true velocities versus the measured.

Manufacturers calibration lines for both scale ranges 0 to 0.5 $m.s^{-1}$ and 0 to 5 $m.s^{-1}$ are shown by Figures 5.36 and 5.37, where it can be seen from these figures that there is a good agreement of these two calibration lines.

Figure 5.38 is the recorded tracings of voltage responses of both temperature (lower values) and velocity for an identical flowrate using six comparable instruments. Following is the statistical analysis and discussion on this calibration.

As Figures 5.35 and 5.38 show there is a difference of readings between each instrument. Each pair of instruments were compared and a t-test statistic was calculated, and the hypothesis that there is no significant difference between the means of measurement was tested. Also a t-test on the comparison of mean of manufacturers calibration data (Figures 5.36 and 5.37), and laboratory calibration data (Fig.5.35) showed that with a 95% confidence limit, there was no significant difference between means obtained in the laboratory and from the manufacturers calibration. The existing differences are due to the different procedure of calibration conditions, execution error and the total number of readings with each instrument (i.e. 4 flow rates in laboratory, five flow rates at factory) (for calculation detail see attached AT5.1).

2.3 Calibration of the Simmon Shielded hot wire anemometer.

This anemometer has a range selecting switch which enables to be measured three ranges of velocities for the same

length of galvanometer deflection scale (i.e. 150 mm). Velocity response to galvanometer deflection is non-linear. Therefore, calibration data for the ranges of measurement is provided by manufacturer. These data are plotted separately for each range of measurement (i.e. 0 to 0.12 MS^{-1}, 0 to 0.6 MS^{-1}, and 0 to 1.5 MS^{-1}). The manufacturers calibrations are done on a whirling arm over the range of air speed. The sensitivity of measurement on each scale range is very good and the main direction of development of this instrument has been for the measurement of very low air movement. Omer et al. (1966) states that the maximum speed in each scale can be measurable with an error of less than $\pm$ 0.5%.

A comparison measurement with this instrument and one of the AVM502 velocity meters, showed that although the relationship was not a good linear one for practical purposes, a line calibration between reasonably close pairs of readings could be assumed. Figures 5.39, 5.40, 5.41 and 5.42 are the calibration lines for this instrument.

3. Calibration of inclined manometers.

Inclined manometers are calibrated against an accurate micromanometer. Flow rate was fixed at a known volume, then a pitot-static tube was traversed vertically (or horizontally) at six positions following the log-linear rule. Total pressure and static pressure legs of the pitot-static tube were connected to the manometers to read the velocity pressure at each traverse position.

System layout is shown schematically by Fig. 5.43 Velocity pressure reading with micromanometer was recorded, Figures 5.44 and 5.45 show the pressure fluctuation at each

traverse point. Figure 5.43 shows that the flow is turbulent, but figures 5.44 to 5.45 clarify that the flow is a steady turbulent flow. Also these recorded velocity pressures show the variation of velocity at each layer of air flow. Average velocity calculated from micromanometer readings is 8.33 m/sec. The ratio of average velocity to the centre velocity is 0.95. This ratio,which is called duct coefficient, may be taken as practically constant for all velocities (Hughes 1911). An average duct coefficient for five different flow rates was 0.9 Table T5.1 contains all the measured velocities.

Figure 5.46 shows graphically the relationship between velocity calculated from pressure readings by micromanometer and inclined manometers. These data were analysed statistically. The statistical inferences are that:

i) there is a high linear correlation between (R = 0.94,0.92) the measurements taken by micromanometer and inclined manometers.

ii) Assuming the difference of readings by different manometers has a normal distribution, then it follows that the differences should have a zero mean. To verify this hypothesis, a two tailed pair t-test was a quite appropriate test. Calculation of this statistic showed that for a significant level of 0.05 and 4 (= 5-1) degrees of freedom, the above hypothesis was not rejected.

As previously stated, due to the physical characteristics of inclined manometer No.2, the readings are higher than the standard instrument. On the other hand the readings with inclined No.1 is lower than the standard readings. These differences are mainly due to experimental and systematic instrumentation error. As a

whole the adjustable inclination tube manometer due to its long limb and the facility of adjusting the inclination proved better manometer than the industrial desk type one. Average percentage errors based on micromanometer were -0.81 and 5.06 respectively for inclined No.1 and No.2.

Figure 5.47 shows the calibration line for inclined No.2 versus inclined No.1. These data are for a range of velocity measurements. As it shows, there is a good linear relationship between the readings. The industrial desk type manometer has a wide range of measurement (up to 35 m/sec or 75 mm WG of velocity pressure), whereas inclined No.1 ranges up to about 30 m/s (50 mm WG pressure difference). Therefore, this calibration line gives a facility for the correction of readings taken with less accurate manometers. Table T5.2 gives the data for this calibration. A similar t-test to that in the previous section was calculated for these data. For the same assumptions and hypothesis, the calculation showed that the hypothesis is not rejected for 0.05 level of confidence.

4. Errors.

The experimental errors are the errors due to positioning of the pitot tube at the traverse positions and scale readings of pressure difference as well as the variation of flow rates, due to the traverse plane which was not at the 10 diameter distances away from any change of the system cross section.

5. Calibration of Averaging pressure tube.

As previously mentioned, pitometry for two diameter traverse plane at right angles, either by the log-linear rule or tangential rule, requires a special cross section plane of a

round duct and correct positioning of the pitot static tube. The accuracy of the pitometry method of integration, without taking into account any errors of positioning or requirement of local velocity pressures, is about ± 0.5% (Wintarnitz et al. 1957). The fulfilment of the requirements was difficult because of the physical limitations. The characteristics of the averaging pressure tube has been mentioned previously. The accuracy of ± 6.5 measurement is mentioned by William (1966). But this accuracy is for velocities from 3 m/sec. up to 7 m/sec. Also this is for two averaging pressure tubes and four static pressure ports at four right-angled planes. In this research just one horizontally placed averaging pressure tube with 3-static pressure ports connected to a common rubber tube, were the permanent flow rating devices. Fig. 5.48 shows the position of the averaging tube and static ports. Both ends of the averaging pressure tube were connected to a common point, and also three static pressure ports were connected to a common point, and then connected to a manometer to read the average velocity pressure.

Flowmetering, by following the British Standard method of pitot-static tube anemometry compared with averaging pressure tube for flow rate measurement, was performed.

For five different flow settings a number of log-linear pitot-static tube readings were recorded for the calibration of the averaging pressure tube.

Table T5.3 contains the average velocities by pitometer method and the velocities calculated from velocity pressures measured with an averaging pressure tube.

Statistical analysis and discussion.

Statistical analysis of data revealed that:

i) there is no significant difference between these two ways of flowmetering (see Table T5.5);

ii) there is a high linear correlation between these two methods (Figure 5.19);

iii) even using an adjustable inclination tube manometer for pressure measurement, a maximum of 5% and minimum of -7%, based on averaging pressure tube, was the range of variation of measuring error for air velocities from 6-30 MS^{-1} (see Table T5.5). Fig. 5.29 shows the velocity calculated from velocity pressure measured with these two different methods.

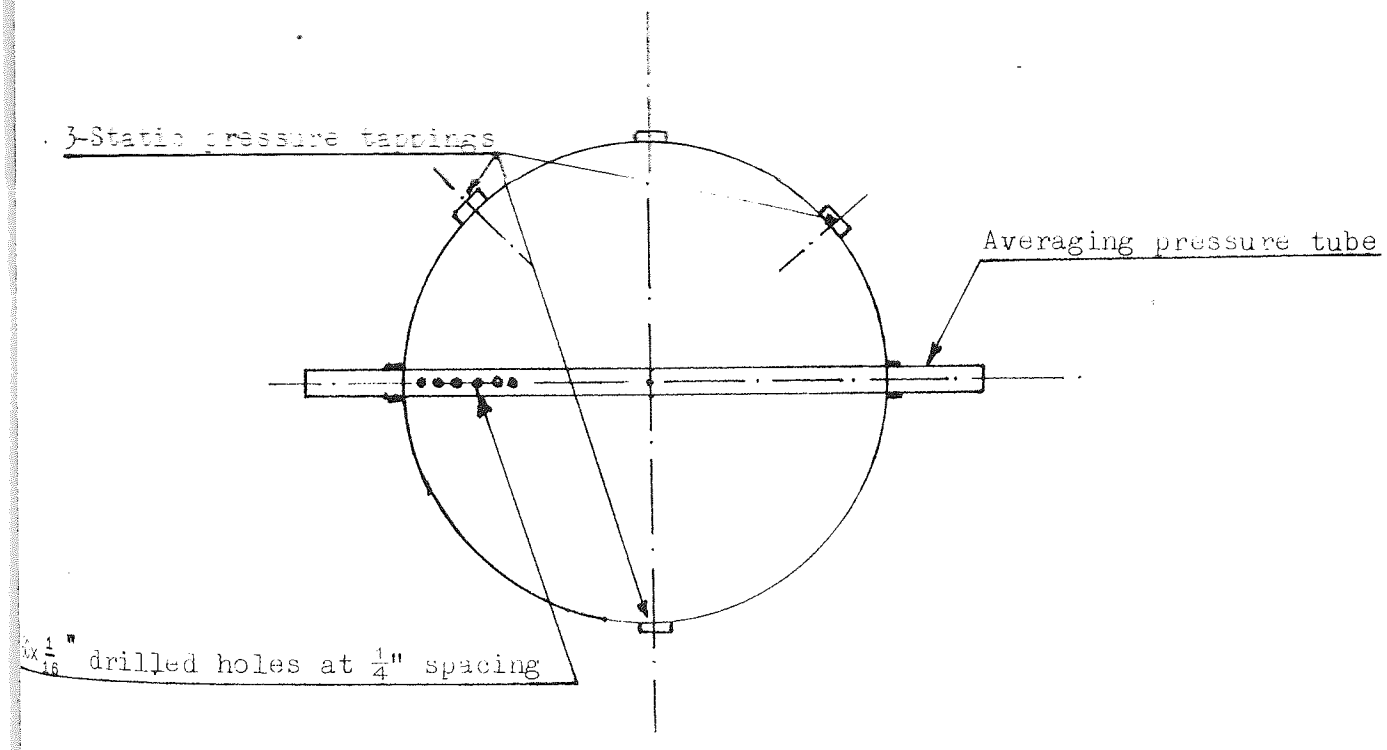

FIG. 5.30 Position of static pressure tapes and averaging pressure tube.

As previously stated, the object is to find the minimum variation between the different types of anemometers. The standard way of flowrate measurement in a round duct is pitot-static tube anemometry (as mentioned earlier). The present experiment showed that the averaging pressure tube method is a very convenient and practically accurate way of airflow

Attach AT5.1

CALIBRATION OF AVM 502

Test for Homogenicity of variance

The purpose of preliminary tests is to provide a partial check on whether or not the observed data tends to be consistent with the factory's calibration data.

Assumption is that the variances should be equal. A test on means by assuming that the variances are homogeneous can be performed by a multiple comparison of means. This test is usually called honesty significant difference (HSD) test or Tukey's method of comparison of means. Following tables are the computation and decision on each AVM 502 labelled from probe no's 1 to 6.

Probe No. 1 Both ranges 0 to 0.5m/sec and 0 to 5.0m/sec

Manufacturer Calibration (extracted from curve corrected for T)	Laboratory Calibration (Measured data corrected for T)
N_F=10 0.102, 0.208, 0.315, 0.416, 0.507, 1.066, 2.030, 3.045, 4.009, 5.024	N_L=4 2.065, 4.225, 4.957, 3.873
$\Sigma V_F = 16.722$ $\Sigma V_F^2 = 56.42$	$\Sigma V_L = 15.12$ $\Sigma V_L^2 = 61.68$
$T_1 = N_F \Sigma V_F^2 - (\Sigma V_F)^2 = 284.58$	$T_2 = N_L \Sigma V_L^2 - (\Sigma V_L)^2 = 246.72 - 228.61 = 18.11$
$S_F^2 = \frac{284.58}{10\,(10-1)} = 3.162$	$S_L^2 = \frac{18.11}{4 \times 3} = 1.51$
$\bar{V}_F = \frac{16.722}{10} = 1.672$	$\bar{V} = \frac{15.12}{4} = 3.78$

$$t^2 = \frac{(N_F + N_L - 2)\,(N_L\,\Sigma V_L - N_F\,\Sigma V_F)^2}{(N_F + N_L)\,(N_F\,T_1 + N_L\,T_2)}$$

$$t^2 = \frac{(10 + 4 - 2)(4 \times 15.12 - 10 \times 16.722)^2}{(4 + 10)(10 \times 284.58 + 4 \times 18.11)} = \frac{136721.16}{399925} =$$

$$t^2 = \frac{136721.16}{399925} = 3.43$$

$$t^2 = \pm 1.85$$

Hypothesis $H_1 : \mu_F - \mu_L = 0$

$\alpha = 0.05$

Decision criterion:

Reject H_1 if t_{obs} $\begin{cases} < -2.13 \\ > 2.13 \end{cases}$

Otherwise do not reject H_1

Since $t_{obs} = -1.85, +1.85$, H_1 is not rejected.

Decision rules are:

Reject H_1 if $t^2_{obs} > 4.54$

otherwise do not reject H_1

In this case $t^2_{obs} = 3.42$; hence H_1 is not rejected.

$$F_{1-\alpha}(1, N_F + N_L - 2) = t^2_{1-(\alpha/2)}(N_F + N_L - 2)$$

Therefore the difference between the calibration of probe no. 1 given by factory and calibration of this probe at lab is in part a function of the difference in the procedure of the two calibration and in part a function of the difference between the average experimental error associated with each of the means.

Probe No. 1 Range 0.0 to 5.0 m/sec scale

Manufacturer Calibration Data	Laboratory calibration data
1.066	2.065
2.03	4.225
3.045	4.957
4.009	3.873
$N_F = 5$ 5.024	$N_L = 4$
$\Sigma V_F = 15.174$	$\Sigma V_L = 15.12$
$\Sigma V_F^2 = 55.842$	$\Sigma V_L^2 = 61.68$

$T_1 = 279.20 - 230.25 = 48.95$

$S_F^2 = \frac{48.95}{20} = 2.4475$

$\bar{V}_F = \frac{\Sigma V_F}{N_F} = \frac{15.174}{5} = 3.0258$

$T_2 = N_L \Sigma V_L^2 - (\Sigma V_L)^2 =$

$246.72 - 228.61 = 18.11$

$S_L^2 = \frac{T_2}{4x3} = \frac{18.11}{12} = 1.51$

$\bar{V} = \frac{15.12}{4} = 3.78$

$F = t^2 = \frac{(5 + 4 - 2)(4 \times 15.12 - 5 \times 15.174)^2}{(5 + 4)(5 \times 4 \times 18.11)} = \frac{1657.9}{2854.7} = 0.581$

$t = \pm 0.762$

Hypothesis $H_1 : \mu_F - \mu_L = 0$

$\alpha = 0.05$

Decision criterion:

Reject H_1 if t_{obs} <-2.13 or >2.13

Otherwise do not reject H_1

Since $t_{obs} = -0.762, 0.762$, H_1 is not rejected.

Probe No. 2 Range 0 to 5.0 m/sec

Manufacturer Calibration Data	Laboratory Data
1.071	1.771
2.040	3.480
2.978	4.286
3.998	3.349
5.024	
$N_F = 5$	$N_L = 4$
$\Sigma V_F = 15.09$	$\Sigma V_L = 12.87$
$\Sigma V_F^2 = 57.39$	$\Sigma V_L^2 = 44.84$
$T_F = 286.95 - 227.71 = 59.24$	$T_L = 179.36 - 165.64 = 13.72$
$S_F^2 = \frac{T_F}{N_F (N_F-1)} = 2.96$	$S_L^2 = \frac{T_L}{N_L (N_L-1)} = 1.14$
$\bar{V}_F = 3.02$	$\bar{V}_L = 3.22$

$$F = t^2 = \frac{(5 + 4 - 2)(4\ \Sigma V_L - 5\Sigma V_F)^2}{(5 + 4)(4\ T_L + 5\ T_F)} = \frac{4021.92}{1142.37} = 3.52$$

$t = \pm 1.8761$

H_1 is the same as before

Since $t_{obs} = -1.8761, 1.876$, H_1 is not rejected.

Probe No. 3 Range 0 to 5.0 m/sec

Manufacturer Calibration Data	Laboratory Data
0.995	1.695
2.015	3.155
3.035	3.901
4.055	3.024
5.100	
$N_F = 5$	$N_L = 4$
$\Sigma V_F = 15.18$	$\Sigma V_L = 11.76$
$\Sigma V_F^2 = 56.71$	$\Sigma V_L^2 = 37.18$
$T_F = 283.55 - 230.43 = 48.12$	$T_L = 148.72 - 138.30 = 10.42$
$S_F^2 = \frac{48.12}{20} = 2.41$	$S_F^2 = \frac{10.42}{12} = 0.87$
$\bar{V}_F = 3.04$	$\bar{V}_L = 2.94$

$$F = t^2 = \frac{(7)\ (47.04 - 75.9)^2}{(9)\ (240.60 + 41.68)} = \frac{3985.1}{2540.52} = 1.57$$

$t = \pm 1.253$

H_1 is the same as probe no. 1

Decision: H_1 is not rejected.

Probe No. 4 Range 0 to 5.0 m/sec

Manufacturer Calibration Data	Laboratory Data
1.076	1.626
2.05	3.130
3.177	3.748
4.228	3.077
5.253	
$N_F = 5$	$N_L = 4$
$\Sigma V_F = 15.76$	$\Sigma V_L = 11.56$
$\Sigma V_F^2 = 60.92$	$\Sigma V_L^2 = 35.96$
$T_F = 304.6 - 248.38 = 56.22$	$T_L = 143.84 - 133.63 = 10.21$
$S_F^2 = 2.81$	$S_L^2 = \frac{10.21}{12} = 0.85$
$\bar{V}_F = 3.15$	$\bar{V}_L = 2.89$

$$F = t^2 = \frac{7(46.24 - 78.80)^2}{9(281.1 + 40.84)} = \frac{7421.05}{2933.46} = 2.53$$

$t = \pm 1.5905$

H_1 is the same as probe No. 1

Decision: H_1 is not rejected.

Probe No. 5 Scale Range 0 to 5 m/sec

Manufacturer Calibration Data	Laboratory Data
0.515	1.718
1.020	3.22
2.111	3.915
4.068	3.024
5.047	
$N_F = 5$	$N_L = 4$
$\Sigma V_F = 12.74$	$\Sigma V_L = 11.86$
$\Sigma V_F^2 = 47.79$	$\Sigma V_L^2 = 37.79$
$T_F = 238.95 - 162.31 = 76.64$	$T_L = 151.16 - 140.66 = 10.50$
$S_F^2 = \frac{T_F}{20} = 3.83$	$S_L^2 = \frac{10.50}{12} = 0.88$
$\bar{V}_F = 2.55$	$\bar{V}_L = 2.97$

$$F = t^2 = \frac{7\ (47.44 - 63.7)^2}{9\ (383.2 + 42.0)} = \frac{1850.73}{3826.8} = 0.48$$

$t = \pm 0.69$

H_1 is the same as probe no. 1

Decision: H_1 is not rejected.

Probe No. 6 Range 0 to 5 m/sec

Manufacturer Calibration Data	Laboratory Data
0.181	1.779
0.518	3.065
1.009	3.976
2.044	3.054
5.149	
$N_F = 5$	$N_L = 4$
$\Sigma V_F = 8.87$	$\Sigma V_L = 11.85$
$\Sigma V_F^2 = 32.01$	$\Sigma V_L^2 = 37.69$
$T_F = 160.05 - 78.68 = 81.37$	$T_L = 150.76 - 140.42 = 10.34$
$S_F^2 = 3.93$	$S_L^2 = \frac{T_L}{12} = \frac{10.34}{12} = 0.86$
$\bar{V}_F = 1.77$	$\bar{V}_L = 2.96$

$$F = t^2 = \frac{7\ (47.40 - 44.35)^2}{9\ (406.85 + 41.36)} = \frac{83.70}{4216.95} = 0.02$$

$t = \pm 0.1414$

H_1 is the same as probe No. 1

Decision: H_1 is not rejected.

TABLE T5.1 Velocity calculated from two diameter pitometry using inclined manometer for pressure readings.

Case No.	Pitch Angle	Vertical Traverse		Horizontal Traverse	
		Inclined 1	Inclined 2	Inclined 1	Inclined 2
1	2	8.26	8.73	9.03	9.67
2	4	17.85	17.13	16.47	16.92
3	6	20.39	20.73	20.65	20.83
4	8	24.95	25.24	25.83	26.18
5	10	27.32	27.49	27.74	28.20
Average		19.75	19.86	19.94	20.36
Standard deviation		6.64	6.62	6.74	6.66
Coefficient of variation		0.34	0.33	0.34	0.33

NOTE: Detailed data is given in Appendix AT5.2

TABLE T5.2 Velocity calculated from velocity pressure reading with pitometry method and three manometers.

Case No.	Pitch Angle	Six points vertical Traverse (log-linear rule) Inclined No.1	Inclined No.2	Macro-manometer	Error % based on Micromanometer Incl.1	Incl.2
1	2	6.94	7.5	6.94	0.0	8.07
2	"	7.39	8.5	8.02	-7.86	5.98
3	"	8.02	8.96	8.31	-3.49	7.82
4	"	9.49	9.48	9.32	1.82	7.08
5	"	9.14	8.96	9.14	0.0	-1.97
6	"	8.60	8.5	8.22	4.62	3.41
Average		8.26	8.73	8.33	-0.81	5.06
Standard deviation		0.9	0.74	0.78	3.97	3.51
Coefficient of variation		0.11	0.085	0.093	-4.9	0.69

NOTE: Detailed data is given in Appendix AT5.2

TABLE T5.3 Data for the calibration of the averaging pressure tube.

Case No.	Flow Rate Setting	Inclined No.1		Inclined No.2		Error % based on Averaging Pressure Tube	
		Averaging Pressure Tube	Pitot-Static Tube	Averaging Pressure Tube	Pitot-Static Tube	Inclined 1	Inclined 2
1	PA = 2	8.4	8.64	8.5	9.20	2.86	8.23
2	PA = 4	16.37	17.16	16.42	17.03	4.83	3.71
3	PA = 6	21.83	20.52	20.46	20.78	-6.0	1.56
4	PA = 8	26.7	25.38	26.82	25.71	-4.91	-4.13
5	PA = 10	29.67	27.53	30.37	27.84	-7.21	-8.33
Average		20.59	19.85	20.51	20.11	-2.086	0.208
Standard deviation		7.59	6.68	7.72	6.63	4.93	5.83
Coefficient of variation		0.37	0.34	0.38	0.33	-2.36	28.05

NOTE: Detailed data is given in Appendix AT5.2

ATTACH AT5.2

CALIBRATION OF AVERAGING PRESSURE TUBE AND MANOMETERS

VELOCITY PRESSURE MEASUREMENT WITH DIFFERENT MANOMETERS CONVERTED TO VELOCITY OF AIR MOVEMENT

Pitot-Static tube Position	Pitch angle = 2				Temp. = 20				BP = 770 mm Hg				Error % bas on vert. trave. rea. of aver. pres. reading				Remarks
	Vertical plane Traverse				Horizontal Trav. plane				Averaging Pressure tube				Vert. Compared	Averaging pressure compared with:			
	Inclin 1*	Inclin 2**	Micro-Mano.	Duct Coef.	Inclin 1	Inclin 2	Micro-Mano.	Duct Coef.	Inclin 1	Inclin 2	Micro-Mano.	Remark	with 2 diam	Vert. trav.	Aver. 2 dia.	Horiz Trav.	
1	6.94	7.5	6.94		8.41	7.5	6.94										
2	7.39	8.5	8.02		10.45	9.65	9.82										
3	8.02	8.96	8.31		9.32	10.22	10.83										
Centre	8.73	8.96	8.78	0.95 0.97 0.94	11.05	9.98	10.83		0.81 0.97 0.91	8.4	8.5	8.31					
4	9.49	9.98	9.32		11.19	10.98	10.76										
5	9.14	8.96	9.14		10.45	9,82	10.61										
6	8.60	8.5	8.22		8.67	9.82	10.75										
Average of six reading	8.26	8.73	8.33		9.03	9.67	9.95										
Average of Incl. No.1	8.64	-	-	-									4.60	-1.66	2.85	7.5	
Average of Incl. No.2	-	9.20	-	-									5.38	2.7	7.29	13.76	
Average of micro mano	-	-	9.14	-									9.72	0.24	9.99	19.73	
Standard dev 6 read.	0.90	0.74	0.78		1.14	1.06	1.36										
Coefficient of variat.	0.11	0.085	0.093		0.126	0.109	0.136										

* Inclined manometer with adjustable inclination limb mark MK5

** " " " fixed " " " MK4 Industrial desk type

CONTINUED

VELOCITY PRESSURE MEASUREMENT WITH DIFFERENT MANOMETERS CONVERTED TO VELOCITY OF AIR MOVEMENT

Pitot-Static tube Position	Pitch angle = 4	Temp. = 20	BP = 749 mm Hg										Error % bas on vert. trave. rea. or aver. pres. reading				Remarks
	Vertical plane Traverse				Horizontal Trav. plane				Averaging Pressure tube				Vert. Compared	Averaging pressure compared with:			
	Inclin 1*	Inclin 2**	Micro-Mano.	Duct Coef.	Inclin 1	Inclin 2	Micro-Mano.	Duct Coef.	Inclin 1	Inclin 2	Micro-Mano.	Remark	with 2 diam	Vert. trav.	Aver. 2 dia.	Horiz Trav.	
1	13.77	14.3	Off Scale		14.24	14.85	Off Scale										
2	15.66	16.67	"		16.17	16.67	"										
3	19.92	17.85	"		17.34	18.08	"										
Centre	19.96	18.75	"	0.89 0.91	18.44	18.75	"	0.89 0.90	16.37	16.42	Off Scale						
4	20.13	18.96	"		18.44	18.96	"										
5	19.32	18.08	"		17.62	17.62	"										
6	18.29	16.91	"		15.02	15.39	"										
Average of six reading	17.85	17.13	-		16.47	16.92											
Average of Incl. No.1	17.16	-	-										-3.86	9.04	4.83	0.61	
Average of Incl. No.2	-	17.03											-0.58	4.32	3.71	3.05	
Average of micro mano	-	-	"										-	-	-	-	
Standard dev 6 read.	2.25	1.44			1.44	1.44											
Coefficient of variat.	0.126	0.08			0.087	0.085											

* Inclined manometer with adjustable inclination limb mark MK5
** " " " fixed " " " MK4 Industrial desk type

ATTACH AT5.2 CONTINUED (1)

VELOCITY PRESSURE MEASUREMENT WITH DIFFERENT MANOMETERS CONVERTED TO VELOCITY OF AIR MOVEMENT

Pitot-Static tube Position	Pitch angle = 6				Temp. = 21				BP = 775 mm Hg				Error % bas on vert. trave. rea. of aver. pres. reading				Remarks
	Vertical plane Traverse				Horizontal Trav. plane				Averaging Pressure tube				Vert. Compared	Averaging pressure compared with:			
	Inclin 1*	Inclin 2**	Micro-Mano.	Duct Coef.	Inclin 1	Inclin 2	Micro-Mano.	Duct Coef.	Inclin 1	Inclin 2	Micro-Mano.	Remark	with 2 diam	Vert. trav.	Aver. 2 dia.	Horiz Trav.	
1	16.65	17.26	Off Scale		19.16	19.24	Off Scale										
2	19.49	20.06	"		21.23	20.66	"										
3	20.92	21.04	"		22.34	22.7	"										
Centre	22.56	22.87	"	0.90 0.90	22.56	22.34	"	0.91 0.93	21.83	20.46	Off Scale						
4	23.26	23.05	"		21.98	22.7	"										
5	21.83	22.34	"		21.23	20.85	"										
6	20.22	20.66	"		17.94	18.22	"										
Average of six reading	20.39	20.73	"		20.65	20.83	"										
Average of Incl. No.1	20.52	-					-						0.63	-6.6	-6.0	-5.40	
Average of Incl. No.2	-	20.78					-						0.24	1.34	1.56	1.81	
Average of micro mano	-	-	"				"						Off Scale				
Standard dev 6 read.	1.96	1.85			1.56	1.51											
Coefficient of variat.	0.096	0.089			0.075	0.072											

* Inclined manometer with adjustable inclination limb mark MK5
** " " " fixed " " " MK4 Industrial desk type

CONTINUED

VELOCITY PRESSURE MEASUREMENT WITH DIFFERENT MANOMETERS CONVERTED TO VELOCITY OF AIR MOVEMENT

ATTACH AT5.2 CONTINUED(3)

Pitot-Static tube Position	Pitch angle = 8				Temp. = 23.5				BP = 749 mm Hg				Error % bas on vert. trave. rea. or aver. pres. reading				Remarks
	Vertical plane Traverse				Horizontal Trav. plane				Averaging Pressure tube				Vert. Compared	Averaging pressure compared with:			
	Inclin 1*	Inclin 2**	Micro-Mano.	Duct Coef.	Inclin 1	Inclin 2	Micro-Mano.	Duct Coef.	Inclin 1	Inclin 2	Micro-Mano.	Remark	with 2 diam	Vert. trav.	Aver. 2 dia.	Horiz Trav.	
1	21.7	22.14	Off Scale		23.5	24.51	Off Scale										
2	24.53	24.92	"		26.51	26.2	"										
3	26.82	26.51	"		26.63	27.1	"										
Centre	27.54	27.42	"	0.90 0.92	27.83	27.86	"	0.92 0.93	26.7	26.82	Off Scale						
4	27.36	27.12	"		26.7	27.86	"										
5	25.70	26.80	"		26.7	26.51	"										
6	23.57	23.92	"		24.92	24.92	"										
Average of six reading	24.95	25.24			25.83	26.18											
Average of Incl. No.1	25.39	-												-6.5	-4.91	-3.26	
Average of Incl. No.2	-	25.71												-5.91	-7.13	-2.38	
Average of micro mano	-	-	"														
Standard dev 6 read.	1.93	1.77			1.12	1.17											
Coefficient of variat.	0.077	0.07			0.043	0.045											

* Inclined manometer with adjustable inclination limb mark MK5
** " " " fixed " " " MK4 Industrial desk type

VELOCITY PRESSURE MEASUREMENT WITH DIFFERENT MANOMETERS CONVERTED TO VELOCITY OF AIR MOVEMENT

ATTACH AT5.2 CONTINUED(4)

Pitot-Static tube Position	Pitch angle = 10	Temp. = 24			BP = 748 mm Hg								Error % bas on vert.trave. rea. of aver.pres.reading				Remarks
	Vertical plane Traverse				Horizontal Trav. plane				Averaging Pressure tube				Vert. Compared	Averaging pressure compared with:			
	Inclin 1*	Inclin 2**	Micro-Mano.	Duct Coef.	Inclin 1	Inclin 2	Micro-Mano.	Duct Coef.	Inclin 1	Inclin 2	Micro-Mano.	Remark	with 2 diam	Vert. trav.	Aver. 2 dia.	Horiz Trav.	
1	23.65	23.89	Off Scale		24.84	24.88	Off Scale										
2	27.07	27.04	"		26.89	28.35	"										
3	29.18	30.0	"		29.67	28.91	"										
Centre	30.32	30.32	"	0.90 0.90	30.0	30.92	"	0.92 0.91	29.67	30.37	Off Scale						
4	30.0	30.0	"		29.46	30.92	"				-						
5	28.8	28.35	"		29.18	28.77	"				-						
6	25.23	25.67	"		26.41	27.34	"				-						
Average of six reading	27.32	27.49	"		27.74	28.20	"		-	-	-						
Average of Incl. No.1	27.53	-											0.77	-8.22	-7.2-	-6.5	
Average of Incl. No.2	-	27.84	-										1.2	-9.48	-8.33	-7.15	
Average of micro mano	-	-	"										-	-	-		
Standard dev 6 read.	2.25	2.22			1.79	1.82											
Coefficient of variat.	0.082	0.080			0.064	0.065											

* Inclined manometer with adjustable inclination limb mark MK5
** " " " fixed " " " MK4 Industrial desk type

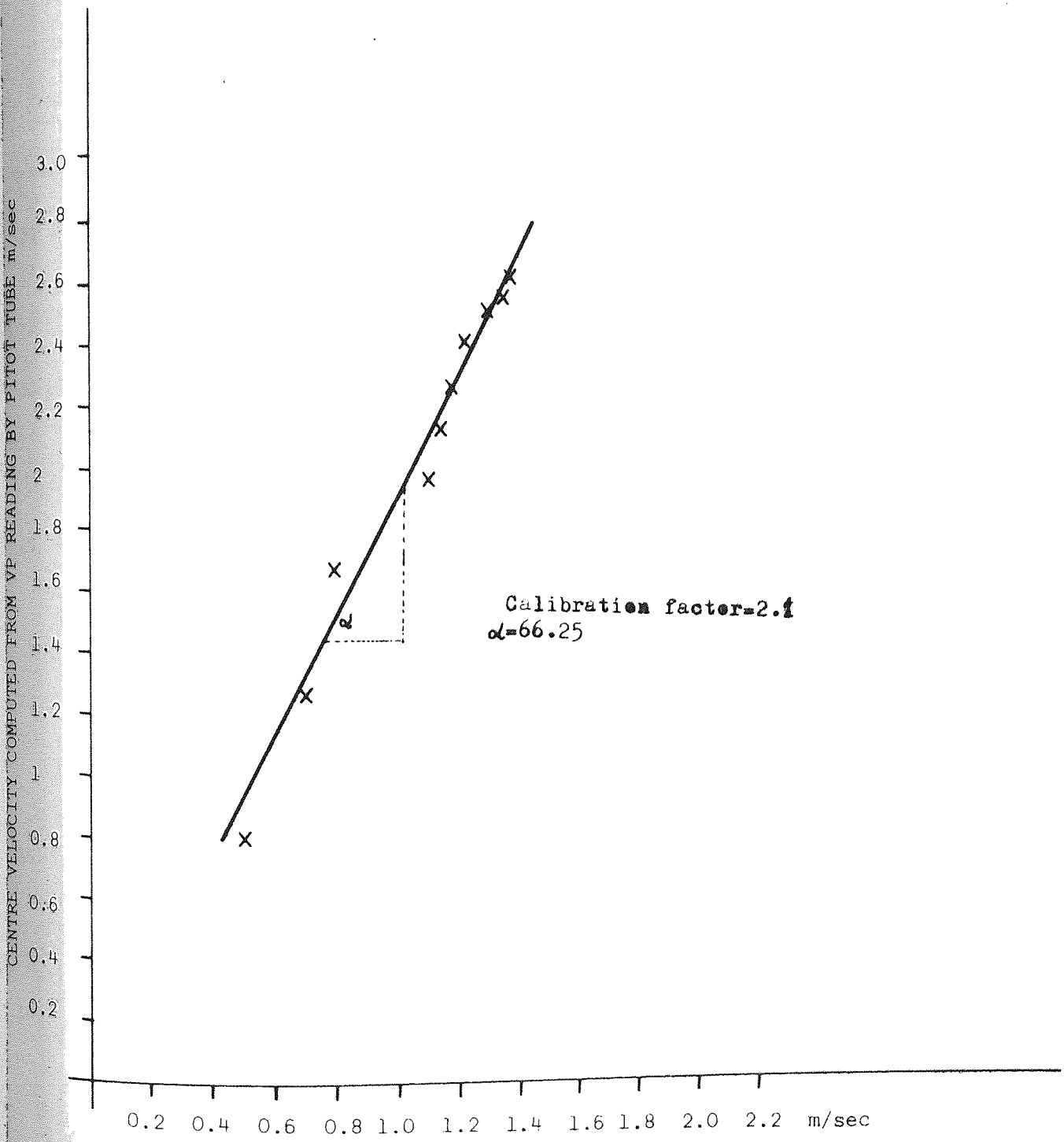

CENTRE POINT VELOCITY AT FACE (DIRECT READING WITH AVM501F (SCALE RANGE 0 TO 10 m/Sec)

Figure 5.31 CALIBRATION OF AVM501F

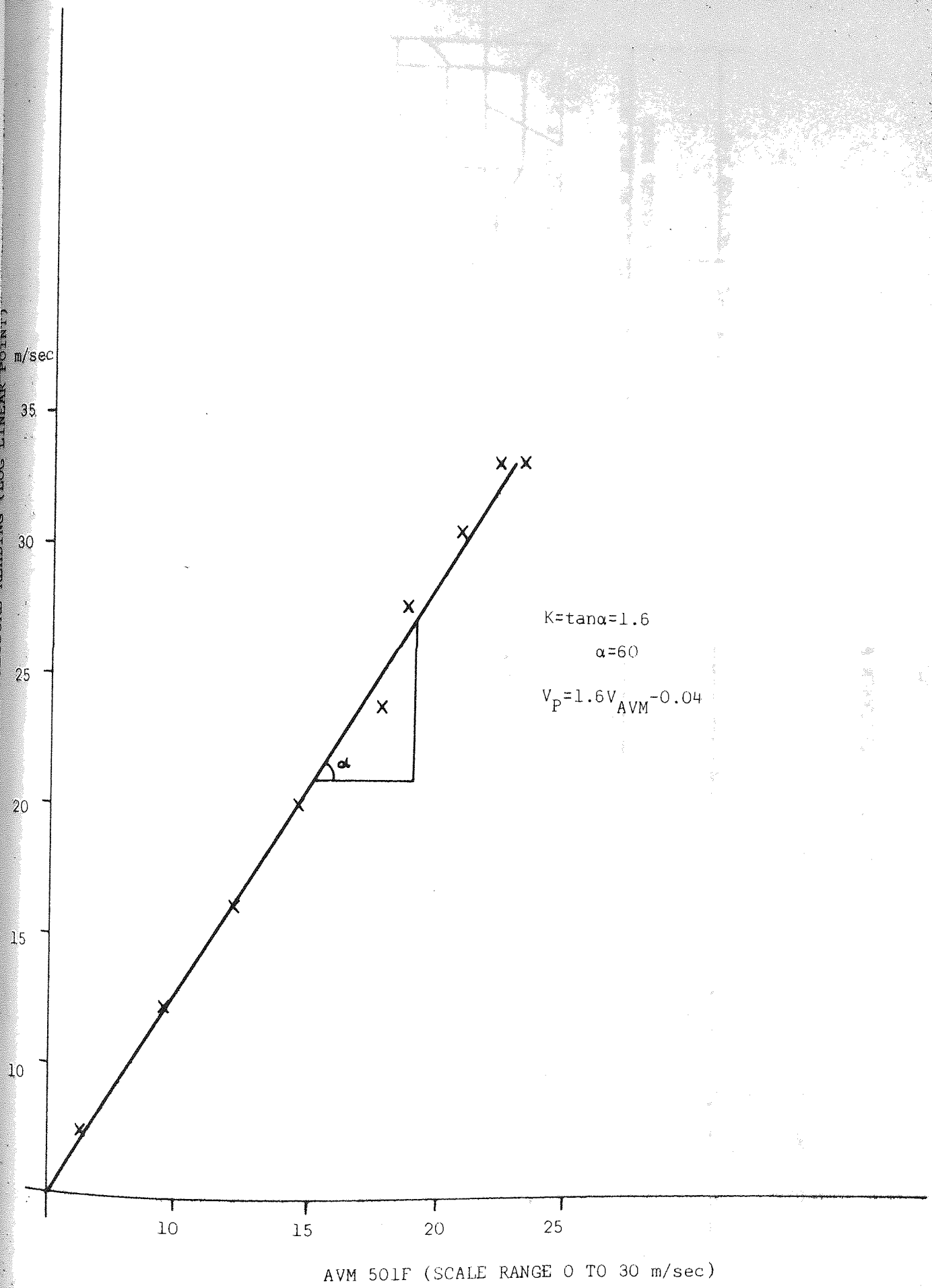

Figure 5.32 CALIBRATION OF AVM 501F

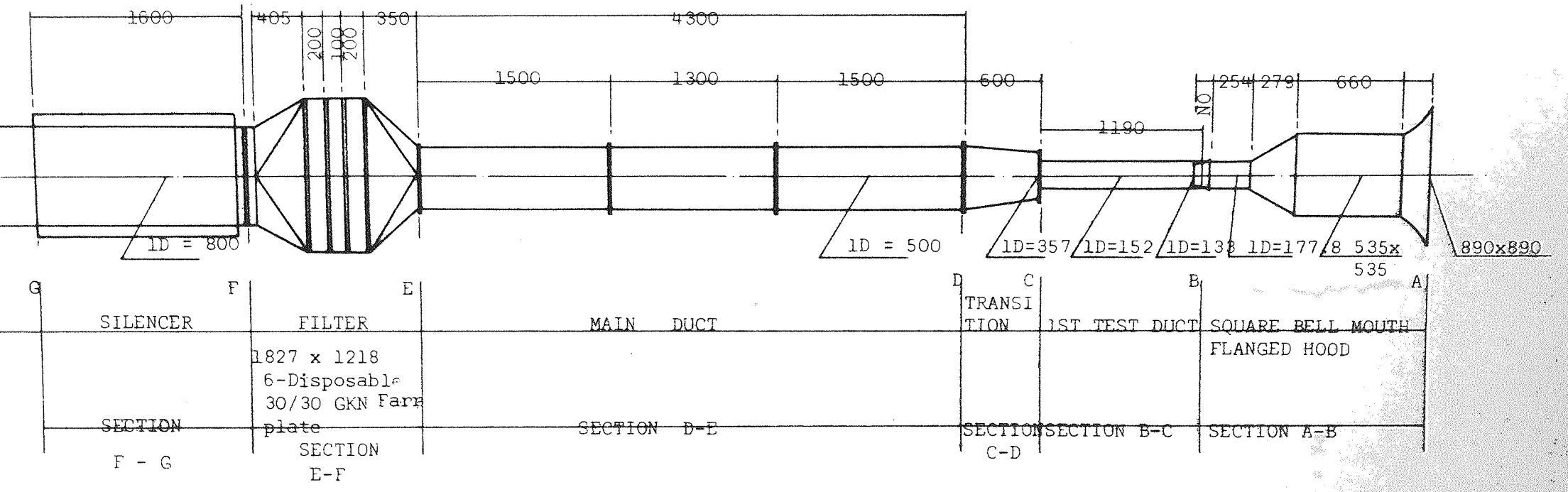

Note: (i) All dimension in mm (2) Dormat scale

Figure 5.3 SCHEMATIC OF RESEARCH WIND TUNNEL

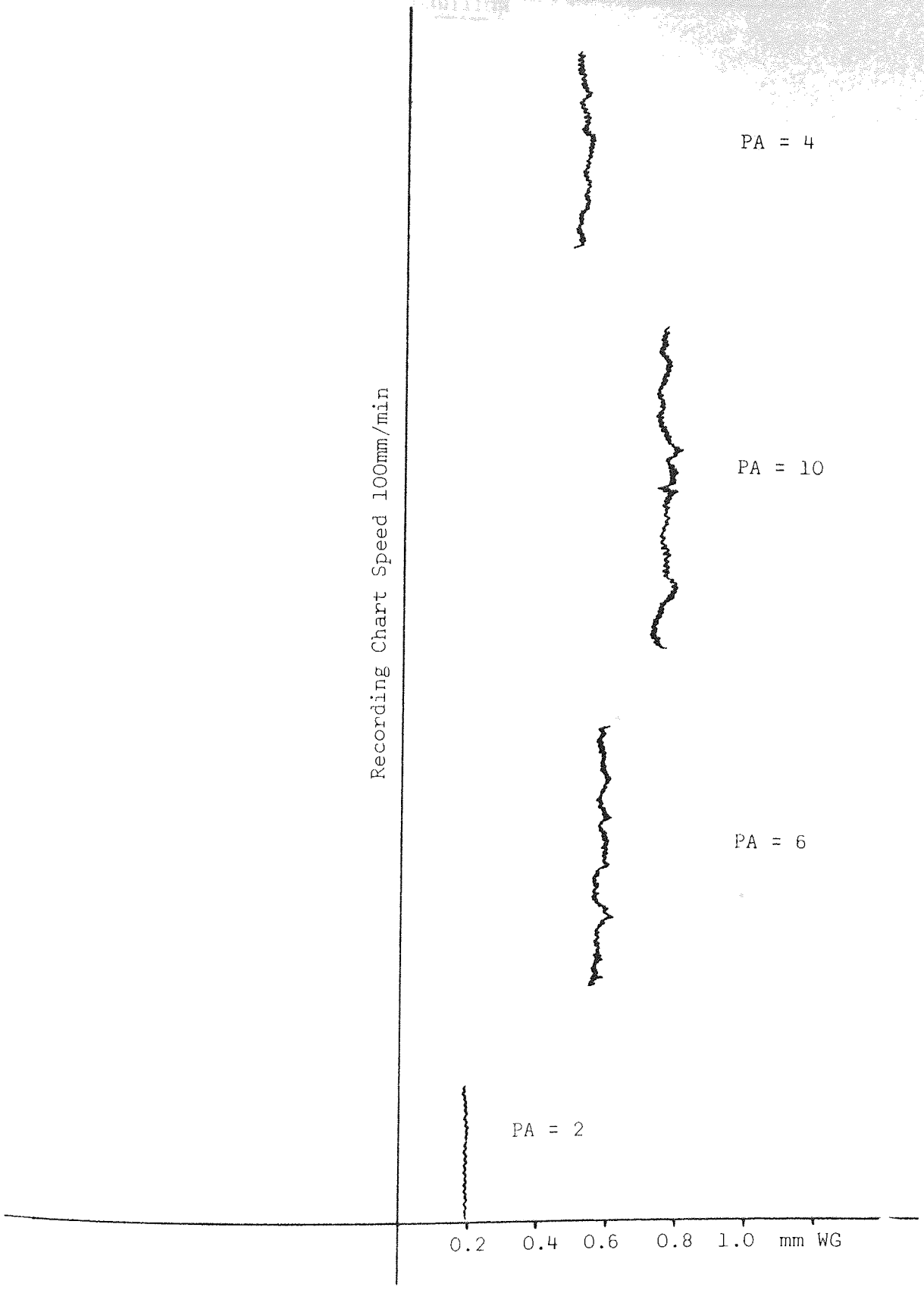

FIGURE 5.34 VELOCITY PRESSURE MEASUREMENT RECORDING DURING THE CALIBRATION OF AVM 502 (MICROMANOMETER AND LINSEIS CHART RECORDER)

Figure 5.35 CALIBRATION OF AIR VELOCITY METER AVM 502 (SCALE 0 TO 5m/sec) LABORATORY CONDITION

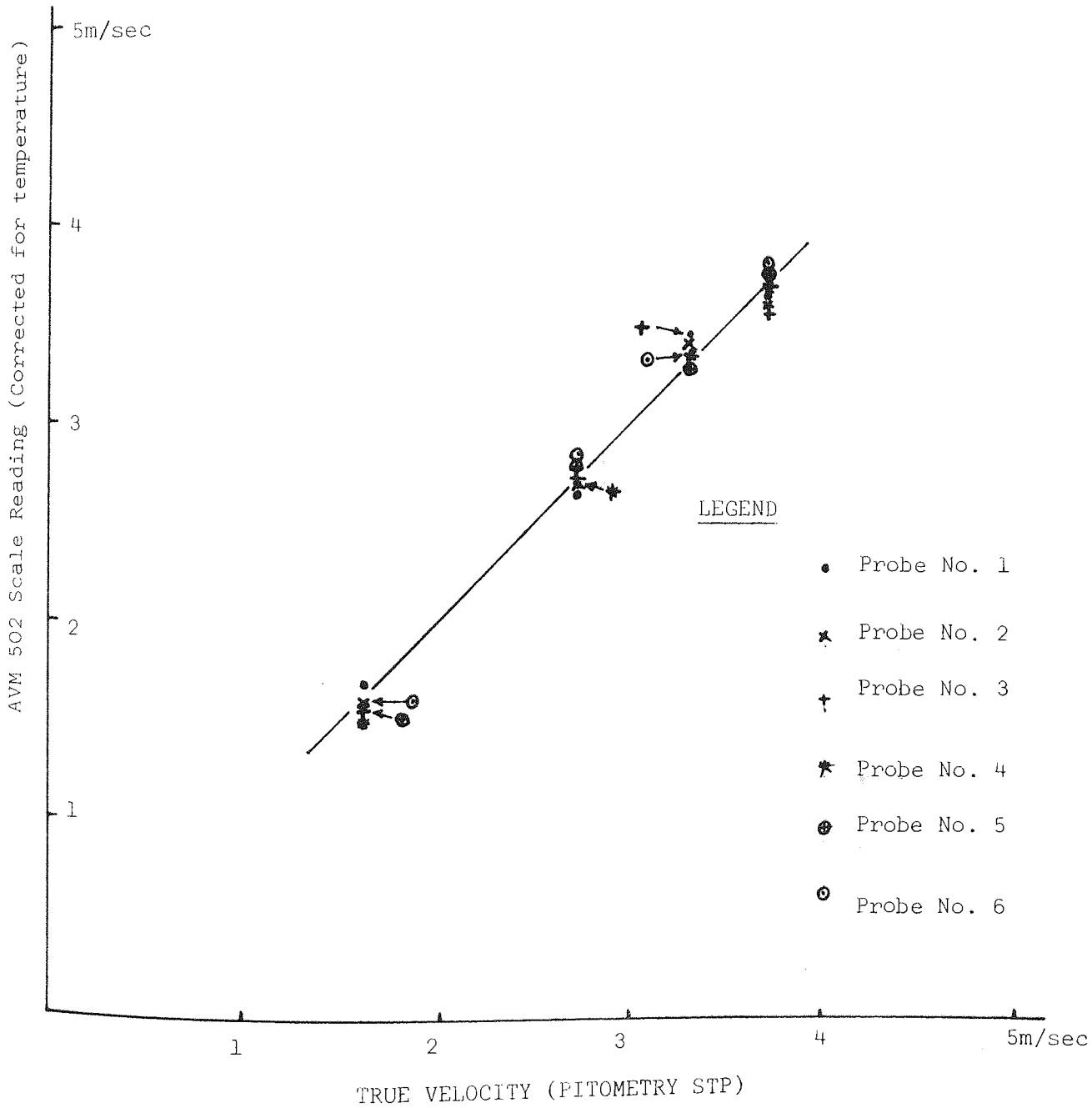

FIGURE 5.36 CALIBRATION OF AIR VELOCITY METER (AVM 502, O TO 0.5m/sec)
(FACTORY DATA)

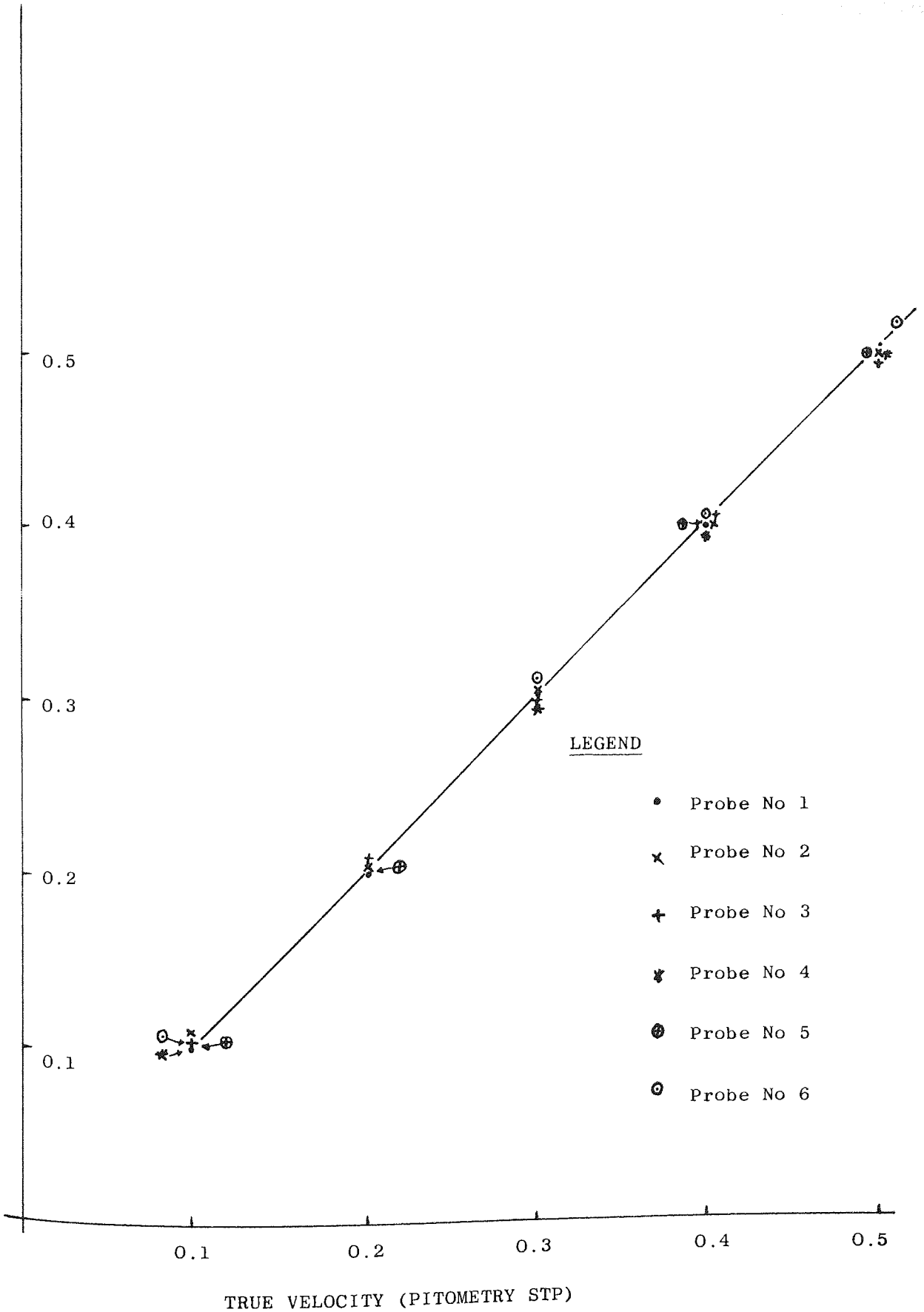

FIGURE 5.37 CALIBRATION OF AIR VELOCITY METER (AVM 502, 0 TO 5 m/sec) (FACTORY CALIBRATION)

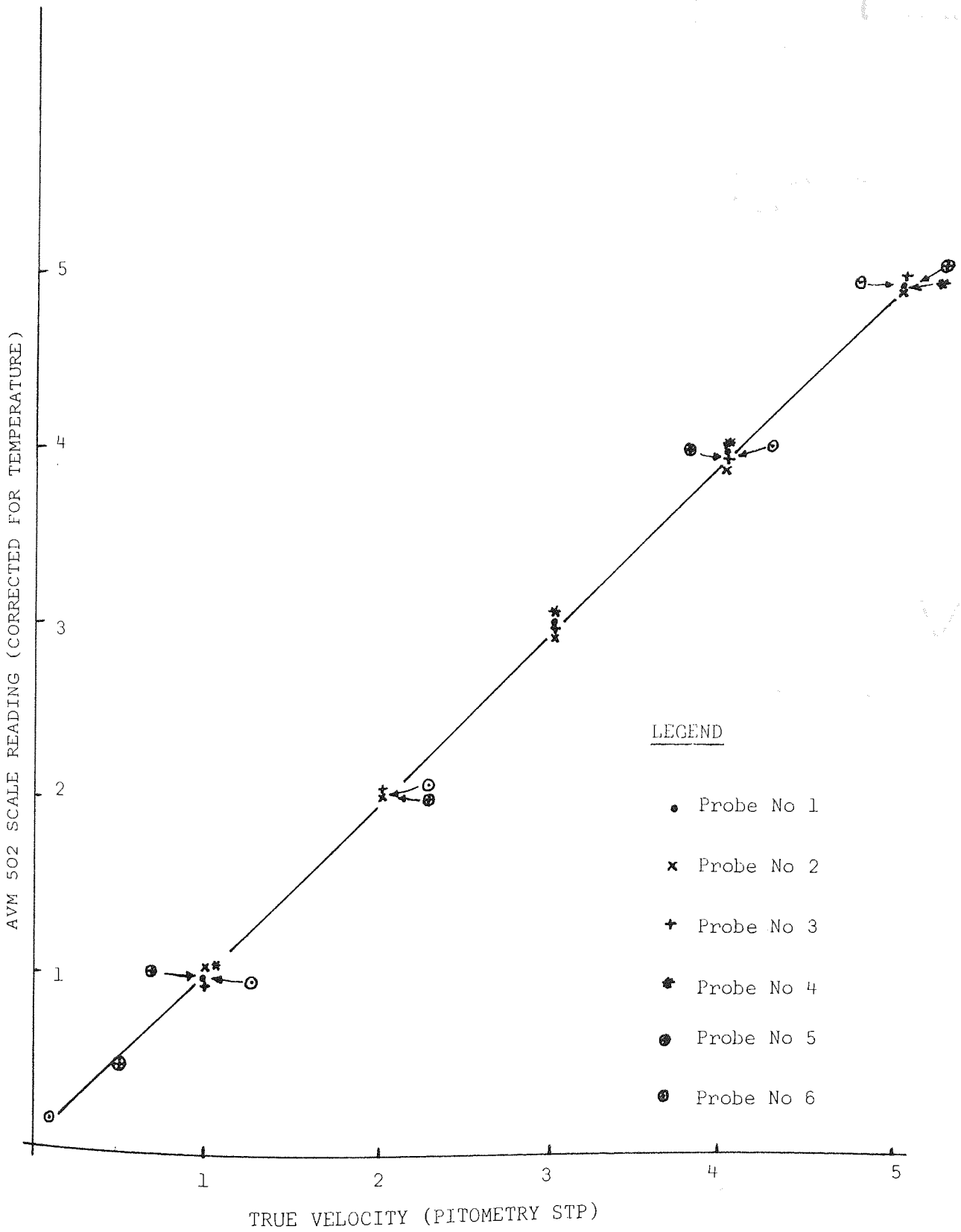

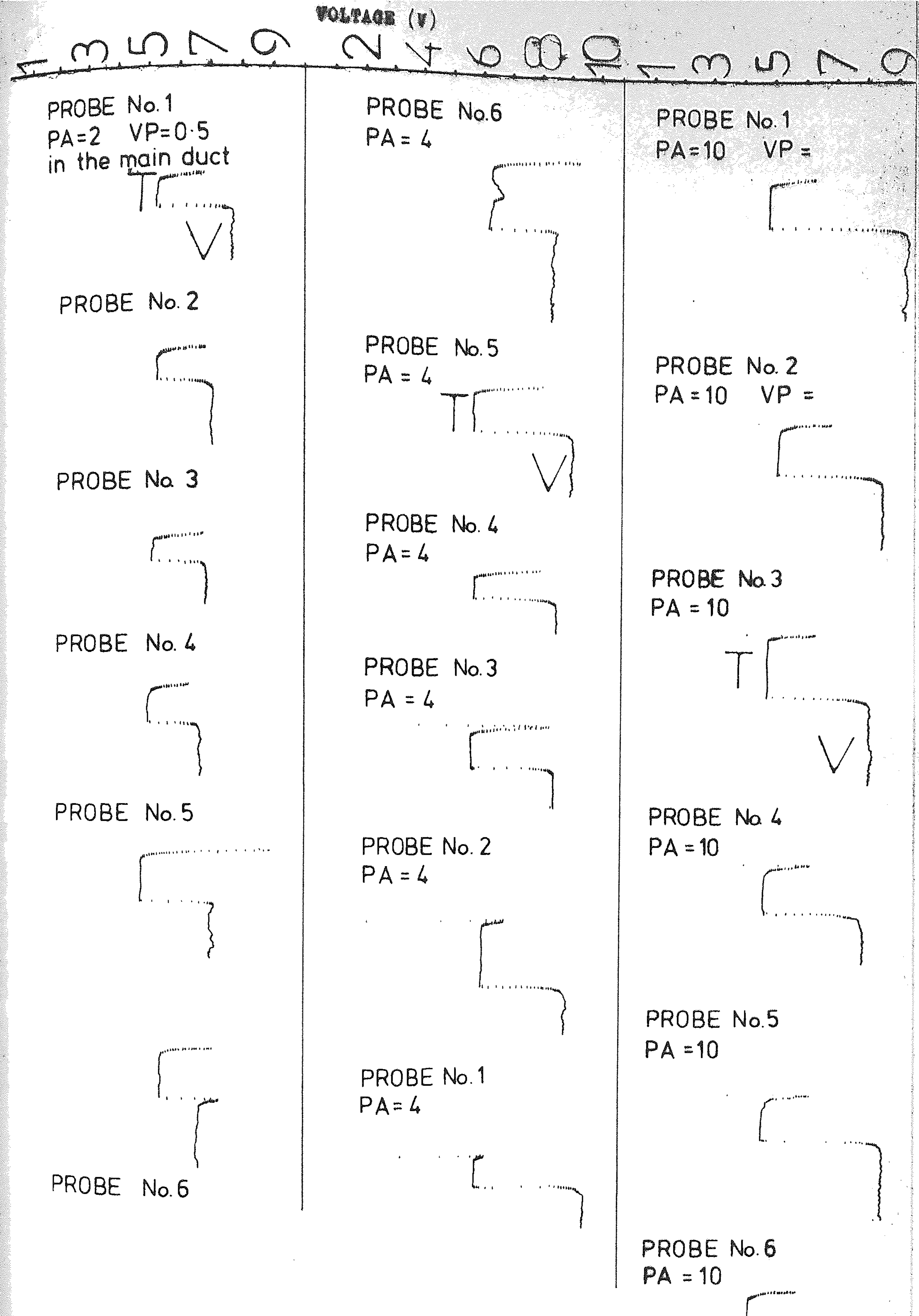

Figure 5.38 Voltage variation corresponding to temperature and velocity recorded during the calibration of AVM502 direct (thermistor) velocity metres.

Note: Recorder chart speed is 24 inches per hour

FIGURE 5.39 CALIBRATION OF

SIMMONS SHIELDED HOT WIRE ANEMOMETER

(TYPE 5115 F - SCALE RANGE ZERO – 0·4 ft/sec.)

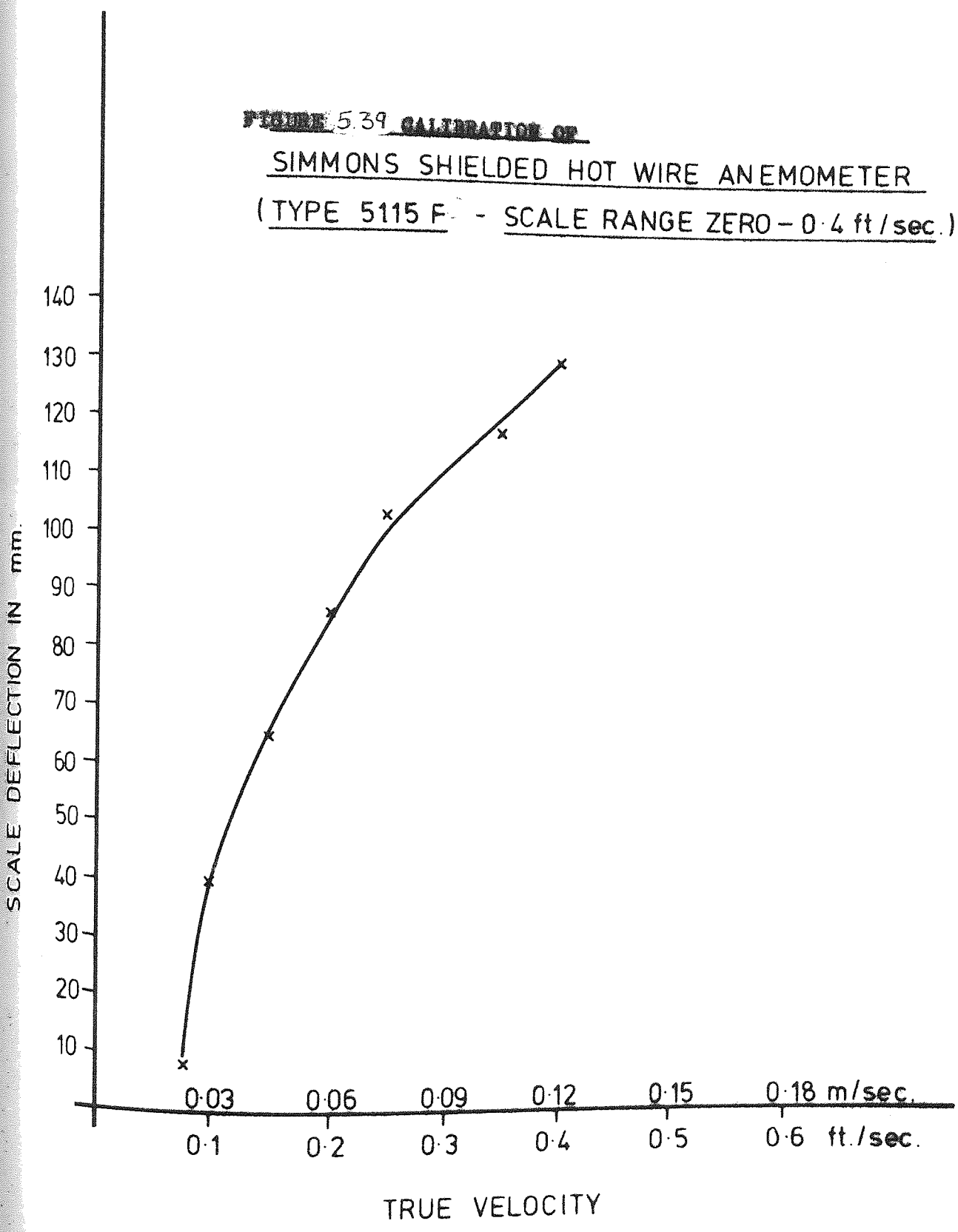

FIGURE 5.40 CALIBRATION OF

SIMMON SHIELDED HOT WIRE ANEMOMETER
(TYPE 5115 F - SCALE RANGE ZERO - 2 ft./sec.)

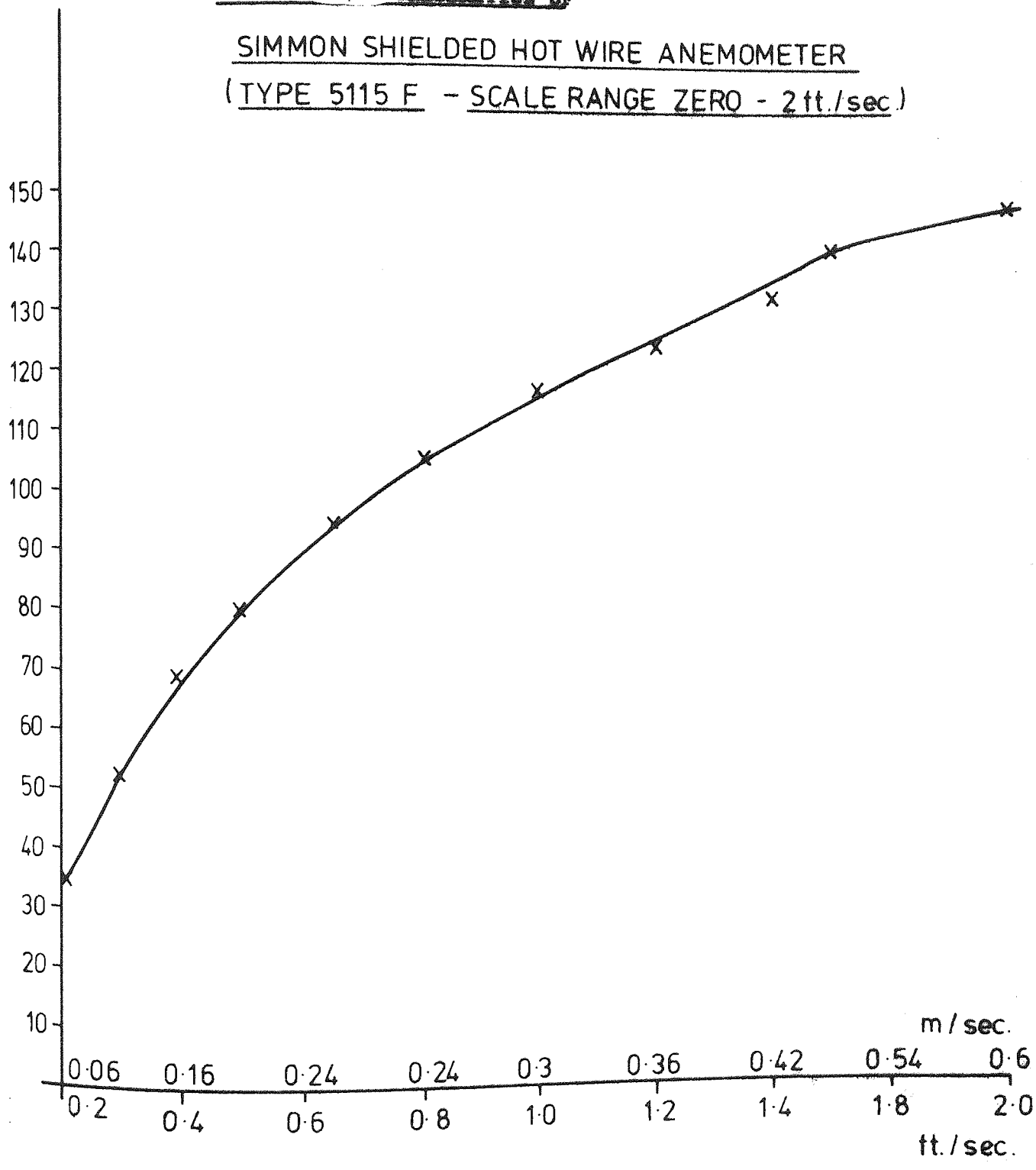

FIGURE 5.41 CALIBRATION OF

SIMMONS SHIELDED HOT WIRE ANEMOMETER

(TYPE 5115 F - SCALE RANGE ZERO - 5 ft/sec.)

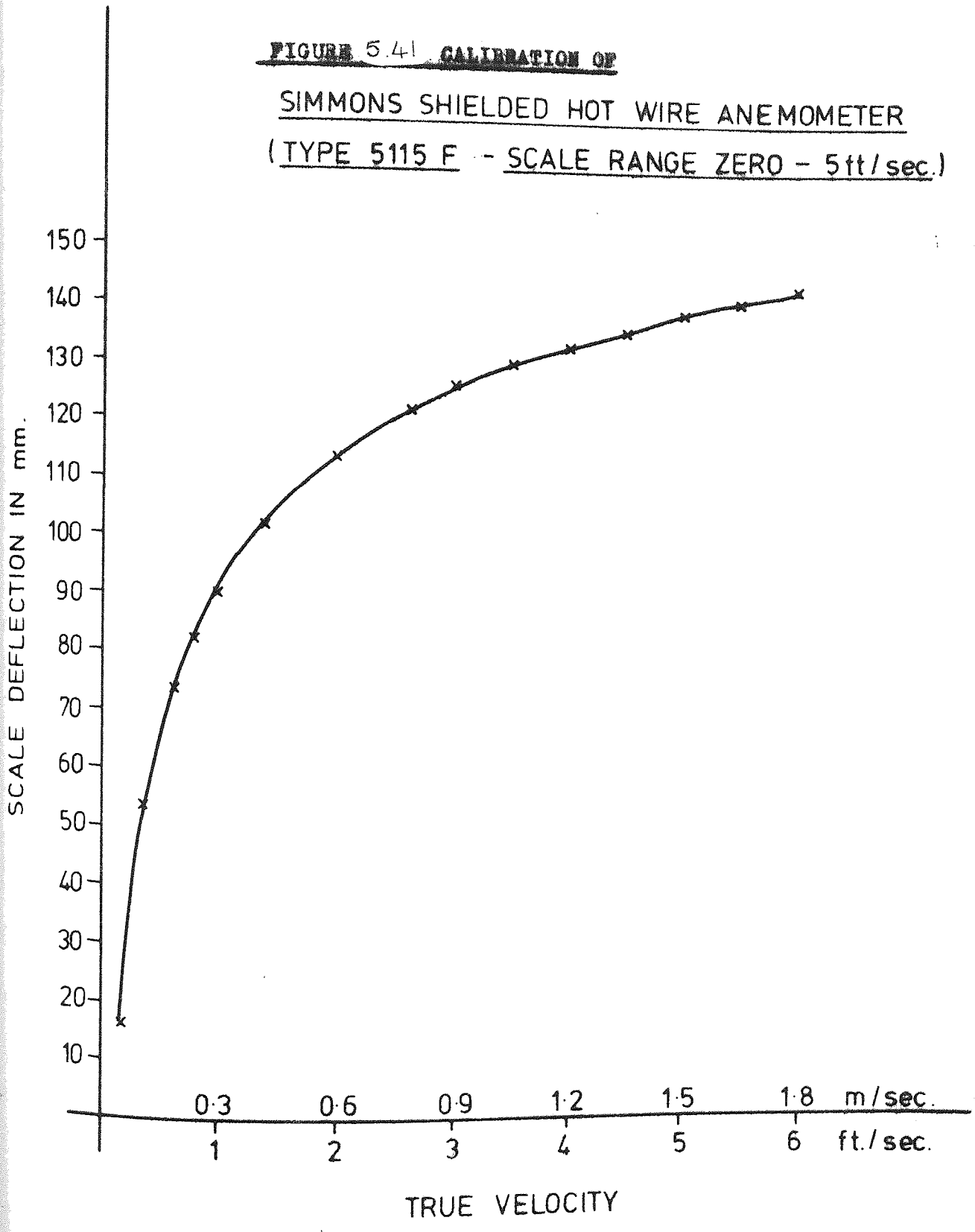

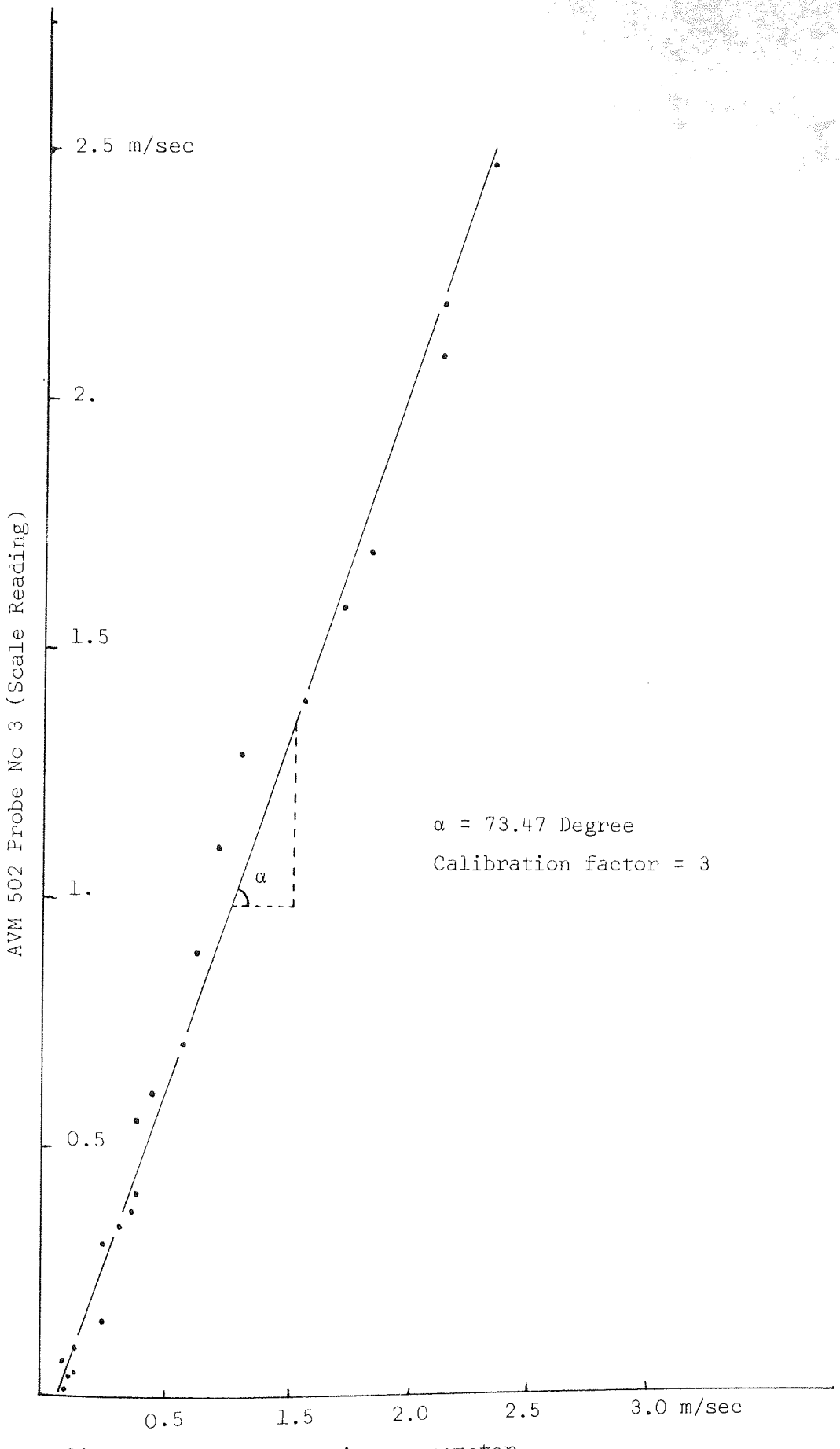

FIGURE 5.42 AVM 502 VERSUS SIMMON SHIELDED HOT WIRE ANENOMETER

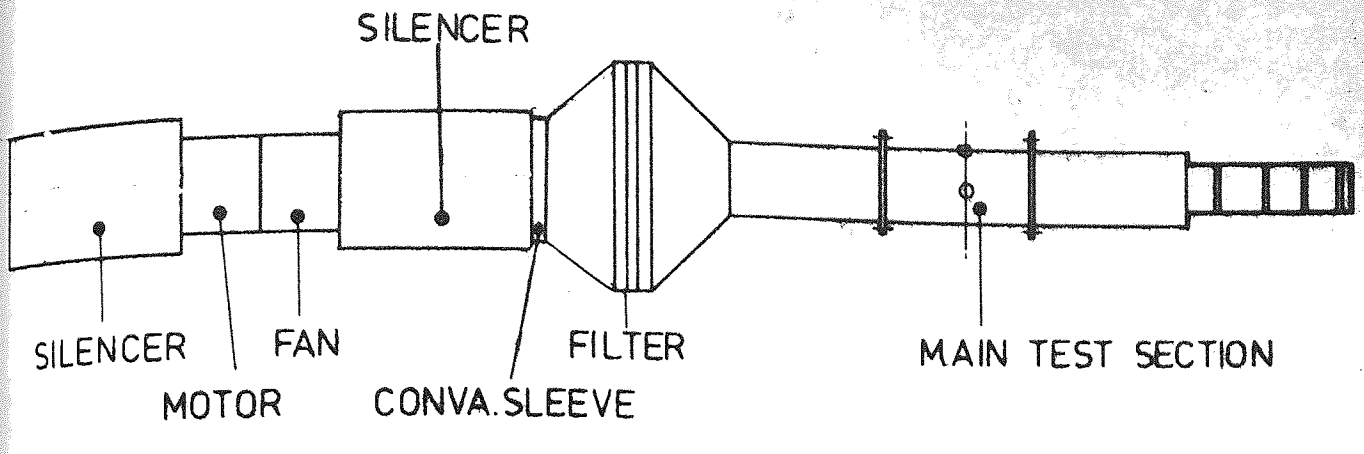

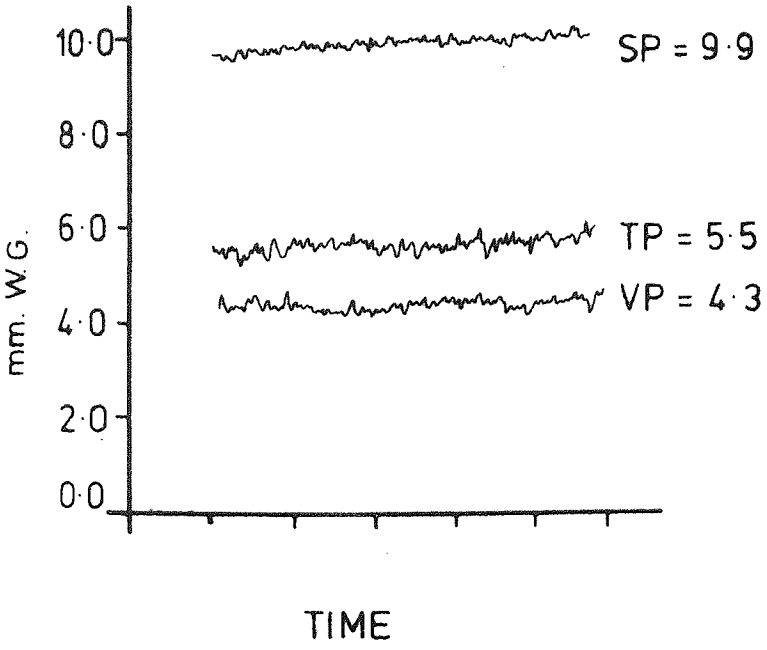

FIGURE 5.43

AVERAGING PRESSURE TUBE ANEMOMETRY (PA 2·0) AT THE MIDDLE DUCT OF MAIN DUCT SYSTEM

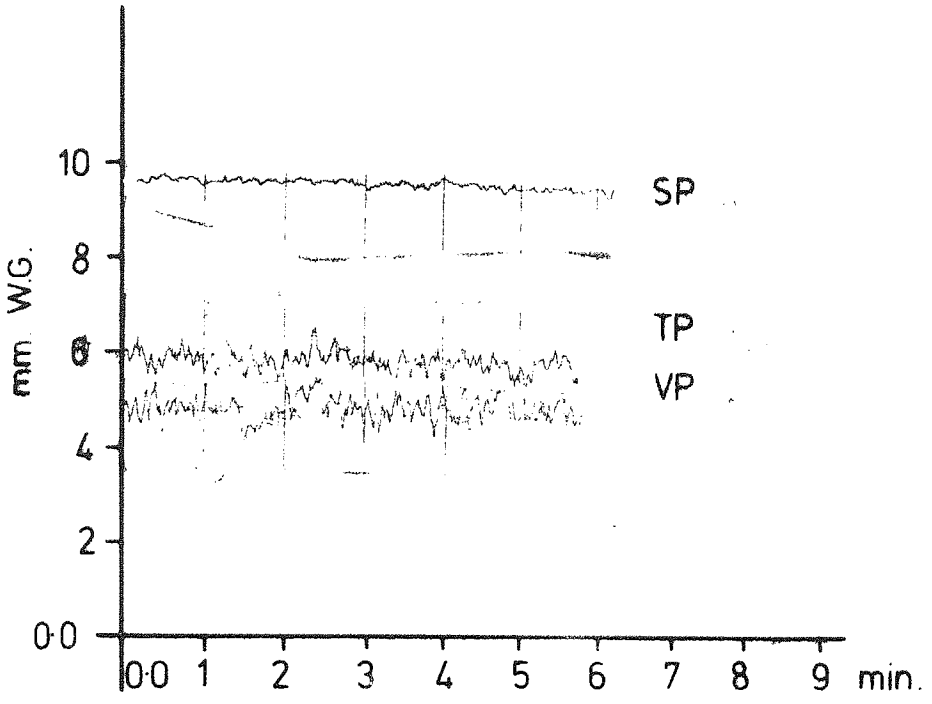

FIGURE 5.44

FLUCTUATION OF VELOCITY , TOTAL AND STATIC PRESSURE AT THE CENTRE LINE OF THE MAIN DUCT SYSTEM.

(PA = 2 , Duct assembly same as Fig. 5.44

PITOT STATIC TUBE ANEMOMETRY,
VERTICAL PLANE TRAVERSE

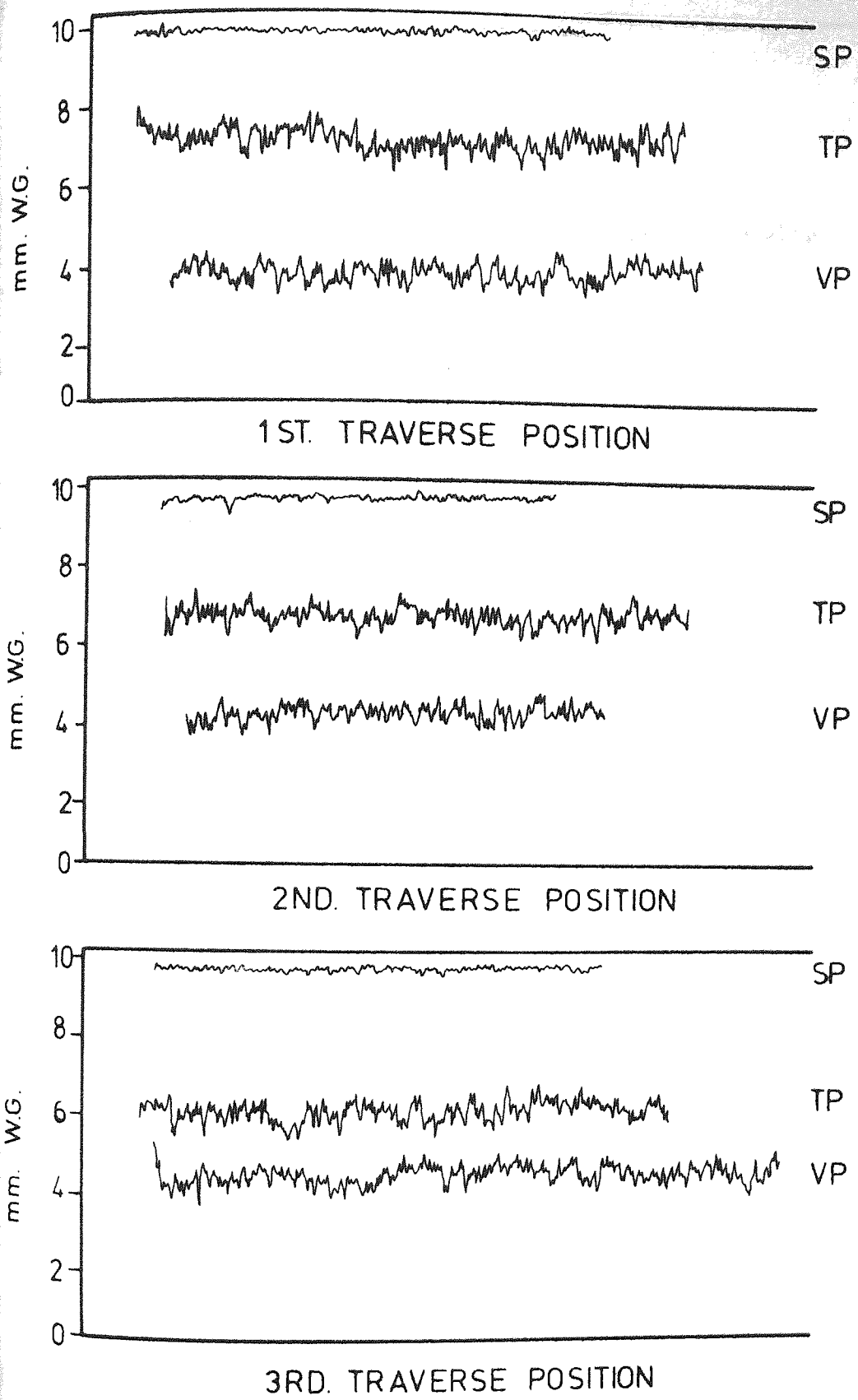

FIGURE 5.45

PITOT STATIC TUBE ANEMOMETRY AT VERTICALPLANE

(PA=2 SCHEMATIC ASSEMBLY SEE FIG. 5.43)

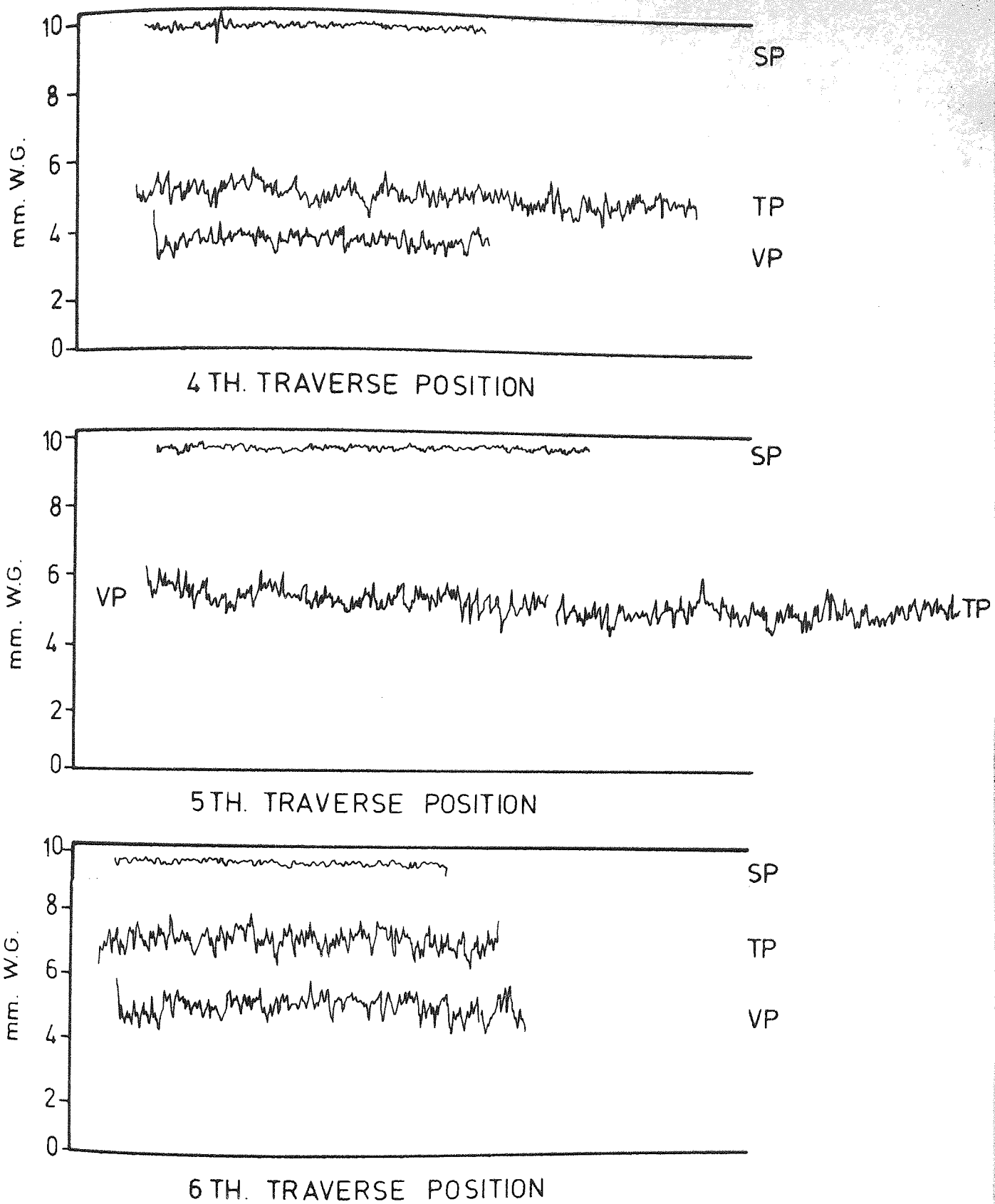

Figure 5.46

FIG. 5.45 CONTINUED

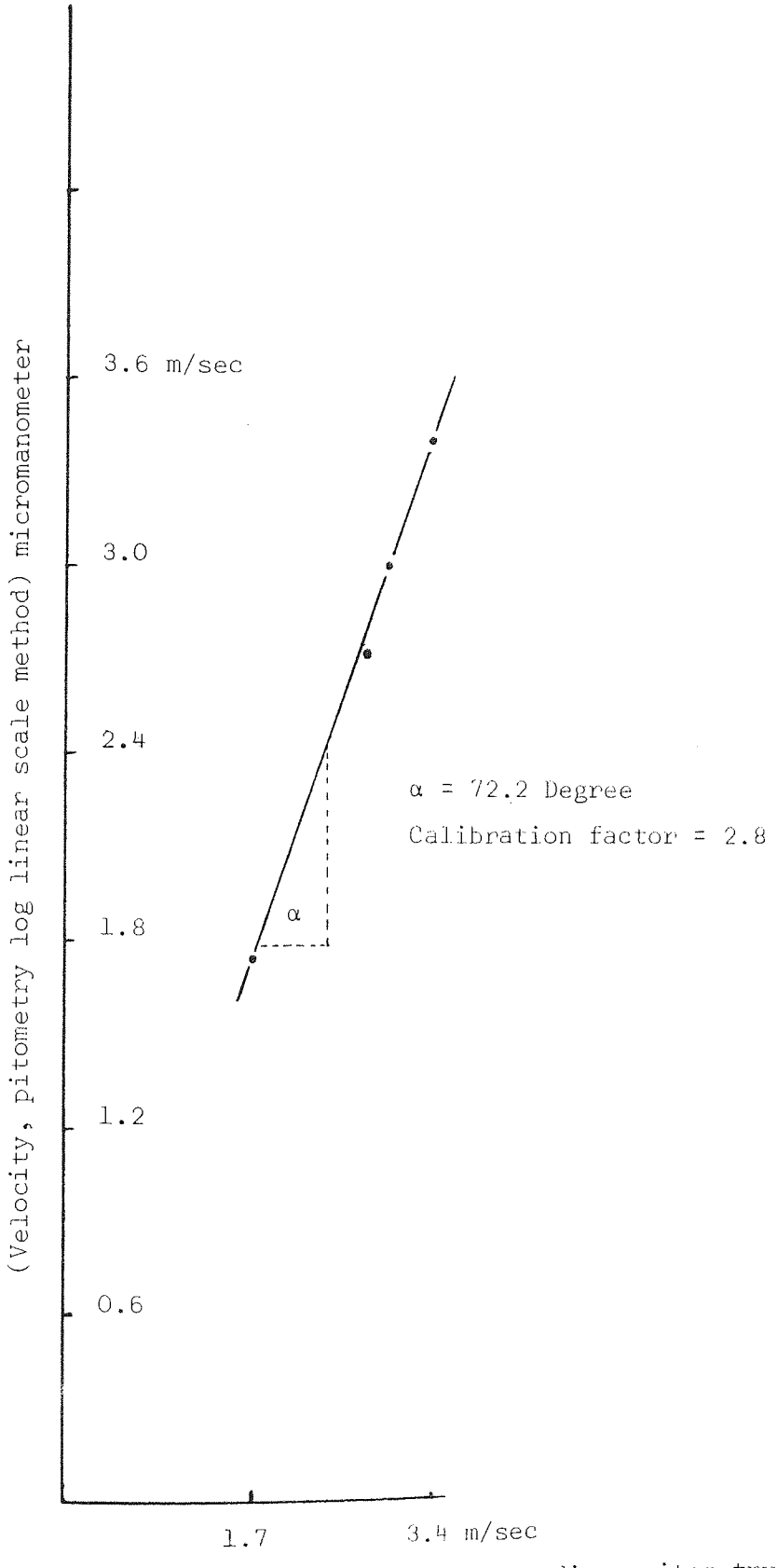

FIGURE 5.47 CALIBRATION OF INCLINED MANOMETER

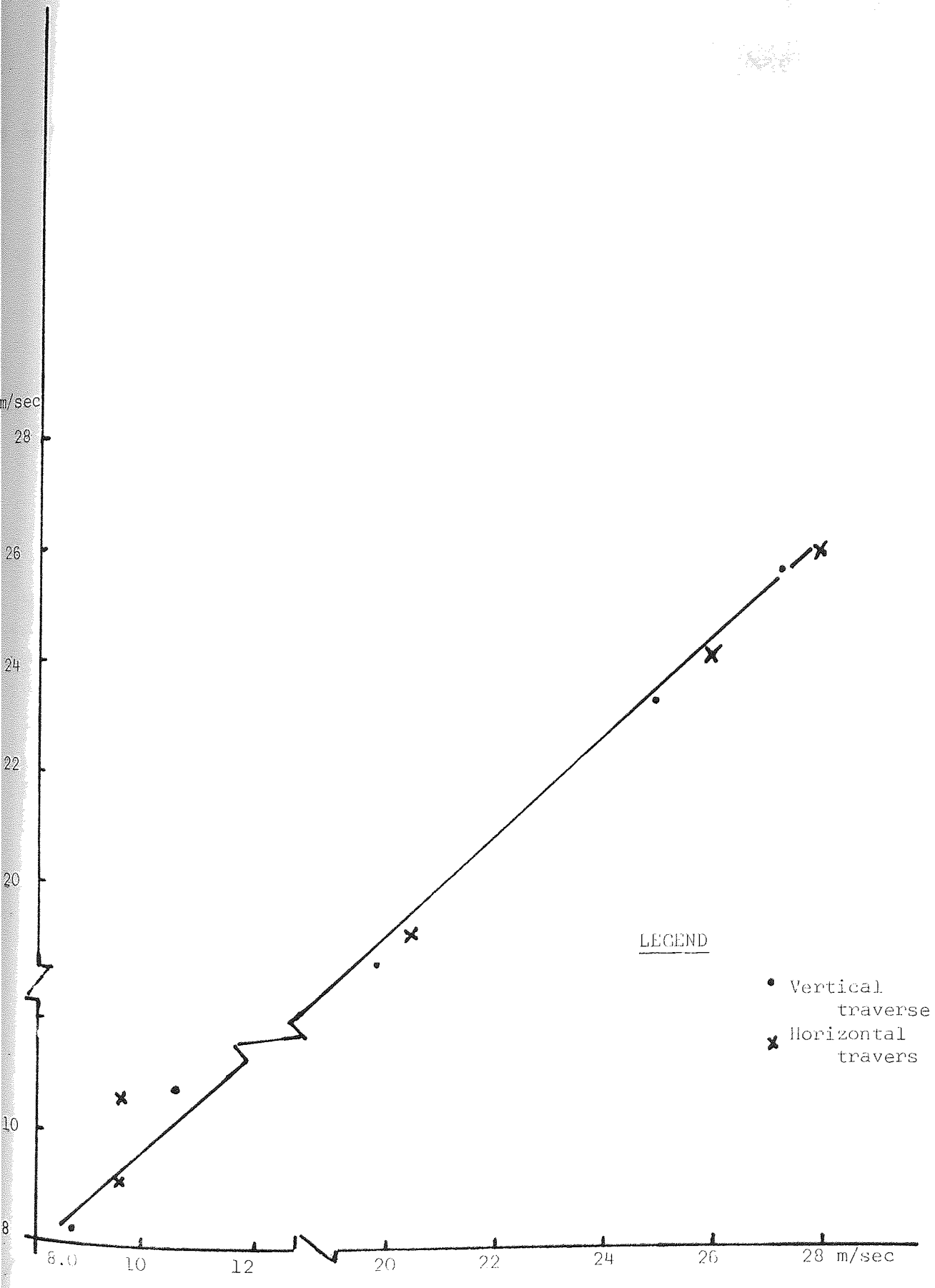

FIGURE 5.48 PITOT-STATIC TUBE ANENOMETRY WITH INCLINED MANOMETERS

FIGURE 5.49 AVERAGING PRESSURE TUBE ANENOMETRY VERSUS PITOT-STATIC TUBE ANENOMETRY (LOG-LINEAR RULE , ROUND DUCT, ID = 0.5 METRES)

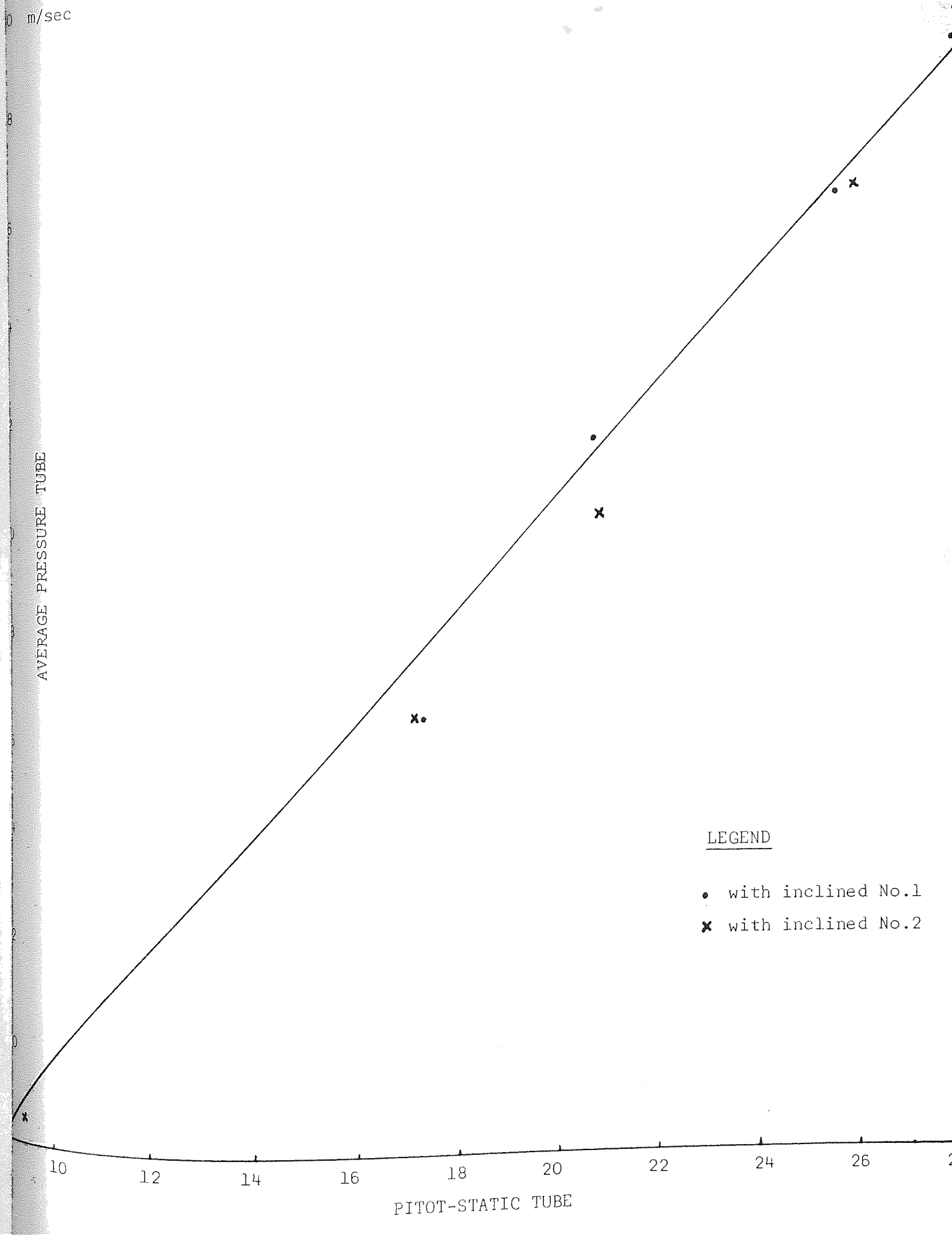

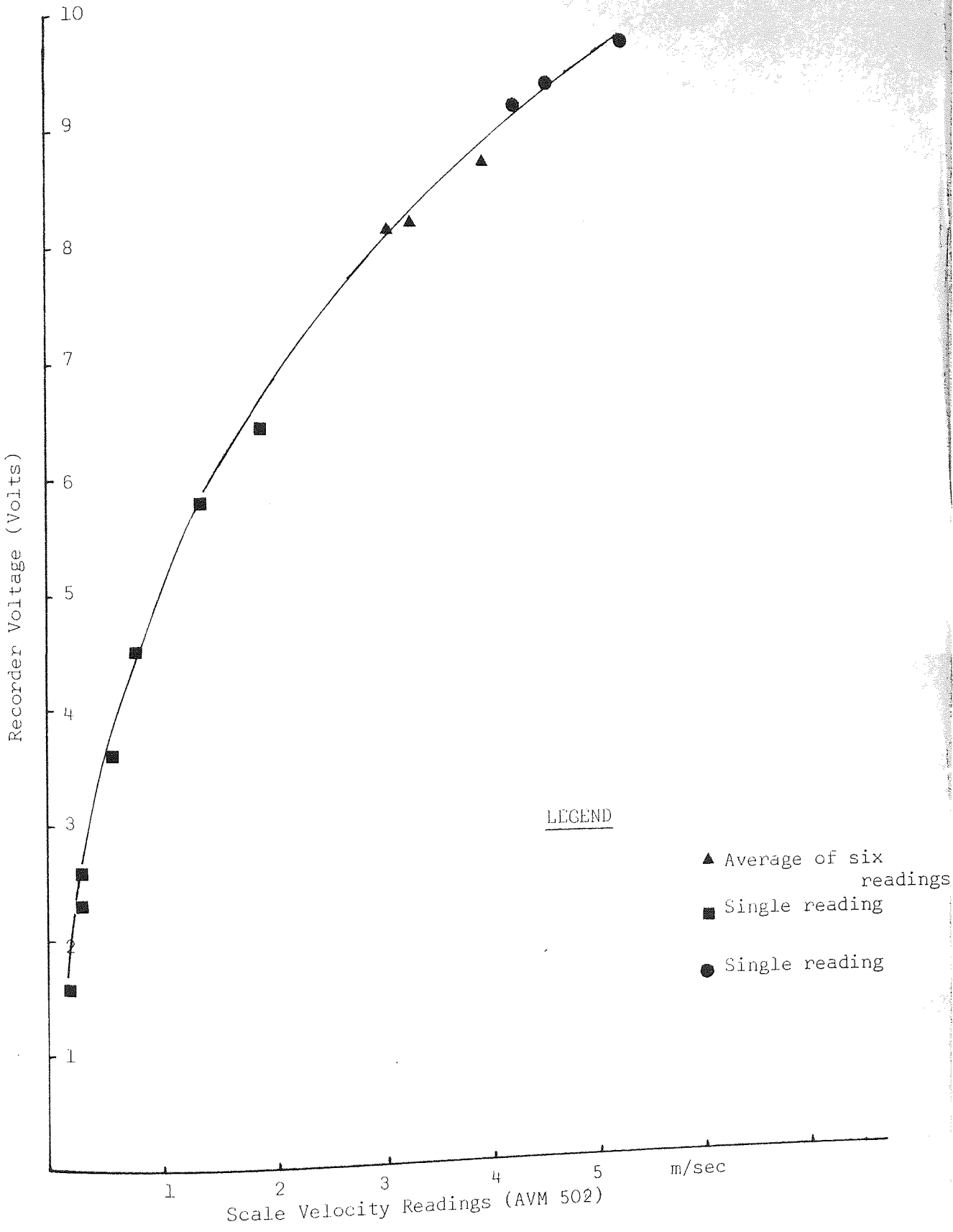

FIGURE 5.30 VOLTAGE VELOCITY RESPONSE OF AIR VELOCITY METER AVM 502

APPENDIX 5.2

LITERATURE ON SOME OF THE INSTRUMENTS

AVM500 Serie

Air Velocity Meters

APPENDIX 6.1

Computer programme ,experimental data,paramerters appraisal and computational output.

```
CL126

RUN NAME              NO NAME
VARIABLE LIST         V X XP1 YP1 ZP1 Q VBA DEQ AR ARE F1 FFF FF HR XHR
                      SET ALF F
N OF CASES            58
INPUT FORMAT          FREEFIELD
COMPUTE                   DL=LG10(DEQ)
COMPUTE                   D=DEQ
COMPUTE                   Y=YP1
COMPUTE                   Z=ZP1
COMPUTE               VL=LG10(V)
COMPUTE               XL=LG10(ABS(X))
COMPUTE               V0=V/VBA
COMPUTE                 V00=V0*100.0
COMPUTE                 P1=V00/(100.0-V00)
COMPUTE                 PL=LG10(P1)
COMPUTE               X1=X/DEQ
COMPUTE               X3=X/SQRT(ARE)
COMPUTE                 X3L=LG10(X3)
COMPUTE                 VF=V*ARE/Q
COMPUTE                  VFL=LG10(VF)
COMPUTE                 XHRL=LG10(XHR)
COMPUTE                 Y=YP1
COMPUTE                 F11=(X/HR)**(-1.7)
COMPUTE                 V1=VBA*F11/(1.0+F11)
COMPUTE                 F22=(X/HR)**(-1.4)
COMPUTE                 V2=VBA*F22/(1.0+F22)
COMPUTE                 F33=0.034*DEQ**(2.08)*X**(-1.91)
COMPUTE                 V3=F33*VBA/(1.0+F33)
COMPUTE                 V4=(.0177*VBA/(X/SQRT(ARE))**(-0.544)
COMPUTE                 V5=VBA/(3.1*(X*X/ARE)+1.0)
COMPUTE                 V6=VBA/(4.45*X**(2.0)/ARE+1.0)
COMPUTE                     V7=0.17*VBA*(SQRT(ARE/Y*X))**(-1.5)
COMPUTE                   F44=1/(1.0+0.259*((1-AR)/AR)**1.19)
COMPUTE                    F55=0.083*(ARE**(1.04))*(X**(-1.91))*F44
COMPUTE                 V8=VBA*F55/(1.0+F55)
COMPUTE                     F77=0.2*(X/ARE)**(-0.3 )
COMPUTE                 F66=X*AR**F77/SQRT(ARE)
COMPUTE                 V9=VBA/(0.93+8.5*F66**2)
COMPUTE                 V10=VBA*(1-X/D*SQRT((X/D)**2+(.2..))
```

```
PUTE          F88=0.11982*((D/X)**1.91)*D**(.1[illegible]
PUTE          V11=V9A*F88/(1+F88)
MENT          ABOVE IS THE ORKAL VERSION OF DALLAVALLE S METRIC FOR
TE CASES      (2X,9(F6.3,2X)/2X,9(F6.3,2X)/2X,13(F6.3,2X)/2X,9(F6.3,2X))
              V,X,XP1,YP1,ZP1,Q,VBA,AR,ARE,F1
              FFF,FF,HR,XHR,BET,ALF,F,DEQ
             ,VL,XL,VG,VOO,P1,PL,XO,
              X3,X3L,VF,VFL,V1,V2,V3,V4,V5,V6,V7,V8,V9,V10,V11
IONS                2,3
D INPUT DATA
```

3.392	0.205	0.165	0.001	0.001	1.464	37.813	0.191	0.600
.039	0.858	0.0[illegible]0	0.081	0.048	4.304	0.200	1.154	0.027
1.790	0.[illegible]	0.065	0.001	0.001	1.464	37.813	0.191	0.600
.039	0.858	0.02[illegible]	0.031	0.048	6.404	0.200	1.717	0.013
0.961	0.410	0.165	0.001	0.001	1.464	37.813	0.191	0.600
.039	0.858	0.013	0.021	0.048	8.609	0.200	2.308	0.007
0.619	0.510	0.165	0.001	0.001	1.464	37.813	0.191	0.600
.039	0.858	0.01[illegible]	0.014	0.048	10.709	0.200	2.[illegible]71	0.005
0.426	0.610	0.165	0.001	0.001	1.464	37.813	0.191	0.600
.039	0.858	0.0[illegible]6	0.010	0.048	12.808	0.200	3.4[illegible]4	0.003
0.349	0.[illegible]	0.065	0.001	0.001	1.464	37.813	0.191	0.600
.039	0.858	0.005	0.00[illegible]	0.048	13.963	0.200	3.744	0.003
2.74[illegible]	0.[illegible]	0.120	0.001	0.001	1.464	37.813	0.191	0.600
.039	0.858	0.0[illegible]2	0.052	0.048	5.459	0.200	1.464	0.017
1.308	0.[illegible]70	0.120	0.001	0.001	1.464	37.813	0.191	0.600
.039	0.858	0.017	0.02[illegible]	0.048	7.559	0.200	2.027	0.009
0.80[illegible]	0.465	0.120	0.001	0.001	1.464	37.813	0.191	0.600
.039	0.858	0.010	0.017	0.048	9.764	0.200	2.618	0.006
0.449	0.565	0.120	0.001	0.001	1.464	37.813	0.191	0.600
039	0.858	0.007	0.011	0.048	11.864	0.200	3.1[illegible]1	0.004
0.371	0.665	0.120	0.001	0.001	1.464	37.813	0.191	0.600
039	0.858	0.005	0.008	0.048	13.963	0.200	3.744	0.003
.307	0.7[illegible]	0.1[illegible]	0.001	0.001	1.464	37.813	0.191	0.600
039	0.858	0.00[illegible]	0.007	0.048	15.118	0.200	4.053	0.002
.591	0.[illegible]1[illegible]	0.170	0.001	0.001	1.464	37.813	0.191	0.600
039	0.858	[illegible]	0.037	0.048	6.509	0.200	1.745	0.012
.964	0.410	0.170	0.001	0.001	1.464	37.813	0.191	0.600
039	0.858	0.01[illegible]	0.021	0.048	8.609	0.200	2.308	0.007
.648	0.510	0.170	0.001	0.001	1.464	37.813	0.191	0.600
039	0.858	[illegible]	0.014	0.048	10.314	0.200	2.[illegible]99	0.005
.377	0.615	0.170	0.001	0.001	1.464	37.813	0.191	0.600
039	0.858	0.0[illegible]6	0.010	0.048	12.913	0.200	3.4[illegible]2	0.003
.280	0.715	0.170	0.001	0.001	1.464	37.813	0.191	0.600
039	0.858	0.[illegible]5	0.007	0.048	15.013	0.200	4.0[illegible]5	0.002
.275	0.770	0.170	0.001	0.001	1.464	37.813	0.191	0.600
039	0.858	0.0[illegible]4	0.006	0.048	16.168	0.200	4.335	0.002
.18[illegible]	0.[illegible]	0.220	0.001	0.001	1.464	37.813	0.191	0.600
039	0.858	0.017	0.02[illegible]	0.048	7.559	0.200	2.0[illegible]7	0.009
.770	0.4[illegible]	0.220	0.001	0.001	1.464	37.813	0.191	0.600
039	0.858	0.011	0.017	0.048	9.659	0.200	2.590	0.006
.540	0.565	0.220	0.001	0.001	1.464	37.813	0.191	0.600
039	0.858	0.007	0.011	0.048	11.864	0.200	3.1[illegible]1	0.004
.324	0.665	0.220	0.001	0.001	1.464	37.813	0.191	0.600
039	0.858	0.005	0.008	0.048	13.963	0.200	3.744	0.003
.259	0.765	0.220	0.001	0.001	1.464	37.813	0.191	0.600
039	0.858	0.004	0.006	0.048	16.063	0.200	4.3[illegible]6	0.002
.255	0.[illegible]20	0.220	0.001	0.001	1.464	37.813	0.191	0.600
039	0.[illegible]5[illegible]	0.004	0.005	0.048	17.21[illegible]	0.200	4.616	0.002
.410	0.[illegible]	0.460	0.001	0.001	1.464	37.813	0.191	0.600
039	0.858	0.016	0.010	0.048	12.59[illegible]	0.200	3.[illegible]78	0.003
.286	0.700	0.460	0.001	0.001	1.464	37.813	0.191	0.600
039	0.858	0.00[illegible]	0.007	0.048	14.69[illegible]	0.200	3.941	0.003
216	0.[illegible]05	0.460	0.001	0.001	1.464	37.813	0.191	0.600
039	0.858	0.014	0.006	0.048	16.903	0.200	4.5[illegible]2	0.002
194	0.905	0.460	0.001	0.001	1.464	37.813	0.191	0.600
39	0.858	0.003	0.004	0.048	19.003	0.200	5.095	0.002

0.140	1.005	0.460	0.001	0.001	1.464	37.513	0.191	0.600
0.039	0.859	0.002	0.004	0.048	21.102	0.200	5.658	0.001
0.122	1.006	0.460	0.001	0.001	1.464	37.513	0.191	0.600
0.039	0.857	0.002	0.003	0.048	22.257	0.200	5.967	0.001
2.800	0.134	0.010	0.001	0.001	0.710	18.342	0.191	0.600
0.039	0.859	0.001	0.142	0.048	3.150	0.200	0.844	0.049
1.117	0.470	0.010	0.001	0.001	0.710	18.342	0.191	0.600
0.039	0.859	0.004	0.056	0.048	5.249	0.200	1.407	0.018
0.589	0.355	0.010	0.001	0.001	0.710	18.342	0.191	0.600
0.039	0.858	0.013	0.028	0.048	7.454	0.200	1.998	0.009
0.302	0.495	0.010	0.001	0.001	0.710	18.342	0.191	0.600
0.039	0.858	0.011	0.017	0.048	9.554	0.200	2.561	0.006
0.202	0.555	0.010	0.001	0.001	0.710	18.342	0.191	0.600
0.039	0.858	0.007	0.012	0.048	11.654	0.200	3.124	0.004
0.145	0.610	0.010	0.001	0.001	0.710	18.342	0.191	0.600
0.039	0.858	0.004	0.010	0.048	12.808	0.200	3.434	0.003
4.472	0.190	0.010	0.001	0.001	1.123	29.001	0.191	0.600
0.039	0.858	0.001	0.142	0.048	3.150	0.200	0.844	0.049
2.070	0.270	0.010	0.001	0.001	1.123	29.001	0.191	0.600
0.039	0.858	0.004	0.056	0.048	5.249	0.200	1.407	0.018
1.011	0.375	0.010	0.001	0.001	1.123	29.001	0.191	0.600
0.039	0.858	0.013	0.028	0.048	7.454	0.200	1.998	0.009
0.567	0.475	0.010	0.001	0.001	1.123	29.001	0.191	0.600
0.039	0.858	0.011	0.017	0.048	9.554	0.200	2.561	0.006
0.304	0.555	0.010	0.001	0.001	1.123	29.001	0.191	0.600
0.039	0.858	0.007	0.012	0.048	11.654	0.200	3.124	0.004
0.294	0.610	0.010	0.001	0.001	1.123	29.001	0.191	0.600
0.039	0.858	0.004	0.010	0.048	12.808	0.200	3.434	0.003
5.627	0.190	0.010	0.001	0.001	1.255	32.424	0.191	0.600
0.039	0.858	0.001	0.142	0.048	3.150	0.200	0.844	0.049
2.299	0.270	0.010	0.001	0.001	1.255	32.424	0.191	0.600
0.039	0.858	0.004	0.056	0.048	5.249	0.200	1.407	0.018
1.134	0.375	0.010	0.001	0.001	1.255	32.424	0.191	0.600
0.039	0.858	0.013	0.028	0.048	7.454	0.200	1.998	0.009
0.627	0.475	0.010	0.001	0.001	1.255	32.424	0.191	0.600
0.039	0.858	0.011	0.017	0.048	9.554	0.200	2.561	0.006
0.417	0.555	0.010	0.001	0.001	1.255	32.424	0.191	0.600
0.039	0.858	0.007	0.012	0.048	11.654	0.200	3.124	0.004
0.329	0.610	0.010	0.001	0.001	1.255	32.424	0.191	0.600
0.039	0.858	0.004	0.010	0.048	12.808	0.200	3.434	0.003
2.565	0.260	0.010	0.001	0.001	1.375	35.519	0.191	0.600
0.039	0.858	0.004	0.056	0.048	5.249	0.200	1.407	0.018
1.260	0.375	0.010	0.001	0.001	1.375	35.519	0.191	0.600
0.039	0.858	0.013	0.028	0.048	7.454	0.200	1.998	0.009
0.707	0.475	0.010	0.001	0.001	1.375	35.519	0.191	0.600
0.039	0.858	0.011	0.017	0.048	9.554	0.200	2.561	0.006
0.45	0.555	0.010	0.001	0.001	1.375	35.519	0.191	0.600
0.039	0.858	0.007	0.012	0.048	11.654	0.200	3.124	0.004
0.407	0.610	0.010	0.001	0.001	1.375	35.519	0.191	0.600
0.039	0.858	0.004	0.010	0.048	12.808	0.200	3.434	0.003
2.763	0.260	0.010	0.001	0.001	1.464	37.813	0.191	0.600
0.039	0.858	0.004	0.056	0.048	5.249	0.200	1.407	0.018
1.371	0.375	0.010	0.001	0.001	1.464	37.813	0.191	0.600
0.039	0.858	0.013	0.028	0.048	7.454	0.200	1.998	0.009
0.754	0.475	0.010	0.001	0.001	1.464	37.813	0.191	0.600
0.039	0.858	0.011	0.017	0.048	9.554	0.200	2.561	0.006
0.485	0.555	0.010	0.001	0.001	1.464	37.813	0.191	0.600
0.039	0.858	0.007	0.012	0.048	11.654	0.200	3.124	0.004
0.434	0.610	0.010	0.001	0.001	1.464	37.813	0.191	0.600
0.039	0.858	0.004	0.010	0.048	12.808	0.200	3.434	0.003

```
NONLINEAR       VARIABLES=V,X,VMA,HR,AR,ARF,N$ B/1.0,-1.7,1.0,1.0,1.0
MODEL           F=F(A)*(X/HR)**F(2)
                YHAT=VMA*F(3)*F/(1.0+F)
PARAMETERS      B(1)=1.0 $ B(2)=-1.7 $  F(3)=1
OPTIONS         3,4,5,6,7,8
STATISTIC       4,5,6,7,8,9
```

```
           F(V) IS PRUZNER EMPIRICAL FORMULA
COMMENT     FOLLOWING IS THE PRUZNER EMPIRICAL FORMULA
COMMENT    VARIABLES=V,X,ARE,AR,HR,VBA,NB=3/0.8,-1.4,1,1,0.95
NONLINEAR  F=B(1)*(X/HR)**B(2)
MODEL      YHAT=VBA*B(3)*F/(1.0+F)
           B(1)=0.8 $ B(2)=-1.4 $  B(3)=0.95
PARAMETERS 3,4,5,6,7,8
OPTIONS    4,5,6,7,8,9
STATISTIC   FOLLOWING IS THE DALLAVALL EMPIRICAL FORMULA
COMMENT     DALLAVALLE EMPIRICAL FORMULA FOR SQUARE OR RECTAN
COMMENT    DALLAVALLE FORMULA,FOR ROUND UNFLANGED DUCT
COMMENT        MODIFIED PITOT TUBE AND MINV 0.5M. X BETW ZERO TO 0.25M
COMMENT    VARIABLES=V,X,VBA,DEQ,NB=4/0.034,2.08,-1.91,1.0
NONLINEAR  F=B(1)*DEQ**B(2)*X**B(3)
MODEL      YHAT=B(4)*F*VBA/(1.0+F)
               B(1)=0.034 $ B(2)=2.08 $ B(3)=-1.91 $ B(4)=1.0
PARAMETERS 3,4,5,6,7,8
OPTIONS    4,5,6,7,8,9
STATISTIC  J.L.ALDEN FORMULA OF PLOTING DALLAVALLE DATA
COMMENT    VARIABLES=V,X,ARE,VBA,NB=2/
NONLINEAR  YHAT=VBA*B(1)*(X/SQRT(ARE))**B(2)
MODEL       3,4,5,6,7,8
OPTIONS     4,5,6,7,8,9
STATISTICS     SILVERMAN  FLANGED ROUN DUCT
COMMENT        VARIABLES=V,X,ARE,VBA,AR,NB=3/
NONLINEAR      YHAT=VBA/(B(1)*(X*X/ARE)**B(3)+B(2))
MODEL          B(1)=3.1 $ B(2)=1.0 $ B(3)=1.001
PARAMETERS     3,4,5,6,7,8
OPTIONS        4,5,6,7,8,9
STATISTIC  SILVERMAN CORRECTION ON DALLAVALLE FORMULA FOR ROUDUC
COMMENT     UNFLANGED
COMMENT    VARIABLES=V,X,ARE,VBA,NB=3/
NONLINEAR  YHAT=VBA/(B(1)*(X**B(2)/ARE)+B(3))
MODEL          B(1)=4.45 $ B(2)=2.0 $ B(3)=1.0
PARAMETERS  3,4,5,6,7,8
OPTIONS     4,5,6,7,8,9
STATISTICS    SILVERMAN EMPIRICAL FORMULA FOR ROUND UNFLANGED
COMMENT      VARIABLES=V,X,ARE,VBA,NB=2/B(1)=0.17, B(2)=1.5
NONLINEAR    YHAT=VBA*B(1)*(SQRT(ARE/X*X))**B(2)
MODEL         B(1)=0.17 $ B(2)=1.5
PARAMETERS    3,4,5,6,7,8
OPTIONS       4,5,6,7,8,9
STATISTICS      SQUARE AND RECTENGULAR DUCT DALLAVALLE MODIFIOT AR 1,0.75
COMMENT           UNFLANGED DUCT
COMMENT         VARIABLES=V,X,AR,ARE,VBA,NB=6/
NONLINEAR       FAR=1/(1.0+B(5)*((1.0-AR)/AR)**B(6))
MODEL            F=B(1)*(ARE**B(2))*(X**B(3))*FAR
                YHAT=VBA*B(4)*F/(1.0+F)
                B(1)=0.083 $ B(2)=1.04 $ B(3)=-1.91 $ B(4)=1.0 $
PARAMETERS     B(5)=0.259 $ B(6)=1.
                3,4,5,6,7,8
OPTIONS         4,5,6,7,8,9
STATISTICS    FLETCHER EMPIRICAL FORMULA FOR RECTANGULAR UNFLANGED DUCT
COMMENT       VARIABLES=V,X,ARE,AR,BET,ALF,VBA,NB=5/B(1)=0.2,
NONLINEAR        B(2)=-0.33,B(3)=1.0,B(4)=BET,B(5)=0.93,B(6)=8.5
MODEL          BET=B(1)*(X/ARE)**B(2)
               ALF=B(3)*X*AR**BET/SQRT(ARE)
               F=1/(B(4)+B(5)*ALF**2)
               YHAT=VBA*F
PARAMETERS     B(1)=0.2 $ B(2)=-0.33 $ B(3)=1.0     B(4)=0.93
               B(5)=8.5
OPTIONS         3,4,5,6,7,8
STATISTICS     4,5,6,7,8,9
NONLINEAR            VARIABLES=VO,X,Z,NB=2/
MODEL                YHAT=X**2/B(1)+Z**2/B(2)
PARAMETERS             B(1)=1.0001 $ B(2)=1.0001
```

```
OPTIONS          ,4,5,6,7,8
STATISTICS       4,5,6,7,8,9
NONLINEAR          VARIABLES=VO,X,Z,NR=4/
MODEL              YHAT=X**(B(2))/B(1)+Z**B(4)/B(3)
PARAMETERS           B(1)=1.0001 $ B(2)=1.0001   B(3)=1.0001 $ B(4)=1.0
OPTIONS          ,4,5,6,7,
STATISTICS       4,5,6,7,8,9
COMMENT            DRKAL METRIC VERSION OF DALLAVALL S FORMULA
NONLINEAR           VARIABLES=V,X,D,VRA,NF=3/0.119 2,1.91,0.17
MODEL          F  =B(1)*((D/X)**B(2))*D**B(3)
                 YHAT=VRA*F 8/(1+F88)
PARAMETERS       (1)=0.1198  $ B(2)=1.91 $ B(3) 0.17
OPTION             3,4,5,6,7,
STATISTICS       4, ,6,7,8,9
COMMENT          D KAL THEOPETICAL FORMULA FOR FLANGED ROUND DUCT
NONLINEAR      VA IABLES=V,X,D,VRA,NP=2/B(1)=2.0, ( )=0.24
MODEL          YHAT=VFA*(1.0-X/D*SQRT((X/D)**B(1)+B(2)))
PARAMETERS     B(1)=2.0 $ B(2)=0.25
OPTIONS           ,4,5,6,7,8
STATISTICS        4,5,6,7, ,9
NONLINEAR     VARIA LES=VO,X,Y,Z,NR=3/
MODEL         YHAT=X**2.0/ (1)+Y**2.0/B(2)+Z**2.0/ ( )
OPTIONS        ,4,5,6,7,
STATISTICS     4, ,6,7,8,9
NONLINEAR       VA IABLES=VO,X,Y,Z,NP=6/
MODEL           YHAT=X**(B(2))/ (1)+Y**B(4)/B(5)+  **  ( )/B(5)
OPTIONS          , ,5,6,7,
STATISTICS      4, ,6,7,8,9
NONLINEAR       VA IABLES=VO,X,Y,NB=2
MODEL           Y  T=X**2.0/B(1)+Y**2.0/B( )
OPTIONS          , ,5,6,7,
STATISTICS      4, , , , ,9
NONLINEAR       V  IABL    P1,A F,X,DE ,NP= /
MODEL             YHAT= (1)*DE **B(2)*X**B( )
OPTIONS            ,4,5,6,7,
STATISTICS         , ,6,7,8,9
NONLINEAR      VA  IA L S=P1,AF,ARE,X,NP=5
MODEL               F A=(1.0+B( )*((1.0-AR)/ R)**B( ))
           Y  T=(  (1)*X** (2)*ARE**B(5))/FRA
OPTIONS            ,4,5,6,7,8
STATISTICS         4,5,6,7,8,9
NONLINEAR           VARIABLES=V,XL,DL,N =3
MODEL         A1= (1)+ (2)*DL
             YHAT=100.0*(1.0-1.0/(1.0+2.718**B(3)*(XL-A1)))
PARAMETERS          (1)=-0.7 $ B(2)=1.2 $ B(3)=4.6
OPTIONS               3,4,5,6,7,8
STATISTICS              4,5,6,7,8,9
PLOT            PLOTS=V WITH X/V WITH XP1 /V WITH Y 1/ V WIT  ZP1/
                V WITH XPR/VO WITH XO/VO WITH X /VL WITH XL/
                 VPL WITH X3L/PL WITH XL/
                TITLE=VELOCITY VERSUS DISTANCE
               SIZE=-6.0,-6.0
                SYMBOLS=1,2,3,4,5,6,7, , ,10,11,12,1 ,14,15
OPTIONS      4,
STATISTICS      ALL
PLOT                PLOTS=VO V   V1 V2 V  V4 V  V6   V8 V
                 V11 WITH X/V10(0.0,30.0) WITH X/
                TITLE=VELOCITY VERSUS DISTANCE
               SIZE=-6.0,-6.0
                SYMBOLS=1,2,3,4,5,6,7,8,9,10,11,12,1 ,14,15
OPTIONS         4,9
STATISTICS        ALL
FINISH
####S
```

APPENDIX 8.2

Observed, predicted and graph of residuals for model $F=b_1\ (X/HR)^{b_2}$
$V=b_3 V_{BA} F/(1+F)$

F I N A L F U N C T I O N V A L U E S A N D R E S I D U A L S
ROOT MEAN SQUARE RESIDUAL = 8.7594908E-02 D.F. = 55
THIS IS THE SCALE UNIT IN THE GRAPH OF THE RESIDUALS.

PREDICTION	OBSERVATION	RESIDUAL
3.7139541E+00	[illegible].3920000E+00	-3.2195412E-01
1.7[illegible]7319[illegible]+00	1.7900000E+00	4.[illegible]14[illegible]E-02
[illegible]15[illegible]17[illegible]E-01	[illegible].6100000E-01	2.841[illegible]255E-02
6.1065611E-01	[illegible].1900000E-01	8.34[illegible]917E-03
4.2[illegible]1073E-01	4.2600000E-01	5.6[illegible]9668E-03
[illegible].5[illegible]7149[illegible]E-01	3.4900000E-01	-1.714[illegible]748E-03
2.[illegible]01E+00	[illegible].2470000E+00	-1.31[illegible]009E-01
1.24[illegible]922[illegible]+00	1.3080000E+00	5.9[illegible]7891E-02
7.[illegible]94952[illegible]E-01	[illegible].0300000E-01	6.3[illegible]4719E-02
4.93[illegible]5051E-01	4.4900000E-01	-4.4350597E-02
3.5[illegible]714[illegible]7E-01	[illegible].2100000E-01	-2.9714775E-02
2.9676248E-01	3.0700000E-01	1.0237519E-02
1.6[illegible]4661[illegible]E+00	1.5910000E+00	-9.4466075E-02
[illegible]15[illegible]17[illegible]E-01	[illegible].6400000E-01	5.[illegible]1[illegible]5[illegible]E-02
5.9[illegible]948[illegible]E-01	6.4800000E-01	4.9600517E-02
4.1[illegible]1[illegible]613[illegible]E-01	[illegible].7700000E-01	-3.6[illegible]61311E-02
3.0114598E-01	2.8000000E-01	-2.1145982E-02
2.5763277E-01	[illegible].7500000E-01	1.7[illegible]67723E-02
1.24[illegible]9322E+00	1.1[illegible]0000E+00	-6.0[illegible]93219E-02
7.5619[illegible]44[illegible]E-01	7.7000000E-01	1.3[illegible]01564E-02
4.[illegible]5051E-01	[illegible].4000000E-01	4.6649493E-02
3.5[illegible]714[illegible]7E-01	[illegible].2400000E-01	-2.[illegible]214975E-02
2.6119437E-01	2.5900000E-01	-2.1943687E-03
2.[illegible]19[illegible]4[illegible]E-01	[illegible].5500000E-01	2.9[illegible]059[illegible]E-02
4.[illegible]197[illegible]E-01	4.1000000E-01	-2.51[illegible]7351E-02
[illegible].16[illegible]79[illegible]E-01	[illegible]E-01	-2.[illegible]E-02
[illegible]1[illegible]E-01	[illegible].1500000E-01	-1.[illegible]1377E-02
1.[illegible]1[illegible]E-01	1.9400000E-01	1.0[illegible]1104[illegible]E-02
1.4[illegible]758[illegible]1E-01	1.4000000E-01	-6.7[illegible]8094E-03
1.[illegible]1[illegible]E-01	1.2200000E-01	-9.0992964E-03
[illegible]26[illegible]E+00	[illegible]E+00	-2.7[illegible]60[illegible]E-01
1.2[illegible]406[illegible]E+00	1.1170000E+00	-1.2[illegible]660[illegible]E-01
6.2[illegible]0795[illegible]E-01	5.8200000E-01	-4.0[illegible]95371E-02
3.751[illegible]10[illegible]E-01	[illegible].0200000E-01	-7.3131031E-02
2.4[illegible]566[illegible]E-01	2.0200000E-01	-4.6[illegible]6605E-02
2.0[illegible]047E-01	1.4500000E-01	-5.8880467E-02
4.8603172E+00	4.8720000E+00	1.1682808E-02
1.9770243E+00	2.0760000E+00	1.0897575E-01
9.[illegible]5165[illegible]E-01	1.0110000E+00	2.5[illegible]7195E-02
5.9[illegible]0822E-01	5.6200000E-01	-[illegible].1[illegible]08221E-02
[illegible].9214615E-01	[illegible].0700000E-01	-8.674615[illegible]E-02
[illegible].2[illegible]6056E-01	2.9400000E-01	-2.[illegible]4056[illegible]E-02
5.4[illegible]9824E+00	5.6370000E+00	2.0[illegible]0175[illegible]E-01
2.1991929[illegible]E+00	2.2990000E+00	9.9[illegible]706[illegible]E-02
1.1014464E+00	1.1330000E+00	3.1[illegible]551E-02
6.6[illegible]2483E-01	6.3900000E-01	-2.4[illegible]24[illegible]3[illegible]E-02
4.3910214E-01	4.1200000E-01	-2.7102143E-02
3.6040[illegible]1[illegible]E-01	3.3900000E-01	-2.140[illegible]912E-02
2.4091147E+00	2.5650000E+00	1.5[illegible]8533E-01
1.2065839E+00	1.2600000E+00	5.3416098E-02
7.2653228E-01	7.0700000E-01	-1.9[illegible]228[illegible]E-02
4.8161619E-01	4.5800000E-01	-2.[illegible]01619[illegible]E-02
3.9481138E-01	4.0700000E-01	1.21[illegible]622E-02
2.5647077E+00	2.7820000E+00	2.1729230E-01
1.2845113E+00	1.3710000E+00	8.64[illegible]694E-02
7.7345548E-01	7.3800000E-01	-3.5455483E-02
5.1208370E-01	4.8500000E-01	-2.7052696E-02

GRAPH OF RESIDUALS

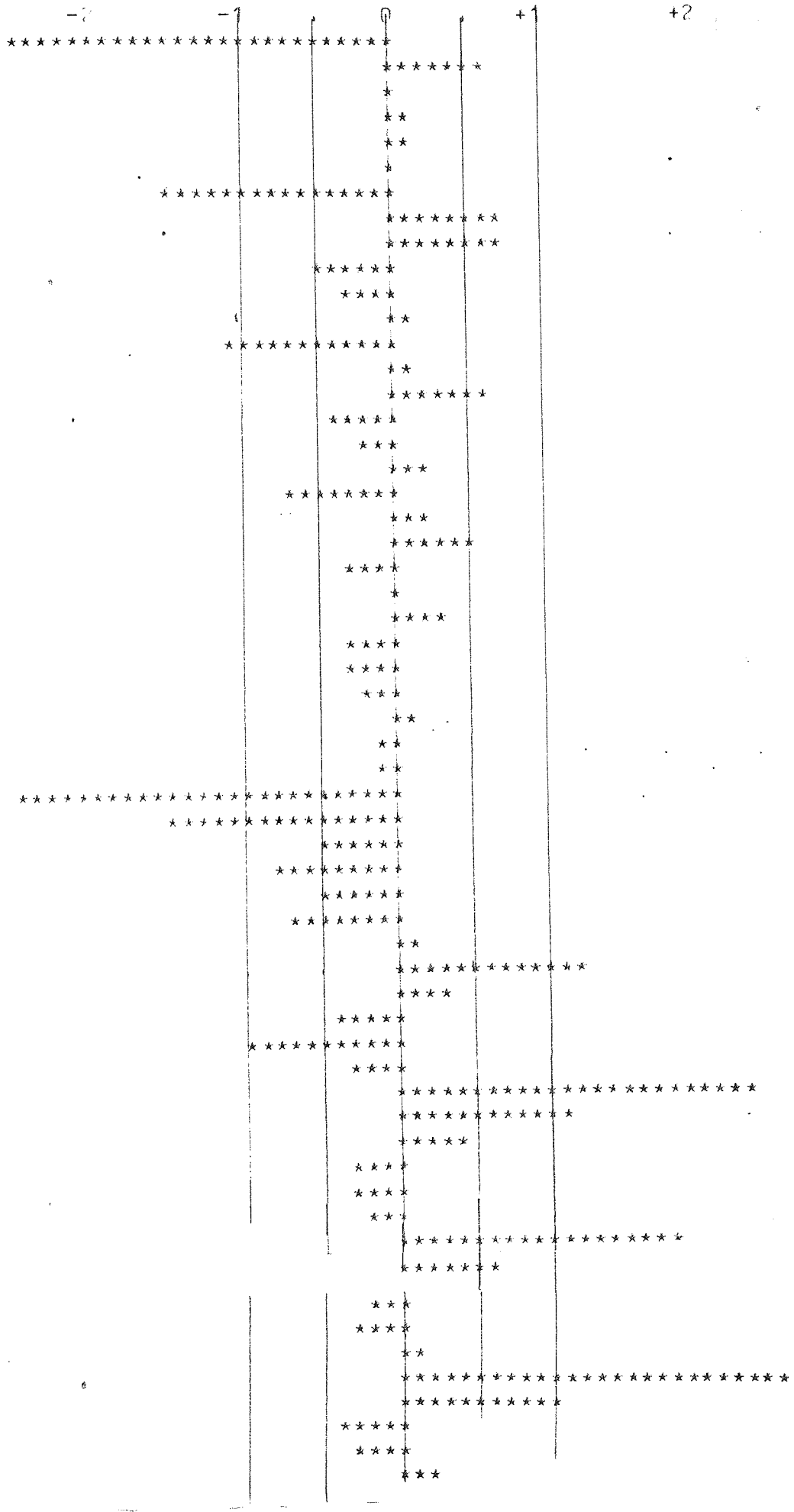

Appendix 6.3. Extract of Nonlinear Regression Analysis on Data of the combination of measurements of two tests on centre line velocities in front of rectangular suction opening (i.e. AR=0.6, HR=0.048m, CE126 is the data Document)

	1	2	3	4	5	6	7	8	9	10	11	12	13	14	15	16
				Parameter				(Prediction-Observed)=Re						Angle		Remark
Reference	No of Observation	MODEL	Shape of Suction Opening	No of Parametre	Initial Value of Parametre or Default	Final Value of Parametre	(5)-(6)	Root Mean Square Residual RMSR	Degree of Freedom	No of Residual Less Than ½RMSR	No of Residual Greater Than RMSR	No of Residual Equal to RMSR	Residual Sum of Square	Base Point	Test Point	
Pruzner	58	$X=b_1(X/HR)^{b2}$ $V=b_3V_{BA}F/(1+F)$	Rectan	1 2 3	1.0 -1.7 1.0	3.833 -2.129 0.664	-2.83 0.43 -0.33	0.087	55	20	8	3	0.422	89.0	83.	
			Round& Square	1 2 3	0.8 -1.4 0.95	3.82 -2.129 0.664	-3.02 0.729 0.28	0.088	55	22	9	3	"	88.0	87.	
Dalla Valll	"	$F=b_1(D_{eq})^{b2}X^{b3}$ $V=b_4V_{BA}F/(1+F)$	Round	1 2 3 4	0.034 2.08 -1.91 1.0	0.183 2.07 -2.129 0.664	-0.149 -0.01 0.219 0.336	0.088	54	20	10	2	0.422	62.0	70.0	
Hypothe-tical	"	$V=b_1V_{BA}(X/\sqrt{A})^{b2}$	Anyshap	1 2	Defa* "	0.1016 -1.88		0.0698	56	32	7	-	0.546	0.28	0.29	
Silver-man	"	$F=b_1(X^2/A)^{b3}+b2$ $V=V_{BA}/F$	Round	1 2 3	3.1 1.0 1.001	8.011 1.51 1.065	-4.9 -0.51 0.064	0.088	55	21	9	3	0.422	87.1	87.	

* Default=1.0001

Continue......

Appendix 6.3 Continued(1)

Silver-man	58	$F=b_1X^{b2}/A+b_3$ $V=V_{BA}/F$	Round	1 2 3	4.45 2.0 1.0	9.88 2.128 1.51	5.43 0.129 0.51	0.088	55	21	8	3	0.422 75. 77.
Alden	"	$V=V_{BA}b_1(A/X2)^{b2}$	Round	1 2	0.17 1.5	0.316 1.5	0.146 0.0	1.16	56	27	"	-	7.537 0.0 0.0
DallaValle	"	$F_1=1/(1+b_1((1-AR)/AR)^{b6})$ $F=b_1A^{b2}X^{b3}F_1$ $V=b_4V_{BA}F/(1+F)$	Rectangular	1 2 3 4 5 6	0.033 1.04 -1.91 1.0 0.259 1.0	0.184 1.01 -2.129 0.664 0.254 0.98	0.101 -0.03 0.219 -0.336 -0.005 -0.02	0.09	52	19	"	3	0.422 75.7 72.0
DallaVa	"	$V=p_1V_{BA}/(1+p_1)$ $p_1=b_1(D_{eq})^{b2}X^{b3}$	Rectang	1 2 3	Default " "	0.409 2.747 -2.014	-	0.004	55	16	9	8	0.009 50. 29.4
DallaValle	"	$V=F_1V_{BA}/(1+p_1)$ $F_1=b_1X^{b2}A^{b5}/F$ $F=(1+b_3((1-AR)/AR)^{b4}$	Rectangula	1 2 3 4 5	" " " " "	0.852 -2.01 0.998 0.976 1.469	-	0.004	53	15	9	8	0.0009 85 26.0
Fletcher	"	$\beta=b_1(X/A)^{b2}$ $\alpha=b_3X(AR)^{\beta}/\sqrt{A}$ $V=VBA/(b_4+b_5\alpha^2)$	Rectangular	1 2 3 4 5	0.2 -0.33 1.0 0.93 8.5	2.09 -0.07 2.496 1.52 8.65	-1.89 0.259 1.496 0.59 0.15	0.089	53	19	10	3	0.422 90. 90.

Continue.....

Hypothet	58	$F=b_1(D_{eq}/X)^{b2}D_{eq}^{b3}$ $V=V_{BA}F/(1+F)$	Any Shape	1 2 3	0.11988 1.91 0.17	0.16 2.038 0.164	0.043 0.128 -0.006	0.089	55	24	10	8	0.439	17.	34.
Von Fr Drkal	"	$V=V_{BA}(1-X/D\sqrt{(X/D)^{b1}+b2})$	Round Flat Fla	1 2	2.0 0.25	0.725 -0.496	-1.275 0.746	118.3	56	33	17	4	7.8E5	0.0	27.5
Hypothetical	"	$V_0=X^2/b_1+Z^2/b_2$ $V_0=V/V_{BA}$	Any Sha	1 2	Defau "	35.4 -5.99E4	-	0.048	56	20	10	9	0.13	0.0	0.0
	"	$V_0=X^{b2}/b_1+Z^{b4}/b_3$ $V_0=V/V_{BA}$	Any Shape	1 2 3 4	" " " "	99.49 -1.56 2.285 2.553	- - - -	0.016	54	50	9	-	0.014	10.0	86.

REFERENCES

1. ABBIS,J.B., CHUBB,T.W., and PIKE,E.R. "Laser Doppler Anemometry" Optics and Laser Technology 1974 Dec. 249-61

2. Airflow Developments Ltd. "Air Flow Demonstration Equipment for Schools, Colleges & Universities, High Wycombe, Bucks Tel. 0494 25252.

3. ALDEN,J.L., "Design of Industrial Exhaust System" 2nd Edition 1948 N.Y. Industrial Press.

4. American Conference of Governmental Industrial Hygienists (ACGIH) "Industrial Ventilation:- A Manual of Recommended Practice" 14th Edition 1974 Michigan U.S.A., ACGIH,

5. Amercian Standard Association (ASA) "Fundamentals Governing the Design and Operation of Local Exhaust System " 1960 Z9.2-1960 N.Y, Amercian Standard Association.

6. " " "American Standard Safety Code for Ventilation and Operation of Open Surface Tanks" 1951 Z9.1-1951 N.Y, ASA.

7. American Society of Heating Refrigeration and Air Conditioning Engineers (ASHRAE) "Handbook of Fundamentals" 1972, New York, ASHRAE.

8. Amercian Society of Heating Refrigeration and Air Conditioning Engineers (ASHRAE) "Handbook and Data book:- Equipment" 1972, New York, ASHRAE.

9. ATHERLY,G.R.C. "Occupational Health and Safety Concepts:- Chemical and Processing Hazards" 1978, London, Applied Science Publishers.

10. BATURIN,V.V. "Fundamentals of Industrial Ventilation" 1972,Oxford, Pergamon Press.

11. British Standards Institutions(BSI) "Methods of Test for Air Filters Used in Air Conditioning and General Ventilation" BS2831 Nos.1 and 2.

12. British Standards Institutions (BSI) "Methods for the Measurement of Fluid Flow in Pipes" 1964 BS1042 Part 1.

13. British Standards Institutions (BSI) "Methods for testing Fans for General Purposes" 1963 BS848 Part 1

REFERENCES (contd)

14. The British Cast Iron Research Association (BCIRA) "Foundry Ventilation and Dust Control" Harrogate Conference 27th-29th April 1955 England, BCIRA 1956.

15. BRYER,D.W. and PANKHURST,R.C. "Pressure-Probe Methods for Determining Wind Speed and Flow Direction" 1971 London, Her Majesty's Stationery Office (HMSO).

16. BRYER,D.W. and PANKHURST,R.C. "The Determination of Wind Speed and Flow Direction by Pressure-Sensing Instruments" National Physical Laboratory, Notes on Applied Science, London, HMSO.

17. COXON,W.E. "Flow Measurement and Control" 1959 London, Haywood Co.Limited.

18. DEAN,D. "The Effectiveness of Exhaust Ventilations with Specific reference to pedestal grinding Machines" M.Sc. Project, Department of Health and Safety, The University of Aston in Birmingham.

19. DALLA VALLE,J.M. "Velocity Characteristics of Hoods under Suction" American Society of Heating and Ventilation Engineer Transaction 1932, 38 387-

20. DALLA VALLE J.M. "The Control of Industrial Dust" Mechanical Engineering 1933, 55 621-24

21. DALLA VALLE J.M. "The Importance of Velocity Characteristic in the Design of Local Exhaust Hoods" Journal of Industrial Hygiene & Toxicology 1938, 15 18-26

22. DALLA VALLE,J.M. "Exhaust Hoods" The N.Y.Industrial Press Ltd. 148 Lafayette Street.

23. DALLA VALLE J.M. and HATCH,T. "Studies in the Design of Local Exhaust Hoods" Transaction of the American Society of Mechanical Engineers WD1-54-10 1939 31-37

24. DALY,B.B. "Woods Practical Guide to Fan Engineering" 1978 England, Woods of Colchester.

25. DAWS,L.F. "Movement of Air Streams Indoors" Journal of the Institute of Heating and Ventilation Engineers 1970 (Feb) 241-253.

REFERENCES (contd)

26. DAWS,L.F. PENWANDEN,A.D. and WATERS,G.T."A Visualization Technique for the Study of air movement in rooms" Ibid 1965 (April) 24-29

27. DRKAL Von Fr. "Stromungsvenhaltnisse bei runden Saugoffnungen mit Flansch" Zeitchnift Fuer Heizung,Leuftung, Klimatechnik Haustechnik (HLH) 1970 21 8 August 271-73

28. DRKAL Von Fr. "Theoretical Determination of Aerodynamic Condition at Exhaust Intake slits" Ibib 1971 22 5 May 167-72

29. EZIHE,C.A. "Maintenance of Local Exhaust Ventilation Systems" 1976 M.Sc. Project, Department of Health and Safety, The University of Aston in Birmingham

30. FIALKOVSKAYA,T.A. "Extract Hoods and Chambers" Ventyazhnye Zanty I Shafy Strouzdat 1947 (Russian)

31. FLETCHER,B. "Centre-Line Velocity Characteristics of Rectangular Unflanged Hoods and Slots Under Suction" The Annals of Occupational Hygiene 1977 20 141-46

32. FLETCHER,B. "Effect of Flanges On the Velocity In Front of Exhaust Ventilation Hoods" Ibid 1978 21 265-269

33. FRAZER,D.A. "An Innocuous Tracer Technique for Testing the Performance of Ventilgation Systems" Journal of the Institute of Heating and Ventilating Engineers 1965 (Sept-Dec) 490-97

34. G.K.N.Farr Filtration Limited "30/30 Disposable Panel Air Filter" Trade Publication undated.

35. GILL, F.S. "Extract Ventilation, its Problems" Polytechnic of South Bank (Unpublished, undated).

36. Great Britain Factory Act 1961 Section 63

37. Great Britian Health and Safety Executive "Principle of Local Exhaust Ventilation: First Report of the Sub-Committee on Dust and Fumes" 1975 London, HMSO

38. HALE,W.B. "Thermistor as Instruments of Thermometry and anemometry" Bulletin American Metallurgical Society 1948, 29, 10 494-99.

39. HARTLEY,H.O. "The modified Gauss-Newton method for fitting of non-linear regression fuction by least squares" Technometrics 1961 3 269-80

40. HARROLD,G. "Getting Rid of Air Contaminants" National Safety News 1941 (December 20-21) 68-9

41. HARTLEY,H.O. and BROOKEN,A. "Non-Linear Least Squares Estimation" Annal of Mathematical Statistics 1965 36 638-50

42. HATCH,T. "Fundamental relating to the Design and Operation of exhaust system" American Standard Association (ASA) 1936 ASA-29 NY, ASA.

43. HATCH,T. "Fundamental Factors in the Design of exhaust system" Mechanical Engineering 1936 58 109-113

44. HATCH,T. "Design of Exhaust Hoods for Dust-Control Systems" "Journal of Industrial Hygiene and Toxicology 1936 18 No.9 595-603

45. HUGHES,H.J. and SEFFARD,A.T. "A Treaties on Hydraulics 1911 New York, The Macmillan Co.

46. Institute of Heating and Ventilating Engineers (IHVE) "Guide Books:
Book A Design Data
Book B Installation and Equipment Data
Book C Reference data"
1970 London, IHVE

47. LAMB,H. "Hydrodynamics" 1906 3rd Edition, Cambridge, At the University Press.

48. LAPPLE,C.E. "Using the Velocity Head Concept in Pressure Calculation" Heating Piping & Air Conditioning 1945 17 179-99, 262-67, 319-24

49. LEGG,R.C. "The Calibration of Anemometers in a six-inch Open Jet Wind Tunnel" Heating and Ventilation Engineers 1970 (August) 57-63

50. LOVELOCK,J.E. and WASILEMSKA,E.M. "An Ionization Anemometer" Journal of Scientific Instruments 1949 26 367-70

51. METZLER,C.M., ELFRING,G.L. and McEVAN A.J. "A User Manual for non-linear and Associated Programming Research Biostatistics" The Up John Company Kalamazoo Michigan 1974 (April) 20

52. MILLER,D.S. and ZANKER,J. "Flow Measurements by Integration and Point Velocities" Report No.RR957 Pembroke Power Station Cooling Water System Aug 1968 British Hydro-Mechanical Research Association

53. International Telephon and Telecommulcation (ITT) "Thermistor Data" 1977-78 2nd Edition Thermistor Division 6513/2066E.

54. MURRAY,W.L. and BEARDSHALL,D. "A Reed Anemometer for measuring Air Speeds in Coal-Dust Explosion" Safety in Mine Research Establishment

55. MYLES,D.J, WHITAKER,J. and JONES,M.R. "A Simplified Integration for measuring Volume Flow in Rectangular Ducts" Ministry of Technology National Engineering Laboratory Report No.251 1966

56. McBAIN,G., COLE,C.W. and SHEPHERD,R.D. "Pneumoconiosis in a group of large Iron and Light Alloyed Foundries 1962 Transassociation Industrial Medical Officers (April) 12 17-29

57. NOON,C.L.B. "Aerofoil Fans in Variable Volume Systems" Woods of Colchester Publication, undated.

58. Nottingham Algorithm Group Library "NAGLIB" 1973 3 Document No.510 England, Nottingham University

59. OPPL,L. "Vetrani v Prumyslr 1957 Prague,Statni nake Technik Litratry

60. OWEN,E. "The Measurement of Air Flow" 1949 London, London Chapman & Hall Ltd.

61. OWEN,E. and PANKHURST,R.C. "The Measurement of Air Flow" 1966 England, Pergamon Press

62. PATTERSON,T.N.L. "The Optimum Addition of Points to Quadrature Formulae" Mathematics Computation 1968 22 848-56 and 877-81

63. PIPES,L.A. "Applied Mathematics for Engineers and Physicists" 1946 1st Edition, New York

64. PRUZNER,A.S. "Flow Structure in the Zone of Action of Suction Appertures" Otopleniye I Ventilyetsize 1939 3 13-21

65. SILVERMAN,L. "Fundamental Factors in the Design of Exhaust Hoods" Ph.D. Thesis, Harvard University 1960

66. SILVERMAN,L. "Velocity Characteristics of narrow exhaust slot" Journal of Industrial Hygiene and Toxicology 1942 24 267-76

67. SILVERMAN.L. "Centre-line Velocity Characteristics of Round Openings Under Suction" Ibid 1942 No.9 259-66

68. NIE,N.H., HULL,C.H., JENKINS,J.G., STEINBRENNER,K. and BENT,D.H. "Statistical Package for Social Sciences (SPSS)" 1975 2nd Edition, N.Y., McGraw Hill Book Co.,

69. University of Manchester Regional Computer Centre (UMIST) "SPSS Version 7 Procedures Volume 1 - Regression" 1979 (August) UMIST

70. University of Manchester Regional Computer Centre (UMIST) "SPSS Version 6 Procedure Volume 1-Regression" 1977 UMIST

71. U.S.A.National Institute for Occupational Safety and Health (NIOSH) "The Recirculation of Industrial Exhaust Air" Symposium Proceedings 1978 U.S.A.Department of Health & Education and Welfare, Washington (April)

72. United States Air Moving and Conditioning Association (AMCA) "Standard Test Code" 1975 AMCA 500-75

73. WHITAKER,J. "Fan Performance Testing Inlet Measuring Methods" National Engineering Laboratory Reprint from the Institute of Mechanical Engineering Conference On Fan Technology 6517

74. WHITERIDGE,W.N. "Here's Methods for Figuring Industrial Exhaust Systems" Heating Piping and Air Conditioning 1945 (March) 121-24.

75. WITHERIDGE,W.N. "Control of Industrial Atmospheres:- Dusts, Fumes,Mists,Vapours and Gases" Transactions American Society of Heating and Ventilating Engineers 1945 (January) No.1275 227-42

76. WILLIAM,Y.L. "The Averaging Pressure Tubes Flowmeter for the Measurement of the rate of Air Flow in Ventilating Ducts and for the Balancing of Air Flow Circuits in Ventilating Systesm" Ph.D.Thesis, Glasgow University (1966)

77. WINTERNITZ,F.A.L. "Probe Measurements in Three-Dimensional Flow:- A Comparative Survey of Different types of Instrument" Fluid Flow 1956 (August 28 273-

78.WINTERNITZ,F.A.L. and FISCHL,C.F. "A Simplified Integration Technique for Pipe Flow Measurement" Water Power 1957 9 No.6 225-34

79. YAGLOU,C.P. "The Heated Thermometer Anemometer" The Journal of Industrial Hygiene and Toxicology 1938 20 No.8 497-510